Hormonal regulation of the Sertoli cell tight junction

Mark McCabe

Doctor of Philosophy

2008

Hormonal regulation of the Sertoli cell tight junction

Thesis submitted in fulfilment of the requirements for the degree of Doctor of Philosophy

Mark McCabe
B App Biol/Biotech (Hons)

School of Applied Science, Science Engineering and Technology
RMIT University
July, 2008

Declaration

I, Mark James McCabe, declare that all material presented within this thesis is my own work conducted since the commencement of my degree attaining to the Doctor of Philosophy. No work contained within this thesis has been submitted on any other previous occasion for the award of any other degree or diploma at any other institution. Furthermore, this thesis contains no previously published material except for where due reference is given. All work conducted in this thesis was as per approved ethical guidelines.

Mark McCabe

Prince Henry's Institute of Medical Research

Monash Medical Centre, Clayton, Victoria

Australia 3168

25th July, 2008

Acknowledgements

Well, what a journey it has been. One of the toughest components of finishing this thesis was not 'what' or 'how' to write the end, but how to sum up the findings of this thesis and let it represent the four years of hard work and committed help from my supervisors, family and friends both at Prince Henry's Institute of Medical Research at the Monash Medical Centre, Clayton, and outside as well.

Justifiably, I wish to thank my supervisor Dr Peter Stanton first and foremost. Your guidance, friendship, patience and sense of humour have been inspirational to me throughout not only my PhD but Honours as well. That's 5.5 years! You have gone out of your way to make every aspect of my PhD as educational, enjoyable, inspirational and beneficial for my future as possible, and I am very grateful for all you have done. I feel that the conferences I have attended through your provision in Perth, New Zealand and Canada and the ability to visit labs for potential post doc work have also been very beneficial for my future and again I am grateful for that. Thankyou for your encouragement and while at times you thought I might have been showing too much commitment to the PHI footy tipping, just remember that had I have shown more you would probably be several thousand dollars richer by now!!

Thankyou also to my RMIT supervisor, Dr Peter Smooker. I am also immensely grateful for your encouragement, sense of humour, help and friendship throughout my PhD studies, especially for your correspondence regarding reports, requirements and bureaucracies!!

I also duly acknowledge the contributions made to my research by others. Thank you to Mrs Enid Pruysers for conducting the serum LH and FSH assays (Chapter 5) and to Ms Fiona McLean for conducting the serum androgen assays (Chapter 5) and teaching me scintillation spectrophotometry. Thankyou also to Dr Sarah Meachem and Mrs Georgia Balourdos for conducting the stereological analyses of germ cell types and numbers (Chapter 5). Also thankyou to Dr Michael Lynch for teaching me how to design primers for RT-PCR analysis for use throughout this thesis. I'm sure my primers worked all the better due to your in-depth knowledge on the subject! I appreciate immensely how each of you have given up your time and used your areas of expertise to further my results. Thankyou.

Professor David 'Robbo' Robertson, thankyou for your help, friendship and sense of humour as well. I appreciate everything you have done for me too and Collingwood will do well at some stage,

trust me. Any time you need me to watch your houses in Glen Waverley or the south of France, let me know and I won't re-train the cat this time, I promise!

Sarah Meachem you have also been a great help. Thankyou for your help and friendship as well and letting me cut the human sections all on my own!! Thankyou to Prof Rob McLachlan and Dr Kati Matthiesson for providing me with human testis samples to conduct my work on (Chapter 7). If I've used too many, I'll find some other volunteers to replace them for you.

Saleela (Saaaal), you were always the most senior PhD student, by one week to me, but we were both well aware of your superior position. Thankyou so much for your friendship and help. It's been great having private chats with you and Caroline, and you have both been great to bleed my heart out too. Thanks Saleela for helping me inject the rats when I was too scared at first. You instilled the confidence in me to do it well! And thankyou Caroline for teaching all of the experimental techniques to me in the beginning and being a back-up whenever I needed it!

Gerard, your wisdom with immunohistochemistry in particular has been a true blessing for my thesis and without your help, I would not have produced the quality images I have. I am very grateful to you for all or your help, support, insight, suggestions and friendship.

To James, Ileana, Yao, Melinda, Maree, Ellen and Mai over in the West Wing. You have all been great mates and it's been fantastic to be able to come over to your side and socialise with you and go out for dinners and just relax. I've appreciated every moment of it. Jim, I'll miss our table tennis games in the 'med students only' room. We may forget the code to get in every time, but we'll break that door down if we have too. I'm sure we'll both hear from Dutchy soon!

To everyone else in the Reproductive Hormones Laboratory and Male Reproductive Endocrinology Laboratory, thank you all for your friendship and support.

Outside of my PhD, thankyou to Andrew and Freda Ioannou, for having me at your business in Lorne over the course of my tertiary education. Working with and for you has been a pleasure, and has provided me with further income to live closer to Prince Henry's, and achieve goals such as travelling overseas and learning to fly planes. I treasure the close friendship we have built between us.

To all of my other mates, thank you for keeping me sane and entertained over the past few years. Luke and Kris, it's been unreal flying with you and exploring this passion. One of my best memories is of making comments over the air-waves after Collingwood was defeated by Geelong in

the 2007 Preliminary Final and being called a traitor by Qantas pilots. We landed pretty quickly after that!

To my wonderful family. Thankyou for all of your encouragement and support during this journey. I may have been difficult at times, but I appreciate everything and how you have stuck by me through it all! It has been a wonderful experience and I don't know how I could have done it without you. I am who I am, because of you.

To my beautiful fiancé Leyla. Thankyou for all of your patience, encouragement, generosity and love. I feel very special that you have kept flying out here from England to help keep our relationship as strong and as close as it has been. I also don't know how I could have done it without you and you have also made me a stronger person. I can't wait to make all of that travelling and emotional farewells at airports up to you and begin our lives together.

Table of Contents

Section

Title Page **i**

Declaration **ii**

Acknowledgements **iii**

Table of Contents **vi**

Publications arising from this thesis **xv**

List of Abbreviations **xvi**

List of Tables **xix**

List of Figures **xx**

Summary **1**

Chapter 1: Literature Review **4**

1.1 Introduction 4

1.2 Overview of spermatogenesis 6

1.2.1 The mammalian testis 6

1.2.2 Spermatogenesis 7

1.2.3 Cycles of spermatogenesis 8

1.2.4 The Sertoli cell 10

1.2.5 Cell-cell interactions 12

a. Anchoring junctions 12

b. Gap junctions 14

c. Tight junctions 14

1.3 The tight junction 15

1.3.1 Tight junction ultrastructure 15

1.3.2 Molecular composition and architecture of the tight junction 16

a. Membrane components 16

b. The cytoplasmic plaque 19

1.4 The function of the tight junction 19

1.4.1 Qualitative assessment of tight junction function 19

1.4.2 Quantitative assessment of tight junction function 21

1.4.3 The size-selective nature of the tight junction 24

1.4.4 The role of occludin and the claudins in tight junction function 26

a. Occludin 26

b. Claudins 27

1.5 The role of phosphorylation in tight junction assembly 29

1.6 The inter-Sertoli cell tight junction 33

1.6.1 The structure of the Sertoli cell tight junction 33

1.6.2 Regulation of tight junction proteins within the Sertoli cell 35

a. Protein phosphorylation 35

b. The role of the extracellular matrix 36

c. The role of local paracrine factors 37

d. The endocrine system 39

1.7 Gonadotrophin suppression models and their effects on spermatogenesis 41

1.7.1 Hormone suppression by GnRH immunisation 42

1.7.2 Hormone suppression by GnRH antagonism 45

1.7.3 Hormone suppression by Testosterone/Estradiol administration 46

1.7.4 The hypogonadal mouse 47

1.7.5 Hormone suppression in men 49

1.8 Knockdown of gene expression by RNA interference 50

1.9 Conclusion 53

1.10 Hypothesis and aims 56

Chapter 2: Materials and Methods **57**

2.1 Animals 57

2.2 Immunohistochemistry 57

a. Fixed tissue 57

b. Frozen tissue 60

2.3 Real-time reverse transcriptase-polymerase chain reaction (RT-PCR) 60

analysis

2.3.1 Total RNA extraction and isolation 60

2.3.2 DNase-free treatment 61

2.3.3 Total RNA quantification 61

a. Ultraviolet spectrophotometry 61

b. RiboGreen assay 62

2.3.4 Reverse transcription 62

2.3.5 Real-time RT-PCR 63

a. The LightCycler system 63

b. Primer optimisation 64

c. Sample preparation for RT-PCR 64

2.4 DNA sequencing 65

2.4.1 DNA agarose gel 65

2.4.2 DNA sequencing 65

2.5 Western blot analysis 66

2.5.1 Protein extraction 66

2.5.2 Protein quantification 67

2.5.3 SDS-Polyacrylamide gel electrophoresis (SDS-PAGE) 67

2.6 Statistical analysis 68

Chapter 3: The contribution of claudin-11 and occludin to the function of the Sertoli cell tight junction, *in vitro* **69**

3.1 Introduction 69

3.2 Materials and Methods 70

3.2.1 Animals 70

3.2.2 Immature Sertoli cell isolation 70

3.2.3 Cell plating 71

a. Plating for transepithelial electrical resistance and immunocytochemistry 71

b. Plating for western blot and total RNA extraction 72

3.2.4 Hypotonic shock 72

3.2.5 Measuring transepithelial electrical resistance 72

3.2.6 siRNA cultures 73

3.2.7 Immunocytochemistry 75

a. Cell fixation procedure 75

b. Preparation of fixed cells for immunocytochemical analysis 76

3.2.8 Real-time RT-PCR analysis 76

3.2.9 Western blot analysis 77

3.2.10 Statistical analysis 77

3.3 Results 77

3.3.1 Effect of claudin-11 siRNA on tight junction function 77

3.3.2 Effect of claudin-11 siRNA on claudin-11 localisation 78

3.3.3 Effect of claudin-11 siRNA on the localisation of other junctional proteins 78

3.3.4 Effect of claudin-11 siRNA on claudin-11 and occludin mRNA expression 78

3.3.5 Effect of claudin-11 siRNA on claudin-11 and occludin protein expression 79

3.3.6 Western blot optimisation for claudin-11 detection in Sertoli cell extractions 79

3.3.7 Effect of occludin siRNA and combined claudin-11/occludin siRNA on tight junction function 80

3.3.8 Effect of occludin siRNA and combined claudin-11/occludin siRNA on protein localisation 81

3.4 Discussion 81

Chapter 4: The optimisation and application of tracers for tight junction functional analysis, *in vivo* **88**

4.1 Introduction 88

4.2 Materials and Methods 89

4.2.1 Animals 89

4.2.2 Experimental design for qualitative tight junction function analysis 89

4.2.3 Experimental design for quantitative tight junction function Analysis 90

4.2.4 Statistical analysis 92

4.3 Results 92

4.3.1 Qualitative tracer optimisation 92

a. Intratesticular injection of Trypan Blue dye 92

b. Detection of HRP in frozen and Bouin's fixed testes by fluorescent microscopy 92

c. Detection of HRP in frozen and fixed testes by light microscopy 93

d. Detection of biotin frozen and fixed testes 93

e. Detection of biotin in a prepubertal rat testis 93

4.3.2 Quantitative tracer optimisation 94

a. Effect of glycerol treatment on testis weights and seminiferous tubule accumulation of [^{3}H]methoxy-inulin 94

b. Effect of glycerol treatment on tubule morphology and biotin permeation into the seminiferous tubules 94

4.4 Discussion 95

Chapter 5: Hormonal regulation of the Sertoli cell tight junction in the gonadotrophin releasing hormone (GnRH)-antagonist treated rat, *in vivo* **100**

5.1 Introduction 100

5.2 Materials and Methods 102

5.2.1 Animals 102

5.2.2 Experimental design 102

5.2.3 Glycerol intratesticular injection 104

5.2.4 Immunohistochemistry 104

5.2.5 Western blot analysis 104

5.2.6 Real-time RT-PCR analysis 104

5.2.7 Stereology 104

5.2.8 Serum hormone assays 105

a. LH 105

b. Total androgens 106

c. FSH 107

5.2.9 Statistics 107

5.3 Results 108

5.3.1 Testis and body weights 108

5.3.2 Serum hormone levels 108

a. LH 108

b. Androgens 109

c. FSH 109

5.3.3 Stereological assessment of germ cell types and numbers 109

a. Type A/Intermediate spermatogonia 109

b. Type B/Preleptotene spermatocytes 109

c. Leptotene/Zygotene spermatocytes 110

d. Pachytene spermatocytes stages I-VIII 110

e. Pachytene spermatocytes stages IX-XIV 111

f. Round spermatids stages I-VIII 111

g. Elongated spermatids stages I-VIII 112

h. Elongated spermatids IX-XIV 112

i. Sertoli cell numbers 112

5.3.4 Effect of hormone suppression and short-term replacement on tight junction structure/localisation and function 112

5.3.5 Quantitative analysis of tight junction function 113

a. Tracer accumulation in hormone suppressed and glycerol treated testes 113

b. Comparative tracer accumulations in control, glycerol treated and prepubertal testes 113

5.3.6 Testicular macrophage localisation following hormones suppression and replacement 115

5.3.7 Western blot analysis 115

5.3.8 Real-time RT-PCR analysis 116

5.4 Discussion 116

Chapter 6: Hormonal regulation of the Sertoli cell tight junction in the hypogonadal (*hpg*) mouse, *in vivo* **131**

6.1 Introduction 131

6.2 Materials and Methods 133

6.2.1 Animals 133

6.2.2 Experimental data 133

6.2.3 Immunohistochemistry 134

6.2.4 Real-time RT-PCR analysis 134

6.2.5 Statistical analysis 135

6.3 Results 135

6.3.1 Developmental localisation of claudin-11 and claudin-3 to the tight junction and ZO-1 to the cytoplasmic plaque in pubertal and adult mice 135

a. Wildtype 136

b. *hpg* 136

c. *hpg* + tgFSH 137

6.3.2 Administration optimisation of biotin to the *hpg* mouse testis 137

6.3.3 Testis weights of adult *wt* mice and *hpg* and *hpg* + tgFSH mice after ± DHT treatment 138

6.3.4 Development of tight junction functionality and protein localisation in *hpg* and *hpg* + tgFSH mice treated with DHT 138

a. Wildtype 138

b. *hpg* 138

c. *hpg* + 2 days DHT 139

d. *hpg* + 10 days DHT 139

e. *hpg* + tgFSH 139

f. *hpg* + tgFSH 2 days DHT 139

g. *hpg* + tgFSH 10 days DHT 139

6.3.5 Effects of DHT treatment on mRNA expression in *hpg* and *hpg* + tgFSH mice 140

6.4 Discussion 141

Chapter 7: Hormonal regulation of the Sertoli cell tight junction in the gonadotrophin suppressed human, *in vivo* **151**

7.1 Introduction 151

7.2 Materials and Methods 152

7.2.1 Human testis tissue 152

7.2.2 Experimental design 153

a. Hormone suppression 153

7.2.3 Immunohistochemistry 153

7.2.4 RNA preparation 153

7.2.5 RNA amplification 154

a. First strand cDNA synthesis 155

b. Second strand cDNA synthesis 155

c. cDNA purification 155

d. *In vitro* transcription (IVT) to synthesise amplified RNA (aRNA) 156

e. aRNA purification 156

f. aRNA quantification and reverse transcription 157

7.2.6 Real-time RT-PCR analysis 157

7.2.7 Statistical analysis 157

7.3 Results 158

7.3.1 Effects of gonadotrophin suppression on tight junction protein localisation 158

7.3.2 Effects of gonadotrophin suppression on other junctional protein localisation 159

7.3.3 Comparison of germ cell numbers with claudin-11 localisation 159

a. T+A treatment group 159

b. T+LNG treatment group 160

c. T+LNG+A treatment group 160

d. T+LNG+D treatment group 160

7.3.4 RNA Amplification with MessageAmp II kit for RT-PCR Analysis 161

7.3.5 RT-PCR validation 161

7.3.6 Effects of gonadotrophin suppression on junctional mRNA expression 161

7.4 Discussion 162

Chapter 8: General discussion 169

References 183

Appendices 238

Appendix 1.1: Immature Sertoli cell culture 238

Appendix 1.2: siRNA protocol 244

Appendix 1.3: Serum hormone assays 247

a. LH 247

b. Androgens 249

c. FSH 249

Appendix 1.4: Data for the stereological assessment of germ cell types and numbers 251

Appendix 1.5: Individual human immunos 262

*** Note that data for Appendices 1.3, 1.4 and 1.5 are also presented on CD inside the back cover over this thesis**

Publications arising from this thesis

Abstracts

McCabe MJ, Stanton PG (2005) Contribution of claudin-11 to the inter-Sertoli cell tight junction, *in vitro*. 48th Annual Scientific Meeting of the Endocrine Society of Australia, Perth, Western Australia, Australia

McCabe MJ, Smooker PM, Stanton PG (2007) Effect of gonadotrophin suppression on testicular tight junctions. Inaugural Southern Health Research Week, Monash Medical Centre, Clayton, Victoria, Australia

McCabe MJ, Tarulli GA, McLachlan RI, Stanton PG (2007) Effect of gonadotrophin suppression on testicular tight junctions. 90th Annual Scientific Meeting of the Society of Endocrinology, Toronto, Ontario, Canada

McCabe MJ, Tarulli GA, Smooker PM, Stanton PG (2007) Hormonal regulation of testicular tight junctions. 50th Annual Scientific Meeting of the Endocrine Society of Australia, Christchurch, New Zealand

List of abbreviations

A	Acyline
Ab	Antibody
Adiol	5α-androstane-3α,17β-diol
aRNA	Amplified RNA
bSA	Bovine serum albumin
BTB	Blood-testis barrier
cDNA	Copy DNA
CAR	Coxsackie virus and adenovirus receptor
CNP	C-natriuretic peptide
CNS	Central nervous system
D	Dutasteride
DAB	3,3-diamino-benzidine
DAPI	4',6-diamidino-2-phenylindole dihydrochloride
ddNTP	Dideoxynucleotide triphosphate
DEPC	Diethylpyrocarbonate
DHT	dihydrotestosterone
DNA	Deoxynucleic acid
dNTP	Dexoynucleotide triphosphate
DMEM	Dulbecco's Modified Eagle's Medium
DMPA	Depot Medroxyprogesterone Acetate
dsDNA	Double-stranded DNA
dsRNA	Double-stranded RNA
EBA	Evan's Blue Dye
ED	Ectodermal dysplasia
EDTA	Ethylenediaminetetraacetic acid
ES	Ectoplasmic specialisation
FCS	Fetal calf serum
FGF-2	Fibroblast growth factor-2

FSH	Follicle stimulating hormone
GAPDH	Glyceraldehyde-3-phosphate dehydrogenase
GnRH	Gonadotrophin releasing hormone
hCG	human chorionic gonadotrophin
hpg	Hypogonadal
HPLC	High performance liquid chromatography
HRP	Horse-radish peroxidase
IgG	Immunoglobulin
IL	Interleukin
INSL-3	Insulin like-3
Ip	Intraperitoneal
IVT	In vitro transcription
JAM	Junctional Adhesion Molecule
KRP	Krebs Ringer Phosphate Buffer
LH	Leutinising hormone
LNG	Levonorgestrel
LPS	Lipopolysaccharide
MDCK	Madin-Darby canine kidney cells
MHC	Male hormonal contraception
MRI	Medical resonance imaging
mRNA	Messenger RNA
PAGE	Polyacrylamide gel electrophoresis
PBS	Phosphate-buffered saline
PEG	Polyethylene glycol
PKA	Protein kinase A
PMSF	Phenylmethylsulfonylfluoride
QC	Quality control
rFSH	Rat FSH
rhFSH	Recombinant human FSH

RIA	Radioimmunoassay
RISC	RNA-inducing silencing complex
rLH	Rat LH
rrFSH	Recombinant rat FSH
RNA	Ribonucleic acid
RT	Reverse transcription
RT-PCR	Reverse transcriptase-polymerase chain reaction
SDS	Sodium dodecyl sulfate
shRNA	Short hairpin RNA
siRNA	Small interfering RNA
T	Testosterone
TE	Testosterone/Estradiol
TER	Transepithelial electrical resistance
TGFβ	Transforming growth factor β
tgFSH	Transgenic FSH
TJ	Tight junction
TNFα	Tissue necrosis factor-α
UV	Ultraviolet
wt	Wildtype
ZO	Zonulae occluden

List of Tables

Table 1.1	Localisation and characterisation of members of the claudin superfamily	17
Table 3.1	siRNA designs	73
Table 3.2	Antibodies used for immunohistochemical analysis	76
Table 3.3	Primer sequences and real time RT-PCR conditions for the analysis of siRNA mediated gene silencing of claudin-11 in cultured Sertoli cells	76
Table 3.4	Antibodies and conditions used for western blot analysis	77
Table 4.1	Antibodies used for immunohistochemical analysis	90
Table 4.2	Localisation of HRP tracer in fixed or frozen testes	93
Table 5.1	Antibodies used for immunohistochemical analysis	104
Table 5.2	Antibodies and conditions used for western blot analysis	104
Table 5.3	Primer sequences and RT-PCR conditions for the analysis of mRNA expression in the GnRH-antagonist treated rat	104
Table 5.4	Body and testis weights	108
Table 5.5	Stereological assessment of elongated spermatid and Sertoli cell numbers	112
Table 6.1	Antibodies used for immunohistochemical analysis	134
Table 6.2	Primer sequences and RT-PCR conditions for the analysis of mRNA expression in the *hpg*, and *hpg* + tgFSH mice treated with DHT	134
Table 7.1	Antibodies used for immunohistochemical analysis	153
Table 7.2	Primer sequences and RT-PCR conditions for the analysis of mRNA expression in the human gonadotrophin suppressed testis	157

List of Figures

Figure 1.1	Organisation of the mammalian testis	6
Figure 1.2	Spermatogenesis in the testis	7
Figure 1.3	The spermatogenic wave and spermatogenic cycle	8
Figure 1.4	The spermatogenic cycle in the human	9
Figure 1.5	The junctional complex	12
Figure 1.6	Protein interactions within the tight junction	15
Figure 1.7	Transmembrane components of the tight junction	15
Figure 1.8	Biotin penetration into the seminiferous epithelium	16
Figure 1.9	Co-localisation of tight junction components with biotin tracer	21
Figure 1.10	Migration of germ cells across the Sertoli cell tight junction	35
Figure 1.11	Horse-radish peroxidase tracer penetration into the seminiferous Epithelium	40
Figure 1.12	The small interfering RNA mediated gene silencing pathway	51
Figure 2.1	LightCycler assessment of real-time polymerase chain reaction (RT-PCR)	63
Figure 2.2	DNA agarose gel and subsequent sequencing of RT-PCR pimer products	65
Figure 3.1	Measuring transepithelial electrical resistance (TER)	72
Figure 3.2	Effect of claudin-11 siRNA on TJ function	77
Figure 3.3	Effect of claudin-11 siRNA on claudin-11 localisation to the TJ	78
Figure 3.4	Effect of claudin-11 siRNA on the localisation of occludin to the TJ and β-catenin to the adherens junction	78
Figure 3.5	Real-time RT-PCR analysis of the effect of claudin-11 siRNA on the mRNA expression of claudin-11 and occludin	78
Figure 3.6	Western blot analysis of changes in the protein expression of	79

	occludin in response to claudin-11 siRNA treatment	
Figure 3.7	Optimisation of western blot analysis for claudin-11 protein expression	79
Figure 3.8	Effect of occludin siRNA, and combined claudin-11/occludin siRNA on TJ function	80
Figure 3.9	Effect of occludin siRNA and combined claudin-11/occludin siRNA on protein localisation to the TJ and adherens junction	81
Figure 4.1	Testicular artery perfusions	92
Figure 4.2	Intratesticular injection of Trypan Blue dye	92
Figure 4.3	HRP localisation in frozen and paraformaldehyde and Bouin's fixed testes	92
Figure 4.4	Biotin tracer localisation in frozen and paraformaldehyde and Bouin's fixed testes	93
Figure 4.5	Biotin localisation in prepubertal rat testes	93
Figure 4.6	Effect of glycerol treatment on TJ function	94
Figure 4.7	Effect of glycerol treatment on seminiferous tubule morphology and biotin migration across Sertoli cell TJs	94
Figure 5.1	Effect of hormone suppression and short-term replacement on Serum LH, androgens and FSH	108
Figure 5.2	Stereological assessment of germ cell types and numbers	109
Figure 5.3	Effect of hormone suppression and replacement on TJ function and structure	112
Figure 5.4	Effect of hormone suppression and replacement on the localisation of claudin-11 and JAM-A to the testicular TJ, and ZO-1 to the cytoplasmic plaque	113
Figure 5.5	Quantitative analysis of TJ function in response to hormone	113

	suppression, short-term hormone replacement, and glycerol treatment	
Figure 5.6	Comparison of [^{3}H]methoxy-inulin and [^{14}C]mannitol accumulation in testes from control and glycerol treated adult rats, and in juvenile rats	114
Figure 5.7	Effect of hormone suppression and replacement on macrophage localisation in hormone suppressed and replaced testes	115
Figure 5.8	Effect of hormone suppression and replacement on TJ protein expression	115
Figure 5.9	Effect of hormone suppression and replacement on TJ mRNA expression	116
Figure 5.10	Macrophage localisation in control and disrupted testes	125
Figure 6.1	Occludin staining in control wildtype mouse testes	135
Figure 6.2	Protein localisation in pubertal (20 day old) and adult *hpg* and *hpg* + tgFSH mice	136
Figure 6.3	Optimisation of biotin administration into mice testes	137
Figure 6.4	Mouse testis weights following androgen DHT treatment	138
Figure 6.5	TJ functional and structural analysis following DHT treatment to *hpg*, and *hpg* + tgFSH mice	138
Figure 6.6	Claudin-3 staining in *hpg* + tgFSH mice	139
Figure 6.7	Real-time RT-PCR analysis of tight junction mRNA expression in response to DHT treatment to *hpg* and *hpg* + tgFSH mice	140
Figure 7.1	Localisation of claudin-11 in control and hormone suppressed human testes	158
Figure 7.2	Localisation of ZO-1 in control and hormone suppressed human testes	159

Figure 7.3	Effect of hormone suppression on different junctional types in the human testis	159
Figure 7.4a	Comparison of claudin-11 localisation with extent of spermatocyte suppression in T+A treated men	159
Figure 7.4b	Comparison of claudin-11 localisation with extent of spermatocyte suppression in T+LNG treated men	160
Figure 7.4c	Comparison of claudin-11 localisation with extent of spermatocyte suppression in T+LNG+A treated men	160
Figure 7.4d	Comparison of claudin-11 localisation with extent of spermatocyte suppression in T+LNG+D treated men	160
Figure 7.5	RT-PCR analysis of mRNA expression in hormone suppressed human testes	161
Figure 7.6	RT-PCR analysis of androgen-regulated INSL-3 and housekeeper protein β-actin mRNA expression in response to hormone suppression in men	161
Figure 7.7	Localisation of claudin-3 in hamster, human and rat testes	164
Figure 7.8	Biotin localisation in an adult rat testis biopsy	165
Figure 7.9	Claudin-11 localisation in TE+DMPA and T+A treated men	167
Figure 8.1	Tight junction function and active spermatogenesis	171
Figure 8.2	Cytoplasmic localisation of TJ proteins in gonadotrophin suppressed rodent testes	174

Summary

The Sertoli cell tight junction (TJ) of the seminiferous epithelium is the major component of the blood-testis barrier (BTB), and is important for the developmental process of spermatogenesis as it separates germ cells in the seminiferous tubules from components of the general circulation in the testicular interstitium. Absence of the TJ leads to spermatogenic arrest and infertility. TJs form at puberty as circulating gonadotrophins luteinising hormone (LH) and follicle stimulating hormone (FSH) increase, with LH causing elevated serum and testicular testosterone (T). Several studies have demonstrated hormonal regulation of the two major TJ proteins, claudin-11 and occludin, and also of TJ function *in vitro* and *in vivo*. Men with low levels of circulating gonadotrophins exhibit an immature and dysfunctional TJ phenotype, which is reversed upon the exogenous application of gonadotrophins.

This thesis hypothesises that claudin-11 and occludin are the major contributors to TJ function, and that gonadotrophins regulate TJ function and structure via these two proteins in several species including humans.

This PhD was divided into four separate studies to address these hypotheses. The first study assessed the relative contribution of claudin-11 and occludin to TJ function *in vitro* using small interfering RNA (siRNA)-mediated gene silencing in cultured immature rat Sertoli cells. As a result of silencing both proteins, separately or in combination, TJ function was significantly ($p < 0.01$) reduced as measured by transepithelial electrical resistance (TER). This was associated with marked reductions in the localisation of the siRNA targeted protein to the TJ *in vitro* as shown by immunocytochemistry, with minimal effects on other nearby proteins or cell junctions. A significant ($p < 0.01$) reduction in claudin-11 mRNA expression was also observed following claudin-11 siRNA treatment as assessed by real-time RT-PCR analysis. It was concluded in this study that both claudin-11 and occludin contribute significantly to TJ function *in vitro*.

The second study then aimed to determine the effect of gonadotrophin suppression and short-term hormone replacement on TJ structure and function in a gonadotrophin releasing hormone (GnRH) antagonist-treated rat model *in vivo*. Weekly injections of the GnRH antagonist, acyline, significantly suppressed testis weights, serum LH, FSH, and androgens as well as germ cell numbers.

This was coincident with undetectable occludin staining, and the relocalisation of claudin-11 from the Sertoli cell TJ to the cytoplasm as assessed by immunohistochemistry *in vivo*. Western blot analysis also revealed decreases in the protein expression of both proteins. Disruption to TJ structure was associated with a disruption in TJ function as shown by the penetration of small molecular weight tracer biotin into the seminiferous tubules, which had been excluded to the testicular interstitium in control rats.

Short-term hormone replacement (daily, one week) with human recombinant FSH, human chorionic gonadotrophin (hCG) (to stimulate testicular production of testosterone and FSH), and hCG + FSH antibody (to stimulate testicular production of testosterone alone) partially reversed the acyline-induced effects as shown by significant recoveries in testis weights, serum hormones and germ cell numbers. The reinitiation of spermatogenic activity was associated with some occludin and claudin-11 relocalisation to the TJ, although limited biotin tracer permeation remained . It was therefore concluded that gonadotrophins regulate TJ structure and function *in vivo,* and that re-initiation of spermatogenesis does not require a fully functional TJ.

The third study aimed to analyse the role of gonadotrophin regulation in TJ formation. This aim used the hypogonadal (*hpg*) mouse model, which is a naturally occurring model of hormone deficiency, with basal levels of LH/T, undetectable FSH, arrested spermatogenesis and incomplete TJs. Immunohistochemical analysis revealed extensive claudin-11 staining at the TJ in wildtype testes, whereas claudin-11 localised to the cytoplasm of Sertoli cells in *hpg* testes. Wildtype TJs were fully functional as shown with biotin tracer, whereas *hpg* testes exhibited extensive biotin penetration throughout the tubules indicating dysfunctional TJs.. The presence of transgenic FSH (tgFSH) in *hpg* mice stimulated a redistribution of claudin-11 to the Sertoli cell TJ, which varied from being dysfunctional to functional. Administration of the potent androgen dihydrotestosterone (DHT) to *hpg* mice stimulated claudin-11 redistribution toward the TJ after 2 days, with extensive claudin-11 at a functional TJ by 10

days. The proportion of functional tubules in the *hpg* + tgFSH mice also appeared to qualitatively increase following DHT treatment.

Claudin-3 is a recently-described androgen-regulated protein present at mouse Sertoli cell TJs. It is transiently expressed as germ cells cross the BTB, hence this third study additionally aimed to analyse claudin-3 recruitment to the TJ following DHT treatment and the initiation of spermatogenesis. Claudin-3 staining at TJs was extensive in wildtype mice, but absent in *hpg* mice and predominantly absent in *hpg* + tgFSH mice. Claudin-3 staining was not detectable in *hpg* mice until 10 days of DHT treatment, but was detectable after 2 days of DHT treatment in *hpg* + tgFSH mice. These results indicated a priming role for FSH in the localisation of androgen-dependent claudin-3 to the TJ. It was concluded that gonadotrophins regulate the formation of a structurally and functionally competent TJ in the mouse, which is associated with the recruitment of claudin-3 to the TJ.

The final study of this thesis aimed to examine TJ structure and mRNA expression in men given male hormonal contraception (MHC) for 8 weeks to suppress circulating FSH, LH, and hence testicular spermatogenesis. Claudin-11 staining was extensive at the TJ in control men but generally became punctate following hormone suppression. The extent of claudin-11 disruption was usually associated with the extent of adluminal germ cell suppression which had been quantified previously. TJ mRNA expression levels of claudin-11 did not change following gonadotrophin suppression. It was concluded that gonadotrophins also appear to regulate the structure of the Sertoli cell TJ in men.

In summary, it is concluded that the Sertoli cell TJ is hormonally regulated, and that the major contributors to TJ function *in vivo* and *in vitro* are claudin-11 and occludin. It is hypothesised that the reduction of claudin-11 localisation to the TJ in men may also result in a loss of human Sertoli cell TJ function, suggesting that the TJ may be a potential target of hormonal contraception in men.

Chapter One: Literature Review

1.1 Introduction

Spermatogenesis is the process of germ cell development in the testis, and involves complex interactions between testicular components of the interstitium and seminiferous tubules with each other and the germ cells. In particular, the Sertoli cell of the seminiferous epithelium is the key provider of nutrients and structural support and the key mediator of hormone and other signals essential to the germ cell during spermatogenesis (Aravindan *et al.* 1997, Griswold, 1998, Cheng and Mruk, 2002).

The Sertoli cells also provide the inter-cellular junctions between themselves and the germ cells. These junctions include the gap junctions which specialise in cell-cell communication and the adhesive type junctions such as the desmosomes, ectoplasmic specialisations and the adherens junctions which serve to i) adhere the Sertoli cells to the basement membrane of the seminiferous epithelium or ii) adhere the Sertoli cells to other Sertoli cells or iii) adhere Sertoli cells to germ cells (Russell and Peterson, 1985, Pelletier and Byers, 1992, Mulholland *et al.* 2001, Lui *et al.* 2003a, Lui *et al.* 2003b).

The blood-testis barrier (BTB) which utilises these adhesive junction complexes to regulate germ cell migration into the seminiferous tubules is another provision of the Sertoli cells. The major component of the blood-testis barrier is another junctional type called the Sertoli cell tight junction (TJ) (Setchell, 2004). These TJs provide germ cells with a specialised microenvironment in the seminiferous tubules in which to develop into mature sperm. TJs achieve this by sealing the membranes of adjacent Sertoli cells together and thereby separating the germ cells from the general circulation (Cheng and Mruk, 2002).

In general, TJs form the paracellular pathway between cells, and are size-selective in which solutes or molecules can cross the barrier (Moroi *et al.* 1998). In the testis, the absence of the Sertoli cell TJ means that the germ cells are exposed to components of the blood stream, and spermatogenesis stops, resulting in infertility Chung and Cheng, 2001, Chung *et al.* 2001). TJs are therefore an essential component of the seminiferous epithelium, which form at puberty when hormone levels increase and spermatogenesis starts (Vitale *et al.* 1973, Setchell *et al.* 1981, Russell and Peterson, 1985, Setchell *et al.* 1998).

TJs are not unique to the seminiferous epithelium, in fact they are ubiquitous in all epithelia and form barriers between body cavities or blood vessels and bodily organs. The loss of the TJ from the blood-brain barrier results in excessive fluid accumulation in the brain and can be potentially fatal (Hirase *et al.* 1997). Its absence from the skin results in the death of mice at birth due to massive transepidermal water loss (Furuse *et al.* 2002) and when the intestinal epithelium lacks a TJ, water loss occurs and diarrhoea results (Mitic *et al.* 2000). Over the past several decades, researchers applied *in vivo* and *in vitro* techniques to analyse the changes in TJ function in response to various stimuli and this has enhanced the general understanding of the role of the TJ, but also raised further questions about which components of the TJ are most important for its function, and to what extent a TJ can be disrupted before function is lost (Pelletier, 1986, Pelletier, 1988, Hirase *et al.* 1997, Mitic *et al.* 2000, Tao *et al.* 2000, Furuse *et al.* 2002, Myers *et al.* 2005, Kaitu'u *et al.* 2007, Tarulli *et al.* 2008).

In the testis, the gonadotrophins luteinising hormone/testosterone (LH/T) and follicle stimulating hormone (FSH) regulate spermatogenesis (Griswold, 1998). Evidence shows that gonadotrophins also regulate the Sertoli cell TJ, which forms at puberty as gonadotrophin levels increase as already mentioned. At the molecular level, men exhibiting low levels of circulating gonadotrophins displayed an immature TJ phenotype which was reverted to a mature phenotype upon the exogenous application of gonadotrophins (de Kretser and Burger, 1972). More recent *in vitro* and *in vivo* studies have shown that LH/T and FSH ablation disrupts Sertoli cell TJ structure and function, although this is model dependent (Pelletier, 1988, Florin *et al.* 2005, Meng *et al.* 2005, Myers *et al.* 2005, Tarulli *et al.* 2006, Kaitu'u *et al.* 2007, Tarulli *et al.* 2008). In the Sertoli cell specific androgen receptor knockout mouse, TJs are absent or marginal (Meng *et al.* 2005), and when FSH is given to seasonally regressed testes of the Djungarian hamster which display dysfunctional Sertoli cell TJs, TJ function is restored (Tarulli *et al.* 2008). Disruptions in the function of the Sertoli cell TJs are associated with disruptions to spermatogenesis, suggesting that TJs are pivotal to successful spermatogenesis and that their function is conferred by hormonal regulation.

The scope of this literature review will be to outline the entire process of spermatogenesis, the role of the Sertoli cell, the structural components of the TJ, and studies which have analysed changes in TJ function and size-selectivity in response to various stimuli including gene knockouts and wounding.

1.2 Overview of spermatogenesis

1.2.1 The mammalian testis

The testis is encased in a tough fibrous skin termed the tunica albuginea and is composed of two functional units- i) the interstitium, which contains Leydig cells, peritubular myoid cells, lymphocytes and macrophages and ii) the seminiferous tubules (Ross, 1995), which are highly convoluted structures taking up most of the testis and where germ cell development, or spermatogenesis occurs (Figure 1.1). The seminiferous tubule is composed of the seminiferous epithelium, which comprises germ cells and the somatic Sertoli cells.

Sertoli cells are attached to the basement membrane of the tubule and extend toward the tubule lumen. Throughout spermatogenesis, germs cells occupy niches formed by the Sertoli cells with which they are always in contact via complex cell junction formations (Meachem *et al.* 2001, Sofikitis *et al.* 2008). In later stages of spermatogenesis, germ cells occupy a cavity formed by the invagination of the Sertoli cell (Russell and Clermont, 1976, de Kretser and Kerr, 1988, Russell *et al.* 1990). Because of their close association, it can be assumed that both germ cells and Sertoli cells interact and communicate with each other. Over the past several decades, studies have shown that Sertoli cells provide nutritional and structural support to developing germ cells (Aravindan *et al.* 1997, Griswold, 1998, Cheng and Mruk, 2002). As spermatogenesis progresses, early germ cells move from the basement membrane, across the blood-testis barrier and Sertoli cell TJ which are located close to the basement membrane, toward the tubule lumen until they are released as mature spermatids. These spermatids collect in the rete-testis before exiting the testis through the efferent ducts into the epididymides. The presence of the Sertoli cell TJ therefore produces two compartments of distinct composition within the seminiferous epithelium, these being the basal compartment which contains the earliest germ cell types, and the adluminal compartment which contains the later maturing germ cell types (Cheng and Mruk, 2002).

In the interstitium, Leydig cells are the predominant cell type present, and these synthesise and secrete androgens (Saez, 1994, Setchell, 2004) which play a key regulatory role in spermatogenesis. Macrophages and lymphocytes are present in the interstitium also and appear to play key roles in

Figure 1.1 Organisation of the mammalian testis.

The testis is enclosed within the tunica albuginea (panel A) and is composed of two functional units, the highly convoluted seminiferous tubules and the interstitium in between them (Panel B). The interstitium contains Leydig cells (LC) and peritubular myoid (PTM) cells, as well as blood vessels. Lining the seminiferous tubules are the Sertoli cells which help nurture developing germ cells through spermatogenesis (Panel C) by providing nutrients, hormone signals and the tight junction. The tight junction forms between adjacent Sertoli cells and is located toward the basal aspect of the seminiferous tubules, just above the pre-leptotene spermatocytes. Modified from Cooke and Saunders, (2002).

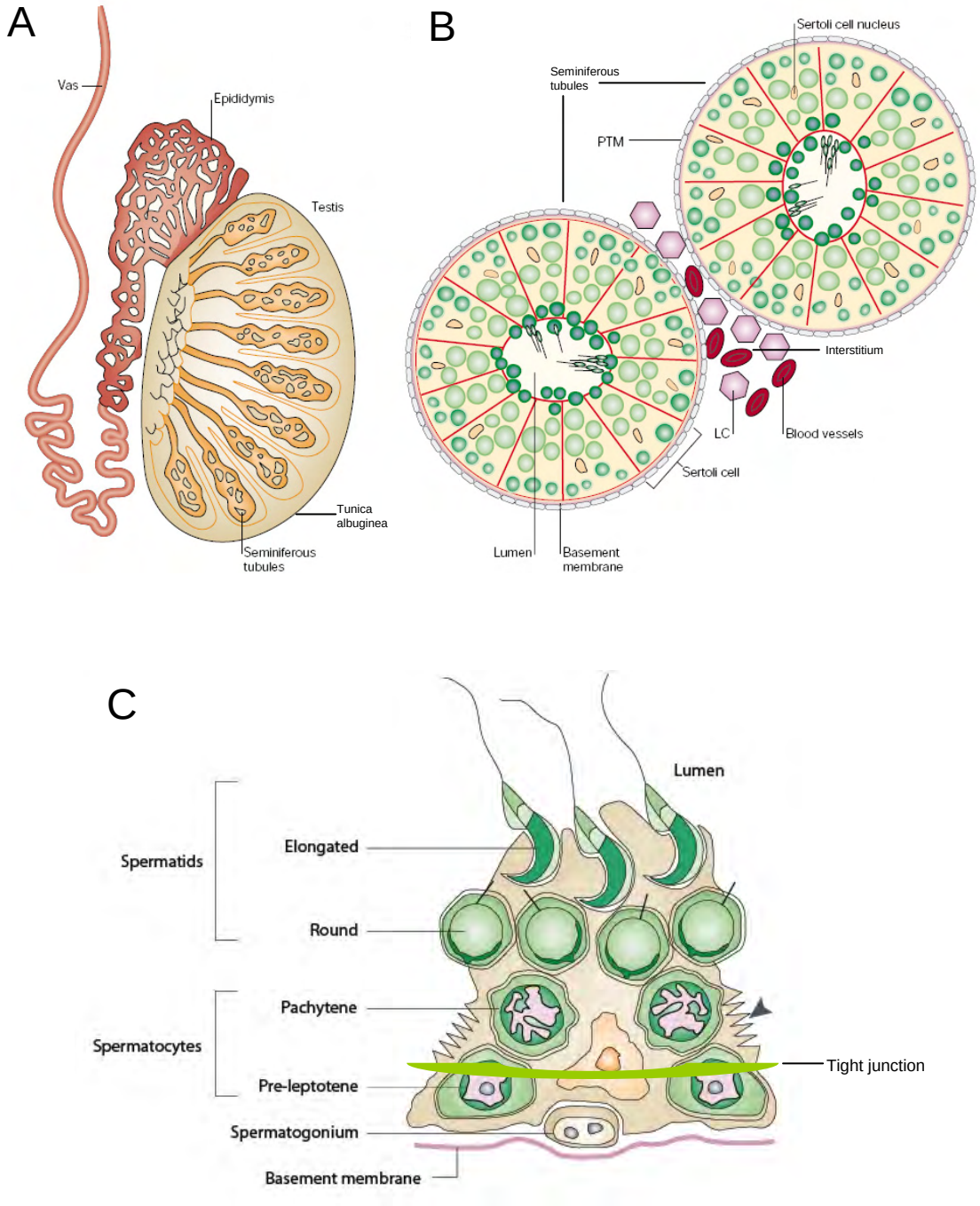
A
Vas
Epididymis
Testis
Tunica albuginea
Seminiferous tubules
B
Sertoli cell nucleus
Seminiferous tubules
PTM
Interstitium
LC
Blood vessels
Sertoli cell
Lumen
Basement membrane
C
Lumen
Spermatids
Elongated
Round
Spermatocytes
Pachytene
Pre-leptotene
Tight junction
Spermatogonium
Basement membrane

regulating both the Leydig cell and spermatogenesis (Hedger, 2002, Hussein *et al.* 2005, Ballow *et al.* 2006).

1.2.2 Spermatogenesis

Spermatogenesis is the dynamic process of germ cell development, where undifferentiated diploid spermatogonial stem cells become highly differentiated haploid spermatozoa (Ballow *et al.* 2006). Only the earliest types of germ cells, the mitotic types A and B spermatogonia, and preleptotene spermatocytes, develop on the basal side of the Sertoli cell TJ, and the latter cells must cross the TJ into the adluminal compartment to continue spermatogenesis (Cheng and Mruk, 2002). The meiotic and haploid spermatocytes on the adluminal side of the Sertoli cell TJ produce antigens which need to be sequestered from the immune system in the interstitium, and the provision of this sequestered space in which to develop is a key function of the Sertoli cell TJ, as in its absence, the latter germ cells are lost, and spermatogenesis stops Chung and Cheng, 2001, Chung *et al.* 2001).

Spermatogenesis can be separated into three separate phases according to germ cell development, these being mitosis, meiosis and spermiogenesis. Diploid spermatogonia are the earliest germ cell types, and are found located basally to the TJ along the basement membrane of the seminiferous tubule (Figure 1.2). Spermatogonia initiate the spermatogenic process and are major players in determining the final sperm output of the testis (for reviews see de Rooij and Russell (2000), Sofikitis *et al.* (2008)). A single spermatogonium can undergo mitotic divisions up to 8 or 9 times before becoming a spermatocyte (Lok and de Rooij, 1983). Spermatogonia are divided into three subgroups, and in order of most primitive to most differentiated, these are type A, intermediate and type B spermatogonia. These are distinguishable by the amount of heterochromatin contained in their nuclei. The most differentiated cell has most heterochromatin (Leblond and Clermont, 1952a, de Rooij and Russell, 2000). Type B spermatogonia divide into the preleptotene spermatocytes, and from this point, spermatogenesis enters the meiotic phase.

Preleptotene spermatocytes are similar in appearance to the type B spermatogonia but smaller (Leblond and Clermont, 1952a). The appearance of a network of thin chromosomic filaments in the nuclei are characteristic of leptotene spermatocyte formation, the first germ cells to appear adluminally

Figure 1.2 Spermatogenesis in the testis.

Spermatogenesis occurs in the seminiferous tubules of the testis and is supported by the Sertoli cells (SC). In the centre of this photo is a seminiferous tubule with interstitial spaces either side. The interstitium contains Leydig cells (LC) and blood vessels (BV). The outer edge of the seminiferous tubules is referred to as the basement membrane (BM) and the closest germ cells to it are the spermatogonia (Sg) and preleptotene spermatocytes (Pl). These early germ cell types reside basally to the Sertoli cell tight junction and among the first germ cells to appear adluminally to the TJ are the pachytene spermatocytes (P). When the pachytene spermatocytes complete meiotic division, they become haploid round spermatids (RS). Spermiogenesis is then commenced and involves the transformation of the round spermatids into elongated spermatids (ES). This photo shows the elongated spermatids with their tails suspended in the lumens of the seminiferous tubules ready for release or spermiation. Those of which have already been released leave behind their cytoplasm which are termed residual bodies (RB).

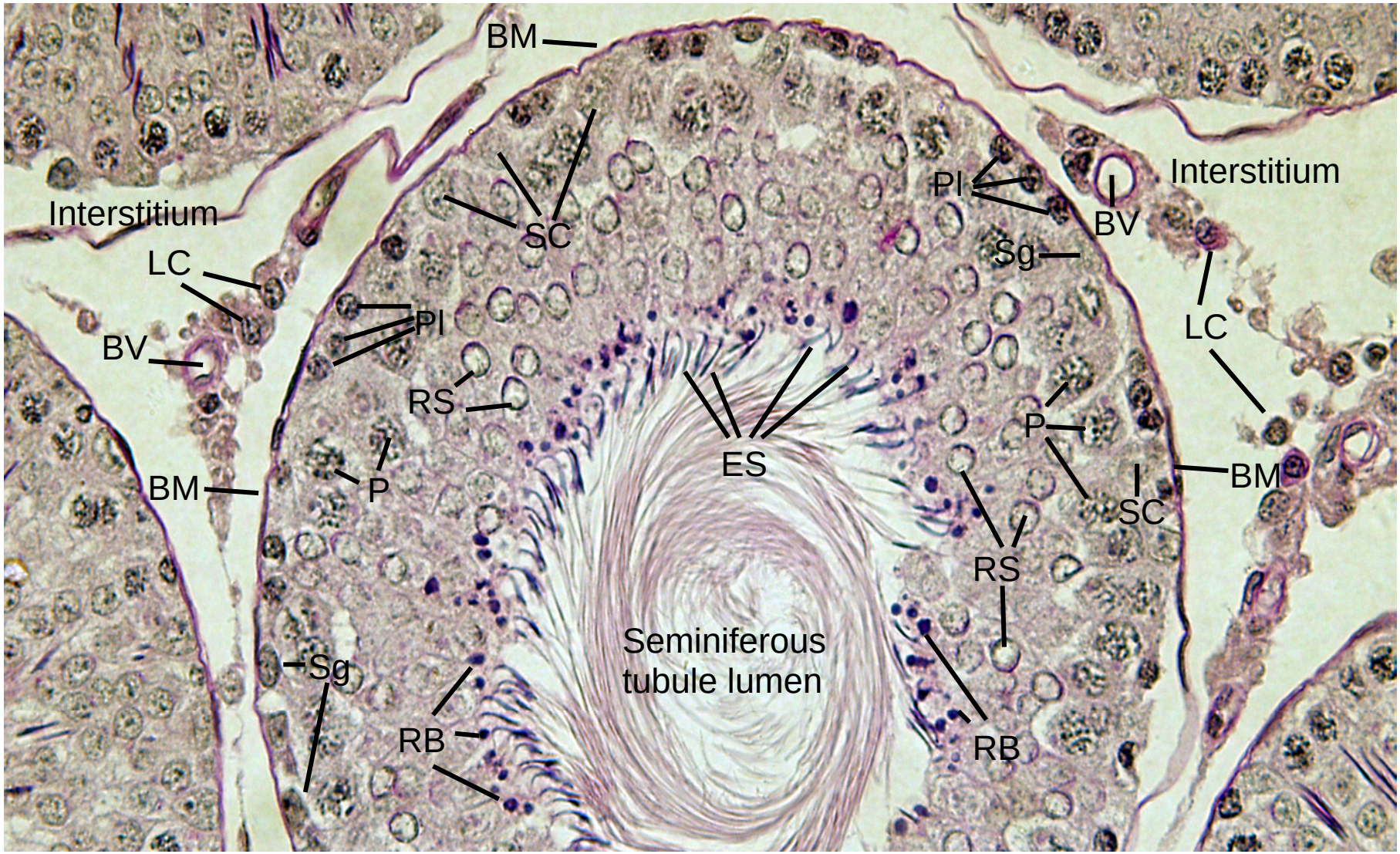
BM
Interstitium
SC
PI
BV
Interstitium
Sg
LC
LC
PI
BV
RS
P
ES
BM
P
BM
SC
RS
Seminiferous
tubule lumen
Sg
RB
RB

to the TJ (Cheng and Mruk, 2002). When these chromosomic filaments pair together, the germ cells are termed zygotene spermatocytes (Leblond and Clermont, 1952a).

The transformation of the zygotene spermatocytes into pachytene spermatocytes involves genetic recombination and is a long process lasting several weeks (Leblond and Clermont, 1952a). Following this phase, the pachytenes undergo rapid division into diplotene and then secondary spermatocytes, before becoming round spermatids, signalling the start of spermiogenesis (Leblond and Clermont, 1952a).

Spermiogenesis is the morphological differentiation of the round spermatids into elongated spermatids, at which point they will be released into the tubule lumen as mature sperm in a process termed spermiation. Spermiogenesis is divided into several phases each consisting of multiple stages (Leblond and Clermont, 1952a). The end result of these phases is the elongation of the round spermatid and its nucleus and the development of an acrosome (head) and filament (tail). For more details see Leblond and Clermont, (1952). Once these phases are complete, the fully mature sperm is ready for release.

The process of germ cell development from spermatogonia to elongated spermatid, is called the spermatogenic wave. The lengths and types of spermatogenic waves vary across species from 40 days in the mouse to 59 days in the rat (Roosen-Runge, 1952, França *et al.* 1998), and given that the scope of this thesis covers TJs and spermatogenesis in the rat, mouse and human, the cycles for these species will be briefly covered below.

1.2.3 Cycles of spermatogenesis

In mammals, different consecutive cell associations and compositions can be observed along the seminiferous tubule (Steinberger and Steinberger, 1975, Cusan *et al.* 1981, França *et al.* 1998) (Figure 1.3). Each of these associations and the period of time for which they exist, are termed ‘stages,’ and these are classified according to the morphology of the developing germ cells which are interacting with the Sertoli cells (Leblond and Clermont, 1952a). Subsequent generations of germ cells are produced before the previous generation has completed its progression, thus spermatogenesis is a continual process, and cross-sections through multiple tubules can reveal any given stage of spermatogenesis (Leblond and Clermont, 1952a). In the rat and mouse, the spermatogenic wave is

Figure 1.3 The spermatogenic wave and spermatogenic cycle.

Spermatogenesis in the rat (panel A) and mouse (panel B) occurs in 14 and 12 stages respectively. Each vertical column in the schematics represents each stage of spermatogenesis as indicated by the roman numerals below each column. Germ cell maturation occurs horizontally across the columns. Each wave consists of 4.6 cycles, and each cycle lasts 12.9 days in the rat and 8.6 days in the mouse. This is equivalent to one wave of spermatogenesis taking 59 days to complete in the rat, and 40 days to complete in the mouse. Germ cells which reside in the basal compartment of the seminiferous tubule are indicated by the hashed box. The point where the preleptotene spermatocytes cross the TJ into the adluminal compartment and give rise to all other adluminal germ cell types is indicated by the arrow. Cross-sections through seminiferous tubules of rats or mice can reveal any given stage of spermatogenesis, and these tables are useful for assigning a stage to a cross-section as it shows which germ cell types appear in which stage, and at which morphology. Modified from França *et al.* (1998).

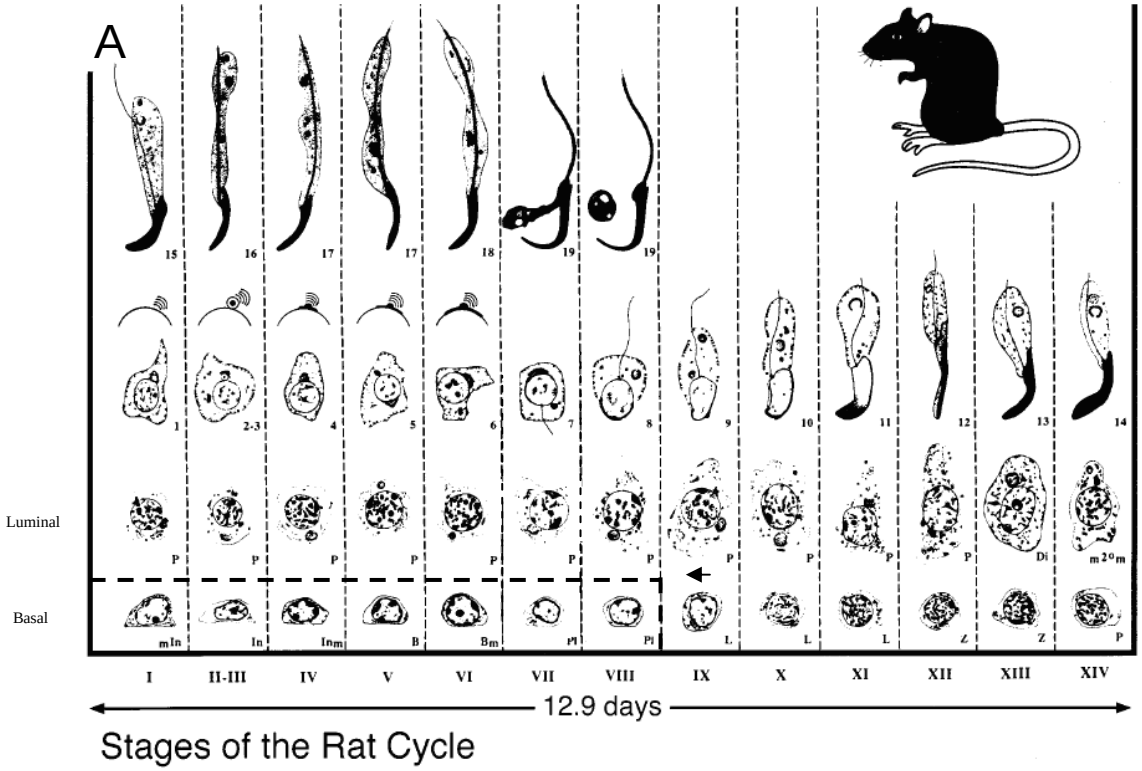

Stages of the Rat Cycle

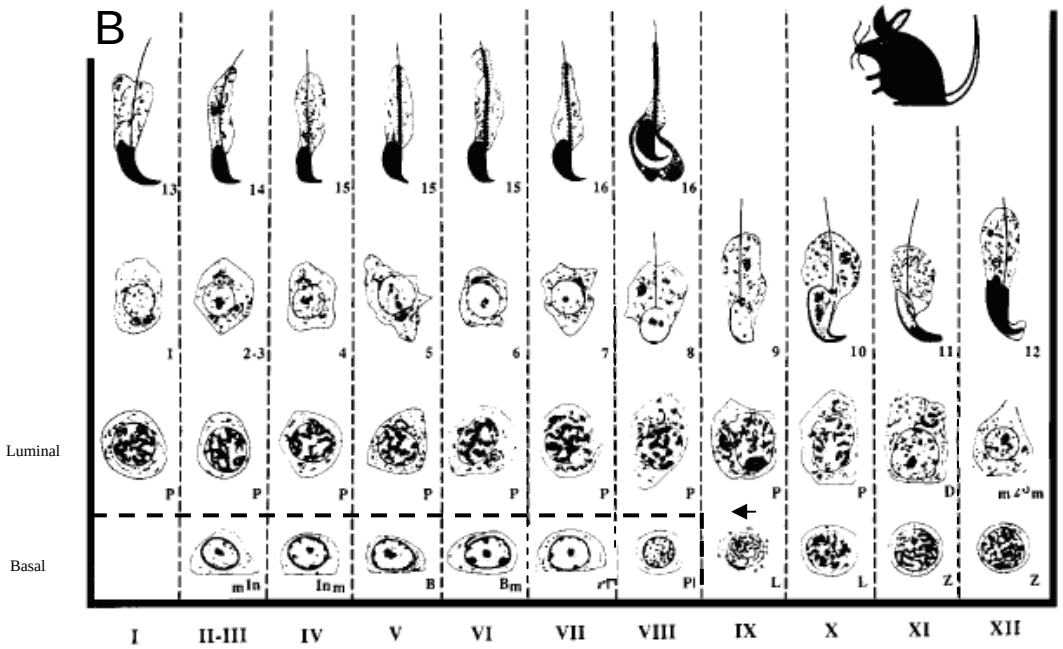

Stages of the Mouse Cycle

'cyclical,' and germ cell development follows an orderly progression through the stages along the seminiferous tubule (França *et al.* 1998, Chiarini-Garcia *et al.* 2001). The characterisation of the rat spermatogenic wave was conducted using the periodic acid-Schiff staining technique (Hotchkiss, 1948, Leblond and Clermont, 1952b, Russell *et al.* 1990) after this stain was found to specifically stain carbohydrates (Clermont and Harvey, 1965). With respect to the germ cell, this stain highlighted acrosome and tail development particularly well (Leblond and Clermont, 1952b). The periodic acid-Schiff stain is still used today extensively, to determine stages in testis tissue cross-sections and to identify germ cell types. The number of stages varies across species, with 14 in the rat, 12 in mice and 6 observed in humans (Roosen-Runge, 1952, Clermont, 1963, França *et al.* 1998). Waves are divided into cycles and in the Sprague Dawley rat, one spermatogenic cycle takes 12.9 days to complete and the development of an immature spermatogonium into a mature elongated spermatid requires 4.6 cycles. One spermatogenic wave therefore takes 59 days to complete (Clermont and Harvey, 1965, França *et al.* 1998). In the mouse, one spermatogenic cycle occurs in 8.6 days, which means one spermatogenic wave in the mouse, is completed in approximately 40 days (Figure 1.3) (Clermont and Trott, 1969, França *et al.* 1998).

The type of spermatogenic wave which occurs in the human is different to that which occurs in rats and mice. In 1902, it was observed that the maturing sperm in the human testis, were less regularly organised in the seminiferous tubules than in other mammals (Clermont, 1963). Later on it was seen that there was no correlation between clumps of differing stages of spermatogenesis within any given area of a tubule, and that unlike in rats, there was no synchronicity of germ cell development (Roosen-Runge and Barlow, 1953). However, Clermont (1963) identified 6 consistent cellular associations across serial sections from adult human testes, and that like in other mammals, these 'stages,' would follow each other in time. Clermont (1963) noted that each stage would appear in several areas across the tubule and that the borders between stages were ill-defined, leading to the apparent 'disorganisation' of spermatogenesis noted in the past. Schulze (1982) noticed that these stages were actually arranged helically along the length of the seminiferous tubule, which led to the helical classification of spermatogenesis in the human and other primates, as opposed to the cyclical classification of rat, mouse and other mammalian spermatogenesis (Figure 1.4) (França *et al.* 1998, Chiarini-Garcia *et al.* 2001).

Figure 1.4 The spermatogenic cycle in the human.

Spermatogenesis in the human is divided into 6 consecutive stages of germ cell maturation as indicated by the roman numerals. Unlike rat or mouse seminiferous tubules, cross sections through human tubules reveal multiple spermatogenic stages which initially made it difficult to stage the spermatogenic cycle and led to the helical term for human spermatogenesis. Lettering in this schematic are: ser, Sertoli cell nuclei; Ad and Ap are types of type A spermatogonia; B, type B Spermatogonia; R, resting primary spermatocytes; L, leptotene spermatocytes; Z, zygotene spermatocytes; P, pachytene spermatocytes; Di, diplotene spermatocytes; Sptc-Im, spermatocytes in division; Sptc-II, secondary spermatocytes in interphase; Sa, Sb, Sc, Sd, spermatids at various spermiogenic stages and RB, residual bodies. Modified from Clermont, (1963).

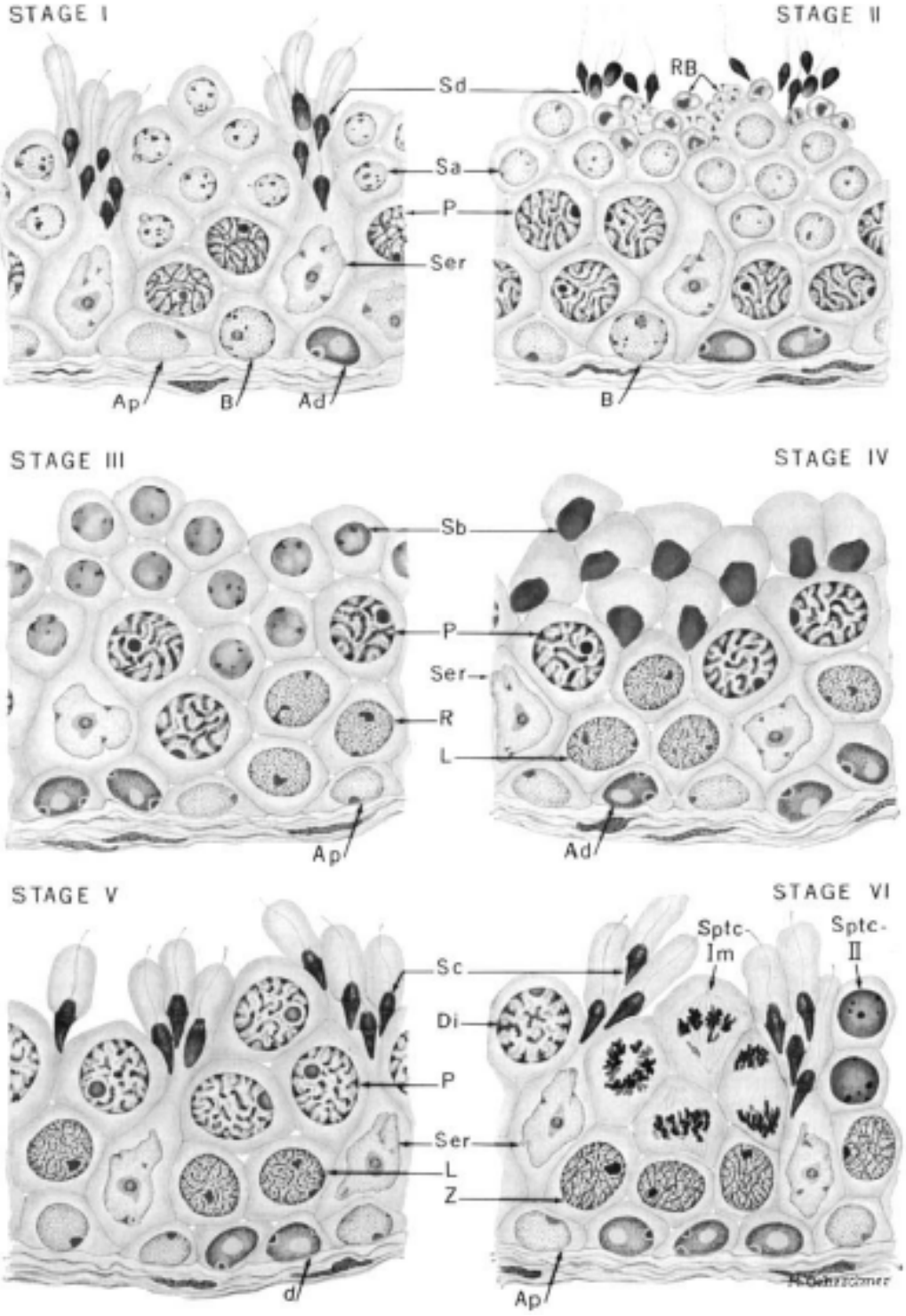
STAGE I
STAGE II
Sd
RB
Sa
P
Ser
Ap
B
Ad
B
STAGE III
STAGE IV
Sb
P
Ser
R
L
Ap
Ad
STAGE V
STAGE VI
Sc
Di
P
Ser
L
Z
Sptc-Im
Sptc-II
d
Ap

The helical arrangement of spermatogenesis in the human has led to the term ‘multi-stage,’ that is, several stages of spermatogenesis can be seen in a single cross-section of a seminiferous tubule, as opposed to the ‘single-stage’ seen in other mammalian species (Wistuba *et al.* 2003). At first it was suspected that the multi-stage arrangement would decrease the efficiency of spermatogenesis (Sharpe, 1994, Johnson, 1995), however the use of the optical dissector technique for quantifying different germ cell types has shown that the spermatogenic efficiency of the human may have been better than first suggested (Wreford, 1995). As reported in Wistuba *et al.* (2003), the finding of highly efficient spermatogenesis in the marmoset despite the presence of multi-stage spermatogenesis has suggested that the topographical arrangement of spermatogenesis in the seminiferous tubules is not related to spermatogenic efficiency (Zhengwei *et al.* 1998, Weinbauer *et al.* 2001, McLachlan *et al.* 2002a, McLachlan *et al.* 2002b). More recently, it was shown that the spermatogenic efficiency was similar across several different species of primates, including in an ancestral primate belonging to the Strepsirrhini sub-order (which includes lemurs) that displayed single-stage spermatogenesis (Wistuba *et al.* 2003). The authors concluded that the presence of a multi/single stage spermatogenesis may simply reflect the germ cell clonal size (Wistuba *et al.* 2003).

In all species, the continuing waves of spermatogenesis allows the testis to continually produce sperm, and this process requires the continual regulatory contributions and complex cell-cell interactions provided by the Sertoli cells.

1.2.4: The Sertoli cell

Sertoli cells are the somatic cells of the seminiferous epithelium and are essential for spermatogenesis (for reviews, see Griswold, (1995), Griswold, (1998), Sofikitis *et al.* (2008)). They are large, highly branched cells, extending from the basement membrane to the tubule lumen, and they are in direct contact with germ cells throughout spermatogenesis (Griswold, 1995, Griswold, 1998, Sofikitis *et al.* 2008). Sertoli cells have several key functions. Firstly, the number of Sertoli cells dictates the spermatogenic output of mature spermatozoa. A rat model which showed a 54% decrease in Sertoli cell number, also displayed a 55% decrease in round spermatid number (Orth *et al.* 1984), yet the ratio of round spermatids to Sertoli cells was the same in the control rats compared to the Sertoli cell-deplete rats. Treatment of neonatal mice for the first 2 weeks of life with the

gonadotrophin follicle stimulating hormone (FSH),stimulated an increase in Sertoli cell number and sperm output by the testis (Singh and Handelsman, 1996). A similar study treated prepubertal mice with FSH which resulted in larger than normal testes and higher numbers of germ cells (Meachem *et al.* 1996). The findings of these studies showed that the production of normal germ cell numbers depends on the size of the Sertoli cell population and that FSH is critical for determining the final Sertoli cell number.

Secondly, Sertoli cells secrete a number of glycoproteins and nutrients that form the basis of Sertoli-germ cell interactions (Griswold, 1993, Setchell, 1993, Griswold, 1995, Griswold, 1998). Griswold (1998), reviewed several pieces of evidence which showed that Sertoli cells secrete various factors such as an abundance of transport or bioprotective proteins, and proteases and protease inhibitors which are essential for tissue remodelling such as required through spermiation and the passage of preleptotene spermatocytes across the blood-testis barrier. Sertoli cells also provide the basement membrane between Sertoli and peritubular myoid cells and secrete growth factors or paracrine factors such as Müllerian inhibiting substance, c-kit ligand and inhibin in low amounts and also the provision of energy metabolites such as lactate and pyruvate (Jutte *et al.* 1983, Griswold, 1998).

Sertoli cells are also the key mediator of the main hormone signals essential for spermatogenesis, FSH and the androgen testosterone, the receptors for which are found on Sertoli cells, but not on germ cells (Lyon *et al.* 1975, Bremner *et al.* 1994, Rannikki *et al.* 1995, Tapanainen *et al.* 1997, Sofikitis *et al.* 2008). As discussed previously, FSH has been shown to be pivotal in determining final Sertoli cell number. In prepubertal rats, FSH increases intracellular cAMP, protein synthesis and estradiol production (Fritz and Rath, 1978). In adult animals, the role of FSH is more controversial and according to Griswold (1998), may vary from species to species and in many cases testosterone may assume the biochemical role of FSH. Either way, there is a change in FSH activity after puberty and this is coincident with the cessation of Sertoli cell proliferation (Zirkin *et al.* 1994, Walker, 2003). On its own, FSH can maintain spermatogenesis through to the round spermatid stage, but after that, spermatogenesis ceases (Singh *et al.* 1995, McLachlan *et al.* 1995). Testosterone also plays key roles in spermatogenesis and the maturation of germ cells. In the absence of FSH in a hypogonadal mouse model, low levels of testosterone were sufficient to drive spermatogenesis (Singh

et al. 1995). This has also been seen in FSHβ subunit gene knockout (Kumar *et al.* 1997) and hormone suppressed rat models under the influence of testosterone alone (Awoniyi *et al.* 1989), albeit at a reduced spermatogenic capacity compared to controls (Kumar *et al.* 1997, Meachem *et al.* 1998). Results from studies which specifically ablated or inhibited the Sertoli cell androgen receptor showed that androgens are essential for germ cell meiosis, the transition from round to elongate spermatids and the final stages of spermiogenesis (O'Donnell *et al.* 1999, Chang *et al.* 2004, de Gendt *et al.* 2004, Holdcraft and Braun, 2004). For a review on the role of testosterone in primate and human spermatogenesis, see McLachlan *et al.* (2002a).

Within the Sertoli cell, the androgen receptor is maximally expressed when TJs form and when germ cells migrate across the blood testis barrier (Russell, 1977, Bremner *et al.* 1994, Zhou *et al.* 2002). Furthermore, testosterone was shown to regulate the localisation and/or mRNA expression of some pivotal Sertoli cell TJ proteins (Kaitu'u *et al.* 2007).

1.2.5 Cell-cell interactions

Cell-cell interactions are ubiquitous in all epithelia and are also another key feature of the Sertoli-germ cell relationship. There are three main types of cell-cell junctions which are morphologically and functionally distinct from each other. Broadly these are the anchoring junctions, gap junctions and TJs (Mruk and Cheng, 2004). In the seminiferous epithelium, these three junctional types contribute to the formation of the blood-testis barrier (Pointis *et al.* 2005). Each are briefly described below and are presented in Figure 1.5.

a. Anchoring junctions

The anchoring junctions connect the cytoskeletons of adjacent cells and can be sub-divided into four smaller groups of junctional types, and these are adherens junctions, cell focal contacts, desmosomes and hemidesmosomes (for reviews see Cheng and Mruk, (2002); Mruk and Cheng, (2004)). Each of these subgroups are present in the testis except for the cell focal contacts, which have as yet not been localised to the testis but are involved in anchoring other epithelial cells to extracellular matrices (Cheng and Mruk, 2002, Xia *et al.* 2005).

Figure 1.5 The junctional complex.

This figure displays diagrammatic representation of junctions between adjacent epithelial cells generally (panel A) and also between adjacent Sertoli cells in the testis (panel B). Panel A shows junctional complexes at the lateral sides of the membranes with electron micrograph representation also. In most epithelia, the tight junctions are the apical junction. Also apparent in panel A are gap junctions, which provide communication channels between adjacent cells, and the desmosomes, which are a type of anchoring junction. In the Sertoli cell figure in panel B, TJs (yellow) are part of a junctional complex composed of adherens junctions (green) and ectoplasmic specialisation (red) and together form the blood-testis barrier. Note that in the Sertoli cells, the TJs are the most basally located junction. Panel A is taken from Oroi and Perrelet, (1975) and panel B is modified from Sluka *et al.* (2006).

A

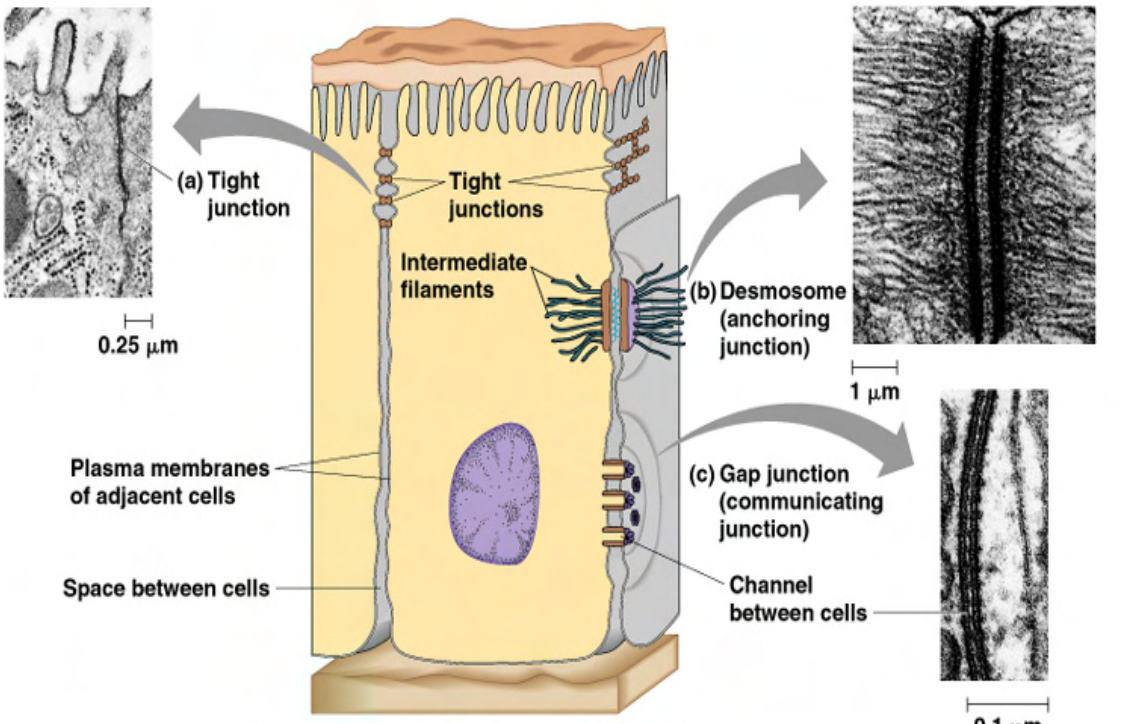

(b) Courtesy of L. Orci and A. Perrelet, Freeze-Etch Histology (Heidelberg: Springer-Verlag, 1975.) ©1975 Springer-Verlag.

B

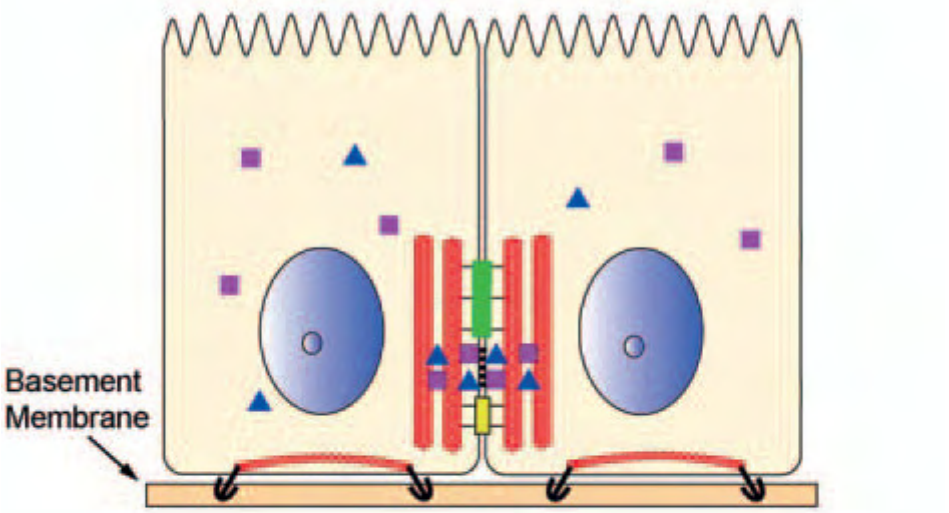

Adherens junctions link neighbouring cells via cytoskeletal actin filaments. In the testis, they are involved with connecting adjacent Sertoli cells to each other and to germ cells (Pointis *et al.* 2005, Cyr *et al.* 2007). A specialised type of adherens junction found only in the testis is the ectoplasmic specialisation (Vogl *et al.* 2000, Mulholland *et al.* 2002, Toyama *et al.* 2003, Pointis *et al.* 2005, Xia *et al.* 2005, Yan *et al.* 2007). These junctions are found basally between Sertoli cells where they stabilise and maintain the blood-testis barrier, and adluminally, where they anchor elongating/elgonated spermatids to the Sertoli cells (Siu *et al.* 2005, Xia *et al.* 2005, Beardsley *et al.* 2006).

Desmosomes are similar to the adherens junction in that they adhere adjacent cells together as well. They have most extensively been studied in the epidermis where they play an important role in maintaining tissue integrity (Cheng and Mruk, 2004). In the testis, they are present at contact points between Sertoli cells and other Sertoli cells, and between Sertoli cells and germ cells. The mechanism of adherence mediated by the desmosomes differs to that mediated by the adherens junction in that the desmosomes are linked to the intermediate filaments of the cytoskeleton rather than the actin filaments (Connell, 1977, Vogl *et al.* 2000, Cheng and Mruk, 2004). Hemidesmosomes in the seminiferous epithelium are restricted to Sertoli cell basal regions, where they anchor the cells to the basement membranes of the seminiferous tubules (Wrobel *et al.* 1979, Vogl, 1988, Cheng and Mruk, 2004).

So that the anchoring junctions can collectively facilitate the movement of germ cells through spermatogenesis, the continual redistribution of the Sertoli cell cytoskeleton is required to ensure that the Sertoli cell is morphologically suitable to each germ cell maturation stage (Russell and Clermont, 1976, Connell, 1977, Parvinen, 1993, Zhu *et al.* 1997, Siu and Cheng, 2004). The regulatory mechanisms behind this process are not well known, but the germ cells themselves may play a role. When rat spermatogonia were transplanted into mouse testes and were interacting with mouse Sertoli cells, they differentiated with cell cycle timing characteristic of rat spermatogenesis and also generated the spermatogenic structural pattern of the rat (França *et al.* 1998). In the same animals, mouse spermatogonia initiated spermatogenic cycles indicative of mouse spermatogenesis. This indicated that germ cells do have roles in regulating their own maturation and more specifically, the cell differentiation process is regulated by the germ cells alone (França *et al.* 1998).

b. Gap junctions

The second type of cell-cell junction, is the gap junction. These form communicative channels between adjacent cells in nearly all epithelia. A channel between two cells is formed by the contribution of a hemichannel called a connexon from each cell (Brehm *et al.* 2007), which in turn are made up of proteins called connexins (For a review, see Sridharan *et al.* (2008)). In the seminiferous epithelium, gap junctions provide the route through which ions and small molecules are exchanged between Sertoli cells and spermatogonia and between Sertoli cells and primary spermatocytes (Brehm *et al.* 2007). Kumar and Gilula (1996), reported that gap junctions in the seminiferous epithelium are pivotal to germ cell growth, differentiation, homeostasis and neoplastic transformation. Upon the Sertoli cell specific knock out of connexin-43, testis weights and spermatogonia were markedly reduced and most of the seminiferous tubules did not show normal spermatogenesis (Brehm *et al.* 2007), thereby indicating the important role that gap junctions also have in maintaining successful spermatogenesis.

c. Tight junctions

The third junction is the TJ. The TJ, as stated previously, is the major component of the blood-testis-barrier and its provision is a separate, key function of the Sertoli cell. In early studies, the rete testis was cannulated and testicular fluid collected (Setchell, 1967, Waites and Setchell, 1969, Dym and Fawcett, 1970). This fluid was found to contain significantly lower amounts of protein, amino acids and ions that are in abundance in the blood plasma and testis lymph (Setchell, 1967, Waites and Setchell, 1969, Dym and Fawcett, 1970). It was concluded that there must be a blood-testis-barrier in the seminiferous epithelium, capable of excluding blood plasma and testis lymph proteins, amino acids and ions from the tubule lumens. Later, a variety of different electron opaque tracers of varying sizes were administered to the testes of guinea pigs and chinchillas. The larger molecules were excluded from the tubules completely, and were restricted to the interstitial side of the myoid cells which surround the seminiferous tubules (Fawcett *et al.* 1970). The smaller tracers, penetrated into the seminiferous tubules and surrounded the spermatogonia, but penetrated no further towards the tubule lumens than that (Fawcett *et al.* 1970). When the tracer lanthanum nitrate was administered to adult rat testes, it was also seen to enter the tubules only as far as the spermatogonia (Dym and Fawcett, 1970).

Electron microscopy revealed that TJs sealed adjacent Sertoli cells just above the spermatogonia and were blocking the progression of the tracer into the adluminal compartment (Dym and Fawcett, 1970). This was the first piece of evidence of the compartmentalisation function of the Sertoli cell TJ.

The function of Sertoli cell TJs has also been tested in *in vitro* culture systems, with Sertoli cells cultured onto bicameral units which are placed into culture wells. Bicameral units have a thin, porous membrane separating the inside of the unit from the outside. In a number of studies it has been shown that Sertoli cells had formed an impermeable barrier between the inside and outside of the bicameral unit as shown by decreased passage of [^{3}H]inulin and electrical currents across the cells, and that most *de novo* synthesised proteins had been secreted into the inside of the bicameral unit (Onoda *et al.* 1990). Subsequent studies have looked at the function of the Sertoli cell TJ and other TJs in different bodily systems, and the remainder of this literature review will focus on the TJ and the regulation of Sertoli cell TJs as revealed by hormone-suppression models.

1.3 The tight junction

1.3.1 Tight junction ultrastructure

TJs were first identified as types of intercellular junctions by ultrathin-section electron microscopy (Farquhar and Palade, 1963) where they appeared as a series of contact points or “kissing points” involving the plasma membranes of adjacent cells (Tsukita and Furuse, 1999). Since the advent of freeze-fracture electron microscopy it has become possible to examine TJs in greater detail (Cereijido and Anderson, 2001). This form of microscopy reveals the membrane components of the TJ, which appear as a mesh like network of continuous, anastomosing strands that wrap around the periphery of epithelial cells (Gonzalez-Mariscal *et al.* 2003). TJ strands on adjacent membranes interact with each other, effectively forming a seal between membranes and eliminating the extracellular space at that point (Figure 1.6) (Furuse *et al.* 1999). This seal is selectively permeable in that it does not allow solutes or water free passage between cells, which is known as the paracellular pathway (Mitic and Anderson, 1998) (discussed later). Hence the seal can form compartments of very different solute and fluid composition between adjacent tissues (Cereijido and Anderson, 2001) as earlier described for in the seminiferous epithelium.

Figure 1.6 Protein interactions within the tight junction.

In this schematic of the testicular Sertoli cell TJs, the extracellular domains of the occludin, claudin-11 and junctional adhesion molecule can be seen interacting with their counterparts on the adjacent cell. The C-termini of each protein binds to the cytoplasmic plaques within the cell, which consist of a complex of large proteins including the zonulae occludens (ZO-1 and ZO-2). This complex links the transmembrane proteins to the cytoskeleton which is depicted here as F-actin in yellow. Taken from Mruk and Cheng, (2004).

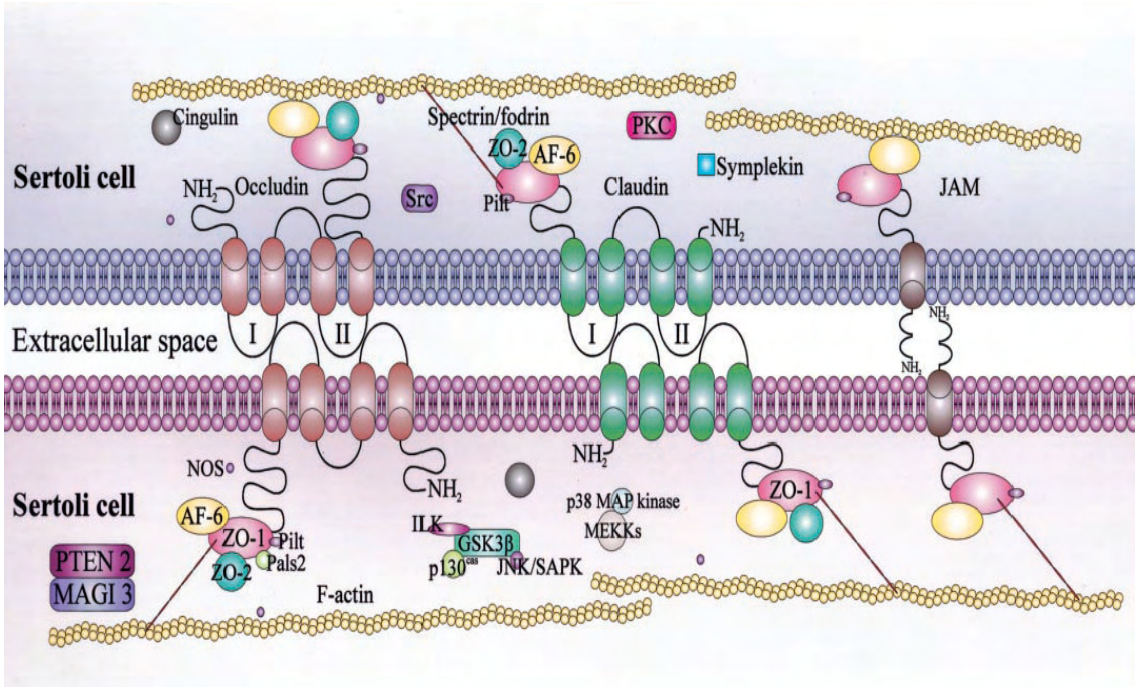
Cingulin
Spectrin/fodrin
ZO-2
AF-6
PKC
Symplekin
Sertoli cell
NH2
Occludin
Src
Pilt
Claudin
NH2
JAM
Extracellular space
I
II
I
II
NH2
NH2
NOS
NH2
NH2
Sertoli cell
AF-6
ILK
p38 MAP kinase
MEKKs
ZO-1
ZO-1
Pilt
GSK3β
PTEN 2
Pals2
p130cas
JNK/SAPK
MAGI 3
ZO-2
F-actin

The composition of the TJ strands has been hotly debated over the past 20 years (Lapierre, 2000). Hypothesised models for TJ composition varied from strands being formed by the polymerisation of integral membrane proteins within plasma membranes (Tsukita and Furuse, 1999), to TJ strands being predominantly lipid in nature, formed by inverted, cylindrical lipid micelles (Mitic and Anderson, 1998). The latter model survived until observations by electron microscopy showed TJ strands were stable in detergent (Stevenson and Goodenough, 1984), suggesting that they were not entirely lipid in nature. Recent work, although not discounting the possible presence of lipids (Lapierre, 2000), has identified at least two pivotal protein components of TJ strands and these are occludin and the claudins, with the latter comprising a large superfamily of more than 20 members (Gonzalez-Mariscal *et al.* 2003).

1.3.2 Molecular composition and architecture of the tight junction

The TJ consists of transmembrane proteins which seal adjacent epithelial cells together through interactions between their extracellular domains. These proteins are linked to the cytoplasmic plaque just inside the cell, which in turn is linked to the cytoskeleton. The next part of this review will look at the transmembrane proteins and the zonnulae occludens of the cytoplasmic plaque.

a. Membrane components

The first transmembrane protein component of the TJ strand was identified in 1993 (Furuse *et al.* 1993). Occludin was isolated from chicken liver as an antigen for monoclonal antibodies raised against a junctional fraction, and was so called after the Latin word ‘occludere’ which means to occlude (Gonzalez-Mariscal *et al.* 2003). After sequencing and cloning occludin from the rat, chicken, human, dog and mouse, Ando-Akatsuka *et al.* (1996) found that the size of occludin is relatively conserved between species at about 65kDa. However, interspecies variation in the sequence of occludin was observed, with greater dissimilarity between chickens and placental mammals, than between placental mammals themselves (Mitic and Anderson, 1998). Occludin spans the membrane four times and has two extracellular loops and one intracellular turn which keeps the N- and C-termini on the cytosolic side of the plasma membrane (Tsukita and Furuse, 1999, Tsukita *et al.* 2001) (Figure 1.7). The first extracellular loop of occludin is characteristically rich in tyrosine and glycine residues

Figure 1.7 Transmembrane components of the tight junction.

Diagrammatic representation of the key transmembrane components of the tight junction; occludin (panel A), claudin (panel B) and junctional adhesion molecule (panel C). Occludin and the claudins are structurally similar as they span the membrane four times, and keep their N- and C-termini within the cell. They are however dissimilar in size and sequence. Junctional adhesion molecule is structurally different to occludin and the claudins. It dimerises with an adjacent junctional adhesion molecule, forming a U-shaped domain in the extracellular space. Taken from Tsukita *et al.* (2001).

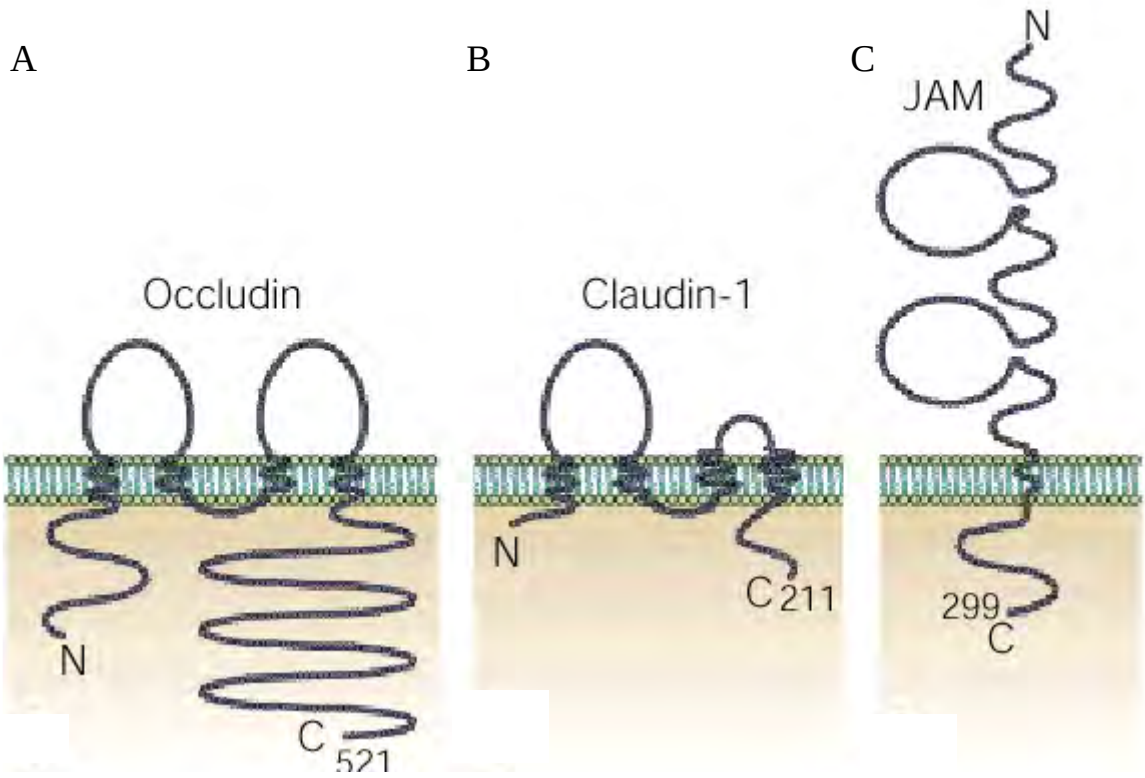
A
B
C
Occludin
Claudin-1
JAM
N
C
521
N
C
211
N
299
C

(60%) and this feature is conserved highly among species. Several lines of evidence suggest that occludin has an important role in defining the TJ barrier (Mitic *et al.* 2000). The addition of a synthetic peptide to cultured *Xenopus* epithelial cells and rat Sertoli cells which corresponded to the sequence of one of the extracellular loops of occludin, decreased TJ function as shown by transepithelial electrical resistance (TER) *in vitro* (Wong and Gumbiner, 1997, Chung *et al.* 2001). Furthermore, the transfection of occludin into fibroblasts lacking occludin and TJs, resulted in the gain of adhesive function between cells (van Itallie and Anderson, 1997). Despite this data supporting the importance of occludin in TJs, occludin knockout mice displayed well developed TJs strands and with respect to the Sertoli cell TJ, these mice were fertile until late adulthood (Saitou *et al.* 2000). Furthermore, epithelial cell morphology was unaltered after the addition of the antagonist peptide mentioned above (Saitou *et al.* 1998). These findings suggested the presence of another protein in these strands.

In 1998, Claudin-1 and Claudin-2 were discovered as 22kDa bands isolated from the same liver fraction used to isolate occludin (Furuse *et al.* 1998) and were named after the Latin word ‘claudere’ meaning, ‘to close.’ Currently, 24 members of the claudin superfamily have been identified as proteins of masses between 20-27kDa (see Table 1.1). They are structurally similar to occludin, spanning the membrane four times, having two extracellular loops (one of which is much larger than the other) and a short tail on the inside of the cell membrane. Despite this structural similarity with occludin (Figure 1.7), there is no similarity in sequence between the claudins and occludin. There is also sequence dissimilarity between members of the claudin superfamily, and these differences lie in the third and fourth membrane spanning domains (Lapierre, 2000). Furthermore, the claudins are distributed differently among different types of tissue (Lapierre, 2000). For example, claudin- 5 is ubiquitously expressed whereas claudin-11 is isolated to the Sertoli cells and central nervous system. All claudin sequences contain a C-terminal PDZ-binding motif, which is a common 80-100 amino acid domain that reside on molecules that target the C-terminal of intracellular and cell-surface proteins (Sidhu *et al.* 2003). The interaction between the PDZ domains and PDZ binding motifs, results in large multiprotein complexes at specific subcellular sites (Craven and Bredt, 1998, Fanning and Anderson, 1999, Sidhu *et al.* 2003). Through their PDZ domains, the claudins bind to the zonulae occluden family of the cytoplasmic plaque beneath the membrane (described in section 1.3.1b) (Itoh *et al.* 1999).

Table 1.1 Localisation and characterisation of members of the claudin superfamily.

To date, 24 members of the claudin superfamily have been identified and characterisation of their localisation and expression is ongoing. Tight junctions consist of one or more claudin components, each apparently with different functional roles. Generally most of the claudins have been well characterised (panel A, taken from Gonzalez-Mariscal *et al.* (2003), with claudin-9, 10, 12, 13, 17 and 19-24 the exceptions and subjects of more recent studies (panel B). There are 7 claudins localised to the testis, with claudin-11 being specific for the Sertoli cell tight junction.

A

Claudin	Distinctive characteristics
1	Present in high-resistance epithelia (e.g. collecting segment) and absent in leaky epithelia (e.g. proximal tubule) (Reyes et al., 2002). Crucial for the mammalian epidermal barrier (Furuse et al., 2002). Absent in most human breast cancer cell lines (Hoevet et al., 2002).
2	Present in leaky epithelia (e.g. proximal tubule) and absent in tight epithelia (e.g. collecting segment) (Reyes et al., 2002; Enck et al., 2001). Present in the choroids plexus epithelium (Wolburg et al., 2001).
3	Also known as RVP1 (Briehl and Miesfeld, 1991). Present in the tighter segments of the nephron (Kiuchi-Saishin et al., 2002). Its expression is elevated in regressing ventral prostate and in prostate adenocarcinomas (Long et al., 2001). Capable of CPE binding (Sonoda et al., 1999).
4	Its expression decreases paracellular conductance through a selective decrease in sodium permeability (Van Itallie et al., 2001). Present in the tighter segments of the nephron (Kiuchi-Saishin et al., 2002). Over expressed in pancreatic and gastrointestinal tumors (Michl et al., 2001). The selective CPE binding gave rise to its alternative name CPE-R (Sonoda et al., 1999).
5	Receives the alternative name of TMVCF, as it is frequently deleted in Velo cardio facial syndrome (Sirotkin et al., 1997). Constitutes TJ strands in endothelial cells (Morita et al., 1999b). Transiently expressed during the development of the retinal pigment epithelium (Kojima et al., 2002).
6	Present in embryonic epithelia (Turksen and Troy, 2001). Its over expression in transgenic mice generates a defective epidermal permeability barrier (Turksen and Troy, 2002).
7	Down regulated in head and neck squamous cell carcinomas (Al Moustafa et al., 2002).
8	Present in the tighter segments of the nephron (Kiuchi-Saishin et al., 2002).
11	Also named OSP. Present in oligodendrocytes and Sertoli cells (Morita et al., 1999a).
14	Expressed in the sensory epithelium of the organ of Corti. Mutations in the gene cause autosomal recessive deafness (Wilcox et al., 2001).
15	Present in endothelial cells (Kiuchi-Saishin et al., 2002).
16	Also known as Paracellin-1. Critical for Mg^{2+} and Ca^{2+} resorption in the human thick ascending limb of Henle (Blanchard et al., 2001; Simon et al., 1999).
18	A downstream target gene for the T/EBP/NKX2.1 homeodomain transcription factor. Expressed in lung and stomach (Niimi et al., 2001).

B

Claudin	Distinctive Characteristics
9	Present in hepatocytes. Potential receptor for HIV virus (Nunes *et al.* 2006; Meertens *et al.* 2008)
10	Absent in vascular epithelia. Present in kidney and jejunum (Inai *et al.* 2005)
12	Present in the blood-brain barrier (Nitta *et al.* 2003)
13	Immunolocalised to the colon in mice (Fujita *et al.* 2006)
17	Immunolocalised to the plasma membrane of cultured human embryonic kidney cells (Hu *et al.* 2006)
19	Immunolocalised to the kidney in mice, rats and humans. Decreased expression in humans with renal disease (Lee *et al.* 2006)
20	mRNA expression detected in duodenum of rats (Charoenphandu *et al.* 2007)
21	Limited data available, although expression detected in human gastric epithelia (Katoh and Katoh, 2003). No rodent data available
22	High mRNA expression in rat duodenum and brain (Charoenphandu *et al.* 2007; Newrzella *et al.* 2007). Implicated in regulation of paracellular pathway in rat duodenum (Charoenphandu *et al.* 2007)
23	mRNA expression detected in duodenum of rats (Charoenphandu *et al.* 2007)
24	Limited data available, although expression detected in human gastric epithelia (Katoh and Katoh, 2003). No rodent data available

Junctional adhesion molecule (JAM) is a third family of proteins consisting of three members (JAM-A, JAM-B, JAM-C) that has been localised to epithelial and endothelial TJs as well as effect on well developed TJs, suggesting that JAM molecules assist in TJ sealing, and once this seal is formed, they are inaccessible (Liu *et al.* 2000, Gonzalez-Mariscal *et al.* 2003).

A good model for studying TJ formation between cells is the mouse trophectoderm, which forms a layer around blastocysts and generates the blastocoel cavity by polarised water and ion transport (Thomas *et al.* 2004). It also initiates attachment and invasion of the uterine endometrium (Thomas *et al.* 2004). Early in the differentiation process of the trophectoderm, JAM-A was seen to localise at cell-cell contact points and co-localise with nectin-2, an adhesion complex protein important for enhancing E-cadherin adhesion for adherens junction formation (Tachibana *et al.* 2000, Honda *et al.* 2003, Takai *et al.* 2003, Thomas *et al.* 2004). E-cadherin has been implicated in providing normal spatial and temporal control of TJ protein assembly and stability (Fleming *et al.* 1989, Javed *et al.* 1993, Sheth *et al.* 2000a, Sheth *et al.* 2000b, Thomas *et al.* 2004), and the localisation of occludin and the claudins does not occur until after the recruitment of E-cadherin to the adherens junction (Fleming *et al.* 1989, Fleming *et al.* 2001, Thomas *et al.* 2004). The early localisation of JAM-A to cell-cell contact points in that study, demonstrated a clear role for JAM-A in TJ assembly mediated through its possible role in also stimulating adherens junction assembly (Thomas *et al.* 2004). This was also seen in Caco-2 cultured cells, where after calcium addition, JAM-A was rapidly recruited to cell-cell contact points to initiate cellular differentiation, prior to the recruitment of occludin and the claudins (Martinez-Estrada *et al.* 2001) and the recruitment of the TJ cytoplasmic plaque protein, ZO-1 (Bazzoni *et al.* 2000) (see below). Thomas *et al.* (2004) also demonstrated that JAM-A migrated to the apical poles of the epithelial cells and co-localised with actin at the microvillus poles after cell-cell contacts had been established, and so it may have a role in epithelial cell polarisation also.

All three members of the JAM family have been localised to the testis, with JAM-A and JAM-B at the Sertoli cell TJ and JAM-C important for the conversion of round spermatids into elongated spermatids (Gliki *et al.* 2004, Mirza *et al.* 2007). The contribution of JAM-A and JAM-B to the Sertoli cell TJ is not well known but recently, JAM-A was also localised in germ cells (Tarulli *et al.* 2008), suggesting that like its role with leukocyte migration across epithelial TJs, JAM-A may also have a

role in mediating germ cell migration across the Sertoli cell TJ (Tarulli *et al.* 2008). Interestingly, while E-cadherin has been localised to the testis in one week old rats (Wu *et al.* 1993), it is not present in Sertoli cells (Byers *et al.* 1994) and therefore does has not appear to be important for blood-testis barrier formation, suggesting that JAM-A may interact with other cadherins or proteins at the time of adherens junction and subsequent TJ formation. This is an area which requires further research.

b. The cytoplasmic plaque

The cytoplasmic plaque is a complex of proteins that interact with each other to link the cytoskeleton to the membrane components of the TJ (Fanning *et al.* 1998) (see Figure 1.6). Zonula occluden-1 (ZO-1) was the first TJ-related protein discovered (Stevenson *et al.* 1986) and has since been shown to be a pivotal component of the cytoplasmic plaque through its interactions with the C-terminal of occludin, the claudins and JAM (Furuse *et al.* 1994, Mitic *et al.* 1999). Since the discovery of ZO-1, ZO-2 and ZO-3 have also been localised to the cytoplasmic plaque. Citi, (2000), also showed that the cytoplasmic plaque acts as targets and effectors of signalling pathways involved in regulating the function of the TJ.

1.4 The function of the tight junction

As has been discussed, the role of the TJ is essential in all epithelia, to form a protective barrier between bodily organs and cavities or blood vessels, and to allow the passage of select solutes across via the paracellular pathway, in a function known as the TJ ‘fence’ function (Gonzalez-Mariscal *et al.* 2008). Over the past several decades, qualitative and quantitative techniques have been employed by researchers to assess the loss or gain of TJ function in response to various stimuli. This section of the review will focus on qualitative and quantitative methods of analysing TJ function, the size-selective nature of the TJ and then move into the apparent roles that occludin and the claudins have in TJ function.

1.4.1 Qualitative assessment of tight junction function

In general, qualitative TJ function analysis has largely involved the use of tracer administration to target tissue *in vivo*, and subsequent visualisation of its localisation with respect to

the TJ by some form of microscopy. Electron microscopy-opaque tracers such as horse-radish peroxidase (HRP) (44kDa) and lanthanum nitrate (433kDa) were originally the more popular tracers for analysis and have been used since the 1970s and 1980s. When administered to the testes of adult minks via arterial perfusion, HRP entered the seminiferous tubules only as far as the Sertoli cell TJ, indicating that the TJ was functioning to exclude the tracer from the adluminal compartment of the seminiferous epithelium. During seasonal testicular regression which coincides with the cessation of spermatogenic activity, the HRP tracer was seen to enter the adluminal compartment of the seminiferous epithelium indicating that the TJs were no longer functioning normally and had become permeable to the tracer (Pelletier, 1986, Pelletier, 1988, Pelletier, 1994). Pelletier, (1994), cast doubt on the validity of lanthanum nitrate as a marker of TJ function, after it was seen on the 'protected' or adluminal side of the epididymal TJ, despite HRP being blocked. It was concluded that lanthanum had affinities for membrane components on the epithelial cells, and was being taken up by the cell, and displayed on the opposite side of the TJ (Pelletier, 1994). A similar result was obtained for the TJ tracer, tannic acid in the liver (Pelletier, 1994). Despite these findings, lanthanum has continued to be used more recently as a marker for Sertoli cell TJ function in the dog (Mann *et al.* 2003).

In the past few years, the use of tracers which can be visualised by immunohistochemistry using fluorescent or light microscopy to analyse TJ function has increased. A biotin (~600Da) tracer containing a long spacer arm which enables it to cross-link primary amines and not cross cell membranes has been used recently as a TJ function marker which can be probed with streptavidin (Furuse *et al.* 2002, Bratt *et al.* 2005, Meng *et al.* 2005). In a superficial keratectomy rat model, biotin readily permeated through wounded corneas, until the epithelium had healed and restored TJ function approximately 72 hours after wounding, at which point, biotin was once more restricted to the outside of the TJ (Hutcheon *et al.* 2007). In a claudin-5 knockout mouse model, biotin was restricted from entering the brain parenchyma by the blood-brain barrier in wildtype mice, yet readily permeated through the TJ and into the brain parenchyma in the knockout, indicating that due to the absence of claudin-5, TJ function had been compromised (Nitta *et al.* 2003). In the testis, biotin was restricted to the interstitium in wildtype mice, but in a Sertoli cell specific androgen receptor knockout mouse model, biotin readily permeated across TJs and spread throughout the seminiferous tubules (Figure 1.8) (Meng *et al.* 2005). This indicated compromised and altered TJ function in the knockout mice

Figure 1.8 Biotin penetration into the seminiferous epithelium.

Fluorescence microscopy was used to demonstrate that biotin tracer (red, arrow) was able to penetrate throughout the seminiferous epithelium of pre-pubertal mice, consistent with the absence of a tight junction which forms at puberty (panel A). In the adult mouse where mature tight junctions have formed, biotin staining was absent from the seminiferous tubules and restricted to the interstitium (panel B). In the adult Sertoli cell-specific androgen receptor knockout mouse, biotin tracer readily permeated throughout the seminiferous tubules as per the pre-pubertal mouse, indicating a non-functional tight junction. Modified from Meng *et al.* (2005). Bar = 50μm.

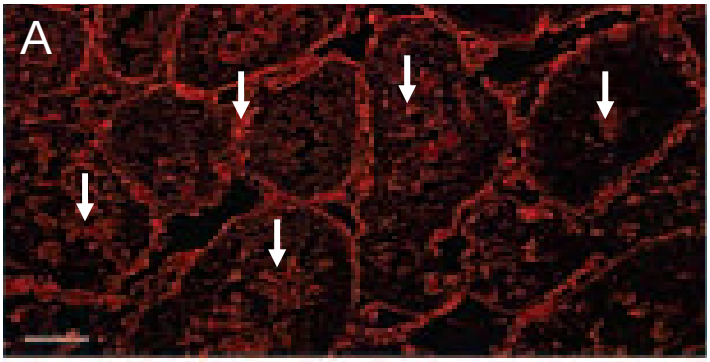
A

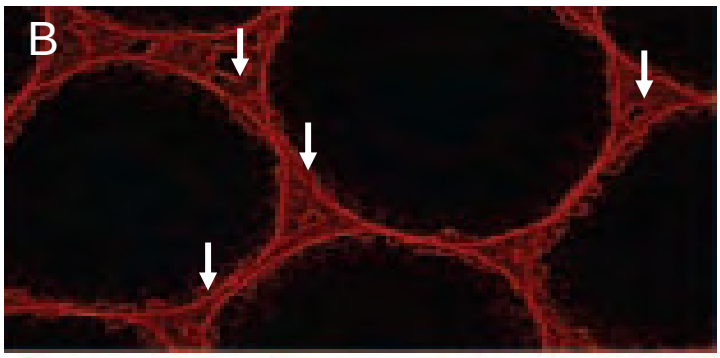
B

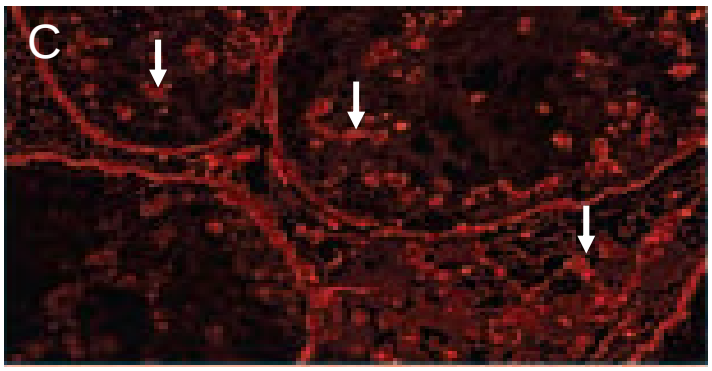
C

(Meng *et al.* 2005). The localisation of biotin in the control testis, was comparable to the localisation of HRP, with both tracers only entering the tubules as far as the TJ (Pelletier, 1986, Meng *et al.* 2005). More recent studies probe for TJ protein components at the same time as TJ function tracers, which means that the degree of TJ disruption can be visualised at the same time as its function (Figure 1.9) (Meng *et al.* 2005, Xia *et al.* 2007, Tarulli *et al.* 2008). Studies have revealed however, that despite tracer permeation, TJs sometimes appear intact by immunohistochemistry and this has displayed the need to study specific TJ components in more detail (discussed below) and their role in regulating both the quantitative function and size-selective discrimination properties of the TJ (Nitta *et al.* 2003, Bratt *et al.* 2005).

1.4.2 Quantitative assessment of tight junction function

Medical resonance imaging (MRI) has been applied to quantify changes in the function of the TJ of the blood-brain barrier in the claudin-5 knockout mouse model analysed in the Nitta *et al.* (2003) study above. Wildtype and claudin-5 mice were injected with a low molecular weight tracer (Gd-DTPA: 742Da) into the heart. In wildtype mice, every organ except for the central nervous system (CNS) displayed positive signalling for the tracer (Nitta *et al.* 2003). In the claudin-5 knockout mice, the CNS stained positively for the tracer in a dose dependent manner. The change in TJ function was quantified by comparing the change in tracer-accessible space/unit volume in the brains of the wildtype mice to the knockout mice. This showed that TJ function was disrupted by approximately 15% due to the claudin-5 knockout (Nitta *et al.* 2003). Thus this study was able to demonstrate both a qualitative decrease in TJ function, and a quantitative decrease.

However, like qualitative TJ functional analysis, quantitative analysis of TJ function *in vivo* largely uses tracers, which are most commonly radio-labelled. Testicular efferent duct ligation leads to fluid retention in the testis, increased testicular turgidity and eventually degeneration of the seminiferous epithelium and the cessation of spermatogenesis (Setchell, 1970, Kumar and Gilula, 1996, Tao *et al.* 2000). The function of the Sertoli cell TJ has been assessed in this efferent duct ligation model in the rat, by the vasculature administration of small molecular weight tracer [^{51}Cr]-EDTA (341 Da), which was monitored by a gamma-counter (Setchell *et al.* 1996, Tao *et al.* 2000).

Figure 1.9 Co-localisation of tight junction components with biotin tracer.

Experiments analysing changes in tight junction structure can be conducted at the same time as analysing changes in tight junction function. These are fluorescent immunomicrographs of biotin tracer (green) and Sertoli cell tight junction protein claudin-11 (blue) localisation in the photoregulated Djungarian hamster. Sertoli cell nuclei are highlighted with GATA-4 (red). In the seasonally regressed testis of the short-day hamster (panel A), biotin permeates throughout the seminiferous tubules and claudin-11 is localised within the cytoplasm of the Sertoli cells and not at the TJ, indicating functionally and structurally incompetent TJs. After 2 days of FSH treatment to these hamsters (panel B), claudin-11 is still cytoplasmic and TJs are still dysfunctional as shown by the continued presence of biotin within the tubules. After 10 days of treatment, claudin-11 has largely redistributed to the TJ, and the permeation of biotin in the tubules gets no further than claudin-11, indicating some restoration in TJ structure and function. Taken from Tarulli *et al.* (2006). Circle indicates junction between biotin and claudin-11 staining. Bar = 50μm.

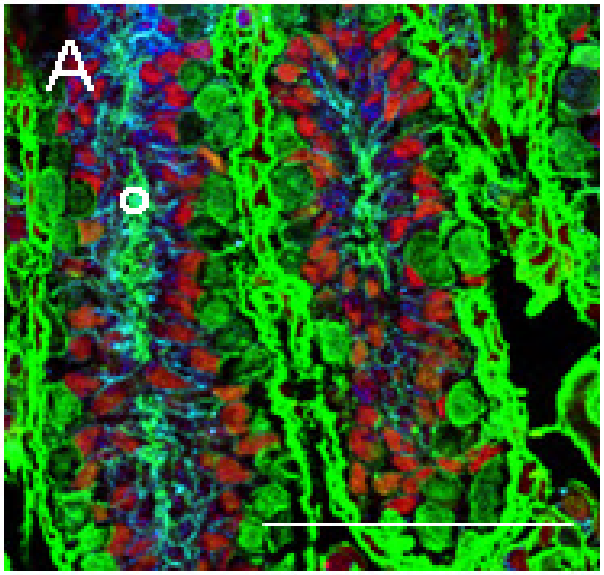
A

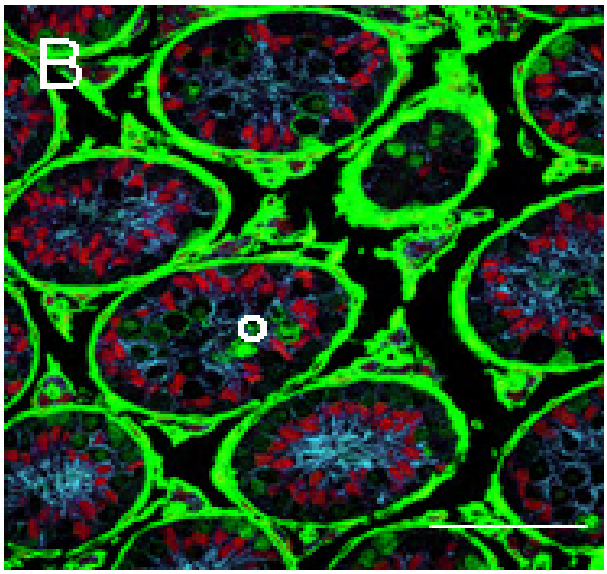
B

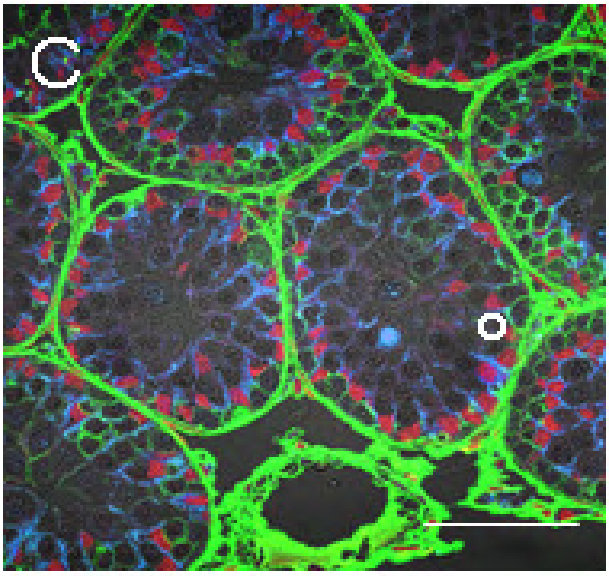
C

The TJ was effective for the first 24 hours of fluid accumulation in the testis, with the concentration of the tracer remaining higher in the interstitium than in the tubules. However after 40-48 hours of duct ligation, the tracer permeated through the tubules and concentrations exceeded that seen in the interstitium, indicating the breakdown of the Sertoli cell TJ (Tao *et al.* 2000). In a similar study, Sertoli cell TJ function was disrupted by the intratesticular injection of glycerol (Eng *et al.* 1994, Igdoura and Wiebe, 1994, Setchell *et al.* 1996). This was shown after seminiferous tubules were collected from control and glycerol-treated testes and incubated in [^{3}H]methoxy-inulin tracer (Eng *et al.* 1994). The accumulation of the tracer inside the seminiferous tubules was ten-fold greater in the glycerol-treated testes than the controls as shown by scintillation spectrometry, indicating that the function of the Sertoli cell TJs had been disrupted (Eng *et al.* 1994). A follow up study showed that the intratesticular injection of glycerol disrupted and disorganised the actin based cytoskeleton and occludin localisation to the Sertoli cell TJ (Wiebe *et al.* 2000). While the seminiferous tubules from the Wiebe *et al.* (2000) study were not incubated in the [^{3}H]methoxy-inulin tracer, there appears to be a connection with the removal of occludin from the Sertoli cell TJ and a loss of function as induced by glycerol (Eng *et al.* 1994, Wiebe *et al.* 2000). However, given that the actin based cytoskeleton was disrupted, it is reasonable to assume that the adherens junction which connects to actin at the blood-testis barrier (Cheng and Mruk, 2004) was also disrupted, meaning that the loss of barrier function in the Eng *et al.* (1994) study could not necessarily be directly attributed to the loss of TJ function, but rather the loss of the blood-testis barrier function as a whole.

Tracers can also be used in *in vitro* culture models for quantitative TJ functional analysis. When rat brain cells were cultured in bicameral units (see section 1.2.5) and incubated in [^{14}C]-inulin, the cells were unable to prevent the passage of the tracer across the filter to the outside of the bicameral unit (Ohtsuki *et al.* 2007). However, when TJ protein claudin-5 was transfected into these cells, the permeability of [^{14}C]-inulin was markedly decreased, indicating that the cells had formed impermeable TJs (Ohtsuki *et al.* 2007). There are not many recent reviews readily available in the literature, but for further details about other methods for measuring TJ function quantitatively *in vivo*, see Vedula *et al.* (2005).

Transepithelial electrical resistance (TER) is another method for *in vitro* quantification of TJ function, and uses the same bicameral unit as above. A current is applied across the cell monolayer,

and the increasing resistance that occurs as TJs form is measured. TER actually measures the permeability of a cell monolayer to Na^+ and Cl^- salts which most culture media contain in an electrically applied field (for reviews see Fanning *et al.* (1999), Matter and Balda, (2003), Gonzalez-Mariscal and Nava, (2005), Vedula *et al.* (2005)). Permeability of cell monolayers to electrical currents varies greatly across bodily epithelia, and this is due to differences in the 'tightness' of different epithelial TJs (Fanning *et al.* 1999). As reviewed in Fanning *et al.* (1999), the leaky mammalian proximal renal tubules recorded TER values of 6-7Ω/cm^2 whereas the very tight bladder epithelium records TER values of 6,000-300,000Ω/cm^2. Results obtained by TER and the application of tracers such as inulin (Dym and Fawcett, 1970) *in vitro* are not comparable. While the TJ permeability measured by TER varies widely across different epithelia, the size selectivity of TJs (detailed in section 1.4.3) from different cultured epithelial cells to any given tracer does not vary to the same extent (Fanning *et al.* 1999). Furthermore, tracers themselves vary in size and so any results obtained for TJ function would reflect the changes in permeability to the particular tracer applied alone. Therefore, TER provides a more global measure of changes in TJ function and while a decreasing trend in TER would correlate to an increasing trend in tracer permeability, final numbers would not be the same. TER is sensitive to changes in media temperature and media volume and so should be measured at a constant temperature of 37^{o}C and in an environment containing the same amount of media on the outside of the bicameral unit as what is inside the unit (Janecki *et al.* 1991, Matter and Balda, 2003).

As mentioned previously in this review, TER was used to show decreases in TJ function in response to the addition of a peptide corresponding to one of the extracellular loops of occludin in cultured *Xenopus* epithelial cells and rat Sertoli cells (Wong and Gumbiner, 1997, Chung *et al.* 2001). TER also showed an increase in TJ function in cultured Madin-Darby canine kidney (MDCK) cells following the over-expression of occludin (McCarthy *et al.* 1996). In cultured Sertoli cells, increases in TER were seen with FSH and testosterone treatment (Janecki *et al.* 1991, Kaitu'u *et al.* 2007) whereas decreases in TER were seen following cytokine TNF-α and TGF-β and phosphatase inhibitor treatment to cultured Sertoli cells (Li *et al.* 2001, Lui *et al.* 2001, Siu *et al.* 2003, Cheng and Mruk, 2004). These data indicate that TER is a versatile means of measuring TJ function in a variety of

cultured epithelial cells, but in order to determine changes in size-selectivity, it would be useful to use tracers of varying molecular weight in the same culture experiments.

Interestingly, TER has also been successfully applied to the insect TJ analogue, septate junctions *in vivo* to measure the effect of a peptide known to regulate the paracellular pathway in the malphigian tubules of the mosquito (Clark *et al.* 1998, Carlson *et al.* 2000). Tubules were incubated in the peptide and then the resistance across the epithelial lining of the individual tubules were recorded. The TER across tubules treated with the peptide was significantly lower than in controls, indicating an alternative means to the use of tracers for analysing TJ function *in vivo* (Clark *et al.* 1998, Carlson *et al.* 2000).

1.4.3 The size-selective nature of the tight junction

Several studies have suggested the existence of size-selective pores in TJs. The blood-brain barrier protects the brain from harmful chemicals in the blood (Nitta *et al.* 2003). It was found in 1885, that when dyes were injected into veins, all organs stained except for the brain (Nitta *et al.* 2003). A major component of the blood-brain barrier is the TJ protein claudin-5 (Nitta *et al.* 2003). When a low molecular weight biotin tracer (443D) was administered to the brains of claudin-5 knockout mice *in vivo*, it readily crossed the TJ into the brain parenchyma, whereas it was restricted to the blood vessels in the control (Nitta *et al.* 2003). When a larger microperoxidase tracer (1.9kDa) was applied to this model, the tracer did not cross the TJ. This data indicated that the claudin-5 knockout reduced TJ function in a size-selective manner. This was further demonstrated by applying a 10kDa dextran-conjugated molecule to the brain mixed with a small nuclear dye. Both stains were observed in the blood vessels, but only the small nuclear dye penetrated through the TJ into the brain parenchyma (Nitta *et al.* 2003). Interestingly, despite the apparent loss of TJ function to low molecular weight molecules, the mice were healthy, there was no morphological difference in the blood-brain barrier compared to controls, and no bleeding or edema was apparent (Nitta *et al.* 2003). This raises the question about how functional and size-selective a TJ needs to be to maintain barrier integrity. Nitta *et al.* (2003) reasoned that the probable cause of loss of blood-brain barrier size-selectivity against low molecular weight tracers and not large molecular weight tracers in the claudin-5 knockout mice, was due to the continued presence of another TJ protein, claudin-12. That is, the loss of claudin-5 reduces

the blood-brain TJ to selectively inhibit small molecular weight molecules passage across the barrier, but the presence of claudin-12 in the absence of claudin-5, maintains the ability of the TJ to discriminate against larger molecular weight molecules and therefore maintain its integrity (Nitta *et al.* 2003).

This phenomenon has also been observed at the Sertoli cell TJ in the rat. Sertoli cell TJs form at puberty, which is coincident with a rise in circulating gonadotrophins and the commencement of spermatogenesis (Russell *et al.* 1989). In the rat, this is at 15 days of age. However, the small molecular weight tracer [^{51}Cr]-EDTA was still able to cross the Sertoli cell TJ after 15 days, and indicated that the barrier function of the TJ is not fully competent until 44 days of age, at a time well into spermatogenesis (Setchell *et al.* 1981, Setchell *et al.* 1988). Such data indicates the further need to study the importance of TJ function and size-selectiveness and the threshold at which TJ interference will result in a non-functional and non-size-selective barrier.

Several studies have analysed size-selectivity in TJs more closely. The permeability of 24 polyethylene glycols (PEG) ranging in molecular radii from 3.5Å-7.4Å was tested in two intestinal-derived model cell lines, Caco-2 and T84 (Watson *et al.* 2001). The molecular radius of PEGs can be converted to molecular weights by the equation: $r\ (Å) = 0.29\ M^{0.454}$ (Ruddy and Hadzija, 1992, Watson *et al.* 2001). Therefore the range of PEGs used was in the molecular weight range of 252Da-1255Da. Watson *et al.* (2001) showed that the permeability of the TJs was inversely proportional to molecular size, and there was a cut-off of molecules penetrating the TJ at a molecular radii of greater than 4.68Å (458Da). The authors of the paper presented other literature which suggested that size-selective pores exist in the TJs and that these are formed by claudins. The larger molecules did eventually cross the TJ and the authors postulated that this was due to possible dilatation of the existing pores, or an increase in pore size and/or number, which may be another separate function of the TJ (Watson *et al.* 2001).

Another study looking at the size-selective nature of the TJ *in vitro*, used mannitol to induce permeation in cultured brain cells (Deli *et al.* 1995). Three radio-labelled tracers of varying molecular weights, [^{14}C]-sucrose (342Da), [^{3}H]-inulin (5kDa) and Evans Blue dye (EBA, 67kDa) were used. A significant increase in permeation to sucrose was observed, as was observed for inulin, although at a 3-fold lower concentration to sucrose which may have been directly due to inulin being a larger

molecule. Evans Blue dye did not cross the TJ in this treatment (Deli *et al.* 1995). This study therefore provided further evidence of the size-selective nature of the blood-brain barrier, where the smallest tracer was able to penetrate the disrupted TJ, as was a slightly larger tracer albeit at a reduced capacity and the largest tracer was completely excluded. Similar data was seen for various radioactive tracers of varying sizes used to analyse TJ function in the alveoli of the lung epithelium in sheep *in vivo* as well (Egan *et al.* 1976).

Therefore, TJs are size-selective across several different types of epithelia and it appears that this property is directly proportional to the functionality of the TJ barrier.

The next question that arises is which of the TJ proteins contribute to the functional and size-selective properties of the TJ. This review will now look at the role occludin and the claudins play in mediating these properties.

1.4.4 The role of occludin and the claudins in tight junction function

a. Occludin

Occludin is localised at membrane fusion points in intact TJs, as shown by immunofluorescence and immunoelectron microscopy (Furuse *et al.* 1993, Clarke *et al.* 2000). In disrupted TJs induced by Ca^{2+} depletion, wound healing, pro-inflammatory cytokines or in the case of the Sertoli cell TJ low circulating gonadotrophins, occludin is localised in intercellular pools within the cytoplasm of the epithelial cells (Ando-Akatsuka *et al.* 1999, Lu *et al.* 2001, Bruewer *et al.* 2003, Bruewer *et al.* 2005, Ivanov *et al.* 2004, Morimoto *et al.* 2005, Tarulli *et al.* 2008). How occludin is distributed to the TJ is the subject of much debate.

As mentioned previously, occludin consists of intracellular C- and N- terminal domains, two extracellular domains and four transmembrane domains (Tsukita and Furuse, 1999) (see Figure 1.7). The C-terminal of occludin while being thought to be important for the localisation of occludin to the TJ, was also seen to mediate the binding of occludin to ZO-1 of the cytoplasmic plaque (Martinez-Estrada *et al.* 2001). Transfected connexin (a gap junction component) chimeras containing the C-terminal of occludin were localised to cell-contact points (Matter and Balda, 1998) but were not integrated into TJ fibrils as seen with different chimeras also containing the occludin C-terminal

(Matter and Balda, 1998). Conversely, chicken occludin lacking the entire C-terminal was also localised to the TJ in MDCK cells and integrated into the TJ fibrils as shown by an increase in TER (Balda *et al.* 1996). A similar phenomenon was also observed in *Xenopus* embryos (Chen *et al.* 1997). These findings suggested that another component of occludin is responsible for it localisation to, and integration into TJ fibrils such as its transmembrane and/or extracellular domains. The removal of the second extracellular loop of occludin resulted in its absence from the TJ (Medina *et al.* 2000), demonstrating that this domain may therefore be important for its integration into the TJ. Furthermore, the extracellular and transmembrane domains of occludin may interact with claudins to form an anchor that binds to the underlying scaffolding complex (cytoplasmic plaque) containing ZO-1, ZO-2 and ZO-3 (Chen *et al.* 1997). As mentioned above, the C-terminal may be important for the interaction with the cytoplasmic plaque, as occludin minus its C-terminal formed discontinuous TJ fibrils and an increase in paracellular flux, suggesting a disruption in the barrier between cells and a loss in TJ function (Chen *et al.* 1997, Hirase *et al.* 1997, Bamforth *et al.* 1999). Interestingly, Occludin is more prevalent in 'tighter' TJs such as in the blood-brain barrier, than in leakier junctions such as those in non-neural tissues (Claude, 1978, Hirase *et al.* 1997), suggesting that occludin may have a regulatory role, rather than a functional role in the TJ (Nusrat *et al.* 2000, Ban *et al.* 2003).

b. Claudins

The claudins have come under close scrutiny since the idea arose that occludin may not be pivotal to the function of the TJ (Nusrat *et al.* 2000, Ban *et al.* 2003). The relative contribution of claudin-1 and claudin-2 to the TJ has been studied (Furuse *et al.* 1998). These two claudins were tagged and transfected into mouse L fibroblasts that were void of TJs to observe the ability of the transfected cells to form TJ strands (Furuse *et al.* 1998). The results showed that fibroblasts transfected with occludin alone, produced TJ strands that were short in length and low in number. However, when the fibroblasts were transfected with the claudins alone, or the claudins in conjunction with occludin, complete TJ fibrils were formed (Furuse *et al.* 1998).

To further demonstrate the importance of claudins to TJs, claudin-1 knockout mice, a type of claudin prevalent in the epidermal layer, died within one day of birth (Furuse *et al.* 2002). These mice displayed a wrinkled phenotype and had died of dehydration due to severe transepidermal water loss

(Furuse *et al.* 2002), indicating that the paracellular regulatory mechanism of the TJ had been compromised. Under the microscope, the layered organisation of the keratinocytes in the dead mice appeared normal and the continuous fibrils of the TJs were visually comparable to those observed in the surviving wildtype mice (Furuse *et al.* 2002). Occludin and claudin-4 were still present in the TJ fibrils. To show, though, that the fibrils were different in the mutant mice, a low molecular weight biotin tracer (~600Da) tracer was injected subcutaneously into both the wildtype and claudin-1 knockout mice. The tracer could not cross the epithelial layer in the wildtype mice, but could in the mutant (Furuse *et al.* 2002), suggesting that the loss of claudin-1 from the TJ fibrils, had disrupted that function of the TJ and altered its size-selectivity properties. In an MDCK cell-line, *Clostridium perfringens* enterotoxin selectively removed claudin-3 and -4 from TJ complexes in an intestinal cell line, resulting in a decrease in TJ function as shown by TER and a large size-selective increase in paracellular flux to 4kDa and 10kDa FITC-Dextran, but not to 40kDa FITC-Dextran (Sonoda *et al.* 1999). In the claudin-5 knockout mouse model mentioned previously with respect to the blood brain barrier, TJ function was compromised in a size-selective manner but was still functional and size-selective enough to prevent bleeding or edema, and the TJ strands looked morphologically normal (Nitta *et al.* 2003). This may have been due to the presence of claudin-12 at the blood-brain barrier, the localisation of which is not effected by the claudin-5 knockout (Nitta *et al.* 2003, Ohtsuki *et al.* 2007). Despite findings that claudin-5 mRNA is expressed 751 fold greater than claudin-12 in cultured rat brain cells (Ohtsuki *et al.* 2007), it may have been possible that claudin-12 was providing the function and enough size-selectivity needed to prevent bleeding in the claudin-5 knockout mice. In wildtype mice, claudin-3 localised to the testicular Sertoli cell TJ at the time of TJ formation, whereas in the Sertoli cell-specific androgen receptor knockout mouse model, claudin-3 staining was absent (Meng *et al.* 2005). When claudin-11 was probed in these androgen receptor knockout mouse testes, the TJs still appeared morphologically normal, however biotin penetration into the seminiferous tubules in these animals showed that TJ function had been compromised and discrimination against low molecular weight tracers had been disrupted (Meng *et al.* 2005). However, evidence also suggests that claudin-11 is essential for TJ function, in that its knockout leads to infertility in the mouse (Gow *et al.* 1999).

In the corneal wounding experiment mentioned previously, low molecular weight biotin permeated through the epithelium until barrier function was restored 72 hours later (Hutcheon *et al.* 2007). The tracer did not penetrate the corneal epithelium anywhere else, including at the regions flanking the wound (Hutcheon *et al.* 2007). Interestingly, the localisation of occludin and ZO-1 remained constant at the TJ even before the wound had healed and barrier function had been restored (Hutcheon *et al.* 2007). The authors did not stain for any of the claudin proteins that may have been involved in the corneal epithelium, but the constant staining pattern of the other TJ proteins in this epithelial layer, and results obtained for the claudins in other epithelia, suggests that the claudins may have been involved with the restoration of barrier function and size-selectivity against biotin in the corneal epithelium also.

Several *in vitro* studies have also demonstrated the importance of the claudins to TJ function. The over-expression of claudin-2 in a MDCK cell-line appeared to decrease TJ function as measured by TER (Amasheh *et al.* 2002). When testing for changes in paracellular flux in the same model, the TJ continued to exclude low molecular weight mannitol (182Da) and higher molecular weight dextran (4kDa) as per the control cells (Amasheh *et al.* 2002). These results reinforce the point made earlier that results obtained from TER are not comparable with results obtained from measuring paracellular flux with tracers. Nonetheless, the negative impact that claudin-2 has on TER is unusual among claudins. For example, the over-expression of claudin-4 in MDCK cells and the localisation of claudin-11 to Sertoli cell TJs, increased TER (van Itallie *et al.* 2001, Kaitu'u *et al.* 2007). As mentioned previously, the extracellular domains of the claudins pair up with their counterparts on adjacent cells and several claudin pairs have been identified. Each 'pairing' has a different effect on the paracellular flux (Mitic *et al.* 2000).

1.5 The role of phosphorylation in tight junction assembly

Phosphorylation and dephosphorylation of some TJ proteins were first seen to be pivotal in regulating their assembly and disassembly in 1991 (Balda *et al.* 1991, Nigam *et al.* 1991, for a review see Gonzalez-Mariscal *et al.* (2008)). The protein kinases and phosphatases involved in regulating the phosphorylation state of TJ proteins are activated in the presence of calcium (Ca^{2+}), which binds to and activates E-cadherin on the extracellular side of the membrane (Yap *et al.* 1997). E-cadherin

activation leads to a cascade of events involving phosphokinases, phospholipases and calmodulin (Farquhar and Palade, 1963) which eventually leads to the phosphorylation of occludin, the claudins and ZO-1, and their subsequent recruitment to the TJ (Gonzalez-Mariscal *et al.* 1985, Sim and Scott, 1999, Matter and Balda, 2003, Gonzalez-Mariscal *et al.* 2008). Cells plated *in vitro* in medium containing low Ca^{2+} concentrations, do not form TJs (Gonzalez-Mariscal *et al.* 1985). However, upon restoration of 'normal' Ca^{2+} levels, TJs formed rapidly (Gonzalez-Mariscal *et al.* 1985). This turning on and off of Ca^{2+}, is termed the calcium switch. This calcium switch has been exploited by many research groups studying the phosphorylation pathways that TJ proteins follow (Citi, 1992, Farshori and Kachar, 1999, Lawrence *et al.* 2002).

Occludin is phosphorylated at TJs in MDCK cells, with non phosphorylated occludin located at the basolateral membrane and not contributing to the TJ (Sakakibara *et al.* 1997, Farshori and Kachar, 1999). By SDS-PAGE gels, occludin bands appear at apparent molecular weights ranging from 62-82kDa (Sakakibara *et al.* 1997), with the heavier bands being those which are more phosphorylated. The removal of phosphate groups by alkaline phosphatase treatment, converged these bands (Sakakibara *et al.* 1997). Less or non-phosphorylated occludin was found to be soluble in 1% NP-40 detergent, and most of the occludin pool was found in this detergent fraction when media concentrations of Ca^{2+} were low. Most occludin however, appeared in an NP-40 insoluble extract upon restoration of Ca^{2+} levels, suggesting it had been phosphorylated (Sakakibara *et al.* 1997). Different detergents also exhibited the same differential solubilisation of occludin (Wong, 1997). The amino acid residues that are phosphorylated on occludin are serine and threonine (Sakakibara *et al.* 1997), but whether their phosphorylation and dephosphorylation is random or sequential is unknown (Sakakibara *et al.* 1997).

Claudins are also targets of phosphorylation by a variety of kinases (Gonzalez-Mariscal *et al.* 2008). The blood-brain barrier and claudin-5 has already been mentioned extensively in this literature review with respect to TJ function and size-selectivity. What has not been mentioned thus far with respect to claudin-5, is that cAMP induces an increase in its mRNA expression, regulates its localisation to the TJ and promotes a switch within the protein from serine phosphorylation to threonine phosphorylation via protein kinase A (PKA) (Ishizaki *et al.* 2003). These events are associated with an increase in TJ function and therefore size-selectivity (Ishizaki *et al.* 2003). When

lung endothelial cells expressed claudin-5 which had a point mutation of a PKA phosphorylation site, the TJ excluded the passage of low molecular weight tracer mannitol (182Da) and large molecular weight tracer inulin (5kDa), whereas in the wildtype the TJ was permeable to mannitol (Gonzalez-Mariscal *et al.* 2008). This data thereby demonstrated the importance of TJ protein phosphorylation and directly implicated the role of phosphorylation in regulating TJ size-selectivity. Serine phosphorylation also appears to be important for claudin localisation to TJs. Serine phosphorylation of claudin-16 as mediated by PKA at residue Ser217, is essential for its localisation to kidney TJs where it acts as a paracellular pore for Mg^{2+} (Simon *et al.* 1999, Mitic *et al.* 2000, Gonzalez-Mariscal *et al.* 2008). Mg^{2+} and Ca^{2+} wastage as seen in some human renal diseases is coincident with claudin-16 not localising to the TJ and displaying mutations in domains of the protein important for phosphorylation, including the C-terminal where Ser217 resides (Simon *et al.* 1999, Kausalya *et al.* 2006, Muller *et al.* 2006, Gonzalez-Mariscal *et al.* 2008). Tyrosine phosphorylation has also been seen to be important for the interaction of claudin-4 with ZO-1 of the cytoplasmic plaque. Phosphorylation of residue Tyr208 which resides on the PDZ binding motif of claudin-4, attenuates its interaction with ZO-1 and actually enhances TJ permeability (Tanaka *et al.* 2005). These results indicate that the phosphorylation of different residues on the claudins has differential effects on TJ function across different epithelia. For a more comprehensive review of claudin phosphorylation see Gonzalez-Mariscal *et al.* (2008).

The zonulae occludens of the cytoplasmic plaque are also phosphorylated proteins, with phosphoamino acid analysis from purified ZO-1 and ZO-2 revealing strong phosphoserine signals (Anderson *et al.* 1988, Balda and Anderson, 1993, Avila-Flores *et al.* 2001, Gonzalez-Mariscal *et al.* 2008). Serine residues of ZO-2 in TJ deficient cells induced by low Ca^{2+} concentrations are significantly more phosphorylated than in monolayers displaying established TJs (Gonzalez-Mariscal *et al.* 2008). According to Gonzalez-Mariscal *et al.* (2008), much of the literature suggests that extensive serine phosphorylation on ZO-1 and ZO-2 results in decreased TJ function *in vitro.* Interestingly, zonulae occluden tyrosine phosphorylation has differential effects on TJ function with increases and decreases in TJ function observed after phosphorylation in different models (for a review see Gonzalez-Mariscal *et al.* (2008)). This is probably due to different amino acid residues being phosphorylated on the target proteins to achieve the desired TJ effect.

Considering that phosphorylation of TJ proteins is important for the maintenance of TJ function, one would expect that dephosphorylation of TJ proteins would also be important. Serine/threonine phosphatase PP2A, was the first TJ-related phosphatase found (Nunbhakdi-Craig *et al.* 2002). Occludin, ZO-1 and claudin-1 were dephosphorylated in its presence in MDCK cells, correlating with a loss of the TJ (Nunbhakdi-Craig *et al.* 2002). PP2A binds to and inhibits protein kinase C which subsequently blocks the phosphorylation of the aforementioned proteins. In the presence of okadaic acid however, this inhibition of PKC was overridden and tight junctions reformed (Nunbhakdi-Craig *et al.* 2002). It is widely agreed that phosphorylation of serine and threonine residues on occludin and ZO-1 results in the formation of the TJ (Chen *et al.* 1997). More recent studies have also implicated a role for claudin phosphorylation as outlined above.

The role of tyrosine phosphorylation in TJ function is controversial, in that it appears to have effects both on TJ assembly and disassembly. ATP depletion stimulates anoxia and the aggregation of occludin, ZO-1 and ZO-2 into large macromolecular aggregates, thereby destroying the TJ barrier (Tsukamoto and Nigam, 1999). After ATP replenishment and the addition of tyrosine kinases, the aggregated macromolecules broke up and regained their original conformation (Tsukamoto and Nigam, 1999). Upon the addition of a tyrosine kinase inhibitor, this recovery of the TJ conformation was blocked. However, Kale *et al.* (2003), showed that tyrosine phosphorylation actually resulted in the disassembly of the TJ in MDCK cells, showing that tyrosine phosphorylation of the C-terminal of occludin, inhibited its interaction with cytoplasmic plaque proteins ZO-1, ZO-2 and ZO-3 (Kale *et al.* 2003). Furthermore, oxidative stress in MDCK and Caco-2 cell monolayers, resulted in the phosphorylation of tyrosine residues on TJ proteins, which were associated with TJ disassembly (Atkinson and Rao, 2001, Kale *et al.* 2003). The addition of tyrosine kinase inhibitors to the Caco-2 cell monolayers prevented oxidative stress and acetaldehyde-induced TJ disruption (Atkinson and Rao, 2001). Due to the apparent biphasic effect of tyrosine phosphorylation on TJ proteins, further research is needed to uncover the exact mechanism of not only this kinase, but also serine and threonine kinases and phosphatases to improve the understanding of TJ regulation by phosphorylation. This topic has been recently reviewed by Gonzalez-Mariscal *et al.* (2008).

1.6 The inter-Sertoli cell tight junction

1.6.1 The structure of the Sertoli cell tight junction

Sertoli cell TJs resemble TJs from other epithelial tissues and are composed of the same types/families of proteins as other TJs, but differ to other TJs in terms of associations with other junctional complexes and also by localisation with respect to the epithelial cell. Sertoli cell TJs are part of a complex made up of several different types of junctions and this complex does not exist in other epithelia. These junctions; TJ, adherens junction, ectoplasmic specialisation, desmosomes, and gap junction, are all packed closely together and are localised at the basal aspect of the Sertoli cell and provide the blood-testis barrier (Russell and Peterson, 1985, Pelletier and Byers, 1992, Mulholland *et al.* 2001, Lui *et al.* 2003a, Lui *et al.* 2003b). TJs in all other epithelial types are located at the apical aspect of their applicable epithelial cell (Morita *et al.* 1999).

The main TJ proteins comprising the Sertoli cell TJ, are occludin and claudin-11, just one of the seven claudins localised to the testis (Morita *et al.* 1999). In more recent years, claudin-3 has been localised to newly formed Sertoli cell TJs in the mouse and hamster (Meng *et al.* 2005, Tarulli *et al.* 2008), but mRNA expression in rat Sertoli cells was undetected and the only part of the rat testis in which claudin-3 protein was detected, was in blood vessels (Kaitu'u *et al.* 2007) .

The importance of occludin in the testis is controversial. When a peptide corresponding to the second extracellular loop of occludin was added to cultured *Xenopus* epithelial cells and rat Sertoli cells, there was a disruption of TJ formation *in vitro* (Wong and Gumbiner, 1997, Chung *et al.* 2001). These results suggest that in part, occludin may be important in the function of the TJ. Furthermore, testosterone and dihydrotestosterone (DHT) regulated the localisation of occludin to cultured rat Sertoli cells *in vitro,* but did not regulate its mRNA expression (Kaitu'u *et al.* 2007). In a hamster model, FSH was seen to also regulate occludin localisation to the Sertoli cell TJ *in vivo* and in the absence of circulating gonadotrophins, occludin mRNA expression increased (Tarulli *et al.* 2008). As has been mentioned previously in this review, there is strong evidence that claudin-11 is pivotal for the working Sertoli cell TJ, as claudin-11 knockout mice were infertile and suffered from massive germ cell loss (Gow *et al.* 1999).

Another protein which may have important roles in the Sertoli cell TJ, is one which has thus far not been mentioned in this literature review.

The Coxsackie virus and adenovirus receptor (CAR) is expressed at most epithelial TJs (Raschperger *et al.* 2006, Mirza *et al.* 2007), where it forms a complex with Junctional Adhesion Molecule-Like (JAM-L) protein to regulate the passage of leukocytes across epithelia (Mirza *et al.* 2007). Studies have shown that CAR has important roles in the heart and muscle and its protein expression is controlled by signals that regulate proliferation, differentiation and inflammatory responses (Carson *et al.* 1999, Nalbantoglu *et al.* 1999, Hutchin *et al.* 2000, Ito *et al.* 2000, Rebel *et al.* 2000, Tallone *et al.* 2001, Vincent *et al.* 2004, Asher *et al.* 2005, Dorner *et al.* 2005, Chen *et al.* 2006, Shaw *et al.* 2006, Mirza *et al.* 2007).

In the adult seminiferous epithelium, CAR is expressed in germ cells when they are migrating across the Sertoli cell TJ (Mirza *et al.* 2007). Wang *et al.* (2007), showed that CAR is also expressed in rat Sertoli cells at the time of TJ formation at Sertoli cell-Sertoli cell contacts *in vitro*. These results suggested that CAR expression in both Sertoli cells and germ cells is important for spermatogenesis, in particular the migration of germ cells across the blood-testis barrier. Interestingly, CAR was shown to be involved in a complex containing JAM-L at the Sertoli cell TJ at the time of germ cell migration (Mirza *et al.* 2007), suggesting that the regulatory processes which allow leukocyte transmigration across epithelia, are very similar to the processes which allow germ cell migration across the blood-testis barrier (Mirza *et al.* 2007). The three subtypes of Junctional Adhesion Molecule (A, B and C) are all found in the testis but their roles are not certain (Gliki *et al.* 2004, Mirza *et al.* 2007). JAM-A and JAM-B partially co-localised with CAR at the Sertoli cell TJ by immunofluorescence (Mirza *et al.* 2007). However, JAM-A and JAM-B were expressed at all stages of the spermatogenic cycle, and no complex association with CAR could be ascertained (Mirza *et al.* 2007) suggesting that there may be no interaction between JAM-A/B and CAR at the Sertoli cell TJ and any common roles in mediating germ cell passage across the blood-testis barrier may involve separate pathways and interactions. However the authors noted that more work in this respect may be required before the role of these proteins in testicular TJ function is fully elucidated (Mirza *et al.* 2007). Recent *in vitro* work in cultured rat Sertoli cells showed that the protein expression of JAM-A and CAR increased as TJs formed. Furthermore, JAM-A protein was seen localised around spermatogonia and preleptotene and

leptotene spermatocytes in a hamster model (Tarulli *et al.* 2008). These results suggest that JAM-A is expressed by both Sertoli cells and germ cells in a similar manner to CAR and therefore JAM-A may also play a role in regulating Sertoli cell TJ assembly and transmigration of germ cell across the blood-testis barrier (Wang *et al.* 2007, Tarulli *et al.* 2008). Interestingly, CAR co-localised with claudin-3 in mouse testes which surrounded migratory germ cells, suggesting both proteins may be involved in TJ remodelling as germ cell crossed (Meng *et al.* 2005, Mirza *et al.* 2007). The Mirza *et al.* (2007) study provided evidence by immunofluorescence that as the CAR positive germ cells traversed the blood-testis barrier, TJ strands formed beneath them, before the adluminal strands broke down (Figure 1.10). This demonstrated nicely the pivotal function of the Sertoli cell TJ to maintain successful spermatogenesis. In order for the TJ to open and close correctly and maintain its own integrity and that of the seminiferous epithelium, tight regulatory controls are necessary.

1.6.2 Regulation of tight junction proteins within the Sertoli cell

a. Protein phosphorylation

Occludin in most epithelia appears to be phosphorylated when the protein is localised at the TJ. When phosphatase inhibitors were added to cultured Sertoli cells *in vitro*, there was a disruption at the TJ level as shown by a decrease in TER, and a rise in permeability (Li *et al.* 2001). It is noteworthy at this point that such inhibitors would alter various phosphorylation dependent pathways and proteins, and not just the TJ. The result obtained for occludin by Li *et al.* (2001), was unexpected as the phosphatase inhibitors were expected to prevent dephosphorylation of occludin and should have maintained TJ integrity. A possible explanation for this dilemma is that the pool of dephosphorylated occludins as mentioned previously residing at the basolateral membrane may be there in case the TJ needs to expand suddenly and rapidly (Li *et al.* 2001). Indeed, TER soared quickly after the addition of trypsin to MDCK cells (Lynch *et al.* 1995), showing that mammalian cells have a mechanism which can quickly assemble TJs. The interaction between preleptotene/leptotene germ cells with TJ membrane proteins just before and after they traverse the barrier could occur within a specialised microenvironment. Data has shown that as preleptotene spermatocytes cross the TJ, new TJ strands form beneath the germ cell before TJ strands above the germ cell break down, thereby maintaining

Sertoli cell TJ integrity and the exclusion of the adluminal compartment of the seminiferous epithelium from the basal compartment (Setchell, 1967, Zhou *et al.* 2002) (Figure 1.10). In order to achieve this the germ cell may contain the stimulus required to quickly alter the phosphorylation state of occludin in the TJ (Li *et al.* 2001). Therefore, phosphorylation appears to be an important process for establishing TJ function in Sertoli cells, however it may well not be the key regulatory mechanism concerned with TJs. Chen *et al.* (2000) observed claudin-1 forming fibrils with claudins in apposing membranes of MDCK cells were largely unphosphorylated, suggesting that the opening and closing of Sertoli cell TJs may be regulated by many pathways. Furthermore, the addition of phosphatase inhibitors did not completely abolish TJ assembly (Li *et al.* 2001). The contribution of phosphorylation to TJ regulation still needs to be fully elucidated.

b. The role of the extracellular matrix

The extracellular matrix that constitutes the basement membrane of Sertoli cells, is composed of collagen types I and IV (Hadley *et al.* 1985, Siu *et al.* 2003, Cheng and Mruk, 2004) and is regulated by metalloproteases and metalloprotease inhibitors (Siu *et al.* 2003). Due to the unusual position of Sertoli cell TJs at the basal aspect of these cells, the extracellular matrix is within close proximity, hence it may be possible that the constituent proteins of the extracellular matrix contribute to or regulate the opening and closing of the TJ. Previous data has shown that Sertoli cells secrete collagen I into the extracellular matrix (Hadley *et al.* 1985, Lee *et al.* 2007), and germ cells secrete collagen IV (Siu *et al.* 2003). The rising concentration of collagen correlates with TJ formation (Siu *et al.* 2003). Upon the addition of a collagen antibody to cultured rat Sertoli cells, TJ disassembly was observed by a decrease in TER *in vitro* (Siu *et al.* 2003). Collagen may have a biphasic effect on the Sertoli cell TJ proteins however, in that upon exogenous addition of cytokine TNFα, collagen levels rose, but TJs were disassembled (Siu *et al.* 2003). This cytokine enhances TJ disassembly and as would be expected, endogenous levels of TNFα are low in Sertoli cells at the time of TJ formation (Siu *et al.* 2003). This shows that other pathways are possibly involved in Sertoli cell TJ regulation, and the evidence provided above for TNFα indicates that regulation by local cytokines may be another regulatory pathway.

Figure 1.10 Migration of germ cells across the Sertoli cell tight junction.

In this immunomicrograph representation of preleptotene spermatocytes (blue, asterisk) migrating from the basal compartment of the seminiferous tubule into the adluminal compartment, the formation of tight junction strands containing the protein occludin (red, arrow) basally to the germ cell can be seen occurring before the breakdown of the tight junction adluminally to the germ cell, thereby demonstrating the ability of the tight junction to maintain the integrity of the specialised microenvironment in the adluminal compartment during germ cell migration. Taken from Mirza *et al.* (2007).

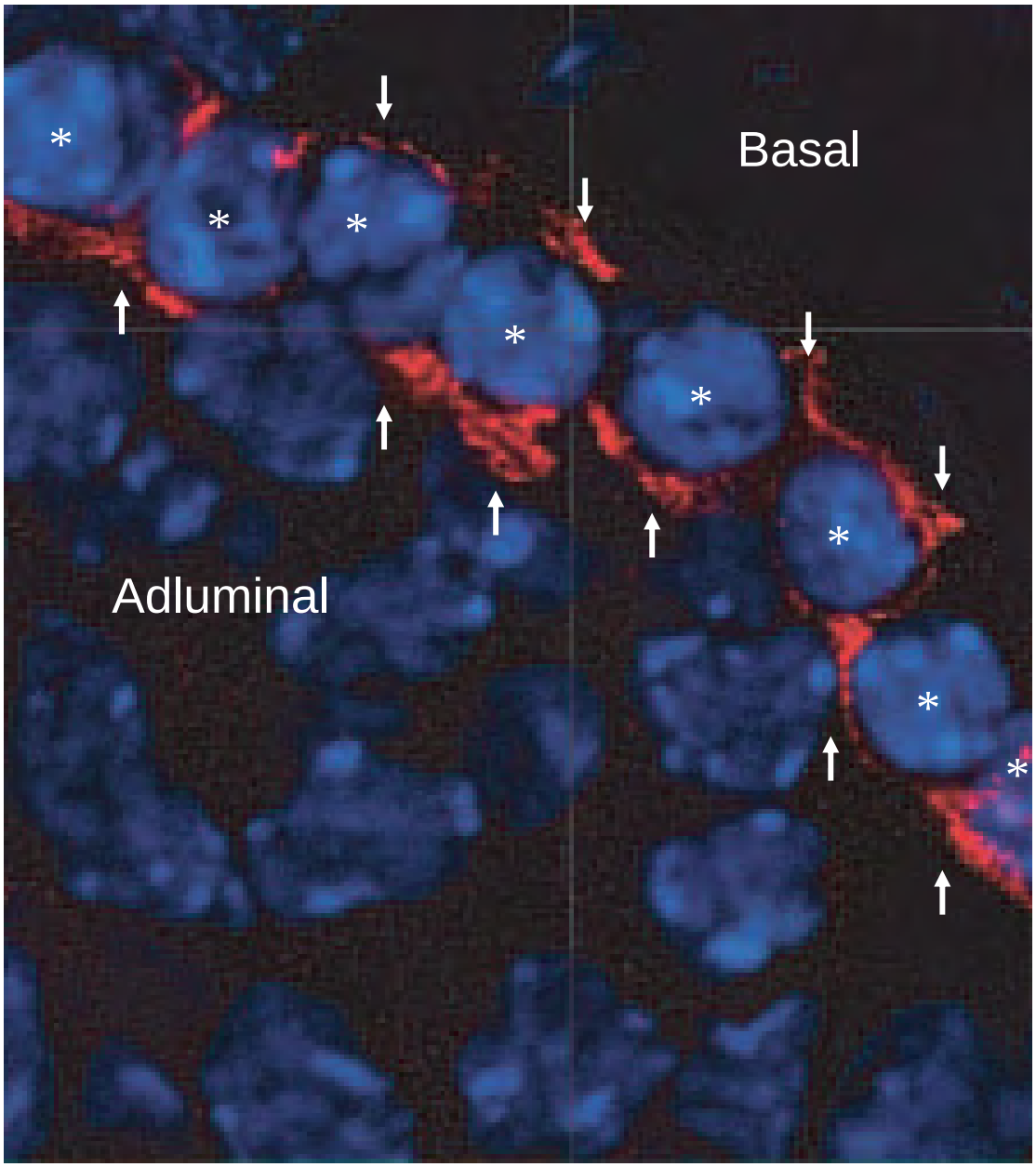
Basal
Adluminal

c. The role of local paracrine factors

Until recently, the role of local cytokine regulation of the Sertoli cell TJ was largely unknown (Xia *et al.* 2007) and only now is becoming clearer. While many cytokines have been implicated in the regulation of other epithelial TJs (see Mruk and Cheng, (2004)), most of the work conducted in the testis has involved looking at the roles of tumour necrosis factor-α (TNF-α) and transforming growth factor-β3 (TGF-β3) (Hellani *et al.* 2000, Siu *et al.* 2003, Cheng and Mruk, 2004, Wong *et al.* 2004, Xia and Cheng, 2005, Lui and Lee, 2006). TNF-α is secreted by Sertoli cells, pachytene spermatocytes and round spermatids, but is minimally expressed as germ cells cross the Sertoli cell TJ (Siu *et al.* 2003, Lui and Lee, 2006). Its administration to rats, results in the loss of germ cells *in vivo*, as well as reductions in occludin and claudin-11 mRNA and protein expression and reduced occludin localisation to the Sertoli cell TJ, indicating that this cytokine can disrupt the structure of the Sertoli cell TJ. Increased permeability of the TJ to a fluorescent dye after TNF-α treatment in the Lui and Lee (2006) study indicated that TJ function had also been disrupted thereby indicating an additional aspect of cytokine regulation.

TGF-β3 appears to have similar regulatory roles to TNF-α, in that at the time of Sertoli cell TJ formation *in vitro*, TGF-β3 levels decrease (Lui *et al.* 2001, Lui *et al.* 2003a). Treatment of these cultured Sertoli cells with TGF-β3 perturbed the TJ and prevented the localisation of occludin, claudin-11 and ZO-1 to the TJ *in vitro* (Lui *et al.* 2001). *In vivo* studies have shown that blood-testis barrier disruption induced by $CdCl_2$ treatment is associated with an increase in TGF-β3 levels and a loss of occludin and ZO-1 from the Sertoli cell TJ (Lui *et al.* 2003b, Wong *et al.* 2004). These studies therefore provide further evidence of local cytokine regulation of the Sertoli cell TJ.

A recent study also implicated the role at the Sertoli cell TJ of a peptide called C-natriuretic peptide (CNP) which belongs to a family of 2 other peptides which regulate blood pressure and volume, fat metabolism and steroidogenesis in the testis (Lucas *et al.* 2000, Potter *et al.* 2006, Xia *et al.* 2007). Sertoli cells and germ cells both secrete CNP although the receptors for CNP have only been localised to the Sertoli cells and not the germ cells (Xia *et al.* 2007). Furthermore, CNP is secreted at stage VIII of the spermatogenic cycle in rats, which is when germ cells cross the BTB barrier (Xia *et al.* 2007). When administered to cultured rat Sertoli cells, CNP-22 synthetic peptide disrupted the localisation of JAM-A and occludin to the TJ *in vitro* and induced a transient increase of

CNP in the cells (Xia *et al.* 2007). When CNP was administered to rat testes via an intratesticular injection *in vivo*, the blood-testis barrier became permeable to low molecular weight protein FITC (389Da) (Xia *et al.* 2007) demonstrating that CNP regulates TJ function *in vivo*. Given that CNP is expressed maximally at the time of germ cell migration into the adluminal compartment of the seminiferous epithelium and that it has since been shown to regulate TJ protein localisation and function, there appears to be an important role for this peptide in regulating spermatogenesis.

The effects of other cytokines on the Sertoli cell TJ are largely unknown, but in the normal testis, anti-inflammatory cytokines such as macrophage migrating inhibitory factor, interferon-γ and pro-inflammatory cytokines such as TNF-α and interleukin-1 (IL-1)-α/β circulate (Gerprasert *et al.* 2002, Hedger, 2002, Hedger *et al.* 2005, O'Bryan *et al.* 2005). Bacterial lipopolysaccharide (LPS) treatment to the testis induces a pro-inflammatory response (Hedger *et al.* 2005) and recently it was shown that LPS disrupted the maturation of leptotene/zygotene spermatocytes which are the first germ cells adluminal to the blood-testis barrier (Liew *et al.* 2007). These germ cells and the more mature round spermatids were released prematurely from the testis within 6 days of LPS treatment which was associated with an increase in germ cell apoptosis (Liew *et al.* 2007). While the Liew *et al.* (2007) study did not analyse the effects of LPS on the Sertoli cell TJ or the blood-testis barrier, the results obtained for the adluminal germ cells suggest that they may have been exposed to the pro-inflammatory cytokines, which may have been mediated by changes in the TJ. The role of the pro-inflammatory cytokine TNF-α has already been discussed with respect to the Sertoli cell TJ in this section of the review, but interestingly, pro-inflammatory cytokines IL-1α and IL-6 have been shown to disrupt TJ function in thyrocytes and umbilical vein endothelial cells in other studies, suggesting that these cytokines might also effect the Sertoli cell TJ (Nilsson *et al.* 1998, Desai *et al.* 2002, Cheng and Mruk, 2004). Furthermore, anti-inflammatory cytokine interferon-γ has also been implicated in regulating TJs in cultured intestinal T84 cells, suggesting that it too may play a role in regulating the Sertoli cell TJ (Madara and Stafford, 1989, Youakim and Ahdieh, 1999, Cheng and Mruk, 2004).

This section of the literature review has revealed some of the important and necessary regulatory mechanisms of local paracrine factors in the testis on the Sertoli cell TJ. For a more global picture of cytokine regulation of the Sertoli cell TJ, much more work needs to be conducted on the extensive array of cytokines yet to be analysed in the testis, but which have shown propensities to

regulate TJs in other tissues. There appears to be co-operation between all of the TJ regulatory pathways so far reviewed from protein phosphorylation, to components of the extracellular matrix and now the paracrine system in maintaining Sertoli cell TJ dynamics. The fourth regulatory process which may also work in co-operation with these other pathways is the gonadotrophin-based endocrine system.

d. The endocrine system

Several lines of evidence suggest that gonadotrophins are involved in Sertoli cell TJ formation and regulation. The formation of inter-Sertoli cell TJs is delayed until the onset of puberty, during which time there is a rise in the levels of the gonadotrophins or hormones- luteinising hormone (LH) and FSH (Russell and Peterson, 1985). In the absence of these hormones, TJ formation is delayed or prevented (Bressler, 1976). In addition, inter-Sertoli cell TJs in hypogonadotrophic hypogonadal men display a prepubertal phenotype. These men have low levels of circulating gonadotrophins, and when these are given exogenously, the TJs change to display a mature phenotype both in morphological and functional terms (de Kretser and Burger, 1972). Gonadotrophin effects on TJ formation can also be observed in animals. The season in which animals breed may depend on the photoperiod length during that season (Bergmann, 1987). The Djungarian hamster is such an animal and during short photoperiods, circulating gonadotrophin levels are low, the testes are regressed, and seminiferous tubule lumens disappear. As a result of all this, spermatogenesis ceases and inter-Sertoli cell TJ proteins are redistributed into the Sertoli cell cytoplasm, rather than at the cell-cell contact points (Bergmann, 1987, Tarulli *et al.* 2006, Tarulli *et al.* 2008). The restoration of gonadotrophin levels during longer photoperiods correlates with the relocalisation of Sertoli cell TJ proteins to the TJ and reappearance of testicular lumens, restoration of the testicular function and spermatogenesis begins again (Tarulli *et al.* 2006, Tarulli *et al.* 2008, for a review, see Bergmann, (1987)).

As mentioned briefly in the above paragraph, fluctuations in circulating gonadotrophins also effects the state of seminiferous tubule lumens, the presence of which is indicative of a functional Sertoli cell TJ and the absence of which is indicative of a non-functional TJ (Pelletier, 1990). Interestingly in other seasonal breeders such as the duck, testicular regression includes only a partial closure of the tubule lumens, which becomes occupied by a lipid plug, and the TJ is still functional

(Pelletier, 1990). When disruption of the basement membrane was induced in guinea pigs by an antibody against laminin, a non-collagenous extracellular matrix component, spermatogenesis was disrupted, testes were regressed and the tubule lumens had closed partially over a lipid plug as seen in the duck (Lustig *et al.* 2000). The Sertoli cell TJ however was still functional, as shown by its continued ability to exclude HRP tracer (Figure 1.11) (Lustig *et al.* 2000). These studies suggest that the loss of TJ function, is associated only with a complete loss of tubule lumens.

Several *in vivo* and *in vitro* studies have demonstrated the regulatory role of androgens and FSH at the molecular level of Sertoli cell TJs. Testosterone and to a lesser extent, FSH, stimulated TJ formation as shown by an increase in TER *in vitro* (Janecki *et al.* 1991, Kaitu'u *et al.* 2007). Furthermore, the mRNA expression of claudin-11 and the localisation of claudin-11 and occludin to the TJ was seen to be regulated by testosterone as well (Kaitu'u *et al.* 2007). In cultured mouse Sertoli cells, FSH was actually seen to decrease claudin-11 mRNA expression (Hellani *et al.* 2000). In two separate *in vivo* studies, androgen antagonist flutamide was administered to rats and caused significant decreases in the mRNA expression of occludin and claudin-11 (Gye and Ohsako, 2003, Florin *et al.* 2005). Interestingly, the presence of androgen receptors on Sertoli cells is maximal at the stage of spermatogenesis when germ cells need to cross the Sertoli cell TJ (Russell, 1977, Bremner *et al.* 1994, Holdcraft and Braun, 2004, Meng *et al.* 2005), and therefore the results of the flutamide studies provide a direct link of androgen regulation of the Sertoli cell TJ. The role of androgens at the Sertoli cell TJ level was further demonstrated in the Sertoli cell specific androgen receptor knockout mouse model (Meng *et al.* 2005). This model showed a small decrease in claudin-11 mRNA expression (Tan *et al.* 2005) but a much larger decrease in claudin-3 mRNA expression, which was associated with a disruption of TJ function as shown by biotin penetration into the seminiferous epithelium (Meng *et al.* 2005). These results showed that androgens do not only regulate the expression and localisation of TJ proteins to the TJ, but also the function of the Sertoli cell TJ (Meng *et al.* 2005). In the seasonally regressed testes of the hamster mentioned above, circulating gonadotrophins are absent and the localisation of Sertoli cell TJ proteins claudin-11, claudin-3, occludin and JAM-A are disrupted *in vivo* (Tarulli *et al.* 2006, Tarulli *et al.* 2008). Furthermore, in control hamsters TJs were seen to be functional by their ability to exclude low molecular weight tracer biotin from entering the seminiferous epithelium, yet in the absence of circulating gonadotrophins, biotin readily permeated

Figure 1.11 Horse-radish peroxidase tracer penetration into the seminiferous epithelium.

Electron micrograph representation of TJ function following HRP perfusion into the testes of adult guinea pigs. HRP (dark line) readily permeated through the seminiferous tubule and surrounded the preleptotene spermatocyte (Pl). The tight junction was able to prevent the passage of HRP into the adluminal compartment (arrow head) as was seen by the lack of staining around the pachytene spermatocyte (P). Taken from Lustig *et al.* (2000)

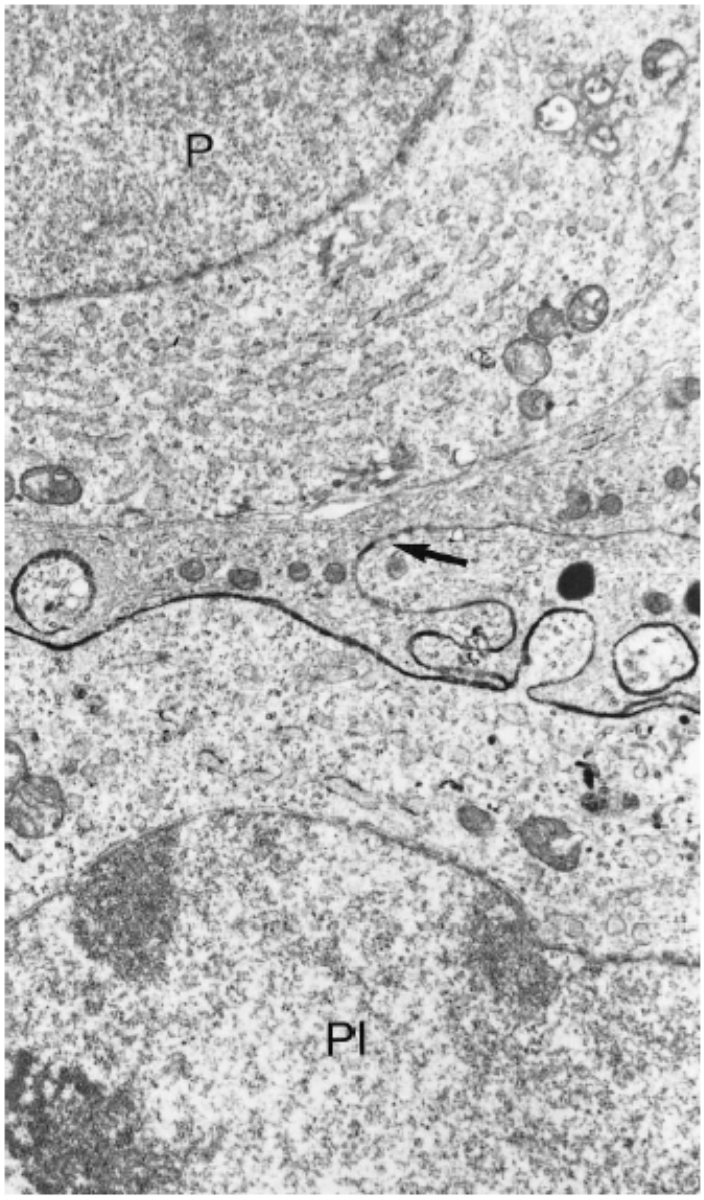
P
Adluminal
Basal
Pl

throughout the tubules indicating the disruption of TJ function *in vivo* (Tarulli *et al.* 2008). FSH replacement was seen to redistribute the TJ proteins back to the TJ and restore function as shown by biotin exclusion (Tarulli *et al.* 2008). It appears therefore, that both androgens and FSH regulate the Sertoli cell TJ according to the literature, and FSH has also been implicated in regulating CAR mRNA expression (Mirza *et al.* 2007). The hamster model is valuable at providing another perspective of gonadotrophin regulation of Sertoli cell TJs *in vivo*. The fact that TJ function and structure is disrupted following the loss of circulating gonadotrophins in this model, shows that gonadotrophins have an important role in the maintenance of the Sertoli cell TJ. When structure and function of the TJ is restored upon gonadotrophin replacement in these animals, results show that gonadotrophins also play a role in Sertoli cell TJ formation.

Therefore, gonadotrophins are essential for the structure and function of the Sertoli cell TJ both from a maintenance point of view, and a formation point of view. The variety of gonadotrophin suppression models used to study the Sertoli cell TJ provides an invaluable means of determining the importance of the Sertoli cell TJ to spermatogenesis and how it fits in with the global gonadotrophin regulation of spermatogenesis.

1.7 Gonadotrophin suppression models and their effects on spermatogenesis

Various animal models exist to study the effect of suppression of testosterone and/or FSH on spermatogenesis and potentially TJs *in vivo*. FSH and LH are released by the pituitary, with the latter gonadotrophin stimulating the release of testosterone from the testicular Leydig cells (Meachem *et al.* 1998). The release of FSH and LH are dependent upon stimulation by the decapeptide gonadotrophin releasing hormone (GnRH), which binds to its receptor on the pituitary after release from the hypothalamus (Herbst, 2003). Hormone suppression models which manipulate circulating hormones use methods such as hypophysectomy (Bartlett *et al.* 1989a, Bartlett *et al.* 1989b, Takase *et al.* 1990a, Takase *et al.* 1990b, Dombrowicz *et al.* 1992), GnRH signal inhibition with immunogens (Mclachlan et al. 1994b, Meachem *et al.* 1998, Pratis *et al.* 2003, Sluka *et al.* 2006, Ruwanpura *et al.* 2008) or antagonists (Hikim and Swerdloff, 1995, Jiang *et al.* 2001, Broqua *et al.* 2002, Herbst *et al.* 2002, Hild *et al.* 2004, Matthiesson et al. 2005b, Porter *et al.* 2006) and steroidal/hormonal negative feedback (Awoniyi *et al.* 1989, Mclachlan et al. 1994a, O'Donnell *et al.* 1994, O'Donnell *et al.* 1996a,

O'Donnell *et al.* 1996b, Meachem *et al.* 1998, Pratis *et al.* 2003). Alternatively, some models such as the hypogonadal (*hpg*) mouse (Charlton *et al.* 1983, Handelsman *et al.* 1999, Allan *et al.* 2001, Walker, 2003, Allan *et al.* 2004, Bruewer *et al.* 2005b, Myers *et al.* 2005), photoregulated Djungarian hamster (Tarulli *et al.* 2006, Tarulli *et al.* 2008) and other seasonal breeders (Pelletier, 1986, Pelletier, 1988, Pelletier, 1994) are naturally occurring hormone deficient models.

Each of these models can be grouped into the information they provide about hormonal regulation of spermatogenesis and therefore potentially the Sertoli cell TJ as well. In gonadotrophin suppression models (by hypophysectomy, GnRH immunisation/antagonism or steroidal negative feedback), normal circulating gonadotrophins exist in the animals prior to suppression (Bartlett *et al.* 1989a, Bartlett *et al.* 1989b, Hikim and Swerdloff, 1995, Meachem *et al.* 1998, Jiang *et al.* 2001). Therefore, these models are used for analysing the role of hormonal maintenance on spermatogenesis. In the *hpg* mouse, a naturally occurring deletion in the GnRH gene (see section 1.7.4) deprives the animal of circulating gonadotrophins and no spermatogenic activity (Ando *et al.* 1990, Singh *et al.* 1995, Ebling *et al.* 2000, Myers *et al.* 2005). Gonadotrophin treatment to these animals therefore allows the study of spermatogenesis from an initiation point of view, which may include the initiation of TJ formation. The seasonal breeders offer models which analyse spermatogenesis from both a maintenance and initiation point of view due to naturally occurring hormone suppression and restoration (Pelletier, 1986, Pelletier, 1988, Tarulli *et al.* 2006, Tarulli *et al.* 2008). This section of the review will focus on some of these models.

1.7.1 Hormone suppression by GnRH immunisation

Up until the early 1990s, there was a lack of suitable hormone suppression models, which could suppress testosterone and/or FSH, without affecting other hormonal systems (Mclachlan et al. 1994b). Hypophysectomy, which involves the surgical removal of the pituitary, not only suppresses testosterone and FSH, but also other pituitary hormones such as prolactin (Bartlett *et al.* 1989a, Bartlett *et al.* 1989b, Takase *et al.* 1990a, Takase *et al.* 1990b, Dombrowicz *et al.* 1992) and thyroid stimulating hormone (Ebling *et al.* 2000), both of which are also important for Sertoli cell function (Takase and Tsutsui, 1997). Hypophysectomised rats tend to be less healthy and underweight as well compared to intact rats (Awoniyi *et al.* 1992a, Awoniyi *et al.* 1992b). Hypophysectomy in rats, results

in significantly reduced numbers of pachytene spermatocytes and round and elongated spermatids (Bartlett *et al.* 1989a, Bartlett *et al.* 1989b). The subsequent administration of testosterone to these rats, showed that it could only maintain a reduced level of spermatogenesis compared to intact rats (Huang *et al.* 1987, Awoniyi *et al.* 1992a, Awoniyi *et al.* 1992b). Under the regulation of FSH alone, spermatogenesis stopped at the round spermatid level (Bartlett *et al.* 1989a, Bartlett *et al.* 1989b). The reasons for these spermatogenic defects however, were not necessarily due to the absence of the 'other' hormone in these experiments, but possibly due to the absence of other pituitary factors as well (Huang *et al.* 1987, Awoniyi *et al.* 1992a, Awoniyi *et al.* 1992b). This necessitated the advent of a model which would specifically suppress both testosterone and FSH, such that any observations made with respect to spermatogenesis, could be directly attributed to these hormones or their derivatives (Awoniyi *et al.* 1992a, Awoniyi *et al.* 1992b).

To suppress both LH and FSH, GnRH immunisation has been employed in the rat. This method works by stimulating the recipient animal to produce antibodies against its own GnRH (Mclachlan et al. 1994b). When administered every 4 weeks for 12 weeks to healthy male rats, a significant reduction in testis weights occurred with severe spermatogenic regression at all stages, with serum FSH, LH and testosterone reduced below assay sensitivity (Meachem *et al.* 1998, Pratis *et al.* 2003). It is possible to replace FSH alone in this model and study its effects on spermatogenic restoration in the short term (1-7 days) (Awoniyi *et al.* 1989), but when replacing testosterone alone, FSH levels return to near-normal levels via a GnRH independent mechanism (Mclachlan et al. 1994b). As a result, it is necessary to add an FSH antibody to suppress endogenous FSH production after the exogenous application of testosterone (Meachem *et al.* 1998, Pratis *et al.* 2003). Such FSH antibodies neutralise at least 90% of serum FSH without effecting serum testosterone (Meachem *et al.* 1998). The disadvantage of this model, is that to date, only recombinant human FSH (rhFSH) has been available for FSH replacement, and this stimulates rat antibodies against the rhFSH within 2 weeks (Meachem *et al.* 1998), thereby restricting FSH replacement times to short-term experiments of approximately 1 week (Meachem *et al.* 1998, Pratis *et al.* 2003). The same problem is applicable for the FSH antibody used to suppress endogenous FSH production in testosterone-alone replacement experiments (Meachem *et al.* 1998).

One recent study, did administer recombinant rat FSH (rrFSH) to GnRH immunised rats in the long-term (Ruwanpura *et al.* 2008). Decreases in testis weights in the Ruwanpura *et al.* (2008) study following GnRH immunisation were comparable to those recorded previously with the same treatment (Mclachlan et al. 1994b, Meachem *et al.* 1998, Pratis *et al.* 2003). There were no significant recoveries in testis weights or serum FSH following long-term rrFSH treatment, but significant recoveries in the early germ cell types through to the pachytene spermatocytes were obtained (Ruwanpura *et al.* 2008). While it was expected that long-term FSH treatment would lead to significant recoveries in testis weights and serum FSH, the failure to obtain such results could have been due to a suboptimal dose of the rrFSH (Ruwanpura *et al.* 2008).

There have not been many studies which have applied either this GnRH immunised model, or the similar GnRH-antagonised model (see section 1.7.2 below), to studying Sertoli cell TJs *in vivo*. However, a recent study looked at the effects of FSH and testosterone on the re-organisation of the adherens junction and ectoplasmic specialisation following GnRH immunisation (Sluka *et al.* 2006) by electron and confocal microscopy. In control animals, pan-cadherin stained extensively at the adherens junction and actin and espin both co-localised extensively at the ectoplasmic specialisation. Both junctions formed characteristic ‘scalloped’ appearances at cell contacts between Sertoli cells. Following GnRH immunisation, pan-cadherin re-localised to the Sertoli cell cytoplasm and was perpendicular to the basement membranes of the seminiferous tubules (Sluka *et al.* 2006). Actin and espin no longer co-localised at the ectoplasmic specialisation but were detected in the Sertoli cell cytoplasm also, with espin being perpendicular to the basement membranes of the seminiferous tubules like pan-cadherin (Sluka *et al.* 2006). The administration of FSH (but not testosterone) for 7 days to this model was sufficient to induce the re-establishment of the adherens junction and the ectoplasmic specialisation, with actin and espin re-colocalising at the latter (Sluka *et al.* 2006). As this model has therefore been successfully applied to the study of the adherens junctions and ectoplasmic specialisation, it may be presumed that such a model could be applied to studying the effects of hormone suppression and replacement on the nearby Sertoli cell TJ.

1.7.2 Hormone suppression by GnRH antagonism

The effect of GnRH antagonism is similar to GnRH immunisation in that LH/testosterone and FSH are suppressed to undetectable levels (Jiang *et al.* 2001, Broqua *et al.* 2002, Herbst *et al.* 2002, Hild *et al.* 2004, Matthiesson et al. 2005b, Porter *et al.* 2006) and germ cell numbers are significantly suppressed in the human (Herbst *et al.* 2002, Matthiesson et al. 2005b). Rather than stimulating an immune response against native GnRH like the immunogens, antagonists competitively bind to the GnRH receptor on the pituitary and block the GnRH signal for gonadotrophin release (for a review, see Herbst, (2003)). The GnRH antagonism model is preferred to GnRH agonism models, as these result in an initial gonadotrophin surge before suppression, and this may not be desirable (Herbst, 2003). However, GnRH agonist models do appear to be useful, after the GnRH agonist leuprolide acetate was shown to support the formation of mouse donor germ cell colonies and the area they occupied in recipient infertile tubules (Dobrinksi *et al.* 2001). Given the similarities with the GnRH immunised model, hormone replacement techniques in the GnRH antagonised model are much the same.

Thousands of GnRH antagonists exist (Herbst, 2003) and while most of the major antagonists all suppress LH/testosterone and FSH to the same extent as each other, it is the duration of efficacy, and the affinity for the stimulation of histamine inflammation after administration that differs among them (Jiang *et al.* 2001, Broqua *et al.* 2002). Most antagonists, such as Nal-Glu, Cetrorelix, Abarelix, and Ganirelix, suppress gonadotrophins for 1 day after single doses of 2mg/kg in adult male rats (Kangasniemi *et al.* 1995, Jiang *et al.* 2001, Broqua *et al.* 2002), whereas Azaline B and Acyline, suppress hormones from 1-2 weeks after a single dose of 2mg/kg (Jiang *et al.* 2001, Hild *et al.* 2004, Porter *et al.* 2006). All of these peptide antagonists are based on native GnRH (Herbst, 2003). A newer antagonist, Degarelix, has been shown to suppress hormones for approximately 6 weeks, before hormones slowly return to control levels over the ensuing 6 weeks, after a single 2mg/kg dose into adult male rats (Jiang *et al.* 2001, Herbst, 2003). Newer antagonists such as acyline and Degarelix, have greater hydrophilicity and solubility, a lower propensity to form gels in aqueous solutions, reduced affinities for histamine release and a greater number of hydrogen bonds available, all of which appear to increase affinity for the GnRH receptor (Beckers *et al.* 2001, Jiang *et al.* 2001, Broqua *et al.*

2002). The design of newer antagonists is essential for potential application in the treatment of cancers in the human and also in male contraceptive treatments (Herbst, 2003).

The GnRH antagonist induced suppression of circulating LH/testosterone and FSH also disrupts spermatogenesis. Hikim and Swerdloff (1995), showed that 4 weeks of Nal-Glu treatment, significantly suppressed preleptotene and pachytene spermatocytes to approximately 25% of control numbers. The elongated spermatids were only occassionally detectable and the numbers of the early type A and B spermatogonia did not change compared to control animals. FSH treatment partly restored pachytene spermatocyte and elongated spermatid numbers and also significantly increased the numbers of type B spermatogonia available to enter meiosis (Hikim and Swerdloff, 1995). Other studies looking at the effect of other GnRH antagonists on spermatogenesis are difficult to find as are studies looking at the effect of gonadotrophin (particularly androgen) replacement on spermatogenesis. As an exception, there are studies which have looked at the effect of GnRH antagonist treatment on irradiated testes which exhibit no spermatogenesis and abnormally high levels of LH/testosterone and FSH (Porter *et al.* 2006). After antagonist treatment, LH/testosterone and FSH levels return to normal and spermatogenesis resumes (Shetty and Meistrich, 2005, Porter *et al.* 2006).

Studies which have used GnRH antagonism to suppress hormones and spermatogenesis have not analysed the effects of suppression on the Sertoli cell TJ or other testicular junctions in general. Considering that GnRH antagonism appears to be very similar to GnRH immunisation in terms of hormone suppression, decreases in testis weights and spermatogenic disruption, it can be presumed that the GnRH-antagonist treated rat model is also an appropriate model for analysing changes in the Sertoli cell TJ following hormone suppression.

1.7.3 Hormone suppression by Testosterone/Estradiol administration

Testosterone/Estradiol (TE) treatment is a common, established method of LH/T suppression in male rats (Awoniyi *et al.* 1989, Mclachlan et al. 1994a, O'Donnell *et al.* 1994, O'Donnell *et al.* 1996a, O'Donnell *et al.* 1996b, Meachem *et al.* 1998, Pratis *et al.* 2003). Low doses of testosterone and estradiol are administered via subcutaneous silastic implants (3cm testosterone and 0.4cm estradiol) which act to slightly increase endogenous serum testosterone and estradiol levels. This suppresses LH secretion from the pituitary to undetectable levels via a negative feedback system,

while leaving serum FSH at normal or partially reduced (70% of control) levels (Mclachlan et al. 1994a, O'Donnell *et al.* 1994, O'Donnell *et al.* 1996a, O'Donnell *et al.* 1996b, Awoniyi *et al.* 1990). The reduced LH causes a reduction in intratesticular testosterone production to 3% of control levels (O'Donnell *et al.* 1994, O'Donnell *et al.* 1996a, O'Donnell *et al.* 1996b). Spermatogenesis is also suppressed following 8 weeks of TE treatment in rats and only proceeds to midspermatogenic germ cell types, with a complete block at the androgen-dependent step VII to step VIII round spermatid transition (Mclachlan et al. 1994a). The low dose of testosterone applied in this treatment can still support some spermatogenic activity, as application of the androgen receptor antagonist flutamide, resulted in a further decrease in germ cell types (Mclachlan et al. 1994a). Data collected from these models indicate that FSH alone is not sufficient to drive complete spermatogenesis (Mclachlan et al. 1994a) and that testosterone is required for the latter part of spermatogenesis, at least from the conversion of round spermatids to elongated spermatids (Mclachlan et al. 1994a). When the TE implants were replaced with high dose (24cm) testosterone implants, intratesticular testosterone levels were restored to 7-12% of control levels, serum testosterone to 20-30% of control levels and serum FSH to controls levels (Awoniyi *et al.* 1989, Mclachlan et al. 1994a, O'Donnell *et al.* 1994). After 2-4 days, high dose testosterone was sufficient to induce round spermatid maturation and restored elongated spermatid numbers to normal (Awoniyi *et al.* 1989, Awoniyi *et al.* 1990, Mclachlan et al. 1994a, O'Donnell *et al.* 1994). Hence this model is principally one of androgen suppression and replacement, with FSH remaining at near normal levels.

The effect of TE treatment on Sertoli cell TJs is unknown. However considering the points presented that FSH is not suppressed and that spermatogenesis proceeds as far as the round spermatid level, it can be assumed that the TJs are functional and as such this model does not appear to be appropriate for studying the role of hormone regulation on TJ function.

1.7.4 The hypogonadal mouse

The hypogonadal (*hpg*) mouse involves a naturally occurring major deletion of 2 of the 4 exons encoding the mouse GnRH gene, leaving it with infantile testes, undetectable FSH and < 10% of normal LH/testosterone levels (Cattanach *et al.* 1977, Charlton *et al.* 1983, Mason *et al.* 1986a, Huang *et al.* 1987, Allan *et al.* 2001). The reproductive tract however is functionally competent, in that

spermatogenesis and fertility can be initiated by transplantation of the GnRH gene (Mason *et al.* 1986b), multiple injections of GnRH (Charlton *et al.* 1983) or by the application of testosterone by silastic implants (Haywood *et al.* 2003, Walker, 2003). Estradiol administration unusually induced FSH production in the *hpg* mice and this was able to establish qualitatively normal spermatogenesis also (Ebling *et al.* 2000, Baines *et al.* 2005). Allan *et al.* (2001), produced a *hpg* mouse model which contained a transgene for the α and β subunits of human FSH. These mice were produced to study the effect of FSH alone on spermatogenesis in the mouse in the absence of LH (Allan *et al.* 2001, Haywood *et al.* 2003). These transgenic *hpg* mice, exhibited phenotypes indicative of FSH treatment such as increased testis weights compared to *hpg* mice, mature Sertoli cells, mature postmeiotic germ cells and significantly higher levels of Sertoli cell cAMP production.

Spermatogenesis in *hpg* mice produces spermatogonia and primary spermatocytes (preleptotene, leptotene and zygotene) at 11% and 2% respectively of wildtypes (Singh *et al.* 1995, Allan *et al.* 2004, Myers *et al.* 2005). FSH production in the *hpg* + tgFSH mice is sufficient to drive spermatogenesis to the round spermatid stage with the occasional appearance of early elongated spermatids (Allan *et al.* 2001, Allan *et al.* 2004). Androgen treatment alone to *hpg* mice initiates qualitatively normal spermatogenesis with fertile sperm, thereby displaying the requirement of androgens for complete spermatogenesis in the mouse. (Handelsman *et al.* 1999, Walker, 2003). The separate roles of FSH and androgens in regulating spermatogenesis in mice and rats are therefore conserved between the two species (Mclachlan et al. 1994a , Hikim and Swerdloff, 1995).

With respect to the Sertoli cell TJ, some electron microscopy work has been conducted in *hpg* mice to visualise its structure and showed that TJ strands were discontinuous and incomplete (Charlton *et al.* 1983, Myers *et al.* 2005). No TJ specific proteins have been targeted in this model but the nearby ectoplasmic specialisation displayed weak espin staining in the *hpg* mice compared to wildtypes (Myers *et al.* 2005).

The *hpg* mouse therefore provides a unique opportunity to study the initiation of spermatogenesis and the formation of the TJ, as opposed to the GnRH immunised/antagonised and TE models, where studies are restricted to the maintenance of spermatogenesis and the TJs.

1.7.5 Hormone suppression in men

Male hormonal contraception is based on the use of testosterone or synthetic androgens to suppress LH and FSH, but particularly intratesticular testosterone to suppress spermatogenesis, while maintaining adequate androgen action at other sites within the body (Matthiesson et al. 2005b). Studies have successfully suppressed intratesticular testosterone by 98% by combining exogenous testosterone with some other hormonal treatment regimen (Morse *et al.* 1973, McLachlan *et al.* 2002c, Coviello *et al.* 2004, Matthiesson et al. 2005b, Matthiesson et al. 2005a), but very few studies have looked at the direct effects on spermatogonia number and their relationship with intratesticular testosterone levels (Matthiesson et al. 2005b). Three types of hormones have been combined with testosterone for hormonal suppression. The first types are the progestins such as Depot Medroxyprogesterone Acetate (DMPA) or Levonorgestrel (LNG) (Matthiesson et al. 2005b, McLachlan *et al.* 2002c, Matthiesson et al. 2005a). Progestins help to increase the rate, but not depth of spermatogenic suppression, and may also have some direct effects upon the Sertoli cell after the mRNA for progestin receptors was found there (Ebling *et al.* 2000, Gadkar-Sable *et al.* 2005, Shah *et al.* 2005). The second type of hormonal treatment is the 5α-reductase inhibitor. O'Donnell *et al.* (O'Donnell *et al.* 1999), proposed a role for the potent androgen dihydrotestosterone (DHT), a derivative of testosterone, in restoring the maturation of round spermatids when intratesticular testosterone levels were exceedingly low. The enzyme which converts testosterone to DHT is 5α-reductase. When testosterone was administered to adult rats which had been hormonally suppressed with TE implants, spermatogenesis was restored, but the addition of a 5α-reductase inhibitor blocked the maturation of round spermatids into elongated spermatids (O'Donnell *et al.* 1999), suggesting a role for the enzyme in the amplification of residual androgen levels (O'Donnell *et al.* 1999). In men undergoing contraceptive treatment, some maintained a reduced level of sperm production despite suppressed LH and testosterone, and this may have been due to them converting testosterone through 5α-reductase to DHT (Anderson *et al.* 1996, Anderson *et al.* 1997). The 5α-reductase inhibitors dutasteride and finasteride have been used therefore to suppress this conversion of testosterone to DHT in recent papers (Matthiesson et al. 2005b). The third type of hormonal treatment with testosterone is GnRH antagonism, most recently with acyline and cetrorelix, the actions of which were described in section 1.7.2. Another GnRH antagonist, Teverelix, has also been used in rhesus

monkeys, but was shown to be slightly less efficient at suppressing FSH than most other antagonists (Erb *et al.* 2000).

Matthiesson *et al.* (2005a) showed that when combining testosterone with i) LNG, ii) acyline, iii) LNG + acyline, iv) dutasteride, all germ cell types from Type B spermatogonia up, were significantly suppressed. Despite a further suppression in intratesticular androgens with dutasteride, there was no difference between the extent of germ cell suppression between any of the groups (Matthiesson *et al.* 2005a). Interestingly, the extent of germ cell suppression did not correlate with intratesticular testosterone levels, with some heterogeneity in germ cell response to all of the treatments, suggesting intrinsic differences in susceptibility to gonadotrophin suppression between individual men (Matthiesson et al. 2005b). This therefore requires more study of human spermatogenesis and its regulation.

TJs in low levels of circulating gonadotrophins in men are permeable to the electron opaque tracer lanthanum and appear immature by electron microscopy (de Kretser and Burger, 1972). These phenotypes are restored upon the exogenous application of gonadotrophins (de Kretser and Burger, 1972), indicating potential regulation of TJ structure and function in men.

1.8 Knockdown of gene expression by RNA interference

The previous section of this literature review looked at some hormone suppressed animal models and their application for studying spermatogenesis and the hormonal regulation thereof. In the literature, some of these models have lightly touched on the Sertoli cell TJ or other junctional types in the testis, and as discussed, some appear to be suitable for studying the effect of gonadotrophin suppression on the Sertoli cell TJ in more depth. However studying the Sertoli cell TJ would not involve the study of hormonal regulation exclusively, but also involve studying the relative contribution of protein constituents to the Sertoli cell TJ. One way of conducting this type of study, would be by RNA interference.

Silencing of gene expression by RNA interference, involves the application of small interfering RNA (siRNA) strands to recipient cells, which eventually leads to the cleavage of a target mRNA strand. This method of gene silencing was only discovered in 1998 when double-stranded RNA (dsRNA) was injected into the nematode *Caenorhabditis elegans* leading to sequence-specific

gene silencing (Wang and Barr, 2005, Fire, 2007). Since this first example of gene silencing, siRNA has been successfully applied to block gene expression in plants, Drosophila, mouse oocytes and numerous other organisms (Baulcombe, 1999a, Baulcombe, 1999b, Svoboda *et al.* 2000). For a review, see Dykxhoorn and Lieberman (2005).

The RNA interference pathway (see Figure 1.12) is complex. Briefly, a long dsRNA strand is introduced into a cell where it is cleaved into small siRNA fragments by a Dicer complex, which is an RNase III family member (Dykxhoorn and Lieberman, 2005). These fragments are then unwound into single stranded antisense fragments by an RNA-inducing silencing complex (RISC). These single stranded fragments guide RISC to the target mRNA which is then cleaved, thereby silencing gene expression (Dykxhoorn and Lieberman, 2005). This entire process occurs within the cytoplasm (Hutvagner and Zamore, 2002a, Hutvagner and Zamore, 2002b, Zeng and Cullen, 2002, Kawasaki *et al.* 2003).

One problem with mammalian cells, is that any dsRNA strand of greater than 30 nucleotides appears to induce a sequence non-specific interferon response within the cell, which effectively results in the cleaving of mRNA and a global shutdown of mRNA translation (Stark *et al.* 1998, Elbashir *et al.* 2001a, Elbashir *et al.* 2001b, Elbashir *et al.* 2001c). Most studies involving gene expression knockdown in mammalian cells therefore appear to adopt siRNA fragments of no greater than 23 nucleotides in length (Stark *et al.* 1998, Elbashir *et al.* 2001a, Elbashir *et al.* 2001b, Elbashir *et al.* 2001c).

The potential importance of siRNA as a therapeutic agent has been demonstrated in an *in vivo* study using mice. Mice were injected intravenously with siRNA specific for *Fas*, a gene in the liver which promotes apoptosis (Kondo *et al.* 1997, Siegel and Fleisher *et al.* 1999). Mice injected with the siRNA, survived up to ten days while all control mice had died of liver failure and liver fibrosis within three days (Song *et al.* 2003).

A more recent study has successfully applied RNA interference during spermatogenesis in mice, *in vivo* (Shoji *et al.* 2005). A DNA vector based system was used to deliver siRNA (in this case termed short hairpin siRNA (shRNA)) into the testes of prepubertal mice by electroporation (Shi, 2003, Dorsett and Tuschl, 2004, Shoji *et al.* 2005). The siRNA was targeted against *Dmc1*, a gene which encodes a DNA recombinase and is functionally required in spermatocytes (Shoji *et al.* 2005).

Figure 1.12 The small interfering RNA mediated gene silencing pathway.

Small interfering RNA (siRNA) fragments are derived from longer double stranded DNA molecules which are cleaved into the smaller siRNA fragments by Dicer. These fragments then bind to RNA-inducing silencing complex (RISC), which unwinds the siRNA in an ATP dependent fashion. The now single stranded siRNA molecules guide the RISC complex to the target mRNA molecule and cleaves it in the cytoplasm, silencing its expression. Taken from Dykxhoorn and Lieberman (2005).

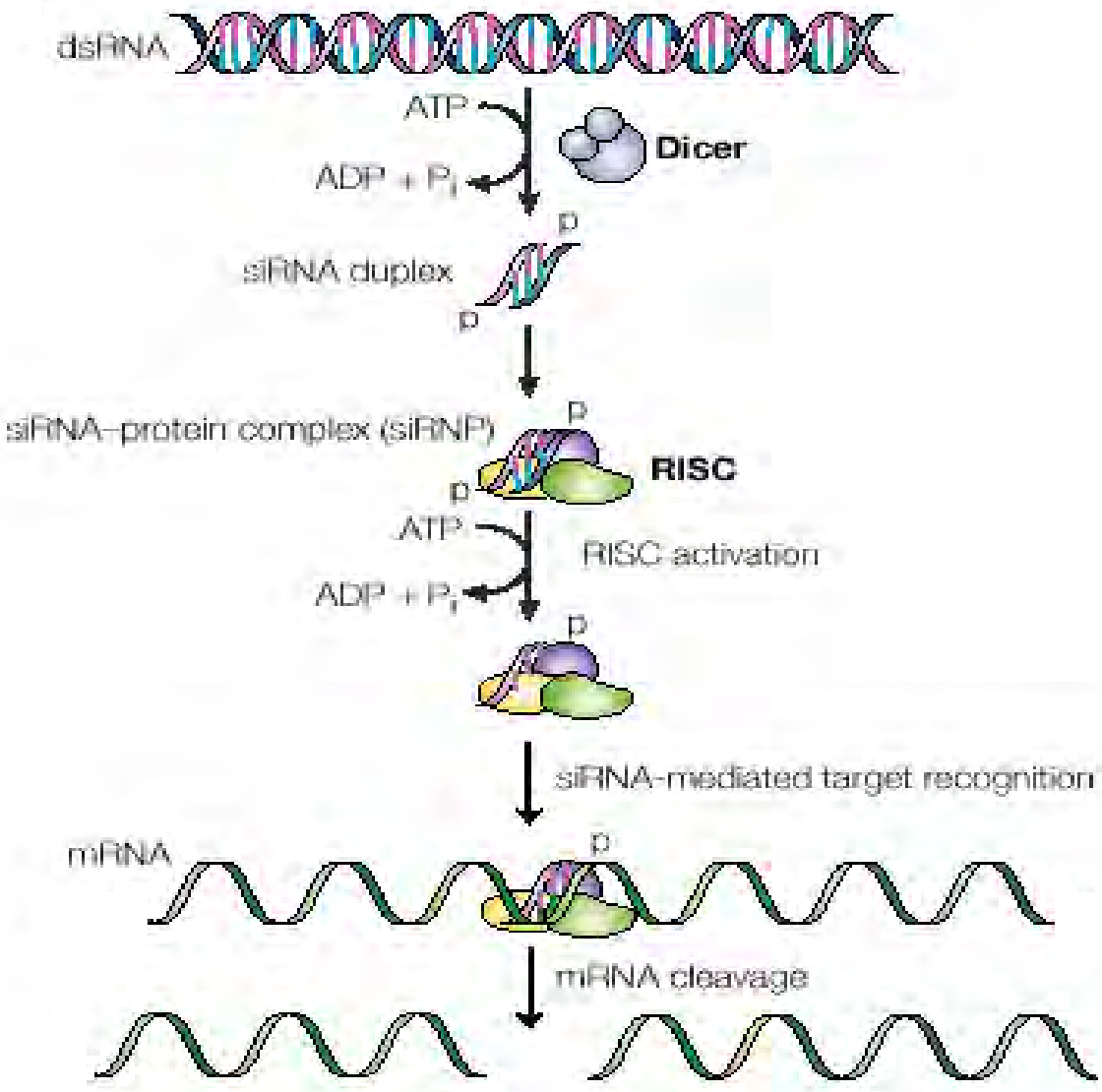
dsRNA
ATP
ADP + P_i
Dicer
siRNA duplex
p
siRNA–protein complex (siRNP)
RISC
RISC activation
siRNA-mediated target recognition
mRNA
mRNA cleavage

The silencing of the *Dmc1* gene, led to meiotic defects in the spermatocytes and this was a similar result to what has been observed in the *Dmc1* null mutant (Shoji *et al.* 2005). This indicates the necessity of Dmc1 in normal spermatogenesis. Other genes which have been silenced in the testis are hard to find, but another testicular gene which has been silenced *in vivo* is the androgen receptor (Compagno *et al.* 2007, Gonzalez-Herrera *et al.* 2006).

Prostate cancers are initially androgen regulated and their growth is inhibited by castration or androgen antagonists, but later on they become resistant to such treatments (Compagno *et al.* 2007). Compagno *et al.* (2007) administered androgen receptor-specific siRNA via an intraperitoneal (ip) injection into mice bearing castration-resistant prostate tumours. The androgen receptor was silenced in the prostate, testis and in the tumours, which inhibited their growth and inhibited angiogenesis, indicating that even after the prostate becomes castration-resistant, they are still androgen sensitive (Compagno *et al.* 2007). These results demonstrated a possible therapeutic role for siRNA.

A second study also silenced the androgen receptor in mice (Gonzalez-Herrera *et al.* 2006). Fibroblast growth factor 2 (FGF-2) is involved in testis development and maintenance, particularly with respect to gamete production and steroid synthesis (Gonzalez-Herrera *et al.* 2006). Its expression is controlled by an androgen regulated protein called IRES, which mediates translation (Gonzalez-Herrera *et al.* 2006). The silencing of the androgen receptor (70% efficiency) led to a decrease in the protein expression of FGF-2 (Compagno *et al.* 2007). This study did not look any further at the effects of the reduced protein expression of FGF-2 with respect to testicular maintenance, which would be an interesting area to follow up and therefore requires more work.

Importantly for this thesis and further research into the field, *in vivo* applications of siRNA mediated gene silencing can offer alternatives to gene knockout or mutation models when studying spermatogenesis and the TJs, and as mentioned previously, it also offers the possibility of studying the importance and contribution of specific protein components to the function of the TJ or other junctions during spermatogenesis, *in vivo*.

Interestingly, the use of siRNA technology appears to be versatile as it has been successfully applied *in vitro* as well. The importance of claudin-4 to the respiratory epithelium has been presented by an *in vitro* pharmaceutical company. Following claudin-4 siRNA treatment, TJ function was decreased by 75% compared to controls as measured by TER (Johnson and Quay, 2005). Furthermore,

application of the siRNA to the same cultured human respiratory cells, prevented TJ formation (Johnson and Quay, 2005). In a cultured human colorectal cancer cell-line, siRNA against claudin-4 increased the motility of invasive cancer cells (Ueda *et al.* 2007) *in vitro*. Conversely in a human ovarian cancer cell-line, siRNA targeted against claudin-3 and claudin-4 reduced the invasiveness and motility of the cancer lines, indicating potentially different roles for the same claudin protein (in this case claudin-4), in different epithelia (Agarwal *et al.* 2005). In recent years, the number of studies looking at the contribution of different claudins to the function of TJs in different cultured epithelial cells using siRNA technology has increased and has included analysis of claudins 1-4, 7 and claudin-12 (see Hou *et al.* (2006) and Fujita *et al.* (2008)). Studies looking at the contribution of occludin to TJ function have also increased although not to the same extent as for the claudins. The silencing of occludin in the retinal pigment epithelium resulted in an increase in TJ permeability to the small molecular weight tracer tetramethylrhodamine (467Da) (Phillips *et al.* 2008) *in vitro*. In cultured MDCK II cells, the silencing of occludin had diverse effects on the function of the TJ and also the cytoskeletons within the epithelial cells (Yu *et al.* 2005). Thus far, the contributions of claudin-11 or occludin to the Sertoli cell TJ have not been analysed.

The transmembrane proteins are not the only TJ proteins to have been studied. In cultured MDCK II cells, siRNA targeted against PALS1, a protein which interacts with ZO-1 of the cytoplasmic plaque and is important for cellular polarisation, also reduced TJ function as shown by TER *in vitro* (Straight *et al.* 2004).

The above studies show that siRNA is a useful technique for analysing the contribution of the key transmembrane proteins, claudin-11 and occludin to the Sertoli cell TJ *in vitro* and potentially *in vivo* as well.

1.9 Conclusion

This review has looked at spermatogenesis and the processes involved to produce mature, fertile sperm. While the length and types of spermatogenic cycles vary across species (Roosen-Runge, 1952, Clermont, 1963, França *et al.* 1998), the pivotal roles that Sertoli cells play in this process are conserved, in that in all species they mediate the provision of nutrients, hormonal signals and cell-cell interactions through junctional complexes, including the essential blood-testis barrier, the major

component of which is the Sertoli cell TJ (Griswold, 1998, Setchell, 2004). This review has covered work studying the proteins involved in TJ formation, regulation and function, as well as reviewing the necessity of TJs in the testis and their role in spermatogenesis. TJ strands are generally composed of two major proteins, occludin and claudin, with contributions from CAR and the junctional adhesion molecules (Bazzoni *et al.* 2000, Gonzalez-Mariscal *et al.* 2003, Mirza *et al.* 2007). These proteins interact with their counterparts on adjacent cells to effectively form a selectively permeable seal in epithelial cells. In forming this seal, compartments of distinct fluid and solute composition are formed (Mitic and Anderson, 1998, Cereijido and Anderson, 2001, Cheng and Mruk, 2002). In observations using freeze fracture electron microscopy, TJs appear as fibrils wrapping around the periphery of cells (Cereijido and Anderson, 2001, Gonzalez-Mariscal *et al.* 2003). Recently, it was determined that these fibrils are proteinaceous and these proteins (occludin and claudin) are linked to the cytoskeleton via the cytoplasmic plaque, a protein complex residing beneath the TJ membrane proteins (Itoh *et al.* 1999, Lapierre, 2000, Gonzalez-Mariscal *et al.* 2003). Progress in understanding the testicular TJ has been made over the past two decades, however some areas still need to be researched further. The dilemma of how occludin localises to the TJ either via its C-terminal or its extracellular and/or transmembrane domains continues to be the subject of much debate. Several discrepancies also lie among separate findings in determining the regulatory role that kinases and phosphatases have on TJ formation. The finding that heavily phosphorylated occludin proteins are integrated into TJ fibrils which still have high paracellular flux, can possibly be explained by the inability of the C-terminal to interact with ZO-1 due to its phosphorylation state (Kale *et al.* 2003). Further research needs to look at the location of phosphorylation residues on occludin and determine if they are actually located on the C-terminal. The role of phosphorylation with respect to the claudins and ZO-1/ZO-2 is also an area which requires further research.

Tracers have been used by many researchers since the late 1960s to analyse the function of the TJ both quantitatively and qualitatively *in vivo* and *in vitro*. Not only have these tracers demonstrated the loss of the function of a TJ by breaching the epithelium they protect, they have also displayed the size-selective nature of TJs and the roles specific proteins have in maintaining size-selectivity and thereby function. Some of the more interesting results have demonstrated that a TJ does not need to be completely ‘functional’ to complete its protective role, as was demonstrated in the claudin-5 knockout

mice (Nitta *et al.* 2003), where despite small molecular weight (443Da) tracers being able to cross the blood-brain barrier into the brain parenchyma, the mice were healthy and suffered no oedemas or bleeding. In the testis, spermatogenesis proceeded after TJs formed at day 15 in the rat, but a [^{51}Cr]-EDTA tracer was still able to cross the blood-testis barrier up until 10 days later (Setchell *et al.* 1981, Setchell *et al.* 1988), indicating that the Sertoli cell TJ did not need to be fully functional for spermatogenesis to commence either. These data have demonstrated that the function of the TJ does not work like an on/off switch, but there are shades of gray where TJ function can be reduced but TJ integrity is not altogether disrupted, and this suggests that considerable work needs to be done to understand the TJ.

In the seminiferous tubules of the testis, TJs need to be constantly disassembled and reassembled to allow passage of early germ cells through to the protected adluminal compartment while maintaining blood-testis barrier integrity, thus providing a good model for studying the regulation of the TJ (Setchell, 1967, Zhou *et al.* 2002). It has been shown that a rise in gonadotrophin levels at puberty correlates with the formation of the inter-Sertoli cell TJ, which does not form beforehand (Russell and Peterson, 1985). Furthermore, androgens and FSH stimulate the expression and localisation of claudin-11 and localisation of occludin to the Sertoli cell TJ (Janecki *et al.* 1991, Florin *et al.* 2005, Meng *et al.* 2005, Tarulli *et al.* 2006, Kaitu'u *et al.* 2007, Tarulli *et al.* 2008). Several hormone suppression models which have successfully enabled the study of the contributions of testosterone and FSH alone or in combination with each other to spermatogenesis, have been presented in this review (Charlton *et al.* 1983, Mclachlan et al. 1994b, Mclachlan et al. 1994a, O'Donnell *et al.* 1994, Hikim and Swerdloff, 1995, O'Donnell *et al.* 1996a, O'Donnell *et al.* 1996b, Meachem *et al.* 1998, Handelsman *et al.* 1999, Allan *et al.* 2001, Jiang *et al.* 2001, Broqua *et al.* 2002, Herbst *et al.* 2002, Pratis *et al.* 2003, Allan *et al.* 2004, Hild *et al.* 2004, Matthiesson et al. 2005b, Porter *et al.* 2006, Sluka *et al.* 2006, Ruwanpura *et al.* 2008). While not a lot of these models have been used to analyse the role of TJs specifically in spermatogenesis, the fact that they suppress FSH and testosterone, and that both of these hormones regulate Sertoli cell TJ proteins makes them potentially suitable models to apply to the study of Sertoli cell TJs.

This review has also briefly looked at a gene silencing technique, RNA interference, which involves the use of small interfering RNA fragments to cleave specific mRNA strands in the

cytoplasm (327). While it has been highly effective in silencing gene expression *in vitro*, more recently, it has been successfully applied to silence the expression of genes important for spermatogenesis *in vivo* (Shoji *et al.* 2005). The implications of this work are that researchers have an alternative to gene knockout and mutation models, but more importantly to this thesis and this field, one can possibly ascertain the importance and contribution of specific TJ proteins to the function of the TJ and therefore spermatogenesis, and then apply this technique more broadly to other junctions *in vivo.*

1.10 Hypothesis and aims

It is hypothesised that the function of the Sertoli cell TJ in the adult testis is regulated by gonadotrophins and that the TJ proteins claudin-11 and occludin are the major proteins regulated by gonadotrophins *in vivo.* Furthermore it is hypothesised that gonadotrophin suppression in men, as a consequence of male hormonal contraception, alters the Sertoli cell TJ.

To address these hypotheses, the following specific aims are presented:

i) To assess the relative contribution of claudin-11 and occludin to Sertoli cell TJ function by employing siRNA methodology to selectively ablate these proteins. The experiments to support this aim form Chapter 3 of this thesis.

ii) To determine the extent to which hormone suppression and replacement in the rat *in vivo,* alters TJ function and TJ protein expression. The experiments to support this aim form Chapter 5 of this thesis.

iii) To examine the effect of the FSH transgene in *hpg* mice as well as androgen DHT administration to *hpg* and *hpg* + tgFSH mice on the initiation of a functionally and structurally competent TJ. This study will also examine the development of the TJ in pubertal wildtype, *hpg* and *hpg* + tgFSH mice into adulthood. The experiments to support this aim form Chapter 6 of this thesis.

iv) To determine the extent to which hormone suppression alters TJ protein localisation and expression in men given male hormonal contraceptive. The experiments to support this aim for Chapter 7 of this thesis.

Chapter Two: Materials and Methods

Chapter 2. Materials and Methods

This Chapter presents the materials and methods used throughout this thesis. In some cases, specific materials and methods were applied to, or optimised for specific Chapters, and details for those can be found within the relevant Chapters.

2.1 Animals

For animal specifics please see relevant Chapters. All animal work conducted within this thesis was approved by the appropriate animal ethics committees. Animals were only used when necessary and were killed humanely at the end of experimentation. Where whole animals or animal parts were not required for this thesis, they were made available to other researchers. Rat work (Chapters 3-5) was conducted under animal ethics numbers MMCB 2002/04, 2002/38 and 2006/19, through Monash Animal Services, Monash University, Clayton, VIC, Australia.

Mouse work at the Anzac Research Institute in Concord, NSW, Australia (Chapter 6) was approved by the University of Sydney and Central Area Health Services Animal ethics committee.

Testicular tissues used in the human study (Chapter 7) came from men who had given prior written consent to experimentation and testicular biopsies. All such work had been approved by the University of Washington, USA.

2.2 Immunohistochemistry

This section is relevant for Chapters 4-7. Immunocytochemistry was used in Chapter 3 for cultured cells and the protocol used for that process can be found in that Chapter.

a. Fixed tissue

The specific fixation methods for each study in preparation for immunohistochemistry can be found in the upcoming Chapters. This section details the procedures performed on all tissue after fixation in Chapters 4-7.

Tissue was dehydrated by gradual ethanol incubations (70%, 2hours, 90%, 2 hours, 100%, 3 x 2 hours) and cleared in histolene (2 x 2 hours) before paraffin wax embedding (2 x 2 hours). Tissues were then mounted on plastic blocks.

Sections were cut to 5μm using a microtome (Leica, Cat # RM 2155) and adhered onto Superfrost-Plus slides (HD Scientific, Melbourne, Australia) before being incubated overnight at 37^{o}C to dry.

Sections were de-waxed in two histolene washes (5 minutes each), and then rehydrated in gradual ethanol incubations (100%, 8 minutes, air-dried 8 minutes, 90%, 8 minutes, 70%, 8 minutes). This was followed by a 5 minute wash in phosphate-buffered saline (PBS, pH 7.4). Antigen retrieval was performed by heating the sections for 10 minutes in 600ml of 1mM EDTA-NaOH (pH 8.0) (Pileri *et al.* 1997) in an 800W microwave. Sections were then allowed to cool in the EDTA-NaOH solution for an hour before being washed for 5 minutes in MilliQ water. Primary antibodies and negative controls were then applied to the sections (at the same concentration as each other) for the appropriate length of time (see details in relevant Chapters for incubation times for all primary and secondary antibodies used in this thesis) in combination with 10% of the normal serum from the species that the secondary antibody was raised in. Sections were then washed in PBS and the secondary antibodies were applied before another wash in PBS. Sections were then subjected to a fluorescent or one of two light microscopy protocols.

For fluorescent microscopy, sections were co-stained after the secondary antibody incubation with the fluorescent nuclear counterstains, DAPI (100nM in PBS/bSA) and TO-PRO-3 (1:100 in DAPI/PBS/bSA, Molecular Probes, Eugene, OR, USA) for 5 minutes before being washed twice in PBS and then mounted in FluorSave (Calbiochem, La Jolla, CA) under 22mm x 50mm coverslips (HD Scientific, Melbourne, Australia). Sections were visualised using a confocal microscope (Fluoview, FV300, Olympus Australia, Mt Waverley, VIC, Australia) or a fluorescent microscope (Olympus, BX-50). Three filter cubes were used on the fluorescence microscope which used a mercury burner light source: i) U-MWG, BP510-550nm (excitation wavelength range), DM570, BA590 (suitable for TRITC and ALEXA-546); ii) U-MWU, BP330-385nm (excitation wavelength range), DM400, BA420, (suitable for DAPI); iii) U-MWB, BP450-480nm (excitation wavelength range), DM500, BA515 (suitable for ALEXA-488 and FITC). The confocal microscope uses the same burner/cube set up for visualising the slides, however for capturing images, laser lines of single wavelengths were used (thus no need for excitation filters) and these were 488nm (green) and 568nm (red). An

ultraviolet (UV) laser line was not available on the confocal microscope, hence the use of TO-PRO-3 which fluoresces at 568nm.

Two protocols were used at different stages for light microscopy in this thesis. Prior to the primary antibody incubations, endogenous peroxidases were inactivated with 3% H_2O_2 (Chemical Ajax, cat # 260) for 30 minutes, and then non-specific binding sites in the tissue were blocked with CAS block (Zymed, San Francisco, CA, USA) containing 10% of normal serum from the animal in which the secondary antibody was raised for a further 20 minutes. Primary and then secondary antibodies were then applied for the appropriate length of time, and it was from after this step that the two detection protocols diverged.

The first protocol used DAB (DAKO, cat # K3466), which acts as a substrate to the HRP conjugated secondary antibodies. Its cleavage produces a brown precipitate which can be visualised by microscopy. The reaction occurs gradually, and so once the positive signal is clear enough, the reaction is stopped by briefly placing the slides into MilliQ water, so as not to enhance any background signal. Sections were then incubated for 30 seconds in hematoxylin (Sigma, St Louis, MO, USA) to highlight cell nuclei, chromatin and ribosomal structures and then rinsed with MilliQ water. Scott's tap water (Sigma, cat # S5134) was then added for a further 30 seconds to enhance hematoxylin staining before a final rinse in MilliQ water. Sections were then dehydrated in 2 x 100% ethanol incubations (30 seconds each), 1 x 70% ethanol incubation (30 seconds), 2 x histolene incubations (5 minutes each). Afterwards the sections were mounted in DPX-resin (BDH, cat # 36029) and visualised and photographed under the fluorescent microscope (Olympus, BX-50) using a FujixHC-2000 high-resolution digital camera (Fujifilm, Tokyo, Japan). The second protocol used a Vecta/VIP (Vector Laboratories, CA, USA) system. Solution ABC (Elite, cat # DK-6100) was prepared by adding 20µl of reagent A to 1ml of PBS, followed by the addition of 20µl of reagent B. The solution was then left at room temperature for 30 minutes before being applied to the sections for 1 hour. Sections were then washed twice in PBS and then incubated in Vecta/VIP (prepared by adding 1 drop of each of four reagents to 1.67ml of PBS and mixing between each addition) for approximately 1 minute, or long enough to allow a clear positive pink signal become apparent under the microscope without letting the background appear. The sections were then washed in MilliQ water to stop the Vecta/VIP reaction. The sections were incubated in hematoxylin for 6 minutes, rinsed in

MilliQ water, incubated in Scott's tap water for 1 minute and then rinsed a final time in MilliQ water. Dehydration and mounting of the tissue was conducted as per the DAB protocol above.

b. Frozen tissue

Frozen testes, microtome blades, slides and forceps were taken to a cryostat (Lecia, cat # CM 1850) and allowed to equilibrate to its conditions (-20^{o}C) for 30 minutes. Testes were then mounted in OCT resin (Optimal Cutting Temp Compound, Sakura, cat # 4583.118), and sectioned at 10μm with a microtome blade inside the cryostat at -20^{o}C. The sections were then placed onto a slide, and a finger placed underneath the slide to warm it up just enough to allow the section to melt onto the slide. The slide was then re-frozen and fixed in 100% acetone for 10 minutes within the crytostat. Alternatively, the slide was stored at -80^{o}C prior to fixation for later use. The fixed sections were allowed to air dry overnight at room temperature, and prior to immunohistochemistry were rehydrated in 2 x 5 minute washes of PBS. Slides were then blocked and followed the remainder of the above protocol for fixed tissue from the primary antibody incubation on.

2.3 Real-time reverse transcriptase-polymerase chain reaction (RT-PCR) analysis

2.3.1 Total RNA extraction and isolation

The following protocol was applied to each Chapter except all bar one of the human testis samples in Chapter 7, where mRNA was already available. mRNA from Chapter 7 underwent further preparation prior to the quantification protocol mentioned in Section 2.3.3. For details see Chapter 7.

Total RNA was extracted from cultured cells or whole testis tissue using the Qiagen RNeasy total RNA Isolation Kit (Qiagen: Hildens, Germany) according to the manufacturer's directions. Total RNA extraction involved lysing tissue and cells with Buffer RLT/1% β-mercaptoethanol (2-Mercaptoethanol; BioRad Laboratories, CA, USA). Homogenisation was then conducted, which for tissue involved repeated passes through syringe needles of decreasing thickness, starting with a 19G needle, 21G needle, then a 25G needle. For cultured cells, homogenisation was conducted by mashing them with the plunger of a 1ml syringe while still in the culture wells, and then passing them through a pipette tip 5 times. One volume of 70% ethanol was then added to each solution and then mixed. Each

solution was then transferred to an RNeasy column stored in a 2ml collection tube. The column was centrifuged for 15 seconds at 10,000rpm (Microfuge) and the flow through discarded. For cultured cells, this procedure was repeated until each well of a particular treatment group was pooled into one RNeasy column. Buffer RW1 was then applied to wash the columns, and after further centrifugation at 10,000rpm (Microfuge) for 15 seconds, the flow through was discarded. 500µl of Buffer RPE (volume of ethanol was added to the buffer beforehand according to manufacturer's instructions) was then added to the RNeasy column and centrifuged for 2 minutes at 10,000rpm. Another 500µl volume of Buffer RPE was added to the columns and centrifuged for a further minute. The columns were then transferred to a 1.5ml collection tube. RNA was eluted from the columns by adding 30µl of RNase-free water followed by a 1 minute centrifugation period at 10,000rpm. This last step was repeated again to have a final volume of 60µl, because a yield of greater than 30µg of total RNA was expected (manufacturer's recommendations). The total RNA extracts were snap frozen and stored at -80^{o}C.

2.3.2 DNase-free treatment

Any contaminating DNA was removed from the total RNA extracts via the use of a DNA-free kit (Ambion, cat# 1906) according to manufacturer's directions. 6µl of 10x DNase 1 Buffer and 1µl of DNase 1 (2 units) were mixed into the RNA samples, which were then incubated for 20-30 minutes at 37^{o}C. Any condensation was removed by a quick centrifugation. DNase Inactivation reagent was resuspended before adding 6.7µl of it to the RNA samples. The samples were then incubated for 2 minutes at room temperature with occasional flicking of the tubes to disperse the DNase Inactivation reagent. Following this, the tubes were centrifuged for 1 minute to pellet the inactivation reagent and then stored as above.

2.3.3 Total RNA quantification

a. Ultraviolet spectrophotometry

RNA samples were diluted 1:20 in MilliQ water, with the remainder of the sample being snap frozen and stored at -80^{o}C. 100µl of these dilutions were added into a plastic cuvette and read on an

ultraviolet spectrophotometer (BioPhotometer, Eppendorf) with OD set to 260/280nm. An OD reading of >1.82 was considered to indicate a pure sample of total RNA. Absorbance readings were taken as a means of quantitating the amount of RNA in a sample.

b. RiboGreen Assay

This assay for total RNA quantification was used in Chapter 3 only, as an addition to ultraviolet spectrophotometry RNA quantification. This assay employs a RiboGreen Quantification Reagent kit (Molecular Probes, Oregon, USA), a method which uses a fluorescent dye to bind to the RNA. A 96 well plate (Nunc Maxicorp, Denmark) was used for each assay, with each well accommodating 100µl of solution. A standard curve was constructed with amounts of RNA ranging between 0-80ng/well. The standards were constructed using Molecular Probes rRNA, whereby a stock solution of 100µg/ml was diluted 1:125 in 1 x TE Buffer (diluted 1:20 from stock; 200mM Tris, 20mM EDTA buffer, pH 7.5) to achieve a solution of 800ng (RNA)/ml, or 80ng/100µl. This solution underwent a series of double dilutions to obtain standards of concentrations; 40, 20, 10, 5 and 2.5ng/100µl. To ensure RNA samples were diluted so as to fit the standard curve, calculations were conducted based upon ultraviolet spectrophotometry results. A strong significant correlation between RiboGreen Assay and ultraviolet spectrophotometry had been determined previously but due to its extra sensitivity, the results obtained from RiboGreen were used for further analysis (Sluka *et al.* 2002). Furthermore, quality controls of known RNA concentration were diluted 1:1000 and 1:2000 for the RiboGreen assay to check for consistency and reproducibility between assays. Following the addition of 100µl of each sample into the appropriate wells, 100µl of RiboGreen (diluted 1:500 in 1x TE Buffer) was added to each well. Plates were then agitated on a plate shaker for 5 minutes, at maximum speed. RNA was quantified by the use of a Victor 1420 multilabel counter (Perkin Elmer, Life Sciences).

2.3.4 Reverse transcription

The required volume of total RNA extracts to reverse transcribe into cDNA was 5.2µl, and in this volume 125ng-1000ng of RNA was needed. To achieve this, calculations were conducted based upon the amount of DNA in the extracts as determined by UV spectrophotometry (or RiboGreen

Assay for Chapter 3). Once determined, the appropriate amount of sample was removed from the total RNA extracts and made up to 5.2µl with DEPC-H_2O (DEPC- diethylpyrocarbonate, inactivates RNase). The remainder of the total RNA was snap frozen and stored at -80^oC. To each 5.2µl sample, 14.8µl of master mix was added. The master mix was composed of 4µl of 5x RT Buffer (Roche, Germany), 8µl of deoxynucleoside triphosphates (dNTPS; dATP, dCTP, dTTP, dGTP; diluted 1:40 in DEPC-H_2O from a 100mM stock to 2.5mM), 2µl of random hexamers [pd(N)6], 0.5µl AMV-RT (reverse-transcriptase) (25U/µl) and 0.3µl of RNasin (40U/µl). Samples were spun briefly and then incubated for 1.5 hours at 46^oC. Afterwards, samples were boiled for 2 minutes and then snap frozen and stored at -20^oC or -80^oC.

2.3.5 Real-time RT-PCR

a. The LightCycler system

The LightCycler (Roche, Germany) system provides convenient monitoring of PCR samples in real-time and so was used in preference to conventional PCR. The melting temperature of DNA is dependent on its GC content and so each PCR product has a unique melting temperature. This melting temperature is a good way of identifying the product (see Figure 2.1) and this is a feature of the LightCycler system. The LightCycler works by detecting a fluorescent dye which is added to each PCR sample and binds to DNA. The amount of DNA in each sample can therefore be quantified in comparison to standards which contain a known amount of DNA. The LightCycler system allows for calculating the starting amount of DNA in a sample by the use of a ‘crossing-point’ calculation. The crossing-point equals the number of PCR cycles it takes for the fluorescence of a sample to increase in a log linear fashion. The crossing points of each unknown DNA can be compared to a standard curve which enables the calculation of the starting concentration of DNA in each sample. For each study, a testicular cDNA standard from untreated animals was prepared and assigned arbitrary unitage (rats, mice, humans). Each primer set was amplified in conjunction with at least 3 doses of this standard, with two-fold differences between each dose, and the top dose typically assigned an arbitrary unitage of 100. Hence the resultant standard curve was linear over an 8-fold range. For real-time PCR, the

Figure 2.1 LightCycler assessment of real-time polymerase chain reaction (RT-PCR).

The LightCycler provides convenient monitoring of PCR samples in real time and has several useful features. The melting curve (panel A) is a good way to identify a particular product, since each product has a characteristic melting curve, seen here at 91^{o}C. The peak at 81^{o}C corresponds to primer dimerization. Multiple peaks, or broad single peaks can indicate a non-specific DNA product being amplified and so the solutions which were subjected to the PCR analysis can then be run on agarose gels to check.

The LightCycler system works by detecting a DNA-binding fluorescent dye that is added to the PCR samples. By the use of a crossing point calculation (panel B), the LightCycler can determine the amount of DNA starting material in each of the samples. The crossing point calculation equals the number of PCR cycles it takes for the fluorescence of a sample to increase in a log linear fashion. The values obtained for this calculation are then fitted to a standard curve (panel C) from which the starting concentrations of DNA in each sample are obtained.

A

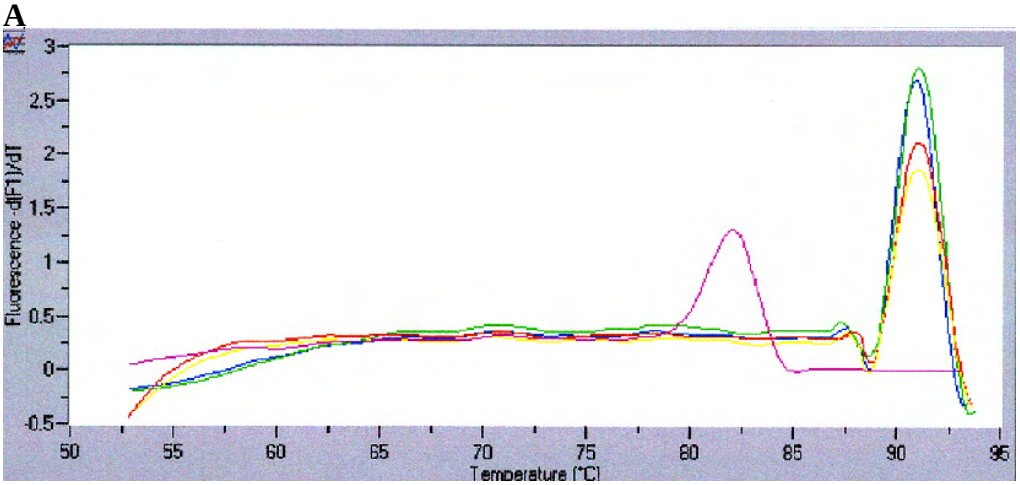
Fluorescence -d(F1)/dT
Temperature (°C)

B

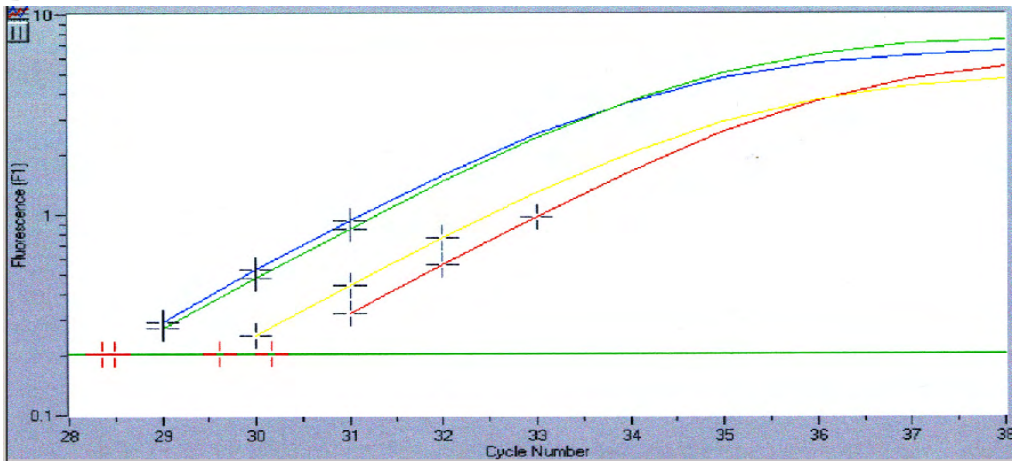
Fluorescence (F1)
Cycle Number

C

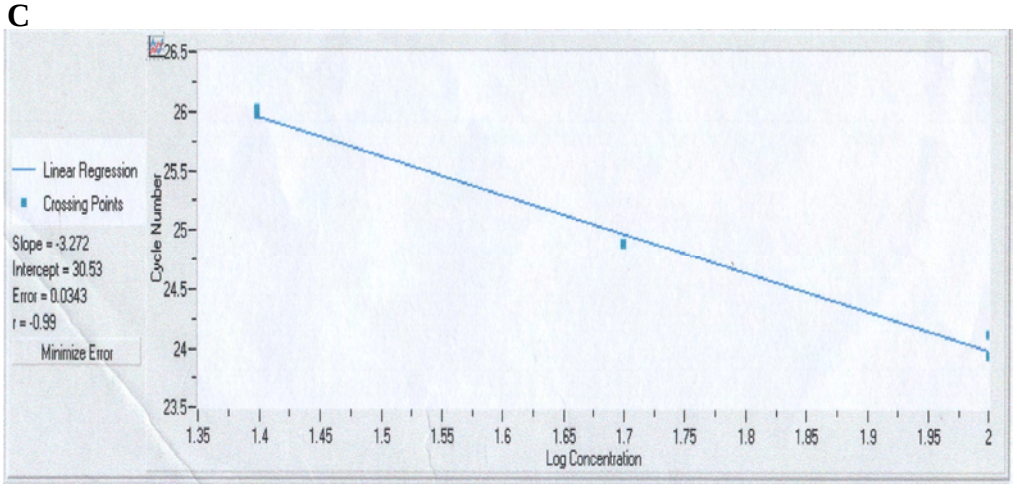
Linear Regression
Crossing Points
Slope = -3.272
Intercept = 30.53
Error = 0.0343
r = -0.99
Minimize Error
Cycle Number
Log Concentration

concentration of the standard was adjusted so that quantification occurred between cycles 25-30. As each primer set was quantified individually against the standard, differences in amplification efficiency were not an issue.

A separate quality control was included in each run in triplicate, and analysed separately. Within assay variation was typically 7% (n = 3), while between assay variation varied from 3%-13% (n = 3-4) depending on the primer set.

b. Primer optimisation

Oligonucleotide primers were designed using the Primer3 program online (http://frodo.wi.mit.edu/primer3/input.htm) or obtained from published sources (for details see Tables in relevant Chapters). Mg^{2+} concentration and annealing temperatures were all optimised on the LightCycler, and primers which produced a single product band on a DNA agarose gel, were processed for DNA Sequencing (see Section 2.4).

c. Sample preparation for RT-PCR

All cDNA samples were diluted in DEPC-H_2O. A master mix was prepared by using the FastStart DNA Master SYBR-green 1 system (Roche Diagnostics, Mannheim, Germany). The master mix for each reaction contained the appropriate concentration of $MgCl_2$, 1µl primer mix (equal volumes of forward and reverse primers had been mixed prior to addition to master mix), 1µl of FastStart SYBR green (FastStart solution contained Taq DNA polymerase, reaction buffer, dNTP mix, SYBR green I dye, 10mM $MgCl_2$), and made up to 9µl final volume with DEPC-H_2O. FastStart SYBR green was supplied in two vials; 1a and 1b, with 1b being kept in the dark at all times. To activate the FastStart SYBR green solution, 10µl of vial 1a was added to vial 1b. The remainder of the solution that was not used in the experiment was stored in the dark, at 4^oC for up to 7 days. The master mix was flicked and then spun down before being added to capillaries in a cold block (9µl per capillary). 1µl of each cDNA sample was added to the capillaries and these were capped. They were then centrifuged and loaded into a carousel and the LightCycler was activated. Cycle details for each primer set are also supplied in each relevant Chapter.

2.4 DNA sequencing

2.4.1 DNA agarose gel

Following each primer optimisation experiment, RT-PCR products were run on a DNA Agarose gel to determine if a single band, indicating a single product, was produced. The gel was prepared by dissolving 4.0g of agarose (Invitrogen, cat # 15510-027) in 200ml of TBE buffer (54g Tris-base (Sigma, cat # T-1503), 27.5g Boric Acid (BHT, Kilsyth, Victoria, Australia), 3.74g EDTA disodium salt (Merck), 1L MilliQ water) in an 800W microwave for 2 minutes. 12µl of 10mg/ml ethidium bromide (Sigma, cat # E-8751) was added to the boiling solution, mixed and then quickly poured into a sealed cassette, and a 20 lane comb was immediately inserted. The gel was then allowed to set at room temperature, for 30 minutes.

The preparation of the samples, involved centrifuging the RT-PCR capillaries into 1.5ml eppendorf tubes (Sarstedt, Germany), which contained 2µl-3µl of sample loading buffer (4M urea, 50% sucrose, 50mM EDTA pH 8.0, and some bromophenol blue). 5µl of sample was then loaded into the wells formed by the comb into the set gel. The gel was then submerged in TBE buffer containing 20µl ethidium bromide/L, and samples were run at 100V, for 50-70 minutes on a running apparatus (BioRad Laboratories, CA, USA) The gel was then imaged on a GelDoc (Ultraviolet Transilluminator; Bioimaging Systems, Upland, CA, USA), and pictures taken of the resultant bands.

2.4.2 DNA sequencing

Gels were imaged on an ultraviolet transilluminator. Single bands which corresponded to the expected product size for each PCR primer were cut out of the gel using scalpel blades, and placed into 1.5ml eppendorf tubes (Figure 2.2a). To extract DNA from the gels, the QIAquick Gel Extraction Kit was used (Qiagen, Germany) as per manufacturer's directions. Six volumes (according to gel weight) of buffer QG was added to dissolve the gel in the eppendorf tubes, and incubated for 10 minutes at 50^{o}C with occasional vortexing, to produce a yellow-coloured solution. One gel volume of isopropanol was then added to the solution to enhance DNA recovery. The sample was then placed into a QIAquick column in a 2ml collection tube and centrifuged for 1 minute at 10,000rpm to bind

Figure 2.2 DNA agarose gel and subsequent sequencing of RT-PCR primer products.

Following primer optimisation by RT-PCR in this thesis, all primer products were run on a DNA agarose gels (panel A). When a single band was obtained (note 8 different products for 8 different primers in panel A), it was cut, prepared for and then subjected to DNA sequencing analysis (panel B) to determine the gene product that had been amplified by RT-PCR, and that it matched what was expected for the primer pair. DNA sequencing was conducted at The Gandel Charitable Trust Sequencing Centre which adds fluorescently labeled ddNTPs to solutions containing the sample DNA, a single primer (either forward or reverse to target sequence) and a DNA polymerase. DNA fragments were separated by capillary electrophoresis where an analyzer detects the specific wavelengths of the labeled ddNTPs and assigns a color to the corresponding dNTP and produces the DNA sequence graph shown in the figure where blue = cytosine, black = guanine, red = thymine and green = adenine. The sequences were typed into a BLAST search engine to determine sequence homologies.

A

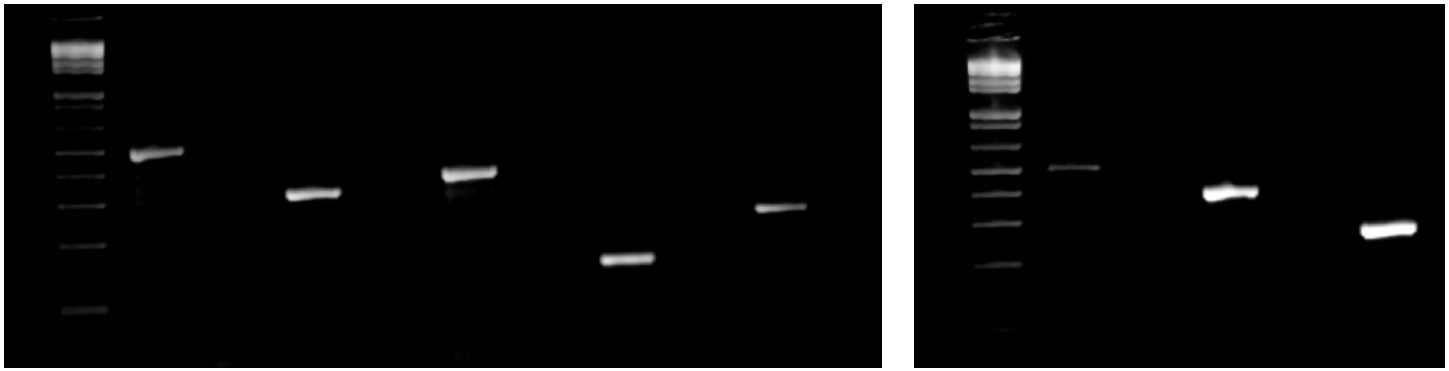

B

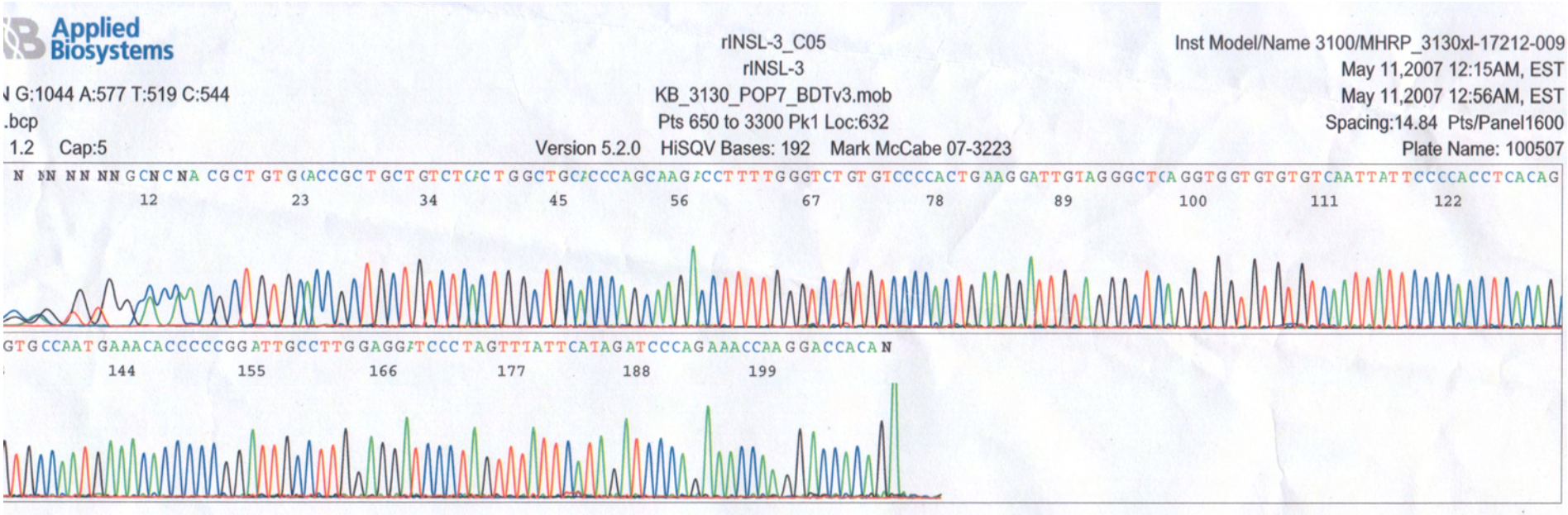
Applied Biosystems
rINSL-3_C05
rINSL-3
KB_3130_POP7_BDTv3.mob
Pts 650 to 3300 Pk1 Loc:632
Version 5.2.0 HiSQV Bases: 192 Mark McCabe 07-3223
Inst Model/Name 3100/MHRP_3130xl-17212-009
May 11,2007 12:15AM, EST
May 11,2007 12:56AM, EST
Spacing:14.84 Pts/Panel1600
Plate Name: 100507
G:1044 A:577 T:519 C:544
.bcp
1.2 Cap:5

the DNA to the column. A further 500µl of QG was then added to the solution, and this was centrifuged for a further minute at 10,000rpm (microfuge). 750µl of Buffer PE was then added to the column and incubated at room temperature for 5 minutes, before a further 1 minute centrifugation. The flow-through was discarded and the column centrifuged again to remove any residual Buffer PE. The column was then placed into a clean 1.5ml eppendorf tube, and to elute the DNA, 30µl of Buffer EB was applied to the column, incubated at room temperature for 1 minute and then centrifuged for 1 minute at 10,000rpm. To maximise yield of DNA, a further 10µl of Buffer EB was applied to the column and centrifuged through.

The resultant solution of DNA was then quantified on the ultraviolet spectrophotometer. Samples were diluted 1:20 and the concentration of DNA calculated to µg/µl. 10ng of DNA along with 3.2pmol of either the forward or reverse primer of each pair was forwarded to the DNA sequencing laboratory (The Gandel Charitable Trust Sequencing Centre, Monash Medical Centre, Clayton, VIC, Australia). Resultant readouts (Figure 2.2b) were then BLAST searched, and if the sequence corresponded to the desired protein, the primer pair was used for all future RT-PCR analyses.

2.5 Western blot analysis

2.5.1 Protein extraction

Protein was extracted from cultured Sertoli cells (Chapter 3) using boiling 2X SDS non-reduced sample buffer (5.0ml MilliQ water, 5ml 0.5M Tris, pH 6.8, 5ml glycerol, 5ml 10% w/v SDS, bromophenol blue), or from frozen rat testes using a buffer containing 1% SDS (MP Biomedicals, Solon, Ohio, USA), 0.125M Tris (Sigma, cat # T-1503), 2mM EDTA (Merck, Damstadt, Germany), 2mM N-ethylmaleimide (Sigma, cat # E-3876), 2mM phenylmethylsulfonylfluoride (PMSF, Sigma, cat # P7626), 1mM sodium orthovanadate (Gordon, 1991), 0.1µM sodium okadate (Calbiochem, Germany) and 1.6% β-mercaptoethanol (BioRad, CA, USA)/water (reduced/non-reduced sample) on ice (pH 6.8, (Wong *et al.* 2004)).

Cultured cells were mashed with the plunger of a 1ml syringe in the extraction buffer and homogenized in the tip of a 1ml pipette. Samples were then centrifuged for 5 minutes at 10,000rpm, snap frozen and stored at -80^{o}C.

For frozen testis samples, 100mg of tissue was cut and homogenized with 19G, 23G and 26G needles in the extraction buffer before being centrifuged at 4^{o}C at 10,000rpm for 10 minutes. Samples were then boiled for 3 minutes, centrifuged at room temperature for 10 minutes (10,000rpm) and then snap frozen and stored at -20^{o}C short-term, or -80^{o}C long-term.

2.5.2 Protein quantification

An aliquot of protein extract was diluted 1:80 in PBS and quantified for protein content using the BCA protein assay kit (Pierce, Rockford, IL, USA).

2.5.3 SDS-Polyacrylamide gel electrophoresis (SDS-PAGE)

Total protein (15μg and 40μg for occludin from Sertoli cell and whole testis protein extracts respectively (reduced), 120μg for claudin-11 from Sertoli cell and whole testis protein extracts (non-reduced)) was diluted in 2X SDS non-reduced (or reduced) sample buffer and then separated by SDS-PAGE on a 4%-20% pre-cast gel (BioRad, Cat # 345-0033) at 200V for 60-90 minutes. Proteins were then being transferred onto PVDF membranes (Immobilon-P, Millipore) for western blotting. Membranes were blocked in 5% skim-milk in PBS at 4^{o}C overnight. Primary antibodies were rabbit anti-occludin (Zymed #71-1500, 2.0μg/ml) and rabbit anti-claudin-11 (CovalAb #284-BM8, 1:200), and were applied to the membranes for 2 hours and co-stained with rabbit anti-β-actin (Sigma #A-2066, 1:1000). For band detection, Infrared 800-conjugated goat anti-rabbit secondary antibody (1:5000, Rocklands Immunochemicals, Inc., Gilbertsville, PA, USA, Cat # 610132121) was added following primary antibody incubation for a further 2 hours. The membranes were scanned onto an infrared imaging system (Odyssey IR imaging scanner, Li-Cor Biosciences, Lincon, NE, USA) at a resolution of 169μm and at an intensity of 5. Results were quantified by densitometry software provided with the system and normalised to β-actin.

2.6 Statistical analysis

Data was tested for normal distribution and equal variance. If data was deemed normally distributed it was then subjected to ANOVA testing for differences (when comparing more than 2 groups). When differences were detected, the post-hoc Student Newman-Keuls test was applied to determine where the differences lay. If the data was non-parametric, data was $\log_{10}$ treated and re-tested for normal distribution and subjected to the same testing as above if successful. If the data remained non-parametric, the determination of differences between groups was determined by the Kruskal-Wallis test, followed by the post-hoc Newman-Keuls analogue (Equal N's) or Dunn's Method tests to determine where the differences lay.

When comparing 2 groups, data was tested for normal distribution and equal variance before being subjected to a t-test. If the equal variance test failed, the t-test analogue Mann-Whitney Rank Sum test was conducted.

All statistical analysis in this thesis was performed using the SigmaStat program for Windows Version 3.5 (Jandel Corporation, CA, USA). Presentation of the statistical analyses will be specified in each Chapter.

Chapter Three: The contribution of claudin-11 and occludin to the function of the Sertoli cell tight junction, *in vitro*

Chapter 3. The contribution of claudin-11 and occludin to the function of the Sertoli cell tight junction, *in vitro*

3.1 Introduction

The Sertoli cell TJ forms in mammals at puberty along with an increase in circulating gonadotrophins (FSH and testosterone), and plays an essential role in spermatogenesis as the major component of the blood-testis barrier, separating and protecting the adluminal germ cells from the general circulation (Russell and Peterson, 1985). Low levels of circulating gonadotrophins leading up to puberty results in the delay or prevention of TJ formation and a lack of spermatogenic activity, a phenotype which in men and hamsters can be reversed by the exogenous application of gonadotrophins (de Kretser and Burger, 1972, Tarulli *et al.* 2006, Tarulli *et al.* 2008).

As mentioned in Chapter 1, the role of occludin in TJs is controversial. Evidence suggests that occludin may play a regulatory TJ role (Nusrat *et al.* 2000, Ban *et al.* 2003), in that it is extensive in 'tighter' TJs such as the blood-brain barrier, but not in leakier junctions such as the intestine (Claude, 1978, Hirase *et al.* 1997). Furthermore, the occludin knockout mouse displayed continuous TJ strands in the testis and was fertile until at least late adulthood (Saitou *et al.* 1998), showing that this protein is not essential for the onset of spermatogenesis. The claudin-11 knockout mouse model on the other hand is infertile (Gow *et al.* 1999), suggesting an important role for claudin-11 in TJ function.

At the molecular level, testosterone has been shown to regulate the localisation of the key TJ transmembrane proteins, occludin and claudin-11 to the TJ in an immature rat Sertoli cell culture model, with testosterone also regulating the mRNA expression of the latter protein (Kaitu'u *et al.* 2007). Furthermore, in the Sertoli cell specific androgen receptor knockout mouse model, claudin-11 mRNA expression is significantly reduced *in vivo* as is TJ function (Meng *et al.* 2005, Tan *et al.* 2005). However, claudin-11 staining is still present at the TJ in this model and Meng *et al.* (2005) showed that another claudin (claudin-3) may also play an important role in the mouse Sertoli cell TJ, as its mRNA expression is disrupted and localisation to the TJ absent in the same model. Interestingly however, claudin-3 is not expressed at the rat Sertoli cell TJ as shown by RT-PCR and immunocytochemical analysis (Kaitu'u *et al.* 2007). In cultured mouse Sertoli cells, FSH has also been shown to play an important role in regulating the mRNA expression of claudin-11 (Hellani *et al.*

2000). Therefore, it appears that occludin and claudin-11 may contribute to the function of the Sertoli cell TJ but to what extent each protein does so is unknown. It is thus hypothesised that both claudin-11 and occludin contribute to the rat Sertoli cell TJ *in vitro*, with claudin-11 contributing significantly more so.

The aim of the work described in this Chapter is to determine the relative contribution of occludin and claudin-11 to Sertoli cell TJ function *in vitro* by selectively silencing gene expression with siRNA targeted specifically against both proteins separately, and in combination.

This Chapter will use an established immature rat (19-21 days old) Sertoli cell primary culture model. Proliferation of Sertoli cells stops at 15 days of age in the rat (Orth, 1984), hence the number of Sertoli cells will remain constant throughout the cultures. Transepithelial electrical resistance (TER) will be used to monitor TJ development from the day of culture up to and including days 5-6 of culture when siRNA will be added. At the end of the culture, cells will either be fixed for immunocytochemical analysis of claudin-11 and occludin localisation, as well as the localisation of β-catenin to the nearby adherens junction, or be extracted for real-time RT-PCR or western blot analyses.

3.2 Materials and Methods

3.2.1 Animals

Twelve male Sprague-Dawley outbred rats aged 19-21 days were used for all cultures. Rats were obtained from Monash Animal Services, Monash University Clayton as approved by the Animal Ethics Committee (ethics numbers: MMCB 2002/04 and MMCB 2002/38), Monash Medical Centre Clayton.

3.2.2 Immature Sertoli cell isolation

The method used for immature rat Sertoli cell isolation follows that of Perryman *et al* (1996), as recently applied to the study of rat Sertoli cell TJs (Kaitu'u *et al.* 2007). A detailed protocol is provided in Appendix 1.1. In brief, the 12 rats for each culture were sacrificed by carbon dioxide asphyxiation, and testes were removed, decapsulated and chopped finely before being digested in

trypsin (in Dulbecco's Phosphate Buffer Saline- PBS; Gibco, NY, USA) to remove interstitial tissue. Digestion lasted 25 minutes at 37^{o}C using an orbital shaker at 90rpm. Digestion was stopped by the addition of PBS/DNase containing 10% foetal calf serum (FCS; Trace Biosciences, Sydney Australia). Seminiferous tubules were separated by unit gravity sedimentation, after which tubules were washed once in 10% FCS in PBS/DNase and three times in DNase (20μg/ml)/PBS. The tubules were allowed to sediment between each wash and after the last wash, the seminiferous tubules were resuspended in PBS containing 1% (w/v) bSA (Sigma, cat# A-7906) and 10μg/ml DNase. Cells were then homogenised by slow depression through a sterile glass/Teflon tissue homogeniser tube with a pistle eight times by hand. Following homogenisation, cells were pelleted by a 5 minute centrifugation process at 1000rpm (94g). The pellet was resuspended in PBS before being filtered through sterile nylon mesh (80μm). The filtered cells were centrifuged again as above, washed twice in PBS and centrifuged further after each wash. After the final wash, the pellet was resuspended in 10ml of appropriate culture medium. 20μl of this solution was diluted 1:2 in Trypan Blue (Trace Biosciences, Sydney, Australia) for cell counting and analysis of viability with the use of a haemocytometer. Cells were then plated in media (DMEM/F12, Sigma, cat# D-2906) as described below.

3.2.3 Cell plating

a. Plating for transepithelial electrical resistance and immunocytochemistry

Millicell-PCF bicameral chambers (Millipore, MA, USA) were used for cell culturing for TER measurements and immunocytochemistry. These bicameral chambers had small PCF filters (12mm diameter, 0.4μm membrane pore size), and fitted easily into wells of a 24-well plate. 50μl of matrigel diluted 1:8 in medium was added to the chambers and spread with a syringe plunger. Both the apical and basal chambers of the bicameral units were filled with a final volume of 600μl of solution. Cells were then incubated at 37^{o}C in a humidified incubator with 5% CO_2 and 95% air throughout the culture.

b. Plating for western blot and total RNA extraction

Cells were plated into regular 24-well plates which had been coated with 20µl of matrigel diluted 1:8 in medium and spread with a syringe plunger. Excess matrigel was then removed, and the plates allowed to set for at least an hour in an incubator at 37^{o}C. Cells were plated at a density of 5.0 x 10^6 cells/ml, with 250µl of the cell suspension per well, for a final cell density at plating of 0.625 x 10^6 cells/cm^2. The final volume of solution in the wells was 1ml.

For details of mRNA and protein extraction from these cells, see sections 2.3 and 2.5.

3.2.4 Hypotonic shock

Contaminating germ cells were removed on day 3 of culture by using a low salt medium to deliver a hypotonic shock. Sterile MilliQ H_2O containing 10% DMEM/F12 was administered to all cells for 45 seconds. For bicameral TER wells, 300µl of this low salt solution was added to the apical side of the bicameral chamber, and then washed out with 300µl of prepared culture medium. The wash was then replaced with 600µl of culture medium on both sides of the bicameral chamber. Similarly for western blot/RNA extraction wells in 24 well plates, 500µl of low salt medium was added, and then washed with 500µl of prepared culture medium before finally being replaced with 1ml of medium containing treatments.

3.2.5 Measuring transepithelial electrical resistance

Transepithelial electrical resistance (TER) was measured daily with the use of a Millipore Millicell- ERS system (Millipore, MA, USA) from the day of cell plating through to the last day of culture. Before measuring TER, the Millicell-ERS electrodes were sterilised for 10 minutes in 70% ethanol, and then equilibrated in DMEM/F12 for 20 minutes at room temperature. Cells were equilibrated to room temperature during the half hour preparation of the Millicell-ERS apparatus. For TER measurements, the long arm of the electrodes sat between the bicameral chamber and the wall of the culture well with the short arm inside the bicameral chamber (see Figure 3.1). An alternating current was applied across the Sertoli cell monolayer until a stable resistance reading was recorded. Each well was read twice. Electrodes were rinsed briefly in 70% ethanol, PBS and then DMEM/F12 between each treatment group.

Figure 3.1 Measuring transepithelial electrical resistance (TER).

Diagrammatic representation of TER measurements. Electrode arms are inserted into the inside and outside of the bicameral chamber (panel A). An electrical current is applied across the cells and as tight junctions form (red) the resistance met by the current increases giving a direct indication of tight junction function. Tight junctions will only form if cells are plated densely (panel B) and this will result in a high TER. If cells are not dense enough (panel C), tight junctions will not form thus giving low TER readings. Modified from Onoda *et al.* (1990)

A

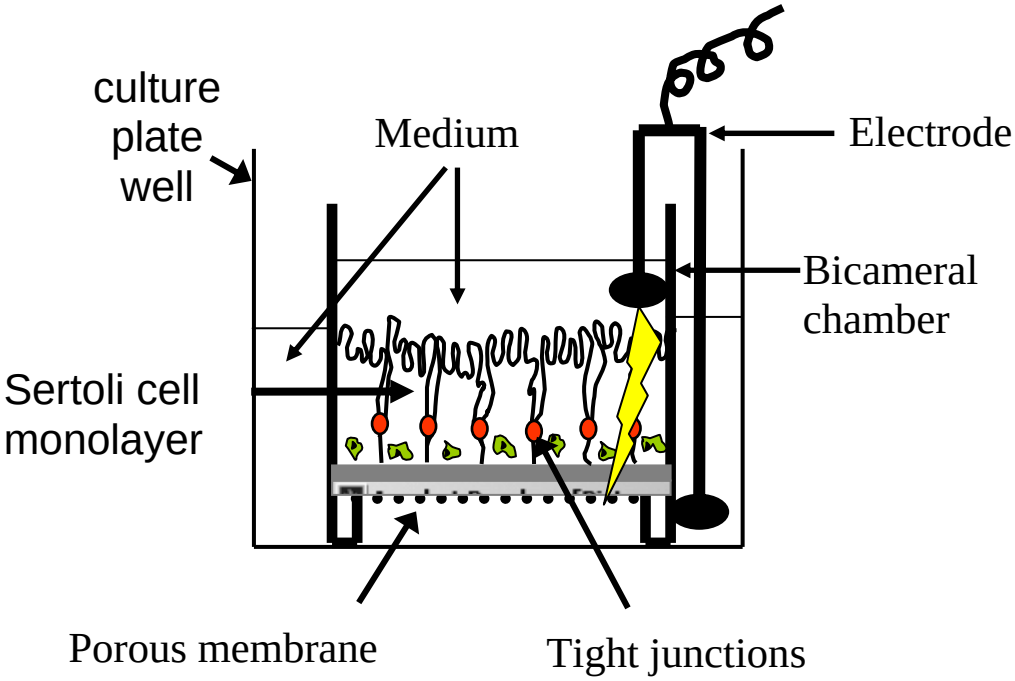
culture
plate
well
Medium
Electrode
Bicameral
chamber
Sertoli cell
monolayer
Porous membrane
Tight junctions

B

C

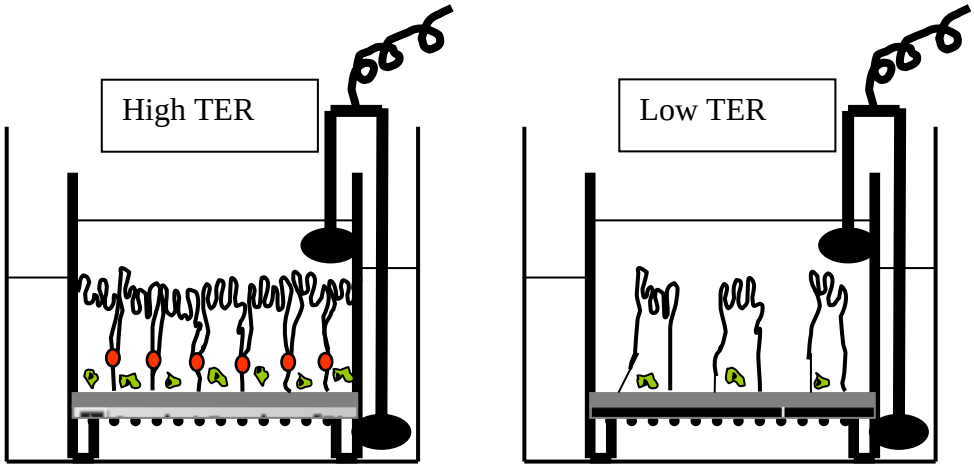
High TER
Low TER

Final TER results were determined by averaging each of the two resistance (Ω) readings from each culture well recorded. The average of TER readings recorded for bicameral chambers coated with matrigel but containing no cells was subtracted from the averages of the wells that did have cells. This final result was then divided by 0.6, the surface area of the bicameral chamber ($0.6cm^2$), to give the TER results in units of Ω/cm^2. Means and standard deviations were determined from triplicate culture wells.

3.2.6 siRNA cultures

siRNA for claudin-11 had been designed previously, and the ratio to which the siRNA was to be diluted in transfection reagent before administration to Sertoli cells optimised (McCabe, 2003). In that study, a range of siRNA:transfection reagent ratios were tested from 1:3 to 1:9 according to the manufacturer's directions (McCabe, 2003). While each of the ratios reduced the function of the cultured Sertoli cells significantly after 3 days of treatment, as measured by TER, ratios greater than 1:3 were seen to be toxic to the cells as shown by immunocytochemistry (McCabe, 2003). The density of the Sertoli cells was low and their nuclei appeared shrivelled and bright (McCabe, 2003). The 1:3 ratio however displayed healthy, dense cells and so this ratio was chosen for all further experiments (McCabe, 2003). Subsequently, 1μg of siRNA was diluted in 3μl of transfection reagent before being added to the culture media which was administered to Sertoli cells for 2 days, a time course recommended by the manufacturer (McCabe, 2003). siRNA fragments of 21 nucleotides in length had been designed for claudin-11 using the web-based siRNA design program through the Whitehead Institute (http://jura.wi.mit.edu/bioc/siRNAext/home.php; "siRNA selection program," Whitehead Institute for Biomedical Research). Two strands which were specific for mouse claudin-11 (accession number: NM_008770) which is exactly the same as rat claudin-11 (accession number: NM_053457) were selected and obtained from Qiagen (Germany) and designated Clau-11-A and Clau-11-B (see Table 3.1). For this thesis, two siRNA strands were also designed for occludin using the same software. These fragments were also obtained from Qiagen (Germany) and were specific for rat occludin (accession number: NM_031329), and were designated Occ-A and Occ-B (Table 3.1). All sequences underwent a BLAST search to show that they only corresponded to the desired gene and no other. Several design aspects of the siRNA fragments needed to be taken into consideration as

Table 3.1 siRNA designs.

siRNA for silencing claudin-11 and occludin was designed on a web-based siRNA design program through the Whitehead Institute (http://jura.wi.mit.edu/bioc/siRNAext/home.php; "siRNA selection program," Whitehead Institute for Biomedical Research). The program's design settings were left at default. Two fragments of 21 nucleotides in length were designed for each protein and were obtained from Qiagen. The G/C content, typically between 30%-70%, needed to be taken into consideration according to the manufacturer. These details, as well as the siRNA are presented in this table.

siRNA fragment	Species/Accession number	Target DNA Sequence (5'-3')	G/C %
Clau-11-A	Mouse NM_008770	AAACCGTTTCTATTACTCTTC	33
Clau-11-B	Mouse NM_008770	GACTGCGTCATGGCCACTGGT	62
Occ-A	Rat NM_031329	AACGATAACCTAGAGACACCT	43
Occ-B	Rat NM_031329	AATTATCACACATCAAGAGGA	33

recommended by the manufacturer such as G/C content (Table 3.1) and the absence of triplicate nucleotides. According to the manufacturer, there was an 88% chance that one of the two specific siRNA fragments for either protein would knockdown gene expression.

For the negative control, siRNA directed against Lamin A/C was also obtained from Qiagen. Lamin A/C, which is present in Sertoli cells, is part of the nuclear lamina and its main function is to provide strength and support in the nucleus of developing animals, although it is not an essential protein (Moss *et al.* 1993, Vester *et al.* 1993, Stuurman *et al.* 1998, Harborth *et al.* 2001). In the McCabe (2003) study, fluorescent siRNA was also used as a positive control to show that cells had taken up the siRNA as shown by immunocytochemistry. This test was not repeated in this thesis, but all siRNA preparation and treatment protocols used in McCabe (2003) were followed in this thesis.

In brief, immature rat Sertoli cells were cultured and allowed to form TJs over 5-6 days, with TJ formation being monitored daily by TER. At the end of this period, the siRNA was prepared for administration. This involved adding 1ml of Sterile Suspension Buffer (Qiagen, Germany) to the claudin-11 and occludin siRNA, and 0.25ml of Sterile Suspension Buffer to the Lamin A/C siRNA, bringing all of the fragments to a final concentration of 20μM. These fragments were heated for 1 minute at 90^{o}C and then incubated for 1 hour at 37^{o}C. Following this step, fragments could either be frozen and stored at -20^{o}C, or used.

The next step was to prepare the siRNA/transfection reagent (TransiFect, Qiagen, Germany) solution at the appropriate ratio (see Appendix 1.2 for detailed calculations). The calculated amount of siRNA was then added to phenol-red free DMEM/F12 culture media (Sigma, catalogue # D-2906), which according to the manufacturer, was necessary as the phenol red interfered with the fluorescent siRNA positive control. While this was not an issue for this thesis as the positive control was not used as already mentioned, the phenol red-free media was still used to keep with the established protocol from McCabe (2003). The solution was vortexed briefly. The appropriate amount of transfection reagent was then added to achieve the desired 1:3 siRNA:transfection reagent ratio. This solution was again vortexed for 10 seconds and allowed to incubate for 10-15 minutes at room temperature to allow transfection reagent-siRNA complexes to form. During this incubation, media was removed from all culture wells, and 450μl of siRNA/transfection reagent free media added to the inside and outside of bicameral chambers, and 750μl added to RT-PCR/western blot wells. The transfection reagent-siRNA

complexes were then added drop-wise into the appropriate wells; 150μl into the inside and outside of bicameral chambers and 250μl into the RT-PCR and western blot wells.

Claudin-11 specific and occludin specific siRNA fragments were added individually at the same concentration as each other. Additional treatments included i) combining the two types of claudin-11 siRNA together, ii) combining the two types of occludin siRNA together and iii) combining Clau-11-B with Occ-B to silence the genetic expression of both claudin-11 and occludin at the same time. The final total siRNA concentration of the mixed samples equalled that of the individual samples.

For controls, cells either received i) additional siRNA/transfection reagent free media, or ii) media with transfection reagent alone or iii) media containing Lamin A/C siRNA and transfection reagent at the same ratio as the other siRNA:transfection reagent treatments.

Treatments were added for two days and changes in TJ function monitored by TER. At the end of the treatment period, cells in bicameral units were fixed for immunocytochemical analysis (see section 3.2.5), and the localisation of claudin-11, occludin and the adherens junction related protein β-catenin analysed. This was done to assess the response of TJ components, or components of nearby junctions to the siRNA fragments. It was also considered, that should the localisation of either occludin or claudin-11 to the TJ be reliant on the presence of the other, that knocking one of them out by siRNA interference could give a false negative result of the specificity of the siRNA fragment. It was thought that β-catenin would be a better indicator of the specificity of the TJ siRNA.

Cells in conventional 24 well plates which received the siRNA treatments at the same time points as the TER cells, had total RNA extracted for RT-PCR analysis and protein extracted for western blot analysis 2 days after treatment addition.

3.2.7 Immunocytochemistry

a. Cell fixation procedure

Cells on PCF membrane filters were pre-extracted on ice for 2 minutes in 0.2% Triton X-100 in phosphate buffer saline (PBS: 0.01M PBS with 0.9% NaCl). Following this, they were then fixed in 3% paraformaldehyde (paraformaldehyde: 3g dissolved in 100ml PBS at 60^{o}C, filtered, wrapped in

foil and stored at room temperature) for 30 minutes in the dark, at room temperature. After the fixing procedure, cells were permeabilised on ice with 0.05% TX-100 (0.5ml Triton X-100 in 100ml PBS). Cells were then washed three times in PBS and stored at 4^{o}C until use.

b. Preparation of fixed cells for immunocytochemical analysis

PCF membrane filters containing the fixed cells, were cut into quarters with a scalpel blade. One quarter was placed into one well of a 48-well plate, with the remaining quarters being stored in PBS at 4^{o}C for later use. The quarter in the well was then washed in 150µl of Phosphate Buffer Saline (PBS)/bSA (0.01M/0.1% w/v bSA/0.9% w/v NaCl) twice for 5 minutes each. Following the washes, the membrane quarter was incubated for 20 minutes in 150µl of CAS block (Zymed, San Francisco, CA, USA) in 10% normal sheep serum to block non-specific binding sites. Quarters were allowed to incubate in 150µl of primary antibody or negative control (at the same concentration as each other) overnight at room temperature (see Table 3.2 for primary and secondary antibody details for this Chapter). Quarters then underwent two 5 minute washes in PBS/bSA before being incubated for one hour in the secondary antibody in the dark. The quarters were then subjected to two 5 minute washes in PBS again before being counterstained with the fluorescent nuclear counterstains, DAPI (100nM in PBS/bSA) and TOPRO-3 (1:100 in DAPI/PBS/bSA from a 1mM stock in DMSO; Molecular Probes, Eugene, USA) for 5 minutes. Quarters were then washed three times for 5 minutes in PBS/bSA and mounted with FluorSave (Calbiochem, Germany) reagent. Quarters were visualised and photographed using a confocal microscope (Fluoview, FV300, Olympus Australia, Mt Waverley, VIC, Australia).

3.2.8 Real-time RT-PCR analysis

Total RNA extraction through to RT-PCR analysis was conducted as outlined in Section 2.3 for cultured cells. Primers for claudin-11, occludin and GAPDH had been previously optimised (Tso *et al.* 1985, Drummond *et al.* 2000, Chung *et al.* 2001, Lui *et al.* 2001, Kaitu'u *et al.* 2007) and so no DNA agarose gels or sequencing was conducted. Details for the primers used in this Chapter are displayed in Table 3.3.

Table 3.2 Antibodies used for immunohistochemical analysis.

Tabulated data for the antibodies used in Chapter 3 of this thesis include details regarding the primary and secondary antibody hosts, working concentrations (conc.)/dilutions, incubation (Inc.) times and company details with catalogue numbers.

Protein	**Primary (1^o) antibody host**	**Company** (cat #)	**Conc.** (μg/ml)	**Negative control**	**1^o Inc. time**	**Secondary (2^o) antibody**	**Company**	**2^o Dilution**	**2^o Inc. time** (mins)
Claudin-11	Rabbit	Zymed (36-4500)	2.0	Normal rabbit IgG	Overnight	Goat α rabbit Alexa-488	Molecular Probes (Oregon, USA)	1:400 of stock	60
Occludin	Rabbit	Zymed (71-1500)	2.5	Normal rabbit IgG	Overnight	Goat α rabbit Alexa-488	Molecular Probes (Oregon, USA)	1:400 of stock	60
β-catenin	Mouse	BD Transduction Laboratories (610154)	0.5	Normal mouse IgG	Overnight	Goat α mouse Alexa-488	Molecular Probes (Oregon, USA)	1:400 of stock	60

Table 3.3 Primer sequences and real-time RT-PCR conditions for the analysis of siRNA mediated gene silencing of claudin-11 in cultured Sertoli cells.

Primers were obtained against TJ proteins claudin-11 and occludin to analyse the effect on the mRNA expression of both proteins after silencing claudin-11 siRNA. A primer pair was also obtained for the housekeeper protein GAPDH which was used to form ratios with claudin-11 and occludin for analyses. Data included in the table are forward and reverse primer sequences, Mg^{2+} concentration, and annealing and acquisition temperatures.

Protein	**Species/Accession number**	**Primer sequences (5'- 3')**	**Product size** (bp)	**[Mg^{2+}]** (mM)	**Anneal temp.** (^{o}C)	**Acquisition temp.** (^{o}C)
Claudin-11 (Chung *et al.* (2001))	Rat NM_053457	Forward: TTAGACATGGGCACTCTTGG Reverse: ATGGTAGCCACTTGCCTTC	624	2.5	68	85
Occludin (Lui *et al.* (2001))	Rat NM_031329	Forward: CTGTCTATGCTCGTCATCG Reverse: CATTCCCGATCTAATGACGC	294	2.5	64	72
GAPDH (Tso *et al.* (1985))	Mouse NM_008084	Forward: GACCCCTTCATTGACCTCAAC Reverse: GATGACCTTGCCCACAGCCTT	560	2.5	60	72

3.2.9 Western blot analysis

Protein was extracted from culture wells with 2 X non-reduced sample buffer as outlined in Section 2.5. 15μg of protein was loaded into gel lanes for occludin protein analysis, whereas claudin-11 protein was difficult to detect and needed further optimisation in this Chapter. For antibody details used for western blot analysis in this Chapter, see Table 3.4. Protein detection for occludin and claudin-11 used ECL (Western Blotting Detection Reagents, Amersham Biosciences) chemicals, which were added to membranes after the wash following the secondary antibody incubation for 5 minutes. Films (Amersham Hyper) were exposed to the membranes for 30 seconds and 1, 2, and 5 minutes and then developed.

3.2.10 Statistical analysis

Triplicate culture wells were used per treatment with 2-3 cultures conducted for each endpoint. Differences in TER and RT-PCR between treatments within cultures were measured as outlined in section 2.6 and expressed as mean ± SD. If no statistical differences between the siRNA treatments were observed within cultures, data was grouped and then tested for differences between cultures by t-test (n = 2 cultures) or ANOVA (n = 3) cultures. If still no statistical differences between the cultures were observed for the siRNA treatments, the final mean and SD were calculated based on the compared cultures' data.

3.3 Results

3.3.1 Effect of claudin-11 siRNA on tight junction function

TJ function increased from the day of cell plating to the day of claudin-11 siRNA addition (day 6) (Figure 3.2a). When claudin-11-A and claudin-11-B siRNA were added to Sertoli cells either separately, or in combination, a decrease of 47%, 76% and 58% respectively ($p < 0.01$, n = triplicate wells/treatment) in TJ function over 2 days of treatment was observed (Figure 3.2a). Over three cultures, differences between the effect of any of the siRNA treatments on TJ function were not significant with each other, giving a final decrease in TJ function of approximately 55% ($p < 0.01$). The graph presented in Figure 3.2a is representative of three separate cultures. When the siRNA

Table 3.4 Antibodies and conditions used for western blot analysis.

Tabulated data for the antibodies used in Chapter 3 of this thesis include details regarding the primary and secondary antibody hosts, working concentrations (conc.)/dilutions, incubation (Inc.) times and company details with catalogue numbers.

Protein	**Primary (1^o) antibody host**	**Company** (cat #)	**Conc.** (μg/ml)	**Negative control**	**Tween20** (v/v) (%)	**1^o Inc. time** (hrs)	**Secondary (2^o) antibody**	**Company**	**2^o Dilution**	**2^o Inc. time** (hrs)
Claudin-11	Rabbit	Zymed (36-4500)	2	Normal rabbit IgG	0.1% primary and secondary	2	Goat α-rabbit HRP conjugated **or** goat α-rabbit IRDye 800	Silenus (Melbourne Australia) **or** Rockland Immunochemicals (Pennsylvania, USA)	1:10000 of stock (HRP) or 1:5000 of stock (IRDye)	2
Claudin-11	Rabbit	AbCam (ab7474)	1:200 of antiserum	Normal rabbit serum	0.1% primary and secondary	2	As above	As above	As above	2
Claudin-11	Rabbit	CovalAb (pep0006)	1:200 of antiserum	Normal rabbit serum	0.1% primary and secondary	2	As above	As above	As above	2
Occludin	Rabbit	Zymed (71-1500)	1	Normal rabbit IgG	0.1% primary and secondary	2	Goat α-rabbit HRP-conjugated	Silenus (Melbourne, Australia)	1:10000 of stock	2
β-actin	Mouse	Sigma ascites fluid (A4700)	1:1000 of stock	Normal mouse IgG	0.1% primary and secondary	2	Goat α-mouse HRP conjugated **or** goat α-mouse IRDye 800	Silenus (Melbourne, Australia) **or** Rockland Immunochemicals (Pennsylvania, USA)	1:10000 of stock (HRP) or 1:5000 of stock (IRDye)	2

Figure 3.2 Effect of claudin-11 siRNA on TJ function.

Immature rat Sertoli cells were cultured and allowed to develop TJs over 5-6 days as measured by transepithelial electrical resistance (●). At day 6 of one culture as indicated by the arrow (panel A), one group of cells was treated with siRNA transfection reagent alone (○), while the other three treatments received clau-11-A siRNA (□), clau-11-B siRNA (Δ) or both siRNA strands together (◊) for 2 days (panel A). In a separate culture at day 5 as indicated by an arrow (panel B), cells either received siRNA transfection reagent alone (○) or the Lamin A/C specific siRNA (x) for 2 days. At the end of the treatment period, cells were fixed for immunocytochemical analysis. Data is mean ± SD, n = triplicate wells/treatment. ** = $p < 0.01$ compared to day of treatment addition.

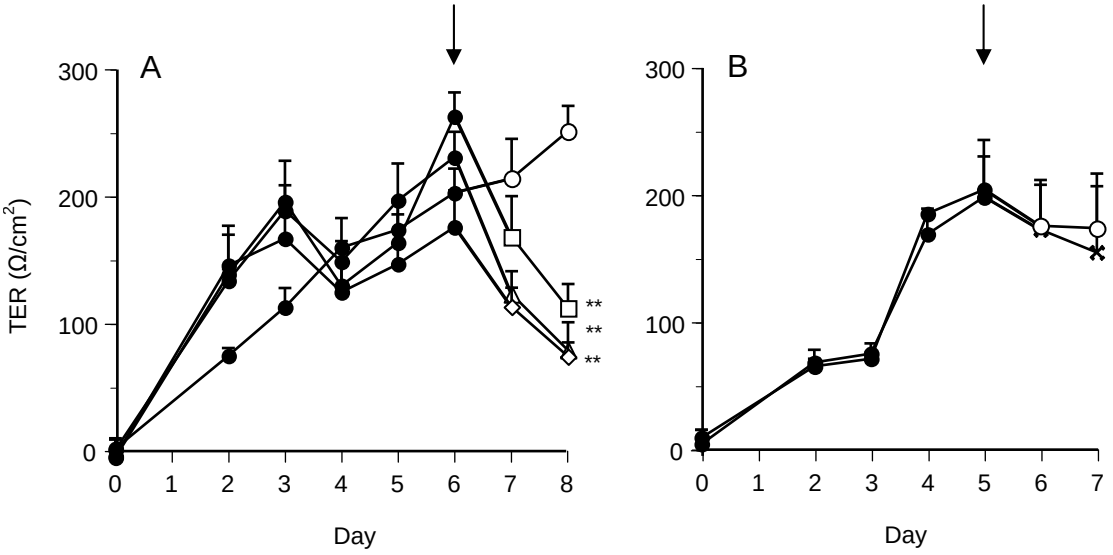
A
B
TER (Ω/cm²)
300
200
100
0
0 1 2 3 4 5 6 7 8
0 1 2 3 4 5 6 7
Day
Day
**
**
**
*

transfection reagent or the non-TJ specific Lamin A/C siRNA (Figure 3.2a/b) were added for two days of culture, no decrease was seen in response to the transfection reagent, but a small, non-significant 22% decrease was observed for Lamin A/C siRNA.

3.3.2 Effect of claudin-11 siRNA on claudin-11 localisation

The same cultured Sertoli cells that gave the changes in TER in Section 3.3.1 were fixed at the end of the culture and processed for immunocytochemical analysis. In medium-only treated cells, or cells treated with the siRNA transfection reagent, or Lamin A/C specific siRNA, claudin-11 localisation to the TJ was extensive (Figure 3.3) although claudin-11 and nuclear staining were less intense in the latter treatment group. After treatment with claudin-11-A or claudin-11-B siRNA separately, or in combination, claudin-11 localisation to the TJ was markedly reduced, with only punctate staining apparent at the TJ (Figure 3.3).

3.3.3 Effect of claudin-11 siRNA on the localisation of other junction proteins

The effect of claudin-11 specific siRNA on the localisation of occludin to the TJ, and β-catenin to the nearby adherens junction was also analysed after two days of treatment. The localisation of occludin (Figure 3.4c) and β-catenin (Figure 3.4e) was extensive in the siRNA transfection reagent alone treatment but was partially reduced after claudin-11 siRNA treatment (Figure 3.4d/f), although not to the same extent as was observed for claudin-11 after claudin-11 specific siRNA (Figure 3.4a/b).

3.3.4 Effect of claudin-11 siRNA on claudin-11 and occludin mRNA expression

Note that unless otherwise stated, all statistical analyses in the ensuing paragraph are comparisons between the time of transfection reagent/siRNA addition and 2 days after exposure, when the Sertoli cell culture was stopped.

Total RNA was extracted from cultured Sertoli cells two days after siRNA treatment. Transfection reagent had no negative impact on claudin-11 or occludin mRNA expression in the claudin-11-A and claudin-11-B samples (Figure 3.5 top panels) but caused a significant ($p < 0.05$) 30% decrease in claudin-11 mRNA expression and a 55% decrease ($p < 0.01$) in occludin mRNA expression in the combined claudin-11-A and claudin-11-B samples (Figure 3.5 bottom panels).

Figure 3.3 Effect of claudin-11 siRNA on claudin-11 localisation to the TJ.

Immature rat Sertoli cells were fixed in paraformaldehyde 2 days after claudin-11 siRNA treatment and analysed by confocal microscopy. Claudin-11 (green) localisation to the TJ around the Sertoli cell nuclei (red) was stained in control cells which received medium alone (panel A), transfection reagent alone (panel B), Lamin A/C specific siRNA (panel C), as well as in cells which received clau-11-A siRNA (panel D), clau-11-B siRNA (panel E) or both siRNA strands in combination with each other (panel F). Bar = 50μm. Inset = negative control for claudin-11.

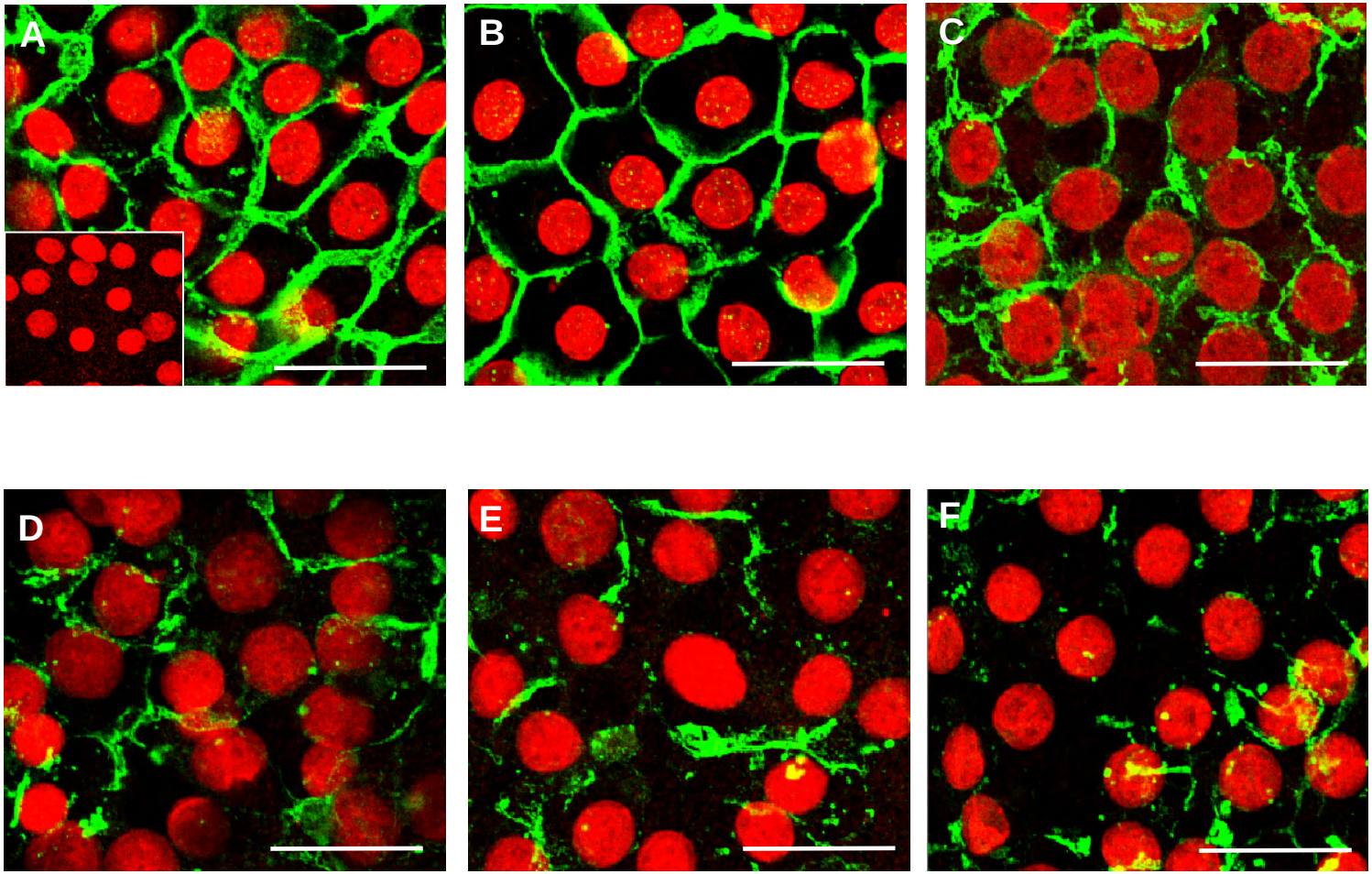
A
B
C
D
E
F

Figure 3.4 Effect of claudin-11 siRNA on the localisation of occludin to the TJ and β-catenin to the adherens junction.

Cultured immature rat Sertoli cells were fixed after 2 days of claudin-11 siRNA treatment. Immunocytochemical analysis was conducted on claudin-11 (green) localisation around the periphery of Sertoli cell nuclei (red) at the TJ in cells which received transfection reagent alone (panel A) or clau-11-A/B siRNA treatment (panel B). Staining for occludin (green) at the Sertoli cell TJ was also conducted in transfection reagent (panel C) and clau-11-A/B siRNA treated cells (panel D). To test for any effects of claudin-11 siRNA on other junctional types, β-catenin (green) of the adherens junction was also stained in transfection reagent (panel E) and siRNA (panel F) treated cells. Bar = 50μm. Inset = negative controls for claudin-11, occludin and β-catenin.

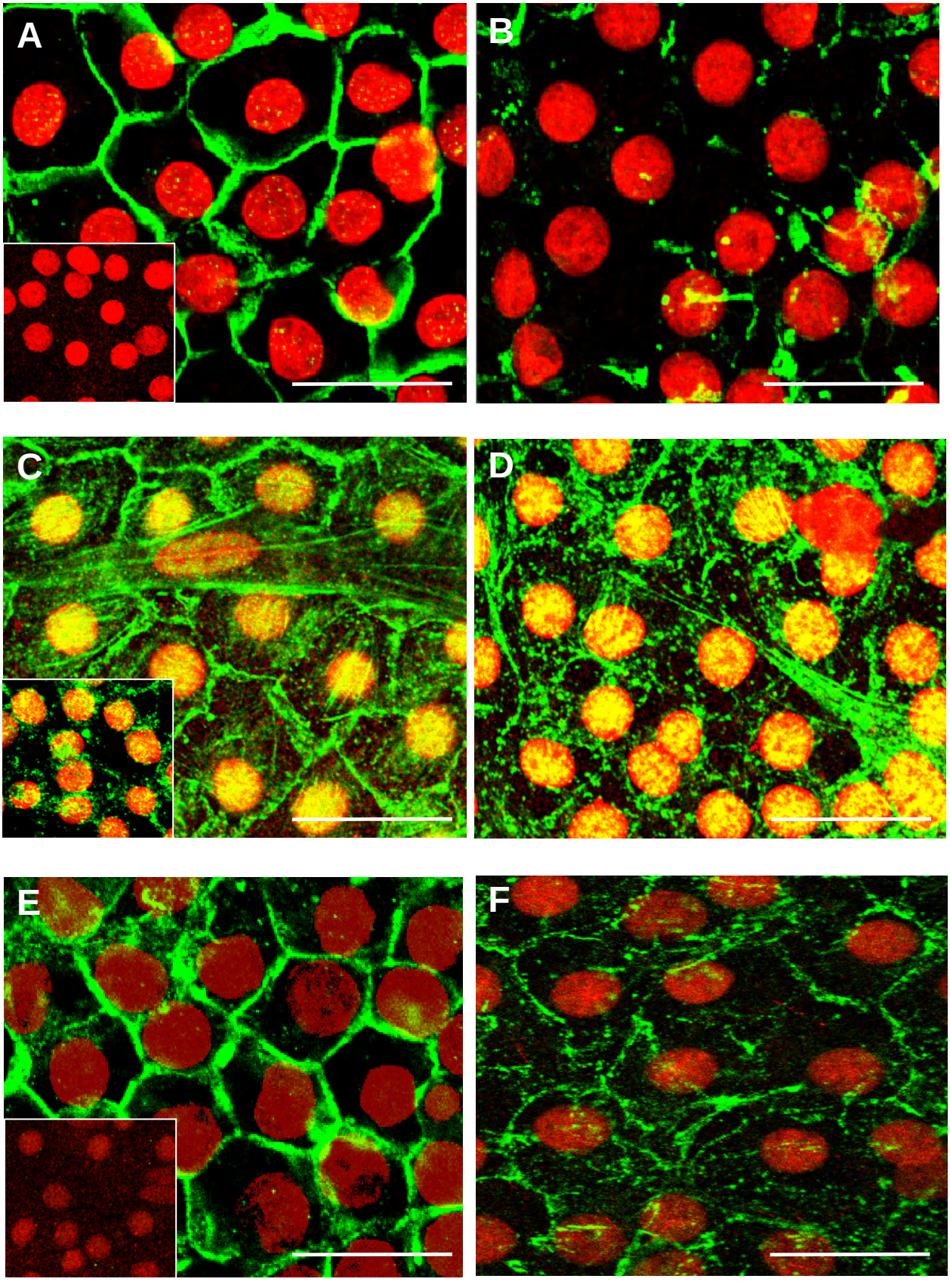
A
B
C
D
E
F

Figure 3.5 Real time RT-PCR analysis of the effect of claudin-11 siRNA on the mRNA expression of claudin-11 and occludin.

Claudin-11 siRNA was added to cultured immature rat Sertoli cells at day 6 of culture. Total RNA was extracted two days after addition and processed for RT-PCR analysis of changes in claudin-11 (left graphs) and occludin (right graphs) mRNA expression. The treatment groups analysed in the top graphs were the siRNA transfection reagent alone (○), Lamin A/C siRNA (x), clau-11-A siRNA (□) and clau-11-B siRNA (Δ). In the lower graphs are transfection reagent (○) and the effects of the combined siRNA strands (◊). Data is mean ± SD, n = 3 wells/treatment. Data has been expressed as a percent versus the GAPDH ratio at the day of siRNA addition (day 0) until the day of total RNA extraction (day 2). ns = not significant, * = $p < 0.05$, ** = $p < 0.01$.

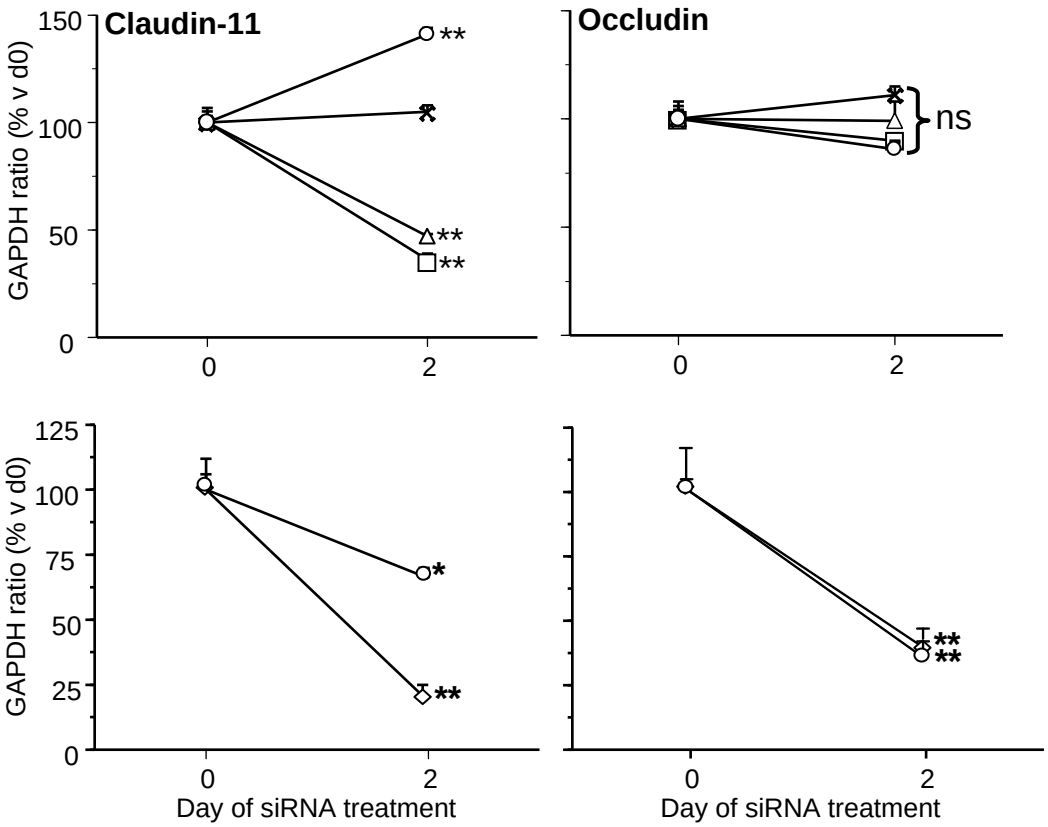
Claudin-11
Occludin
GAPDH ratio (% v d0)
150
100
50
0
125
75
25
**
*
ns
0
2
Day of siRNA treatment

Claudin-11 mRNA expression in response to siRNA treatment was reduced by 71% ($p < 0.01$, n = triplicate wells/treatment, n = 3 cultures (Figure 3.5). The graphs shown in Figure 3.5 are representative of the data obtained from the 3 cultures. The decrease in claudin-11 mRNA expression in response to claudin-11-A + B was significantly greater ($p < 0.01$) than the decrease induced by the transfection reagent. Furthermore, the decrease ($p < 0.01$) in occludin mRNA expression in the same treatment group was of the same magnitude as that induced by the transfection reagent alone (Figure 3.5), ie) the presence of claudin-11 siRNA had no further effect on occludin mRNA expression. Lamin A/C had no effect on the mRNA expression of either protein (Figure 3.5).

3.3.5 Effect of claudin-11 siRNA on claudin-11 and occludin protein expression

Protein was extracted from cultured Sertoli cells two days after siRNA treatment. Claudin-11 protein was undetectable by Western blot analysis in control or siRNA treated extracts, indicating that further optimisation would be required (see section 3.3.6). Occludin protein expression appeared at a consistent level between controls and claudin-11 siRNA treatment (Figure 3.6).

3.3.6 Western blot optimisation for claudin-11 detection in Sertoli cell extracts

Claudin-11 was not detected in any of the Sertoli cell extracts which had been treated with ± claudin-11 siRNA, so a series of optimisation experiments was conducted, some of which are displayed in Figure 3.7. The first experiment examined three different claudin-11 antibodies from Zymed (Goat anti-rabbit, cat # 36-4500), CovalAb (Goat anti-rabbit, cat # pep0006) and AbCam (Goat anti-rabbit, cat # ab 7474), using mouse brain and rat testis tissue as positive controls (Figure 3.7a). Claudin-11 was never detected in reduced samples and was only detected at 22kDa in mouse brain extracts in non-reduced samples using the CovalAb and AbCam primary antibodies. Claudin-11 was not detected in the rat testis extracts with any of these antibodies

Given the failure to detect claudin-11 in the testis protein extract from 2 X non-reduced sample buffer, three other protein extraction buffers were used. These were the 1% SDS buffer outlined in section 2.5.1 (Wong *et al.* 2004), RIPA buffer (25mM Tris.HCl (Sigma), 150mM NaCl (Merck), 1% NP-40 (Sigma), 1% sodium deoxycholate, 0.1% SDS, pH 7.6) and RW buffer (20mM PBS, pH 7.2, 150mM NaCl (Merck), 50mM NaF (Sigma, cat # S-1504), 0.5mM Na_3VO_4 (MP

Figure 3.6 Western blot analysis of changes in the protein expression of occludin in response to claudin-11 siRNA treatment.

Protein was extracted from cultured immature rat Sertoli cell cultures two days after siRNA treatment with combined clau-11-A and clau-11-B siRNA. Claudin-11 was undetectable and so was omitted from this figure, but further optimisation pictures are presented in Figure 3.7. Occludin was positively stained at 64kDa as indicated by the arrow. Numbers above the western blot correspond to the lanes which consisted of the following: 1) control extract on day of siRNA addition; 2) control extract 2 days after siRNA addition; 3) siRNA treated extract on the day of siRNA addition; 4) siRNA treated extract 2 days after siRNA addition.

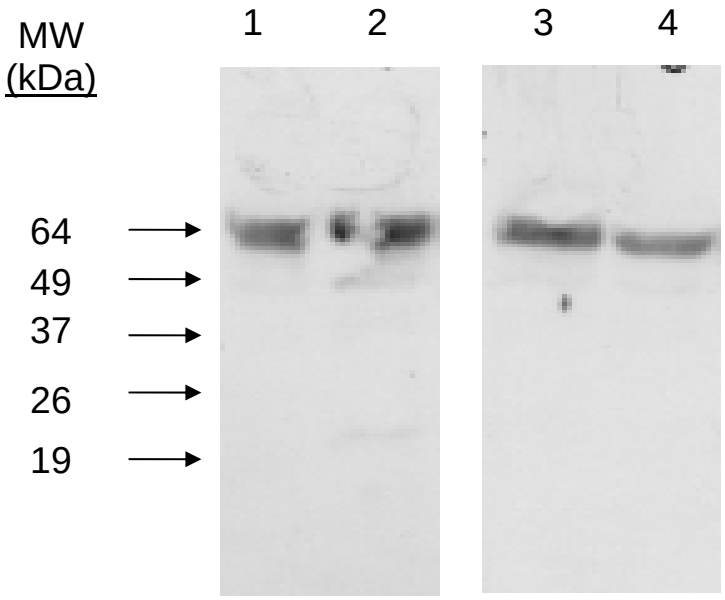
MW
(kDa)
1
2
3
4
64
49
37
26
19

Figure 3.7 Optimisation of western blot analysis for claudin-11 protein expression.

Following the inability to detect claudin-11 in Sertoli cell extracts, several experiments were conducted to optimise conditions for its detection in Sertoli cells, three of which are shown in this figure. The first experiment (panel A) was to detect claudin-11 in mouse brain as a control tissue, and rat testis extracts, with claudin-11 primary antibodies as follows: Lanes 1-2 are Zymed; Lanes 3-4 are CovalAb and Lanes 5-6 are AbCam. Lanes 7-8 are the negative controls for the mouse brain and rat testis respectively. Claudin-11 is indicated by the asterisk at 22kDa.

In the next experiments (panel B), three different protein extraction buffers were used to solubilise protein from mouse brain and rat testis, and the presented data in this Figure is for the AbCam antibody for claudin-11 detection. Lanes 1-3 are mouse brain extracts, with RIPA buffer, 1% SDS buffer, RW buffer. Lanes 4-6 are rat testis extracts with the buffers in the same order as for the mouse. Positive claudin-11 bands at 26kDa and 22kDa are indicated by the asterisks. Lane 7 is the negative control from a rat testis extract.

A final experiment attempted to detect claudin-11 (with the AbCam primary antibody) and β-actin as a loading control. Increasing amounts of protein from Sertoli cells extracted in 1% SDS were loaded as follows: 1) 7.5μg protein; 2) 15μg protein; 3) 30μg protein; 4) 60μg protein; 5) 120μg protein and 6) 120μg protein from a 1% SDS extract of rat testis. Claudin-11 staining at 22kDa and β-actin staining at 43kDa are indicated by asterisks.

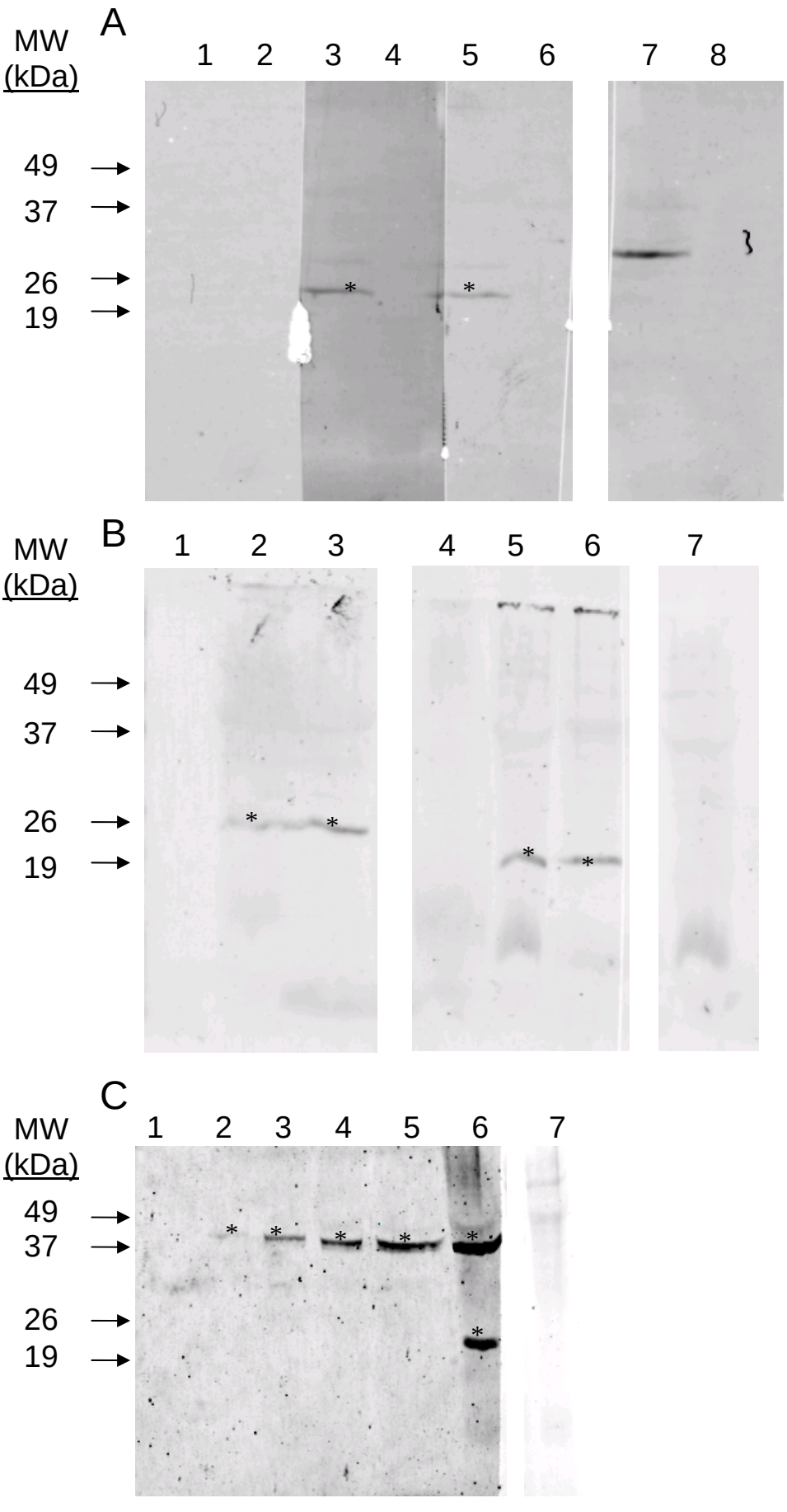
A
MW
(kDa)
1 2 3 4 5 6 7 8
49
37
26
19
*
*
B
MW
(kDa)
1 2 3 4 5 6 7
49
37
26
19
*
*
*
*
C
MW
(kDa)
1 2 3 4 5 6 7
49
37
26
19
*
*
*
*
*
*

Biomedicals, cat # 159664), 2% Triton-X100 (Sigma, cat # 57H0650) and 1 protease inhibitor complex tablet (PIC; EDTA-free, Roche, cat # 1873580), pH 7.2 (Chapin *et al.* 2001)). Each of the three new buffers contained protease inhibitors to stop degradation of protein in the extracts which may have been hindering claudin-11 detection. This second part of the experiment also used fluorescent second antibody detection with Odyssey software (section 2.5.3) instead of ECL.

Each of the three antibodies were again used in this part of the experiment and the result for AbCam is shown in Figure 3.7b. No claudin-11 staining was detected in either the mouse brain or rat testis extracts in RIPA buffer. Positive bands at 26kDa for the mouse brain and at 22kDa in the rat testis were obtained in the 1% SDS and RW buffers (Figure 3.7b). Staining was similar for the CovalAb antibody, but no positive staining was obtained using the Zymed antibody. Western blots for the latter two antibodies are not included in the Figure.

Based on this experiment, the 1% SDS buffer was chosen as the buffer of choice for extracting proteins from cultured Sertoli cells and the next experiment tested Sertoli cell extracts with doubling amounts of total sample protein concentration, using the AbCam primary antibody (Figure 3.7c). No claudin-11 was seen in any of the Sertoli cell extracts, despite increasing amounts of β-actin staining as a loading control. The rat testis positive control stained for both β-actin and claudin-11 (Figure 3.7c).

Subsequent westerns attempted protein extraction from Sertoli cells with RIPA and RW buffers, both to no avail. Further westerns were attempted to concentrate protein extracts, alter primary antibody and blocking protein preparations, alter incubation times, as well as treating extracts with endonucleases to rid samples of contaminating DNA. While claudin-11 was always detected in the rat testis, it was never detected reliably in Sertoli cell extracts. It was therefore decided to omit this endpoint from this study. It is noted that clear differences in claudin-11 expression could be observed by immunocytochemistry of these same cells.

3.3.7 Effect of occludin siRNA and combined claudin-11/occludin siRNA on tight junction function

Occludin specific occ-A and occ-B siRNA fragments were added separately or in combination with each other to cultured Sertoli cells with established TJs (Figure 3.8). After two days of treatment, TJ function had decreased by 51% for all three siRNA treatments ($p < 0.01$, n = 3 wells/treatment, n =

Figure 3.8 Effect of occludin siRNA, and combined claudin-11/occludin siRNA on TJ function.

Immature rat Sertoli cells were cultured and allowed to develop TJs over 6 days as measured by transepithelial electrical resistance (●). At day 6 as indicated by the arrow, one group of cells was treated with siRNA transfection reagent alone (○), while the other three treatments received occ-A siRNA (□), occ-B siRNA (Δ), both occludin siRNA strands together (◊) or a mixture of clau-11-B and occ-B siRNA (☆) for 2 days. At the end of the treatment period, cells were fixed for immunocytochemical analysis. Data is mean ± SD, n = triplicate wells/treatment. ** = $p < 0.01$ compared to day of treatment addition.

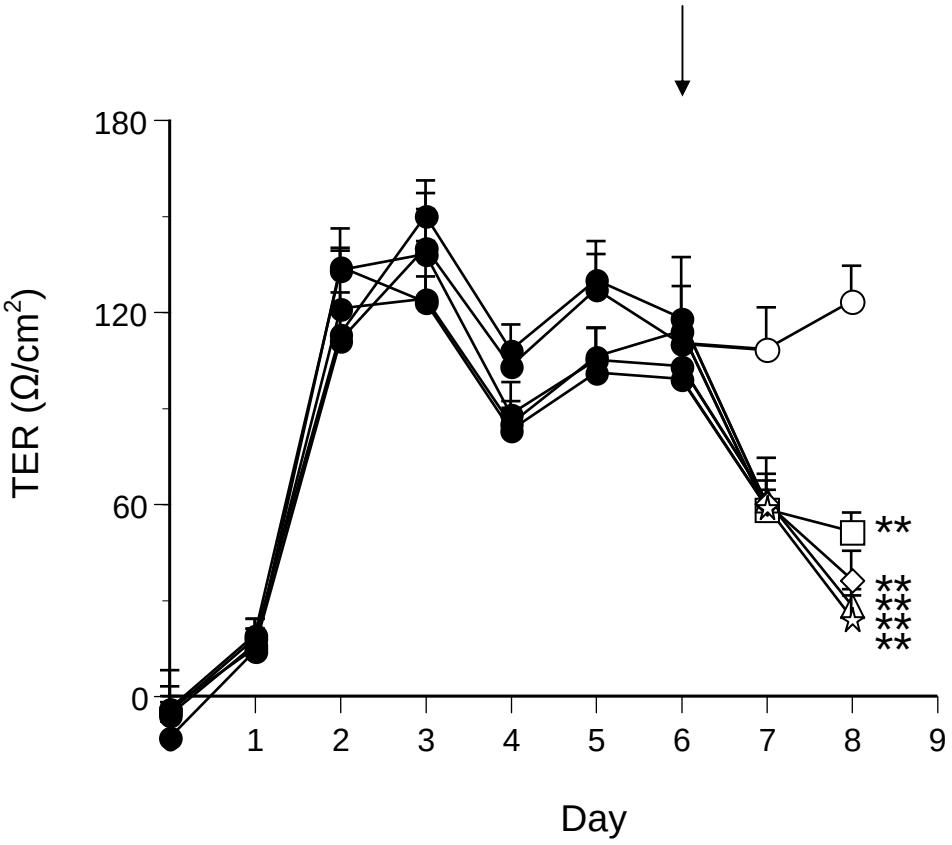
180
120
60
0
TER (Ω/cm2)
1
2
3
4
5
6
7
8
9
Day
**
**
**
**
**

2 cultures). The effect of treating Sertoli cells for 2 days with combined claudin-11-B siRNA and occludin-B siRNA was a 62% ($p < 0.01$, n = 3 wells/treatment, n = 1 culture) decrease in TJ function (Figure 3.8). This decrease was significant ($p < 0.01$) compared to the total 51% and 55% decrease in TJ function induced by occludin siRNA and claudin-11 siRNA separately over multiple cultures.

3.3.8 Effect of occludin siRNA and combined claudin-11/occludin siRNA on protein localisation

Cultured Sertoli cells were fixed after two days of siRNA treatment. Occludin siRNA reduced occludin localisation to the TJ (Figure 3.9). Claudin-11 localisation was extensive at the TJ and β-catenin was also extensive at the adherens junction yet appeared more punctate than seen in Figure3.4. The combination of claudin-11 siRNA with occludin siRNA reduced the localisation of both proteins to the TJ, while β-catenin was still extensive at the adherens junction (Figure 3.9).

3.4 Discussion

The aim of the work described in this Chapter was to determine the contribution of claudin-11 and occludin to rat Sertoli cell TJ function *in vitro*, using specific siRNA-mediated gene silencing. The immature rat Sertoli cell culture model was chosen as it is a well established culture model (Perryman *et al.* 1996, Kaitu'u *et al.* 2007), and because at 19-21 days of age, the only contaminating germ cells that are isolated along with the Sertoli cells are the most immature types (Chung *et al.* 1998), which were removed a few days after culturing by hypotonic shock treatment with a low-salt media. Hence, this method provides high purity Sertoli cells (>90% (Perryman *et al.* 1996)), with the remaining cells being predominantly peritubular myoid cells (Perryman *et al.* 1996).

Cultured Sertoli cells formed stable TJs 5-6 days after plating as shown by high TER readings. When the siRNA transfection reagent was added to the cells for 2 days, there was no decrease in TJ function demonstrating that it was not toxic to the cells over this time period. In response to 2 days of treatment with the siRNA control which targeted Lamin A/C, a protein of the nuclear envelope and unrelated to the TJ (Moss *et al.* 1993, Vester *et al.* 1993, Stuurman *et al.* 1998, Harborth *et al.* 2001), a non-significant reduction in TJ function of 22% was observed, thus indicating that any changes in TJ function with the TJ specific siRNA was not due to other non-specific effects. Other studies have also reported no significant effects of Lamin A/C-specific siRNA on TER (Mandell *et al.* 2005).

Figure 3.9 Effect of occludin siRNA and combined claudin-11/occludin siRNA on protein localisation to the TJ and adherens junction.

Cultured immature rat Sertoli cells were fixed after 2 days of occludin siRNA treatment and a combination of claudin-11 and occludin siRNA treatment. Immunocytochemical analysis was conducted for occludin, claudin-11 and the adherens junction protein β-catenin (all green) in response to the siRNA transfection reagent alone, occ-A siRNA and clau-11-B/occ-B siRNA. Sertoli cell nuclei are highlighted in red. Bar = 50μm. Inset = negative controls for occludin, claudin-11 and β-catenin.

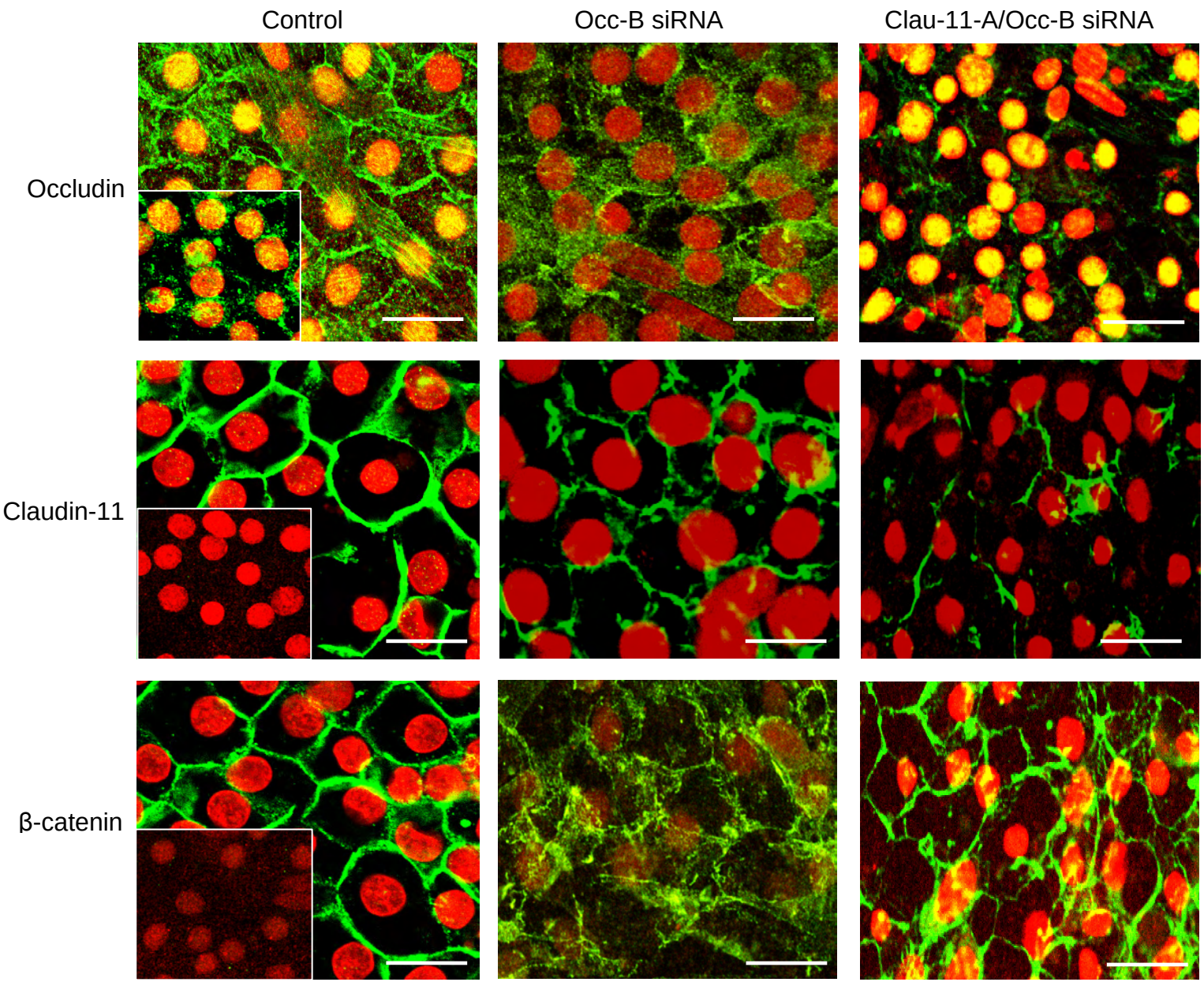
Control
Occ-B siRNA
Clau-11-A/Occ-B siRNA
Occludin
Claudin-11
β-catenin

When claudin-11-specific siRNA was added to stable TJs for 2 days, a decrease of 55% was recorded in TJ function as measured by TER. Similarly, a decrease of 51% in TER was observed after the addition of occludin-specific siRNA to established TJs, indicating the contribution of both proteins to TJ function was approximately 50%. This percentage figure could be argued as being relative to the experimental model, as the experiment had limitations on the siRNA:transfection reagent ratio and treatment time course (McCabe, 2003). As mentioned earlier, the McCabe (2003) study showed that breaching the 1:3 siRNA:transfection reagent ratio or using the ideal ratio for any longer than 2 days caused Sertoli cell death and their sloughing from the bicameral membranes. Therefore, it can only be concluded that both claudin-11 and occludin contribute to the function of the Sertoli cell TJ significantly, and that while this contribution may not be able to be given an empirical value in this model, the contribution of both proteins to TJ function is similar to each other.

This result was surprising, as it was expected that claudin-11 would have contributed more to TJ function than occludin, given the infertile phenotype of the claudin-11 knockout mouse (Gow *et al.* 1999), and the fertile phenotype seen in the young occludin knockout mouse (Saitou *et al.* 2000). In the claudin-11 and occludin knockout models, the ablation of either protein would have been 100%, and while no functional assays were conducted in those studies, to induce infertility it is presumed that knocking out claudin-11 reduced TJ function sufficiently. The percentage of claudin-11 or occludin ablation in the immature rat Sertoli cell culture model used herein could not be measured, although in the immunocytochemical analyses of protein localisation to the TJ following silencing, some staining of the ‘silenced’ protein was still apparent, albeit markedly reduced compared to controls (discussed later), thereby indicating that the ablation of claudin-11 or occludin was not 100%. This could have indicated the need to expose the cultured cells to the siRNA solution for longer but as already mentioned this was not feasible. The results obtained herein therefore raises the questions as to what extent claudin-11 needs to be removed from the TJ before its function is sufficiently suppressed to induce infertility, and also whether there are any differences between the contribution of claudin-11 and occludin to the TJ. The immature rat Sertoli cell culture model cannot answer the first question and due to the limitations on the methodologies used herein it cannot answer the second question either.

With the development of targeted delivery of siRNA to the testis *in vivo* (Shoji *et al.* 2005), it may be possible to deliver claudin-11 or occludin specific siRNA and observe the effect on spermatogenesis. With the increasing use of tracers (see Chapters 5 & 6) for TJ functional analysis, changes in TJ function both qualitatively and quantitatively could therefore be determined *in vivo*. As outlined in Chapter 1 (Section 1.4.2), tracers can provide a more detailed indication of changes in TJ function than TER. While TER measures fluctuations in TJ permeability, the use of tracers of varying sizes can measure changes in the size-selectivity of the TJ (Fanning *et al.* 1999).

It was expected in this study that silencing both claudin-11 and occludin in combination with each other would have caused a much greater suppression of TJ function than silencing either one of these proteins alone. This was not the case, with only a 62% decrease in TJ function recorded after 2 days of siRNA treatment against both proteins. Several reasons could be attributed to this result. Firstly, in order to maintain the appropriate siRNA:transfection reagent ratio, the experimental design employed in this Chapter was that the total siRNA component was comprised of a 50:50 mix of claudin-11 and occludin, thereby treating the cells with less than optimal amounts of either siRNA fragments and reducing the overall ablation of both proteins. Secondly, the treatment time may not have been long enough to completely silence both genes, and an extended time may have been required for the reduced amounts of siRNA, which was not feasible. Thirdly, the failure to completely suppress TJ function *in vitro* could have been due to other components of the TJ which contribute to its function. Such components could have been JAM-A, where siRNA targeted against this protein for three days in a human intestinal cell-line induced an 80% decrease in TER and a 5-fold increase in permeability to FITC-dextran (4kDa) (Mandell *et al.* 2005). Recently, another transmembrane protein called tricellulin was localised to the TJ at tricellular contacts between epithelial cells (Ikenouchi *et al.* 2005). While little work has been published with respect to tricellulin, siRNA targeted against it in a cultured mammary cell-line prevented TJ formation as shown by basal TER values compared to controls which had high TER readings (Ikenouchi *et al.* 2005). Furthermore, the permeability of the tricellulin-specific siRNA treated cells was 12-15 fold greater than controls to 4kDa FITC-dextran but not 250kDa FITC-dextran (Ikenouchi *et al.* 2005), indicating the potential contribution that tricellulin has to mammary TJ function. Ikenouchi *et al.* (2005) also showed that in the absence of tricellulin at the mammary TJ *in vitro*, occludin and claudin-3 staining had been altered suggesting that tricellulin

might maintain TJ structure and organisation as a whole. Similar findings were observed at the insect TJ analogue. Gliotactin, which is localised at tricellular contacts within the septate junction, was shown to establish its overall organisation (Schulte *et al.* 2003), suggesting a conserved trend for TJs and its analogues between different species. In the human, mutations in the tricellulin gene has been shown to cause deafness (Riazuddin *et al.* 2006, Chishti *et al.* 2008). These interesting findings present another possible protein contributing to the function of the Sertoli cell TJ, and while tricellulin has thus far not been localised to the Sertoli cell TJ, further analyses into its presence and/or role in the seminiferous epithelium should be conducted.

Cultured Sertoli cells were fixed 2 days after siRNA treatment for immunocytochemical analysis of claudin-11 and occludin, as well as any effects on the nearby adherens junction using β-catenin as the marker. The localisation of all three proteins was extensive in cells treated with the transfection reagent and Lamin A/C siRNA as also seen previously (Mandell *et al.* 2005). Interestingly, claudin-11 staining was marginally less intense in the Lamin A/C treatment group which may have reflected the non-significant 22% decrease in TJ function as recorded by TER. However staining was still extensive and these results therefore indicate that the Lamin A/C siRNA and transfection reagent had no significant effects on TJ or adherens junction structure. When cells were treated with claudin-11 siRNA for 2 days, claudin-11 staining was markedly reduced from the TJ compared to the controls, although not completely absent. Occludin and β-catenin staining were also partially reduced compared to controls although not to the same extent as claudin-11, thereby suggesting that the reduction of claudin-11 at the TJ may have some local effects on other TJ protein components such as occludin, and also have knock-on effects on other junctional types such as the adherens junction.

Similar data was obtained with the occludin siRNA treatment, where all three proteins were extensively stained in controls, but occludin staining was markedly reduced following 2 days of treatment. Claudin-11 and β-catenin localisation were also partially reduced compared to controls, indicating that the removal of occludin may also have some local and broader effects on other junctional types. When siRNA was targeted against both claudin-11 and occludin, the localisation of both proteins was reduced at the TJ, whereas β-catenin staining was still apparent at the adherens junction.

Total RNA was extracted from the cultured Sertoli cells 2 days after claudin-11 siRNA addition for RT-PCR analysis of changes in mRNA expression. The transfection reagent and Lamin A/C siRNA controls had zero to minor effects on claudin-11 mRNA expression, yet following claudin-11 siRNA treatment, there was a marked 71% reduction in claudin-11 mRNA expression. While occludin mRNA decreased in the claudin-11 siRNA treated cells, it also decreased in the control cells demonstrating that the decrease in the former treatment was not due to a non-specific effect of the siRNA. The reduction of claudin-11 mRNA expression was in good agreement with the reduction of claudin-11 protein localisation to the TJ, which caused the significant loss in TJ function.

Unfortunately, the relationship between changes in mRNA and protein expression as a result of the claudin-11 specific siRNA could not be determined. Several different methods of attempting to optimize claudin-11 detection by western blot analysis failed to provide a suitable method for the quantitation of this protein in cultured Sertoli cells. These methods included i) use of different extraction buffers containing various detergents to solubilise claudin-11 from the cultured cells, ii) the inclusion of protease inhibitors to prevent protein digestion in the extracts, iii) the addition of DNA endonucleases to prevent the ‘sticky’ genetic material of the cells that is released after lysing from interfering with protein extraction, iv) modifying extracting conditions (boiled buffers versus room temperature), protein reduction or non-reduction, use of different claudin-11 antibodies in conjunction with various incubation conditions and detection protocols and v) concentrating protein samples within extracts to maximize detection. Some of the results from these experiments were displayed in Figure 3.7, but none of these methods worked to enable claudin-11 detection from Sertoli cells, and so this endpoint was not completed. Claudin-11 expression was observed in rat testis, hence it is presumed that the issue was related to sensitivity, but this was not proven.

In contrast, occludin was much easier to detect by western blot analysis, and showed no change in response to 2 days of claudin-11 siRNA treatment, again displaying the specificity of the siRNA for claudin-11. The expected result for the claudin-11 western would have been a marked reduction in claudin-11 protein expression. This appears to be a feasible assumption as claudin-11 siRNA reduced claudin-11 mRNA expression and protein staining in the Sertoli cells, which points to a reduction in protein content as well. Interestingly, when testis quality controls (QCs) were included in the western blot optimisation experiments, claudin-11 was easily detectable. It may be simply that

the number of plated Sertoli cells was not enough to provide detectable claudin-11. It may also be plausible in future to conduct an siRNA study *in vivo* as mentioned previously and analyse changes in claudin-11 expression in the whole testis where it is easier to detect. In the testis, claudin-11 is only localised to the Sertoli cell TJ (Lapierre, 2000), so any positive staining would be specific for this site, and not other testicular cell types.

Interestingly, this was not the first study to apply siRNA targeted against epithelial TJ proteins. PALS1 is a protein involved in a complex that binds to ZO-3 of the cytoplasmic plaque and is involved in establishing cellular polarity (Straight *et al.* 2004). siRNA targeted against PALS1 in MDCKII cells, delayed the polarisation of the MDCKII cells and TJ formation as shown by basal TER values compared to control *in vitro* (Straight *et al.* 2004). Interestingly, the loss of PALS1 also disrupted the localisation and expression of another protein (PATJ) involved in the same complex and disrupted complex-complex interactions essential for polarisation establishment. It is interesting that siRNA targeted against one protein can indirectly effect the expression of another. Similarly in this study, the localisation of occludin was effected by the reduction of claudin-11 localisation at the Sertoli cell TJ. Neither of these results appeared to be due to non-specific siRNA effects. Hence, it is hypothesised that a further use of siRNA could be to indirectly enhance the understanding of protein-protein and even complex-complex interactions by observing what happens to some proteins after the loss of another.

siRNA targeted against claudin-4 in cultured human respiratory epithelial cells, caused an approximate 75% reduction in TJ function as measured by TER *in vitro* (Johnson and Quay, 2005). Furthermore, claudin-4 specific siRNA was able to inhibit TJ formation in freshly cultured cells (Johnson and Quay, 2005). It was the aim of that study to determine how siRNA could aid in changing the function of the TJ for potential nasal drug deliveries. In the testis, siRNA has also significantly reduced TJ function when targeted against claudin-11 and occludin. It may also therefore provide a tool at identifying a suitable Sertoli cell TJ target protein for hormonal based contraception in men. As reviewed in Chapter 1 (Section 1.8), several studies have now analysed the contributions of other claudins and occludin to other epithelial types and have shown that both proteins have significant roles in maintaining TJ function and integrity (Agarwal *et al.* 2005, Yu *et al.* 2005, Hou *et al.* 2006, Ueda *et al.* 2007, Fujita *et al.* 2008, Phillips *et al.* 2008).

In conclusion, claudin-11 and occludin contribute significantly to the function of the Sertoli cell TJ *in vitro*. Selective knock-down of claudin-11 and occludin has indicated that both proteins appear important to the role of the TJ in maintaining its functional and structural integrity. Given that both proteins contributed approximately 50% to TJ function *in vitro* after 2 days of siRNA treatment in this model, it is necessary to conduct further studies to i) analyse the contribution of other integral transmembrane components such as JAM-A and possibly tricellulin to TJ function and/or ii) to conduct *in vivo* siRNA studies to further define the role of these proteins to Sertoli cell TJ function with the use of quantitative tracers.

Chapter Four: The optimisation and application of tracers for tight junction functional analysis, *in vivo*

Chapter 4. The optimisation and application of tracers for tight junction functional analysis, *in vivo*

4.1 Introduction

The previous Chapter revealed the importance of claudin-11 and occludin to the function of the Sertoli cell TJ *in vitro*, after selective ablation of both proteins using siRNA- mediated gene silencing. The ensuing three Chapters of this thesis will look at the *in vivo* changes in protein localisation, protein expression and/or mRNA expression of TJ proteins in the absence of circulating hormones, and what happens when hormones are given or replaced. As well as these endpoints, a functional test is needed to analyse the changes in TJ function following hormone withdrawal and replacement *in vivo*.

In the previous Chapter, TER was used to analyse TJ function *in vitro*. For *in vivo* analyses, small molecular weight tracers have been used for the past several decades to analyse changes in TJ function induced by various causes (Egan *et al.* 1976, Setchell *et al.* 1981, Pelletier, 1986, Pelletier, 1988, Setchell *et al.* 1988, Eng *et al.* 1994, Setchell *et al.* 1996, Lustig *et al.* 2000, Furuse *et al.* 2002, Nitta *et al.* 2003, Meng *et al.* 2005, Hutcheon *et al.* 2007, Tarulli *et al.* 2008). These have included genetic knockouts (Furuse *et al.* 2002, Nitta *et al.* 2003, Meng *et al.* 2005) and keratectomy (Hutcheon *et al.* 2007) among other causes (for full details, see Chapter 1, Section 1.4). For example, low molecular weight tracer biotin (~600Da) could not penetrate intact TJs in wildtype mice but readily crossed the blood-brain barrier in the claudin-5 knockout mice (Nitta *et al.* 2003) and the epidermal TJ in the claudin-1 knockout mice (Furuse *et al.* 2002). The application of a tracer (Gd-DTPA; 742Da) detectable by MRI to the claudin-5 null blood-brain barrier showed that TJ function had decreased by 15% (Nitta *et al.* 2003), thus providing an *in vivo* model in which TJ function had been analysed both qualitatively with the biotin tracer, and quantitatively with the MRI tracer (Nitta *et al.* 2003).

In the testis, tracers for the qualitative assessment of TJ function such as HRP (44kDa) (Pelletier, 1986, Pelletier, 1988, Lustig *et al.* 2000) and biotin (~600Da) (Tarulli *et al.* 2008, Meng *et al.* 2005) are both restricted to the interstitium and only enter the seminiferous tubules as far as the Sertoli cell TJ in various control animal models which are undergoing normal spermatogenesis (Pelletier, 1986, Pelletier, 1988, Lustig *et al.* 2000, Meng *et al.* 2005, Tarulli *et al.* 2008). These results

indicate the presence of functional TJs. Yet, when spermatogenesis ceases in the same animal models, either due to seasonal testicular regression or genetic knockouts, both tracers have been seen to permeate throughout the tubules indicating dysfunctional TJs (Pelletier, 1986, Pelletier, 1988, Pelletier, 1994, Meng *et al.* 2005, Tarulli *et al.* 2008).

Quantitative TJ functional analyses as outlined in Chapter 1 often utilise radiolabelled tracers such as [^{3}H]methoxy-inulin (~5kDa), to allow a measure of functionality to be made. A 10-fold increase in the accumulation of the [^{3}H]methoxy-inulin tracer compared to controls, has been observed in the seminiferous tubules from rats whose Sertoli cell TJs were disrupted via an intratesticular injection of glycerol (Eng *et al.* 1994).

The aim of the work presented in this Chapter is to optimise methodologies to allow Sertoli cell TJ function to be assessed both qualitatively and quantitatively *in vivo*, for use in the ensuing Chapters of this thesis. These methodologies will include an assessment of the administration route for the tracers, as well as subsequent testis processing for optimal TJ function analyses.

For quantitative TJ functional analyses, this Chapter will use the published glycerol-treated rat model to open testicular TJs (Eng *et al.* 1994), in an attempt to replicate the results obtained for [^{3}H]methoxy-inulin accumulation in seminiferous tubules after 4 weeks of glycerol treatment.

4.2 Materials and Methods

4.2.1 Animals

Male outbred-Sprague Dawley rats at 9 days of age (juvenile) and 75-90 (adult) days of age were obtained from Monash University Animal Services, Monash University (Melbourne, Australia). All experimental work conducted on rats was approved by the Monash Medical Centre Animal Ethics Committee (ethics number: MMCB 2006/19). Following experimentation, rats were killed by CO_2 asphyxiation. Nine day old rats were killed by cervical dislocation.

4.2.2 Experimental design for qualitative tight junction function analysis

Immediately after death, testes were dissected from rats and injected with 30mg/ml HRP (Type II (Sigma cat # P8250)) in saline (Lustig *et al.* 2000) or 10mg/ml Biotin (EZ-Link Sulfo-NHS-

LC-Biotin (Pierce, cat # 21335, Rockford, IL, USA) in PBS + 1mM $CaCl_2$ (Meng *et al.* 2005) at 10% testis volume. This volume was approximately 200µl for adult rat testes using a 1ml syringe (Becton Dickinson, Singapore) attached to a 26G needle (Terumo, Tokyo, Japan), and 2µl into juvenile (9 day old) rat testes using a displacement syringe (5µl, SGE, Australia).

Testes were then left at room temperature for 30 minutes to allow the tracer to spread throughout (Russell *et al.* 1989, Meng *et al.* 2005). For the HRP tracer, testes were then snap frozen on dry ice, or fixed in one of the following fixatives; Bouin's (Meachem *et al.* 1996), paraformaldehyde (3g paraformaldehyde (BDH-Merck, Kilsyth, Vic, Australia) in 100ml PBS), formalin (10g formaldehyde (BDH-Merck, Kilsyth, Vic, Australia) in 100ml PBS), carnoys (10% acetic acid (Merck, Damstadt, Germany), 60% ethanol (Ajax Finechem, Seven Hills, NSW, Australia), 30% chloroform (BDH, Poole, England, UK) and methacarn (10% acetic acid, 60% methanol (Merck, Damstadt, Germany), 30% chloroform) for varying lengths of time at room temperature (except for methacarn which was done on ice). For the biotin tracer, testes were snap frozen or fixed for 5 hours in Bouin's or paraformaldehyde at room temperature.

Testes were then processed for immunohistochemistry as outlined in Section 2.2, and stained for HRP or biotin, and sometimes occludin as the TJ marker. For HRP and occludin antibody incubation details, see Table 4.1. Light and fluorescent microscopy were conducted on the sections.

Staining for biotin was conducted directly using the streptavidin SA Alexa-488 (diluted 1:100 (adult) and 1:800 (9 day old); Molecular Probes, Eugene, USA) probe. When co-staining with another protein (ie. occludin), the SA Alexa-488 was diluted into the secondary antibody solution for that protein. When staining for biotin alone, SA Alexa-488 was diluted in PBS and administered to the tissue section after antigen retrieval for 30 minutes. Afterwards, the sections were washed three times in PBS and mounted as per the desired immunohistochemistry protocol in Section 2.2.

4.2.3 Experimental design for quantitative tight junction functional analysis

Adult rats were anaesthetised with isofluorane (Abbott, UK) and received intratesticular injections of 20% glycerol to open the blood testis barrier, or vehicle (sterile saline) (n = 5/group) at a volume of 10% of the testis weights using a 26G needle attached to a 1ml syringe (Eng *et al.* 1994). It was assumed that the testis weights for these animals would have been approximately 2.0g, based on

Table 4.1 Antibodies used for immunohistochemical analysis.

Tabulated data for the antibodies used in Chapter 4 of this thesis include details regarding the primary and secondary antibody hosts, working concentrations (conc.)/dilutions, incubation (Inc.) times and company details with catalogue numbers.

Protein	**Primary (1^o) antibody host**	**Company** (cat #)	**Conc.** (μg/ml)	**Negative control**	**1^o Inc. time**	**Secondary (2^o) antibody**	**Company**	**2^o Dilution**	**Inc. time** (mins)
Occludin	Rabbit	Zymed (71-1500)	2.0	Normal rabbit IgG	30 minutes	Goat α rabbit Alexa-488	Molecular Probes	1:400 of stock	30
HRP	Mouse	AbCam (ab8326)	5.0	Normal mouse IgG	Overnight	Goat α mouse Alexa-546 **or** goat α mouse HRP conjugated	Molecular Probes (Alexa) **or** Silenus	1:400 (Alexa) **or** 1:100 (Silenus)	30

published data (Meachem *et al.* 1998). To minimize localised pain, rats received a subcutaneous injection of the analgesic carprofen (Rimadyl: Lypard, cat # ZEKE, Victoria, Australia) at 5mg/kg in the shoulder immediately after the glycerol injection, while still anaesthetised. Rats were then allowed to recover, and monitored daily for 3 days, and thereafter every 3 days for 4 weeks to check for any adverse reactions to the intratesticular injections. No such reactions were ever observed.

Four weeks after the glycerol injection, rats were killed by CO_2 asphyxiation. Testes were dissected from 4 of the rats/group and trimmed of all connective tissue, fat and epididymides and then weighed. The testes from the fifth rat from each group was also trimmed and then injected with biotin for qualitative TJ functional analysis as outlined above.

The first set of testes from above were decapsulated in a tissue culture laminar flow cabinet and seminiferous tubules were isolated. Three segments of approximately 80mg were taken from each isolated clump of seminiferous tubules and incubated in 1ml of [^{3}H]methoxy-inulin (0.5μCi; MP Biomedicals, cat # 0127029H-2) in Krebs Ringer Phosphate Buffer (KRP: 130mM NaCl, 5mM KCl, 1.3mM $CaCl_2$, 1.3mM $MgSO_4$, 10mM Na_2HPO_4, pH 7.4) (Chaika *et al.* 1999) at 34^{o}C for 1 hour. Tubules were then rinsed three times in cold KRP and then suspended in 5ml of MilliQ water in 15ml Falcon tubes (Sarstedt, South Australia, Australia). The suspensions were then homogenised (Polytron, PT 10 20 3500, top speed, 10 seconds) and a 0.5ml aliquot taken and resuspended in 1.5ml of tissue solubilizer (Soluene-350, PerkinElmer, Boston, MA, USA) overnight at room temperature. The remainder of the homogenate was snap frozen and stored at -20^{o}C. The following day, the homogenate/tissue solubiliser solution was incubated at 50^{o}C in a water bath for 5 hours to dissolve the tissue. At the end of this period, 2 x 100μl additions of 3% H_2O_2 was pipetted into the solutions and left to incubate for a further 30 minutes at 50^{o}C. Afterward, 10ml of scintillation fluid (LSC Cocktail, Perkin Elmer, cat # 6013389) was added to the solution, which was vortexed vigorously and left at room temperature for 24 hours, before the radioactivity that had accumulated in the seminiferous tubules was read and quantified on a scintillation spectrophotometer (Packard, 2500TR Liquid scintillation analyser, Amersham Biosciences (GE)).

4.2.4 Statistical analysis

Statistical analysis was conducted as outlined in Section 2.6 for 2 samples. Data has been presented as mean ± SD with n = 4 rats/group.

4.3 Results

4.3.1 Qualitative tracer optimisation

a. Intratesticular injection of Trypan Blue dye

Methods of delivering substances to the testis have included whole body perfusions through other arteries or veins (Meachem *et al.* 1996, Setchell *et al.* 1996, Meachem *et al.* 1998, Tao *et al.* 2000) or perfusions directly into the testicular artery (Lustig *et al.* 2000, Cambrosio *et al.* 2003), which is easily distinguishable in rats, mice and rabbits due to its wavy or coiled morphology (Chubb and Desjardins, 1982). The latter method was attempted with some success (Figure 4.1) however replicating the results was difficult so an alternative method was sought.

The intratesticular injection was considered to be the easiest and most direct means of tracer administration to the testis. The efficacy of injecting a tracer into a freshly isolated testis of a dead adult rat at 10% testis weight was analysed using Trypan Blue dye (Figure 4.2). The dye immediately spread throughout the testis and could be seen through the scrotum. The testis was then frozen and 10μm sections cut on a microtome in the cryostat, which showed the inner part of the testis as a pale blue color. This test established that intratesticular injection was a suitable technique for delivery of dye-containing solutions throughout the organ.

b. Detection of HRP tracer in frozen and Bouin's fixed testes by fluorescent microscopy

TJ qualitative tracer HRP was probed in frozen and paraformaldehyde- or Bouin's-fixed rat testes to determine which tissue fixation method was best for detection (Figure 4.3). No HRP staining was apparent in the sections using either fixation protocol although high background was detected in the paraformaldehyde-fixed testis. HRP was co-localised with the TJ protein occludin which was detected in each of the fixed testes (Figure 4.3). In the frozen testes, bright HRP staining was observed

Figure 4.1 Testicular artery perfusions.

A direct method of administering tracers to the testis is through the testicular artery itself, either by cannulating it or perfusing into it via a thin haematocrit tube. The testis is dissected, trimmed of all fat and connective tissue and placed so that the testicular artery (arrow) is facing up at the researcher (panel A). The haematocrit tube (panel B) is rubbed along the artery with saline running through until it ruptures as indicated by the release of blood. At this point, the haematocrit is held in position and the saline or tracers are released directly into the testis through the perforated artery. A successful perfusion is indicated by the drainage of the artery and all testicular veins which turns the testis into an opaque white (panel C, right).

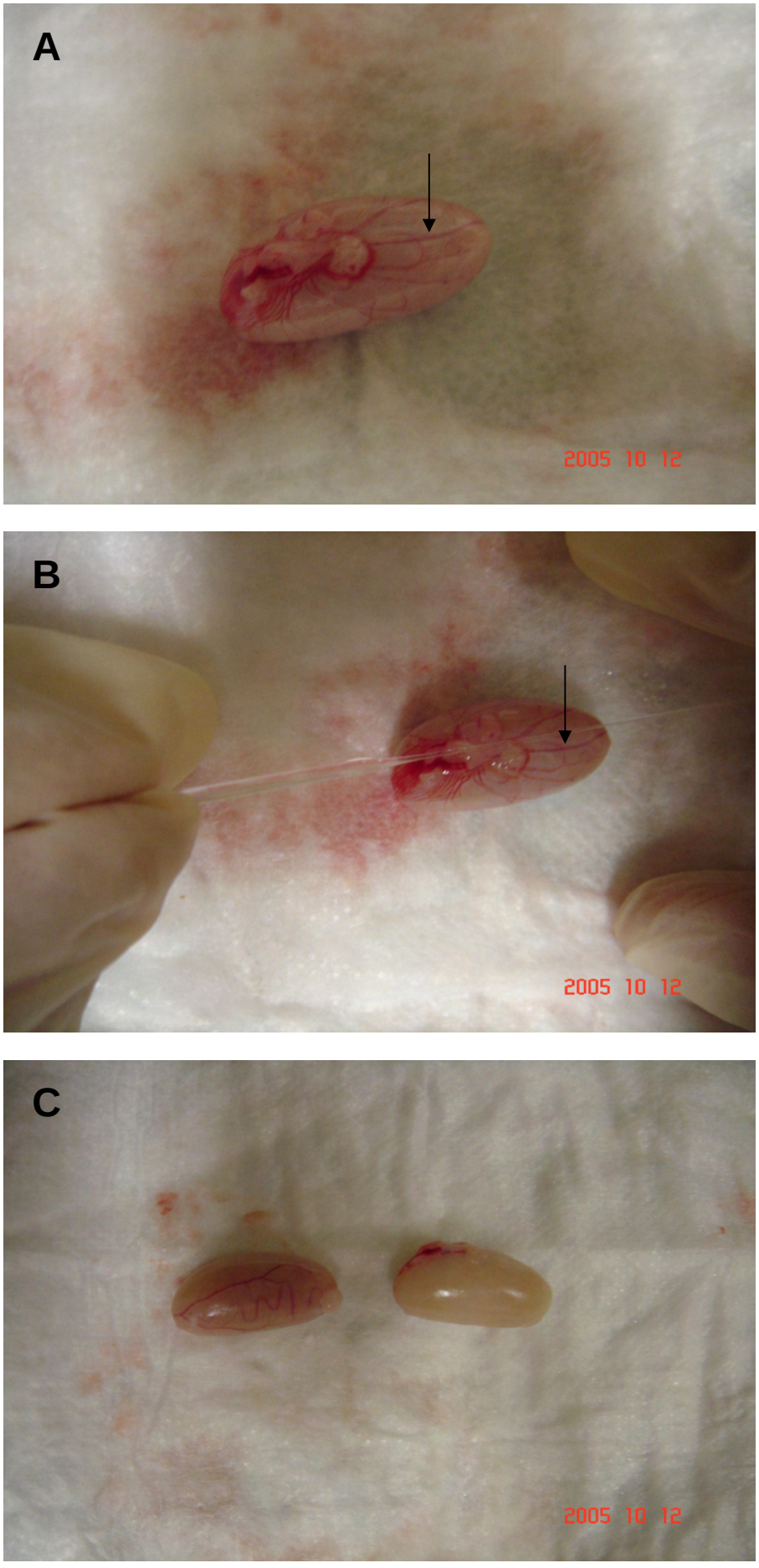
A
2005 10 12
B
2005 10 12
C
2005 10 12

Figure 4.2 Intratesticular injection of Trypan Blue dye.

For the intratesticular injection, the testis was held under a bright lamp and the testicular artery visualized for orientation (panel A). A 26G needle was inserted through to one pole of the testis and the solution injected while withdrawing the needle through the other pole. Trypan blue dye was injected into the left testis (asterisk, panel B) of a freshly killed adult rat at 10% testis volume (200µl) with PBS being injected into the right testis. The extent of spread was apparent after the testis was dissected out of the animal and trimmed of all fat and connective tissue (panel C, left). To check that the dye had spread throughout the inside of the testis and not just around the edge, the testis was frozen, and cut on the cryostat. The internal color of the Trypan Blue injected testis (panel D) was compared with the internal color of the PBS injected testis (panel E).


A


B
*

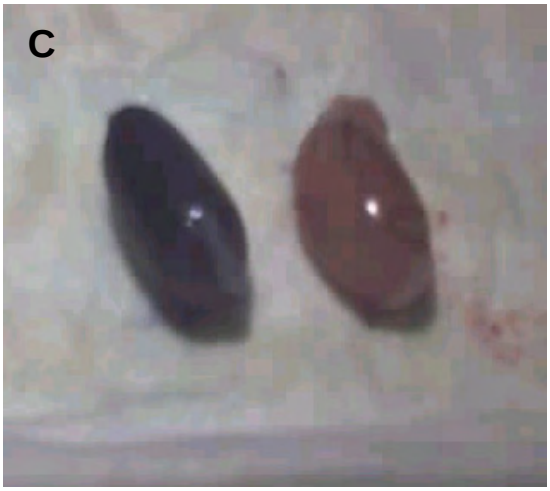
C

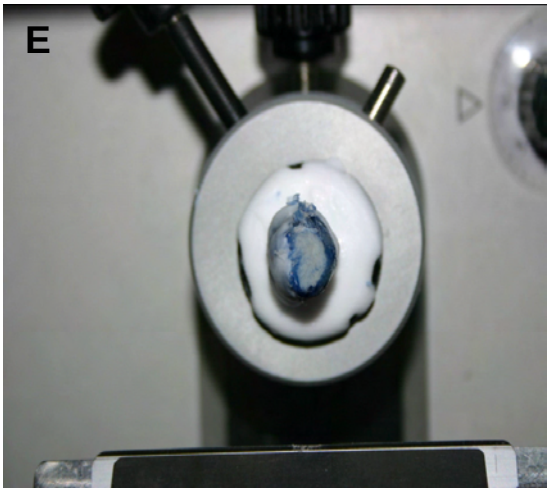
E

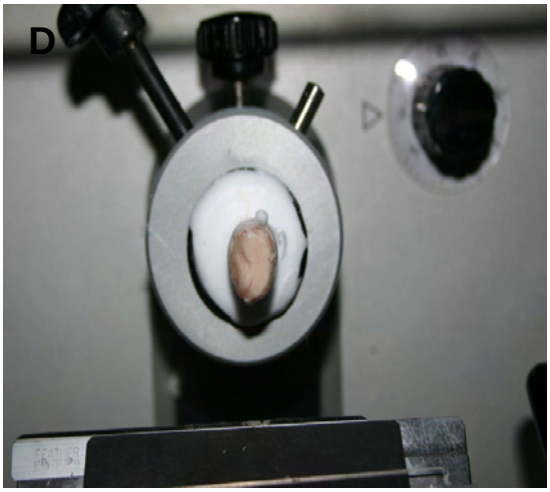
D

Figure 4.3 HRP tracer localisation in frozen and paraformaldehyde, and Bouin's fixed testes.

HRP was administered to testes via an intratesticular injection at 10% testis weight before testes were frozen (panel A), or fixed in paraformaldehyde (panel B) or Bouin's (panel C) for 5 hours. HRP (red, asterisk) was co-localised with occludin (green, arrows) to mark the Sertoli cell TJs. The co-localisation of HRP with occludin gives a yellow color. Bar = 50μm. Inset = negative controls for HRP and occludin except in panel B, where left and right insets are separate negatives for occludin and HRP respectively.

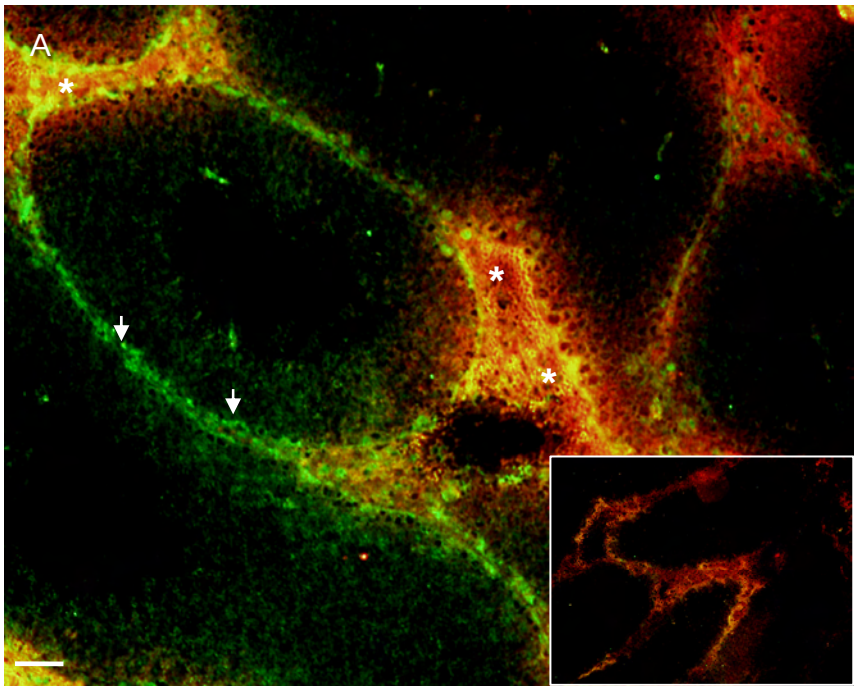
A

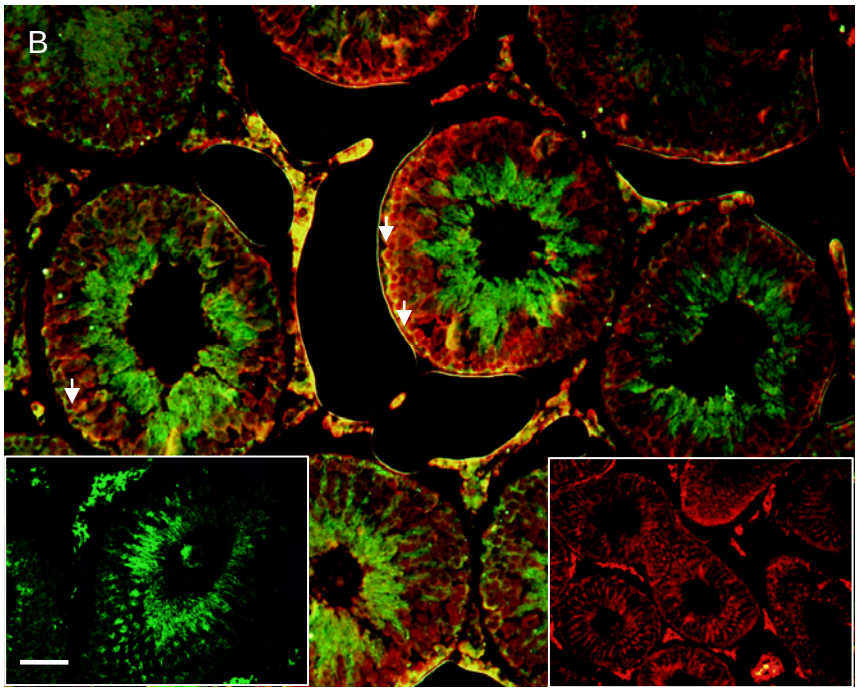
B

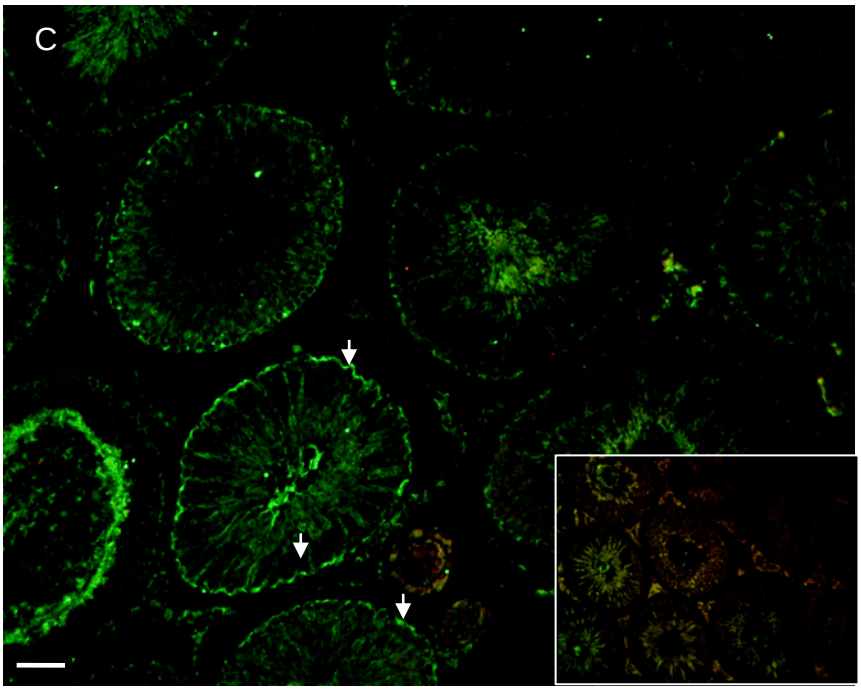
C

in the interstitium and only permeated the seminiferous tubules as far as the TJ as highlighted by occludin (Figure 4.3). The negative control displayed a duller version of the HRP stain in the interstitium.

c. Detection of HRP tracer in frozen and fixed testes by light microscopy

As the previous experiment had shown that HRP staining was sensitive to fixation, an additional experiment was conducted to monitor HRP immunoactivity in testes which had been fixed for varying lengths of time in various aldehyde containing fixatives (Bouin's, paraformaldehyde, formalin), non-aldehyde containing fixatives (carnoys, methacarn), and in testes which had been snap frozen on dry ice (Table 4.2). HRP was not detectable in any of the fixed testes at any of the fixation time points, despite heavier background being apparent in some sections (Table 4.2). However, HRP staining was readily apparent in the interstitium of the frozen testes, and this staining did not permeate throughout the seminiferous tubules (Table 4.2). The negative control for the frozen testis displayed a fainter version of the positive control, indicating the probable presence of endogenous peroxidases in the interstitium. This experiment indicated that HRP staining was only detectable in frozen testis tissues.

d. Detection of Biotin tracer in frozen and fixed testis

Biotin was probed with streptavidin Alexa-488 in adult frozen testes as well as Bouin's and paraformaldehyde fixed testes. In each testis, biotin stained strongly in the interstitium and did not enter the seminiferous tubules (Figure 4.4). By light microscopy, biotin was seen entering the seminiferous tubules only as far as the spermatogonia (Figure 4.4d and e).

e. Detection of Biotin in a prepubertal rat testis

To ensure that biotin could access the entire seminiferous epithelium in situations where TJs were not functional, testes from immature (day 9) rats which lack TJs were examined. Biotin was probed in a Bouin's fixed, 9 day old rat testis, and co-stained with occludin for fluorescent microscopy. No occludin staining was visible, and biotin was extensive in the interstitium and permeated throughout the seminiferous tubules (Figure 4.5a). In tubules which were injected with the

Table 4.2 Localisation of HRP tracer in fixed or frozen testes.

Testes were extracted from adult rats and injected with 30mg/ml HRP at 10% testis weight and left at room temperature for 30 minutes. The testes were then either snap frozen on dry ice or fixed in Bouin's, paraformaldehyde, formalin, carnoys or methacarn for different lengths time as indicated in the table. Testes were then processed for immunohistochemical analysis of HRP localisation (asterisk), using the DAB light microscopy protocol. Bar = 50μm. Inset = negative control.

Time / Fixative	1 hour	2 hours	5 hours	Overnight
Bouin's		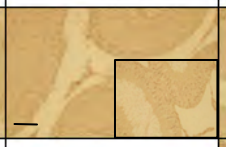		
Paraformaldehyde	N/A	N/A		
Formalin	N/A	N/A	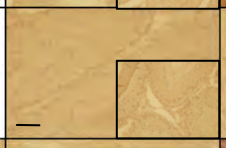	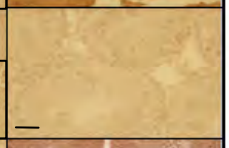
Carnoys		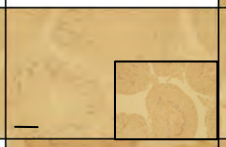	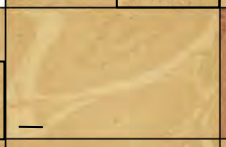	
Methacarn	N/A	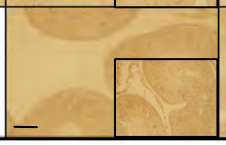		

Frozen

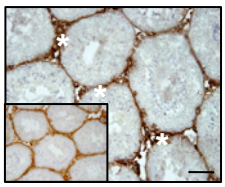

Figure 4.4 Biotin tracer localisation in frozen and paraformaldehyde and Bouin's fixed testes.

Biotin was administered to rat testes at 10% testis weight and incubated for 30 minutes at room temperature. The testes were then i) snap frozen on dry ice (panel A), ii) fixed in paraformaldehyde for 5 hours (panel B) or iii) fixed in Bouin's for 5 hours (panel C) before being processed by immunohistochemistry. Analysis was conducted by fluorescent microscopy (panels A-C) for biotin (green, asterisk) and occludin (red, arrow, with co-localisation giving a yellow appearance. Analysis was also conducted by VIP light microscopy (panel D) for biotin (arrow heads) localisation with respect to different germ cell types. A higher magnification of a biotin perfused testis analysed by light microscopy is shown in panel E. Bar = 50μm. Inset = negative control

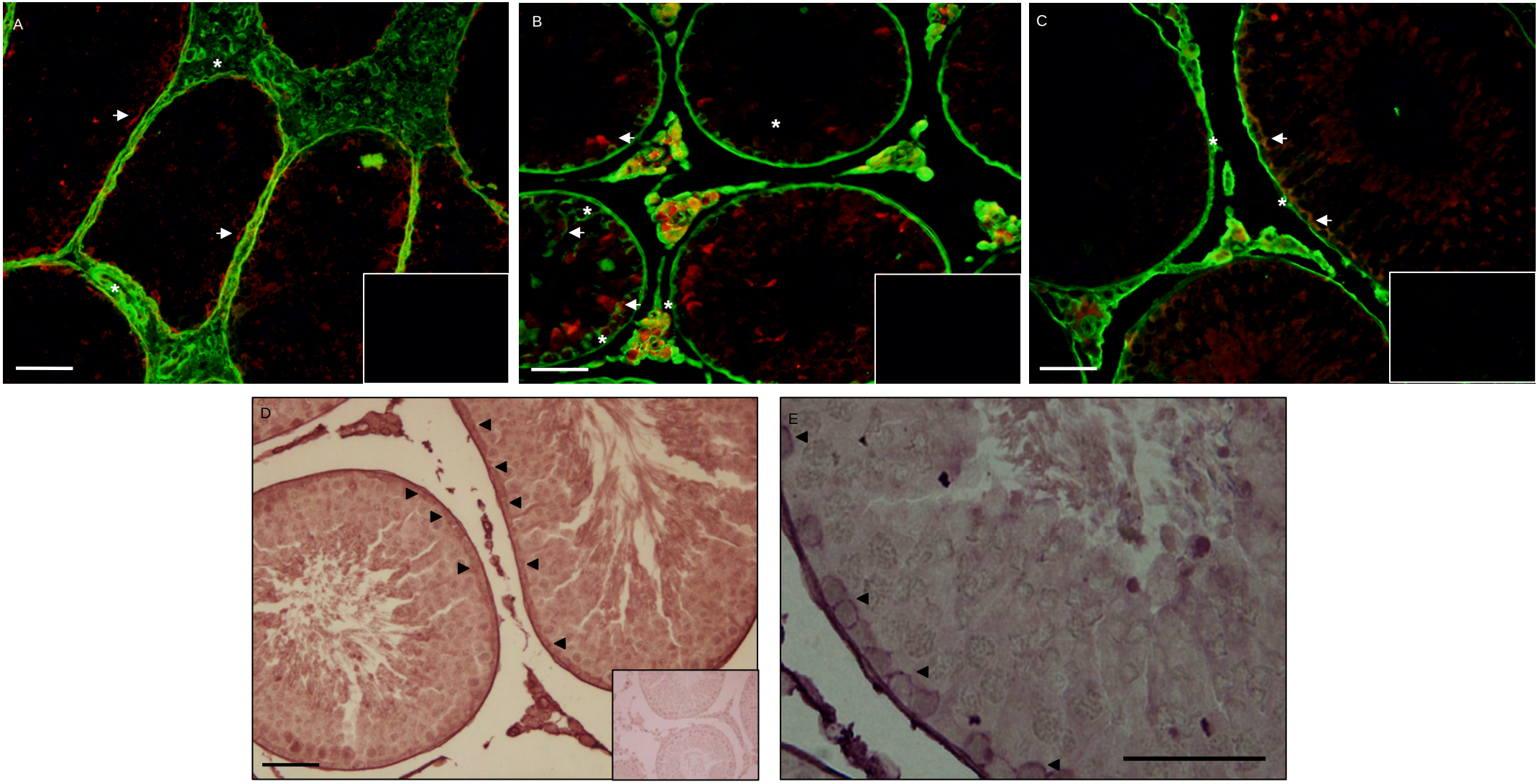
A
B
C
D
E

Figure 4.5 Biotin localisation in prepubertal rat testes.

Biotin was administered to the testes of a 9 day old rat at 10% testis weight, which was then fixed in Bouin's fixative and processed for immunohistochemistry. Streptavidin was used to probe biotin by fluorescent microscopy (panel A, green, asterisk), and co-localised with occludin (red). Testes had also been injected with PBS as vehicle control and were also probed for biotin (only) as a negative control (panel B). In addition, Vector VIP light microscopy was conducted for biotin detection in testes which had been injected with biotin (panel C, brown, asterisk), or with the PBS vehicle control (panel D). Bar = 50μm. Inset = negative control. Note that panel A is a confocal micrograph.

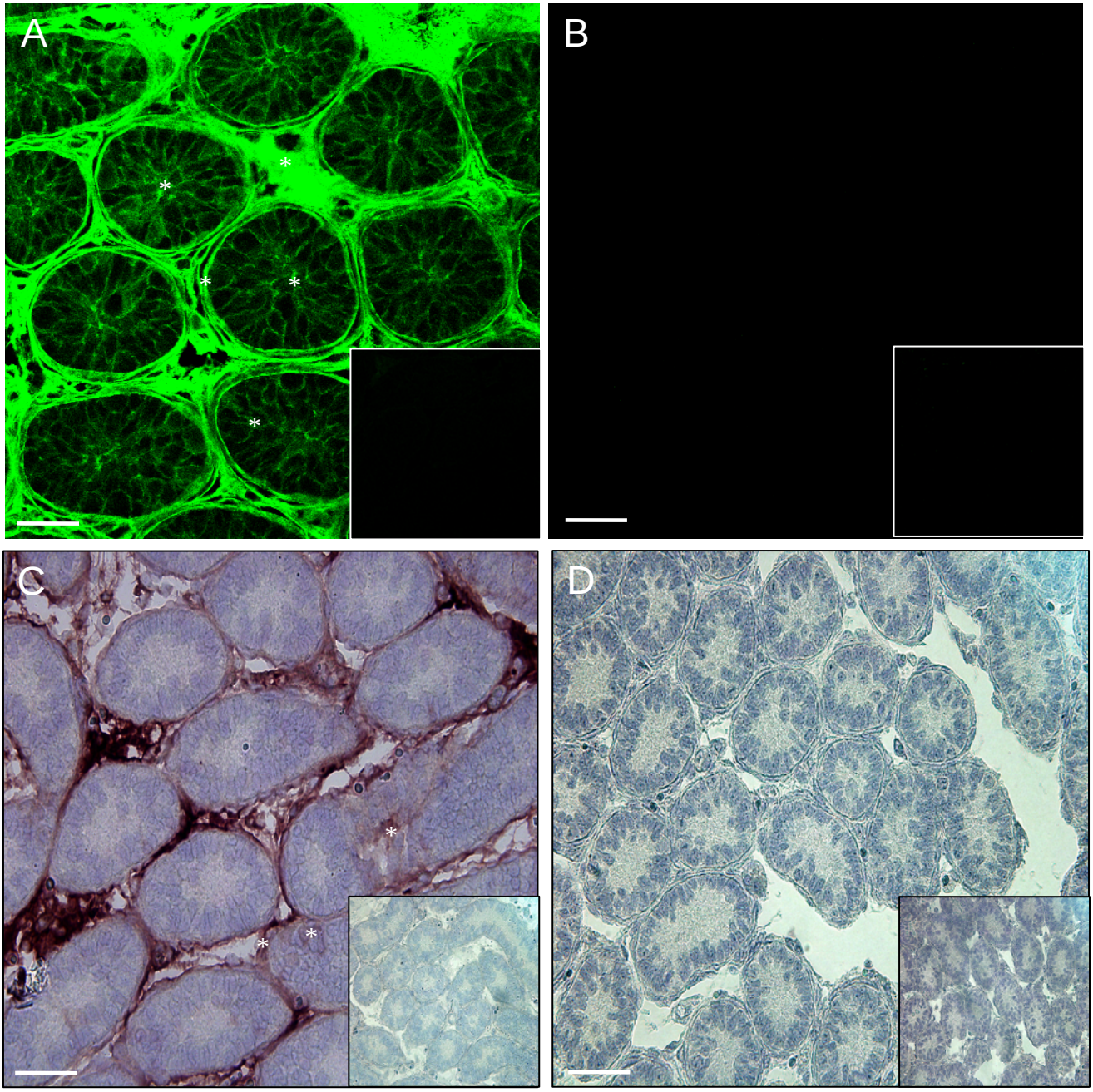
A
B
C
D

biotin vehicle control (PBS) and probed for biotin only, no biotin was detected (Figure 4.5b). By light microscopy, biotin staining was visible in the interstitium, and inside the seminiferous tubules (Figure 4.5c). The PBS vehicle control showed no biotin staining by light microscopy (Figure 4.5d).

4.3.2 Quantitative tracer optimisation

Eng *et al.* (1994) demonstrated with [^{3}H]methoxy-inulin tracer (~5kDa) that TJ function had quantitatively decreased 10 fold following an intratesticular injection of 20% glycerol. This was coincident with occludin no longer localised at the Sertoli cell TJ (Wiebe *et al.* 2000). Maximal disruption was achieved within 2 weeks of glycerol treatment with no further changes to TJ function over one year (Eng *et al.* 1994). This Chapter follows the experimental design of Eng *et al.* (1994) to determine the suitability of [^{3}H]methoxy-inulin for quantitative TJ functional analyses and the use of the glycerol treated rat model as a positive control for Chapter 5.

a. Effect of glycerol treatment on testis weights and seminiferous tubule accumulation of [^{3}H]methoxy-inulin

As mentioned above, maximal disruption of TJ function was achieved 2 weeks after 20% glycerol treatment in a published study, with no further changes in proceeding weeks (Eng *et al.* 1994). A dose higher than 20% caused damage to seminiferous tubules (Igdoura and Wiebe, 1994), therefore for this thesis, a dose of 20% glycerol for four weeks was chosen for experimentation.

Four weeks after glycerol treatment body weights had not changed, but testis weights were reduced to 61% ($p < 0.001$) of controls (Figure 4.6a and b respectively). Glycerol treatment reduced TJ function to 55% of controls ($p < 0.001$) as shown by a 45% greater accumulation of the [^{3}H]methoxy-inulin tracer in the glycerol treated seminiferous tubules (Figure 4.6c).

b. Effect of glycerol treatment on tubule morphology and biotin permeation into the seminiferous tubules

Four weeks after glycerol treatment varying degrees of seminiferous tubule disruption were seen. Four common phenotypes were observed; i) morphologically normal seminiferous tubules with extensive biotin permeation throughout (Figure 4.7a), ii) morphologically normal tubules with some

Figure 4.6 Effect of glycerol treatment on TJ function.

20% glycerol or saline was injected directly into the testis at 10% of testis weights while animals were under isofluorane anaesthesia. Four weeks after the injection, rats were killed and body weights (panel A) and testis weights (panel B) measured. Seminiferous tubules were then isolated and exposed to the radioactive tracer [^{3}H]methoxy-inulin for 1 hour at 34^{o}C. Tracer accumulation in glycerol and control tubules was measured by scintillation spectrophotometry (panel C). Data is mean ± SD, n = 4/group, *** = $p < 0.001$.

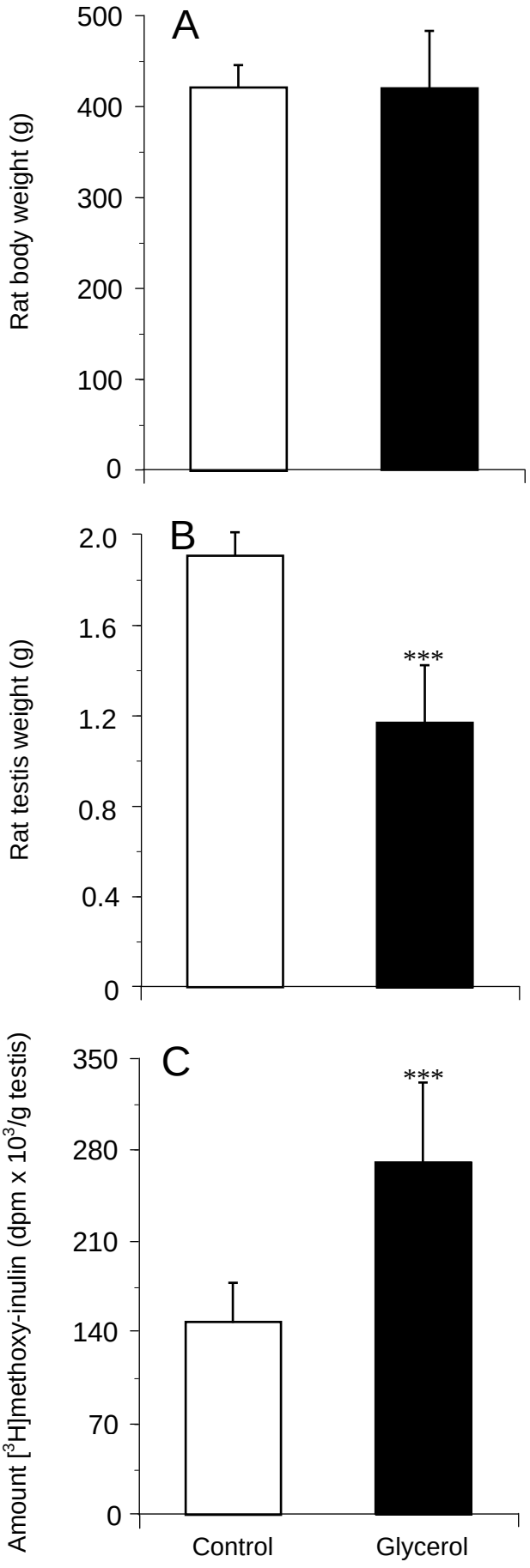
A
500
400
300
200
100
0
Rat body weight (g)
B
2.0
1.6
1.2
0.8
0.4
0
***
Rat testis weight (g)
C
350
280
210
140
70
0
***
Amount [3H]methoxy-inulin (dpm x 10^3/g testis)
Control
Glycerol

Figure 4.7 Effect of glycerol on seminiferous tubule morphology and biotin migration across Sertoli cell TJs.

Four weeks after an intratesticular injection of 20% glycerol, testes were collected from adult rats, fixed in Bouin's fixative and processed for confocal immunohistochemical analysis of biotin (green) and TJ protein occludin (red) localisation. Several phenotypes were observed and are displayed here. Bar = 50μm. Inset = negative control.

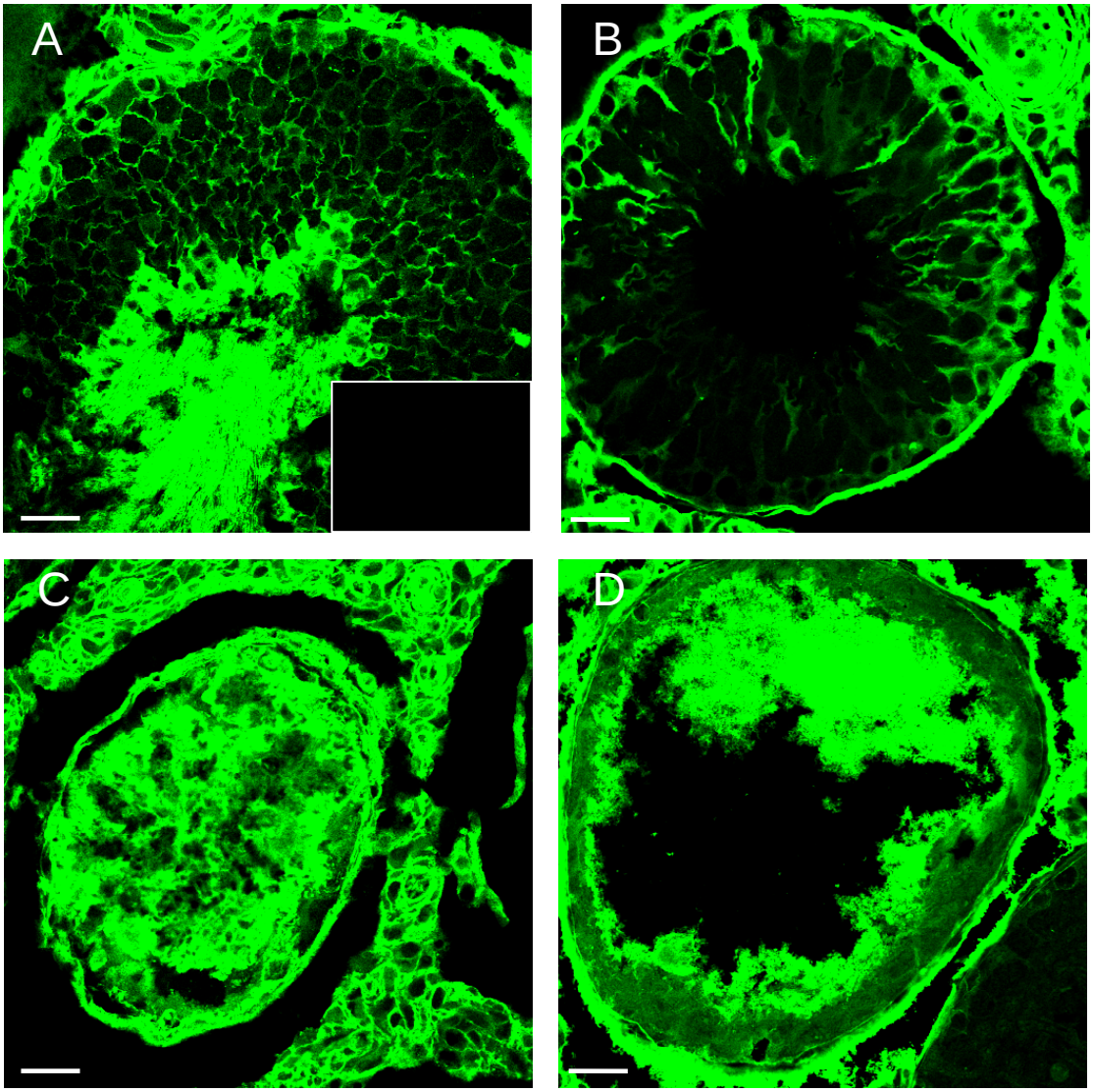
A
B
C
D

biotin permeation (Figure 4.7b), iii) shrunken tubules with no lumens and extensive biotin permeation (Figure 4.7c), and iv) tubules with large lumens and very few cell types with extensive biotin permeation (Figure 4.7d). This positive control further demonstrated that the biotin permeability technique worked as expected.

4.4 Discussion

Studies presented in this Chapter aimed to optimise tracers for qualitative and quantitative TJ functional analysis in the testis for the ensuing *in vivo* studies.

In order to achieve the above aim, it was necessary to optimise a route of administration for the tracers. While the perfusion of the tracers into the testis through the testicular artery proved difficult, the ease and feasibility of directly injecting the tracer into the testis was shown after a Trypan Blue dye injection spread immediately throughout the testes. This result was similar to published data which showed that a smaller injection of Trypan Blue spread 2cm through the testes within 5 minutes, and throughout the testes within 2 hours (Russell *et al.* 1987). Russell *et al.* (1987) further demonstrated that the injection itself caused no damage to the seminiferous tubules (Russell *et al.* 1987). Injection volumes vary in the literature from 40-400µl/g testis weight, with most studies using 100-200µl/g (O'Shaughnessy, 1980, Russell *et al.* 1987, Eng *et al.* 1994, Chung *et al.* 2001, Melaine *et al.* 2003). The amount used in studies presented herein were 100µl/g, which was a value in the middle of the range of published injection volumes.

For qualitative TJ functional analysis, HRP was the first attempted tracer optimisation. HRP was undetectable in testes which had been fixed in Bouin's or paraformaldehyde for 5 hours, but was visible in frozen testes. The use of frozen tissue was not ideal however, as the negative controls gave a weaker version of the positive stain in the interstitial tissue, and the testis morphology was poor, which is a typical feature when using frozen tissue sections (Whiteland *et al.* 1997).

For better morphology, it was considered necessary to fix the testes, and so a follow up experiment tested the ability to detect HRP in testes fixed for varying lengths of time (1, 2 and 5 hrs, and overnight) in Bouin's, paraformaldehyde and formalin, as well as in the non-aldehyde containing fixatives carnoys and methacarn. For better visualisation of the tracer with respect to the germ cells in the seminiferous epithelium, HRP was stained using the DAB light microscopy protocol. HRP was

undetectable in any of the fixatives at any of the time-points, although morphology was generally well preserved. This result was surprising particularly for carnoys and methacarn, as further review of the literature found that fixation in aldehyde containing fixatives for greater than 50 minutes destroys the HRP signal which accounted for why the tracer was undetectable in Bouin's, paraformaldehyde or formalin. In the frozen testes, HRP was visible in the interstitium, only permeating the tubules around the spermatogonia as seen previously by electron microscopy (Pelletier, 1986, Pelletier, 1988, Pelletier, 1994). Again the morphology was sub-optimal and biotin was sought as a better alternative.

The biotin tracer technique has recently been successfully applied to evaluate blood-testis barrier function in the Sertoli cell specific androgen receptor knockout mouse model (Meng *et al.* 2005). The testis sections in that study were again frozen. This Chapter was able to replicate those results successfully in adult rat testes, as shown by strong biotin staining in the interstitium and permeation into the seminiferous tubules only as far as the TJ marker occludin. However, the morphology was again sub-optimal as evidenced by the shrunken appearance of the seminiferous tubules. In contrast, in testes fixed in either Bouin's or paraformaldehyde, a similar biotin staining pattern was observed to the frozen testes, but with ideal morphology. This was in direct contrast with the HRP tracer which was undetectable in the fixed testis sections. Light microscopy displayed biotin staining at the TJ just above the early spermatogonial cells, with no biotin staining adluminally to the spermatogonia, indicating fully functional TJs (Pelletier, 1986, Pelletier, 1988, Lustig *et al.* 2000, Meng *et al.* 2005).

As a positive control for TJ function, biotin localisation was assessed in a 9 day old prepubertal rat testis, which lacks TJs. Biotin staining localised extensively in the interstitium and permeated throughout the seminiferous tubules, and this was coincident with an absence of occludin staining. Based on the success of the biotin localisation in conjunction with the good morphology in Bouins-fixed tissues, this tracer technique was chosen for all *in vivo* qualitative TJ functional analysis in this thesis.

[^{3}H]methoxy-inulin was assessed as a tracer for the quantitative functional analysis of testicular TJs, based on its previous application to testicular tissues (Eng *et al.* 1994). To determine the effectiveness of this tracer, it was necessary to employ a model which is known to disrupt TJs as a positive control. Testicular glycerol treatment has been associated with the restructuring of

cytoskeleton to which the TJ is indirectly linked, so in effect, causes TJ disassembly (Wiebe *et al.* 2000). These tissues displayed an absence of occludin localisation to the TJ after a 2 week treatment period with 20% glycerol, and this phenotype persists for at least 1 year, despite glycerol reportedly being cleared from the general circulation within 24 hours (Wiebe *et al.* 1986, Eng *et al.* 1994, Wiebe *et al.* 2000). Various glycerol concentrations had been tested in previous studies ranging from 10%-70% (Eng *et al.* 1994, Igdoura and Wiebe, 1994, Wiebe *et al.* 2000). An injection of 70% glycerol resulted in focal destruction of tubules, and some of these were acellular (Weinbauer *et al.* 1985, Wiebe *et al.* 1986), whereas in testes which received smaller glycerol concentrations (10%-20%), spermatogenesis was suppressed without damage to the tubules (Igdoura and Wiebe, 1994). Therefore, an injection directly into the tests containing 20% glycerol was chosen for this study. At no stage did the rats display any sign of pain or discomfort as a result of the injection.

Four weeks after glycerol treatment to adult rats no effect on body weights compared to controls was observed, but testis weights were significantly reduced 39%. This was comparable with a 37% decrease in testis weights obtained in a separate study using 20% glycerol (Igdoura and Wiebe, 1994). These authors also analysed testis weights at 1, 2, 8 and 56 weeks after glycerol administration, and found no differences across this time course (Igdoura and Wiebe, 1994), suggesting that extending the exposure of rats in this study to glycerol would have had no additional effect on the testes. Some scarring at the injection site and among the seminiferous tubules in the immediate vicinity of the injection site was apparent in this study, but nothing was visible deeper within the testis.

Seminiferous tubules were isolated from glycerol-treated and control- (vehicle treated) testes and exposed to [^{3}H]methoxy-inulin according to a published protocol (Eng *et al.* 1994). Accumulation of the tracer in glycerol tubules was approximately 2 fold higher than in control tubules, suggesting a quantitative disruption in TJ function after 4 weeks of glycerol treatment. The degree of disruption however, was somewhat lower than expected, as in the Eng *et al.* (1994) study a 10-fold accumulation of the tracer was observed in tubules following 4 weeks of glycerol treatment. This difference between the results could be due to the experimental protocol which appeared to be crude in design. Other means of measuring [^{3}H]methoxy-inulin penetration of the TJ would technically have been possible to improve this design, such as collecting and measuring tracer accumulation in rete testis fluid, seminiferous tubule fluid, interstitial fluid or the whole testis (Eng *et al.* 1994).

Alternatively, the extent to which glycerol had induced TJ disruption may have been important. Fluorescent microscopy of the glycerol treated testes which received the biotin tracer, showed disruption of TJ function qualitatively as indicated by the permeation of biotin into the seminiferous tubules. Interestingly, it was also seen that four phenotypes or degrees of tubule and/or spermatogenic disruption existed (see Figure 4.7), which were comparable to similar phenotypes previously published (Wiebe *et al.* 2000).

As shown in Figure 4.7 of this Chapter, 'normal' spermatogenesis appeared to be taking place, with all germ cell types adluminal to the TJ present (Figure 4.7a). However, biotin had readily permeated through the TJ and was surrounding these adluminal germ cell types, suggesting that the TJ was not entirely functional, and that it did not need to be entirely functional for spermatogenesis to continue. In other words, the effect of glycerol had not disrupted TJs sufficiently to disrupt their function in some tubules. Other studies have also demonstrated that the TJ in the blood-testis-barrier, as well as in the blood-brain-barrier does not need to be fully functional to main barrier integrity (Setchell *et al.* 1981, Setchell *et al.* 1988, Nitta *et al.* 2003). This possibility may also explain why the quantitative difference in TJ function between glycerol and control testes was so small, in that inulin (5kDa) was too large to cross the marginally disrupted TJ, which had become permeable to biotin (~600Da). More definitive experiments are needed to confirm this hypothesis. Also evident, were some tubules in Figure 4.7 appeared completely disrupted, with an apparent acellular morphology as reported with higher doses of glycerol (Weinbauer *et al.* 1985, Wiebe *et al.* 1986). The biotin accumulation in these tubules was great, and it would be expected that inulin accumulation in those tubules would also be great. The other two pictures in Figure 4.7 displayed phenotypes which appeared to be in between 'normal' spermatogenesis and completely disrupted spermatogenesis. The final outcome on quantitative TJ functional analysis would therefore depend on the proportion of tubules with completely disrupted TJs compared to those with marginally disrupted TJs. This proportion was not determined in this thesis, but may be required in the future with similar experiments. Regardless, the [^{3}H]methoxy-inulin tracer will be used for quantitative TJ functional analysis in the next Chapter, which will look at the effect of hormone suppression and replacement on the TJ *in vivo*.

In conclusion, methods to assess the qualitative and quantitative function of testicular TJs *in vivo* have been examined, with biotin tracer and [^{3}H]methoxy-inulin respectively chosen as the two methods to be used. Biotin was readily detectable in Bouin's fixed tissue, which is important as Bouin's maintains good tubule morphology and allows easy identification of germ cell types and biotin localisation. HRP on the other hand would only work in frozen tissue sections, which does not maintain good morphology. [^{3}H]methoxy-inulin accumulation in glycerol treated testes was 2-fold higher than in control testes, suggesting its availability as a quantitative TJ functional marker for the next study.

Chapter Five: Hormonal regulation of the Sertoli cell tight junction in the gonadotrophin releasing hormone (GnRH)-antagonist treated rat, *in vivo*

Chapter 5. Hormonal regulation of the Sertoli cell tight junction in the gonadotrophin releasing hormone (GnRH)-antagonist treated rat, *in vivo*

5.1 Introduction

Hormone suppression using various animal models has been used in the past to analyse the regulatory roles of testosterone and/or FSH on spermatogenesis (see Chapter 1 section 1.7). GnRH is a hormone released from the hypothalamus and stimulates the pituitary to release i) FSH, which interacts directly upon Sertoli cells, and ii) LH, which stimulates testicular Leydig cells to produce testosterone which then acts on Sertoli cells. GnRH antagonism involves inhibiting the GnRH stimulus at the pituitary level by administration of a GnRH antagonist, typically by subcutaneous injection.

All published GnRH antagonists suppress LH/testosterone and FSH to basal levels soon after the initial injection, and given that hormonal suppression is maintained, the testis regresses with reductions in germ cell numbers, leading to a cessation of spermatogenesis (Jiang *et al.* 2001, Broqua *et al.* 2002, Herbst *et al.* 2002, Hild *et al.* 2004, Matthiesson et al. 2005b, Porter *et al.* 2006). Where GnRH antagonists vary is in their duration of effectiveness after a single dose (Jiang *et al.* 2001, Broqua *et al.* 2002) and propensity to stimulate histamine release (Jiang *et al.* 2001, Broqua *et al.* 2002) Most antagonists such as Nal-Glu, Cetrorelix, Abarelix and Ganirelix, suppress gonadotrophins for 1 day (Kangasniemi *et al.* 1995, Jiang *et al.* 2001, Broqua *et al.* 2002) therefore requiring multiple doses to maintain suppression for any given period of time. Degarelix, which is a relatively new GnRH antagonist, suppresses gonadotrophins for 6 weeks after a single dose (Jiang *et al.* 2001, Herbst, 2003) but at the time of experimentation, this antagonist was not commercially available.

Another GnRH antagonist acyline, has very low histamine release properties (Jiang *et al.* 2001, Broqua *et al.* 2002), and is relatively long acting at suppressing hormones, where a single subcutaneous dose in the rat suppresses LH/T for approximately 10 days (Porter *et al.* 2006). Furthermore, it is still effective at fully suppressing hormones after multiple doses (Hild *et al.* 2004). Acyline treatment has been applied to rats (Jiang *et al.* 2001, Hild *et al.* 2004, Porter *et al.* 2006) and humans (Herbst, 2003, Matthiesson et al. 2005b). Hence, its effects on spermatogenesis are well known, which makes it a good candidate for studying the effect of hormone suppression on the rat Sertoli cell TJ *in vivo*.

It is hypothesised that gonadotrophin suppression with acyline in adult rats will disrupt Sertoli cell TJ function and structure and that short-term hormone replacement will restore TJ function and structure. The aim of the work presented in this Chapter is therefore to determine the effect of gonadotrophin suppression and subsequent short-term hormone replacement on Sertoli cell TJ function and structure.

Gonadotrophin suppression will be induced by weekly doses of acyline to groups of rats for 7-8 weeks to fully suppress spermatogenic activity. This time-point was chosen as rats were rendered azoospermic and infertile after 8 weeks of GnRH immunisation in a previous study using a similar model (Awoniyi *et al.* 1992b, Awoniyi *et al.* 1993). Furthermore, these rats displayed testis weights which were comparable to another study which used the same GnRH immunisation protocol for 12 weeks (Meachem *et al.* 1998). Therefore, 7-8 weeks of acyline treatment was considered sufficient to cause maximal suppression of spermatogenesis which was thought necessary to induce changes in the Sertoli cell TJ. Following hormone suppression, hormones will be selectively replaced via a short-term (1 week) treatment regimen using i) human recombinant FSH (hrFSH) (Pratis *et al.* 2003, McLachlan *et al.* 1995); ii) human chorionic gonadotrophin to stimulate testicular production of testosterone and FSH (Pratis *et al.* 2003) and iii) human chorionic gonadotrophin + FSH antibody to stimulate the testicular production of testosterone alone. This short-term replacement regimen was chosen based on published protocols from very similar GnRH immunisation models (McLachlan *et al.* 1995, Meachem *et al.* 1998, Pratis *et al.* 2003), which have quantified changes in germ cell numbers and serum/testicular steroids and FSH thus potentially drawing some interesting and useful parallels between this study and the GnRH immunisation studies.

For qualitative and quantitative TJ functional analysis, the biotin and [^{3}H]methoxy-inulin tracers which were optimised in the previous Chapter, will be used respectively. Changes in TJ protein localisation as well as protein and mRNA expression will be monitored by immunohistochemistry, western blot analysis and real-time RT-PCR analysis after hormone suppression and short-term replacement. Results from this Chapter will describe the role hormones have in maintaining the Sertoli cell TJ.

5.2 Materials and Methods

5.2.1 Animals

Male outbred-Sprague Dawley rats at 75-90 days of age were obtained from Monash University Animal Services, Monash University (Melbourne, Australia). All experimental work conducted on rats was approved by the Monash Medical Centre Animal Ethics Committee (ethics number: MMCB 2006/19). Following experimentation, rats were killed by CO_2 asphyxiation.

5.2.2 Experimental design

FSH and LH/T were suppressed by weekly subcutaneous injections of acyline (donated by Dr Richard Blye, National Institute of Health, MD, USA) for 7 weeks into adult rats at 1.5mg/kg in sterile 5% mannitol/MilliQ water (Porter *et al.* 2006), administered as single injections to the hind flank or shoulder (500µl/site). Control rats received a subcutaneous injection of the vehicle alone (n = 10). The preparation of acyline involved dissolving 0.3g of acyline powder (which had been stored at 4^{o}C until use) in 100ml of sterile 5% mannitol/MilliQ water in a tissue culture laminar flow cabinet. This gave a final concentration for acyline of 3mg/ml. 10ml aliquots were snap frozen on dry ice and stored at -20^{o}C for the duration of the experiment (maximum = 8 weeks). Aliquots were only thawed once when required for use, with residual amounts being re-frozen and stored at -20^{o}C in case extra acyline was required.

After gonadotrophin suppression, rats (n = 10/group) in the eighth week received an additional dose of acyline in conjunction with short-term hormone replacement (daily, for 7 days) by subcutaneous injections with one of the following; i) hrFSH (25 IU/kg) (Puregon; Organon, Holland) (Meachem *et al.* 1998, Pratis *et al.* 2003), ii) hCG (2.5 IU/kg) (Pregnyl; Organon, Holland) + FSH Antibody (Ab) (sheep anti-rat, 2mg/kg) to investigate testicular production of testosterone alone (Meachem *et al.* 1998) and iii) hCG (2.5 IU/kg) + normal sheep immunoglobulins (2mg/kg) to investigate testosterone and FSH production (Meachem *et al.* 1998). Three more groups of rats (n = 10/group) continued to receive i) acyline vehicle, ii) acyline + FSH Ab (daily, sheep anti-rat, 2mg/kg) to suppress residual FSH, and iii) acyline + normal sheep immunoglobulins (daily, 2mg/kg) (Meachem *et al.* 1998, Pratis *et al.* 2003), daily for a further week. Note that the dose of FSH Ab chosen has

previously been shown to neutralise >90% of circulating FSH in a very similar rat model (Meachem *et al.* 1998). Note also that the acyline + normal sheep immunoglobulin group meant that one of the rat groups in this study, received acyline alone for a total of 8 weeks.

hrFSH, hCG, FSH Ab and normal sheep immunoglobulins were all prepared fresh on the day of use and were injected into the hind flank or shoulder in a 0.5ml volume. Preparation details were as follows: 150 IU hrFSH was dissolved in 1ml of saline (0.9% NaCl in MilliQ water). This was then diluted in 5ml of saline to give a final concentration of 25 IU/ml. 500 IU of hCG was dissolved in 1ml of saline and then diluted 1:10 to give a final concentration of 50 IU/ml. This was then diluted a further 1:20 to give a final concentration of 2.5 IU/ml. 10mg of FSH Ab and 20mg of normal sheep immunoglobulins was weighed out and dissolved in saline at volumes of 5ml and 10ml respectively to give final concentrations of 2mg/ml for both products.

At the end of the experiment, rats were killed and testes were excised and weighed immediately. The right testis from each animal was processed for quantitative TJ functional analysis using [^{3}H]methoxy-inulin (n = 10/group) (see section 4.2.3 for the protocol). Five of the left testes per treatment group were snap-frozen in dry ice for RT-PCR and western blot analyses. The remaining 5 left testes from each group were injected pole to pole with either the qualitative TJ functional tracer biotin (10mg/ml, EZ-Link Sulfo-NHS-LC-Biotin, Pierce, Rockford, IL, USA) (n = 4) (Meng *et al.* 2005) in a volume of 10% testis weight, or the biotin vehicle (PBS + 1mM $CaCl_2$) (n = 1) at 10% testis weight. Testes were then incubated at room temperature for 30 minutes (Meng *et al.* 2005) before immersion fixation in fresh Bouin's fixative for 5 hours. Testes were then randomly sampled by a systematic uniform approach (Wreford, 1995) for stereological or immunohistochemical assessment.

Shortly after killing rats, blood was taken by cardiac puncture with an 18G needle connected to a 10ml syringe, and stored overnight at 4^{o}C before being spun down in a centrifuge at 1288g (2,500rpm, Beckman Coulter, Model J-6B) for 15 minutes. Serum was then collected by centrifugation, aliquotted, snap-frozen and then stored at -80^{o}C for analysis of FSH, LH and androgen concentrations.

5.2.3 Glycerol Intratesticular injection

The glycerol treatment that was used in the previous Chapter for biotin-functional tracer optimisation (n = 10/group (glycerol and control)), was again used in this Chapter as a positive control to decrease TJ function. The treatment protocol was conducted as outlined in section 4.2.3.

5.2.4 Immunohistochemistry

Bouin's-fixed, paraffin-embedded tissue underwent the immunohistochemistry protocol outlined in section 2.2 with confocal/fluorescent microscopy as the endpoints. Primary and secondary antibody incubation conditions for occludin, claudin-11, claudin-3, JAM-A and ZO-1, as well as the macrophage markers ED1 and ED2 are presented in Table 5.1. When probing for biotin, the Streptavidin Alexa-488 probe was diluted into the secondary antibody solutions as outlined in section 4.2.2. Biotin negative controls simply omitted the probe from the secondary solutions. All images are confocal microscopy unless otherwise stated.

5.2.5 Western blot analysis

Protein was extracted from frozen rat testes and prepared for western blot analysis of occludin and claudin-11 protein expression as outlined in section 2.5. Primary and secondary antibody conditions are presented in Table 5.2.

5.2.6 Real-time RT-PCR analysis

Total RNA was extracted from frozen rat testes and prepared for RT-PCR analysis as outlined in section 2.3. Primers for occludin, claudin-11, JAM-A, ZO-1, the androgen-regulated protein INSL-3, or housekeepers GAPDH and β-actin, were either taken from published sources or designed using the online Primer3 program (http://frodo.wi.mit.edu/primer3/input.htm) and parameters are presented in Table 5.3.

5.2.7 Stereology

The total number of cells per testis was calculated using the optical dissector method as previously described (Wreford, 1995, Meachem *et al.* 1998). Germ cells were identified using the

Table 5.1 Antibodies used for immunohistochemical analysis.

Tabulated data for the antibodies used in Chapter 5 of this thesis, including details regarding the primary and secondary antibody hosts, working concentrations (conc.)/dilutions, incubation (Inc.) times and company details with catalogue numbers.

Protein	**Primary (1^o) antibody host**	**Company (cat no.)**	**Conc.** (μg/ml)	**Negative control**	**1^o Inc. time (mins)**	**Secondary (2^o) antibody**	**Company**	**2^o Dilution**	**2^o Inc. time** (mins)
Claudin-11	Rabbit	Zymed (36-4500)	2.0	Normal rabbit IgG	60	Goat α rabbit Alexa-488 **or** Alexa-546	Molecular Probes	1:400 of stock	30
Occludin	Rabbit	Zymed (71-1500)	2.5	Normal rabbit IgG	30	Goat α rabbit Alexa-488 **or** Alexa-546	Molecular Probes	1:800 of stock	30
ZO-1	Rabbit	Zymed (61-7300)	1.25	Normal rabbit IgG	60	Goat α rabbit Alexa-488 **or** Alexa-546	Molecular Probes	1:800 of stock	30
JAM-A	Rabbit	Zymed (36-1700)	0.625	Normal rabbit IgG	Overnight	Goat α rabbit Alexa-488 **or** Alexa-546	Molecular Probes	1:400 of stock	30
ED1	Mouse	Serotec (MCA341)*	1:200 into ED2	Normal mouse IgG	Overnight	Goat α mouse Alexa-488	Molecular Probes	1:400 of stock	30
ED2	Mouse	Suspended in supernatants from hybridoma cultures*	Neat	Normal mouse IgG	Overnight	Goat α mouse Alexa-488	Molecular Probes	1:400 of stock	30

* Monash Institute of Medical Research, courtesy of Dr Mark Hedger (see Dijkstra *et al.* (1985))

Table 5.2 Antibodies and conditions used for western blot analysis.

Tabulated data for the antibodies used in Chapter 5 of this thesis, including details regarding the primary and secondary antibody hosts, working concentrations (conc.)/dilutions, incubation (Inc.) times and company details with catalogue numbers.

Protein	**Primary (1^o) antibody host**	**Company** (cat no.)	**Conc.** (μg/ml)	**Negative control**	**Tween20 (v/v) (%)**	**1^o Inc. time** (hrs)	**Secondary (2^o) antibody**	**Company**	**2^o Dilution**	**2^o Inc. time** (hrs)
Claudin-11	Rabbit	AbCam (ab7474)	1:200 of antisera	Normal rabbit serum	0.1% secondary only	2	Goat α rabbit IRDye 800 or goat α rabbit Alexa-680	Rocklands Immunochemicals or Molecular Probes	1:5000 of either secondary	2
Occludin	Rabbit	Zymed (71-1500)	2	Normal rabbit IgG	0.1% primary and secondary	2	As above	As above	As above	2
B-actin	Mouse	Sigma ascites fluid (A4700)	1:1000 of stock	Normal mouse IgG	0.1% primary and secondary	2	Goat α mouse IRDye 800	Rocklands Immunochemicals	1:5000 of stock	2

Table 5.3 Primer sequences and real-time RT-PCR conditions for the analysis of mRNA expression in the GnRH-antagonist-treated rat.

Primers were designed against the TJ proteins claudin-11, occludin, JAM-A, and the cytoplasmic plaque protein ZO-1, to quantitate mRNA expression following hormone suppression and short-term replacement. Primers were also designed against insulin-like 3 (INSL-3) which is androgen regulated and served as a useful positive control for hormone suppression on mRNA expression. The housekeepers used in this study were GAPDH and β-actin. Data included in the table are forward and reverse primer sequences, Mg^{2+} concentration, and annealing and acquisition temperatures.

Protein	**Species Accession no.**	**Primer Sequences (5'- 3')**	**Product size** (bp)	**[Mg^{2+}]** (mM)	**Anneal temp.** (^oC)	**Acquisition temp.** (^oC)
Claudin-11 (Chung *et al.* (2001))	Rat NM_053457	Forward: TTAGACATGGGCACTCTTGG Reverse: ATGGTAGCCACTTGCCTTC	624	2.5	68	85
Occludin (Lui *et al.* (2001))	Rat NM_031329	Forward: CTGTCTATGCTCGTCATCG Reverse: CATTCCCGATCTAATGACGC	294	2.5	64	75
JAM-A (Primer3)	Mouse NM_172647	Forward: TATAGCCGTGGATACTTT Reverse: GTCAGCCCAGCCACTATTACT	425	2.5	64	72
ZO-1 (Primer3)	Rat NM_009386	Forward: AGAGAGGAAGAGCGAATGTCTA Reverse: TTCATGCTGGGCCTAAGTA	248	3.0	60	72
β-actin (Primer3)	Rat NM_031144	Forward: CCGTAAAGACCTCTATGCCAACA Reverse: GCTAGGAGCCAGGGCAGTAATC	103	2.0	67	72
INSL-3 (Primer3)	Rat NM_053680	Forward: CTTCCTCACCAGGCTTCTCA Reverse: CTGTGGTCCTTGGTTTCTGG	241	2.0	58	72
GAPDH (Tso *et al.* (1985))	Mouse NM_008084	Forward: GACCCCTTCATTGACCTCAAC Reverse: GATGACCTTGCCCACAGCCTT	560	2.5	60	72

criteria of Russell *et al.* (1990) as published previously (McLachlan *et al.* 1995) and approximately 100 germ cells of each type was counted per animal (Gundersen, 1986).

Germ cells were divided into subgroups including type A/intermediate spermatogonia, type B/preleptotene spermatocytes, leptotene/zygotene spermatocytes, pachytene spermatocytes (associated with stages I-VIII and IX-XIV), round spermatids and elongated spermtids (associated with stages I-VIII and IX-XIV).

Cell counting was performed using a 100X objective lens on an Olympus BX-50 microscope (Tokyo, Japan) with a microcator (Heideinhain D83301: Traunreut, Germany) attached to the stage to measure the depth scanned. A Pulinix TMC-6 video camera coupled to a Pentium personal computer captured the image. The software package DH CASTGRID version 1.10 (Olympus, Munich, Germany) was used to superimpose a set of unbiased counting frames (of known areas) on to the video image. Unbiased fields were selected within the frames by a systematic uniform random sampling method for cell counting (McLachlan *et al.* 1995, Meachem *et al.* 1998). The number of assigned fields for each germ cell type was determined by their frequency (Meachem *et al.* 1998). Estimation of the number of cells per testis was determined by dividing the total number of cells by the total volume sampled. Volume sampled was determined by multiplying the total number of fields counted by the volume sampled in each field (volume sampled in each field equals the area of the unbiased frames multiplied by the depth scanned (10μm)). This is then multipled by the total testis volume. The final screen magnification was 2,708X and no correction for tissue shrinkage was necessary as determined previously (McLachlan *et al.* 1995, Meachem *et al.* 1996, Meachem *et al.* 1998).

All cell counting for this experiment was conducted by Mrs Georgia Balourdos at Prince Henry's Institute of Medical Research, Clayton, Victoria, Australia.

5.2.8 Serum hormone analyses

a. LH

Serum LH assay was conducted by Mrs Enid Pruysers at Prince Henry's Institute of Medical Research according to a published protocol (Robertson *et al.* 2001). The assay kit used was the Delfia hLH assay (Wallac). 96 well plates (Wallac) were coated with the B1 LH antibody which detects the

LHβ subunit. In brief, plates were washed with wash buffer and rLH standards (diluted 1:2 in buffer (TSA/5% bSA) from a starting concentration of 500pg/25µl to 7.8pg/25µl) and serum samples (diluted 1:2 over 5 doses in buffer (TSA/5% bSA) added to appropriate wells in triplicate in 25µl volumes. The plate was then incubated at room temperature for 2 hours while shaking and then washed twice. Europium (Eu)-labelled A2 antibody (targeted against the LHα subunit) was then added overnight at room temperature without shaking. The plate was then washed six times with wash buffer and enhancement solution added prior to reading on a time resolved Wallac 1234 Fluorometer. Assay sensitivity was 0.012ng/ml and cross-reactivity with hCG was 4% (Haavisto *et al.* 1993).

b. Total androgens

The concentration of serum total androgens was determined using a published protocol (O'Donnell *et al.* 1996b) and performed by Ms Fiona McLean at Prince Henry's Institute of Medical Research. Serum samples were loaded into separate homogenisation tubes for total androgen (testosterone, DHT, 5α-androstane-3α,17β-diol (Adiol)) extraction. To follow androgen recoveries throughout processing, 5000cpm radiolabelled [1α,2α-N-^{3}H]T], (DuPont, New England Nuclear, Melbourne, Australia; SA, 40-60Ci/nmol) was added to each sample. Homogenates were centrifuged (20 minutes, 9391g, 4^{o}C (10,000rpm, Eppendorf, Germany)) and the supernatants kept on ice. Pellets were resuspended in homogenisation buffer, vortexed, sonicated for 3 minutes and then centrifuged as above. Combined supernatants were diluted 1:3 in HPLC-grade deionised H_2O and 0.1% trifluoroacetic acid and loaded onto Sep-Pak C_{18} disposable columns (MilliQ system, Millipore, Milford, MA, USA). Androgens were eluted with 0.1% (vol/vol) trifluoroacetic acid and 60% acetonitrile and lyophilised. The O'Donnell *et al.* (1996b) study then separated the individual androgenic steroids by HPLC, with subsequent quantification by radioimmunoassay (RIA) using a primary antibody that cross-reacted with all androgens. This Chapter aimed to determine total androgen content in the serum without HPLC separation, hence samples were analysed directly by RIA as per the O'Donnell *et al.* (1996b) protocol. Samples were suspended in assay buffer (0.1% wt/vol gelatine in 0.1M PBS (0.154M NaCl), pH 7.4). Primary antibody Cox 0457 (Sirosera, Sydney, Australia) diluted 1:400,000 in 1:800 normal sheep serum was added to the solutions along with the tracer iodinated histamine-T (10,000cpm/100µl) (O'Donnell *et al.* 1996b). The assay was incubated

overnight at 4°C and then the secondary antibody (100µl donkey antisheep IgG diluted 1:20 in assay buffer) was added for 30 minutes at room temperature. Following this, 1ml of 6% Polyethylene Glycol 6000 (Merck, Darmstadt, Germany) was added and incubated for 30 minutes at 4°C, after which an additional aliquot of potato starch was added to ensure pelletisation. Tubes were then centrifuged (40 minutes, 1503g, 4°C (4,000rpm, Eppendorf)), drained and counted on a Wallac (Turku, Finland) γ-counter. The assay sensitivity was 0.013ng/ml.

c. FSH

Serum rat FSH assay was conducted as previously published (Robertson *et al.* 2001) by Mrs Enid Pruysers at Prince Henry's Institute of Medical Research. The assay used was a sensitive immunofluorometric assay (Delfia, rFSH kit no. A0710201). Briefly, 96 well plates pre-coated with the FSH monoclonal antibody 36306 were obtained from Wallac (Robertson *et al.* 2001) and washed once with wash solution. Rat FSH standard (diluted 1:2 in buffer (TSA-SM) from a starting concentration of 2000pg/100µl to 1.95pg/100µl) or the serum samples (diluted 1:2 in buffer (TSA-SM) over 5 doses) were added to the wells (in triplicate at 100µl) and incubated at room temperature for 3 hours, with shaking. Wells were then washed twice and Eu-labelled FSH monoclonal antibody (50ng/well, BD10) added and incubated for a further 30 minutes without shaking. Plates were washed 6 times before enhancement solution was added prior to determining fluorescence in a time resolved fluorometer. The assay sensitivity was 0.015ng/ml. Cross-reactivity with human FSH was 1.3% (Jimenez *et al.* 2005).

5.2.9 Statistics

Statistical analysis was conducted as outlined in Section 2.6. Data has been presented as mean ± SD unless otherwise stated, and the total number of animals/group is outlined in each result section of this Chapter.

Note that raw data for serum hormone assays and stereology of germ cell numbers have been supplied in Appendices 1.3 and 1.4 respectively and are on CD inside the back cover of this thesis.

5.3 Results

5.3.1 Testis and body weights

At the end of the hormonal or glycerol treatment protocols, freshly killed rats were weighed to obtain body weights (n = 10/group). No change in body weight was obtained in response to hormone suppression or replacement, and no change in body weight was obtained in response to the glycerol intratesticular injection compared to control (Table 5.4).

Testes were then excised, trimmed of all fat and connective tissue and then weighed before further experimentation. Hormone suppression with acyline for 7 weeks resulted in a significant decrease ($p < 0.001$) in testis weights to 19% of controls (Table 5.4). No further significant decrease was observed after the addition of the FSH Ab for another week, where testis weights were at 17% of control.

Short-term hormone replacement with hrFSH, hCG + FSH Ab (to observe the effect of testosterone alone) or hCG + control IgG (to observe the effect of both testosterone and endogenous rat FSH) all gave a significant ($p < 0.001$) partial recovery in testis weights to 24%-27% of controls (Table 5.4).

Four weeks after a single intratesticular injection of glycerol, testis weights had significantly decreased to 68% ($p < 0.001$) of control weights (Table 5.4).

5.3.2 Serum hormone levels

a. LH

Hormone suppression with acyline significantly decreased serum levels of rat LH to 16% ($p < 0.05$) (Figure 5.1a) of control, and the addition of the FSH Ab in the eighth week resulted in a further decrease in serum LH of 11% ($p < 0.05$). Short-term hrFSH and hCG replacement had no effect on suppressed serum LH levels, whereas short-term replacement of hCG + FSH Ab resulted in a further significant decrease of rat LH ($p < 0.05$).

Table 5.4 Body and testis weights.

Rats were killed after 8 weeks of hormone suppression/replacement, or 4 weeks after an intratesticular injection of glycerol. Body weights were measured, after which testes were excised, trimmed of all fat, connective tissue and epididymides, and then weighed. Data for the hormone experiment is presented in Table A, and the glycerol experiment in Table B. All data is mean ± SD, n = 10/group. Difference between letters is $p < 0.001$.

A

Treatment	Control	Acyline	Acyline + FSH Ab	Acyline + FSH	Acyline + hCG + FSH Ab	Acyline + hCG
Body weights (g)	438.6 ± 37.7	402.7 ± 21.7	401.8 ± 37.3	415.9 ± 39.9	412.5 ± 13.7	418.6 ± 20.3
Testis weights (mg)	1754.5 ± 90.6[a]	331.5 ± 44.4[b]	299.2 ± 46.6[b]	425.8 ± 33.0[c]	432.9 ± 53.5[c]	481.5 ± 74.4[c]

B

Treatment	Control	Glycerol
Body weights (g)	409.0 ± 12.4	388.5 ± 25.1
Testis weights (mg)	1752.2 ± 89.0[a]	1195.8 ± 241.7[b]

Figure 5.1 Effect of hormone suppression and short-term replacement on serum LH, androgens and FSH.

Serum concentrations of LH (panel A), androgens (panel B) and rat FSH (panel C) in control rats, animals suppressed with acyline for 8 weeks, and in animals suppressed with both acyline and given short-term hormone replacement for 7 days. Full details of treatment groups are given in Section 5.2. Data is mean ± SD, n = 9-10 rats/group (serum androgens), 6-8 rats/group (serum FSH), 5-8 rats/group (serum LH). Significant differences ($p < 0.05$ or greater) between treatment groups are indicated by letters, as specified in Results. NA = not assessed.

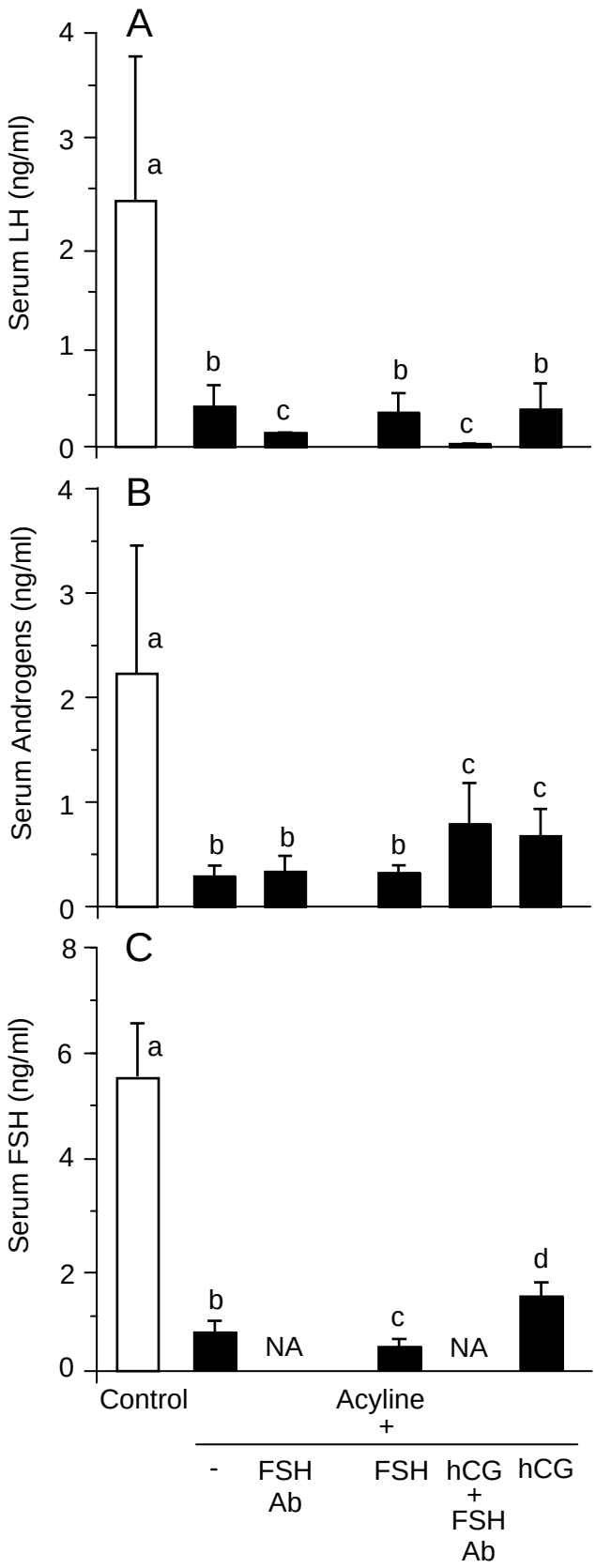
A
B
C
Serum LH (ng/ml)
Serum Androgens (ng/ml)
Serum FSH (ng/ml)
0
1
2
3
4
6
8
a
b
c
d
NA
Control
Acyline
+
-
FSH
Ab
FSH
hCG
+
FSH
Ab
hCG

b. Androgens

Acyline treatment reduced serum total androgens to 13% ($p < 0.001$) of control, and the addition of the FSH Ab caused no further decrease (Figure 5.1b). Short-term hormone replacement with hrFSH had no effect on serum androgen levels, but a significant recovery was achieved with short-term replacement of hCG which lifted serum androgens to 30% of control ($p < 0.01$), and hCG + FSH Ab which lifted serum androgens to 35% of control ($p < 0.001$).

c. FSH

Serum FSH was reduced to 12% ($p < 0.01$) of controls in response to acyline treatment (Figure 5.1c). The FSH Ab interfered with the assay and so the effect of this treatment on serum FSH alone, and in combination with hCG could not be measured. However, the short-term replacement of hrFSH further decreased serum rat FSH levels to 7% of control ($p < 0.05$), whereas the addition of hCG induced a significant recovery to 25% of control ($p < 0.001$).

5.3.3 Stereological assessment of germ cell types and numbers

a. Type A/Intermediate spermatogonia

Hormone suppression with acyline for 8 weeks significantly ($p < 0.001$) reduced Type A and intermediate spermatogonia to 66% of controls, and the addition of the FSH Ab caused a further significant reduction compared to acyline alone ($p < 0.05$) of these cell types to 46% of controls (Figure 5.2). Short-term hormone replacement with FSH, or the stimulation of testicular production of testosterone ± FSH kept germ cell numbers at values significantly lower than the controls ($p<0.001$), or acyline treated ($p<0.05$) but no differences were observed between the replacement groups and the Acyline + FSH Ab group (Figure 5.2).

b. Type B/Preleptotene spermatocytes

No significant decrease ($p = 0.242$) following acyline treatment with germ cells at 76% of control (Figure 5.2). The addition of the FSH Ab did achieve a significant ($p < 0.05$) reduction in type B/preleptotene spermatocytes to 65% of control levels. Short-term FSH replacement restored

Figure 5.2 Stereological assessment of germ cell types and numbers.

Stereological assessment by the optical dissector method was used to determine the effect of the various hormone treatments on germ cell types and numbers. Germ cells were divided into the following subgroup; i) Type A/intermediate spermatogonia, ii) Type B/preleptotene spermatocytes, iii) Leptotene/zygotene spermatocytes, iv) Pachytene spermatocytes stages I-VIII, v) Pachytene spermatocytes stages IX-XIV, vi) Round spermatids stages I-VIII, all of which are presented in the Figure. For elongated spermatids (stages I-VIII and IX-XIV) and Sertoli cell numbers, see Table 5.5. A full description of the treatment groups is given in Section 5.2. Data is Mean ± SD, n = 5 rats/group. Significant differences ($p < 0.05$ or greater) between treatment groups is denoted by different letters, with full details given in the text. Note the logarithmic y-axes for the 2 lower right graphs.

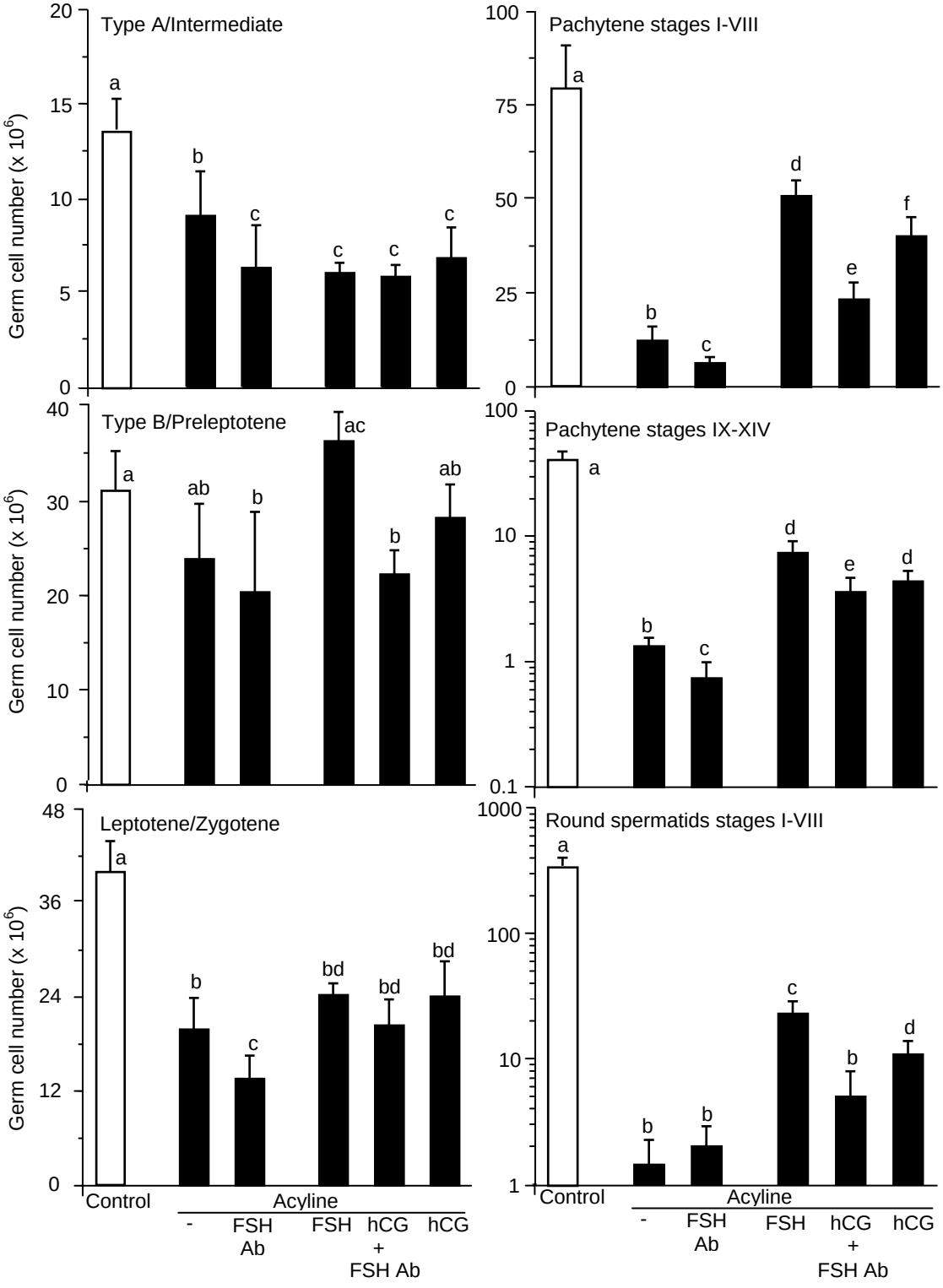
Type A/Intermediate
Germ cell number (x 10^6)
20
15
10
5
0
a
b
c
c
c
c
Pachytene stages I-VIII
100
75
50
25
0
a
b
c
d
e
f
Type B/Preleptotene
40
30
20
10
0
a
ab
b
ac
b
ab
Pachytene stages IX-XIV
100
10
1
0.1
a
b
c
d
e
d
Leptotene/Zygotene
48
36
24
12
0
a
b
c
bd
bd
bd
Round spermatids stages I-VIII
1000
100
10
1
a
b
b
c
b
d
Control
Acyline
-
FSH Ab
FSH
hCG + FSH Ab
hCG

germ cell numbers to control levels ($p < 0.001$ versus FSH Ab) but the stimulation of testosterone alone had no effect on type B/preleptotene spermatocytes recovery (Figure 5.2). Germ cell numbers did not change from suppressed levels following the stimulation of both testosterone and endogenous rat FSH in the hCG-alone group, however these numbers were also no longer significantly different to control levels either (Figure 5.2).

c. Leptotene/Zygotene spermatocytes

Acyline reduced leptotene/zygotene spermatocyte numbers to 50% of control ($p < 0.001$), and the addition of the FSH Ab caused a further decrease to 34% of control ($p < 0.001$ versus control, $p < 0.01$ versus acyline alone) (Figure 5.2). None of the short-term hormone replacements induced significant recoveries in these germ cell types from acyline induced numbers. This was despite increases to 61% of control numbers in response to FSH replacement, 51% response to the effect of testosterone alone (as determined with hCG + FSH Ab treatment group) and 60% following the simulation of both testosterone and endogenous rat FSH with hCG.

d. Pachytene spermatocytes Stages I-VIII

Acyline decreased pachytene spermatocytes in stages I-VIII to 15% ($p < 0.001$) of controls, and the addition of the FSH Ab further reduced numbers to 8% of control ($p < 0.001$ versus control, $p < 0.05$ versus acyline) (Figure 5.2). hrFSH-alone replacement increased germ cell numbers significantly ($p < 0.001$ versus acyline) to 64% of control, while testosterone alone (induced by hCG + FSH Ab treatment) also significantly ($p < 0.001$) increased pachytene spermatocyte (stages I-VIII) numbers to 29% of control, but this result was significantly ($p < 0.001$) lower than the hrFSH-induced recovery. The stimulation of both testosterone and endogenous rat FSH with hCG treatment resulted in a recovery of germ cell numbers to 51% of control, which was significantly higher than the recovery induced by testosterone alone ($p < 0.001$) but significantly lower than the recovery induced by hrFSH alone ($p < 0.001$) (Figure 5.2).

e. Pachytene spermatocytes Stages IX-XIV

Acyline treatment reduced pachytene spermatocytes at stages IX-XIV to 3% of control ($p < 0.001$), with a further significant suppression to 2% of control numbers with the FSH Ab treatment ($p < 0.05$ versus acyline) (Figure 5.2). rhFSH treatment stimulated a recovery in these germ cells to 18% of control numbers ($p < 0.05$). Testosterone alone (induced by hCG + FSH Ab treatment) resulted in a recovery to 9% of control values ($p < 0.05$), which was significantly less ($p < 0.05$) than rhFSH alone. The stimulation of both testosterone and endogenous rat FSH using hCG treatment resulted in a recovery of germ numbers to 11% of control ($p < 0.05$) (Figure 5.2). Data testing for each treatment group was found to be non-parametric. This was after $\log_{10}$ treatment of the raw data which did not result in a normal distribution. The differences between groups were then determined by the Kruskal-Wallis test, followed by the post-hoc Newman-Keuls analogue (Equal N's) to determine where the differences lay.

f. Round spermatids Stages I-VIII

Acyline treatment resulted in a significant ($p < 0.001$) reduction in round spermatids at stages I-VIII to 0.4% of control numbers, with no further significant reduction following treatment with the FSH Ab (Figure 5.2). rhFSH treatment resulted in a partial but significant ($p < 0.05$) recovery of germ cell numbers to 6.5% of controls (Figure 5.2). Testosterone alone (induced by hCG + FSH Ab treatment) also stimulated a significant ($p < 0.05$) recovery to 1.4% of control numbers, but this was significantly ($p < 0.05$) less than the numbers obtained with hrFSH alone. The stimulation of both testosterone and endogenous rat FSH with hCG treatment resulted in a significant ($p < 0.05$) germ cell recovery to 3.1% of controls, but this was still significantly ($p < 0.05$) less than the germ cell numbers reached with rhFSH alone replacement (Figure 5.2). Data testing for each treatment group was non-parametric. As above, this was determined after $\log_{10}$ treatment of the raw data which did not result in a normal distribution. Subsequently, a Kruskal-Wallis test was conducted to determine if there were any differences between the groups and the Newman-Keuls analogue (Equal N's) tests was then conducted to determine where the differences lay.

g. Elongated spermatids Stages I-VIII

Acyline treatment ± FSH Ab completely suppressed the elongated spermatids at stages I-VIII with none detected ($p < 0.001$). Short-term replacement with any of the hormone treatment groups gave no recovery in numbers, with no germ cells detected (Table 5.5).

h. Elongated spermatids Stages IX-XIV

Acyline reduced the number of elongated spermatids at stages IX-XIV to 0.2% of control ($p < 0.001$), with no further significant reduction obtained with the FSH Ab. None of the hormone replacements gave any recovery in these germ cell numbers (Table 5.5).

i. Sertoli cell numbers

Sertoli cell numbers were unchanged with hormone suppression or short-term replacement compared to the control (Table 5.5).

5.3.4 Effect of hormone suppression and short-term replacement on tight junction structure/localisation and function

Control rats displayed large seminiferous tubules with lumens, extensive occludin staining at the TJ and biotin functional tracer staining restricted to the interstitium and only entering the tubules as far as the TJ (Figure 5.3a). Occasional endogenous biotin staining was visible within the control seminiferous tubules and the occludin antibody cross-reacted with the spermatid heads in the same animals. Non-specific staining in the interstitium was also occasionally visible.

In acyline treated and FSH Ab treated (Figures 5.3b and 5.3c respectively) testes, tubule and lumen diameters had markedly decreased. Occludin staining was undetectable and biotin permeated throughout the tubules and surrounded all remaining germ cell types which based on stereological analysis were spermatogonia, leptotene/zygotene spermatocytes and some pachytene spermatocytes.

Short-term hormone replacement for 7 days with either hrFSH, hCG + FSH Ab or hCG alone (Figure 5.3d-f) gave increased tubule and lumen diameters with some positive but limited occludin staining at the TJ (mostly in panels E and F). Biotin generally permeated throughout the tubules, but in some cases was excluded to the interstitium (Figures 5.3g-i) The proportion of tubules excluding

Table 5.5 Stereological assessment of elongated spermatid and Sertoli cell numbers.

Stereological data for elongated spermatids (stages I-VIII and IX-XIV) and Sertoli cell numbers. Quantification was conducted as per the earlier germ cell types presented in Figure 5.2. Data is mean ± SD, n = 5 rats/group

Treatment / Germ cell	Control	Acyline	Acyline + FSH Ab	Acyline + FSH	Acyline + hCG + FSH Ab	Acyline + hCG
Elongated spermatids stages I-VIII	3.63E+08 ± 5.86E+07[a]	0.00E+00 ± 0.00E+00[b]	0.00E+00 ± 0.00E+00[b]	0.00E+00 ± 0.00E+00[b]	0.00E+00 ± 0.00E+00[b]	0.00E+00 ± 0.00E+00[b]
Elongated spermatids stage IX-XIV	9.45E+07 ± 8.35E+06[a]	1.42E+05 ± 1.93E+05[b]	2.39E+04 ± 3.48E+04[b]	3.69E+05 ± 4.10E+05[b]	1.22E+05 ± 2.42E+05[b]	3.32E+05 ± 4.04E+05[b]
Sertoli cells	4.11E+07 ± 3.06E+06[a]	4.44E+07 ± 8.81E+06	4.71E+07 ± 1.51E+07	5.18E+07 ± 1.17E+07	5.54E+07 ± 1.64E+07	5.18E+07 ± 1.15E+07

Figure 5.3 Effect of hormone suppression and replacement on testicular TJ function and structure.

Immunofluorescence of occludin (red) and biotin functional tracer (green) in testes from rats given hormone suppression and replacement. TJ structure and function was initially visualised in a normal control testis (panel A), and compared to testes which had been hormonally suppressed with acyline alone for 8 weeks (panel B) or with acyline for 7 weeks plus the FSH Ab for an additional week (panel C). Following hormone suppression the effect of short-term hormone replacement with hrFSH alone (panel D), hCG + FSH Ab to investigate the effect of testosterone alone (panel E) and hCG to stimulate both testosterone and endogenous rat FSH (panel F) on TJ function and structure was analysed. Panels G-I represent a much smaller proportion of TJ phenotypes observed with each of the short-term hormone treatments listed above respectively. Such phenotypes were never observed for acyline treatment alone. Bar = 50μm. Inset = negative control with positive nuclear stain. Note this Figure presents conventional fluorescent micrographs (not confocal).

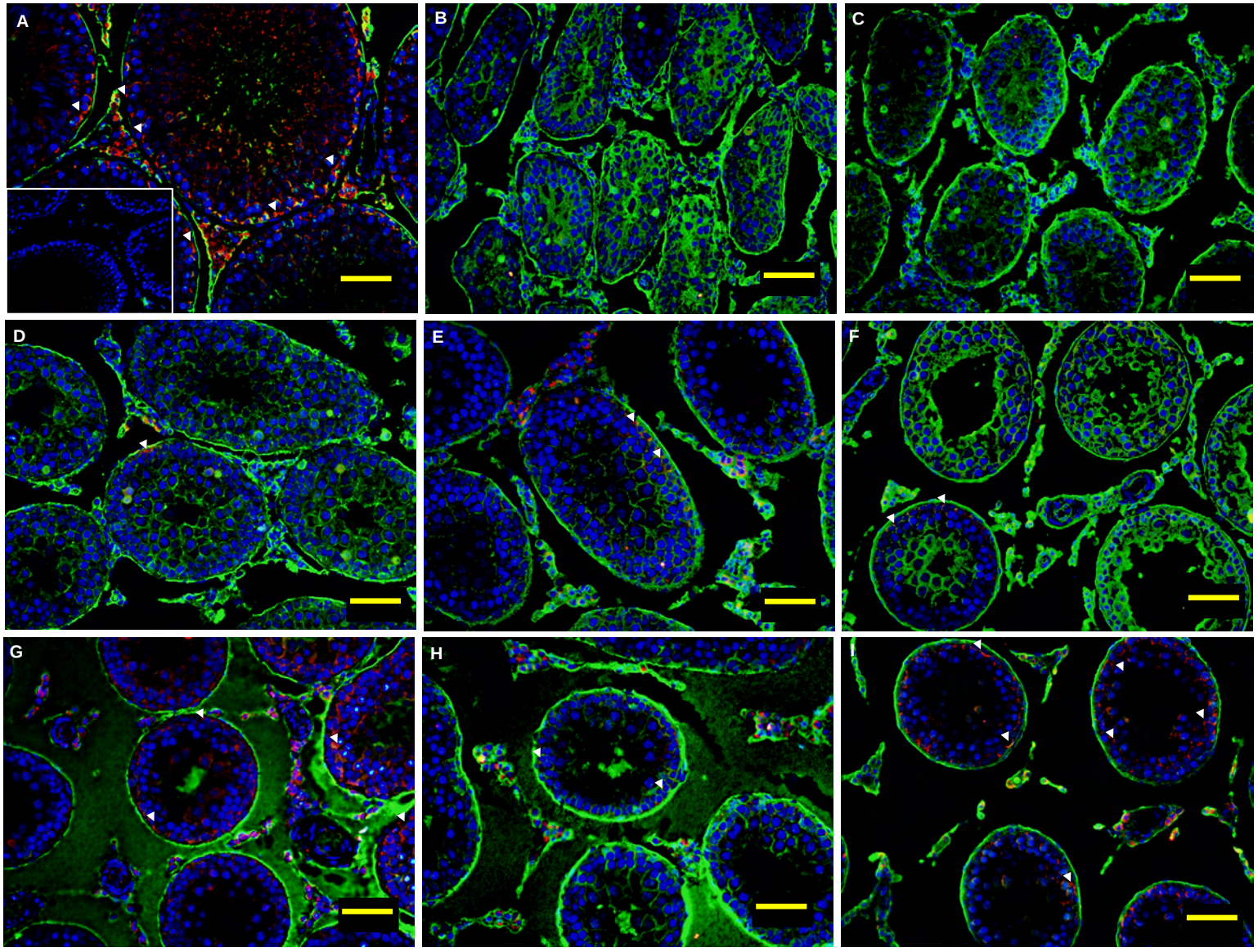
A
B
C
D
E
F
G
H
I

biotin was not able to be quantitated, but qualitative observation indicated that this was low (<5% of tubules/cross-sections). This phenotype was never observed in the acyline treatment groups.

In control rats, the localisation of claudin-11 and JAM-A was extensive at the TJ, as was ZO-1 localisation at the cytoplasmic plaque (Figure 5.4). Under hormone suppressed conditions, claudin-11 protein remained present, but was localised to adluminal Sertoli cell cytoplasm in the tubules. JAM-A localisation responded in a similar manner to claudin-11 in hormone suppressed animals (acyline, acyline + FSH Ab) and was cytoplasmic and adluminal. ZO-1 staining was cytoplasmic and appeared more adluminal than in controls (Figure 5.4).

ZO-1 of the cytoplasmic plaque had re-localised toward the outer edge of the seminiferous tubules in each of the short-term hormone replaced treatments (Figure 5.4).

5.3.5 Quantitative analysis of TJ function in response to hormone suppression and short-term replacement

a. Tracer accumulation in hormone suppressed and glycerol treated testes

Unexpectedly, the accumulation of [^{3}H]methoxy-inulin in seminiferous tubules from the acyline-treated testes was significantly ($p < 0.05$) lower than in control testes at 80% of control values (Figure 5.5a). Inulin accumulation remained at control levels in the acyline + FSH Ab treatment group, and was 52% and 20% greater than controls in the short-term replaced hrFSH and hCG + FSH Ab groups respectively. Inulin accumulation in the hCG-treated group was the same as control (Figure 5.5a).

Four weeks of glycerol treatment resulted in a significant ($p < 0.001$) 27% greater accumulation of [^{3}H]methoxy-inulin accumulation in seminiferous tubules compared to control (Figure 5.5b).

b. Comparative tracer accumulations in control, glycerol treated and prepubertal testes

The absence of any quantitative difference in [^{3}H]methoxy-inulin accumulation in the seminiferous tubules of the hormone suppressed testes compared to controls, and the small difference obtained for the glycerol-treated testes, led to a subsequent repeat experiment which tested the

Figure 5.4 Effect of hormone suppression and replacement on the localisation of claudin-11 and JAM-A to the testicular TJ, and ZO-1 to the cytoplasmic plaque.

Immunohistochemical analysis of the localisation of claudin-11 (green) and JAM-A (red) to the TJ, and ZO-1 (red) to the cytoplasmic plaque in control, hormone-suppressed, and short-term replaced groups. Bar = 50μm. Inset = negative control.

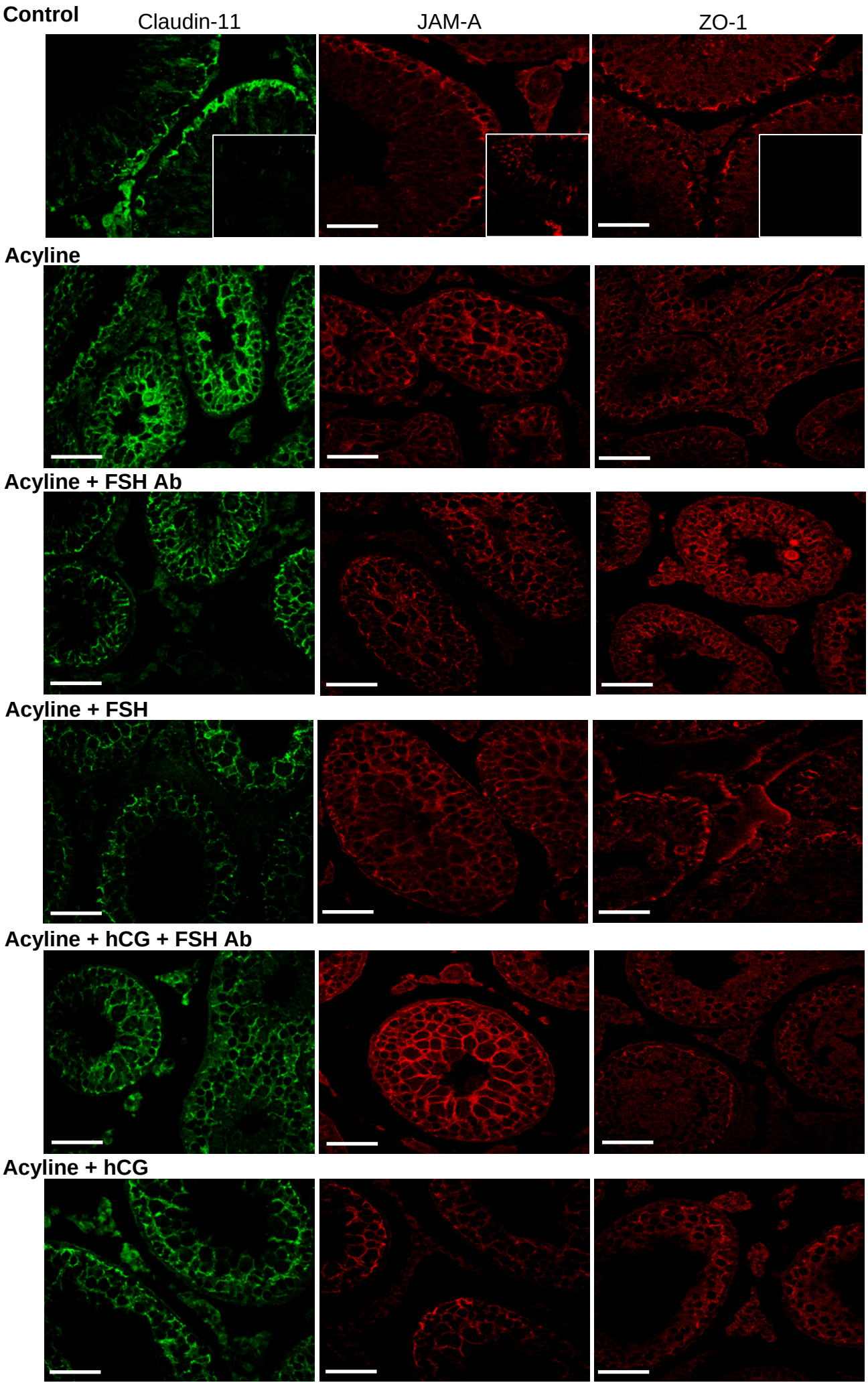
Control
Claudin-11
JAM-A
ZO-1
Acyline
Acyline + FSH Ab
Acyline + FSH
Acyline + hCG + FSH Ab
Acyline + hCG

Figure 5.5 Quantitative analysis of TJ function in response to hormone suppression, short-term hormone replacement, and glycerol treatment.

Testes were excised from freshly killed rats which had undergone hormone suppression with acyline and short-term hormone replacement (panel A), or rats which had undergone 4 weeks of glycerol treatment as a positive control for TJ disruption (panel B). Seminiferous tubules were incubated in 0.5μCi of [^{3}H]methoxy-inulin for 1 hour at 34^{o}C, before being homogenised and dissolved. Solutions were made up with scintillation fluid before final radioactive counts were determined for each treatment by scintillation spectrophotometry. Data is mean ± SD, n = 5/group. Difference between letters is $p < 0.05$. *** = $p = 0.001$. Note that the controls between the two panels are different vehicle controls for acyline (panel A) and glycerol (panel B). Therefore no statistical analyses were conducted between these two different experiments.

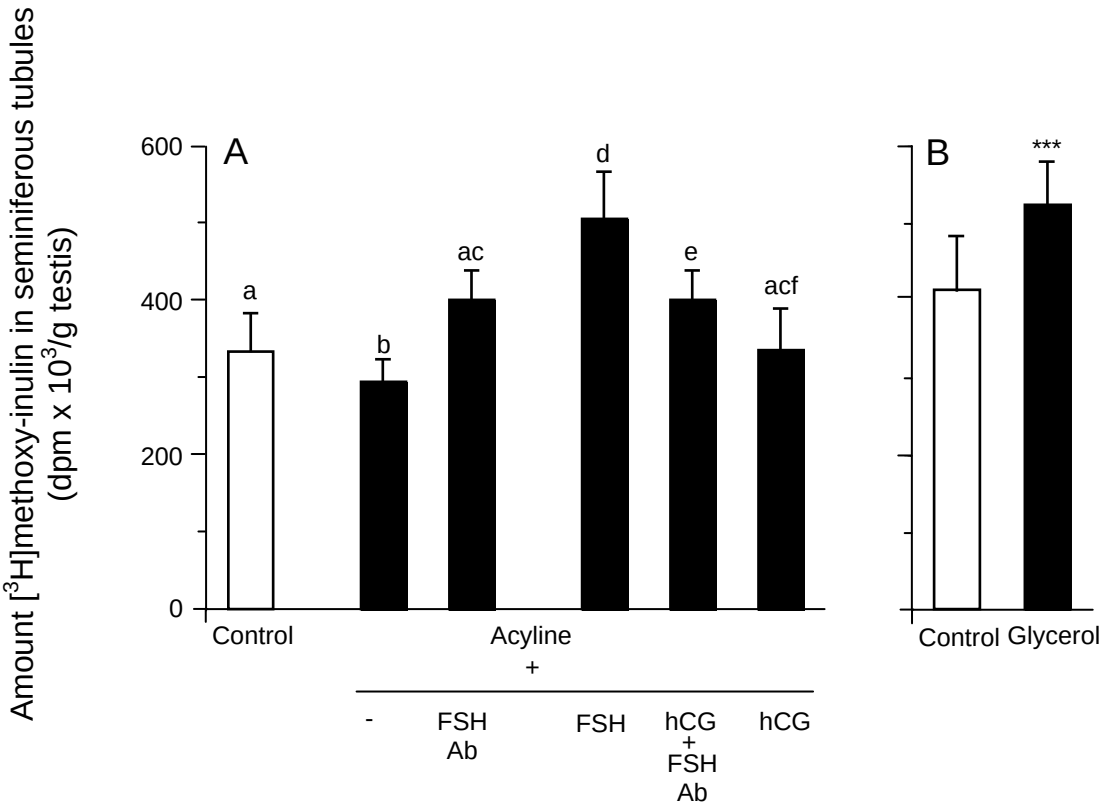
Amount [3H]methoxy-inulin in seminiferous tubules
(dpm x 10^3/g testis)
600
400
200
0
A
a
b
ac
d
e
acf
Control
Acyline
+
-
FSH
Ab
FSH
hCG
+
FSH
Ab
hCG
B
***
Control
Glycerol

accumulation of [^{3}H]methoxy-inulin and that of a much lower molecular weight tracer [^{14}C]mannitol (182Da, 0.5μCi; Amersham Biosciences (GE), cat # CFA-238)) in the seminiferous tubules of control, and glycerol-treated adult rats (n = 6/group). An additional group (n = 6) of prepubertal (9 day old) juvenile rats was included in this experiment as a positive control to examine tracer permeability in tubules from testes in which TJs had not yet formed. It was hypothesised that the testicular TJ is size-selective for tracers. The protocols for glycerol administration and tracer incubations were the same as outlined in section 4.2.3, with tubules from the right testes being incubated in wells containing both [^{3}H]methoxy-inulin and [^{14}C]mannitol tracers in combination. As the prepubertal testes were very small, tubules isolated from each testis were not fragmented into 3 sections, rather they were put whole into the tracer wells. An addition to the standard protocol was an intratesticular injection into each left testis of a solution containing both tracers at 10% testis volume. This was conducted to mimic the methodology of the biotin-permeation experiment as closely as possible. The testes were incubated for 30 minutes at room temperature following the injection, before tubules were isolated and rinsed in KRP prior to suspension in 5ml of MilliQ water as outlined in section 4.2.3.

Glycerol treatment for 4 weeks reduced testis weights to 67% of control ($p < 0.001$). Prepubertal testis weights were 3% ($p < 0.001$) of adult control testis weights as shown in the table below:

Rat group	**Control**	**Glycerol treated**	**9 day old Juvenile**
Testis weights (mg)	1885 ± 117	1289 ± 385	53 ± 8

When glycerol-treated seminiferous tubules were incubated in the tracers, the accumulation of either [^{3}H]methoxy-inulin or [^{14}C]mannitol was not significantly different to the accumulation in the control tubules (Figure 5.6a). However, the accumulation of [^{14}C]mannitol in glycerol and control tubules was always significantly ($p < 0.05$) greater than [^{3}H]methoxy-inulin accumulation. When seminiferous tubules from juvenile testes were incubated in the tracers, there was a significant 1.6 fold and 1.3 fold greater accumulation of [^{3}H]methoxy-inulin and [^{14}C]mannitol respectively compared to controls (Figure 5.6a).

In testes which received an intratesticular injection of the tracers, glycerol-treated tubules accumulated a non-significant ($p = 0.098$) 1.5 fold greater amount of [^{3}H]methoxy-inulin and a non-

Figure 5.6 Comparison of [^{3}H]methoxy-inulin and [^{14}C]mannitol accumulation in testes from control and glycerol treated adult rats, and in juvenile rats.

Testes were excised from controls (white bars), glycerol-treated (4 weeks) (black bars) and 9 day old juvenile rats (grey bars) to compare differences in the accumulation of [^{3}H]methoxy-inulin and [^{14}C]mannitol in testes within each group, and for any differences between the groups. Seminiferous tubules were isolated from the right testis of each animal and incubated in a solution containing both tracers (panel A) for 1 hour at 34^{o}C before being homogenised, solubilised and quantitated by scintillation spectrophotometry. The left testis from each animal was injected with a solution containing both tracers (panel B) at 10% testis weight and incubated and processed as per the right testis. Data is mean ± SD, n = 6 testes/group. Difference between letters is $p < 0.05$, ** = $p < 0.01$, *** = $p < 0.001$.

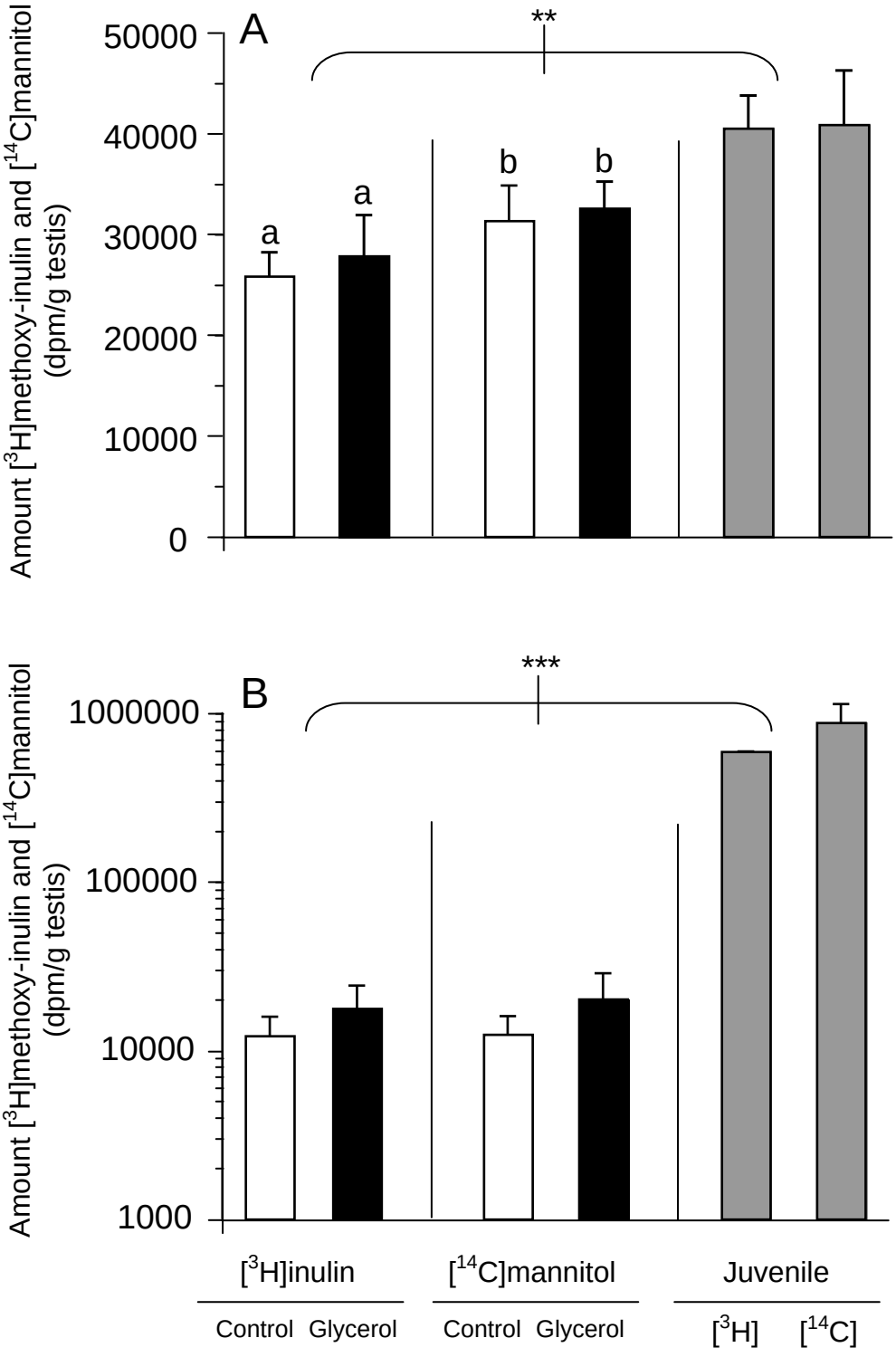
A
**
50000
40000
30000
20000
10000
0
a
a
b
b
Amount [3H]methoxy-inulin and [14C]mannitol (dpm/g testis)
B
***
1000000
100000
10000
1000
[3H]inulin
[14C]mannitol
Juvenile
Control
Glycerol
Control
Glycerol
[3H]
[14C]

significant ($p = 0.133$) 1.6 fold greater amount of [^{14}C]mannitol compared to controls (Figure 5.6b). Juvenile testes accumulated a significant ($p < 0.001$) 49 fold greater amount of [^{3}H]methoxy-inulin and 71 fold greater amount of [^{14}C]mannitol in their tubules compared to controls following the intratesticular injection (Figure 5.6b).

5.3.6 Testicular macrophage localisation following hormone suppression and replacement

An autoimmune response to hormone suppression and replacement was analysed by targeting ED1 and ED2 macrophage antigens (Figure 5.7). Control rat testes had very few macrophages which appeared predominantly localised in the blood vessels. Most tubules had very few macrophages surrounding them (Figure 5.7). In acyline treated rats, macrophage numbers appeared to qualitatively increase and had localized to the outer edges of the seminiferous tubules or in same cases had penetrated into the seminiferous epithelium (Figure 5.7). Rats treated with acyline + FSH Ab displayed a very similar macrophage number and localisation to the acyline alone treated group (Figure 5.7). Each of the short-term hormone replacement treatments appeared to result in a qualitative decrease in macrophage numbers compared to acyline treated (Figure 5.7), although these were still localized to the outer edges of the seminiferous tubules and were in greater number than in control. Glycerol treatment (to open TJs) when compared to the acyline treatment, appeared to stimulate a similar or marginally greater increase in macrophage number around the seminiferous tubules (Figure 5.7).

5.3.7 Western blot analysis

Control rat testis protein extracts displayed single bands corresponding to occludin at 64 kDa (Figure 5.8a) and claudin-11 at 22 kDa (Figure 5.8b). The latter protein was co-stained with β-actin (43kDa) to ensure consistent protein loadings across each sample. Fainter bands were also present in each of the gels but were also detectable in the negative control. Hormone suppression resulted in a marked decrease in occludin protein expression to beyond the limit of detection with the Odyssey system (Figure 5.8a). Recoveries in protein expression for occludin remained undetectable following short-term hormone replacement (Figure 5.8a). Similarly for claudin-11, protein expression was suppressed to beyond the limit of detection following hormone suppression (Figure 5.8b), with no

Figure 5.7 Effect of hormone suppression and replacement on macrophage localisation in hormone suppressed and replaced testes.

Bouin's fixed testes were processed for immunohistochemical analysis of the macrophage markers ED1 and ED2, which labels all resident and circulating macrophages of the testis. Macrophages (green) were visualized by confocal microscopy with transillumination to highlight the seminiferous tubules in control testes, hormone suppressed testes, short-term hormone replaced testes and glycerol treated testes acting as positive control for open TJs. The bottom right panel is another control testis section taken at a lower magnification to display whole seminiferous tubules (dashed black line) and the number of macrophages (arrow) surrounding them. Bar = 50μm. Inset is negative control.

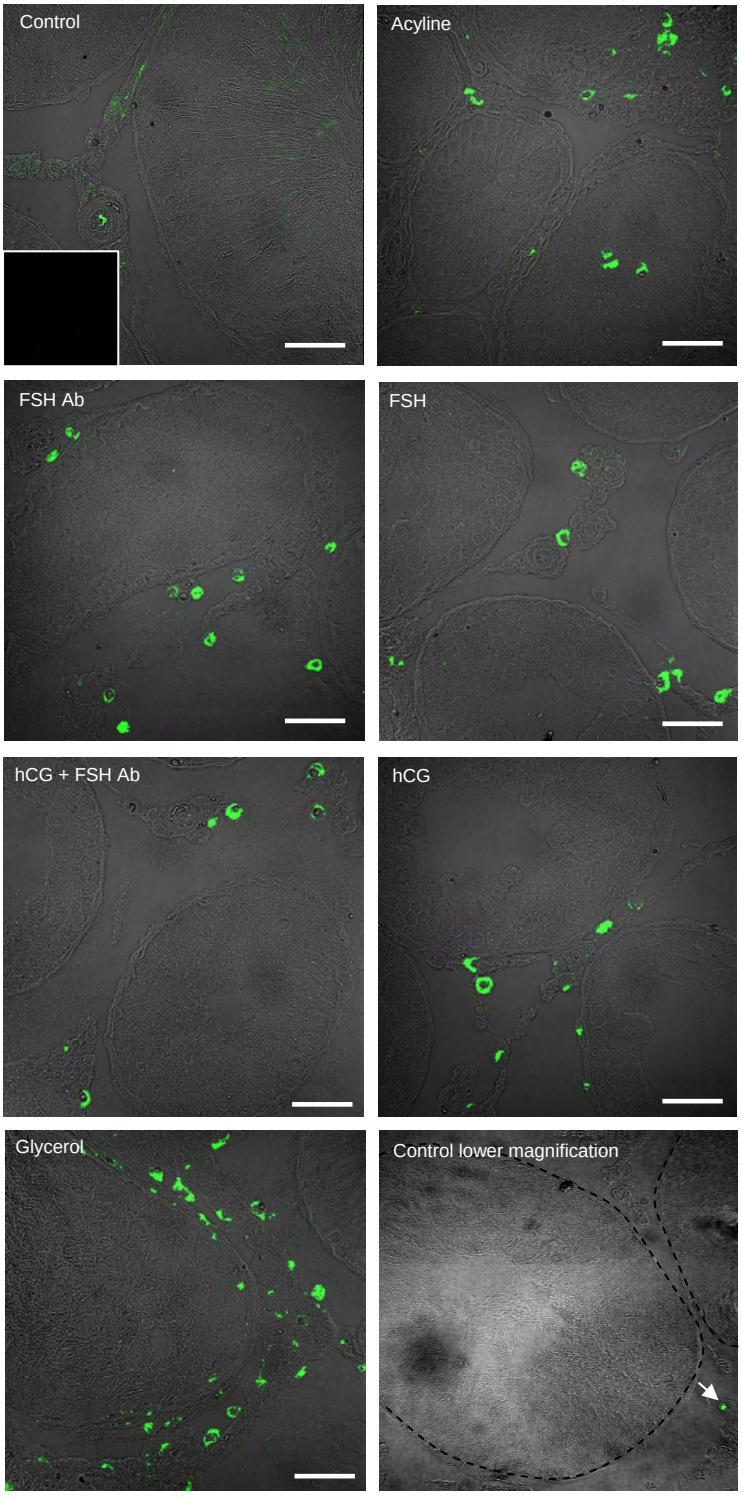
Control
Acyline
FSH Ab
FSH
hCG + FSH Ab
hCG
Glycerol
Control lower magnification

Figure 5.8 Effect of hormone suppression and replacement on TJ protein expression.

Western blot analysis of occludin (40μg total protein per lane, reducing conditions, Panel A, 64kDa) and claudin-11 (120μg total protein per lane, non-reducing conditions, Panel B, 22kDa). Detection of both proteins with fluorescently labeled secondary antibodies with Odyssey software. The house-keeping protein β-actin (43kDa) was also probed in each lane on the claudin-11 gel. Lanes are: 1) control, 2) acyline, 3) acyline + FSH Ab, 4) Acyline + FSH, 5) Acyline + hCG + FSH Ab, 6) Acyline + hCG, 7) Glycerol testis control, 8) Glycerol, 9) Negative control.

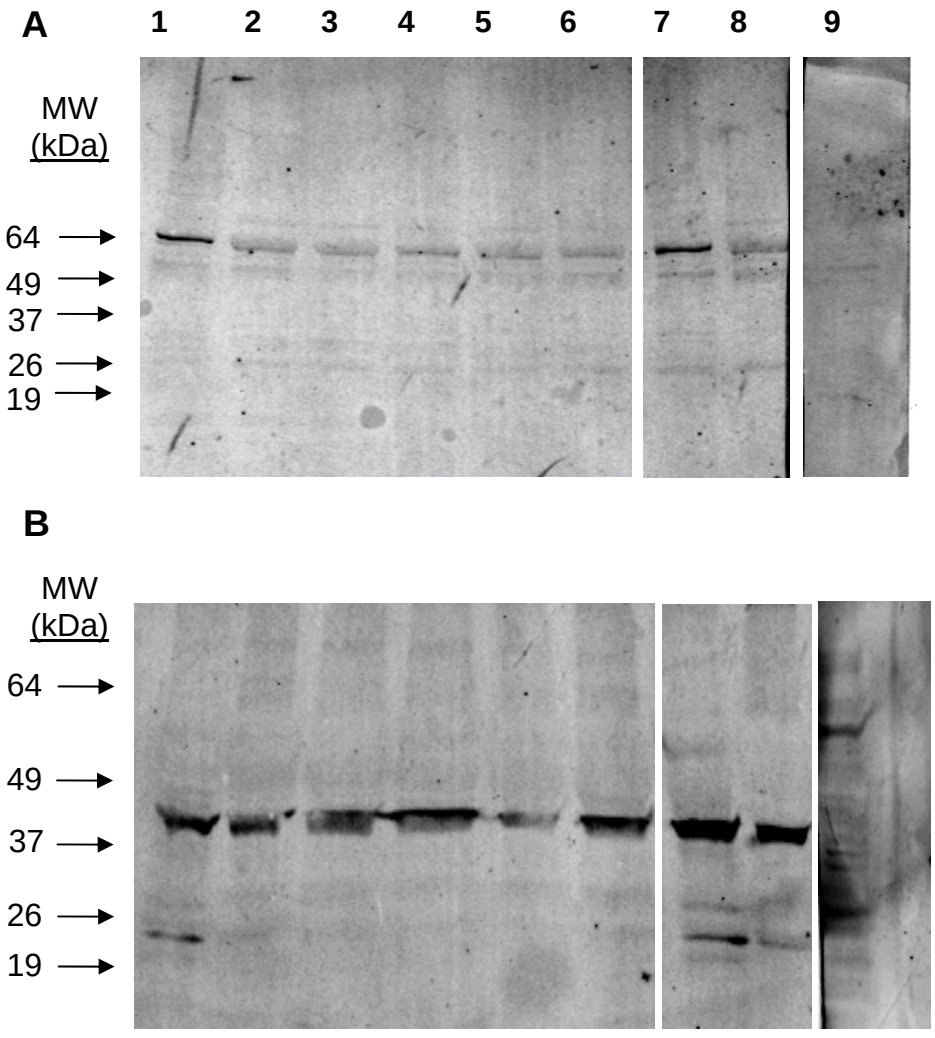
A
1
2
3
4
5
6
7
8
9
MW
(kDa)
64
49
37
26
19
B
MW
(kDa)
64
49
37
26
19

detectable recovery following any of the short-term hormone replacement regimens. β-actin protein expression did not change with any of the treatments compared to control (Figure 5.8b).

5.3.8 Real-time RT-PCR analysis

Hormone suppression with acyline resulted in a significant ($p < 0.001$) ~4 fold increases in claudin-11 and occludin mRNA expression, and an approximate 3 fold ($p < 0.001$) increase in JAM-A mRNA expression (Figure 5.9). Short-term hormone replacement with each of the treatments resulted in another significant ($p < 0.001$) change in both claudin-11 and occludin mRNA expression levels, back towards control levels. It was noteworthy that both claudin-11 and occludin expression levels decreased to the same extent regardless of the short-term replacement group (FSH alone, hCG +FSH Ab, or hCG). However, JAM-A levels remained high in all treatment groups (Figure 5.9). Hormone suppression and short-term replacement had no effect on ZO-1 mRNA expression compared to the controls (Figure 5.9). Androgen regulated INSL-3 mRNA expression was suppressed 12 fold following hormone suppression (Figure 5.9). Short-term hormone replacement with hrFSH had no effect on suppressed levels of INSL-3 whereas stimulation of androgen production with either hCG or hCG + FSH Ab resulted in a recovery of INSL-3 back to control levels (Figure 5.9). β-actin mRNA expression remained unchanged following hormone suppression and replacement compared to control (Figure 5.9).

5.4 Discussion

The hormones LH/T and FSH were suppressed in the studies presented in this Chapter by the use of a GnRH antagonist-treated rat model, and then selectively replaced in the short-term, with the aim of studying potential changes in the function and structure of the Sertoli cell TJ. The antagonist acyline had no major effects on the animals' health as shown by a lack of change in body weights compared to controls. Acyline has previously been used in rat and human studies (Herbst *et al.* 2004, Hild *et al.* 2004, Porter *et al.* 2006), and has been shown to have no propensity to stimulate histamine release, which is a problem associated with other GnRH antagonists (Herbst, 2003). After 8 weeks of treatment, testis weights had decreased by 81% of control weights. The addition of the FSH Ab to suppress any remaining FSH (Meachem *et al.* 1998) had no further significant effect on testis weights

Figure 5.9 Effect of hormone suppression and replacement on TJ mRNA expression.

Real-time RT-PCR quantitation was conducted for the TJ proteins claudin-11 (panel A), occludin (panel B) and JAM-A (panel C) as well as the cytoplasmic plaque protein, ZO-1 (panel D). As a positive control for hormone suppression and replacement, RT-PCR analysis was also conducted on the androgen regulated gene INSL-3 (panel E), which is plotted on a log-scale. All data has been presented as a ratio with the housekeeper GAPDH. To check for any changes in GAPDH mRNA across the various treatment groups, an additional ratio was made between GAPDH and a second housekeeper, β-actin (panel F). Data is mean ± SD, n = 5/group. Differences between letters is $p < 0.001$.

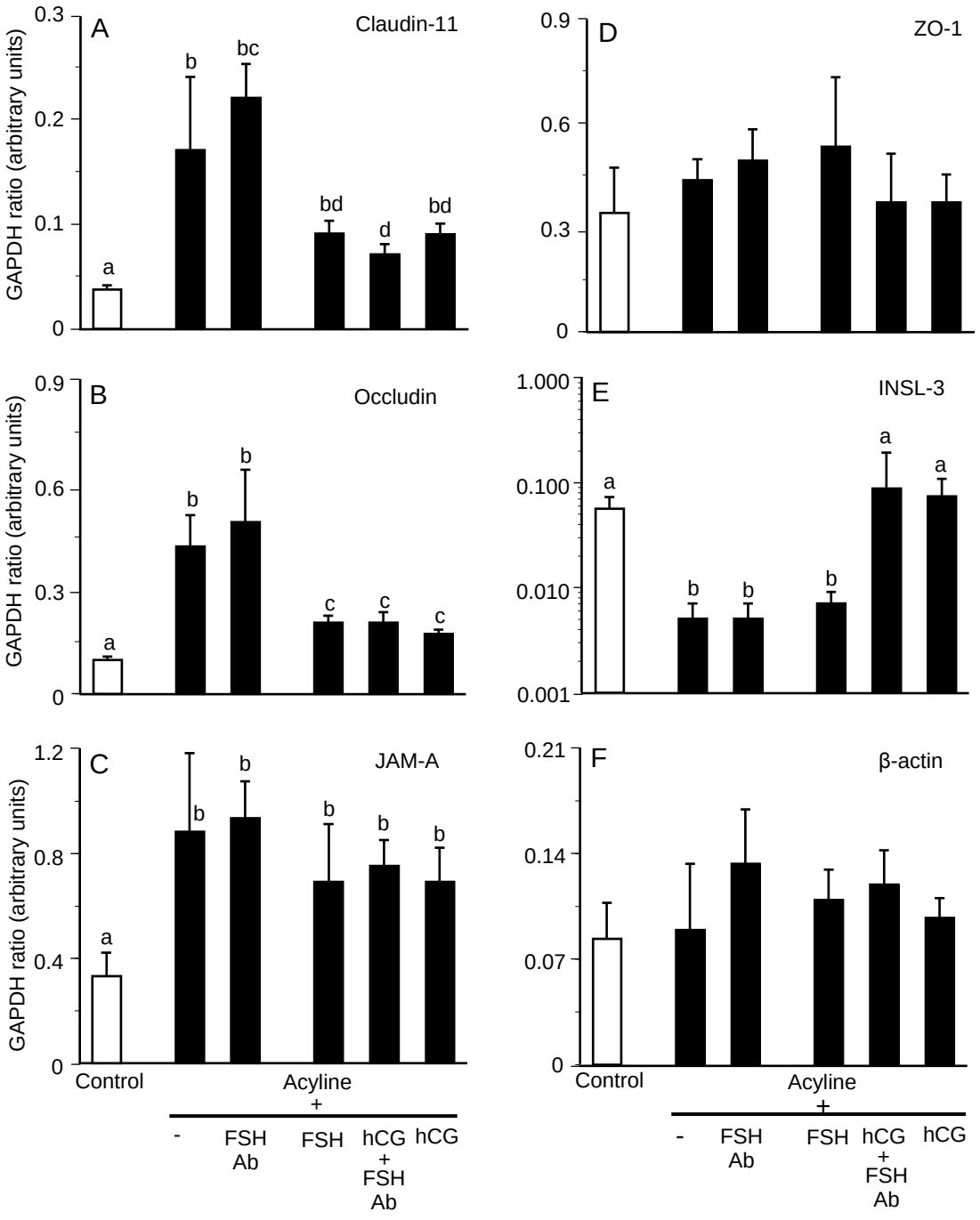
A
Claudin-11
GAPDH ratio (arbitrary units)
0.3
0.2
0.1
0
a
b
bc
bd
d
bd
D
ZO-1
0.9
0.6
0.3
0
B
Occludin
0.9
0.6
0.3
0
a
b
b
c
c
c
E
INSL-3
1.000
0.100
0.010
0.001
a
b
b
b
a
a
C
JAM-A
1.2
0.8
0.4
0
a
b
b
b
b
b
F
β-actin
0.21
0.14
0.07
0
Control
Acyline
+
-
FSH Ab
FSH
hCG + FSH Ab
hCG

which were at 17% of controls after a further week of treatment. The level of suppression achieved in this Chapter was marginally better or similar to other data which used a GnRH immunogen to suppress hormones, with testis weights being reduced by 71%-81% (Mclachlan et al. 1994b, Meachem *et al.* 1998, Pratis *et al.* 2003). Most studies analysing the effect of acyline on rat testis weights in the literature have not looked at normal healthy rats (Hild *et al.* 2004, Porter *et al.* 2006). However recent studies using short-term administration of acyline in normal rats, have shown decreases in testis weights to 47% of control after 14 days in Sprague Dawley rats (Vera *et al.* 2006), and 33% of control after 10 days of treatment in another rat species (Pareek *et al.* 2007). The TE suppression model, which suppresses testosterone but not FSH, generally reduced testis weights by 67%-68% in other studies (O'Donnell *et al.* 1999, Pratis *et al.* 2003).

Serum hormone levels were significantly suppressed following treatment with acyline, with an 84% reduction in LH, an 87% reduction in androgens and an 88% reduction in FSH. The addition of the FSH Ab caused a further significant reduction in serum LH but had no effect on the level of serum androgens. Due to antibody interference with the FSH assay, serum FSH was not analysed in response to this treatment. However, other data obtained in this study from testis weights and stereology demonstrated that the FSH Ab had suppressed residual FSH successfully. The suppression of LH in response to the FSH Ab treatment compared to acyline alone, while unexpected, was reported in another GnRH immunogen study which combined the FSH Ab with hCG (Pratis *et al.* 2003). On its own, the immunogen suppressed LH to a similar extent to acyline (Pratis *et al.* 2003). In the hCG + FSH Ab treatment in the Pratis *et al.* (2003) study, the LH concentration was lower than the immunogen alone treatment but did not achieve significance. In this study, the FSH Ab alone or in conjunction with hCG stimulated decreases in LH which were significantly lower than the acyline-induced concentration. The cause of such a decrease in response to the FSH Ab is not readily available in the literature and so the reasons remain uncertain, although it may be possible that there is some cross-talk between the FSH and LH signalling systems.

Acyline suppression of serum LH (84%) and serum androgens (87%) was similar to studies which used the GnRH immunogen where an 88% decrease in serum LH (Pratis *et al.* 2003) and 92% decrease in serum testosterone (Meachem *et al.* 1998) were obtained. These decreases were in line with other antagonist studies using acyline, as well as other antagonists (Jiang *et al.* 2001, Broqua *et*

al. 2002, Herbst, 2003, Hild *et al.* 2004, Matthiesson et al. 2005b, Porter *et al.* 2006, Vera *et al.* 2006, Pareek *et al.* 2007). Where the antagonist differed from the immunogen was in the suppression of FSH. While FSH was suppressed to just 12% of controls with acyline, FSH was still at 34%-54% of controls in the immunogen studies (Meachem *et al.* 1998, Pratis *et al.* 2003), which demonstrates that GnRH antagonism is more effective at suppressing hormones, and therefore spermatogenesis, compared to GnRH immunisation, which is expected to account for the smaller testes observed in this Chapter as well.

Most studies in recent years using acyline and other GnRH antagonists in rats have not looked at the effects of antagonism on serum FSH (Jiang *et al.* 2001, Broqua *et al.* 2002, Herbst, 2003, Hild *et al.* 2004, Matthiesson et al. 2005b, Porter *et al.* 2006). An exception to this is one recent study in rats which showed that 48 hours of acyline treatment reduced serum FSH to ~20% of controls (Pareek *et al.* 2007), which was marginally higher than the suppression obtained herein. In studies conducted in the 1980s and 1990s which used the GnRH antagonist Nal-Glu in rats, serum FSH was seen to significantly decrease below the assay sensitivities, although these were less sensitive than the assay used in this Chapter (Rea *et al.* 1986, Bhasin *et al.* 1987, Arslan *et al.* 1989, Rodin *et al.* 1989, Dubourdieu *et al.* 1993). In more recent human studies, acyline was seen to have a dose dependent effect on serum FSH suppression, with a maximal dose of 300μg/kg suppressing FSH to 10% of control values (Herbst, 2003, Herbst *et al.* 2004). This compares well with the suppression of FSH to 12% of control values achieved with rats in this study.

Short-term hormone replacement had some differential effects on the serum hormones studied. When hrFSH was replaced for 7 days, no effect on suppressed levels of LH or androgens was obtained. In GnRH immunised models, hrFSH replacement also had no effect on suppressed LH or androgen (Meachem *et al.* 1998, Pratis *et al.* 2003). hrFSH administration in this study however saw a further significant reduction in endogenous production of FSH. This was possibly a result of the hrFSH suppressing the residual endogenous FSH via a negative feedback system, which may have been produced via the GnRH-independent pathway (Rea *et al.* 1986, Bhasin *et al.* 1987). Increases in testis weights and germ cell numbers (described later) seen in response to hrFSH treatment in this Chapter were therefore most likely due to the exogenously applied hormone alone. The Meachem *et al.* (1998) and Pratis *et al.* (2003) studies did not look at the effects of hrFSH on suppressed FSH

levels due to concerns of interference with the rat FSH assay, but further investigations (Jimenez *et al.* 2005) showed that the hrFSH as used in this Chapter had a low 1.3% cross reactivity with the rat FSH assay (Jimenez *et al.* 2005), and hence was no cause for concern on data obtained herein.

The stimulation of testicular testosterone alone using hCG required the addition of the FSH Ab to suppress endogenous rat FSH levels which rise under the influence of testosterone stimulation (Rea *et al.* 1986, Bhasin *et al.* 1987). The result for hCG + FSH Ab for LH was interesting, in that levels were again suppressed to the same extent as observed in animals treated with acyline plus FSH Ab. This appears to be a specific effect of the FSH antibody itself, as when FSH was suppressed with hrFSH, LH levels were not. Further investigations need to be conducted into the FSH antibody used in this study to determine if it has any LH content. Again, the FSH Ab used in this particular treatment meant serum FSH levels could not be determined, but the endogenous stimulation of testosterone with hCG did increase serum androgens (3-fold), as was expected based on previous studies using the same hormone dose (Pratis *et al.* 2003).

When hCG (which has a low 4% cross-reactivity with the rat LH assay used herein (Haavisto *et al.* 1993)) was used to stimulate both testosterone and FSH production, no effect was seen on suppressed LH levels, but serum androgens and endogenous rat FSH levels increased significantly as expected (Meachem *et al.* 1998, Pratis *et al.* 2003). Suppressed rat FSH levels recovered 2 fold to 25% of control levels in this study. In the GnRH immunised rat, hCG or androgen testosterone administration for the same period of time led to similar fold increases in FSH, although the final concentration was much higher than this study (Meachem *et al.* 1998, Pratis *et al.* 2003). This would have been due to the far greater suppression of FSH induced by acyline compared to the GnRH immunogen and so similar recoveries in FSH would have required longer hCG administration which was not possible (Meachem *et al.* 1998, Pratis *et al.* 2003).

The effect of hormone suppression on germ cell numbers in this study was analysed by optical dissector stereology. This form of stereology is assumption free and unbiased, and is also good for quantifying non-spherical objects such as spermatogonia and spermatids (Wreford, 1995, Meachem *et al.* 1998).

Acyline treatment significantly reduced the numbers of the early type A/intermediate spermatogonia to 66% of controls, but did not achieve a significant suppression of type B/preleptotene

spermatocyte numbers, despite a reduction to 76% of controls. The addition of the FSH Ab resulted in a further suppression of these germ cell types which was significantly greater than acyline alone, showing the requirement to fully suppress FSH to achieve better spermatogenic suppression.

In a closely related study examining the effect of GnRH immunisation on testicular germ cell numbers, type A/intermediate spermatogonia and type B/preleptotene spermatocytes were all suppressed to approximately 50% of control levels (Meachem *et al.* 1998) which was a greater suppression than that obtained in this study. This was despite the similar reductions in testis weights and serum androgens between the two studies, and a greater suppression of serum FSH in this study. It has been suggested that the presence of FSH promotes cell survival (McLachlan *et al.* 1995, Shetty *et al.* 1996), and so with the lower amounts of serum FSH following acyline treatment compared to immunogen treatment (Meachem *et al.* 1998, Pratis *et al.* 2003), it was expected that the early germ cell types in this study would have been similar to, if not lower than the numbers obtained in the immunogen study. The failure of this to be the case demonstrates that the GnRH-antagonist treated rat model is different to the GnRH immunised rat model. Alternatively, the GnRH studies suppressed hormones for 12 weeks (Mclachlan et al. 1994b, McLachlan *et al.* 1995, Meachem *et al.* 1998, Pratis *et al.* 2003) as opposed to the 8 week suppression conducted herein. It is possible that full spermatogenic suppression was not achieved after 8 weeks of acyline treatment hence the higher numbers of these spermatogonia and preleptotene spermatocytes. Another possibility is that distinguishing type A/intermediate spermatogonia from Type B/preleptotene spermatogonia can be difficult due to the severely regressed tubules encountered in GnRH immunised or antagonist treated rats (Meachem *et al.* 1998), and errors could have been made in the count. Future studies could benefit from an additional endpoint as back-up for final germ cell number results.

Short-term hormone replacement with hrFSH kept the type A/intermediate spermatogonia at the same levels as observed for the acyline + FSH Ab treatment group, which again was unexpected. The same phenotype was seen in the hCG + FSH Ab treatment group, and the hCG alone group. In the Meachem *et al.* (1998) GnRH immunisation study, exogenous FSH and/or testosterone stimulated a significant recovery in these germ cell types compared with the GnRH immunised group. It may be possible in this GnRH antagonist model that FSH initiated a survival mechanism in the early spermatogonia by promoting their conversion to type B spermatogonia. This mechanism is supported

by a recovery back to control numbers after short-term hrFSH replacement or stimulation of FSH production with hCG, but not with testosterone stimulation alone. This is a potential novel finding for a role for FSH in type A spermatogonial maturation. Interestingly, this appears to be similar to effects observed in a hormone-suppressed human model, where spermatogenesis was suppressed using T plus the progestin DMPA (Matthiesson *et al.* 2006). In that study, 6 weeks of hormone suppression led to a 17% reduction in type A spermatogonia compared to controls. Even though the difference was not significant, short-term hormone replacement with FSH and hCG, kept type A spermatogonia at approximately 17% of control values as well (Matthiesson *et al.* 2006), meaning that type A spermatogonial numbers were not effected by either hormone treatment (Matthiesson *et al.* 2006). The type B spermatogonia were significantly suppressed in that study with T + DMPA, and hormone replacement led to recoveries back to control levels (Matthiesson *et al.* 2006). It appears therefore that the GnRH-antagonist treated rat model mimics responses observed in the human model for early spermatogonial maturation.

Suppression of leptotene/zygotene spermatocytes, as well as pachytene spermatocytes and round spermatids, with acyline in this study was significant and comparable with the extent of suppression observed with the GnRH immunogen (Meachem *et al.* 1998). Each short-term hormone replacement regimen did not give significant recoveries in leptotene/zygotene spermatocyte numbers compared to the acyline-treated group (50% of control). Numbers also remained significantly lower than controls. These results appeared to reflect those obtained in the Meachem *et al.* (1998) study.

The reduction in pachytene spermatocyte numbers to 15% (stages I-VIII) and 3% (stages IX-XIV) of control as well as the later germ cell types with acyline occurred in tubules where a marked disruption in blood-testis barrier function was demonstrated. Interestingly, treatment with the FSH Ab resulted in further significant suppression in pachytene spermatocyte numbers at both stages I-VIII, and IX – XIV as well, reinforcing the need for FSH in pachytene spermatocyte maturation. Encouragingly, all short-term hormonal treatments appeared to stimulate significant recoveries in pachytene spermatocytes. hrFSH alone appeared to give significantly better recoveries of pachytene spermatocytes than the hCG treatments. The same significant recovery was seen for round spermatids which was probably a flow on effect of the increase in pachytene spermatocyte number (Meachem *et al.* 1998). The extent of flow-on in the spermatogenic wave is dictated by the number of days of short-

term treatment (Meachem *et al.* 1998). The maturation of step 8 round spermatids into elongated spermatids takes 13 days (Meachem *et al.* 1998) and so no change in elongate numbers was expected after 7 days of short-term hormone replacement. The increase in round spermatids was again largely FSH driven, although the stimulation of testosterone alone also gave a significant recovery. Similar results were obtained in the Meachem *et al.* (1998) study. Interestingly, hrFSH stimulated significantly greater numbers of type B spermatogonia/preleptotene spermatocytes, early pachytene spermatocytes and round spermatids than the hCG-induced rat FSH suggesting that the former treatment had greater biological effect than the latter treatment. The data obtained has demonstrated the importance of FSH in spermatogenesis and while testosterone alone can maintain spermatogenesis albeit at a reduced capacity (Singh *et al.* 1995), it appears that FSH is an essential hormone in early to mid spermatogenesis.

Immunohistochemical analysis showed that the suppression of hormones with acyline treatment disrupted TJs both functionally and structurally. In control testes, the localisation of occludin, claudin-11 and JAM-A at the TJ and ZO-1 at the cytoplasmic plaque was extensive in the control animals. This was coincident with a functional barrier as shown by extensive biotin staining in the interstitium and permeation into the seminiferous tubules only as far as the occludin marked TJ. Acyline treatment for 8 weeks resulted in marked changes in occludin, claudin-11 and JAM-A localisation. Occludin became difficult to detect by confocal-immunofluorescence whereas claudin-11 and JAM-A both localised to the Sertoli cell cytoplasm. Some JAM-A staining continued at the basal aspect of the Sertoli cells and this may have been spermatogonial as seen in the Djungarian hamster model (Tarulli *et al.* 2008). ZO-1 staining was also disrupted in this model and had become more adluminal with respect to the basement membrane of the tubules. The localisation of each of these proteins was similar to that seen in the gonadotrophin deplete testis of the short-day Djungarian hamster model (Tarulli *et al.* 2006, Tarulli *et al.* 2008) except for occludin, where staining continued and had re-localised to the Sertoli cell cytoplasm as per the other proteins (Tarulli *et al.* 2008). The disruption in TJ protein localisation in this study was associated with the disruption of TJ function as shown by extensive penetration of biotin throughout the seminiferous tubules to surround any remaining pachytene and round spermatid germ cells. These results were indicative of the observations made in the Sertoli cell specific androgen receptor knockout mouse model (Meng *et al.* 2005), the

prepubertal rat testis displayed in the previous Chapter (recall Figure 4.5) and the seasonally regressed testis of the Djungarian hamster (Tarulli *et al.* 2008). The TJ in the short-day hamster model had originally been shown to be non-functional with the use of tracers and electron microscopy (Bergmann, 1987). Interestingly, occludin and claudin-11 were present at the TJ in the Sertoli cell specific androgen receptor knockout mouse (Meng *et al.* 2005) and the change in TJ function was attributed to the loss of claudin-3 (Meng *et al.* 2005). As mentioned in the previous Chapter, claudin-3 mRNA expression and localisation at the rat Sertoli cell TJ were undetectable in another study (Kaitu'u *et al.* 2007). These data point to some inter-species differences between Sertoli cell TJ components and their response to hormonal fluctuations (Meng *et al.* 2005, Tarulli *et al.* 2006).

Short-term hormone replacement led to a partial re-localisation of occludin, claudin-11, JAM-A and ZO-1 to their respective junctions, although this was not complete, presumably because a longer period of stimulation was needed. Following ten days of FSH treatment in gonadotrophin suppressed hamsters, claudin-11 had largely re-localised to the Sertoli cell TJ (Tarulli *et al.* 2006, Tarulli *et al.* 2008). Furthermore, these hamster TJs had become functional again by their ability to exclude biotin tracer. In the acyline study presented here, biotin still largely permeated beyond the TJ and throughout the seminiferous tubules after 7 days of short-term hormone replacement. This suggested that despite some re-establishment of TJ structure, TJs were still non-functional. The effect of hormone administration on TJ structure and function had also been observed in an immature Sertoli cell culture model, where hormone treatment lead to claudin-11 and occludin localisation to the TJ as well as an increase in TJ function as measured by TER (Kaitu'u *et al.* 2007). Therefore, there are similarities between the localisation of TJ proteins and subsequent functional phenotypes in both normal and disrupted spermatogenesis in two different species.

Marked decreases in tubule diameters and the disappearance of lumens was apparent in immunofluorescent micrographs following hormone suppression. This has been associated with disrupted TJ function in the past (Tarulli *et al.* 2006, Tarulli *et al.* 2008, Bergmann, 1987, Pelletier, 1990). Short-term hormone replacement with each of the treatments also led to the re-establishment of tubule lumens which indicated the reformation of functional TJs (Bergmann, 1987, Tarulli *et al.* 2006, Tarulli *et al.* 2008). As mentioned above however, the majority of tubules were still readily permeable to biotin, and this was despite significant increases in the numbers of pachytene spermatocytes and

round spermatids indicating some spermatogenic restoration, which reportedly requires functional TJs (Bergmann, 1987, Chung and Cheng, 2001, Chung *et al.* 2001,). However, this data suggests otherwise, and that the Sertoli cell TJ does not need to be fully functional for spermatogenesis to proceed. Rather it needs to be dynamic to allow spermatogenesis to proceed into the meiotic stages of germ cell development. This dynamic activity may be directly related to changes in the size-selective nature of the Sertoli cell TJ. The data presented for biotin suggests that spermatogenesis can proceed even when the TJ cannot selectively-exclude tracers of at least 600Da in size. Interestingly, a recent study showed that small molecular weight immunosuppressive molecules (496Da-522Da) are present in the testes (Foulds *et al.* 2008). While this paper looked at the role of these molecules in adult rats which exhibit normal spermatogenesis and TJs, one might hypothesise that these molecules effectively protect germ cells at the initiation of spermatogenesis in younger rats, when the TJ is not completely functional. Other examples of TJs not being fully functional to maintain epithelial integrity have already been documented in this thesis for biotin in the blood-brain barrier (Nitta *et al.* 2003), and ^{51}Cr-EDTA permeation across the blood-testis barrier in young rats just beginning the spermatogenic cycle (Setchell *et al.* 1981, Setchell *et al.* 1988).

Occasionally complete occludin localisation to the TJs and complete biotin exclusion was seen after just one week of hormone replacement in this model. While the percentage of tubules displaying this ‘repaired’ phenotype was not determined, it appeared very small, and could therefore not account for the large recoveries of pachytene and round spermatid germ cells that were observed. The presence of these ‘repaired’ tubules could be explained as either a more rapid recovery of tubular function under hormonal stimulus, or by an incomplete suppression in all tubules by the acyline treatment. As no evidence for this latter point was observed, it is suggested that tubule recovery was heterogeneous. A quick restoration of TJ function has been reported in the past for wounded eye epithelia (Hutcheon *et al.* 2007), and suggests that a longer term hormone replacement experiment (7 to 21 days) should be conducted following suppression to see if TJ disruption is completely reversible. With the current experimental design, this would not be possible because of antibody response to heterologous protein hormones (McLachlan *et al.* 2002b). A recent study has administered recombinant rat FSH (rrFSH) in the long term to GnRH immunised rats, but this failed to rescue reduced testis weights or suppressed serum hormone (including FSH) levels (Ruwanpura *et al.* 2008). This was despite significant

recoveries for type A/intermediate spermatogonia, leptotene/zygotene and early pachytene spermatocytes (Ruwanpura *et al.* 2008). However, no assessment of blood-testis barrier function or TJ protein localisation was attempted in this particular study.

As mentioned in the literature review, one of the key roles of the blood-testis barrier is to ensure that adluminal germ cell antigens are sequestered from the immune system (see Chapter 1, Section 1.2.2). It was therefore expected in this model that the disruption in TJ function and subsequent significant losses of adluminal germ cells could in some part be attributed to an immunological response. Immunohistochemistry was therefore conducted for the macrophage-specific markers ED1 and ED2 (Gerdprasert *et al.* 2002). ED2 highlights the majority of the macrophages in the testis, whereas ED1 highlights the remaining circulating monocytes/macrophages which are ED2 negative (Gerdprasert *et al.* 2002). In the control rat testes of this Chapter, very few macrophages, surrounded the seminiferous tubules, and none were observed on the adluminal side of the BTB. In the hormone-suppressed testes, there qualitatively appeared to be higher numbers of macrophages surrounding the tubules, although very few had actually entered them. Macrophage numbers appeared to decrease again following short-term hormone replacement. These results are similar to another study which used bacterial lipopolysaccharide (LPS) to induce an immune response in the adult rat testis (Gerdprasert *et al.* 2002). As a result, increased numbers of $ED1^{+}$ macrophages were seen proliferating in the interstitium and lining up on the outside of the seminiferous tubules after LPS treatment, compared with control tissues. This information has been reprinted here in this Chapter (Figure 5.10), and compared with the response seen for acyline suppression.

LPS reportedly lowers testosterone levels by blocking LH production and Leydig cell steroidogenesis (Gerdprasert *et al.* 2002). One of the key roles of the testicular Leydig cells is to regulate pro- and anti-inflammatory cytokines of the testis and recruit macrophages (Hedger *et al.* 2005). Testosterone has been shown to regulate the levels of the anti-inflammatory cytokines, including macrophage migrating inhibitory factor, interferon-γ, transforming growth factor (TGF)-β and activin A (Hedger *et al.* 2005) in the rat testis. These cytokines are highly expressed in control and inflamed testes, which attenuates the propensity of the macrophages to stimulate the release of pro-inflammatory cytokines including tissue necrosis factor (TNF)-α and interleukin-1 (IL-1)-α/β (Hedger,

Figure 5.10 Macrophage localisation in control and disrupted testes.

Comparative immunohistochemical analysis of macrophage localisation in adult rat testes from Gerdprasert *et al.* (2002) (panels A and B), and the GnRH antagonist study presented herein (panels C and D). Inflammation was induced by bacterial lipopolysaccharide (LPS) treatment in the Gerprasert *et al.* (2002) study and macrophages (purple) were stained for ED1 and ED2. Comparisons were made between the normal control testis (panel A) and LPS treated testis (panel B). Macrophages from this GnRH antagonist study were also stained for ED1 and ED2 (green) and comparison drawn between the normal control testis (panel C) and the hormone suppressed testis (panel D). Bar = 10μm.

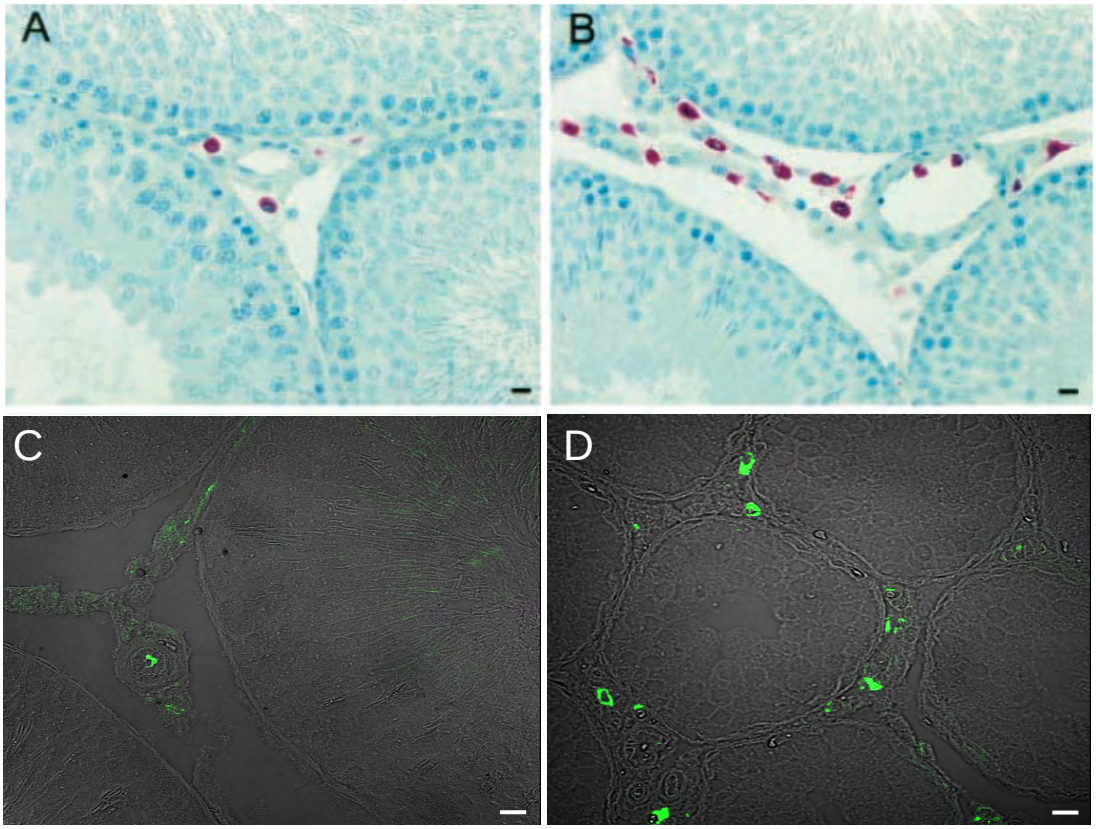
A
B
C
D

2002, Hedger *et al.* 2005, O'Bryan *et al.* 2005). This phenomenon is not observed in other tissues including the liver, which deems the testis an immunologically privileged site which helps protect the germ cells (Hedger *et al.* 2005). In low testosterone levels induced by LPS treatment, the testis mounts an overt pro-inflammatory response, which is reversed by the exogenous application of testosterone (Gerdprasert *et al.* 2002, Hedger *et al.* 2005, O'Bryan *et al.* 2005).

It is reasonable therefore considering the phenotypic similarities of macrophage localisation and suppressed/replaced testosterone in the LPS study, and the acyline study with its concomitant low levels of testosterone presented in this Chapter, that these low androgen concentrations could have caused a pro-inflammatory response with cytokines possibly including TNF-α and IL-1α/β, both of which are known to disrupt testicular TJ structure and function (Cheng and Mruk, 2004, Lui and Lee, 2006, Sarkar *et al.* 2008). It is therefore hypothesised that the Sertoli cells and remaining germ cells may have been exposed to factors derived from the immune system in the acyline-treated rat testis, which in turn could have played a part in germ cell decline. For more conclusive results, it would be necessary to conduct quantitative analysis of macrophage numbers in the hormone suppressed/replaced testis, with additional mRNA/protein expression analysis of the main candidate pro- and anti-inflammatory cytokines. Furthermore, it would also be interesting to analyse the response of the small molecular weight (496Da-522Da) immunosuppressive molecules (Foulds *et al.* 2008) mentioned above to hormone suppression and short-term replacement.

The disruption of the TJ structure as demonstrated by immunohistochemistry was also associated with a decrease in occludin and claudin-11 protein expression as shown by western blot analysis. Short-term hormone replacement did not appear to stimulate any recovery in either protein's expression despite their apparent re-localisation to the TJ as shown by immunohistochemical analysis. This may have been a detection sensitivity issue of the Odyssey software used for analysis. Alternatively, the poor cross-reactivity of the primary antibodies with the SDS protein extracts could also have been a reason for the limit detectability. An increased protein load was attempted but to not avail. Therefore, no quantitative analysis was conducted on protein expression due to these difficulties, which were outlined in Chapter 3.

In contrast to the protein responses, mRNA levels of occludin and claudin-11 both significantly increased in response to hormone suppression, and short-term hormone replacement led

to further significant changes back toward control levels. Such a result is difficult to explain, as it goes against the trend for function and localisation, but it may be that the Sertoli cells were trying to re-establish the blood testis barrier by producing more protein through a rescue mechanism, but hormone suppression had put a block at the protein translation point and/or at protein localisation. Several studies have shown the existence of cytoplasmic pools of TJ proteins (Ando-Akatsuka *et al.* 1999, Lu *et al.* 2001, Bruewer *et al.* 2003, Ivanov *et al.* 2004, Bruewer *et al.* 2005, Meng *et al.* 2005, Morimoto *et al.* 2005, Tarulli *et al.* 2008). Claudin-11 and JAM-A were also seen in the cytoplasm of the acyline treated rats in this study. In a recent report, testosterone was shown to enhance the internalisation of TJ proteins occludin and JAM-A (Yan *et al.* 2008) and the recycling of these proteins back to the TJ as a possible mechanism of disassembling and then reassembling TJs as germ cells cross the blood testis barrier (Yan *et al.* 2008). Despite the resolution of the images presented herein not being sufficient enough to observe these proteins in defined cytoplasmic vesicles, the data is strong enough to allow the hypothesis that testosterone and FSH may be doing the same thing in this acyline-treated rat model. The mRNA data obtained herein was shown to hold true for two different housekeepers (β-actin and GAPDH), as there were no significant differences in the ratio of these two transcripts across the various treatments, despite the very large changes in testicular weights, and germ cell types and numbers between the various treatment groups. No changes in Sertoli cell specific GATA-6 mRNA expression were also observed in the Djungarian hamster model despite large fluctuations in testis weights in response to hormone suppression/replacement in those animals (Tarulli *et al.* 2008). Furthermore, the mRNA expression of the known androgen-regulated protein INSL-3 significantly decreased 10 fold after hormone suppression, and recovered to control levels only in the androgen-stimulated treatment groups, confirming that the real-time RT-PCR expression analysis method used in this model was not suffering from artefacts.

Differences between the protein and mRNA expression could be explained by the recycling of TJ proteins between the TJ and the cytoplasm, rather than decreases in their protein expression. Following hormone withdrawal as seen in this study, or the seasonally regressed Djungarian hamster testis (Tarulli *et al.* 2008) or the pro-inflammatory cytokine treated rat testis (Sarkar *et al.* 2008), cytoplasmic localisation of claudin-11 and/or occludin was observed. Upon restoration of TJ function, the protein appears to be recycled and re-localised to the new TJ, and may not involve the translation

of any new protein. This could be due to phosphorylation events occurring within the Sertoli cells, which has been shown to recruit certain TJ components to the TJ (Gonzalez-Mariscal *et al.* 1985, Sim and Scott, 1999, Matter and Balda, 2003, Gonzalez-Mariscal *et al.* 2008), indicating an interplay between phosphorylation and hormonal control of the TJ.

Quantitative TJ functional analysis with [^{3}H]methoxy-inulin in this Chapter showed no great change in TJ function in response to hormone suppression or replacement. While various significant differences were recorded across the treatments (recall Figure 5.5), this was most likely due to the high number of samples per group used, making minor differences between groups significant. Given that biotin readily permeated TJs after hormone suppression, this Chapter had already qualitatively shown that TJ function was disrupted and so it was expected that quantitatively there would have been a significant increase in [^{3}H]methoxy-inulin accumulation within the seminiferous tubules. However, there were unexpected problems with the quantitative tracer technique. In the previous Chapter, blood-testis barrier disruption with glycerol resulted in a limited 2 fold accumulation of [^{3}H]methoxy-inulin compared with controls, whereas in this Chapter, only a 1.2 fold increase was observed, despite a similar testis weight reduction. Hence, the dynamic range of this test was not sufficient to quantitate permeability changes in the acyline study. It was suggested in the previous Chapter that this small increase in tracer accumulation could have been due to tracer size and crude protocol techniques, and so in a separate study conducted in this Chapter, the accumulation of [^{3}H]methoxy-inulin in control, glycerol treated and pre-pubertal rat testes was compared to the accumulation of the much smaller tracer [^{14}C]mannitol. The tracer administration method was also modified to allow comparisons between tubules incubated with the tracers (as done previously), or direct injection via an intratesticular injection as per the biotin technique.

When seminiferous tubules from control, glycerol treated and pre-pubertal rats were incubated in the tracers, the accumulation of [^{14}C]mannitol was significantly higher by 18% and 14% than that of [^{3}H]methoxy-inulin in the control and glycerol testes respectively, but not in the juvenile testes, which were yet to form TJs as they were prepubertal (Russell and Peterson, 1985, Russell *et al.* 1989). The data suggested that the tubules were more permeable to the smaller tracer than the larger one, which would be expected. However, when testes from each rat group were injected with the tracers, tubules were equally permeable to [^{14}C]mannitol as they were to [^{3}H]methoxy-inulin for reasons unclear. Pre-

pubertal testes always accumulated significantly more of either tracer on a dpm/g testis basis than the adult control and glycerol testes, which was expected due to the lack of TJs in these tissues (Russell and Peterson, 1985, Russell *et al.* 1989). However, it was of concern that no differences were seen between glycerol-treated or control rats for either tracer. This result was in contrast to the studies presented in this and the previous Chapters and was in despite of testis weights having decreased by comparable amounts. Given the discrepancy in tracer accumulation and the relatively small difference testing [^{14}C]mannitol accumulation made, it appears that the experimental protocol itself needs further optimisation rather than the tracer size being the issue. A measure of tracer uptake efficiency should be included in future experiments using this protocol. Compounding this point was a recently published paper, which showed increased inulin-fluorescein labelled isothiocyanate accumulation in seminiferous tubules after treatment with IL-1α to disrupt TJ function (Sarkar *et al.* 2008). While that study was qualitative in nature, it demonstrated that a molecule the size of inulin could cross a disrupted TJ barrier. A second potential improvement would be to administer the tracer via the jugular vein, which is a popular route of tracer administration in other studies (Setchell *et al.* 1981, Setchell *et al.* 1988) including the Sarkar *et al.* (2008) report. In summary, the failure to achieve a quantitative difference in TJ function in response to hormone suppression was not due to i) a fully functional TJ in the absence of hormones as shown by biotin permeation or ii) inappropriate molecular weight of the [^{3}H]methoxy-inulin tracer used, but due to experimental techniques which need further optimisation.

In conclusion, the data reported in this Chapter demonstrates that the rat Sertoli cell TJ is regulated by hormones *in vivo*. Hormone suppression resulted in a decrease in TJ function as shown by an increased permeability to biotin, which was coincident with a change in TJ protein localisation and expression and loss of tubule lumens, as well as a loss of adluminal germ cells and a qualitative increase in macrophage number surrounding the seminiferous tubules. Short-term hormone replacement with FSH and/or hCG partially reversed the suppressive effects of acyline. This was demonstrated by the renewed proliferation of adluminal germ cell types, some relocalisation of TJ proteins to the TJ, reappearance of tubule lumens and some biotin exclusion from the seminiferous tubules, which were all indicative of a partial restoration of TJ function. Finally, this Chapter has demonstrated the essential roles that both FSH and testosterone have in regulating the TJ both

functionally and structurally *in vivo*, in terms of protein expression and localisation as well as mRNA expression, and how essential the TJ is to successful spermatogenesis.

Chapter Six: Hormonal regulation of the Sertoli cell tight junction in the hypogonadal (*hpg*) mouse, *in vivo*

Chapter 6. Hormonal regulation of the Sertoli cell tight junction in the hypogonadal (*hpg*) mouse, *in vivo.*

6.1 Introduction

The previous Chapter used a GnRH-antagonist treated rat model to determine the effects of gonadotrophin suppression and short term gonadotrophin replacement on TJ function and structure. Upon gonadotrophin suppression, TJ structure was disrupted as shown by changes in protein expression and localisation to the TJ, as well as changes in mRNA expression. Furthermore, the function of the TJ was disrupted following gonadotrophin suppression, as shown by a marked permeation of the tubule by the qualitative TJ functional tracer, biotin. Short-term gonadotrophin replacement partially restored TJ structure and function in some cases. These results demonstrated a role for gonadotrophins in the *maintenance* of Sertoli cell TJ structure and function in the adult rat. However, the extent to which gonadotrophins are required for the *initiation* of TJ structure and function remains to be determined. Several lines of evidence associate increases in gonadotrophins with the first appearance of TJ proteins at the basal aspect of Sertoli cells in vivo, as reviewed in Chapter 1.6.1 and 1.6.2d. Sertoli cell TJs do not form until puberty which is associated with an increase in circulating gonadotrophins (Russell and Peterson, 1985). Furthermore, in the absence of circulating gonadotrophins, TJ formation is delayed or prevented (Nitta *et al.* 2003). Men displaying low levels of circulating gonadotrophins also displayed an immature TJ phenotype, which was reverted to a mature phenotype upon the exogenous application of gonadotrophins (de Kretser and Burger, 1972). In order to study the role of FSH and LH/T in the initiation of TJ structure and function, it was decided to employ the *hpg* mouse model which lacks spermatogenesis due to an absence of GnRH action at the pituitary level.

The *hpg* mouse is deficient in circulating gonadotrophins due to a large mutation in the GnRH gene resulting in the deletion of two of the four GnRH exons (Mason *et al.* 1986a, Handelsman *et al.* 1999), and offers a unique naturally occurring animal model of spermatogenic inactivity. Spermatogonia and primary spermatocytes are arrested at 11% and 2% of wildtype respectively (Singh *et al.* 1995, Ebling *et al.* 2000, Myers *et al.* 2005). The production of human FSH in *hpg* mice via the insertion of a transgene (*hpg* + tgFSH) resulted in the stimulation of spermatogenic activity through to

the production of round spermatids and a few elongated spermatids, but no further (Allan *et al.* 2001, Allan *et al.* 2004). Androgen (DHT or testosterone) application to *hpg* mice via Silastic implants induced qualitatively normal spermatogenesis with fertile sperm (Singh *et al.* 1995, Handelsman *et al.* 1999). These studies demonstrated that inactive spermatogenesis could be stimulated via the application of gonadotrophins. While TJ strands have been observed by electron microscopy in the *hpg* mouse model (Charlton *et al.* 1983, Myers *et al.* 2005), they appeared disorganised in comparison with control tissues, and were presumably dysfunctional, due to the absence of spermatogenesis and the markedly reduced testis weights compared to wildtype mice (Charlton *et al.* 1983, Myers *et al.* 2005). It is hypothesised in this thesis that the administration of gonadotrophins to *hpg* mice will result in the formation of functionally and structurally competent Sertoli cell TJs containing claudin-11 and claudin-3. While the claudin-11 knockout mouse is infertile (Gow *et al.* 1999), the Sertoli cell androgen receptor knockout prevents the localisation of claudin-3 to TJs in mice during germ cell migration (Meng *et al.* 2005). However, a claudin-3 knockout is still required for elucidating its role at the TJ and during spermatogenesis. It is thereforefurther hypothesised that the initiation of TJ formation in this model will lead to the recruitment of claudin-3 to the blood-testis barrier (Meng *et al.* 2005).

The aims of studies presented in this Chapter are to i) study the development of the TJ in wildtype, *hpg*, and *hpg* mice which are transgenic for FSH (tgFSH), at both puberty (20 days of age) and into adulthood, and ii) determine the effect of administration of the pure androgen dihydrotestosterone (DHT) on the establishment of TJ function and the recruitment of claudin-3 into the TJ in *hpg*, and *hpg* + tgFSH mice in the short-term (2 days) and longer-term (10 days). A Silastic implant of 1.0cm in length was chosen as the DHT dose based on published data which showed that this dose gave maximal stimulation of serum DHT and round spermatid numbers (Singh *et al.* 1995). In the photoregulated Djungarian hamster model, changes in TJ structure was observed within 2 days with FSH treatment (Tarulli *et al.* 2006, Tarulli *et al.* 2008), and therefore it was hypothesised that any changes in TJ structure and/or function in the mouse could also occur within 2 days, hence this short-term time point.

For both of the above aims, endpoints will include immunohistochemical localisation and real-time RT-PCR quantification of the TJ proteins claudin-11, occludin and claudin-3. TJ function

analysis will use the biotin tracer technique as employed in the GnRH-antagonist treated rat experiment in Chapter 5.

Experiments in this Chapter were conducted in collaboration with Dr Charles Allan, who provided access to the *hpg* colony at the Anzac Research Institute, Concord Hospital, Concord, Sydney, NSW, Australia.

6.2 Materials and Methods

6.2.1 Animals

All experimental mouse work except for biotin administration was conducted by Dr Charles Allan at the Anzac Research Institute in Concord, NSW, Australia and was approved by the University of Sydney and Central Area Health Services Animal ethics committee. In brief, operative procedures were conducted under 0.5% ketamine (Parke-Davis, Caringbah, NSW, Australia) and xylazine (Bayer Australia Ltd, Botany, NSW, Australia) anaesthesia which was administered by an intraperitoneal (ip) injection (0.01ml/g body weight) (Handelsman *et al.* 1999). At the end of experimentation, mice were killed by anaesthetic overdose (Handelsman *et al.* 1999).

6.2.2 Experimental design

Part 1 of this Chapter used testis sections from pubertal (20 days old) and adult mice which were either wildtype, *hpg* or *hpg* + tgFSH. These sections were provided by Dr Charles Allan from archived sources and required no experimental work to be conducted on animals.

Part 2 of this study required some animal work prior to experimentation. The pure androgen DHT (Merck, Darmstadt, Germany), was administered to adult *hpg* and *hpg* + tgFSH mice via a SILASTIC implant (1.0cm, Dow Corning, Midland, MA, USA) for 2 days or 10 days (n = 3/group). These mice, along with controls (consisting of wildtype and *hpg* and *hpg* + tgFSH minus the DHT implant (n = 3/group)) were killed on the same day. Testes were then excised, trimmed of all fat and connective tissue and then weighed. Biotin was then administered (see below) to the left testis of each animal, which were then incubated for 30 minutes at room temperature before being fixed for 4 hours in Bouin's fixative. One of the control testes was administered PBS/$CaCl_2$ as the biotin negative

control. The right testis from each mouse was immediately snap frozen in liquid nitrogen for RT-PCR analysis. All testes were then transferred to Prince Henry's Institute of Medical Research in Melbourne for further analysis.

As most of the testes were too small for an intratesticular injection of 10% testis weight, a new method for administration had been previously optimised at Prince Henry's Institute of Medical Research in Melbourne using control adult mouse testes. These testes were administered biotin (10mg/ml) either by i) intratesticular injection (as a positive control), ii) slit on the tunica and then incubated whole in the biotin-containing solution, or iii) placed straight into the biotin containing solution after extraction without slitting the tunica. Testes were processed for immunohistochemistry and probed for biotin as outlined in section 2.2 and 5.2.4. Results of this pilot study are presented in the results section of this Chapter. After the Bouin's fixation procedure, all testes were stored in 70% ethanol.

6.2.3 Immunohistochemistry

Fixed testes from Part 2 of this study were processed on the histokinette for immunohistochemical analysis as outlined in section 2.2. All sections, including those from Part 1 of this study were processed for TJ protein localisation by confocal fluorescent microscopy as outlined in Section 2.2. Biotin was probed in Part 2 testes as outlined in Section 4.2.2. For all antibody incubation details see Table 6.1.

6.2.4 Real-time RT-PCR analysis

RT-PCR analysis was conducted on the Part 2 testes. As most of the testis weights were around 20mg or less, total RNA was extracted from whole testes except for wildtype. The protocol followed was identical to that outlined in section 2.3. According to the RNeasy kit manufacturer (Qiagen), testis samples weighing less than 20mg required 350µl of RLT buffer rather than the standard amount of 600µl to extract RNA.

Primers were optimised and sequenced according to section 2.3. Details of the primers used in this study are shown in Table 6.2.

Table 6.1 Antibodies used for immunohistochemical analysis.

Tabulated data for the antibodies used in Chapter 6 of this thesis include details regarding the primary and secondary antibody hosts, working concentrations (conc.)/dilutions, incubation (Inc.) times and company details with catalogue numbers.

Protein	**Primary (1^{O}) antibody host**	**Company** (cat #)	**Conc.** (μg/ml)	**Negative control**	**1^{o} Inc. time**	**Secondary 2^{o} antibody**	**Company**	**2^{o} Dilution**	**2^{o} Inc. time** (mins)
Claudin-11	Rabbit	Zymed (36-4500)	1.25	Normal rabbit IgG	Overnight	Goat α rabbit Alexa-488 **or** Alexa-546	Molecular Probes	1:400 of stock	30
Claudin-3	Rabbit	Zymed (34-1700)	1.25	Normal rabbit IgG	Overnight	Goat α rabbit Alexa-488 **or** Alexa-546	Molecular Probes	1:400 of stock	30
ZO-1	Rabbit	Zymed (61-7300)	1.25	Normal rabbit IgG	Overnight	Goat α rabbit Alexa-488 **or** Alexa-546	Molecular Probes	1:400 of stock	30
β-catenin	Mouse	BD Transduction Laboratories (610154)	1.25	Normal mouse IgG	Overnight	Goat α mouse Alexa-546	Molecular Probes	1:400 of stock	30
Connexin-43	Mouse	Sigma ascites fluid (C8093)	1:400 of stock	Normal mouse IgG	Overnight	Goat α mouse Alexa-546	Molecular Probes	1:400 of stock	30
Vinculin	Mouse	Sigma ascites fluid (V4505)	1:400 of stock	Normal mouse IgG	Overnight	Goat α mouse Alexa-546	Molecular Probes	1:400 of stock	30

Table 6.2 Primer sequences and real-time RT-PCR conditions for the analysis of mRNA expression in the *hpg*, and *hpg* + tgFSH mice treated with DHT.

Primers were designed against the TJ proteins claudin-11, occludin and claudin-3, as well as androgen-regulated INSL-3 and the housekeeper protein β-actin, to check for changes in their mRNA expression following DHT treatment for 2 and 10 days. Data included in the table are forward and reverse primer sequences, Mg^{2+} concentration, and annealing and acquisition temperatures.

Protein	**Species/ Accession number**	**Primer sequences (5'- 3')**	**Product size** (bp)	**[Mg^{2+}]** (mM)	**Anneal temp.** (^{o}C)	**Acquisition temp.** (^{o}C)
Claudin-11 (Primer3)	Mouse NM_008770	Forward: CTACGTGCAGGCTTGTAGAGC Reverse: GGCACATACAGGAAACCAGATG	208	2.5	64	72
Occludin (Primer3)	Mouse NM_008756	Forward: TTTTTGCTGTGAAAACCCGAAG Reverse: CTGTCAACTCTTTCCGCATAGT	178	2.5	64	72
Claudin-3 (Primer3)	Mouse NM_009902	Forward: AACTGCGTACAAGACGAGACG Reverse: GGCACCAACGGGTTATAGAAAT	143	2.5	64	72
β-actin (Primer3)	Rat NM_031144	Forward: CCGTAAAGACCTCTATGCCAACA Reverse: GCTAGGAGCCAGGGCAGTAATC	103	2.0	67	72
INSL-3 (Primer3)	Mouse NM_013564	Forward: CAGTGCCGCCACCAACGCT Reverse: AGGTCATGATGGGGCTTCTTGG	240	2.0	64	72

6.2.5 Statistical analysis

Statistical analysis was conducted as outlined in section 2.6. Data presented herein is either mean ± SD or SEM, n = 3 mice/group.

6.3 Results

6.3.1 Developmental localisation of claudin-11 and claudin-3 to the tight junction and ZO-1 to the cytoplasmic plaque in pubertal and adult mice

The developmental changes in localisation of various junction proteins was first investigated in pubertal and adult mice from the *hpg*, and *hpg* + tgFSH models, to give an indication of other junctional types which may have been altered by the absence of gonadotrophins in the *hpg* model, and how these changed in the *hpg* + tgFSH mice. Claudin-11, claudin-3 and ZO-1 were co-localised with the adherens junction marker β-catenin, the gap junction marker connexin-43 and the ectoplasmic specialisation protein vinculin respectively.

The intention of this Chapter was to also localise occludin in these mice by immunohistochemistry, however staining was undetectable using two different antibodies (Rabbit anti-occludin (Zymed, cat # 71-1500) and Mouse anti-occludin (Zymed, cat # 33-1500) (Figure 6.1) when using EDTA-NaOH antigen retrieval as outlined in Section 2.2a. A second type of antigen retrieval (0.01M citrate buffer (Na-citrate, citric acid, pH 6.0 (Pileri *et al.* 1997)) was attempted. The immunohistochemistry protocol was as per that outlined in Section 2.2 except with the different antigen retrieval buffer. Occludin staining with the Mouse anti occludin primary antibody generally gave no staining for occludin, although occasional positive staining at the outer edges of the section was detected (Figure 6.1c). Due to the inability to reproduce consistent occludin immunostaining, it was decided to omit this endpoint from this study. This was simply an antibody issue and not due to occludin being absent at the mouse Sertoli cell TJ as it was occasionally seen herein as mentioned above and has been successfully stained in mouse testes in another study (Meng *et al.* 2005).

Figure 6.1 Occludin staining in control wildtype mouse testes.

Detection of occludin (green, arrow) was attempted in Bouin's fixed, paraffin embedded adult control mouse testis sections with rabbit anti occludin (Zymed, panel A) and mouse anti occludin (Zymed, panel B) primary antibodies in sections treated with EDTA-NaOH for antigen retrieval. A follow up experiment also using the mouse anti occludin primary antibody was subjected to citrate-buffer antigen retrieval (panel C). Bar = 50μm.

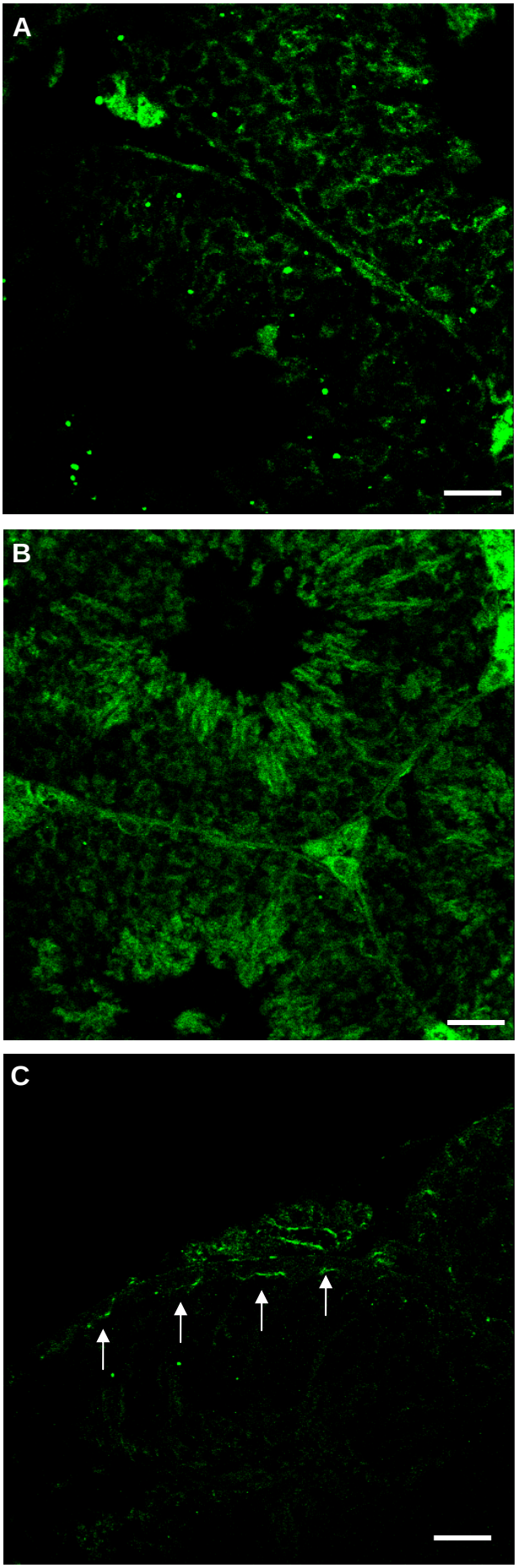
A
B
C

a. Wildtype

Wildtype (*wt*) pubertal mice, which were all 20 days of age and beginning to form round spermatids indicating active spermatogenesis (Sasagawa *et al.* 1998, McCarrey *et al.* 1999, Marh *et al.* 2003, Xu *et al.* 2004), displayed extensive claudin-11 staining which was just adluminal to the spermatogonia (Figure 6.2). β-catenin staining was extensive at the inter-Sertoli cell adherens junction and surrounded spermatogonia, but did not co-localise with claudin-11. Adherens junction staining was also positive around the adluminal germ cells including the pachytene spermatocytes and round spermatids. No claudin-3 was detectable in the *wt* pubertal mice, whereas connexin-43 was extensive toward the outer edge of the tubules at inter-Sertoli cell gap junctions (Figure 6.2). ZO-1 in the *wt* pubertal mouse was extensive at the cytoplasmic plaque toward the outer edge of the tubules, and vinculin staining was extensive throughout the tubules from the basement membrane toward the tubule lumens (Figure 6.2).

In *wt* adult mice all proteins were localised extensively at their respective junctions (Figure 6.2), and this included the appearance of positive staining for claudin-3. All protein 'pairs' co-localised with each other, giving a yellow appearance toward the basement membranes of the tubules, consistent with localisation at inter-Sertoli cell junctions. Of note was that pubertal tissues appeared to display higher levels of background staining than adult tissues, which gave clearer immunohistochemical results. This phenomenon was also apparent in the *hpg* and *hpg + tgFSH* tissue.

b. hpg

In *hpg* pubertal mice, claudin-11 staining was in cytoplasmic pools and disorganised at the centre of the seminiferous tubules (Figure 6.2). In contrast, β-catenin was predominantly localised toward the outer edge of the tubules as per the *wt* mice (Figure 6.2). Claudin-3 was undetectable in pubertal *hpg* testes, and connexin-43 localisation was generally cytoplasmic as per claudin-11, extending toward the outer edge of the tubules. ZO-1 was localised to the cytoplasmic plaque at the outer edge of the tubule, with some cytoplasmic staining evident also. Vinculin staining was predominantly cytoplasmic.

In the adult *hpg* mice, claudin-11 staining was still cytoplasmic and unlike the *wt*, did not co-localise with β-catenin, which was still at inter-Sertoli cell adherens junctions at the outer edge of the

Figure 6.2 Protein localisation in pubertal (20 day old) and adult *hpg* and *hpg* + tgFSH mice.

Bouin's fixed, paraffin embedded testis sections were obtained from pubertal and adult wildtype, *hpg* and *hpg* + tgFSH mice. Sections were processed by immunohistochemistry and stained for TJ proteins claudin-11 (page A) and claudin-3 (page B), as well as the cytoplasmic plaque protein ZO-1 (page C) (all green). These proteins were co-stained with β-catenin (adherens junction), connexin-43 (gap junction) and vinculin (ectoplasmic specialization) (all red) respectively. Bar = 50μm. Inset = negative control.

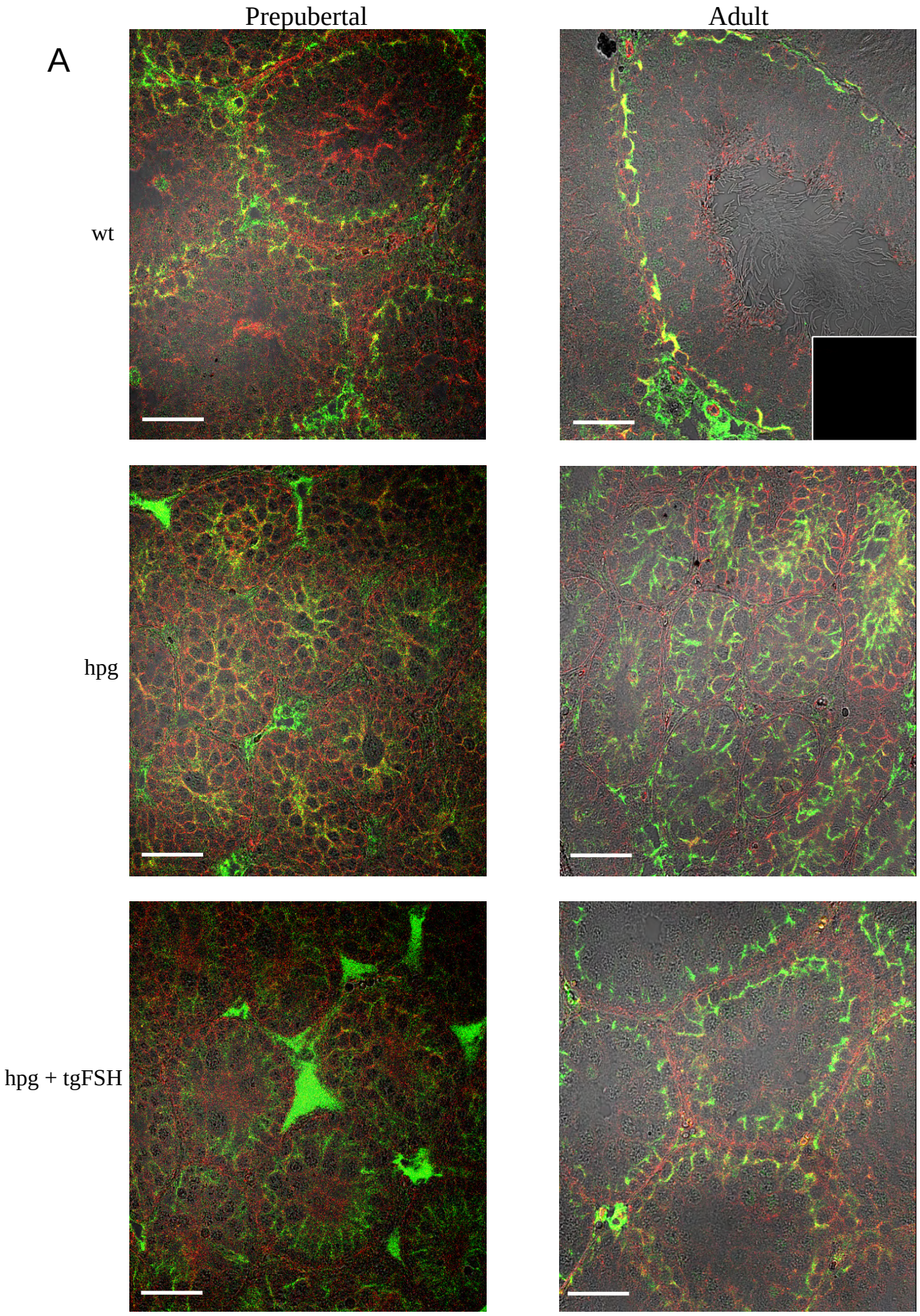
A
Prepubertal
Adult
wt
hpg
hpg + tgFSH

B

Prepubertal

Adult

wt

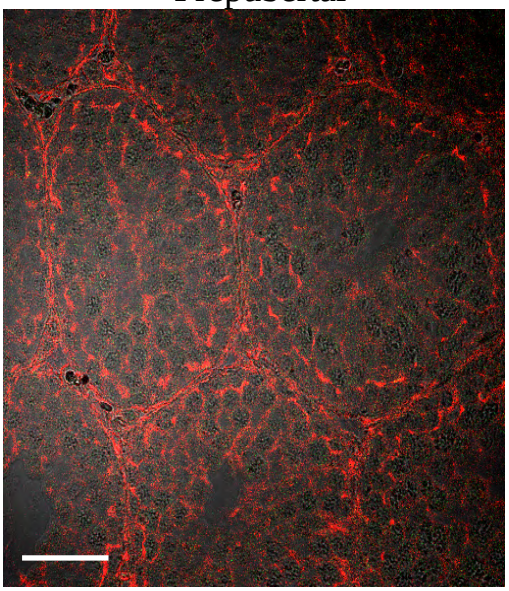

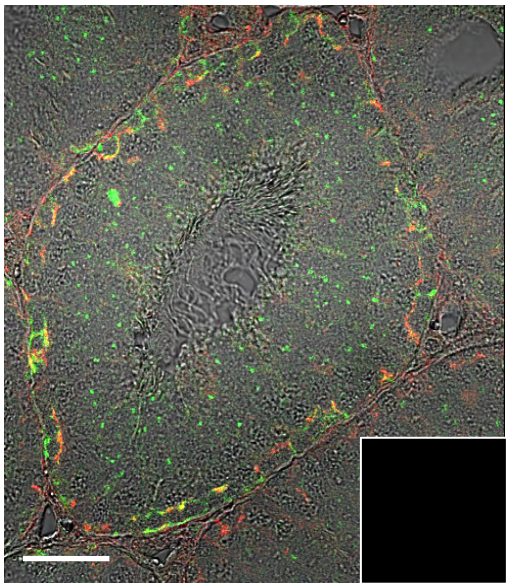

hpg

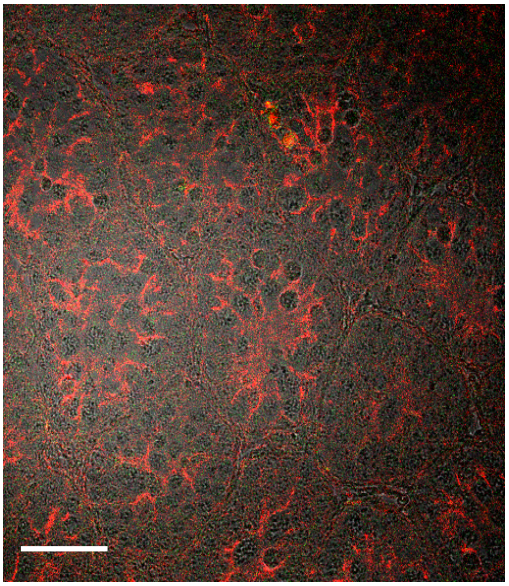

hpg + tgFSH

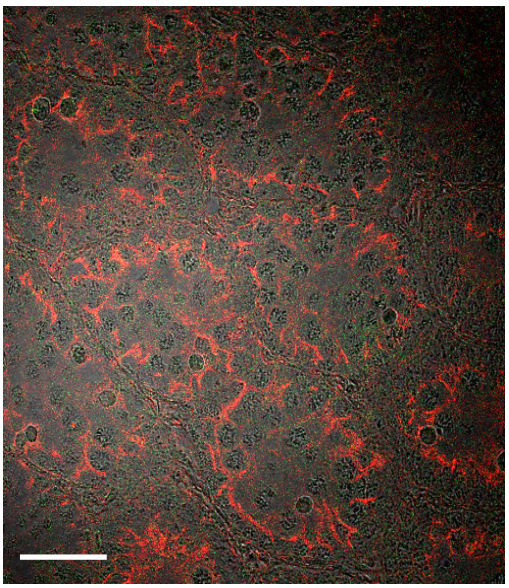

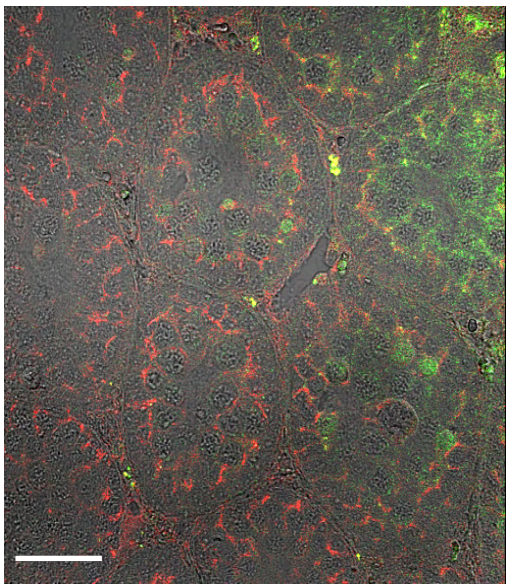

C

Prepubertal

Adult

wt

hpg

hpg + tgFSH

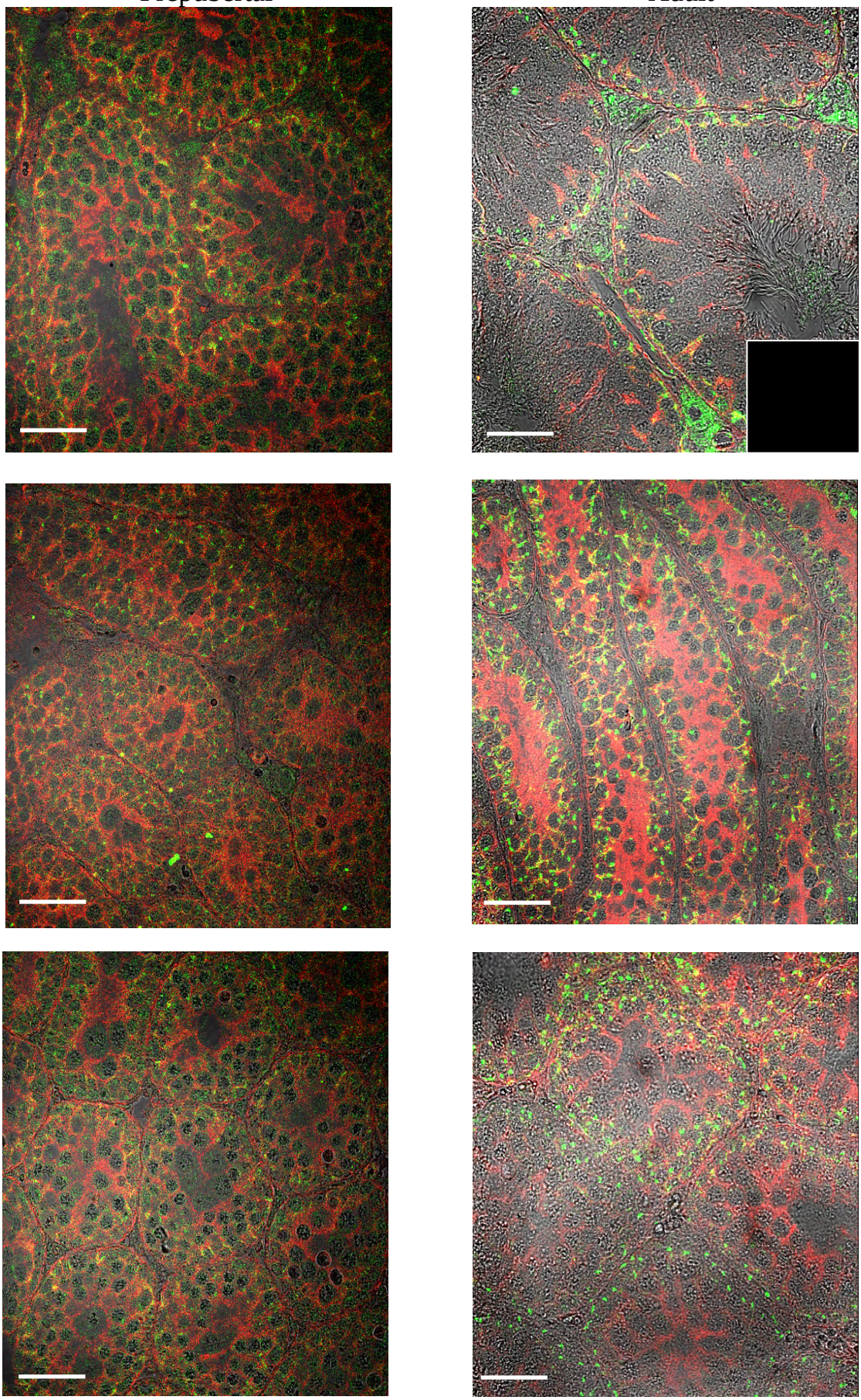

tubules (Figure 6.2). Claudin-3 staining was absent in the adult *hpg,* but connexin-43 stained well at the gap junction toward the basement membrane of the tubules, and was not localised to the cytoplasm unlike the pubertal *hpg* mice, thus resembling the *wt* adult mice (Figure 6.2). ZO-1 localisation was similar to *wt* mice, with staining at the cytoplasmic plaque at the basement membrane, whereas vinculin staining was cytoplasmic and resembled staining in the pubertal *wt* mice (Figure 6.2).

c. hpg + tgFSH

In pubertal *hpg + tgFSH* mice, claudin-11 appeared to be re-distributing from the cytoplasm toward the TJ and appeared slightly more organised than the pubertal *hpg* testes, but much less so than the pubertal *wt* mice (Figure 6.2). β-catenin staining was similar to the *hpg* and *wt* tissue, and was localised at the adherens junction toward the basal aspect of tubules. Claudin-3 staining was also absent, but connexin-43 had begun localising toward the gap junction. Staining was less cytoplasmic compared to *hpg* staining but more so than in pubertal *wt* mice. ZO-1 staining was at the cytoplasmic plaque toward the basal aspect of tubules, and was similar to staining in the *hpg* and *wt* tissue. Vinculin was still cytoplasmic and very similar to the pubertal *hpg* and *wt* testes.

Claudin-11 in the adult mice formed TJs which appeared continuous but irregular compared to the *wt* in that they were more cytoplasmic. This staining resembled the pubertal *wt* mice. β-catenin was extensive at the adherens junction and basal to claudin-11, as per the *wt* pubertal mice (Figure 6.2). Claudin-3 was generally absent in this mouse model, but connexin-43 was present at the gap junction and resembled the *wt* and *hpg* phenotypes. ZO-1 staining was again very similar to its staining in the *wt* and *hpg* testes. Vinculin localisation appeared less concentrated in the cytoplasm compared to *hpg* mice and seemed to be re-localising toward the ectoplasmic specialisation at the basement membrane (Figure 6.2).

6.3.2 Administration optimisation of biotin to the *hpg* mouse testis

Testes from adult *wt* mice were administered biotin by i) intratesticular injection, ii) slit tunica and then incubated in a 10mg/ml biotin solution or iii) intact testis incubation in a 10mg/ml biotin solution (Figure 6.3). In each case, biotin successfully entered the testes and was seen extensively staining the interstitium of each testis, and only entering the tubules as far as the basal germ cells. It

Figure 6.3 Optimization of biotin administration into mice testes.

Testes from adult wildtype mice were excised from freshly killed animals and trimmed of all fat and connective tissue. Testes were then either injected with the biotin (10mg/ml) tracer at 10% weight (panel A), or incubated in the tracer with a slit tunica (panel B), or intact tunica (panel C). Testes were processed by immunohistochemistry and probed for biotin (green) with streptavidin alexa-488. Bar = 50μm. Inset = negative control.

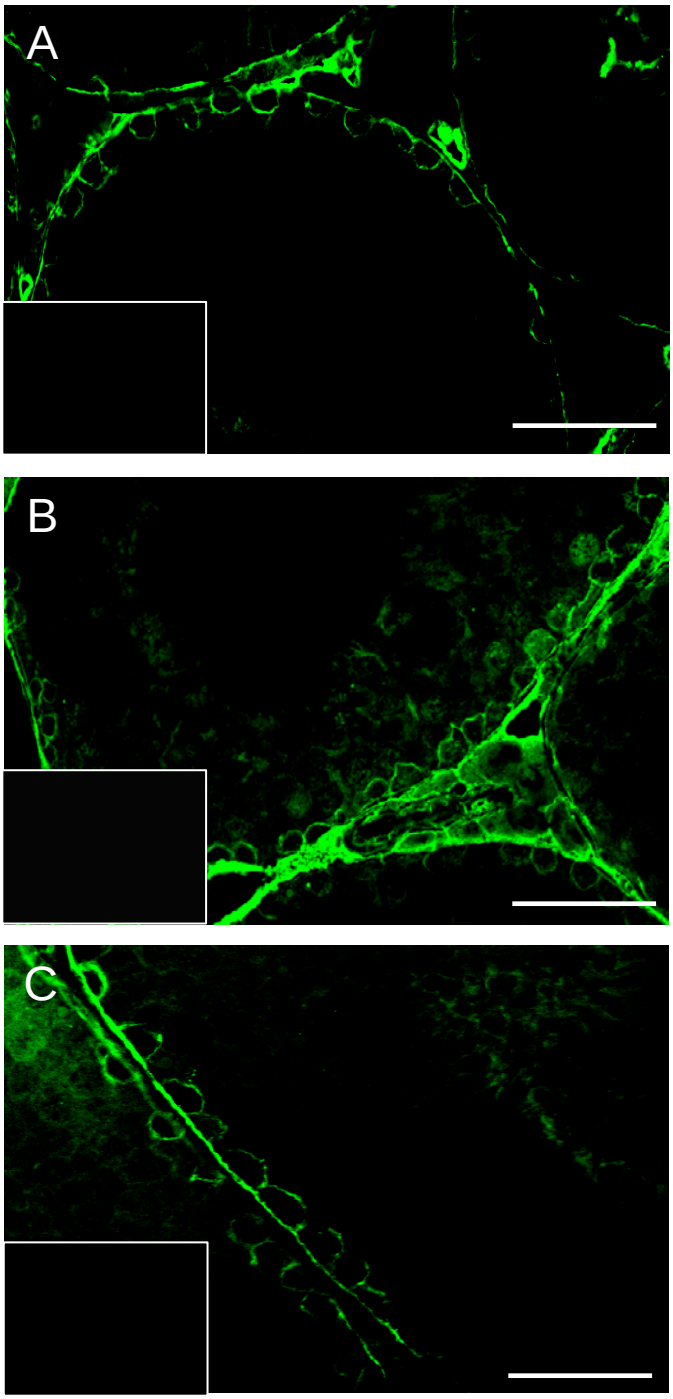
A
B
C

was noted that background staining was present in the incubated testes but absent in the biotin injected testes (Figure 6.3). As a result of these images, it was decided for Part 2 of this study to administer biotin by slitting the tunica and incubating the whole testes in a 10mg/ml biotin solution.

6.3.3 Testis weights of adult *wt* mice and *hpg* and *hpg* + tgFSH mice after ± DHT treatment

Untreated *hpg* testis weights were at 2.5% ($p < 0.001$) of *wt* testis weights, while the untreated *hpg* + tgFSH testis weights were at 17.0% of *wt* testis weights ($p < 0.001$) (Figure 6.4). The difference is testis weights between the untreated *hpg* and untreated *hpg* + tgFSH mice was also significant ($p < 0.01$).

No change in testis weights was observed in *hpg* mice until 10 days of DHT treatment, when the testes had increased to 7.8% of *wt* ($p = 0.016$ compared to *hpg* control) and were no longer significantly different to the untreated *hpg* + tgFSH testes (Figure 6.4).

DHT treatment to the *hpg* + tgFSH testes resulted in no significant change in testis weights after either time point compared to the untreated control (Figure 6.4).

6.3.4 Development of TJ functionality and protein localisation in *hpg* and *hpg* + tgFSH mice treated with DHT

a. Wildtype

Biotin tracer staining was extensive in the interstitium of *wt* testes, and only entered the seminiferous tubules as far as the TJ, which stained extensively for claudin-11 and claudin-3 (Figure 6.5).

b. hpg

In *hpg* testes, biotin staining was extensive in the interstitium and permeated throughout the seminiferous tubules, where it co-localised with claudin-11 which was cytoplasmic and in the centre of the tubules (Figure 6.5). Claudin-3 staining was essentially undetectable in the seminiferous epithelium. The presence of staining in the interstitium was also detected in the negative control as shown with the *wt* picture (Figure 6.5).

Figure 6.4 Mouse testis weights following androgen DHT treatment.

Testes from wildtype, *hpg*, and *hpg* + tgFSH mice treated with DHT for 2 and 10 days were dissected from the mice and trimmed of all fat, epididymides and connective tissue immediately after death and weighed prior to further treatment. Data is mean ± SD, n = 3/group. a v b/c, $p < 0.001$, b v c, $p < 0.01$. Note the log-scale on the y-axis.

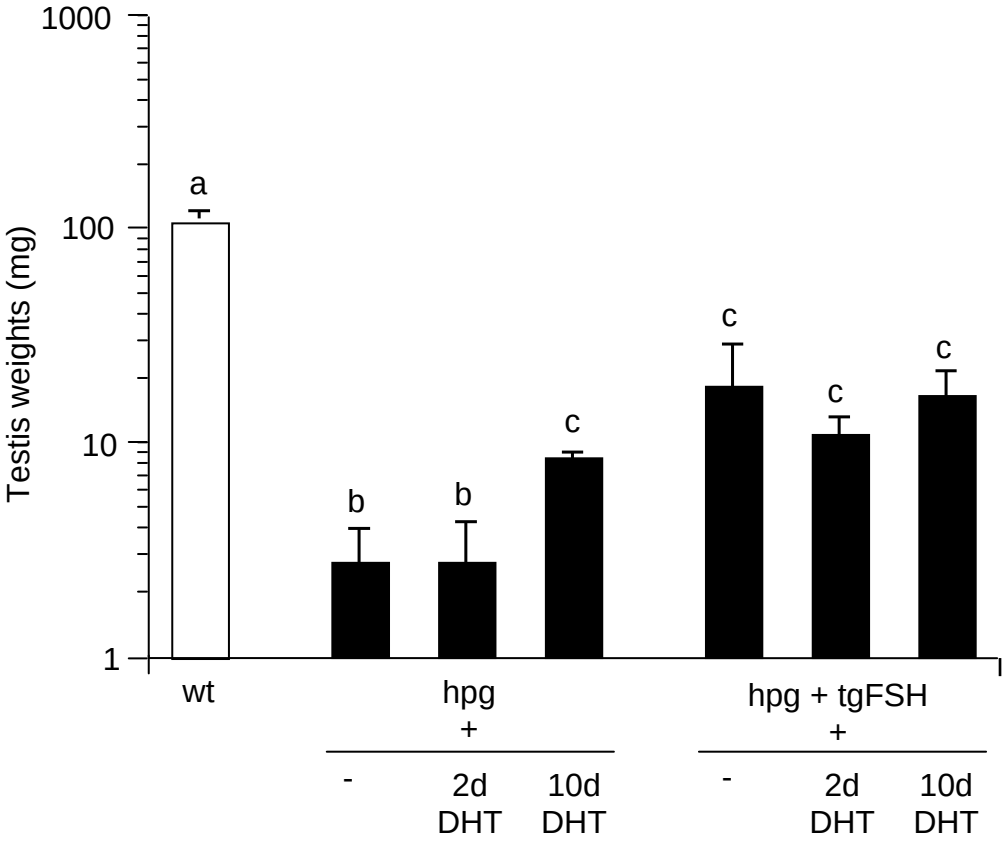
1000
100
10
1
Testis weights (mg)
a
b
b
c
c
c
c
wt
hpg
+
hpg + tgFSH
+
-
2d
DHT
10d
DHT
-
2d
DHT
10d
DHT

Figure 6.5 TJ functional and structural analysis following DHT treatment to *hpg*, and *hpg* + tgFSH mice.

hpg and *hpg* + tgFSH mice were treated with DHT for 2 and 10 days before being killed by anaesthetic overdose. Testes were excised, trimmed of all connective tissue and fat, and then weighed. Tunicas were then slit with a scalpel and testes incubated in biotin at 10mg/ml for half and hour, before being fixed in Bouin's for 4 hours. Testes were then processed by immunohistochemistry for TJ functional analysis with biotin (green) and structural analysis using the TJ markers claudin-11 (page A) and claudin-3 (page B) (both red). Bar = 50μm. Inset = negative control.

A

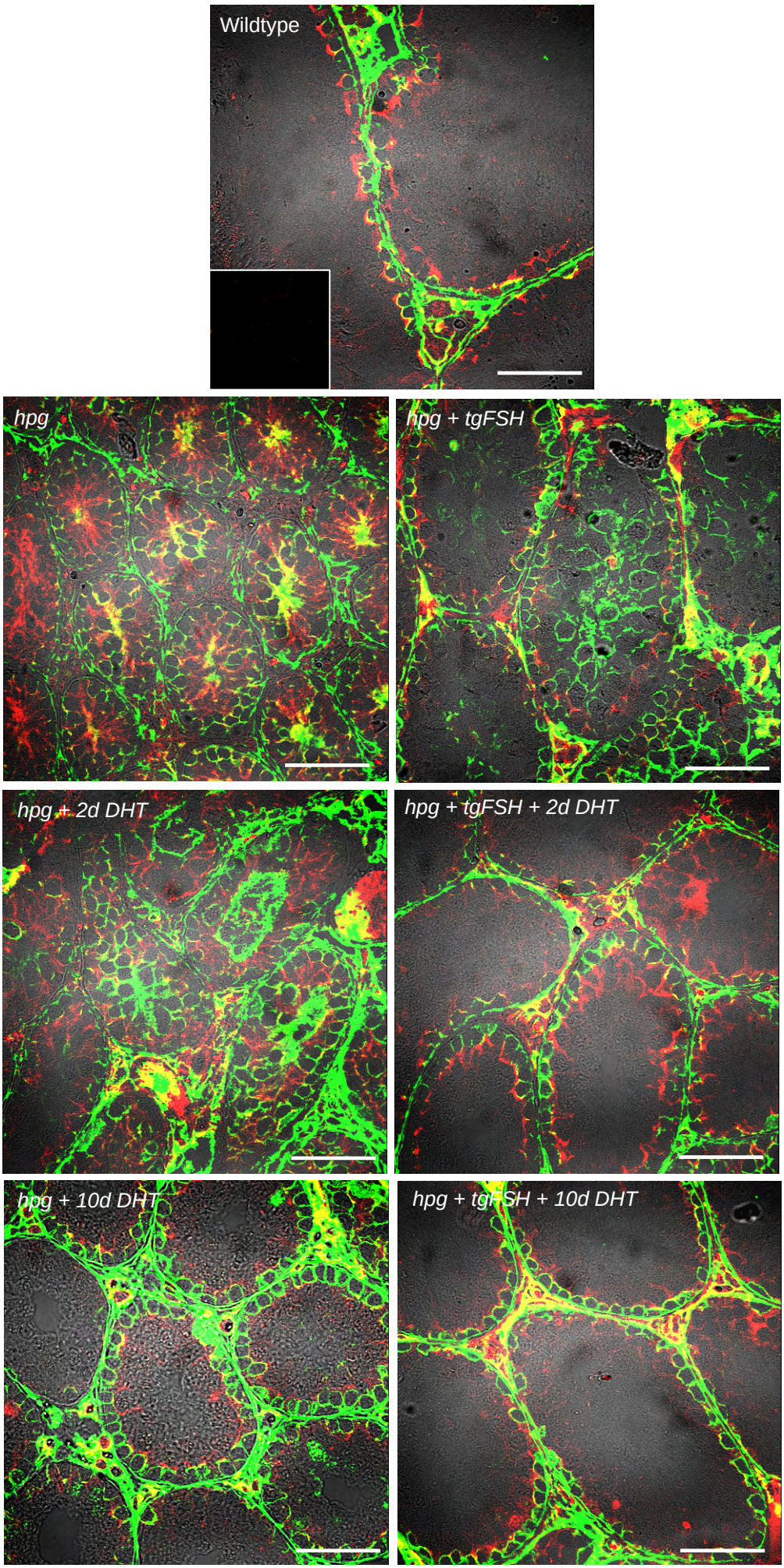
Wildtype
hpg
hpg + tgFSH
hpg + 2d DHT
hpg + tgFSH + 2d DHT
hpg + 10d DHT
hpg + tgFSH + 10d DHT

B

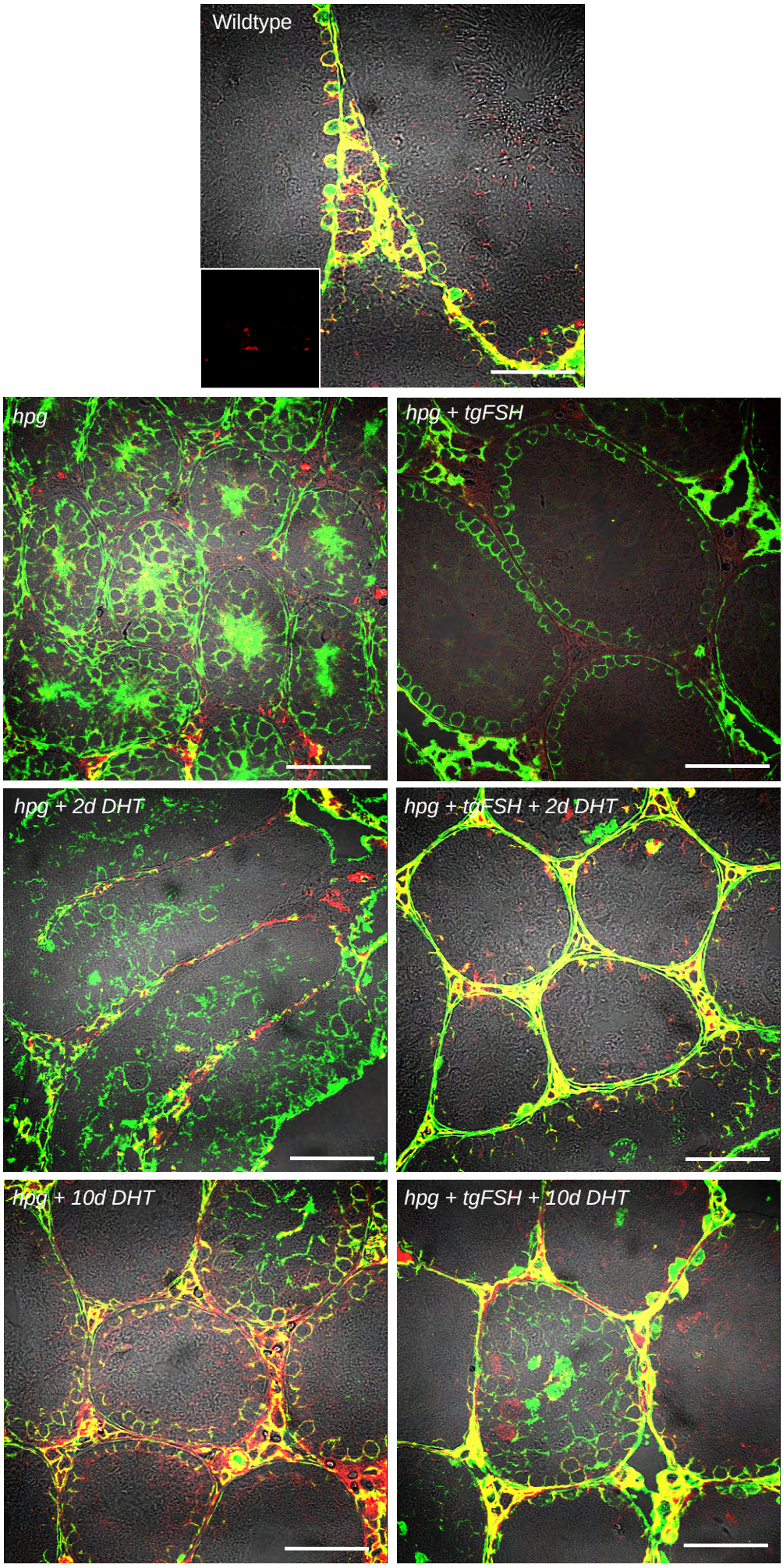
Wildtype
hpg
hpg + tgFSH
hpg + 2d DHT
hpg + tgFSH + 2d DHT
hpg + 10d DHT
hpg + tgFSH + 10d DHT

c. hpg + 2 days DHT

Biotin staining was still extensive in the interstitium and centre of tubules of *hpg* animals treated with DHT for 2 days. Biotin staining no longer co-localised with claudin-11 which had re-distributed basally (Figure 6.5). Claudin-3 staining was still not detectable.

d. hpg + 10 days DHT

Biotin staining was excluded from most of the tubules and remained in the interstitium of *hpg* animals treated with DHT for 10 days, which were extensively stained with claudin-11 and claudin-3 at basal inter-Sertoli cell TJs (Figure 6.5).

e. hpg + tgFSH

Biotin staining was extensive in the interstitium of the *hpg* + tgFSH testes, and permeated throughout some of the seminiferous tubules but was excluded from the remaining tubules (Figure 6.5). Claudin-11 staining was extensive at the TJ just adluminal to the basement membrane, and claudin-3 was generally absent. In some cases, minor staining for claudin-3 was visible in these testes where it was observed to co-localise with biotin (Figure 6.6).

f. hpg + tgFSH + 2 days DHT

Biotin staining was excluded from most of the seminiferous tubules of the *tgFSH* mouse treated with DHT for 2 days, and entered them only as far as claudin-11 staining which was extensive (Figure 6.5). Claudin-3 had become more prominent at the TJ at this time point but staining was not extensive (Figure 6.5).

g. hpg + tgFSH + 10 days DHT

Biotin staining in the *hpg* + tgFSH mice treated with DHT for 10 days was phenotypically similar to the 2 day DHT treatment where it was excluded from most tubules and remained in the interstitium (Figure 6.5). Claudin-11 staining was extensive at the TJ as also seen in the 2 day DHT treatment group (Figure 6.5), although was more basally located, in that the cytoplasmic staining

Figure 6.6 Claudin-3 staining in *hpg* + tgFSH mice testes.

Testes were dissected from adult *hpg* + tgFSH mice which had not received any DHT treatment. Testes were trimmed of all fat, connective tissue and epididymides and fixed in Bouin's fixative for 4 hours. Testes were then processed by immunohistochemistry for biotin (green) and claudin-3 (red) detection. Panel A represents the most common phenotype observed with no claudin-3 staining. In some instances however, minimal claudin-3 staining was apparent (panel B) co-localising with the biotin tracer (yellow, arrow). Bar = 50μm.

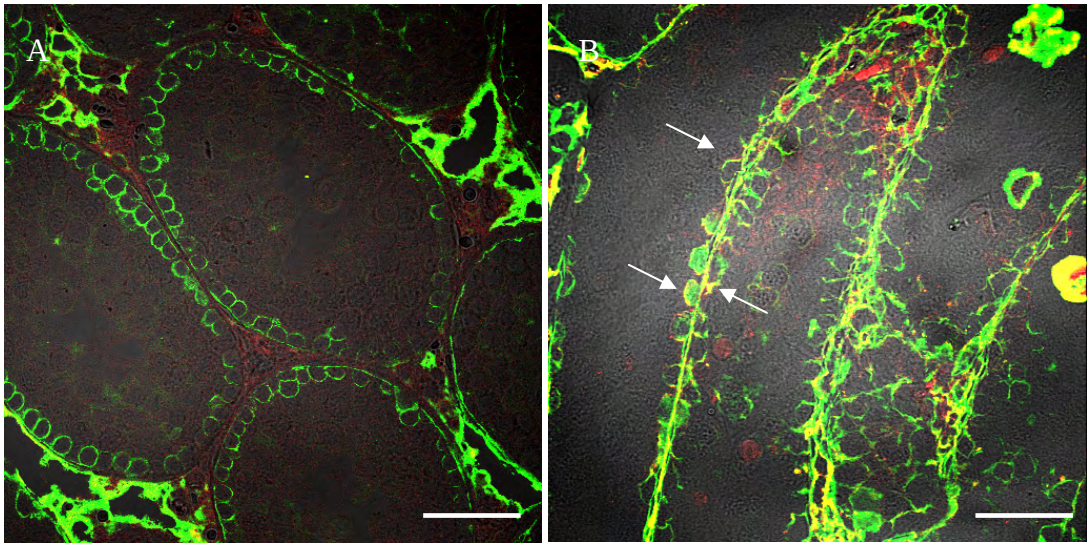
A
B

component seen in day 2, had gone by day 10. Claudin-3 staining had become extensive in some but not all tubules (Figure 6.5).

6.3.5 Effects of DHT treatment on mRNA expression in *hpg* and *hpg* + tgFSH mice

This section addresses RT-PCR analysis of mRNA expression of the TJ proteins claudin-11, occludin and claudin-3, as well as the androgen-regulated INSL-3 in *hpg* and *hpg* + tgFSH mice in response to 2 and 10 days of DHT treatment. The RNA extraction protocol of one of the original control *hpg* testes failed as demonstrated by the inability to amplify any products by RT-PCR from original and repeat cDNA samples produced from the RNA extract concerned. As RNA had originally been extracted from the entire testis, this reduced the number of *hpg* control samples to 2. Fortunately, 2 more cDNA samples from control *hpg* testes of the same age as the original testes were donated by Dr Charles Allan, Anzac Research Institute, Sydney.

Claudin-11 mRNA levels in *hpg* and *hpg* + tgFSH control mice were not different to *wt* levels (Figure 6.7). The same result was obtained for occludin, although the difference between *wt* and *hpg* mice fell just short of significance ($p = 0.057$). Administration of DHT to *hpg* mice led to a non-significant increase in claudin-11 mRNA expression after two days of treatment. After 10 days of treatment, there was a significant decrease ($p < 0.05$) back to control levels of claudin-11 mRNA expression (Figure 6.7). Occludin mRNA expression levels did not change after 2 days of DHT treatment to *hpg* mice. After 10 days of DHT treatment, mRNA expression levels non-significantly decreased toward *wt* levels (Figure 6.7). DHT treatment to *hpg* + tgFSH mice had no effect at the 2 day or 10 days time-point on claudin-11 or occludin mRNA expression levels compared to the *hpg* + tgFSH control (Figure 6.7).

Claudin-3 levels in *wt* mice were significantly ($p < 0.05$) greater than in *hpg* control mice, where it was barely detectable. DHT treatment for 2 and 10 days in *hpg* mice did not result in significant ($p = 0.084$) changes in claudin-3 mRNA expression (Figure 6.7). Claudin-3 mRNA expression levels in *hpg* + tgFSH mice were significantly ($p < 0.05$) lower than in *wt* mice and equal to the levels of claudin-3 expressed in the *hpg* control mice (Figure 6.7). There was no difference in claudin-3 mRNA expression in *hpg* + tgFSH mice compared to *hpg* mice which received DHT for 2

Figure 6.7 Real-time RT-PCR analysis of tight junction mRNA expression in response to DHT treatment to *hpg* and *hpg* + tgFSH mice.

Total RNA was extracted from frozen testes and reverse transcribed for real time RT-PCR analysis of claudin-11, claudin-3, occludin and androgen-regulated INSL-3, in adult wildtype mice, adult *hpg*, and *hpg* + tgFSH mice which had received the androgen DHT for 2 days and 10 days. Data is mean ± SEM, n = 3/group. Exception is *hpg* – DHT where n = 4. Differences between letters are specified in results. * = $p < 0.05$.

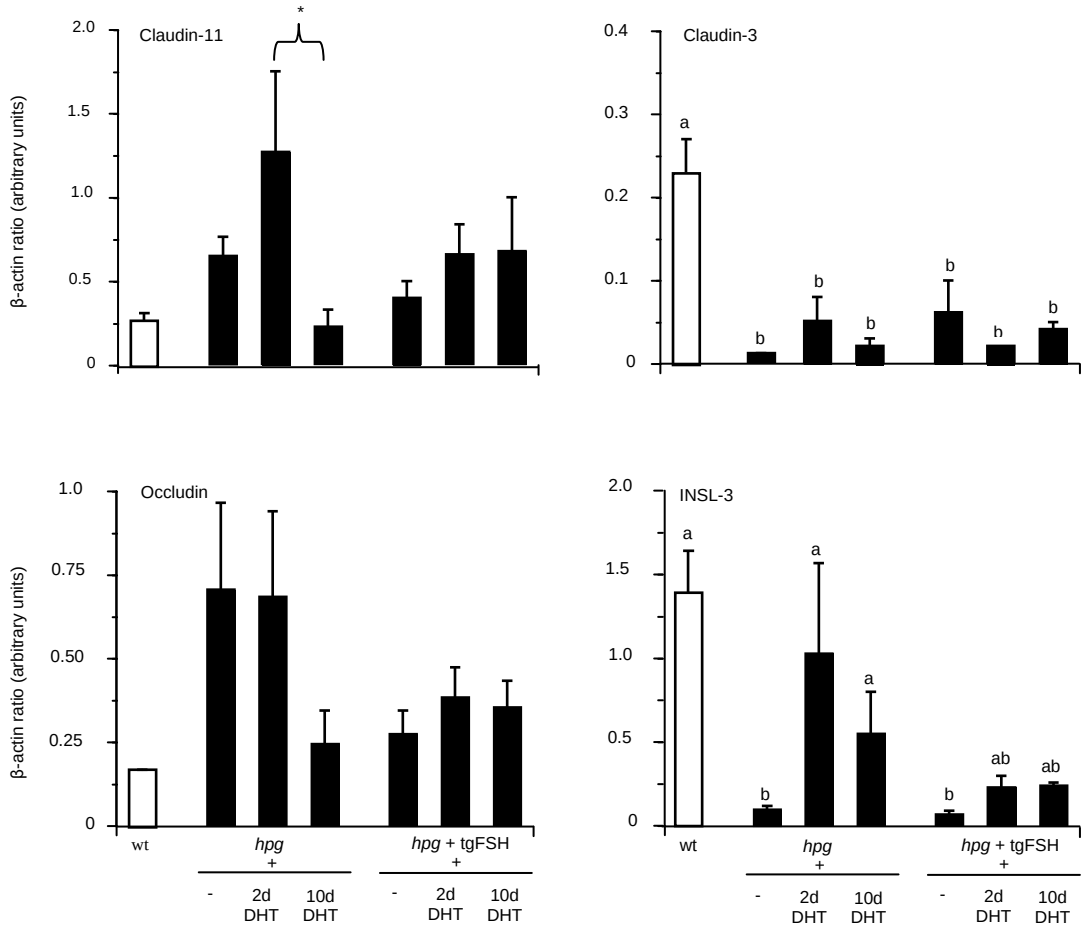
Claudin-11
β-actin ratio (arbitrary units)
2.0
1.5
1.0
0.5
0
*
Claudin-3
0.4
0.3
0.2
0.1
0
a
b
b
b
b
b
b
Occludin
1.0
0.75
0.50
0.25
0
wt
hpg +
hpg + tgFSH +
-
2d DHT
10d DHT
INSL-3
2.0
1.5
1.0
0.5
0
a
b
a
a
b
ab
ab

and 10 days. DHT treatment to the *hpg* + tgFSH mice led to no significant changes in claudin-3 mRNA levels (Figure 6.7).

The androgen-regulated gene INSL-3 was 15 fold ($p < 0.01$) lower in *hpg* control mice and 23 fold lower in *hpg* + tgFSH control ($p < 0.05$) compared to *wt* mice (Figure 6.7). Expression of INSL-3 increased significantly in *hpg* mice after DHT treatment for 2 days ($p < 0.05$) and 10 days ($p < 0.05$). mRNA expression levels of INSL-3 in *hpg* + tgFSH mice remained at control levels following DHT treatment for 2 and 10 days, although expression did increase sufficiently to no longer be significantly different to *wt* levels either.

6.4 Discussion

The aims of studies in this Chapter were to i) analyse the development of the TJ from pubertal to adult in wildytpe, *hpg* and *hpg* + tgFSH mice, and ii) to analyse the changes in TJ function and protein localisation, including the recruitment of claudin-3 to the TJ, in response to DHT treatment for 2 days and 10 days in adult *hpg* and *hpg* + tgFSH mice.

In the first part of the experiment, claudin-11 and claudin-3 were co-localised with the adherens junction marker β-catenin and the gap junction marker connexin-43 respectively, to observe differences in the localisation of proteins to other junctional types in *hpg* and *hpg* + tgFSH mice. In addition, ZO-1 of the cytoplasmic plaque was co-localised with the ectoplasmic specialisation marker vinculin. It would have been useful to include occludin in the immunohistochemistry endpoint, however as mentioned previously, an antibody could not be optimised for its detection in Bouin's fixed tissue.

In adult *wt* mice, claudin-11 staining was extensive at the inter Sertoli cell TJs which were fully functional as shown by complete exclusion of the biotin tracer from the seminiferous tubules. Such staining resembled that obtained in the *wt* mice in the Sertoli cell androgen receptor knockout model (Meng *et al.* 2005), long day Djungarian hamster (Tarulli *et al.* 2008), and in the control adult rat as seen in the previous Chapter. In addition, claudin-11 in the adult *wt* mice presented in this Chapter co-localised with β-catenin at the adherens junction. In the 20 day old pubertal wildtypes, claudin-11 staining was extensive but partly adluminal compared to adults, and did not co-localise with β-catenin which was still at the outer edge of the tubules. This data suggested that at 20 days of

age, the Sertoli cell TJ has not fully formed in the mouse. In adult and pubertal *hpg* mice, claudin-11 was disorganised and located in the cytoplasm of the Sertoli cells toward the centre of the tubules. This phenotype for claudin-11 localisation in an animal lacking gonadotrophins was also displayed in the acyline-suppressed rat testis (Chapter 5), and has also been observed in the short-day Djungarian hamster testis (Tarulli *et al.* 2008), thereby displaying a conserved trend for claudin-11 localisation across several rodent species and a conserved regulatory role for gonadotrophins with respect to localisation. Biotin analysis in the adult *hpg* mice showed that TJs were completely dysfunctional as demonstrated by their inability to excluded biotin from the seminiferous tubules. Interestingly, adherens junctions were not disrupted in *hpg* mice when compared to *wt* mice with β-catenin still extensive at the basal aspect of the tubules, indicating that its localisation is not regulated by gonadotrophins.

hpg + tgFSH adult mice, which produce physiological levels of human FSH (Haywood *et al.* 2003), showed extensive claudin-11 localisation at the TJ which was slightly adluminal compared to the adult *wt*, and closely resembled the phenotype observed in the pubertal *wt* mice. Biotin tracer analysis showed variation in the functionality of the TJs with some tubules able to exclude the tracer and others being permeable to the tracer, with biotin actually seen adluminal to claudin-11. This result is in direct contrast to the Djungarian hamster model, where regardless of the localisation of claudin-11 and the functional state of the TJ, biotin was never adluminal to claudin-11 (Tarulli *et al.* 2008). In the same model, claudin-11 redistribution to the TJ as induced by FSH treatment was always associated with the formation of a functional barrier as shown by biotin exclusion (Tarulli *et al.* 2008). The results obtained in the hamster study and in the *hpg* + tgFSH mice presented herein, could be directly attributable to the size-selective nature of TJs and differences between the models in obtaining this property. Watson *et al.* (2001) presented data demonstrating the existence of size-selective pores and the role claudins have in maintaining these pores. If this is the role of claudin-11 at the Sertoli cell TJ, then one may expect that biotin will penetrate through the seminiferous epithelium only as far as claudin-11 whether it be localised at the TJ, or in cytoplasmic pools. The data in the hamster seems to support this role for claudin-11. This is in contrast to the mouse. Data presented herein suggests that if claudin-11 is important for size-selective pore formation in the mouse testis, it must be localised at the TJ and in sufficient supply of hormonal regulation to obtain its size-selectivity against low molecular

weight tracers such as biotin. While FSH may play a large role in regulating this property in the mouse as in the hamster, there appears to be a requirement for other regulatory mechanisms, such as androgens in the mouse. Further analyses into this feature of the Sertoli cell TJ are required.

In pubertal *hpg* + tgFSH mice, claudin-11 was cytoplasmic but was observed to be re-distributing toward the TJ. The difference between these mice and the *hpg* mice was that pools of claudin-11 were not localised at the centre of the tubule, indicating a role for FSH alone in the localisation of claudin-11 from the Sertoli cell cytoplasmic pools to the TJs at the basal aspect. Again, β-catenin was localised to the outer edge of the tubules in the adult and pubertal animal.

The similarity between claudin-11 localisation in adult *hpg* + tgFSH mice and the 20 day old pubertal *wt* mice is interesting. At 20 days of age, *wt* mice are beginning to display round spermatid production in their seminiferous tubules (Sasagawa *et al.* 1998, McCarrey *et al.* 1999, Marh *et al.* 2003, Xu *et al.* 2004). The production of FSH alone in the *hpg* + tgFSH mouse, is sufficient to drive spermatogenesis past meiosis to the round spermatid level, and also initiate spermiogenesis as indicated by the presence of some elongated spermatids (Allan *et al.* 2001, Haywood *et al.* 2003, Allan *et al.* 2004). At that point, spermatogenesis ceases (Allan *et al.* 2001, Haywood *et al.* 2003, Allan *et al.* 2004), due to the absolute need for androgen to complete spermiogenesis (Zhengwei *et al.* 1998, Allan *et al.* 2001, McLachlan *et al.* 2002b, Haywood *et al.* 2003, Allan *et al.* 2004, Matthiesson et al. 2005b). It appears that spermatogenesis in the adult *hpg* + tgFSH mouse is frozen at approximately the same spermatogenic stage that 20 day old *wt* mice are undergoing. In that case, one might expect that TJ phenotypes between these two mice would be similar, and the data presented herein suggests it is. Furthermore, the tubules in the *hpg* + tgFSH mice which most closely resembled those in the 20 day old *wt* mice with respect to claudin-11 localisation, were also functional, suggesting that the tubules in the 20 day old *wt* mice, were already functional, hence the appearance of the round spermatids (Allan *et al.* 2001, Haywood *et al.* 2003, Allan *et al.* 2004). The difference between the 20 day old mice and the adult *hpg* + tgFSH mice, is that the latter mice lack androgen.

The administration of testosterone to *hpg* + tgFSH mice and *hpg* mice is sufficient to drive qualitatively normal spermatogenesis with fertile sperm (Singh *et al.* 1995, Handelsman *et al.* 1999, Haywood *et al.* 2003). The effect of androgens on TJs was looked at in the second part of this Chapter, and it was shown in *hpg* and *hpg* + tgFSH mice that 2 days of DHT treatment was sufficient to at least

initiate the redistribution of claudin-11 from the cytoplasm of the Sertoli cells toward the basally located TJs. After 10 days of DHT treatment, claudin-11 was extensive at the TJ in both mouse models and this was coincident with a functional barrier as shown by biotin exclusion. It therefore appears that in order for the Sertoli cell TJ to achieve its size-selective nature in the mouse as mentioned before, it requires androgen.

RT-PCR analysis was also conducted on the response of claudin-11 mRNA expression to DHT treatment. Claudin-11 expression was no different in the *hpg* and *hpg* + tgFSH mice ± DHT treatment, suggesting that the mRNA expression of claudin-11 may not be hormonally regulated in the mouse. However, there did appear to be an initial surge in its mRNA expression after 2 days of DHT treatment in *hpg* mice, but this did not achieve significance. The presence of an outlyer in this group of three animals caused a large error bar thus possibly preventing differences from being significant. Therefore future experimental designs should include larger numbers of animals per group (n = 5-7) to avoid this problem. In the acyline treated rat model of the previous Chapter, and in the Djungarian hamster model (Tarulli *et al.* 2008), mRNA expression levels were significantly higher in the hormone suppressed states compared to the controls. In the mouse, *hpg* claudin-11 mRNA levels were not significantly different to *wt* levels, indicating a differential response in mice to the absence of hormones with respect to mRNA expression. Interestingly in the Sertoli cell specific androgen receptor knockout mouse, claudin-11 mRNA expression did decrease, but the decrease in claudin-3 (discussed shortly) mRNA expression was much greater (Myers *et al.* 2005, Tan *et al.* 2005). Furthermore, the localisation of claudin-11 to the TJ in the same model was retained while claudin-3 localisation was absent (Myers *et al.* 2005). These data suggest that the regulation of claudin-11 is different to the regulation of claudin-3 and differences between these proteins was further indicated as shown by the localisation of claudin-3 being more basal than that of claudin-11 (Myers *et al.* 2005).

The mRNA expression of occludin was also analysed in response to DHT and showed a relatively similar profile to claudin-11. Again, no differences in occludin mRNA expression were obtained between *hpg* and *hpg* + tgFSH ± DHT mice, despite high levels of mRNA in the *hpg* control. Large error bars most likely contributed to the inability to achieve significance. There was also no significant change in occludin mRNA expression after 2 or 10 days of DHT treatment in *hpg* mice, despite an apparent decrease to *wt* levels in response to the latter treatment. Similarities between

claudin-11 and occludin mRNA expression in this Chapter, were also seen in the previous Chapter and in the Djungarian hamster model (Tarulli *et al.* 2008), demonstrating shared responses to changes in circulating gonadotrophins.

The testis weights of the *hpg* and *hpg* + tgFSH untreated mice at 3mg and 18mg respectively were comparable to published data (Haywood *et al.* 2003, Allan *et al.* 2004). The commencement of spermatogenesis in the *hpg* mice was shown with significant ($p = 0.016$) increases in testis weights after 10 days of DHT treatment. In a similar study, 8 weeks of DHT treatment in *hpg* mice also stimulated qualitatively normal spermatogenesis which produced fertile sperm (Singh *et al.* 1995). Interestingly, testis weights in *hpg* + tgFSH mice did not change even after 10 days of DHT treatment. This was an unexpected result. While there are no other studies which have treated *hpg* + tgFSH mice with DHT, there has been a study looking at the effect of the androgen testosterone in *hpg* + tgFSH mice (Haywood *et al.* 2003). After 6 weeks of treatment, a significant increase in testis weights was observed, from approximately 16% of *wt* testis weights to 55% of *wt* testis weights (Haywood *et al.* 2003). While testosterone and DHT are different androgens, *hpg* mice treated with either androgen recorded similar increases in testis weights (Singh *et al.* 1995), suggesting that DHT and testosterone should work similarly, at least with respect to testis weights in *hpg* + tgFSH mice. Subsequent RT-PCR analysis in this study, showed that androgen regulated INSL-3 mRNA expression increased 6 fold after 10 days of DHT treatment in *hpg* mice, but only increased 4 fold in the *hpg* + tgFSH mice. The differences between the levels of INSL-3 mRNA expression in the DHT treated *hpg* and *hpg* + tgFSH mice were not significant. The DHT implants used in the *hpg* mice to generate the observed changes in testis weights and mRNA expression in those mice were the same implants used in the *hpg* + tgFSH mice, meaning that the implants themselves were working. The proportion of functional tubules to non-functional in DHT treated *hpg* + tgFSH testes also seemed to increase, although some quantitative analysis would be required to confirm this. Further means to show that the implant had worked though not attempted here, would have been to determine serum androgens and monitor changes in other androgen-dependent organ weights such as seminal vesicle or prostate weights. Hence, the reason(s) for the lack of testis weight response remain unknown, but suggests some other confounding factor. The same factor may have been responsible for the lack of change in claudin-11 and occludin mRNA expression in response to DHT in the *hpg* + tgFSH mice.

Claudin-3 was the next protein of the TJ to be analysed. In adult *wt* mice, its localisation to the TJ was extensive in some seminiferous tubules and absent in others. This was to be expected as claudin-3 is only expressed at stage VIII of the spermatogenic cycle which is when basal germ cells cross the blood-testis barrier into the adluminal region, and any given testis cross section displays various seminiferous tubules undergoing different stages of spermatogenesis (Leblond and Clermont, 1952a, Meng *et al.* 2005). Its expression in the testis is androgen dependent as shown by its absence in the Sertoli cell specific androgen receptor knockout mouse model (Meng *et al.* 2005). No claudin-3 was detectable in pubertal *wt* mice in this study or *hpg* mice regardless of age. Furthermore, claudin-3 mRNA expression was very low in *hpg* mice, showing that claudin-3 is largely absent in these mice. Its absence in this model, which has basal levels of circulating androgen and FSH (Cattanach *et al.* 1977, Charlton *et al.* 1983, Mason *et al.* 1986a, Allan *et al.* 2001), is consistent with the known androgen dependency of this protein (Meng *et al.* 2005). In addition, spermatogenesis is arrested with just 11% and 2% of *wt* spermatogonia and primary spermatocyte (leptotene and zygotene) populations respectively (Singh *et al.* 1995, Ebling *et al.* 2000, Myers *et al.* 2005). TJs are discontinuous and incomplete as revealed by electron microscopy and espin staining at the ectoplasmic specialisation (a component of the blood-testis barrier) is weak in *hpg* mice (Charlton *et al.* 1983, Myers *et al.* 2005). Since TJs do not form, and spermatogenesis does not proceed in this animal, the requirement for claudin-3 at the TJ was not present in these mice. DHT treatment to *hpg* mice for 2 days did not result in a significant change in claudin-3 mRNA expression, despite an apparent 5-fold increase ($p = 0.084$). By 10 days of DHT treatment, claudin-3 mRNA expression levels had decreased again. This expression profile for claudin-3 followed similar patterns to claudin-11 and occludin obtained in this Chapter, suggesting the possibility of conserved regulation of each of these proteins.

Claudin-3 was largely undetectable in the presence of FSH in the *hpg* + tgFSH mice, although was occassionally localised to the TJ, indicating that FSH may play a minor role in the localisation of claudin-3 to the TJ. Androgen DHT treatment to *hpg* mice and *hpg* + tgFSH mice stimulated the appearance of claudin-3 protein and its subsequent localisation to the TJ within 2 days in the *hpg* + tgFSH mice and within 10 days in the *hpg* mice. The more rapid appearance of claudin-3 in the *hpg* + tgFSH mice suggests that FSH may play a priming role in the localisation of claudin-3 to the TJ. Such a priming role for FSH has been well documented in the literature in relation to the regulation of other

Sertoli cell junctions (Muffly *et al.* 1994, Cameron *et al.* 1998, Zhang *et al.* 2003). Supporting information for this argument is also provided by the claudin-11 staining pattern in the pubertal *hpg* + tgFSH model, which appeared to be much more immature than the pubertal *wt* which has both FSH and androgens. These data reinforce the need for both gonadotrophins in maintaining successful spermatogenesis at the level of the TJ.

Low levels of claudin-3 mRNA expression were detected in the untreated *hpg* + tgFSH mice, showing that FSH can to some extent regulate its expression. DHT treatment in these mice had no effect on claudin-3 mRNA expression, but as outlined for claudin-11, occludin and INSL-3, this could have been due to some confounding factor(s) in the testes of these mice.

The absence of claudin-3 staining in pubertal *wt* mice was unexpected. It was hypothesised that the initiation of spermatogenesis which occurs at puberty, would involve the recruitment of claudin-3 to the TJ. TJs need to disassemble to allow germ cells to cross the blood-testis barrier, and then reform underneath them to maintain the integrity of the adluminal compartment (Setchell, 1967, Zhou *et al.* 2002). Currently it is unknown whether claudin-3 is a transient member of disassembling TJs, or a member of reassembling TJs, or both (Meng *et al.* 2005). The absence of claudin-3 at puberty when spermatogenesis is starting and TJs are forming suggests that it is not a member of assembling TJs, but could be a member of disassembling TJs. An argument against this point is that the pubertal mice used in this Chapter were 20 days of age. These animals already have some round spermatids inside the adluminal compartment of the seminiferous tubules, hence TJ formation had probably already occurred. Biotin analysis in tubules which displayed phenotypic similarities to the 20 day old *wt* mice also suggested that these tubules were functional. At 13 days of age, the earliest pachytene spermatocytes appear in the *wt* mouse (Marh *et al.* 2003) and so around this time and each day thereafter until the end of the first spermatogenic wave may be suitable periods to stain for claudin-3 to determine whether it is a member of assembling TJs. Alternatively, one could stain for claudin-3 at the end of the first spermatogenic wave when germ cells are again crossing the TJ.

Claudin-3 was also co-stained with connexin-43 of the inter Sertoli cell gap junction. In *wt* mice, connexin-43 was always at the outer edge/basal aspect of the tubule regardless of age, and in the adult, co-localised with claudin-3. Connexin-43 localisation was cytoplasmic in pubertal *hpg* mice, yet was present at basal gap junctions in the adult *hpg* animal. This indicated that the localisation of

connexin-43 to the gap junction was independent of gonadotrophins. Previous studies have shown that thyroid hormone stimulates connexin-43 action in the Sertoli cells, where it has an important role for normal testicular development and spermatogenesis (St-Pierre *et al.* 2003, Gilleron *et al.* 2006, Brehm *et al.* 2007, Sridharan *et al.* 2007a, Sridharan *et al.* 2007b). In adult and pubertal *hpg* + tgFSH mice, connexin-43 was always localised at the basal gap junctions, indicating that FSH may have a partial role in its localisation.

The cytoplasmic plaque protein ZO-1 was also looked at this Chapter. While staining was not as clear as that for the other proteins already mentioned, its localisation tended to be basal in each mouse genotype, adult or pubertal. While further study may be required to confirm this, it is postulated that the cytoplasmic components of the TJ are appropriately expressed in the absence of gonadotrophins, but that localisation of the key transmembrane TJ proteins (claudin-11, claudin-3 and potentially occludin) require gonadotrophin support.

ZO-1 was co-stained with vinculin of the ectoplasmic specialisation. The phenotype for vinculin localisation supported previous studies that this junction is gonadotrophin-regulated (Muffly *et al.* 1993, Cameron *et al.* 1998, Myers *et al.* 2005, Wong *et al.* 2005, Sluka *et al.* 2006). Hence, vinculin staining was extensive at the ectoplasmic specialisation in adult *wt* mice, but was cytoplasmic in Sertoli cells from *hpg* mice. This pattern was partially rescued by FSH in the *hpg* + tgFSH mice, where vinculin was seen to be re-distributing toward the ectoplasmic specialisation, in a manner similar to the pubertal *wt* animal.

In the GnRH-antagonist treated rat in the previous Chapter, TJs were shown to be dysfunctional by extensive biotin permeation throughout the seminiferous tubules. The hamster, rat and *hpg* mouse models therefore all exhibit dysfunctional and structurally compromised TJs, with significantly reduced or inactive spermatogenesis. Collectively, these data indicate the vital role that TJs have in the maintenance of spermatogenesis. The role gonadotrophins have in regulating the formation of TJ function and structure in *hpg* mice was demonstrated by DHT administration. Within 2 days of DHT treatment, claudin-11 mRNA expression had partially increased and cytoplasmic claudin-11 had begun re-distributing and appeared to have shifted basally toward the TJ, which was still not fully functional as shown by biotin. In the presence of FSH alone, claudin-11 had also shifted basally toward the TJ which varied in functional status as already mentioned. Further evidence that

claudin-11 had shifted basally in response to gonadotrophin treatment was shown by the presence of biotin alone in the centre of the seminiferous tubules, ie) it no longer co-localised with claudin-11. This basal movement of claudin-11 in response to a hormonal stimulus was also observed in the Djungarian hamster model after FSH administration (Tarulli *et al.* 2008). After 10 days of DHT treatment to *hpg* mice, TJs were predominantly functional with biotin being completely restricted from most seminiferous tubules.

The *hpg* mouse provides a different means to study hormone regulation of the TJ compared with the GnRH-antagonist treated rat and also the Djungarian hamster. This is because *hpg* mice have never had circulating hormones in contrast to the other two models, hence the *hpg* mouse is purely a model of TJ formation, and not a TJ maintenance study. The GnRH antagonist treated rat model in the previous Chapter concluded that the maintenance of Sertoli cell TJ function and structure is hormonally regulated *in vivo.* The *hpg* model has added to this knowledge by showing that hormones also regulate the initial formation of the Sertoli cell TJ *in vivo*. While it can be argued that the depletion of circulating gonadotrophins and subsequent regression of the TJ in the seasonally regressed testis of the Djungarian hamster can also demonstrate TJ formation, the fact that these animals had prior exposure to gonadotrophins means that one could argue that the Djungarian hamster model is also a maintenance model. No such argument could be made about the *hpg* mouse model. Either way, it is interesting and noteworthy that, in situations where circulating levels of gonadotrophins are reduced, either through congenital defect or induced through suppression, the key Sertoli cell TJ proteins such as claudin-11 and occludin (as shown in the hamster (Tarulli *et al.* 2006, Tarulli *et al.* 2008)) are always present, albeit localised away from the TJ in the centre of the seminiferous tubules. Presumably occludin was also present at all times in this *hpg* mouse study as well. It appears therefore that the key role of gonadotrophins is to redistribute these proteins to the Sertoli cell TJ.

It is concluded that gonadotrophins (both FSH and LH/testosterone) stimulate the formation of a functionally and structurally competent Sertoli cell TJ by redistributing claudin-11 and claudin-3 to the TJ from Sertoli cell cytoplasmic pools. This redistribution from the cytoplasm is regulated in a very similar manner to that observed for the maintenance of TJs by gonadotrophins. It is further concluded that while FSH is sufficient to stimulate partial TJ formation, androgens are absolutely

required for complete TJ formation and function, and subsequent spermatogenic activity. Although not proven in this study because of low group numbers, the data also suggests that gonadotrophins are able to regulate claudin-11, occludin and claudin-3 mRNA expression.

Chapter Seven: Hormonal regulation of the Sertoli cell tight junction in the gonadotrophin suppressed human, *in vivo*

Chapter 7. Hormonal regulation of the Sertoli cell tight junction in the gonadotrophin suppressed human, *in vivo.*

7.1 Introduction

The previous Chapters have shown that gonadotrophins regulate both the structure and function of Sertoli cell TJs *in vitro* and *in vivo,* and that gonadotrophins maintain TJ integrity and also stimulate its formation.

In order to study gonadotrophin regulation of spermatogenesis in men and to ascertain the specific points of spermatogenesis which testosterone and/or FSH regulate, male hormonal contraception has been induced in several studies through the addition of testosterone or synthetic androgens to suppress LH and FSH but particularly intratesticular testosterone to suppress spermatogenesis (see Chapter 1, Section 1.7.5), while maintaining adequate androgen action at other sites in the body (McLachlan *et al.* 2002a, McLachlan *et al.* 2002b, Matthiesson et al. 2005b, Matthiesson et al. 2005a). Following gonadotrophin suppression, spermatogenesis is stopped in most individuals with LH/testosterone and FSH levels at basal levels and germ cell numbers significantly decreased (Herbst, 2003, Herbst *et al.* 2004, Matthiesson et al. 2005b). These features are similar to the GnRH-antagonist treated rat, for which this thesis has demonstrated changes in TJ structure and function following gonadotrophin suppression, indicating that TJ maintenance is gonadotrophin-dependent. However, the extent to which gonadotrophin suppression alters human testicular TJ function is not known. A direct demonstration of the importance of gondotrophins in the initiation of human Sertoli cell TJ function is provided by a study with hypogonadotrophic hypogonadal men, who have naturally low levels of circulating gonadotrophins, and display a prepubertal TJ phenotype as determined by electron microscopy (de Kretser and Burger, 1972). Following the exogenous application of gonadotrophins, the Sertoli TJ assumed a mature phenotype, with subsequent spermatogenesis and fertility (de Kretser and Burger, 1972).

The aim of the work presented in this Chapter is to determine the effect of gonadotrophin suppression on the localisation and mRNA expression of human Sertoli cell TJ proteins. In addition, the effects of gonadotrophin suppression on the localisation and mRNA expression of protein markers of nearby junction types will also be analysed. These include β-catenin (adherens junction), connexin-

43 (gap junction), vinculin (ectoplasmic specialisation), ZO-1 (cytoplasmic plaque) and β-actin (cytoskeleton). Finally, RT-PCR of the androgen-regulated protein INSL-3 was included as a means to confirm androgen suppression in these men.

To undertake this study, archived human testis fragments and wax-embedded testis sections were generously provided by Drs K Matthiesson and R McLachlan at the Monash Medical Centre (Clayton, Victoria), from a study which examined the effects of various gonadotrophin suppression treatments on germ cell numbers, serum hormones, and sperm output (Matthiesson et al. 2005b). It was hypothesised that gonadotrophin suppression would lead to changes in TJ mRNA and protein localisation in the human testis.

7.2 Materials and Methods

While the only work conducted in this thesis on the human testis tissue was immunohistochemistry and RT-PCR, it is necessary to provide the background of the tissue that was used, and its preparation. A brief outline of the experimental design that led to the provision of the tissue samples is provided below. Full experimental details are published in Matthiesson *et al.* (2005a).

7.2.1 Human testis tissue

Samples for this study came from archived Bouin's fixed human testes or frozen human testis mRNA from a previous study (Matthiesson et al. 2005b). Briefly, the samples were obtained from 29 healthy men who were planning to undergo elective vasectomy through media advertisement (Matthiesson et al. 2005b). For details regarding consent, and inclusion/exclusion criteria, see Matthiesson *et al.* (2005b). Briefly, the Institutional Review Board at the University of Washington, USA, approved all experimental protocols, and subjects gave written informed consent before screening (Matthiesson et al. 2005a).

7.2.2 Experimental design

a. Hormone suppression

The Matthiesson *et al.* (2005a) study was divided into three phases, these being a 2 week screening phase, an 8 week treatment phase, and a 4 week recovery phase. After the screening phase, men were randomly assigned to one of the four hormone suppressive treatments (n = 5-6/group) or to a control group (n = 7) (Matthiesson et al. 2005b). The treatment groups were: 100mg Testosterone enanthate (T; Delstestryl, Bristol-Myers, Squibb, Princeton, NJ, USA), injected intramuscularly, weekly + i) 125μg progestin Levonorgestrel (LNG; Wyeth, Madison, NJ, USA), orally, daily (n = 5), ii) LNG + 0.5mg 5α-reductase inhibitor Dutasteride (D; GlaxoSmithKilne, Research Triangle Park, NC, USA), orally, daily (n = 6), iii) 300μg/kg GnRH antagonist Acyline (A; Multiple Peptide Systems, San Diego, CA, USA), subcutaneously, fortnightly (n = 6), or iv) LNG + A (Matthiesson et al. 2005b).

Following the treatment phase, testicular biopsies were taken from each man in conjunction with a pre-planned vasectomy (Matthiesson et al. 2005b). Biopsies were also taken from control men who went straight through to the surgery (Matthiesson et al. 2005b). Biopsies were then either fixed in Bouin's for 3 hours and embedded in paraffin wax and kept at room temperature, or used for total RNA extraction and kept at -80^{o}C.

7.2.3 Immunohistochemistry

Bouin's fixed, paraffin embedded testes from Matthiesson *et al.* (2005a) were cut and processed by immunohistochemistry for confocal fluorescent microscopy analysis as outlined in section 2.2. For primary and secondary antibody incubation details see Table 7.1. Note that all pictures were taken with the same fluorescent illumination intensities.

7.2.4 RNA preparation

Total RNA had already been extracted from all the archived testis tissue samples from the Matthiesson *et al.* (2005a) study and quantified. As only two prepared control samples were available, it was necessary to extract RNA from a third frozen control human testis biopsy which had been set

Table 7.1 Antibodies used for immunohistochemical analysis.

Tabulated data for the antibodies used in Chapter 7 of this thesis, including details regarding the primary and secondary antibody hosts, working concentrations (conc.)/dilutions, incubation (Inc.) times and company details with catalogue numbers.

Protein	**Primary (1^o) antibody host**	**Company**	**Conc.** (μg/ml)	**Negative control**	**1^o Inc. time (mins)**	**Secondary (2^o) antibody**	**Company**	**Dilution**	**2^o Inc. time** (mins)
Claudin-11	Rabbit	Zymed (36-4500)	2.0	Normal rabbit IgG	60	Goat α rabbit Alexa-488	Molecular Probes	1:400 of stock	30
Claudin-3	Rabbit	Zymed (34-1700)	1.25	Normal rabbit IgG	60	Goat α rabbit Alexa-488	Molecular Probes	1:400 of stock	30
ZO-1	Rabbit	Zymed (61-7300)	1.25	Normal rabbit IgG	Overnight	Goat α rabbit Alexa-488	Molecular Probes	1:800 of stock	30
β-catenin	Mouse	Transduction Laboratories (610154)	0.33	Normal mouse IgG	60	Goat α mouse Alexa-488	Molecular Probes	1:400 of stock	30
Connexin-43	Mouse	Sigma ascites fluid (C8093)	1:800 of stock	Normal mouse IgG	60	Goat α mouse Alexa-488	Molecular Probes	1:400 of stock	30
Vinculin	Mouse	Sigma ascites fluid (V4505)	1:400 of stock	Normal mouse IgG	60	Goat α mouse Alexa-488	Molecular Probes	1:400 of stock	30
β-actin C4 clone	Mouse	MP Biomedicals (69100)	1:200 of stock	Normal mouse IgG	60	Goat α mouse Alexa-488	Molecular Probes	1:400 of stock	30

aside from the Matthiesson *et al.* (2005a) study. Total RNA extraction through to quantification by UV spectrophotometry was conducted as outlined in Section 2.3.1 to 2.3.3. Also, a commercially available total RNA human testis extract was purchased (100μg, Ambion, Cat # 7972) to be the QC and standard curve for the PCR experiments.

As each RNA sample was precious and amount limited (~45μg-140μg in total/sample), a method of RNA amplification was employed to maximise usage and availability of the samples for these and other studies.

7.2.5 RNA Amplification

RNA from the human testis samples was amplified using the MessageAmp II aRNA Amplification Kit (Ambion, Cat # 1751) according to the manufacturer's directions. A detailed protocol is outlined below, but in brief, the RNA samples were incubated with a T7 Oligo(dT) primer and reverse transcription enzyme to produce the typical RNA-cDNA hybrid. The T7 Oligo (dT) primer binds to the poly-A tail of mRNA, and this primer initiates the reverse transcription process. The next step was a second reverse transcription process which replaced the RNA component of the hybrid with DNA, producing double stranded DNA molecules. This was purified and an *in vitro* transcription experiment carried out to produce amplified RNA by linear amplification of the double stranded DNA. The amplified RNA was then reverse transcribed again for final RT-PCR analysis, using random hexamers (as per the reverse transcription protocol outlined in section 2.3.4) instead of the T7 Oligo (dT) due to the loss of the poly-A tail following the initial reverse transcription experiments.

The amplification kit used a reverse transcription enzyme called M-MLV RT Array Script (Ambion, cat # 2048) for the first and second round reverse transcription experiments, which according to the manufacturer has excellent 'processitivity' compared to other reverse transcription enzymes. This means that as the enzyme starts reverse transcribing the RNA molecule from the T7 primer at the 3' end, it will advance further along the RNA toward the 5' end than other commercially available reverse transcription enzymes. It still however displays 3' bias, and so after each reverse transcription event, of which there are three to produce the final cDNA product for RT-PCR, the

molecule becomes progressively shorter from the 5' end. This meant that it was essential to design the primers for RT-PCR analysis, toward the 3' end of the target molecules.

a. First strand cDNA synthesis

1μg of RNA was taken from each sample (based on UV spectrophotometry quantification results), except for the Ambion-supplied human testis RNA sample, from which 4μg was taken and transferred into a non-stick, sterile, RNase-free 0.5ml tube, in a volume not exceeding 10μl. 1μl of T7 Oligo(dT) primer was added to the mixture and the final volume brought to 12μl with nuclease-free water before being centrifuged for 1 minute at 10,000rpm (9391g, Eppendorf, Germany). The samples were then incubated for 10 minutes in a thermal cycler (Applied Biosystems, Gene Amp PCR System 9700, Australia) at 70^{o}C, and then centrifuged briefly to collect condensation at the bottom of the tube.

The final volume of the tube was brought to 20μl with the addition of the reverse transcription master mix (2μl 10X first strand buffer, 4μl dNTP mix, 1μl RNase inhibitor, 1μl ArrayScript), which was mixed into the solution, gently vortexed and then centrifuged briefly and placed on ice. Tubes were then incubated for 2 hours at 42^{o}C in a hybridisation oven (Carbolite, UK), and placed on ice.

b. Second strand cDNA synthesis

Each of the solutions were then made up to 100μl with the addition of a second strand master mix (63μl nuclease-free water, 10μl 10X second strand buffer, 4μl dNTP mix, 2μl DNA Polymerase, 1μl RNase H), which was mixed by gentle vortexing and brief centrifugation. The tubes were then incubated for 2 hours at 16^{o}C in the thermal cycler, before being placed on ice. These samples were safe to store at this point if desired, at -20^{o}C.

c. cDNA purification

The nuclease-free water bottle supplied with the kit was preheated to between 50^{o}C-55^{o}C, being careful not to go over 58^{o}C as directed by the manufacturer.

250μl of cDNA binding buffer was added to each sample and mixed thoroughly, before the entire sample was loaded into the centre of a cDNA filter cartridge. This was centrifuged for 1 minute

at 10,000rpm (9391g) and the flow through discarded. 500µl of wash buffer (a volume of ethanol was added to the buffer beforehand according to manufacturer's instructions) was then added to each cartridge and centrifuged for a further minute at 10,000rpm. The cartridges were then centrifuged again for 1 minute to remove any trace amounts of wash buffer, before they were transferred to a cDNA elution tube.

10µl of the heated nuclease-free water was added to the cDNA filter cartridge, left for 2 minutes at room temperature and then centrifuged for 1.5 minutes at 10,000rpm. A second 10µl dose of nuclease-free water was added and centrifuged, leaving the double stranded cDNA in the eluate in an approximate volume of 16µl. This final aliquot was sub-aliquotted into 4 x 4µl in free standing screw tubes (0.5ml, Astral Scientific, cat # I2120-00, Gymea, NSW, Australia) with screw-cap and o-ring lids (I2001-00 Astral Scientific, Gymea, NSW, Australia), snap frozen and stored at -80^{o}C for extra double stranded cDNA storage.

d. In vitro transcription (IVT) to synthesise amplified RNA (aRNA)

One of the 4µl double stranded DNA sub-aliquots from each sample was subjected to this next protocol. They were made up to 16µl in accordance to manufacturer's requirements.

Each sample was made up to 40µl by the addition of an IVT master mix (4µl T7 ATP (75mM), 4µl T7 CTP (75mM), 4µl GTP (75mM), 4µl T7 UTP (75mM), 4µl T7 10X Reaction buffer, 4µl T7 Enzyme mix) which was mixed well by vortexing and brief centrifugation, before being placed on ice.

Tubes were then incubated at 37^{o}C for 8 hours in the hybridisation oven. According to the manufacturer, the incubation times are important for maximal RNA amplification. Toward the end of this period, the supplied nuclease-free water bottle was heated to 50^{o}C-60^{o}C.

The amplification reaction was stopped by the addition of 60µl of heated nuclease-free water.

e. aRNA purification

Nuclease-free water was preheated to 50^{o}C-60^{o}C before proceeding. An aRNA filter cartridge was placed into an aRNA collection tube. 350µl of aRNA binding buffer was added to the 100µl

aRNA sample. 250µl of ACS grade 100% ethanol was immediately added to the solution and mixed by pipetting up and down 3 times. The samples were not vortexed or centrifuged as per manufacturer's instructions.

The solutions were then immediately transferred onto the centre of an aRNA filter cartridge, which was then centrifuged for 1 minute at 10,000rpm (9391g). The flow-through was discarded, and 650µl of wash buffer added to the cartridge, and centrifuged for a further minute at 10,000rpm. Any trace amount of wash buffer was removed by another 1 minute centrifugation at 10,000rpm.

Filter cartridges were then transferred to aRNA collection tubes. 100µl of the preheated nuclease-free water was added to the centre of the tube, left at room temperature for 2 minutes and then centrifuged for 1.5 minutes at 10,000rpm, leaving the aRNA in the collection tube. This was sub-aliquotted at 10 x 10µl and stored in screw-cap eppendorf tubes, snap frozen and stored at -80^{o}C.

f. aRNA quantification and reverse transcription

The protocols for these next experiments which dealt with quantifying the aRNA and reverse-transcribing it into cDNA for RT-PCR analysis were not part of the manufacturer's directions and were the same protocols used as per the rest of this thesis. See Sections 2.3.3-2.3.4.

7.2.6 Real-time RT-PCR analysis

All RT-PCR work and primer design was conducted as outlined in Section 2.3.5. For primer details, see Table 7.2.

7.2.7 Statistical analysis

Statistical analysis was performed as outlined in Section 2.6 with data expressed as mean ± SEM. Numbers ranged from 3-5 per group. See results section for further details.

Table 7.2 Primer sequences and real-time RT-PCR conditions for the analysis of mRNA expression in the human gonadotrophin suppressed testis.

Primers were designed or obtained from published sources against the TJ proteins claudin-11, claudin-3, occludin, JAM-A and the cytoplasmic plaque protein ZO-1, as well as against adherens junction protein β-catenin, ectoplasmic specialisation protein vinculin and gap junction protein connexin-43. Further analysis was done with the housekeeper and cytoskeletal protein β-actin and androgen-regulated protein INSL-3. Data included in the table are forward and reverse primer sequences, Mg^{2+} concentration, and annealing and acquisition temperatures.

Protein	**Species/ Accession number**	**Primer sequences (5'- 3')**	**Product size** (bp)	**[Mg^{2+}]** (mM)	**Anneal temp.** (^{o}C)	**Acquisition temp.** (^{o}C)
Claudin-11 (Primer3)	Human NM_005602	Forward: CTGGTGGACATCCTCATCCT Reverse: AGCTAGAGCCCGCAGTGTAG	391	3.0	64	72
Occludin (Ghassemifar *et al.* (2002)	Human NM_002538	Forward: ACAAGGAACACATTTATGAT Reverse: ATTGTAAGCTCTTGTATTCC	438	3.0	61	72
Claudin-3 (Primerbank database)	Human NM_001306	Forward: AACACCATTATCCGGGACTTCT Reverse: CGCGGAGTAGACGACCTTG	183	2.0	64	72
β-actin (Primer3)	Human NM_001101	Forward: CGAGCGCGGCTACAGCTT Reverse: TCATACTCCTGCTTGCTGATCC	506	3.5	64	72
β-catenin (Primer3)	Human NM_001904	Forward: CCCACTAATGTCCAGCGTTT Reverse: CTCACGATGATGGGAAAGGT	324	3.0	60	72
Connexin-43 (Chen *et al.* (2006)	Human NM_000165	Forward: CCTTCTTGCTGATCCAGTGGTAC Reverse: ACCAAGGACACCACCAGCAT	154	4.0	64	72
JAM-A (Primer3)	Human NM_016946	Forward: GGACCCTTCTCTGCCCTTAC Reverse: TATTGGCATGTGACCCTTGA	254	4.0	61	72
Vinculin (Primer3)	Human NM_014000	Forward: ATTTCCCAGCACATGAAACC Reverse: AAAGCACATCCGGCATAAAG	396	2.0	64	72
ZO-1 (Primer3)	Human NM_003257	Forward: GGGAGGGTGAAGTGAAGACA Reverse: ACCACCAAATGCACAACGTA	270	3.0	64	72
INSL-3 (Primer3)	Human NM_005543	Forward: GGGATGGGTGCTCACTATCT Reverse: TTTCTGCTTTGGGTCGTTTA	228	2.5	64	72

7.3 Results

7.3.1 Effects of gonadotrophin suppression on tight junction protein localisation

The localisation of claudin-11 at the TJ in each of the control men (n = 3) was extensive and formed continuous stained bands toward the basement membranes of the seminiferous tubules (Figure 7.1). Within each gonadotrophin suppression treatment [T+A (n = 3), T+LNG (n = 2), T+LNG+A (n = 2), T+LNG+D (n = 2)], the staining pattern of claudin-11 was heterogeneous between men receiving the same treatment. The extent of claudin-11 localisation varied from a marked loss of protein staining at the basal aspect of the tubules which appeared very punctate, to a continuous staining resembling the controls (Figure 7.1). For example a comparison between man 102 and man 122 in the T+A group shows claudin-11 as punctate at the TJ in man 102 and continuous at the TJ in man 122 (Figure 7.1). Similar variability in claudin-11 staining patterns was observed in the other treatment groups (Figure 7.1), with no particular treatment producing consistently suppressed claudin-11 staining. It was also noted that, in contrast to the gonadotrophin-suppressed rat model, claudin-11 staining did not appear in Sertoli cell cytoplasm in gonadotrophin-suppressed men. All immunohistochemical experiments were conducted at the same time and repeated up to 3 times with consistent results.

Occludin, JAM-A and claudin-3 were undetectable in the testes sections with the primary antibodies employed, expected to be due to cross-reactivity issues and the type of fixation (Bouin's fixative). However, it was possible to examine the localisation of the cytoplasmic plaque protein ZO-1, and this remained unchanged in any of the men from any of the hormone suppressing treatments, compared with controls (Figure 7.2).

Immunofluorescent images presented in this Chapter are representative of the results observed within treatment groups (typically n = 2-5 per group), and so data from all of the men examined are not shown herein. Furthermore, occasional artefact staining of the basement membrane was detectable in some immunoblots. Images for all men are presented in Appendix 1.5 and CD in cover.

Figure 7.1 Localisation of claudin-11 in control and hormone suppressed human testes.

Bouin's fixed, paraffin embedded human testis biopsies were processed by immunohistochemistry and stained for the TJ protein claudin-11 (green). Biopsies came from men (♂) with hormone suppression induced by T+A, T+LNG, T+LNG+A and T+LNG+D, as well as control men. Presented in this Figure are several of the phenotypes observed within each treatment. Biopsies from different individuals are indicated by patient numbers which were allocated by Matthiesson *et al.* (2005a). Note that another channel (grey) has been added to the confocal microscope for the T+LNG+A #136 man to highlight the localisation of claudin-11 with respect to the seminiferous tubules in the cross section. Bar = 50μm. Inset = negative control.

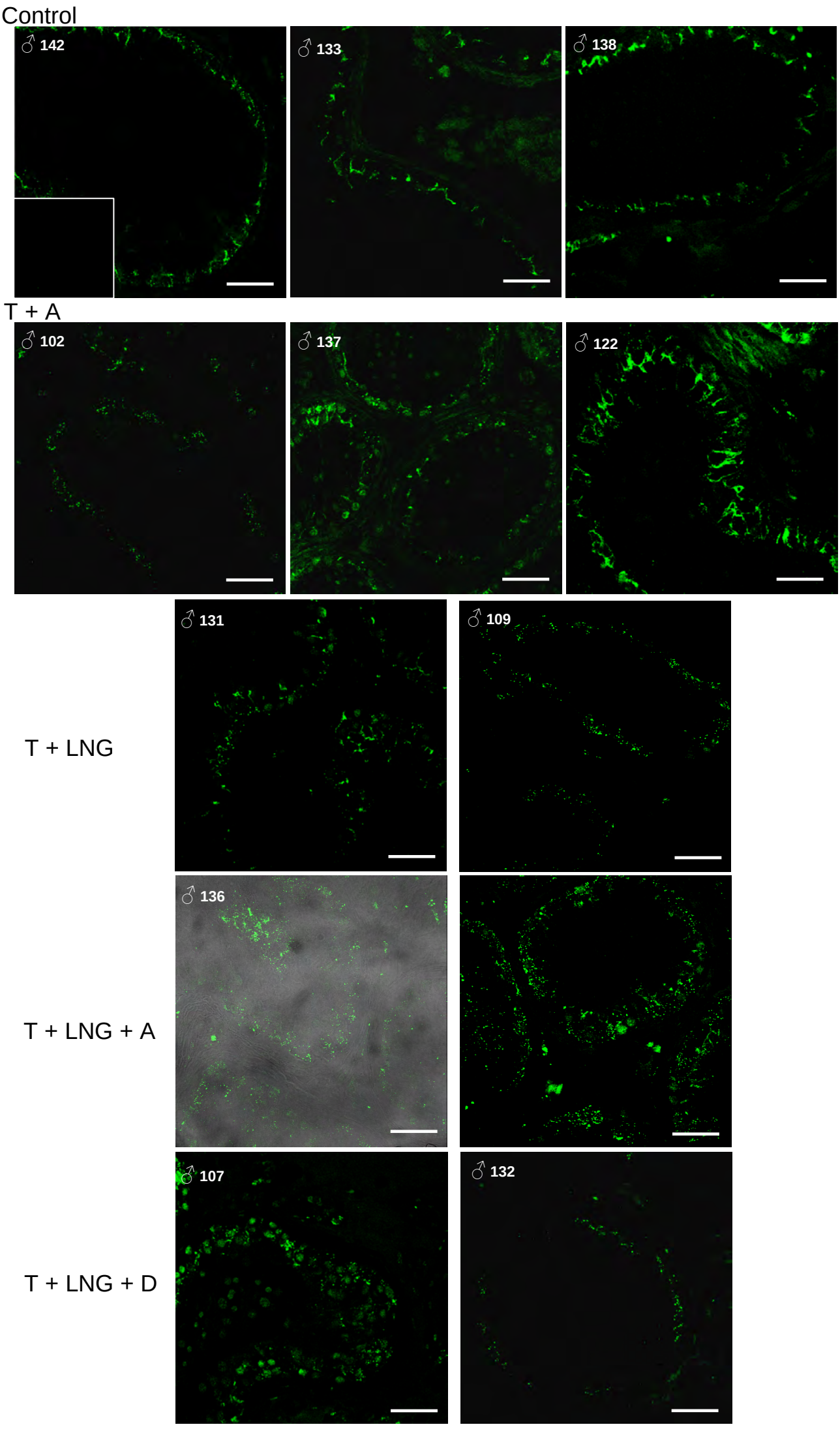
Control
♂ 142
♂ 133
♂ 138
T + A
♂ 102
♂ 137
♂ 122
T + LNG
♂ 131
♂ 109
T + LNG + A
♂ 136
T + LNG + D
♂ 107
♂ 132

Figure 7.2 Localisation of ZO-1 in control and hormone suppressed human testes.

Bouin's fixed, paraffin embedded human testis biopsies were processed by immunohistochemistry and stained for the cytoplasmic plaque protein ZO-1 (green). Biopsies came from men (♂) with hormone suppression induced by T+A, T+LNG, T+LNG+A and T+LNG+D, as well as control men. Presented in this figure are the same biopsies used for claudin-11 in Figure 7.1, where different staining phenotypes were observed within treatments. Biopsies from different individuals are indicated by numbers which were allocated by Matthiesson *et al.* (2005a). Note that another channel (grey) has been added to the confocal microscope for the T+LNG+D #107 man to highlight the localisation of ZO-1 with respect to the seminiferous tubules in the cross section. Bar = 50 μm. Inset = negative control.

Control

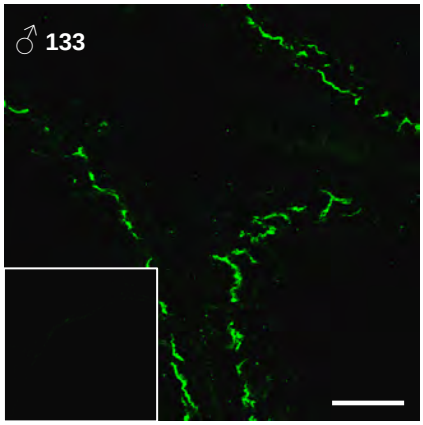

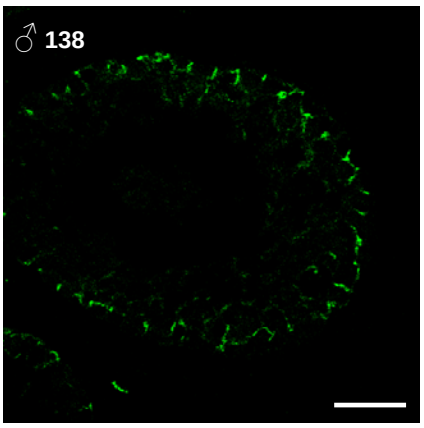

T + A

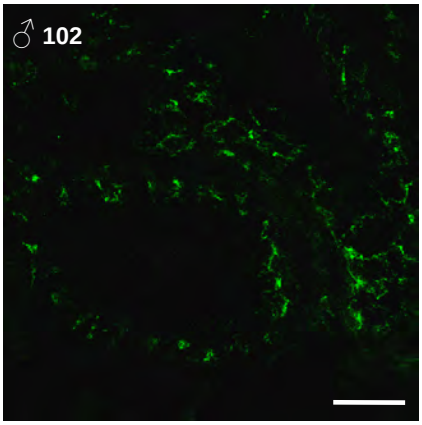

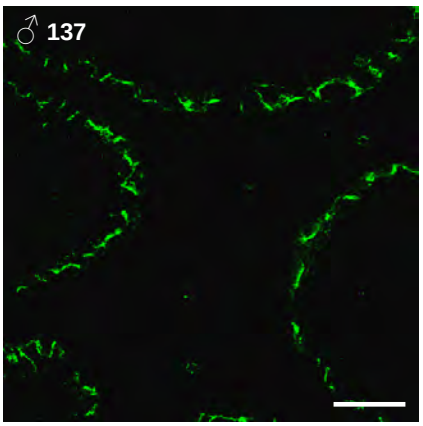

T + LNG

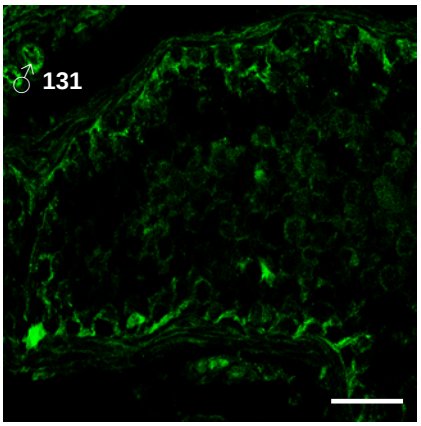

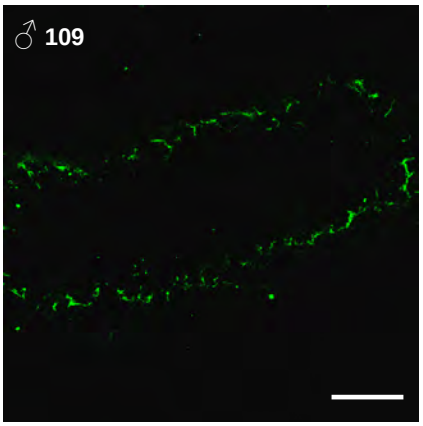

T + LNG + A

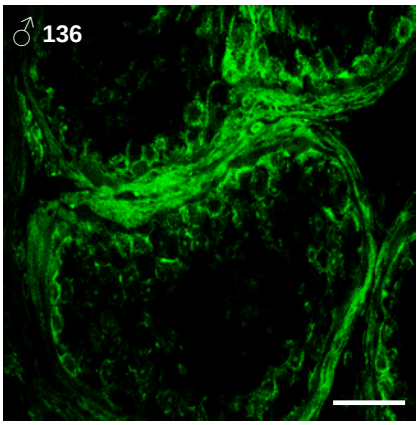

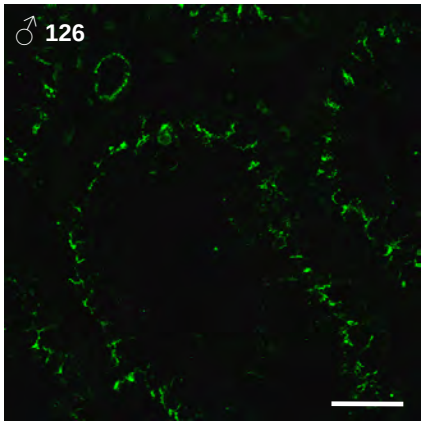

T + LNG + D

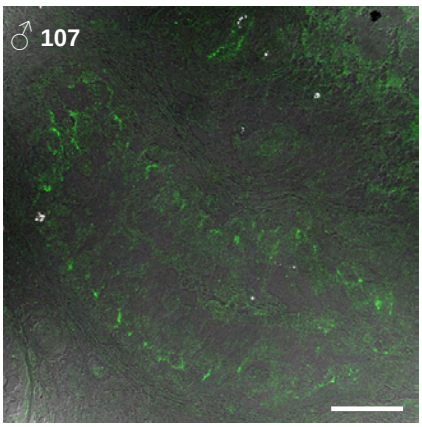

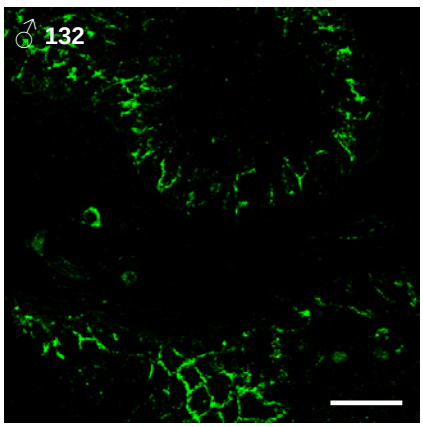

7.3.2 Effects of gonadotrophin suppression on other junctional protein localisation

The effect of hormone suppression on human spermatogenesis was extended to include other junctional markers such as β-catenin (adherens junction), vinculin (ectoplasmic specialisation), connexin-43 (gap junction), and β-actin (cytoskeleton) (Figure 7.3). Each of the above proteins were localised at their respective junctions extensively in the control men (Figure 7.3). Following gonadotrophin suppression with each of the treatments, the localisation of β-actin and vinculin was largely unchanged, although tubule shrinkage appeared to 'squash' the proteins inward. β-catenin staining appeared partly reduced particularly in the T+A treatment group, but was overall unchanged. Connexin-43 staining appeared more diffuse than in control and possibly more cytoplasmic, but was overall similar to the control testes (Figure 7.3).

7.3.3 Comparison of germ cell numbers with claudin-11 localisation

Quantitative data describing the changes in germ cell types and numbers in each of the human testis biopsies used in this Chapter has previously been published (Matthiesson et al. 2005b). A notable feature from the Matthiesson *et al.* (2005a) study was the considerable difference observed in the extent of germ cell suppression between men within the same treatment group. In particular, those germ cells normally found within the adluminal region (leptotene, zygotene and pachytene spermatocytes, round spermatids) remained at 30-50% of controls (Figure 7.4) in some suppressed men, whereas in others this range dropped to < 5-20% It was therefore hypothesised that the extent of TJ protein suppression would be maximal in men who exhibited the greatest suppression of these germ cell types. Changes in claudin-11 localisation were therefore qualitatively compared to the extent of adluminal germ cell (in particular leptotene, zygotene & pachytene spermatocytes) suppression in each biopsy analysed in each treatment (Figure 7.4).

a. T+A treatment group

Men analysed in this treatment group were assigned the numbers 101, 102, 114, 116, 122 and 137. Man number 114 was not available for immunofluorescent analysis. Men 101 and 116 had suppressed leptotene, zygotene and pachytene spermatocytes to < 5% of controls (Figure 7.4a), and claudin-11 staining in these men was very punctate at the TJ. This staining pattern for claudin-11 was

Figure 7.3 Effect of hormone suppression on different junctional types in the human testis.

Bouin's fixed, paraffin embedded human testis biopsies were processed by immunohistochemistry and stained for i) cytoskeletal protein β-actin, ii) adherens junction protein β-catenin, iii) ectoplasmic specialisation protein vinculin and iv) gap junction protein connexin-43 (all green). Biopsies came from men (♂) with hormone suppression induced by T+A, T+LNG, T+LNG+A and T+LNG+D, as well as control men. The hormone suppressed biopsies presented in this figure are from men who showed maximal claudin-11 localisation disruption, demonstrated by the degree of punctate staining. Biopsies from different individuals are indicated by numbers which were allocated by Matthiesson *et al.* (2005a). Bar = 50μm. Inset = negative control.

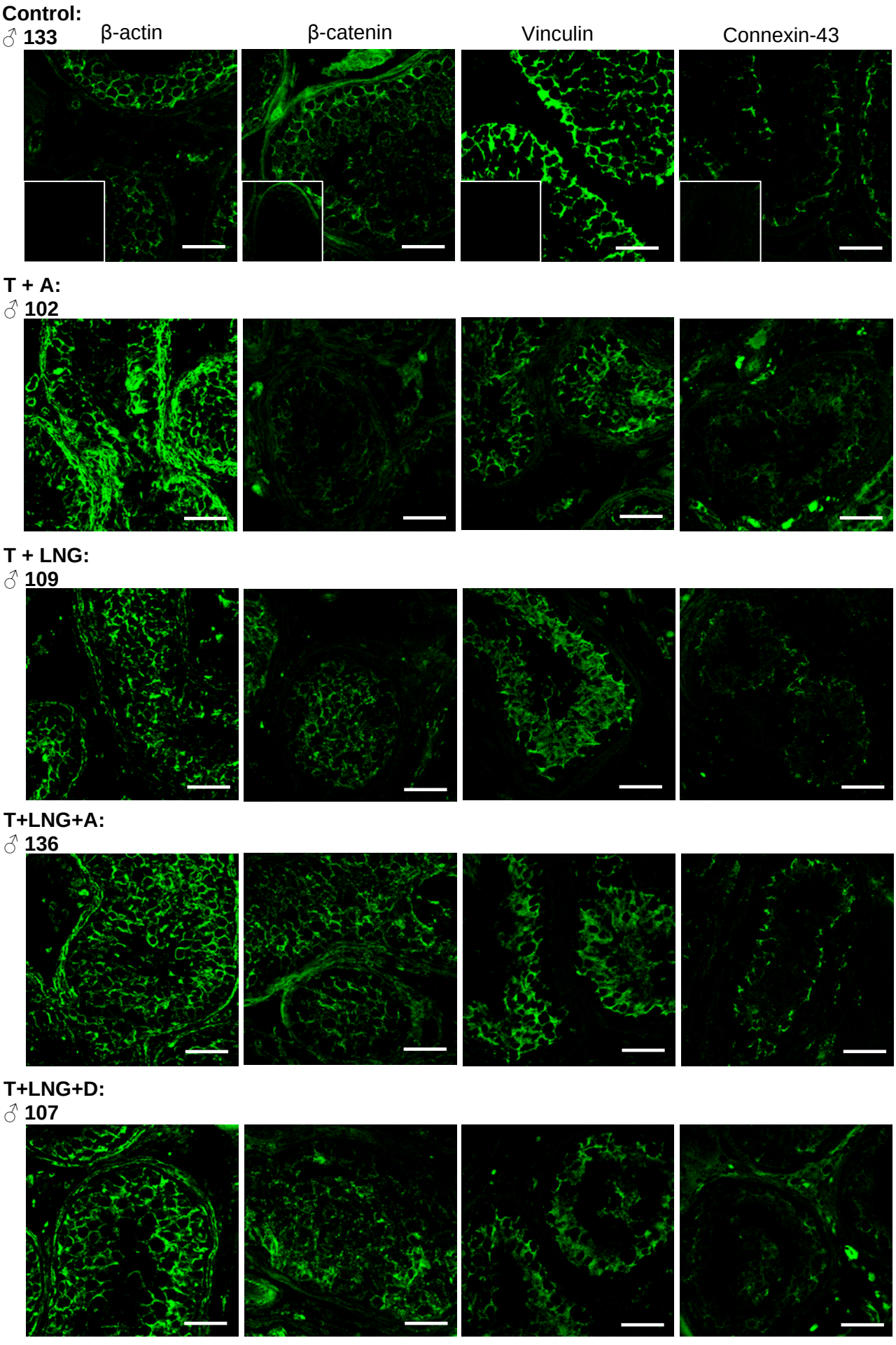
Control:
♂ 133
β-actin
β-catenin
Vinculin
Connexin-43
T + A:
♂ 102
T + LNG:
♂ 109
T+LNG+A:
♂ 136
T+LNG+D:
♂ 107

Figure 7.4a Comparison of claudin-11 protein localisation with extent of spermatocyte suppression in T+A treated men.

Germ cell data for leptotene, zygotene and pachytene spermatocytes (arrows) in men treated with T+A was obtained from Matthiesson *et al.* (2005a), and compared to claudin-11 (green) localisation in testis biopsies obtained from the same men (♂). Different individuals were allocated numbers by Matthiesson *et al.* (2005a) which were 101 (■), 102 (●), 114 (▲), 116 (♦), 122 (□) and 137 (✕). Note that number 114 was not available for immunohistochemical analysis. Germ cell types presented are: All A type spermatogonia (All A), type A dark spermatogonia (Ad), type A pale spermatogonia (Ap), type B spermatogonia (B), preleptotene spermatocytes (Pl), leptotene/zygotene spermatocytes (L-Z), pachytene spermatocytes (PS), round spermatids (rS), step 3-6 elongating spermatids (3-6 ST), step 7-8 elongating spermatids (7-8 ST) and sperm. Bar = 50μm.

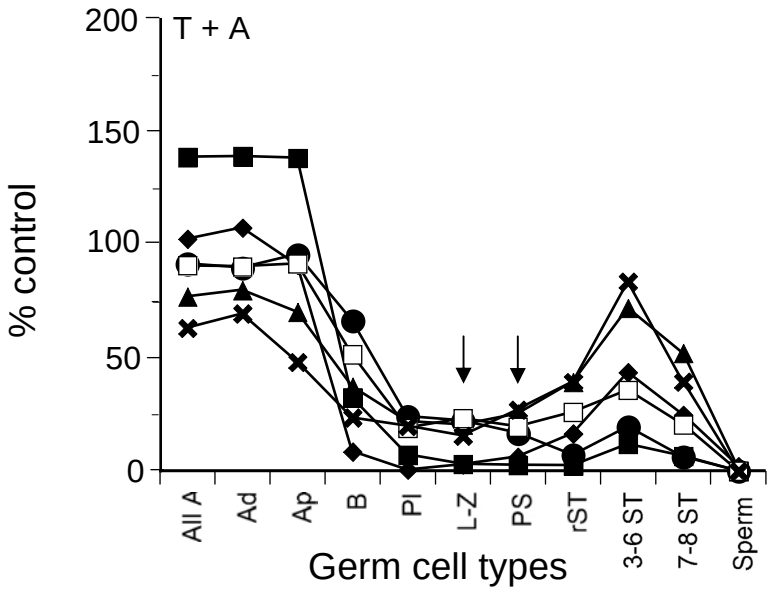
T + A
200
150
100
50
0
% control
All A
Ad
Ap
B
Pl
L-Z
PS
rST
3-6 ST
7-8 ST
Sperm
Germ cell types

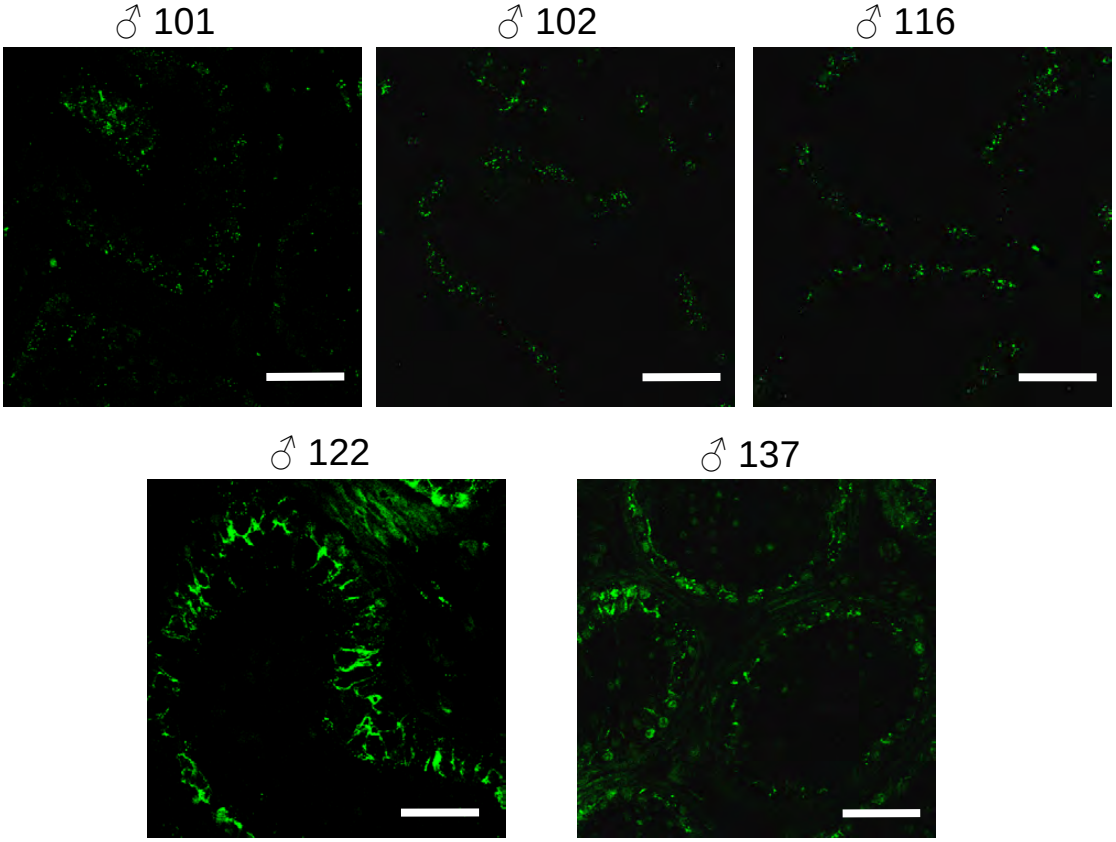
♂ 101
♂ 102
♂ 116
♂ 122
♂ 137

also apparent in man 102, whose spermatocytes had only decreased to approximately 20% of controls. Claudin-11 staining at the basal aspect of tubules was more extensive in men 137 and 122 (particularly in the latter) where spermatocytes had decreased to approximately 30% of controls (Figure 7.4a).

b. T+LNG treatment group

Men treated with T+LNG were assigned the numbers 105, 106, 109, 123, 131, although only numbers 109 and 131 were available for immunofluorescent analysis. Leptotene, zygotene and pachytene spermatocytes in man number 109 had suppressed to < 5% of controls (Figure 7.4b), and gave claudin-11 staining that was punctate at the TJ (Figure 7.4b). In contrast, man number 131 had suppressed spermatocytes to approximately 40% of controls, yet the claudin-11 staining was punctate and very similar to man 109 although some patches of more continuous staining were present (Figure 7.4b).

c. T+LNG+A treatment group

Men treated with T+LNG+A were assigned the numbers 104, 117, 126, 136 and 141. Only numbers 117, 126 and 136 were available for immunofluorescent analysis. Each of these men had suppressed leptotene, zygotene and pachytene spermatocyte number to 10%-15% of controls (Figure 7.4c). Claudin-11 staining in man 117 varied between punctate and continuous staining at the TJ (see two panels in Fig 7.4c), although the total claudin-11 staining appeared low. Man number 126 displayed extensive but punctate claudin-11 staining at the TJ although it was also partly continuous in areas (Figure 7.4c). Number 136 displayed a more punctate phenotype of claudin-11 staining at the TJ than men number 117 and 126 (Figure 7.4c).

d. T+LNG+D treatment group

Men in this treatment group were assigned the numbers 107, 108, 120, 124, 127 and 132. Only numbers 107, 120 and 132 were available for immunofluoescent analysis. The extent of leptotene, zygotene and pachytene spermatocyte suppression between these men differed. Man number 120 had suppressed spermatocytes to < 5% of controls (Figure 7.4d). The testis biopsy section was poor but displayed punctate staining of claudin-11, which was also continuous in areas. Number 107 had

Figure 7.4b Comparison of claudin-11 protein localisation with extent of spermatocyte suppression in T+LNG treated men.

Germ cell data for leptotene, zygotene and pachytene spermatocytes (arrows) in men treated with T+LNG was obtained from Matthiesson *et al.* (2005a), and compared to claudin-11 (green) localisation in testis biopsies obtained from the same men (♂). Different individuals were allocated numbers by Matthiesson *et al.* (2005a) which were 105 (■), 106 (●), 109 (▲), 123 (♦), 131 (□). Only numbers 109 and 131 were available for immunohistochemical analysis. Germ cell types presented are: All A type spermatogonia (All A), type A dark spermatogonia (Ad), type A pale spermatogonia (Ap), type B spermatogonia (B), preleptotene spermatocytes (Pl), leptotene/zygotene spermatocytes (L-Z), pachytene spermatocytes (PS), round spermatids (rS), step 3-6 elongating spermatids (3-6 ST), step 7-8 elongating spermatids (7-8 ST) and sperm. Bar = 50μm.

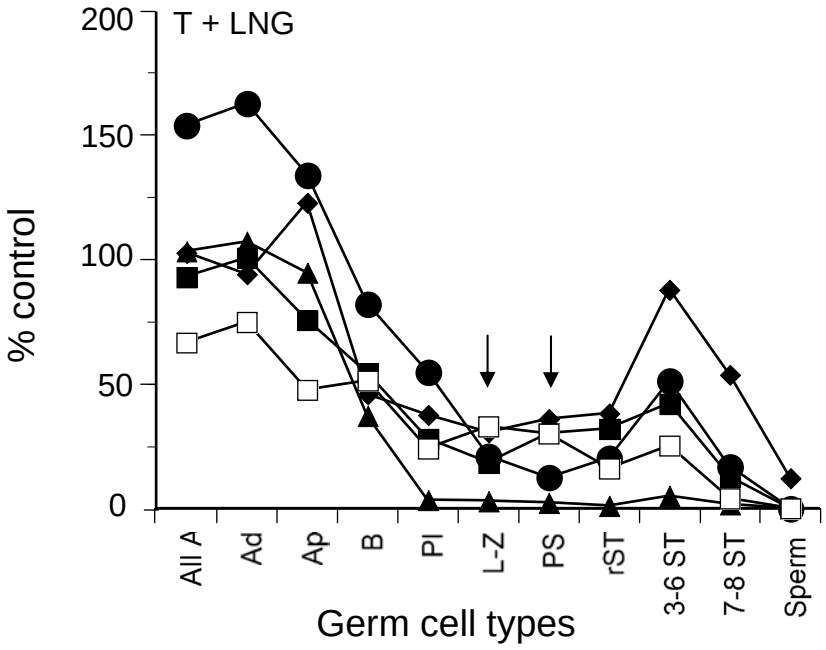
T + LNG
200
150
100
50
0
% control
All A
Ad
Ap
B
Pl
L-Z
PS
rST
3-6 ST
7-8 ST
Sperm
Germ cell types

♂ 109

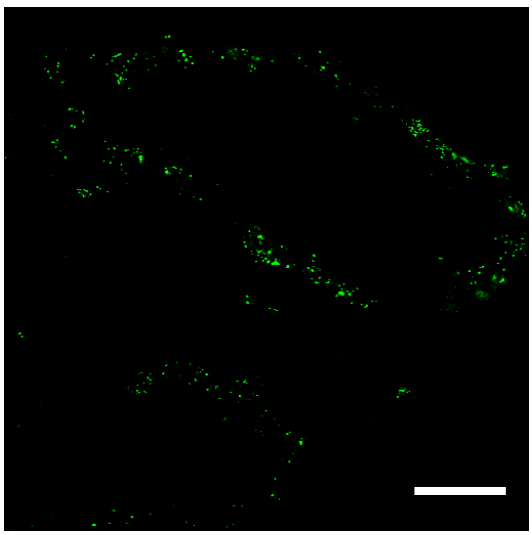

♂ 131

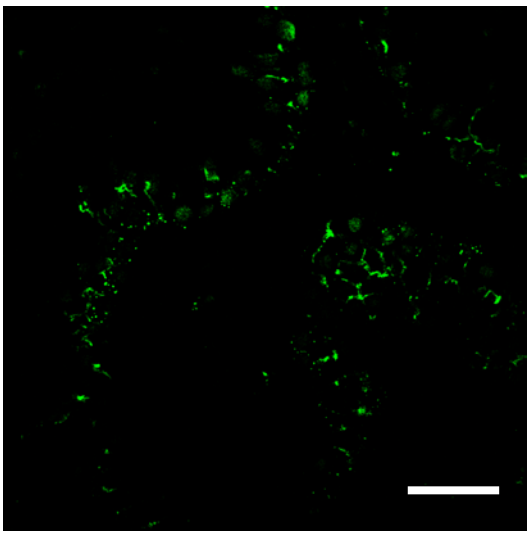

Figure 7.4c Comparison of claudin-11 protein localisation with extent of spermatocyte suppression in T+LNG+A treated men.

Germ cell data for leptotene, zygotene and pachytene spermatocytes (arrows) in men treated with T+LNG+A was obtained from Matthiesson *et al.* (2005a), and compared to claudin-11 (green) localisation in testis biopsies obtained from the same men (♂). Different individuals were allocated numbers by Matthiesson *et al.* (2005a) which were 104 (■), 117 (●), 126 (▲), 136 (♦), 141 (□). Only numbers 117, 126 and 136 were available for immunohistochemical analysis, with the grey channel of the confocal microscope provided for man 136 to highlight claudin-11 localisation with respect to the seminiferous tubules. Germ cell types presented are: All A type spermatogonia (All A), type A dark spermatogonia (Ad), type A pale spermatogonia (Ap), type B spermatogonia (B), preleptotene spermatocytes (Pl), leptotene/zygotene spermatocytes (L-Z), pachytene spermatocytes (PS), round spermatids (rS), step 3-6 elongating spermatids (3-6 ST), step 7-8 elongating spermatids (7-8 ST) and sperm. Bar = 50μm.

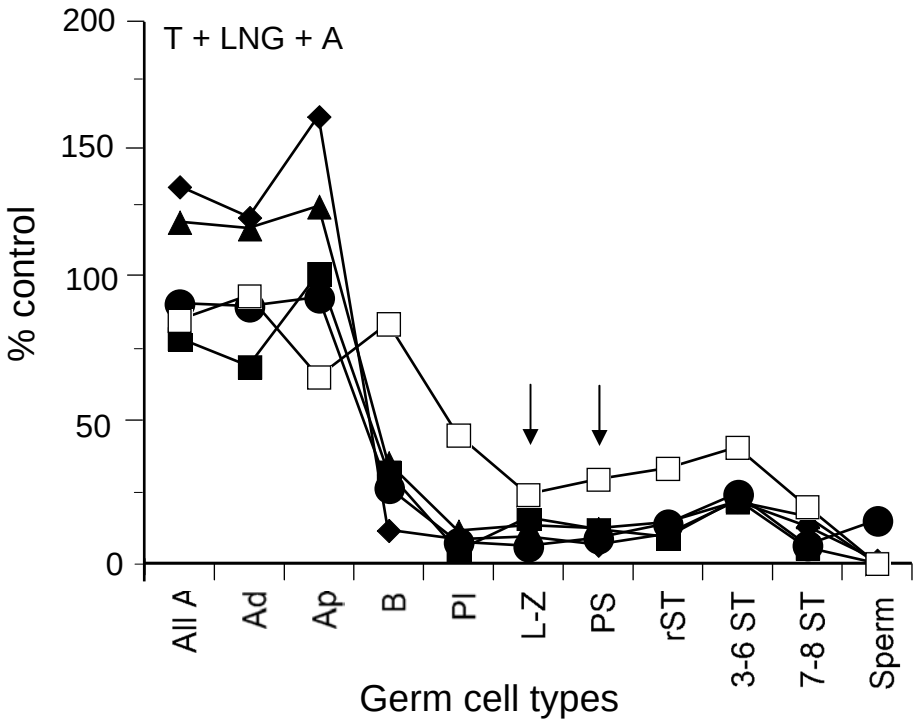
T + LNG + A
200
150
100
50
0
% control
All A
Ad
Ap
B
Pl
L-Z
PS
rST
3-6 ST
7-8 ST
Sperm
Germ cell types

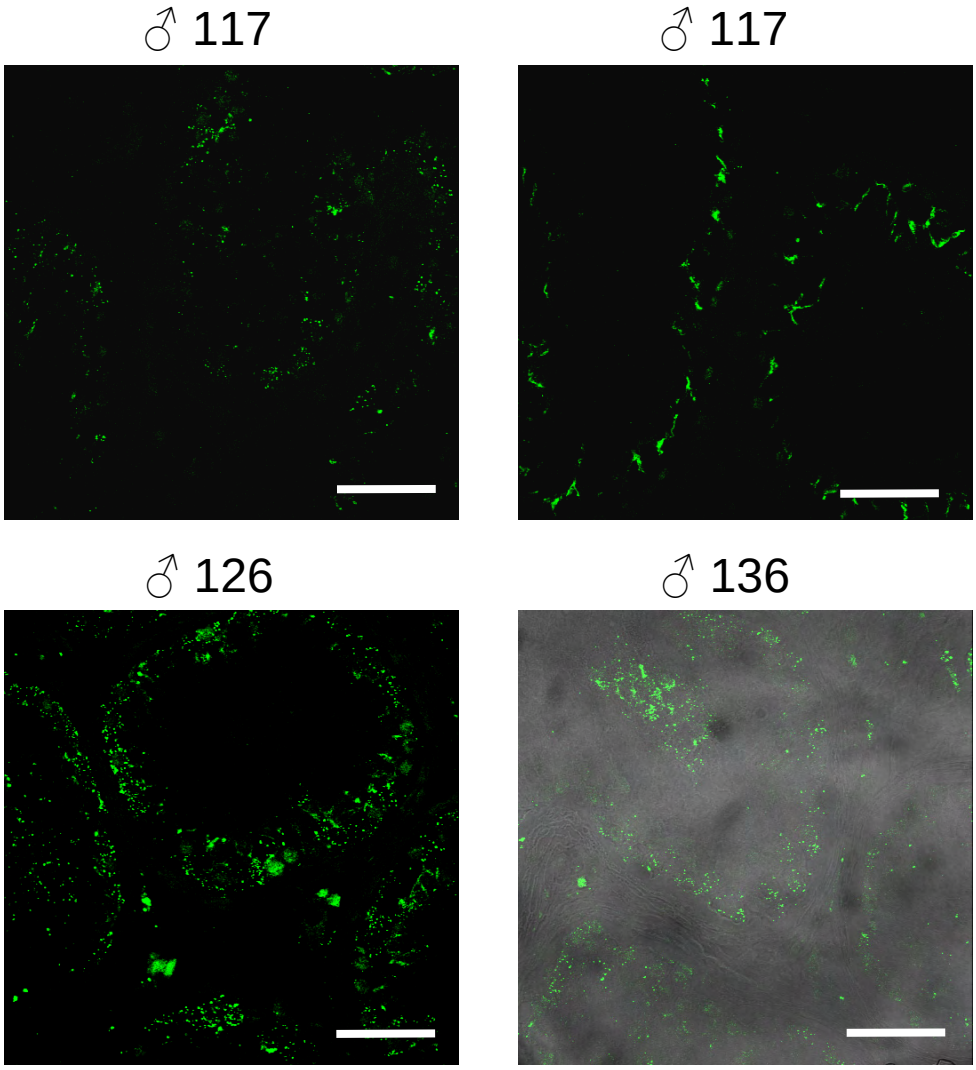
♂ 117
♂ 117
♂ 126
♂ 136

Figure 7.4d Comparison of claudin-11 protein localisation with extent of spermatocyte suppression in T+LNG+D treated men.

Germ cell data for leptotene, zygotene and pachytene spermatocytes (arrows) in men treated with T+LNG+D was obtained from Matthiesson *et al.* (2005a), and compared to claudin-11 (green) localisation in testis biopsies obtained from the same men (♂). Different individuals were allocated numbers by Matthiesson *et al.* (2005a) which were 107 (■), 108 (●), 120 (▲), 124 (♦), 127 (□), 132 (×). Only numbers 107, 120 and 132 were available for immunohistochemical analysis. Germ cell types presented are: All A type spermatogonia (All A), type A dark spermatogonia (Ad), type A pale spermatogonia (Ap), type B spermatogonia (B), preleptotene spermatocytes (Pl), leptotene/zygotene spermatocytes (L-Z), pachytene spermatocytes (PS), round spermatids (rS), step 3-6 elongating spermatids (3-6 ST), step 7-8 elongating spermatids (7-8 ST) and sperm. Bar = 50μm.

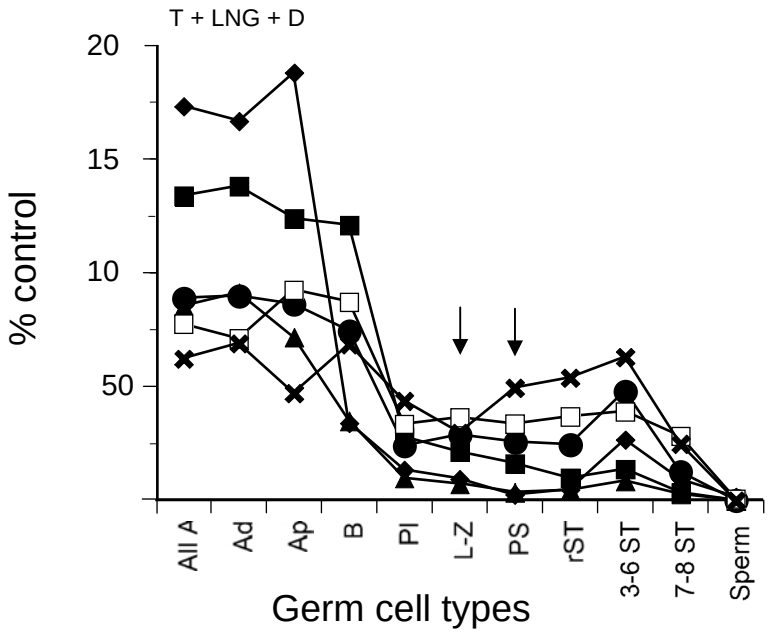
T + LNG + D
20
15
10
50
% control
All A
Ad
Ap
B
Pl
L-Z
PS
rST
3-6 ST
7-8 ST
Sperm
Germ cell types

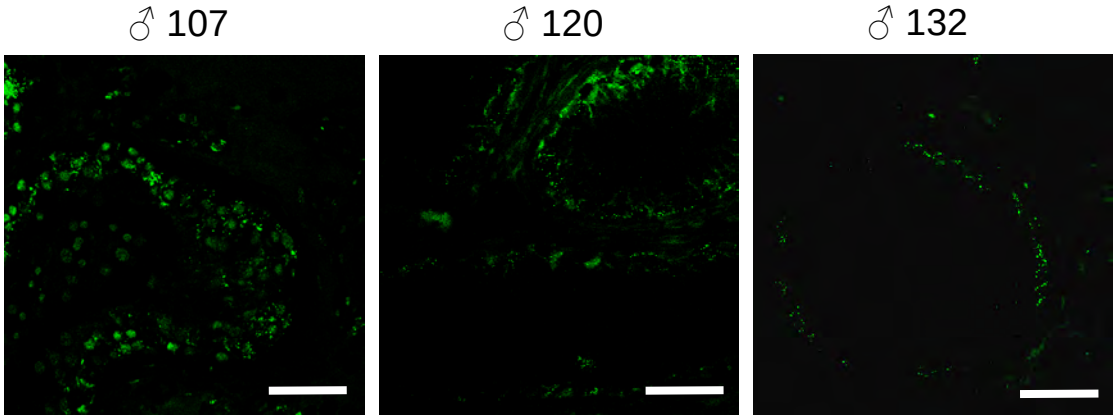
♂ 107
♂ 120
♂ 132

suppressed spermatocyte numbers to approximately 20% of controls, and also demonstrated punctate claudin-11 staining at the TJ. In man number 132, spermatocyte numbers remained at 50% of control. The biopsy section was again poor, but claudin-11 formed continuous TJ strands which resembled that seen in the previous control images (Figure 7.4d).

7.3.4 RNA Amplification with MessageAmp II kit for RT-PCR analysis

Amplification of each testis mRNA sample was successful. The amplification of the human testis QC extract from Ambion was 100 fold, which was the fold-amplification expected for an 8 hour incubation in the IVT buffer for aRNA synthesis (see Section 7.2.5c).

7.3.5 RT-PCR validation

After reverse-transcribing the amplified RNA into cDNA, RT-PCR was conducted using human β-actin primers, and the products separated on an agarose gel. A single band for β-actin was obtained at the expected molecular weight and subsequent DNA sequencing analysis confirmed the identity of the gene. It was therefore concluded that the cDNA produced from the amplified RNA was suitable for subsequent RT-PCR analyses.

7.3.6 Effects of gonadotrophin suppression on junctional mRNA expression

Gonadotrophin suppression did not alter the mRNA expression of any of the TJ proteins tested (claudin-11, claudin-3, occludin, JAM-A), or the cytoplasmic plaque protein ZO-1 (Figure 7.5). A decreasing trend in occludin mRNA expression was evident but this did not achieve significance ($p = 0.203$). Gonadotrophin suppression also had no effect on the mRNA expression of any of the other junctional proteins tested; vinculin, connexin-43 or β-catenin (Figure 7.5).

β-actin mRNA levels remained consistent across the groups (Figure 7.6). Androgen regulated INSL-3 decreased 20-fold ($p < 0.001$) in each of the suppressing treatments compared to control (Figure 7.6).

Figure 7.5 RT-PCR analysis of mRNA expression in hormone suppressed human testes.

mRNA was supplied from control men and men treated with T+A, T+LNG, T+LNG+A and T+LNG+D from Matthiesson *et al.* (2005a). mRNA was amplified to maximise availability, before a final reverse transcription was conducted to produce the cDNA required for RT-PCR. Responses to hormone suppression were analysed for the TJ proteins claudin-11, occludin, JAM-A and claudin-3 as well as for proteins from different junctional types, including ZO-1 (cytoplasmic plaque), vinculin (ectoplasmic specialisation), β-catenin (adherens junction) and connexin-43 (gap junction). Data is mean ± SEM, n = 3-5/group as shown.

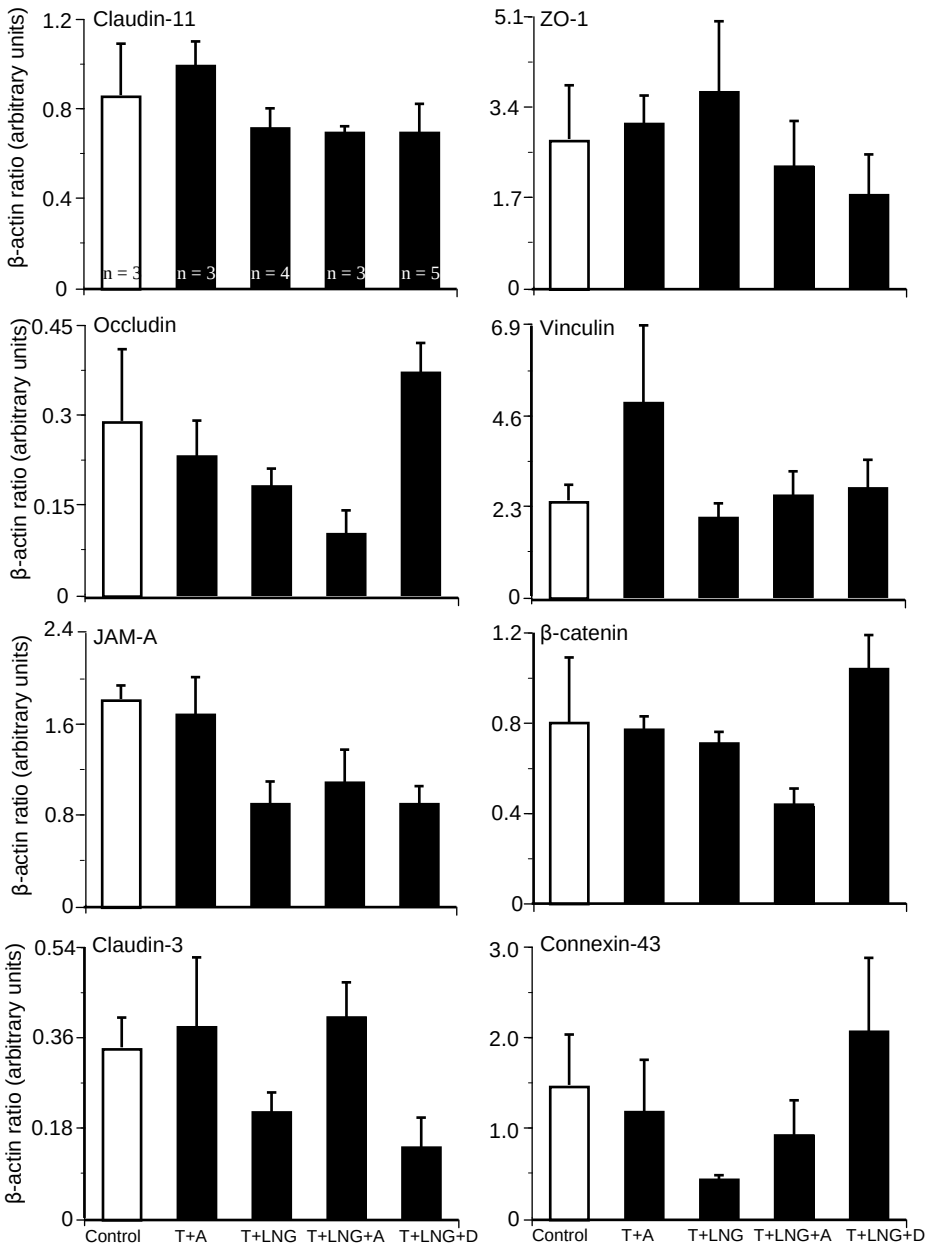
Claudin-11
ZO-1
Occludin
Vinculin
JAM-A
β-catenin
Claudin-3
Connexin-43
β-actin ratio (arbitrary units)
1.2
0.8
0.4
0
5.1
3.4
1.7
0.45
0.3
0.15
6.9
4.6
2.3
2.4
1.6
0.54
0.36
0.18
3.0
2.0
1.0
n = 3
n = 3
n = 4
n = 3
n = 5
Control
T+A
T+LNG
T+LNG+A
T+LNG+D

Figure 7.6 RT-PCR analysis of androgen regulated INSL-3 and housekeeper protein β-actin mRNA expression in response to hormone suppression in men.

mRNA was supplied from control men and men treated with T+A, T+LNG, T+LNG+A and T+LNG+D from Matthiesson *et al.* (2005a). mRNA was amplified to maximise availability, before a final reverse transcription was conducted to produce the cDNA required for RT-PCR. Responses to hormone suppression were analysed for the androgen-regulated protein INSL-3 (note logarithmic y-axis) as well as the housekeeper protein β-actin. Data is mean ± SEM, n = 3-5/group. a versus b = $p < 0.001$.

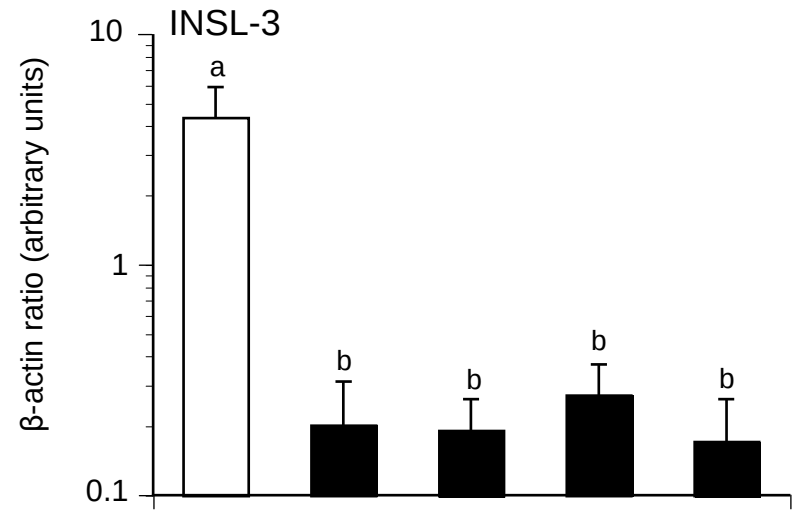
INSL-3
β-actin ratio (arbitrary units)
10
1
0.1
a
b
b
b
b

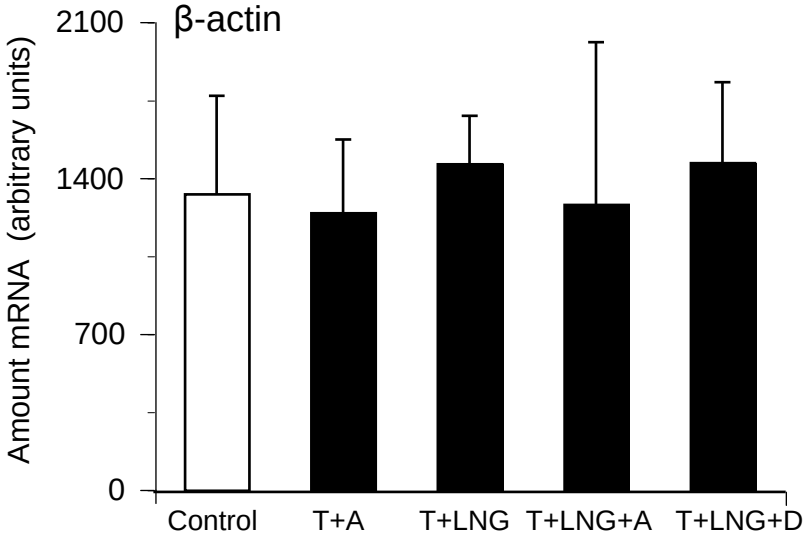
β-actin
Amount mRNA (arbitrary units)
2100
1400
700
0
Control
T+A
T+LNG
T+LNG+A
T+LNG+D

7.4 Discussion

The aims of studies presented in this Chapter were to i) determine the effects of gonadotrophin suppression on the Sertoli cell TJ, as well as other nearby junctional types in men with respect to protein localisation and mRNA expression and ii) determine whether intrinsic differences in germ cell response within each treatment group as reported in Matthiesson *et al.* (2005a) were associated with changes in TJ protein localisation, using claudin-11 as the TJ marker.

Previous data has shown in hypogonadotrophic hypogonadal men that TJs are immature in appearance (de Kretser and Burger, 1972), and this Chapter has shown that at the molecular level, claudin-11 localisation to the TJ is disrupted by gonadotrophin suppression. In the most severely germ cell-deplete testes according to the Matthiesson *et al.* (2005a) study, claudin-11 staining was reduced to a phenotype of primarily punctate staining at the outer edge of the seminiferous tubules. This phenotype was conserved across each gonadotrophin suppression treatment, all of which used a testosterone implant to promote negative feedback at the pituitary in conjunction with different modes of suppression such as GnRH antagonism (acyline), progestin (levonorgestrel) to inhibit androgen production, and a 5α-reductase inhibitor (dutasteride) to block the conversion of testosterone to the more potent androgen DHT (Matthiesson et al. 2005b, Matthiesson et al. 2005a). This suppressed claudin-11 phenotype also marks a departure from the cytoplasmic localisation of claudin-11 and other TJ proteins which occurs in the absence of gonadotrophins in rodent species, as displayed in the rat and mouse in this thesis, and also in the hamster (Tarulli *et al.* 2008).

As there were no significant differences in germ cell numbers for type B spermatogonia and later germ cell types between the various treatments (Matthiesson et al. 2005b), it was expected that the claudin-11 localisation would also be similar between these groups. However, within each treatment group, there was some heterogeneity observed in claudin-11 localisation response between men, from a phenotype with very limited punctate staining at the basal aspect of tubules, to an almost continuous TJ staining phenotype resembling the human control testes. To some extent, this result matched the extent of germ cell suppression for those germ cell types which normally reside within the blood-testis barrier, these being leptotene, zygotene and pachytene spermatocytes (Matthiesson et al. 2005b).

Interestingly, it generally appeared that when the numbers of these germ cells were at their lowest (typically <5% of control values), the regressed claudin-11 phenotype was at its most punctate. For example, in men numbered 122 and 137 who had received T+A for 8 weeks, leptotene, zygotene and pachytene spermatocytes were at approximately 30% of control numbers and claudin-11 was more extensive at the TJ, compared to other men in the same treatment group (numbers 101, 116) who had spermatocytes at < 5% of control and punctate claudin-11 staining. The same pattern was seen in the T+LNG treatment group for man number 131 who had leptotene, zygotene and pachytene spermatocyte numbers at 40% of control and more extensive claudin-11 staining than man 109, who had lower spermatocyte numbers (< 5% of control) and more punctate claudin-11 staining. Again in the T+LNG+D group, spermatocyte numbers were at 50% of control in man number 132, and claudin-11 staining was more extensive at the TJ. In the other two men from this group, spermatocyte numbers were lower and claudin-11 staining was punctate. In T+LNG+A, all spermatocyte numbers were between 10%-15% of control values, and claudin-11 varied from punctate to continuous staining in each of the men. While there seems to be an apparent trend in the data, not all samples conformed to this trend. Man number 102 (T+A treated) presented punctate claudin-11 staining at the TJ despite having leptotene, zygotene and pachytene spermatocyte numbers of approximately 20% of control, which was well above the ~5% of control spermatocyte numbers that men numbers 101 and 116 (from the same treatment group) presented along with reduced claudin-11 staining, and within the range of men who presented with more extensive claudin-11 staining. Therefore this study is an important first indication that the structure of the human TJ may be altered by gonadotrophin suppression, but additional studies will be needed to determine if this is true such as functional testing of the TJ in similar primate models.

It is hypothesised from the data presented herein that there may be a threshold at which once a particular amount of claudin-11 has been ‘lost’ form the Sertoli cell TJ in men, adluminal germ cells including leptotene, zygotene and pachytene spermatocyte numbers decrease and this may be directly related to an existence of a TJ functional threshold. While all men showed reduced spermatocyte numbers, the differences in degrees of reduction may suggest that some men in the treatment groups crossed this hypothesised threshold earlier than others. It may also suggest that the intrinsic differences in germ cell response to hormone suppression in men receiving the same treatment in the

Matthiesson *et al.* (2005a) study was actually attributable to intrinsic differences in TJ response to hormone suppression between men.

Further work is required to confirm the above speculation especially considering that changes in TJ protein localisation induced by gonadotrophin suppression in this Chapter was observed for just a single protein (claudin-11). While the claudin-11 knockout mouse is infertile (Gow *et al.* 1999), it is possible that another TJ protein could be maintaining TJ function and integrity to some extent and could also be accounting for the apparent intrinsic differences in TJ response to hormone suppression with the same treatment between men. Occludin was not able to be immunolocalised in this Chapter and the staining for claudin-3 was the same in the negative control (Figure 7.7). However the mRNA for both proteins was shown to be present in the testis. Claudin-3 was detected in the hamster positive control testis, but only stained the blood vessels in the rat (Figure 7.7) which supported the findings of Kaitu'u *et al.* (2007) where claudin-3 mRNA expression or protein localisation could not be detected in rat Sertoli cells *in vitro*. Alternatively, electron microscopy could be used as an additional assessment of changes in TJ structure in response to gonadotrophin suppression. This technique was successfully applied in the past to analyse the state of the Sertoli cell TJ in hypogonadotrophic hypogonadal men (de Kretser and Burger, 1972). It is hypothesised that in the men analysed in this study, the TJ would display an immature phenotype as it did in the de Kretser and Burger (1972) study.

Evidence for a functional threshold mentioned above of the Sertoli cell TJ was seen in the rat and mouse studies presented in Chapters 5 and 6 respectively. In some seminiferous tubules, spermatogenesis was seen to be proceeding, yet biotin tracer could still cross the TJ indicating it was not completely functional. However, it was functional enough that it was above the threshold for successful spermatogenesis. Unfortunately, this Chapter could not test for changes in TJ function in response to gonadotrophins suppression in men as the testis samples had already been processed previously for immunohistochemical and RT-PCR work.

Future studies investigating hormonal regulation of Sertoli cell TJs in men will therefore need to include a test of TJ function to address the points raised above. The nature of this test is not immediately clear, as the current biotin administration technique will not be practical. However, it may be possible that changes in TJ function *in vivo* could be qualitatively assessed using a testis

Figure 7.7 Localisation of claudin-3 in hamster, human and rat testes.

Hamster testis tissue (panel A) which had been fixed in Bouin's, as well as control human testis (panel B) tissue from Matthiesson *et al.* (2005a) was analysed by immunohistochemistry for claudin-3 (green, arrows) localisation to the Sertoli cell TJ. An adult control rat testis section (panel C) was also analysed for claudin-3 (green, arrows) localisation in seminiferous tubules (highlighted by red hashed line) using a blood vessel (centre) as the positive control. Bar = 50μm. Inset = negative control.

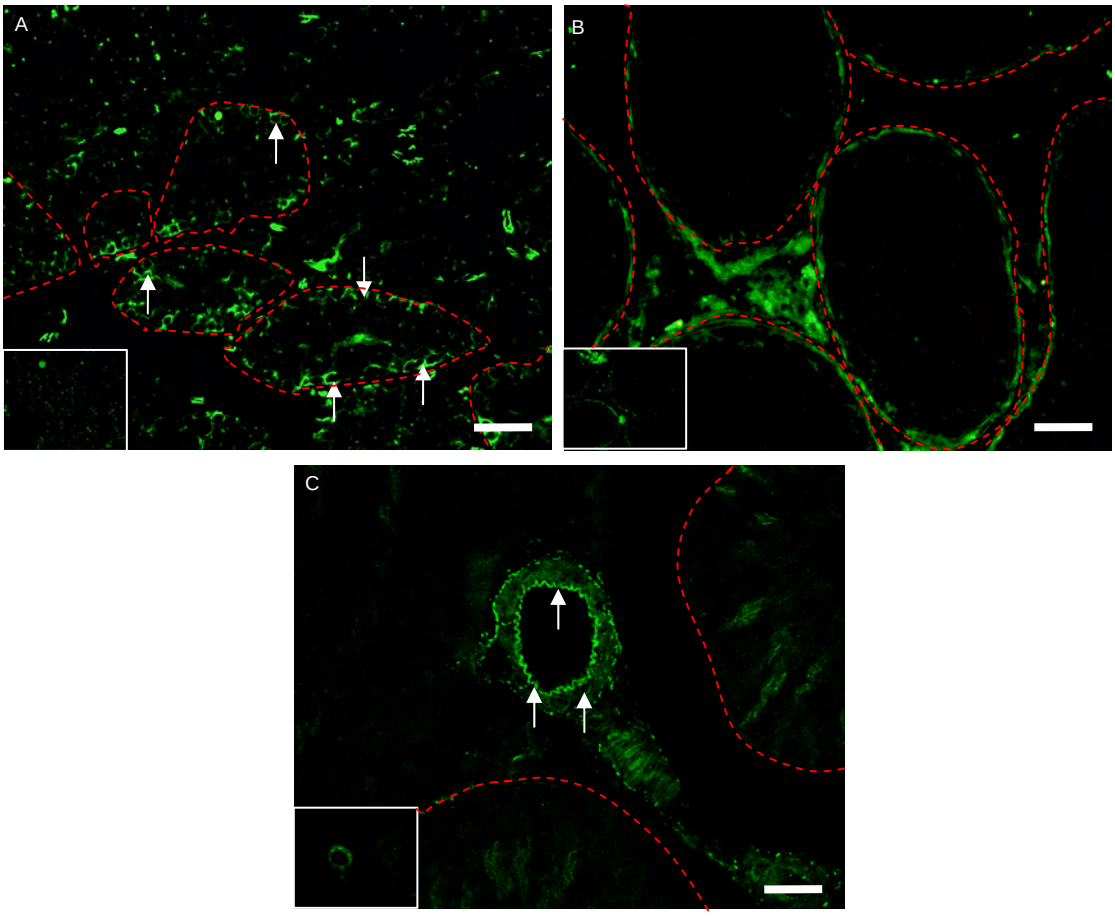
A
B
C

biopsy (~100mg) in conjunction with the biotin tracer technique as conducted in the previous two Chapters. To test this suggestion, a testis biopsy was conducted on a control adult rat testis by slitting the tunica albuginea to expose a portion of the seminiferous tubules to excise and incubate in biotin and then fix in Bouin's for immunohistochemical analysis via the established protocol. The biopsy experiment was conducted to replicate the means by which the human testis samples were obtained. Biotin staining was not only extensive in the interstitium and basal part of the seminiferous tubules, but was also present throughout the seminiferous tubules (Figure 7.8), indicating that the biotin tracer had entered through the severed ends of the tubules. In the intratesticular injection procedure, the tubules remain intact which prevents this problem.

Hence, the use of biotin as a qualitative TJ functional marker on human testis biopsies would not work. An alternative means could be to conduct experiments on primates and administer biotin to the testis via arterial perfusion. Or, for more direct administration to the testis, biopsied seminiferous tubules could be ligated to close the severed ends and then incubated in biotin. While the latter procedure would be more difficult, the ligation of efferent ducts in another study induced the retention of testicular fluid within the testis (Tao *et al.* 2000) and so this technique could be applied to the seminiferous tubules as well.

This Chapter has also shown that gonadotrophin suppression in men appears to specifically affect the TJ but generally not the nearby junctional types. No changes in immunofluorescent localisation of markers for the adherens junction, ectoplasmic specialisation or cytoplasmic plaque were observed after 8 weeks of suppression, with marginal changes seen in the localisation of connexin-43 to the gap junction. These results appear similar to those observed in the *hpg* mouse in Chapter 6, although in that model some disruption of vinculin localisation to the ectoplasmic specialisation was noted. Arguably, an extended period of gonadotrophin suppression to further suppress spermatogenesis and germ cells may result in changes in the other junctional types. Connexin-43 is important to Sertoli-Sertoli cell and Sertoli-germ cell interactions (Drummond *et al.* 2000, Sridharan *et al.* 2008) and the loss of germ cells may have led to the changes in connexin-43 localisation observed. Its continued presence could have been due to some residual FSH in the treatment groups (0.5%-0.8% of control (Matthiesson et al. 2005a)), or thyroid hormone which has

Figure 7.8 Biotin localisation in an adult rat testis biopsy.

One adult rat was killed by CO_2 asphyxiation and one of the testes was excised. The tunica was nicked to expose the seminiferous tubules and a small portion of these were cut from the testis and incubated in biotin (10mg/ml) tracer for 30 minutes before being fixed in Bouin's fixative for 5 hours. The tissue was then embedded in paraffin wax and processed by immunohistochemistry with streptavidin alexa-488 to probe for biotin (green) localisation. Biotin localised basally to the TJ is indicated by arrows and adluminally localised biotin has been indicated by asterisks. Bar = 50μm.

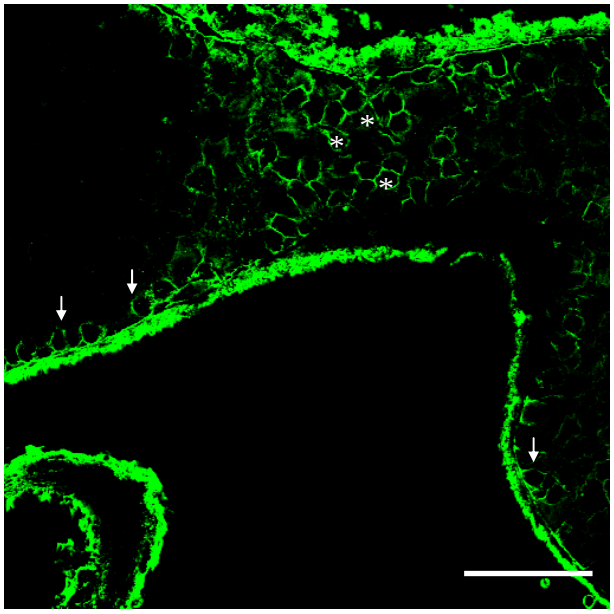

also been shown to regulate connexin-43 (Stuurman *et al.* 1998, Harborth *et al.* 2001, Sridharan *et al.* 2008).

ZO-1 localisation to the cytoplasmic plaque in this study was unaffected by gonadotrophin suppression. This may have been an expected result, as unlike in the rodent models in this thesis, claudin-11 which binds to the cytoplasmic plaque, did not redistribute to the cytoplasm and so there may not have been a requirement for ZO-1 to redistribute either. β-catenin was still localised at the adherens junction in this model, and the adherens junction also binds to the cytoplasmic plaque (Yan and Cheng, 2005). This may also explain the continued presence of ZO-1 at the cytoplasmic plaque in the *hpg* mouse which was also coincident with continued β-catenin staining.

The response of junctional mRNA expression to gonadotrophin suppression in men was also analysed. RNA samples from the Matthiesson *et al.* (2005a) study were amplified to maximise availability for these studies and was shown to be successful through the production of RNA which was viable for RT-PCR. This was after reverse transcription gave a single band for housekeeper protein β-actin on a DNA agarose gel at the expected molecular weight and DNA sequence. Viability was further demonstrated after RT-PCR analysis showed that the mRNA expression levels of β-actin did not change across the treatment groups.

Expression of the androgen-regulated protein INSL-3 was decreased by approximately 20-fold in the gonadotrophin suppressed groups, and is consistent with the low levels of intratesticular androgens as measured in the Matthiesson *et al.* (2005a) study. This INSL-3 mRNA data also resembled the results obtained in the previous two Chapters presented in this thesis, although it is noteworthy that the magnitude of the suppression was considerably greater in humans (22 fold) compared to rats (12 fold) and mice (15 fold).

The mRNA expression of TJ proteins claudin-11, occludin, JAM-A and claudin-3 was unaffected by gonadotrophin suppression. Occludin mRNA expression did appear to decrease with hormone suppression, but this result did not achieve significance ($p = 0.203$). In addition, the mRNA expression of markers of the nearby junctional types was also unaffected. The result for claudin-11 was unexpected as protein staining while still at the TJ, was markedly reduced compared to controls. In the rat and mouse Chapters presented herein, mRNA expression levels for claudin-11 and/or occludin tended to increase when TJ protein localisation to the TJ was disrupted in the absence of

circulating hormones. A similar result was seen in the hamster, where like in the rat, the mRNA expression of claudin-11 and occludin increased in reduced hormone levels (Tarulli *et al.* 2008), indicating that the mRNA expression of both proteins respond differently to hormone suppression in the human than in rodents. This role for gonadotrophin regulation of TJ protein localisation has now been demonstrated in rats, mice and humans which demonstrates a conserved trend of hormonal regulation of the TJ among mammalian species and suggests that the regulation of mRNA expression is mediated by something else either separately to or in conjunction with gonadotrophins, such as local factors.

In the Matthiesson *et al.* (2005a) study, spermiogenesis failed demonstrating the regulatory mechanism of gonadotrophins (particularly androgens) during this point of spermatogenesis. It was argued that since decreases were seen in late spermatid and round spermatid numbers in two other studies which used TE + progestin depot medroxyprogesterone acetate (DMPA) (Zhengwei *et al.* 1998, McLachlan *et al.* 2002a) that decreases in earlier spermatogonia was a flow on effect of the loss of the spermatids. Indeed, when claudin-11 was stained in testis biopsies which had been obtained from one of these studies (McLachlan *et al.* 2002a), its localisation at the TJ, while more diffuse, remained extensive and generally continuous at TJs even after 12 weeks of TE + DMPA treatment and despite large germ cell losses as mentioned (Figure 7.9). Staining was not punctate like that obtained in this thesis. However, as already mentioned in this thesis, the Sertoli cell TJ is essential for spermatogenesis and its absence results in infertility Chung and Cheng, 2001, Chung *et al.* 2001). Given that this Chapter has suggested that gonadotrophins may regulate the Sertoli cell TJ in men and that gonadotrophins also regulate spermiogenesis in men (Zhengwei *et al.* 1998, McLachlan *et al.* 2002a, Matthiesson et al. 2005b), it can be argued that the loss of germ cell types in the human seminiferous epithelium as a response to gonadotrophin suppression is a combined effect of the loss of TJ integrity and spermiogenesis. Differences in claudin-11 localisation in response to TE+DMPA and TE+treatments form this study suggests a different mode of action for the progestin DMPA compared to other treatments used herein. To reinforce this contribution of the TJ, on needs to conduct functional testing in a follow up study.

Figure 7.9 Claudin-11 localisation in TE+DMPA and T+A treated men.

Claudin-11 (green) was probed in Bouin's fixed control human testes (panel A) and testes which had been treated with TE+DMPA for 12 weeks (obtained from McLachlan *et al.* (2002a)) (panel B). Immunohistochemical analyses on these testes was conducted by Gerard Tarulli at Prince Henry's Institute of Medical Research, Melbourne and are representative of all testes probed in these treatment groups. These immunofluorescence micrographs have been presented here as a comparison with the control (panel C) and T+A treated testes (obtained from Matthiesson *et al.* (2005)) (panel D) conducted in this Chapter. Note that claudin-11 in panel A and B was co-stained with gap junction protein connexin-43 (red), hence the yellow staining.

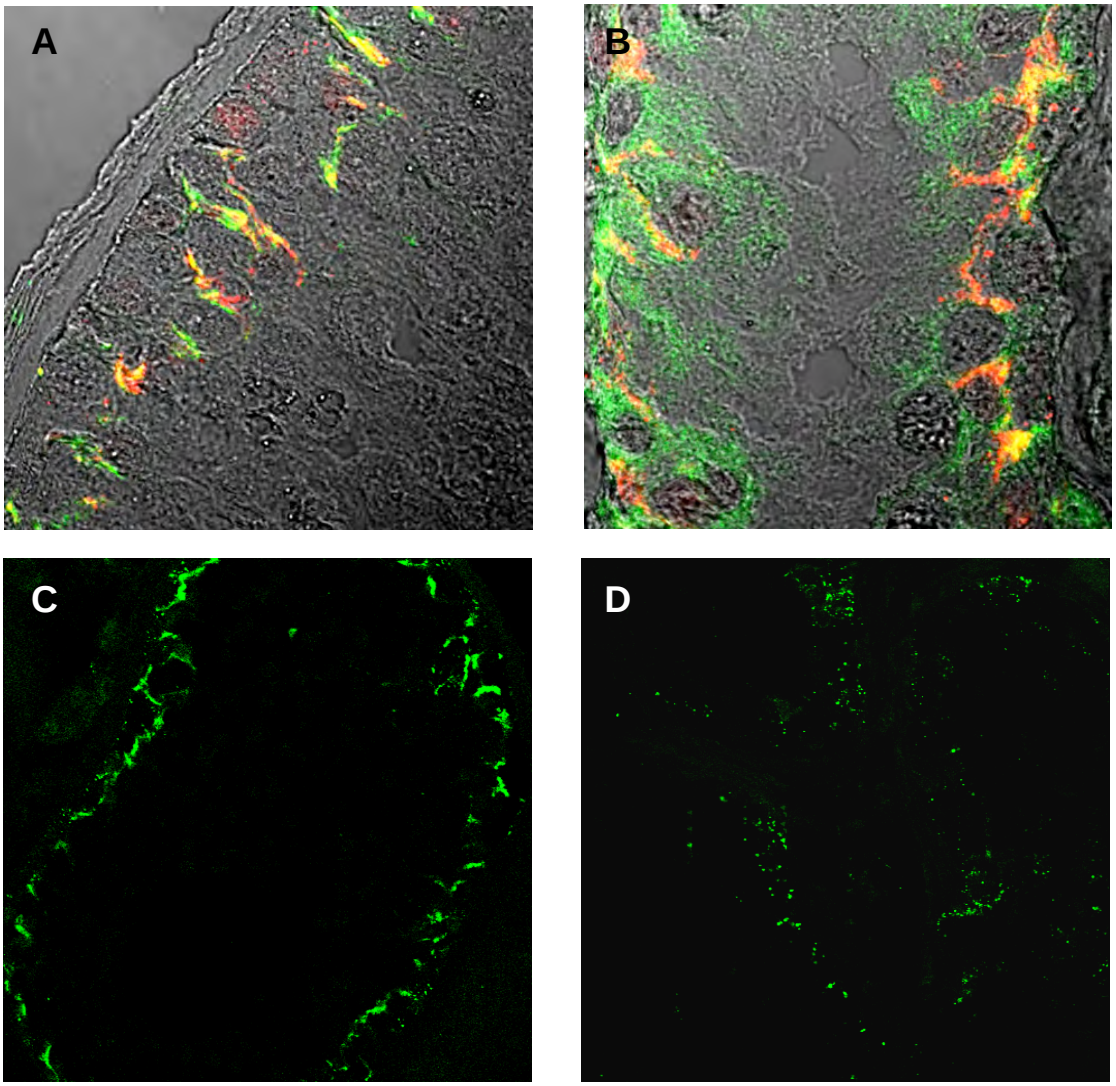
A
B
C
D

In conclusion, evidence is presented here to show that gonadotrophins can regulate the localisation of claudin-11 to the Sertoli cell TJ in men. Intrinsic differences in claudin-11 localisation response to gonadotrophin suppression between men within the same treatment group was observed and seems to be associated with the intrinsic differences observed in germ cell suppression (Matthiesson et al. 2005b). The suppression of circulating gonadotrophins resulted in the reduction of protein staining at the TJ and the cessation of spermatogenesis. The structural integrity of the Sertoli cell TJ in men, is therefore essential for successful spermatogenesis and thus it is speculated that the Sertoli cell TJ could prove to be a potential target of hormonal contraception in men.

Chapter Eight: General Discussion

Chapter 8. General discussion

The aims of the studies described in this thesis were to assess the relative contribution of the integral transmembrane proteins claudin-11 and occludin to the Sertoli cell TJ *in vitro,* and to determine the roles that gonadotrophins have in maintaining and stimulating the formation of Sertoli cell TJ function and structure in the rat and mouse *in vivo.* Furthermore, this thesis aimed to analyse gonadotrophin regulation of the Sertoli cell TJ in gonadotrophin-suppressed men.

Studies in the first part of this thesis demonstrated that both claudin-11 and occludin had important roles in maintaining TJ function in an immature rat Sertoli cell culture model, *in vitro*. The genetic silencing of claudin-11 or occludin with siRNA resulted in a decrease in TJ function of approximately 50% *in vitro* as measured by TER, while silencing both proteins in combination decreased TJ function by 62% *in vitro*. It was concluded that silencing both proteins together had no additive effect on TJ function compared to silencing either protein in isolation as the difference between the results, while significant, was marginal. The disruption to TJ function due to the silencing of claudin-11 *in vitro* is consistent with the infertility phenotype of the claudin-11 knockout mouse (Gow *et al.* 1999). Future studies to determine whether a similar 50% knockdown of claudin-11 *in vivo* would be sufficient to cause a loss of TJ function in an established adult mouse/rat model where spermatogenesis is ongoing would be interesting. Such methodologies could involve the use of siRNA to selectively silence its expression, in conjunction with molecular tracers of varying sizes to establish changes in permeability of the epithelium. The significant TJ functional role found for occludin *in vitro,* was more surprising given that its knockout is fertile in young adults (Saitou *et al.* 2000), which had led to the hypothesis that its contribution to Sertoli cell TJ function would be significantly less than that of claudin-11. In fact, in the *in vitro* Sertoli cell culture both TJ proteins were comparable, at least in terms of TER. The *in vivo* studies using siRNA mentioned above for claudin-11 should also be applied for studying the contribution of occludin to Sertoli cell TJ function *in vivo*.

The literature however, does point to changes in TJ function induced by experiments targeting the occludin protein. For example, the treatment of cultured *Xenopus* embryo epithelial cells or cultured rat Sertoli cells with synthetic peptides corresponding to one of the extracellular loops of occludin increased paracellular permeability *in vitro* (Wong and Gumbiner, 1997, Chung *et al.* 2001). Furthermore the intratesticular injection of one of these peptides into adult rat testes resulted in

massive germ cell loss *in vivo* (Chung *et al.* 2001). A similar increase in paracellular flux was seen in cultured MDCK cells when chicken occludin lacking the entire C-terminal domain was transfected into them Balda *et al.* 1996). Conversely, the over-expression of wildtype occludin in the same cells simulated TER Balda *et al.* 1996). These data implicate a role for occludin in the regulation of TJ function as outlined in Chapter 1 (see Section 1.4.4a). Such regulatory roles for occludin are evident in that 'tighter' TJs such as those found in the bladder epithelium contain more occludin protein than 'looser' TJs such as the intestine, with the Sertoli cell TJ considered to be one of the 'tighter' TJs in the mammalian body (Dym and Fawcett, 1970, Hirase *et al.* 1997, Sluka *et al.* 2006). No such variable phenotype for the claudins has been found with respect to the tightness of TJs. Therefore, the silencing of occludin at the Sertoli TJ with siRNA, may have resulted in a 'looser' TJ, which equated to decreased transepithelial electrical resistance and therefore decreased TJ function, *in vitro*.

However, a recurring theme in this thesis showed that reduced Sertoli cell TJ function does not necessarily equate with spermatogenic inactivity, and that there may be a TJ functional threshold above which spermatogenesis continues to function normally, but below which loss of germ cells and Sertoli cell function occurs. The phenotype of the claudin-11 knockout indicates that the absence of claudin-11 at the Sertoli cell TJ breaches this threshold. The occludin knockout mouse model is less clear (Gow *et al.* 1999). These mice displayed normal spermatogenesis at 6 weeks of age, but by 40 weeks of age, seminiferous tubules displayed atrophy and contained Sertoli cells only (Gow *et al.* 1999). While the reasons for this are uncertain, the authors suggested that the ablation of downstream signalling mechanisms potentially mediated by occludin, could have led to a gradual onset of infertility (Gow *et al.* 1999). This meant that the TJ functional threshold was gradually breached somewhere between 6 weeks and 40 weeks of age. As mentioned earlier, the role of occludin at the TJ still needs to be fully elucidated. While several studies have shown that cytokines or environmental toxicants can affect the function of the Sertoli cell TJ (Lui *et al.* 2001, Lui *et al.* 2003a, Siu *et al.* 2003, Cheng and Mruk, 2004, Lui and Lee, 2006, Zhang *et al.* 2008), no other models apart from the knockouts provide evidence of a functional threshold at the Sertoli cell TJ with respect to active spermatogenesis *in vivo*.

The fact that spermatogenesis does not depend upon a fully functional TJ is very interesting. When spermatogenic activity was suppressed in the GnRH-antagonist treated rat and arrested in the *hpg*

mouse, low molecular weight biotin tracer was present on the adluminal side of the Sertoli cell TJ indicating disrupted TJ function (Figure 8.1). This was coincident with reduced-to-absent tubule lumens, which is taken as a good morphological indicator about the functionality of testicular TJs (Bergmann, 1987, Pelletire, 1990). When hCG, which stimulates testicular testosterone production, and/or FSH were selectively replaced, spermatogenic activity re-initiated as shown by larger tubule diameters with the reappearance of tubule lumens, and reappearance of adluminal germ cells. This was all in the presence of a 'leaky' Sertoli cell TJ as shown by the continued presence of biotin in the adluminal compartment of the seminiferous tubules (Figure 8.1). In the human, some meiotic and post-meiotic germ cell types were present in hormone-suppressed testes, despite markedly reduced claudin-11 staining at the TJ. While no functional analyses were carried out in the human study, it is hypothesised based on the rat and mouse data that the human Sertoli cell TJ was not fully functional, but that sufficient function remained to allow some spermatogenic activity.

Work in this thesis has therefore demonstrated that Sertoli cell TJ functionality should not be regarded as an 'on-off switch' in terms of spermatogenesis in the adult animal, but rather that functionality can vary over a range commensurate with ongoing spermatogenic activity. However, this is not a particularly novel finding for the Sertoli cell TJ, or for TJs in other epithelia, as illustrated by the following examples. The low molecular weight tracer [^{51}Cr]-EDTA (341Da) was still detectable on the adluminal side of the blood-testis barrier in post-pubertal rats at 25 days of age (Setchell *et al.* 1981, Setchell *et al.* 1988), which is well into spermatogenesis as shown by the presence of post-meiotic round spermatids in the epithelium (Meachem *et al.* 1996). In the claudin-5 knockout mouse, the blood-brain barrier was disrupted as shown by the penetration of a low molecular weight biotin tracer (443Da) into the brain parenchyma indicating altered TJ function (Nitta *et al.* 2003). However, these mice were apparently healthy and did not suffer any bleeding or oedemas (Nitta *et al.* 2003). In this same claudin-5 knockout model, a larger microperoxidase tracer (1.9kDa) was excluded by the blood-brain barrier, indicating that the claudin-5 deficient TJ retained a size-selective phenotype. Watson *et al.* (2001) showed that the permeability of cultured Caco-2 and T84 intestinal cells was inversely proportional to the increasing size of 24 polyethylene glycols ranging from 252Da-1255Da *in vitro*, with a cut-off in TJ permeability to tracers of greater than 458Da. In a similar study, mannitol treatment to cultured brain cells induced a significantly higher permeability to the smallest of

Figure 8.1 Tight junction function and active spermatogenesis.

Testes from the GnRH-antagonist treated rat study (panels A – C) and the *hpg* mouse study (panels D – F) were stained for biotin (green, arrow head) and TJ proteins occludin (rat, red, arrow) or claudin-11(mouse, red, arrow). Treatment groups presented in this figure are cross-sections through i) control rat and mice testes (panels A and D respectively); ii) acyline treated rat testes (8 weeks) and *hpg* mouse testes (panels B and E respectively) and iii) hCG + FSH Ab treated (7 days) rat testes and *hpg* + tgFSH mouse testes treated with 10 days of androgen DHT (panels C and F respectively). Bar = 50μm. Inset = negative control.

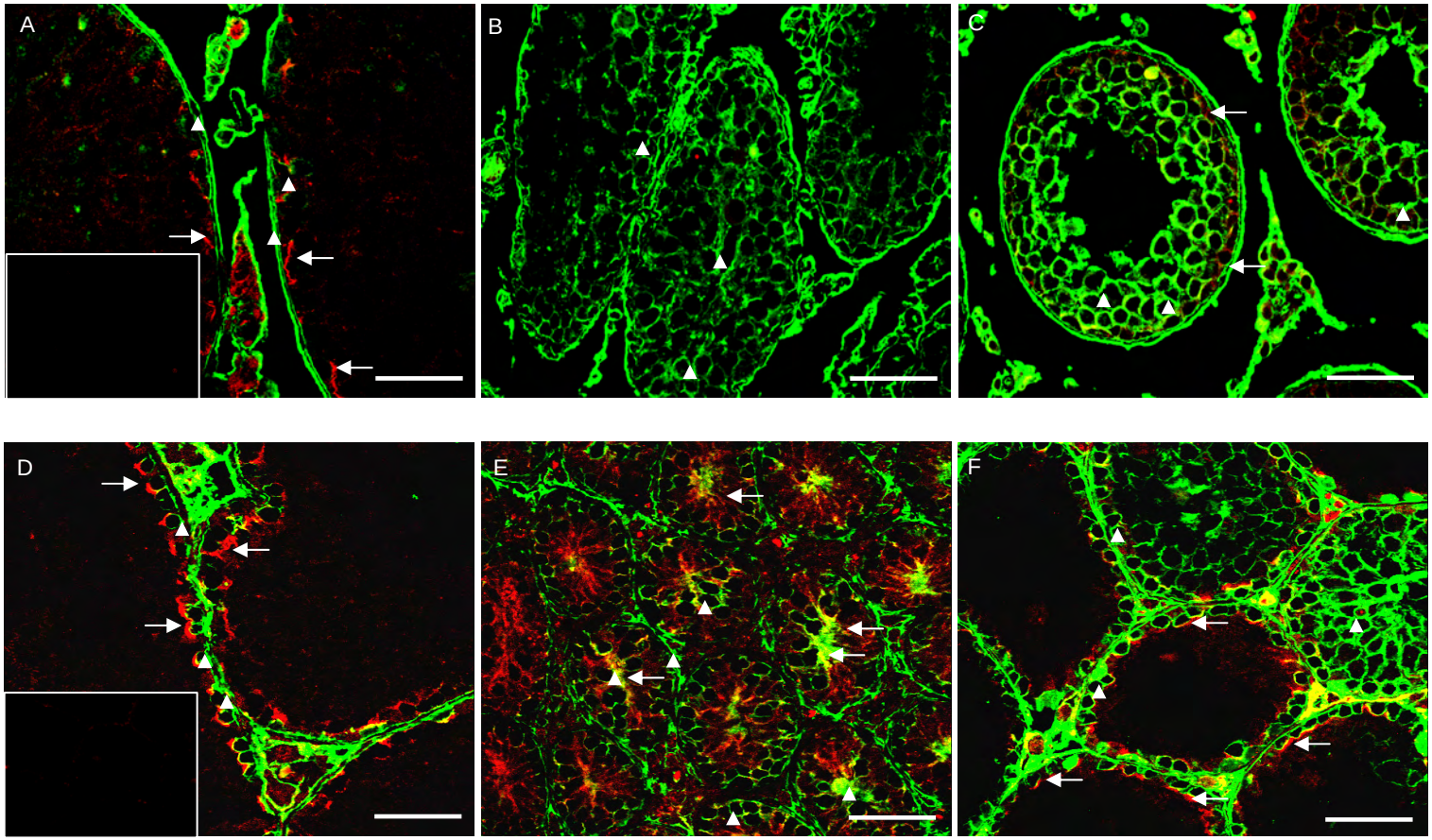
A
B
C
D
E
F

three tracers ([^{14}C]sucrose, 342Da) employed, compared with the next smallest tracer ([^{3}H]inulin, 5kDa) *in vitro*, whereas the third and largest tracer (Evan's Blue Dye, 67kDa) remained impermeable (Deli *et al.* 1995). None of the tracers were permeable to the TJ in the untreated cells (Deli *et al.* 1995). Hence, TJs are size-selective, and the removal of certain protein components alters this size-selective nature (Watson *et al.* 2001, Nitta *et al.* 2003). Most of the literature suggests that the claudins contribute to the size-selectivity of TJs (Watson *et al.* 2001) although changes in the size-selectivity of the Sertoli cell TJ or other epithelial TJs in the occludin knockout mouse, were not analysed (Gow *et al.* 1999), so the contribution of occludin to size-selectivity is not known.

The threshold at which TJ function is completely disrupted is therefore the point at which the TJ cannot selectively maintain the integrity of the microenvironment(s) or compartment(s) it regulates either side of any given barrier. Examples of this include massive transepidermal water loss in the claudin-1 knockout mouse (Furuse *et al.* 2002), and Mg^{2+} and Ca^{2+} wastage in some human renal diseases where claudin-16 failed to localise to the TJ (Simon *et al.* 1999, Kausalya *et al.* 2006, Muller *et al.* 2006, Gonzalez-Mariscal *et al.* 2008). In the testis, a loss of blood-testis barrier integrity could in theory lead to the induction of macrophages or immuno-modulatory factors including TGFβ3, TNFα, IL-1 (α/β) and interferon-γ (Gerdprasert *et al.* 2002, Hedger, 2002, Hedger *et al.* 2005, O'Bryan *et al.* 2005), or possibly an autoimmune response to adluminal germ cell antigens which are normally sequestered from the immune system by the TJ Chung and Cheng, 2001, Chung *et al.* 2001), although evidence for this needs to be elucidated.

In the GnRH antagonist-treated rat study, a greater number of macrophages appeared to increase and localise to the periphery of the seminiferous tubules, with the occasional macrophage actually penetrating into the lumen of some tubules. A similar induction of macrophage localisation to the periphery of seminiferous tubules was seen in LPS-treated rat testes where testosterone production was attenuated, resulting in a pro-inflammatory response (Gerdprasert *et al.* 2002, Hedger *et al.* 2005, O'Bryan *et al.* 2005). This inflammatory response was reversed following the exogenous application of testosterone (Gerdprasert *et al.* 2002, Hedger *et al.* 2005, O'Bryan *et al.* 2005). The very preliminary result for macrophage induction obtained for the GnRH antagonist-treated rat, suggests that there might have been an immune response, similar to LPS treatment, following gonadotrophin suppression and subsequent TJ disruption. Much more work is needed to identify which, if any,

macrophage elements and/or immuno-modulatory factors were elevated in response to the impaired Sertoli cell TJ. However, it is already known that several of these factors, including TNFα and TGFβ3, can negatively regulate blood-testis barrier dynamics (Lui *et al.* 2001, Lui *et al.* 2003a, Siu *et al.* 2003, Cheng and Mruk, 2004, Lui and Lee, 2006), and that their expression levels in the seminiferous epithelium are lowest as TJs form (Lui *et al.* 2001, Lui *et al.* 2003a, Siu *et al.* 2003, Cheng and Mruk, 2004, Lui and Lee, 2006). In addition, intratesticular administration of TNFα to rats resulted in germ cell loss, and the opening of testicular TJs as monitored with a fluorescent dye (FITC) *in vivo* (Li *et al.* 2006). Similarly, TGFβ3 dose-dependently disrupted the function of cultured rat Sertoli cell TJs as shown by decreases in TER *in vitro* (Lui *et al.* 2001). Given the regulatory role these local paracrine factors appear to have with respect to TJ function, it is hypothesised that an interplay between these factors and gonadotrophins can regulate Sertoli cell TJ function in the rat *in vivo*.

The infiltration of biotin into the seminiferous epithelium in low levels of gonadotrophins in this thesis, points to an alteration in the size-selective nature of the Sertoli cell TJ. Two other tracers of differing size ([^{14}C]mannitol, 182Da, and [^{3}H]methoxy-inulin, 5kDa) were also employed in this thesis, but without success primarily due to technical difficulties. However, other tracers such as fluorescently labelled FITC-dextran (4kDa, 10kDa or 40kDa) (Sonoda *et al.* 1999, Nitta *et al.* 2003) are available and might be easier alternatives which could provide a more detailed qualitative analysis of changes in Sertoli cell TJ size-selectivity following hormone suppression and/or replacement/administration. If the TJ was permeable to each of these tracers in the acyline-treated rat or *hpg* mouse, one might be able to analyse changes in the size-selectivity of the TJ as hormones are replaced/administered, and in particular, determine at which specific point with respect to size-selectivity that germ cells normally found in the adluminal compartment, reappear. Evidently, spermatogenesis can re-initiate while TJs are still permeable to small molecules less than or equal to 600Da as shown with biotin. Such data suggests a link between TJ function/size-selectivity and germ cell survival/progression in animal models, which could potentially be useful in predicting the extent to which TJ function has to be suppressed for spermatogenic arrest in the human.

In the low levels of circulating gonadotrophins in the GnRH antagonist-treated rat or *hpg* mouse models, testicular TJ proteins were either undetectable (as for occludin in the rat model), or localised in the Sertoli cell cytoplasm (as for claudin-11 in the rat and mouse models) toward the centre of the

seminiferous tubules. This cytoplasmic localisation of claudin-11 was very similar to that observed in the short-day hamster testis, where occludin was also seen to be cytoplasmic (Tarulli *et al.* 2006, Tarulli *et al.* 2008) (Figure 8.2), suggesting species differences and similarities with respect to hormonal regulation of TJ protein localisation. Unlike the rodent models, claudin-11 in gonadotrophin-suppressed men became more punctate at the Sertoli cell TJ and did not redistribute to the cytoplasm, suggesting differences in the regulatory pathways for TJ proteins between humans and rodents. The human and rodent models did, however, give unexpected results for gonadotrophin regulation of TJ mRNA expression. Given that testosterone has been shown elsewhere to regulate rat Sertoli cell claudin-11 mRNA expression *in vitro* (Kaitu'u *et al.* 2007), and that treatment with the androgen receptor antagonist, flutamide, inhibited claudin-11 mRNA expression *in vivo* (Florin *et al.* 2005), it was expected that gonadotrophin suppression would lead to reduced TJ mRNA expression in the rat, mouse and human models. This was not the case, with mRNA expression for occludin and claudin-11 remaining unchanged in the human following gonadotrophin suppression, but significantly elevated or tending to be increased in the rodent models. Elevated mRNA expression levels of occludin and claudin-11 have also been reported in the rodent short-day hamster model, which has low serum gonadotrophins (Tarulli *et al.* 2008).

These mRNA results are difficult to explain, but suggest a differential response between TJ mRNA expression and TJ protein localisation, with the potential for a block after mRNA transcription. The nature of such a inhibitory function is unknown, but could include the action of local cytokines such as TNFα and TGFβ3, which are known to prevent the localisation of TJ proteins to the TJ *in vitro* (Lui *et al.* 2001, Lui and Lee, 2006). This reinforces the notion made earlier for an interplay between hormonal and paracrine regulation of the Sertoli cell TJ, and also demonstrates that regulation of TJ mRNA expression across rodent species is conserved, but differs to the human.

In the absence of detectable circulating gonadotrophins in the *hpg* mouse, TJ proteins were localised to the Sertoli cell cytoplasm, in a similar manner to that observed in the GnRH-antagonist treated rat, and short day hamster (Tarulli *et al.* 2006, Tarulli *et al.* 2008). The application of exogenous hormones to each of these models stimulated the re-localisation of TJ protein back to the TJ at the basal aspect of the seminiferous epithelium. This observation strengthens the conclusion that TJ protein localisation is hormonally regulated, but does not show the extent to which newly

Figure 8.2 Cytoplasmic localisation of TJ proteins in gonadotrophin suppressed rodent testes.

The Sertoli cell TJ protein claudin-11 was stained in a Bouin's fixed GnRH-antagonist treated rat testis (panel A, green) and a *hpg* mouse testis (panel B, red) to display the cytoplasmic localisation that occurs in low circulating gonadotrophin levels in rodents. This has been compared to a result obtained for occludin (green –open circles) in a short-day hamster testis (panel C) obtained from Tarulli *et al.* (2008). Bar = 50μm and inset = the negative control in panels A and B. In panel C, the bar = 50μm and the inset = an enlarged version of the micrograph.

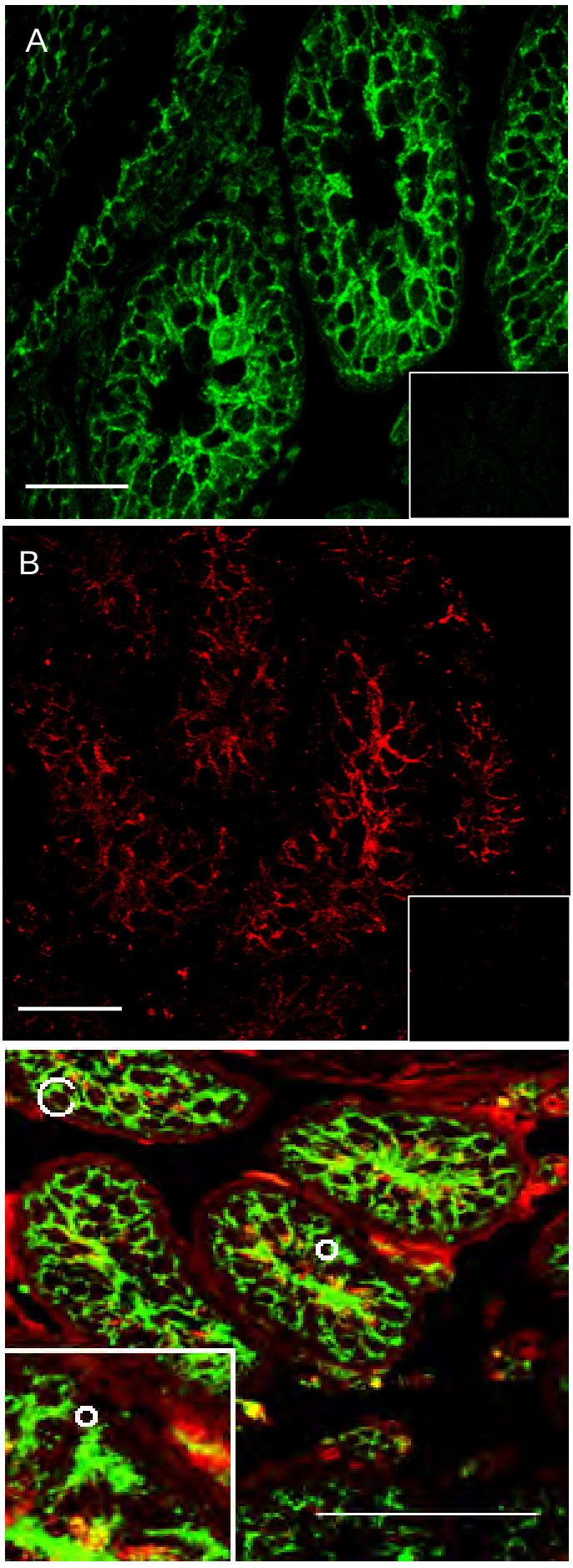
A
B
C

synthesised protein is added to this apparent cytoplasmic pool as part of the relocalisation process.

This cytoplasmic pool of TJ protein may exist in readiness for rapid TJ formation. It could also be important in the mechanism of TJ remodelling needed to allow germ cells to migrate into the adluminal compartment, where a rapid breakdown and reassembly of TJ proteins to maintain blood-testis barrier integrity is required (Setchell, 1967, Zhou *et al.* 2002).

Intracellular pools of claudins and occludin have been observed in Ca^{2+} depleted MDCK cells, in wound healing, and following treatment with proinflammatory cytokines (Ando-Akatsuka *et al.* 1999, Lu *et al.* 2001, Bruewer *et al.* 2003, Ivanov *et al.* 2004, Bruewer *et al.* 2005, Morimoto *et al.* 2005). In fibroblastic baby hamster kidney cells and epithelial MTD-1A cells, it was found that the G-protein Rab13, a member of a family of proteins which regulate the localisation of proteins to the cell surface and control cell polarity (Morimoto *et al.* 2005), regulated the localisation of occludin to the TJ *in vitro* and was co-localised with internalised occludin in the protein pool (Morimoto *et al.* 2005). The existence of a TJ protein pool was further demonstrated by the treatment of cultured polarised T84 intestinal cells with the *Escherichia coli*-derived toxin cytotoxic necrotising factor-1 (Hopkins *et al.* 2003). Upon exposure to the toxin, occludin was internalised and pooled into caveolae, early endosomes and recycling endosomes, and the authors suggested that this could enable occludin to avoid degradation and be recycled back into the TJ (Hopkins *et al.* 2003). Therefore, the existence of a TJ protein pool is not unusual, and hence may also be expected in the Sertoli cell. As mentioned in Chapter 5, images presented herein were not of sufficient resolution to allow visualisation of TJ proteins within defined cytoplasmic vesicles, although the data is strong enough to hypothesise that similar recycling of TJ proteins from the cytoplasm to the Sertoli cell TJ occurs like in other cell types. Recent studies have suggested that this is the case, where the cytokine IL-1α induced the relocalisation of claudin-11 and occludin to the Sertoli cell cytoplasm in rats (Sarkar *et al.* 2008). Furthermore, testosterone was also seen to induce internalisation of these proteins and their subsequent recycling back to the Sertoli cell membrane (Kaitu'u *et al.* 2007, Yan *et al.* 2008). It would be of interest to see whether Rab13 is localised at the Sertoli cell TJ, and is involved in the gonadotrophin-regulated recycling and redistribution of occludin and/or claudin-11 to the TJ.

Claudin-11 and occludin were the key TJ proteins studied in this thesis, but in the mouse and hamster testes, claudin-3 is also present at the TJ, although only when germ cells migrate across the

blood-testis barrier (Meng *et al.* 2005, Tarulli *et al.* 2008). Previous evidence has shown that the mRNA expression of claudin-3 in mice is androgen regulated (Meng *et al.* 2005), whereas the localisation of claudin-3 protein to the TJ in the hamster is FSH regulated (Tarulli *et al.* 2008, Tarulli *et al.* 2006). This thesis confirmed these findings, with androgens seemingly playing a larger role than FSH with respect to claudin-3 localisation to the TJ in mice. Interestingly however, claudin-3 was not localised at the Sertoli cell TJ in rats or humans (recall Figure 7.8), suggesting that a different claudin could be expressed at the Sertoli cell TJ in rats and humans alongside claudin-11. The presence of more than one claudin in any given epithelial TJ is not unusual. Both claudin-5 and claudin-12 are at the blood-brain barrier (Nitta *et al.* 2003), claudin-1 and claudin-2 are present at TJs in the liver (Furuse *et al.* 1998), and claudin-3 and claudin-4 are often co-localised in numerous epithelia including the endometrium and ovary, pancreas, esophagus, breast and lung (Rangel *et al.* 2003, Nichols *et al.* 2004, Gyorffy *et al.* 2005, Tokes *et al.* 2005, Moldvay *et al.* 2007). It may be possible that claudin-4 is also present at the Sertoli cell TJ with claudin-3 (and claudin-11) in the mouse and hamster testis, or instead of claudin-3 in the human and rat testis. The presence of testicular claudin-4 has only been demonstrated using northern blot analyses (Morita *et al.* 1999, Michl *et al.* 2001), hence the particular cells to which it is localised remain unknown. Further analyses are needed to find if other claudins are involved in the restructuring of Sertoli cell TJs as germ cells migrate, with claudin-4 a suitable starting candidate along with other more ubiquitous claudins such as claudin-1 and claudin-5 (Sidhu *et al.* 2003).

In addition to claudin-11 and occludin, this thesis also investigated the regulation and localisation of JAM-A and ZO-1 in response to gonadotrophin suppression. The amount of literature covering JAM-A is limited, but is increasing. It appears that JAM-A is mainly important during TJ formation such as in the trophectoderm, where JAM-A has been shown to recruit adherens junction and TJ components (Thomas *et al.* 2004). Most recently, Tarulli *et al.* (2008) localised JAM-A to Sertoli-germ cell contacts surrounding the most basal spermatogonia in hamster testes, and also at Sertoli-Sertoli cell contact points. Its localisation around human spermatogonia has also been recently observed (Tarulli, personal communication). Following gonadotrophin suppression in the GnRH-antagonist treated rat, JAM-A was predominantly localised to Sertoli cell cytoplasm in a similar manner to claudin-11 and occludin, but staining was also extensive at the basement membrane, which

may reflect spermatogonial staining as seen in the hamster (Tarulli *et al.* 2008) and human (Tarulli, personal communication). Like claudin-11 and occludin, JAM-A mRNA expression increased following gonadotrophin suppression, but in contrast to claudin-11 and occludin, JAM-A mRNA expression levels in the rat did not return back toward control levels upon short-term hormone replacement, which could again be due to a spermatogonial contribution. This early germ cell localisation of JAM-A, which appears conserved between hamsters, rats and men, is very interesting as TJs do not exist between Sertoli and germ cells (Cheng and Mruk, 2004, Sluka *et al.* 2006). JAM-A is known to regulate the passage of leukocytes across microvasculature epithelial cells (Martin-Padura *et al.* 1998, Tsukita and Furuse, 1999, Chavakis *et al.* 2004, Morris *et al.* 2006, Bradfield *et al.* 2007), believed to be conducted by interactions between JAM-A and proteins important for cytoskeletal restructuring. The passage of germ cells across the Sertoli cell TJ requires similar cytoskeletal restructuring, and JAM-A mRNA has been detected in Sertoli cells and germ cells (Chalmel *et al.* 2007), and protein has been detected in spermatozoa from the caudal epididymis (Shao *et al.* 2008). Taking the results from these studies into account, it has been hypothesised that JAM-A in the hamster may play an important role in spermatogenesis by mediating the passage of germ cells across the blood-testis barrier (Tarulli *et al.* 2008). Unfortunately, JAM-A was undetectable in the human in Chapter 7 or *hpg* mouse studies by immunohistochemistry, where its localisation in the *hpg* mouse would have provided a unique opportunity to study the role of this protein in the initiation of spermatogenesis and TJ formation.

The localisation and mRNA expression of the adapter cytoplasmic plaque protein ZO-1 was predominantly unchanged in the Sertoli cells as a result of gonadotrophin suppression across each chapter in this thesis, although it had moved slightly adluminally from the basement membrane in the GnRH-antagonist treated rat. The redistribution of claudin-11 and occludin in the absence of ZO-1 redistribution suggests that both of these proteins had somehow disengaged from ZO-1. A similar disengagement event between ZO-1 and occludin has been observed in the lung following TJ restructuring (Kawkitinarong *et al.* 2004). In the testis, disengagement of Sertoli cell TJ proteins, as well as adherens junction proteins from the cytoplasmic plaque has been shown to be a requirement for blood-testis barrier restructuring as germ cells migrate (Yan and Cheng, 2005). Interestingly, the cytokine TGFβe has been shown to modulate ZO-1 redistribution and disengagement at the time of

germ cell migration (Ahdieh *et al.* 2001, Xia *et al.* 2005, Xia and Cheng, 2005), and other cytokines such as IL-4 and IL-13 have been shown to modulate ZO-1 mRNA and protein expression (Ahdieh *et al.* 2001, Xia *et al.* 2005, Xia and Cheng, 2005). Results obtained from this thesis suggest that occludin/claudin-11 disengagement and engagement from/to ZO-1 could also be hormonally regulated. The results obtained in this thesis also show that the changes in TJ function are directly due to changes in claudin-11 and occludin redistribution and this is further shown by the continued presence of ZO-1 at the outer edge of seminiferous tubules in the claudin-11 knockout mouse (Gow *et al.* 1999). Furthermore, two MDCK cell-lines which record either high or low TERs *in vitro* displayed similar amounts of ZO-1 protein at TJs, suggesting that the amount of ZO-1 in any given tissue does not correlate with the tightness and therefore function of TJs (Stevenson *et al.* 1986).

In the *hpg* mouse and human studies, this thesis also analysed the effect of gonadotrophin suppression on other testicular junctional types in association with the TJ. No changes were seen in β-catenin localisation at the adherens junction, and the fact that this junction is also associated with ZO-1 (Yan and Cheng, 2005), may be another reason as to why there was no ZO-1 protein redistribution. Vinculin as a marker of the ectoplasmic specialisation was localised in the Sertoli cell cytoplasm of the *hpg* mouse, and gonadotrophin administration stimulated vinculin redistribution to the blood-testis barrier. Hormonal regulation of vinculin localisation in the gonadotrophin-suppressed human however was not observed, with any apparent changes in vinculin localisation more likely due to tubular shrinkage as a result of hormone suppression. However, the *hpg* mouse and gonadotrophin-suppressed human are two different models, with the results actually demonstrating that gonadotrophins stimulate the formation of the ectoplasmic specialisation (ES) in mice, but do not regulate its maintenance in humans at least in the time frame (8 weeks) that these men were suppressed. It is arguable however, that a longer suppression phase could produce a greater spermatogenic regression as evidenced by increased germ cell loss, particularly of pachytene spermatocytes and round spermatids, and under these circumstances, ES regulation could well be altered. The results obtained in the *hpg* mice, suggest that in some species, there is a global regulation of the blood-testis barrier (at least in terms of formation) with the regulation of the most important component, the Sertoli cell TJ, being conserved across many species.

In barely-detectable levels of circulating gonadotrophins in the *hpg* mouse, gap junction protein connexin-43 was localised to the Sertoli cell cytoplasm at the centre of the seminiferous tubules in the 20 day old pubertal animals, but had re-localised to the basement membrane by adulthood as per the *wt* adult mouse, indicating a hormone-independent mechanism with respect to its localisation. The presence of connexin-43 at the basement membrane indicated that gap junctions had possibly formed between adjacent Sertoli cells (Drummond *et al.* 2000, Sridharan *et al.* 2008). Handelsman *et al.* (1999), reported that despite *hpg* mice having no circulating gonadotrophins and infantile gonads, that the reproductive system was functionally competent as shown by the initiation of spermatogenesis following testosterone treatment (Singh *et al.* 1995). The continued presence of connexin-43 at gap junctions may also contribute to this functional competency, and thereby have a role in the initiation of spermatogenesis following gonadotrophin treatment. In the gonadotrophin-suppressed human, connexin-43 had moved adluminally toward the centre of the seminiferous tubules and away from the basement membrane. This adluminal movement was marginal however and a greater effect on connexin-43 re-localisation, may have been observed had gonadotrophins been suppressed in the human for longer than 8 weeks.

Overall, it is concluded that gonadotrophin suppression and replacement in the adult animal selectively regulates the Sertoli cell TJ via its effects on claudin-11 and occludin expression and localisation. However, it does not appear that the associated junction types (ectoplasmic specialisation, adherens, and gap junctions) are regulated in the same manner, highlighting the TJ as a potential site of gonadotrophin action. It is known that gonadotrophins regulate different points of spermatogenesis (McLachlan *et al.* 2002a, McLachlan *et al.* 2002b, Allan *et al.* 2001, Allan *et al.* 2004, Matthiesson *et al.* 2006), and while FSH alone is sufficient to drive spermatogenesis through to the start of spermiation in the mouse (Allan *et al.* 2001, Allan *et al.* 2004), testosterone alone is sufficient to drive qualitatively normal spermatogenesis producing fertile sperm (Singh *et al.* 1995, Handelsman *et al.* 1999). In the human, it is generally agreed that both FSH and LH/testosterone can maintain spermatogenesis independently of each other, albeit at a quantitatively reduced capacity (Matthiesson *et al.* 2006). Studies have shown that FSH has key roles in the progression of types A and B spermatogonia (McLachlan *et al.* 2002b), and provides better maintenance of pachytene spermatocytes than LH/testosterone (Matthiesson *et al.* 2006). In contrast, hCG stimulated a better conversion of

pachytene spermatocytes to round spermatids than FSH (Matthiesson *et al.* 2006). Steroid-based contraceptives result in spermiogenic failure (McLachlan *et al.* 2002b), with principle lesions at spermiation and spermatogonial progression (Matthiesson *et al.* 2006). Future male hormonal contraceptive regimens however must ensure to suppress both LH/testosterone and FSH for maximal spermatogenic suppression (Matthiesson *et al.* 2006).

One of the key findings in this thesis is that both gonadotrophins can regulate the Sertoli cell TJ, suggesting a common regulatory pathway which is involved in both the formation and maintenance of Sertoli cell TJs. In men who underwent gonadotrophin suppression, spermatogenesis was arrested at spermiation (Zhengwei *et al.* 1998, McLachlan *et al.* 2002a, McLachlan *et al.* 2002b, Matthiesson et al. 2005b). This led to the conclusion that the reduction in numbers of all of the other types of germ cells was due to a back-flow effect of significant spermiogenic failure. The results obtained in this thesis which showed a reduced claudin-11 localisation at the human Sertoli cell TJ in the presence of markedly reduced pachytene spermatocyte numbers, suggests that the reduction in germ cell numbers is a combined effect of a loss of TJ function and spermiogenic failure.

As mentioned in Chapter 7, functional testing on the Sertoli cell TJ in the gonadotrophin-suppressed man is required to show that the reduced claudin-11 localisation at the TJ is coincident with reduced TJ function. It would also be beneficial to combine this approach with a hormonal suppression regime designed to achieve greater spermatogenic suppression than the model used by Matthiesson et al (2005a). However, considering results obtained from the rat and mouse studies where i) claudin-11, as well as occludin contributed significantly to TJ function *in vitro*, ii) the localisation of both proteins was disorganised in the low levels of circulating gonadotrophins *in vivo* in association with dysfunctional TJs and suppressed spermatogenic activity, and iii) that gonadotrophin suppression in men also disrupts TJ protein localisation, then the Sertoli cell TJ appears to be another potential target of hormonal-based contraception in men.

In conclusion, the formation and maintenance of a structurally and functionally competent Sertoli cell TJ is regulated by the gonadotrophins testosterone and FSH, either separately to, or in combination with each other, *in vivo.* This is achieved through the hormonal regulation of claudin-11 and occludin relocalisation to the Sertoli cell TJ *in vivo*. It is further concluded that the Sertoli cell TJ does not need to be fully functional for spermatogenesis to proceed, as indicated by the continuing

presence of biotin tracer on the adluminal side of the Sertoli cell TJ during active spermatogenesis shortly after gonadotrophin treatment. Thus, it is also concluded that Sertoli cell TJs are size-selective and that there is a dynamic threshold required for spermatogenesis to proceed into the meiotic stages of germ cell development. It is further hypothesised that this threshold is controlled by the amount of the TJ proteins claudin-11 and occludin which are actually present at the Sertoli cell TJ, such that TJ function can be progressively upregulated to a point sufficient to support full spermatogenesis. In presenting this hypothesis, it is recognised that additional features, such as phosphorylation of occludin, or the presence of local cytokines and so on, can also regulate TJ function *in vitro* and *in vivo* (Sakakibara *et al.* 1997, Farshori and Kachar, 1999, Li *et al.* 2001, Lui *et al.* 2001, Lui *et al.* 2003a, Siu *et al.* 2003, Cheng and Mruk, 2004, Lui and Lee, 2006), which have not been investigated in this thesis.

The nature of the Sertoli cell TJ which requires it to continually ‘open’ and ‘close’ during active spermatogenesis, to allow the germ cells to cross the blood-testis barrier to proceed with spermatogenesis, sets this junction apart from other epithelial TJs. Surprisingly though, this thesis concludes that the Sertoli cell TJ also has several characteristics in common with other epithelial TJs. These features include the presence of protein pools in the Sertoli cell cytoplasm for rapid TJ formation, and a potential paracrine regulation of TJ mRNA and protein expression which could operate in conjunction with hormonal regulation. While claudin-3 appears to be important for the process of TJ assembly or disassembly in mice and hamsters to allow germ cell migration into the adluminal compartment of the seminiferous epithelium, it is concluded that its absence at the Sertoli cell TJ in rats and humans means that it is not required in these species. It may be possible that an alternative claudin or other TJ protein is localised at the Sertoli cell TJ in rats and humans with a similar role to claudin-3 in mice and hamsters. An example of another protein could be JAM-A which has been localised to spermatogonia as well as TJs (Tarulli *et al.* 2006) and may play a role in their migration across the blood-testis barrier. Alternatively, it may also be possible that such a mechanism regulated by claudin-3 in mice and hamsters, is not required in rats or humans.

Overall, it is concluded that the Sertoli cell TJ is actively regulated by gonadotrophins and is essential for spermatogenesis, with the TJ proteins claudin-11 and occludin both important in

maintaining TJ integrity in several rodent species, as well as in men. The significance of this work is that the Sertoli cell TJ has been identified as a site of action of hormonal-based contraception in men.

References

References

Agarwal R, D'Souza T, Morin PJ 2005 Claudin-3 and claudin-4 expression in ovarian epithelial cells enhances invasion and is associated with increased matrix metalloproteinase-2 activity. Cancer Research 65:7378-7385

Ahdieh M, Vandenbos T, Youakim A 2001 Lung epithelial barrier function and wound healing are decreased by IL-4 and IL-13 and enhanced by IFN-gamma. American Journal of Physiology 281:C2029-2038

Allan CM, Haywood M, Swaraj S, Spaliviero J, Koch A, Jimenez M, Poutanen M, Levallet J, Huhtaniemi I, Illingworth P, Handelsman DJ 2001 A novel transgenic model to characterize the specific effects of follicle-stimulating hormone on gonadal physiology in the absence of luteinizing hormone actions. Endocrinology 142:2213-2220

Allan CM, Garcia A, Spaliviero J, Zhang FP, Jimenez M, Huhtaniemi I, Handelsman DJ 2004 Complete Sertoli cell proliferation induced by follicle-stimulating hormone (FSH) independently of luteinizing hormone activity: evidence from genetic models of isolated FSH action. Endocrinology 145:1587-1593

Amasheh S, Meiri N, Gitter AH, Schoneberg T, Mankertz J, Schulzke JD, Fromm M 2002 Claudin-2 expression induces cation-selective channels in tight junctions of epithelial cells. Journal of Cell Science 115:4969-4976

Anderson JM, Stevenson BR, Jesaitis LA, Goodenough DA, Mooseker MS 1988 Characterization of ZO-1, a protein component of the tight junction from mouse liver and Madin-Darby canine kidney cells. The Journal of Cell Biology 106:1141-1149

Anderson RA, Wallace AM, Wu FC 1996 Comparison between testosterone enanthate-induced azoospermia and oligozoospermia in a male contraceptive study. III. Higher 5 alpha-reductase activity in oligozoospermic men administered supraphysiological doses of testosterone. The Journal of Clinical Endocrinology and Metabolism 81:902-908

Anderson RA, Kelly RW, Wu FC 1997 Comparison between testosterone enanthate-induced azoospermia and oligozoospermia in a male contraceptive study. V. Localization of higher 5 alpha-reductase activity to the reproductive tract in oligozoospermic men administered supraphysiological doses of testosterone. Journal of Andrology 18:366-371

Ando S, Panno ML, Beraldi E, Tarantino G, Salerno M, Palmero S, Prati M, Fugassa E 1990 Influence of hypothyroidism on in-vitro testicular steroidogenesis in adult rats. Experimental and Clinical Endocrinology 96:149-156

Ando-Akatsuka Y, Saitou M, Hirase T, Kishi M, Sakakibara A, Itoh M, Yonemura S, Furuse M, Tsukita S 1996 Interspecies diversity of the occludin sequence: cDNA cloning of human, mouse, dog, and rat-kangaroo homologues. The Journal of Cell Biology 133:43-47

Ando-Akatsuka Y, Yonemura S, Itoh M, Furuse M, Tsukita S 1999 Differential behavior of E-cadherin and occludin in their colocalization with ZO-1 during the establishment of epithelial cell polarity. Journal of Cellular Physiology 179:115-125

Aravindan GR, Mruk D, Lee WM, Cheng CY 1997 Identification, isolation, and characterization of a 41-kilodalton protein from rat germ cell-conditioned medium exhibiting concentration-dependent dual biological activities. Endocrinology 138:3259-3268

Arslan M, Weinbauer GF, Khan SA, Nieschlag E 1989 Testosterone and dihydrotestosterone, but not estradiol, selectively maintain pituitary and serum follicle-stimulating hormone in gonadotropin-releasing hormone antagonist treated male rats. Neuroendocrinology 49:395-401

Asher DR, Cerny AM, Weiler SR, Horner JW, Keeler ML, Neptune MA, Jones SN, Bronson RT, Depinho RA, Finberg RW 2005 Coxsackievirus and adenovirus receptor is essential for cardiomyocyte development. Genesis 42:77-85

Atkinson KJ, Rao RK 2001 Role of protein tyrosine phosphorylation in acetaldehyde-induced disruption of epithelial tight junctions. American Journal of Physiology Gastrointestinal and Liver Physiology 280:G1280-1288

Avila-Flores A, Rendon-Huerta E, Moreno J, Islas S, Betanzos A, Robles-Flores M, Gonzalez-Mariscal L 2001 Tight-junction protein zonula occludens 2 is a target of phosphorylation by protein kinase C. Biochemical Journal 360:295-304

Awoniyi CA, Santulli R, Sprando RL, Ewing LL, Zirkin BR 1989 Restoration of advanced spermatogenic cells in the experimentally regressed rat testis: quantitative relationship to testosterone concentration within the testis. Endocrinology 124:1217-1223

Awoniyi CA, Sprando RL, Santulli R, Chandrashekar V, Ewing LL, Zirkin BR 1990 Restoration of spermatogenesis by exogenously administered testosterone in rats made azoospermic by hypophysectomy or withdrawal of luteinizing hormone alone. Endocrinology 127:177-184

Awoniyi CA, Kim WK, Hurst BS, Schlaff WD 1992 Immunoneutralization of gonadotropin-releasing hormone and subsequent treatment with testosterone Silastic implants in rats: an approach toward developing a male contraceptive. Fertility and Sterility 58:403-408

Awoniyi CA, Zirkin BR, Chandrashekar V, Schlaff WD 1992 Exogenously administered testosterone maintains spermatogenesis quantitatively in adult rats actively immunized against gonadotropin-releasing hormone. Endocrinology 130:3283-3288

Awoniyi CA, Reece MS, Hurst BS, Faber KA, Chandrashekar V, Schlaff WD 1993 Maintenance of sexual function with testosterone in the gonadotropin-releasing hormone-immunized hypogonadotropic infertile male rat. Biology of reproduction 49:1170-1176

Baines H, Nwagwu MO, Furneaux EC, Stewart J, Kerr JB, Mayhew TM, Ebling FJ 2005 Estrogenic induction of spermatogenesis in the hypogonadal (hpg) mouse: role of androgens. Reproduction (Cambridge, England) 130:643-654

Balda MS, Gonzalez-Mariscal L, Contreras RG, Macias-Silva M, Torres-Marquez ME, Garcia-Sainz JA, Cereijido M 1991 Assembly and sealing of tight junctions: possible participation of G-proteins, phospholipase C, protein kinase C and calmodulin. The Journal of Membrane Biology 122:193-202

Balda MS, Anderson JM 1993 Two classes of tight junctions are revealed by ZO-1 isoforms. The American Journal of Physiology 264:C918-924

Balda MS, Whitney JA, Flores C, Gonzalez S, Cereijido M, Matter K 1996 Functional dissociation of paracellular permeability and transepithelial electrical resistance and disruption of the apical-basolateral intramembrane diffusion barrier by expression of a mutant tight junction membrane protein. The Journal of Cell Biology 134:1031-1049

Ballow D, Meistrich ML, Matzuk M, Rajkovic A 2006 Sohlh1 is essential for spermatogonial differentiation. Developmental Biology 294:161-167

Bamforth SD, Kniesel U, Wolburg H, Engelhardt B, Risau W 1999 A dominant mutant of occludin disrupts tight junction structure and function. Journal of Cell Science 112 (Pt 12):1879-1888

Ban Y, Dota A, Cooper LJ, Fullwood NJ, Nakamura T, Tsuzuki M, Mochida C, Kinoshita S 2003 Tight junction-related protein expression and distribution in human corneal epithelium. Experimental Eye Research 76:663-669

Bartlett JM, Weinbauer GF, Nieschlag E 1989 Differential effects of FSH and testosterone on the maintenance of spermatogenesis in the adult hypophysectomized rat. The Journal of Endocrinology 121:49-58

Bartlett JM, Weinbauer GF, Nieschlag E 1989 Quantitative analysis of germ cell numbers and relation to intratesticular testosterone following vitamin A-induced synchronization of spermatogenesis in the rat. The Journal of Endocrinology 123:403-412

Baulcombe D 1999 Viruses and gene silencing in plants. Archives of Virology Supplementum 15:189-201

Baulcombe DC 1999 Gene silencing: RNA makes RNA makes no protein. Current Biology 9:R599-601

Bazzoni G, Martinez-Estrada OM, Orsenigo F, Cordenonsi M, Citi S, Dejana E 2000 Interaction of junctional adhesion molecule with the tight junction components ZO-1, cingulin, and occludin. Journal of Biological Chemistry 275:20520-20526

Beardsley A, Robertson DM, O'Donnell L 2006 A complex containing alpha6beta1-integrin and phosphorylated focal adhesion kinase between Sertoli cells and elongated spermatids during spermatid release from the seminiferous epithelium. The Journal of Endocrinology 190:759-770

Beckers T, Bernd M, Kutscher B, Kuhne R, Hoffmann S, Reissmann T 2001 Structure-function studies of linear and cyclized peptide antagonists of the GnRH receptor. Biochemical and Biophysical Research Communications 289:653-663

Bergmann M 1987 Photoperiod and testicular function in Phodopus sungorus. Advances in Anatomy, embryology, and cell biology 105:1-76

Bhasin S, Fielder TJ, Swerdloff RS 1987 Testosterone selectively increases serum follicle-stimulating hormonal (FSH) but not luteinizing hormone (LH) in gonadotropin-releasing hormone antagonist-treated male rats: evidence for differential regulation of LH and FSH secretion. Biology of Reproduction 37:55-59

Bradfield PF, Scheiermann C, Nourshargh S, Ody C, Luscinskas FW, Rainger GE, Nash GB, Miljkovic-Licina M, Aurrand-Lions M, Imhof BA 2007 JAM-C regulates unidirectional monocyte transendothelial migration in inflammation. Blood 110:2545-2555

Bratt A, Birot O, Sinha I, Veitonmaki N, Aase K, Ernkvist M, Holmgren L 2005 Angiomotin regulates endothelial cell-cell junctions and cell motility. Journal of Biological Chemistry 280:34859-34869

Brehm R, Zeiler M, Ruttinger C, Herde K, Kibschull M, Winterhager E, Willecke K, Guillou F, Lecureuil C, Steger K, Konrad L, Biermann K, Failing K, Bergmann M 2007 A sertoli cell-specific knockout of connexin43 prevents initiation of spermatogenesis. The American Journal of Pathology 171:19-31

Bremner WJ, Millar MR, Sharpe RM, Saunders PT 1994 Immunohistochemical localization of androgen receptors in the rat testis: evidence for stage-dependent expression and regulation by androgens. Endocrinology 135:1227-1234

Bressler RS 1976 Dependence of Sertoli cell maturation on the pituitary gland in the mouse. The American Journal of Anatomy 147:447-455

Broqua P, Riviere PJ, Conn PM, Rivier JE, Aubert ML, Junien JL 2002 Pharmacological profile of a new, potent, and long-acting gonadotropin-releasing hormone antagonist: degarelix. The Journal of Pharmacology and Experimental Therapeutics 301:95-102

Bruewer M, Luegering A, Kucharzik T, Parkos CA, Madara JL, Hopkins AM, Nusrat A 2003 Proinflammatory cytokines disrupt epithelial barrier function by apoptosis-independent mechanisms. J Immunology 171:6164-6172

Bruewer M, Utech M, Ivanov AI, Hopkins AM, Parkos CA, Nusrat A 2005 Interferon-gamma induces internalization of epithelial tight junction proteins via a macropinocytosis-like process. The Faseb Journal 19:923-933

Byers SW, Sujarit S, Jegou B, Butz S, Hoschutzky H, Herrenknecht K, MacCalman C, Blaschuk OW 1994 Cadherins and cadherin-associated molecules in the developing and maturing rat testis. Endocrinology 134:630-639

Cambrosio Mann M, Friess AE, Stoffel MH 2003 Blood-tissue barriers in the male reproductive tract of the dog: a morphological study using lanthanum nitrate as an electron-opaque tracer. Cells, Tissues, Organs 174:162-169

Cameron DF, Muffly KE, Nazian SJ 1998 Development of Sertoli cell binding competency in the peripubertal rat. Journal of Andrology 19:573-579

Carlson SD, Juang JL, Hilgers SL, Garment MB 2000 Blood barriers of the insect. Annual Review of Entomology 45:151-174

Carson SD, Hobbs JT, Tracy SM, Chapman NM 1999 Expression of the coxsackievirus and adenovirus receptor in cultured human umbilical vein endothelial cells: regulation in response to cell density. Journal of Virology 73:7077-7079

Cattanach BM, Iddon CA, Charlton HM, Chiappa SA, Fink G 1977 Gonadotrophin-releasing hormone deficiency in a mutant mouse with hypogonadism. Nature 269:338-340

Cera MR, Del Prete A, Vecchi A, Corada M, Martin-Padura I, Motoike T, Tonetti P, Bazzoni G, Vermi W, Gentili F, Bernasconi S, Sato TN, Mantovani A, Dejana E 2004 Increased DC trafficking to lymph nodes and contact hypersensitivity in junctional adhesion molecule-A-deficient mice. The Journal of Clinical Investigation 114:729-738

Cereijido M, Anderson JM 2001 Tight Junctions. In: Tight Junctions. 2 ed. Boca Raton, Florida, USA: CRC Press

Chaika OV, Chaika N, Volle DJ, Hayashi H, Ebina Y, Wang LM, Pierce JH, Lewis RE 1999 Mutation of tyrosine 960 within the insulin receptor juxtamembrane domain impairs glucose transport but does not inhibit ligand-mediated phosphorylation of insulin receptor substrate-2 in 3T3-L1 adipocytes. Journal Biological Chemistry 274:12075-12080

Chalmel F, Rolland AD, Niederhauser-Wiederkehr C, Chung SS, Demougin P, Gattiker A, Moore J, Patard JJ, Wolgemuth DJ, Jegou B, Primig M 2007 The conserved transcriptome in human and rodent male gametogenesis. Proceedings of the National Academy of Sciences of the United States of America 104:8346-8351

Chang C, Chen YT, Yeh SD, Xu Q, Wang RS, Guillou F, Lardy H, Yeh S 2004 Infertility with defective spermatogenesis and hypotestosteronemia in male mice lacking the androgen receptor in Sertoli cells. Proceedings of the National Academy of Sciences of the United States of America 101:6876-6881

Chapin RE, Wine RN, Harris MW, Borchers CH, Haseman JK 2001 Structure and control of a cell-cell adhesion complex associated with spermiation in rat seminiferous epithelium. Journal of Andrology 22:1030-1052

Charlton HM, Halpin DM, Iddon C, Rosie R, Levy G, McDowell IF, Megson A, Morris JF, Bramwell A, Speight A, Ward BJ, Broadhead J, Davey-Smith G, Fink G 1983 The effects of daily administration of single and multiple injections of gonadotropin-releasing hormone on pituitary and gonadal function in the hypogonadal (hpg) mouse. Endocrinology 113:535-544

Chavakis T, Keiper T, Matz-Westphal R, Hersemeyer K, Sachs UJ, Nawroth PP, Preissner KT, Santoso S 2004 The junctional adhesion molecule-C promotes neutrophil transendothelial migration in vitro and in vivo. Journal of Biological Chemistry 279:55602-55608

Chen JW, Zhou B, Yu QC, Shin SJ, Jiao K, Schneider MD, Baldwin HS, Bergelson JM 2006 Cardiomyocyte-specific deletion of the coxsackievirus and adenovirus receptor results in hyperplasia of the embryonic left ventricle and abnormalities of sinuatrial valves. Circulation Research 98:923-930

Chen Y, Merzdorf C, Paul DL, Goodenough DA 1997 COOH terminus of occludin is required for tight junction barrier function in early Xenopus embryos. The Journal of Cell Biology 138:891-899

Chen Y, Lu Q, Schneeberger EE, Goodenough DA 2000 Restoration of tight junction structure and barrier function by down-regulation of the mitogen-activated protein kinase pathway in ras-transformed Madin-Darby canine kidney cells. Molecular Biology of the Cell 11:849-862

Chen Z, Evans WH, Pflugfelder SC, Li DQ 2006 Gap junction protein connexin 43 serves as a negative marker for a stem cell-containing population of human limbal epithelial cells. Stem Cells 24:1265-1273

Cheng CY, Mruk DD 2002 Cell junction dynamics in the testis: Sertoli-germ cell interactions and male contraceptive development. Physiological Reviews 82:825-874

Chiarini-Garcia H, Hornick JR, Griswold MD, Russell LD 2001 Distribution of type A spermatogonia in the mouse is not random. Biology of Reproduction 65:1179-1185

Chishti MS, Bhatti A, Tamim S, Lee K, McDonald ML, Leal SM, Ahmad W 2008 Splice-site mutations in the TRIC gene underlie autosomal recessive nonsyndromic hearing impairment in Pakistani families. Journal of Human Genetics 53:101-105

Chubb C, Desjardins C 1982 Vasculature of the mouse, rat, and rabbit testis-epididymis. The American Journal of Anatomy 165:357-372

Chung NP, Cheng CY 2001 Is cadmium chloride-induced inter-sertoli tight junction permeability barrier disruption a suitable in vitro model to study the events of junction disassembly during spermatogenesis in the rat testis? Endocrinology 142:1878-1888

Chung NP, Mruk D, Mo MY, Lee WM, Cheng CY 2001 A 22-amino acid synthetic peptide corresponding to the second extracellular loop of rat occludin perturbs the blood-testis barrier and disrupts spermatogenesis reversibly in vivo. Biology of Reproduction 65:1340-1351

Chung SS, Zhu LJ, Mo MY, Silvestrini B, Lee WM, Cheng CY 1998 Evidence for cross-talk between Sertoli and germ cells using selected cathepsins as markers. Journal of Andrology 19:686-703

Citi S 1992 Protein kinase inhibitors prevent junction dissociation induced by low extracellular calcium in MDCK epithelial cells. The Journal of Cell Biology 117:169-178

Citi S 2000 Introduction: opening up tight junctions. Seminars in Cell and Developmental Biology 11:277-279

Clark TM, Hayes TK, Beyenbach KW 1998 Dose-dependent effects of CRF-like diuretic peptide on transcellular and paracellular transport pathways. The American Journal of Physiology 274:F834-840

Clarke H, Soler AP, Mullin JM 2000 Protein kinase C activation leads to dephosphorylation of occludin and tight junction permeability increase in LLC-PK1 epithelial cell sheets. Journal of Cell Science 113 (Pt 18):3187-3196

Claude P 1978 Morphological factors influencing transepithelial permeability: a model for the resistance of the zonula occludens. The Journal of Membrane Biology 39:219-232

Clermont Y 1963 The cycle of the seminiferous epithelium in man. The American Journal of Anatomy 112:35-51

Clermont Y, Harvey SC 1965 Duration of the Cycle of the Seminiferous Epithelium of Normal, Hypophysectomized and Hypophysectomized-Hormone Treated Albino Rats. Endocrinology 76:80-89

Clermont Y, Trott M 1969 Duration of the cycle of the seminiferous epithelium in the mouse and hamster determined by means of 3H-thymidine and radioautography. Fertility and Sterility 20:805-817

Compagno D, Merle C, Morin A, Gilbert C, Mathieu JR, Bozec A, Mauduit C, Benahmed M, Cabon F 2007 SIRNA-directed in vivo silencing of androgen receptor inhibits the growth of castration-resistant prostate carcinomas. PLoS ONE 2:e1006

Connell CJ 1977 The effect of HCG on pinocytosis within the canine inter-sertoli cell tight junction. A preliminary report. The American Journal of Anatomy 148:149-153

Cooke HJ, Saunders PT 2002 Mouse models of male infertility. Nature Reviews Genetics 3:790-801

Coviello AD, Bremner WJ, Matsumoto AM, Herbst KL, Amory JK, Anawalt BD, Yan X, Brown TR, Wright WW, Zirkin BR, Jarow JP 2004 Intratesticular testosterone concentrations comparable with serum levels are not sufficient to maintain normal sperm production in men receiving a hormonal contraceptive regimen. Journal of Andrology 25:931-938

Craven SE, Bredt DS 1998 PDZ proteins organize synaptic signaling pathways. Cell 93:495-498

Cusan L, Gordeladze JO, Parvinen M, Clausen OP, Hansson V 1981 Protein carboxylmethylase and germ cell adenylyl cyclase at specific stages of the spermatogenic cycle of the rat. Biology of Reproduction 25:915-919

Cyr DG, Gregory M, Dube E, Dufresne J, Chan PT, Hermo L 2007 Orchestration of occludins, claudins, catenins and cadherins as players involved in maintenance of the blood-epididymal barrier in animals and humans. Asian Journal of Andrology 9:463-475

de Gendt K, Swinnen JV, Saunders PTK, Schoonjans, L, Dewerchin M, Devos A, Tan K, Atanassova N, Claessens F, Lecureuil C, Heyns W, Carmeliet P, Guillou F, Sharpe RM, Verhoeven G 2004 A Sertoli cell-selective knockout of the androgen receptor causes spermatogenic arrest in meiosis. Proceedings of the National Academy of Sciences of the United States of America 101:1327-1332

de Kretser DM, Burger H 1972 Ultrastructural studies of the human Sertoli cell in normal men and males with hypogonadotrophic hypogonadism before and after gonadotrophic treatment. New York, USA: Wiley-Interscience

de Kretser DM, Kerr J 1988 Cytology of the testis. In: Knobil E, Neill JD (eds) The Physiology of Reproduction. New York, USA: Raven Press Ltd

de Rooij DG, Russell LD 2000 All you wanted to know about spermatogonia but were afraid to ask. Journal of Andrology 21:776-798

Deli MA, Dehouck MP, Cecchelli R, Abraham AS, Joo F 1995 Histamine induces a selective albumin permeation through the blood-brain barrier, *in vitro*. Inflammation Research 44:S56-S57

Desai TR, Leeper NJ, Hynes KL, Gewertz BL 2002 Interleukin-6 causes endothelial barrier dysfunction via the protein kinase C pathway. Journal of Surgical Research 104:118-123

Dijkstra CD, Dopp EA, Joling P, Kraal G 1985 The heterogeneity of mononuclear phagocytes in lymphoid organs: distinct macrophage subpopulations in the rat recognized by monoclonal antibodies ED1, ED2 and ED3. Immunology 54:589-599

Dobrinski I, Ogawa T, Avarbock MR, Brinster RL 2001 Effect of the GnRH-agonist leuprolide on colonization of recipient testes by donor spermatogonial stem cells after transplantation in mice. Tissue and Cell 33:200-207

Dombrowicz D, Sente B, Closset J, Hennen G 1992 Dose-dependent effects of human prolactin on the immature hypophysectomized rat testis. Endocrinology 130:695-700

Dorner AA, Wegmann F, Butz S, Wolburg-Buchholz K, Wolburg H, Mack A, Nasdala I, August B, Westermann J, Rathjen FG, Vestweber D 2005 Coxsackievirus-adenovirus receptor (CAR) is essential for early embryonic cardiac development. Journal of Cell Science 118:3509-3521

Dorsett Y, Tuschl T 2004 siRNAs: applications in functional genomics and potential as therapeutics. Nature Reviews Drug Discovery 3:318-329

Drummond AE, Dyson M, Thean E, Groome NP, Robertson DM, Findlay JK 2000 Temporal and hormonal regulation of inhibin protein and subunit mRNA expression by post-natal and immature rat ovaries. The Journal of Endocrinology 166:339-354

Dubourdieu S, Le Nestour E, Spitz IM, Charbonnel B, Bouchard P 1993 The combination of gonadotrophin-releasing hormone (GnRH) antagonist and pulsatile GnRH normalizes luteinizing hormone secretion in polycystic ovarian disease but fails to induce follicular maturation. Human Reproduction (Oxford, England) 8:2056-2060

Dykxhoorn DM, Lieberman J 2005 The silent revolution: RNA interference as basic biology, research tool, and therapeutic. Annual Review of Medicine 56:401-423

Dym M, Fawcett DW 1970 The blood-testis barrier in the rat and the physiological compartmentation of the seminiferous epithelium. Biology of Reproduction 3:308-326

Ebling FJ, Brooks AN, Cronin AS, Ford H, Kerr JB 2000 Estrogenic induction of spermatogenesis in the hypogonadal mouse. Endocrinology 141:2861-2869

Egan EA. Nelson RM, Olver RE 1976 Lung inflation and alveolar permeability to non-electrolytes in the adult sheep *in vivo*. The Journal of Physiology 260:409-424

Elbashir SM, Harborth J, Lendeckel W, Yalcin A, Weber K, Tuschl T 2001 Duplexes of 21-nucleotide RNAs mediate RNA interference in cultured mammalian cells. Nature 411:494-498

Elbashir SM, Lendeckel W, Tuschl T 2001 RNA interference is mediated by 21- and 22-nucleotide RNAs. Genes and Development 15:188-200

Elbashir SM, Martinez J, Patkaniowska A, Lendeckel W, Tuschl T 2001 Functional anatomy of siRNAs for mediating efficient RNAi in Drosophila melanogaster embryo lysate. The EMBO Journal 20:6877-6888

Eng F, Wiebe JP, Alima LH 1994 Long-term alterations in the permeability of the blood-testis barrier following a single intratesticular injection of dilute aqueous glycerol. Journal of Andrology 15:311-317

Erb K, Pechstein B, Schueler A, Engel J, Hermann R 2000 Pituitary and gonadal endocrine effects and pharmacokinetics of the novel luteinizing hormone-releasing hormone antagonist teverelix in healthy men--a first-dose-in-humans study. Clinical Pharmacology and Therapeutics 67:660-669

Fanning AS, Jameson BJ, Jesaitis LA, Anderson JM 1998 The tight junction protein ZO-1 establishes a link between the transmembrane protein occludin and the actin cytoskeleton. Journal of Biological Chemistry 273:297

Fanning AS, Anderson JM 1999 Protein modules as organizers of membrane structure. Current Opinion in Cell Biology 11:432-439

Fanning AS, Mitic LL, Anderson JM 1999 Transmembrane proteins in the tight junction barrier. Journal of the American Society of Nephrology 10:1337-1345

Farquhar MG, Palade GE 1963 Junctional complexes in various epithelia. The Journal of Cell Biology 17:375-412

Farshori P, Kachar B 1999 Redistribution and phosphorylation of occludin during opening and resealing of tight junctions in cultured epithelial cells. The Journal of Membrane Biology 170:147-156

Fashena SJ, Thomas SM 2000 Signalling by adhesion receptors. Nature Cell Biology 2:E225-229

Fawcett DW, Leak LV, Heidger PM, Jr. 1970 Electron microscopic observations on the structural components of the blood-testis barrier. Journal of Reproduction and Fertility Supplementum 10:105-122

Fire AZ 2007 Gene silencing by double-stranded RNA. Cell Death and Differentiation 14:1998-2012

Fleming TP, McConnell J, Johnson MH, Stevenson BR 1989 Development of tight junctions de novo in the mouse early embryo: control of assembly of the tight junction-specific protein, ZO-1. The Journal of Cell Biology 108:1407-1418

Fleming TP, Sheth B, Fesenko I 2001 Cell adhesion in the preimplantation mammalian embryo and its role in trophectoderm differentiation and blastocyst morphogenesis. Frontiers in Bioscience 6:D1000-1007

Florin A, Maire M, Bozec A, Hellani A, Chater S, Bars R, Chuzel F, Benahmed M 2005 Androgens and postmeiotic germ cells regulate claudin-11 expression in rat Sertoli cells. Endocrinology 146:1532-1540

Foulds LM, Boysen RI, Crane M, Yuanzhong Y, Muir JA, Smith AI, de Kretser DM, Hearn MT, Hedger MP 2008 Molecular Identification of Lyso-Glycerophosphocholines as Endogenous Immunosuppressives in Bovine and Rat Gonadal Fluids. Biology of Reproduction 79:525-536

França LR, Ogawa T, Avarbock MR, Brinster RL, Russell LD 1998 Germ cell genotype controls cell cycle during spermatogenesis in the rat. Biology of Reproduction 59:1371-1377

Fritz W, Rath FW 1978 [Current diagnostic problems of Hirschsprung's disease]. Kinderarztliche Praxis 46:428-435

Fujita H, Sugimoto K, Inatomi S, Maeda T, Osanai M, Uchiyama Y, Yamamoto Y, Wada T, Kojima T, Yokozaki H, Yamashita T, Kato S, Sawada N, Chiba H 2008 Tight Junction Proteins Claudin-2 and -12 Are Critical for Vitamin D-dependent Ca2+ Absorption between Enterocytes. Molecular Biology of the Cell 19:1912-1921

Furuse M, Hirase T, Itoh M, Nagafuchi A, Yonemura S, Tsukita S, Tsukita S 1993 Occludin: a novel integral membrane protein localizing at tight junctions. The Journal of Cell Biology 123:1777-1788

Furuse M, Itoh M, Hirase T, Nagafuchi A, Yonemura S, Tsukita S, Tsukita S 1994 Direct association of occludin with ZO-1 and its possible involvement in the localization of occludin at tight junctions. The Journal of Cell Biology 127:1617-1626

Furuse M, Fujita K, Hiiragi T, Fujimoto K, Tsukita S 1998 Claudin-1 and -2: novel integral membrane proteins localizing at tight junctions with no sequence similarity to occludin. The Journal of Cell Biology 141:1539-1550

Furuse M, Sasaki H, Tsukita S 1999 Manner of interaction of heterogeneous claudin species within and between tight junction strands. The Journal of Cell Biology 147:891-903

Furuse M, Hata M, Furuse K, Yoshida Y, Haratake A, Sugitani Y, Noda T, Kubo A, Tsukita S 2002 Claudin-based tight junctions are crucial for the mammalian epidermal barrier: a lesson from claudin-1-deficient mice. The Journal of Cell Biology 156:1099-1111

Gadkar-Sable S, Shah C, Rosario G, Sachdeva G, Puri C 2005 Progesterone receptors: various forms and functions in reproductive tissues. Frontiers in Bioscience 10:2118-2130

Gerdprasert O, O'Bryan MK, Muir JA, Caldwell AM, Schlatt S, de Kretser DM, Hedger MP 2002 The response of testicular leukocytes to lipopolysaccharide-induced inflammation: further evidence for heterogeneity of the testicular macrophage population. Cell and Tissue Research 308:277-285

Ghassemifar MR, Sheth B, Papenbrock T, Leese HJ, Houghton FD, Fleming TP 2002 Occludin TM4(-): an isoform of the tight junction protein present in primates lacking the fourth transmembrane domain. Journal of Cell Science 115:3171-3180

Gilleron J, Nebout M, Scarabelli L, Senegas-Balas F, Palmero S, Segretain D, Pointis G 2006 A potential novel mechanism involving connexin 43 gap junction for control of sertoli cell proliferation by thyroid hormones. Journal of Cellular Physiology 209:153-161

Gliki G, Ebnet K, Aurrand-Lions M, Imhof BA, Adams RH 2004 Spermatid differentiation requires the assembly of a cell polarity complex downstream of junctional adhesion molecule-C. Nature 431:320-324

Gonzalez-Herrera IG, Prado-Lourenco L, Pileur F, Conte C, Morin A, Cabon F, Prats H, Vagner S, Bayard F, Audigier S, Prats AC 2006 Testosterone regulates FGF-2 expression during testis maturation by an IRES-dependent translational mechanism. The Faseb Journal 20:476-478

Gonzalez-Mariscal L, Chavez de Ramirez B, Cereijido M 1985 Tight junction formation in cultured epithelial cells (MDCK). The Journal of Membrane Biology 86:113-125

Gonzalez-Mariscal L, Betanzos A, Nava P, Jaramillo BE 2003 Tight junction proteins. Progress in Biophysics and Molecular Biology 81:1-44

Gonzalez-Mariscal L, Nava P 2005 Tight junctions, from tight intercellular seals to sophisticated protein complexes involved in drug delivery, pathogens interaction and cell proliferation. Advanced Drug Delivery Reviews 57:811-814

Gonzalez-Mariscal L, Tapia R, Chamorro D 2008 Crosstalk of tight junction components with signaling pathways. Biochimica et Biophysica Acta 1778:729-756

Gordon JA 1991 Use of vanadate as protein-phosphotyrosine phosphatase inhibitor. Methods in Enzymology 201:477-482

Gow A, Southwood CM, Li JS, Pariali M, Riordan GP, Brodie SE, Danias J, Bronstein JM, Kachar B, Lazzarini RA 1999 CNS myelin and sertoli cell tight junction strands are absent in Osp/claudin-11 null mice. Cell 99:649-659

Griswold M 1993 Actions of FSH on mammalian Sertoli cells. In: The Sertoli Cell. Clearwater, Florida, USA: Cache River Press

Griswold MD 1995 Interactions between germ cells and Sertoli cells in the testis. Biology of Reproduction 52:211-216

Griswold MD 1998 The central role of Sertoli cells in spermatogenesis. Seminars in cell & Developmental Biology 9:411-416

Gundersen HJ 1986 Stereology of arbitrary particles. A review of unbiased number and size estimators and the presenation of some new ones, in memory of William R. Thompson. Journal of Microscopy 143:3-45

Gye MC, Ohsako S 2003 Effects of flutamide in the rat testis on the expression of occludin, an integral member of the tight junctions. Toxicology Letters 143:217-222

Gyorffy H, Holczbauer A, Nagy P, Szabo Z, Kupcsulik P, Paska C, Papp J, Schaff Z, Kiss A 2005 Claudin expression in Barrett's esophagus and adenocarcinoma. Virchows Archiv 447:961-968

Haavisto AM, Pettersson K, Bergendahl M, Perheentupa A, Roser JF, Huhtaniemi I 1993 A supersensitive immunofluorometric assay for rat luteinizing hormone. Endocrinology 132:1687-1691

Hadley MA, Byers SW, Suarez-Quian CA, Kleinman HK, Dym M 1985 Extracellular matrix regulates Sertoli cell differentiation, testicular cord formation, and germ cell development in vitro. The Journal of Cell Biology 101:1511-1522

Handelsman DJ, Spaliviero JA, Simpson JM, Allan CM, Singh J 1999 Spermatogenesis without gonadotropins: maintenance has a lower testosterone threshold than initiation. Endocrinology 140:3938-3946

Harborth J, Elbashir SM, Bechert K, Tuschl T, Weber K 2001 Identification of essential genes in cultured mammalian cells using small interfering RNAs. Journal of Cell Science 114:4557-4565

Haywood M, Spaliviero J, Jimemez M, King NJ, Handelsman DJ, Allan CM 2003 Sertoli and germ cell development in hypogonadal (hpg) mice expressing transgenic follicle-stimulating hormone alone or in combination with testosterone. Endocrinology 144:509-517

Hedger MP 2002 Macrophages and the immune responsiveness of the testis. Journal of Reproductive Immunology 57:19-34

Hedger M, Klug J, Frohlich S, Muller R, Meinhardt A 2005 Regulatory cytokine expression and interstitial fluid formation in the normal and inflamed rat testis are under leydig cell control. Journal of Andrology 26:379-386

Hellani A, Ji J, Mauduit C, Deschildre C, Tabone E, Benahmed M 2000 Developmental and hormonal regulation of the expression of oligodendrocyte-specific protein/claudin 11 in mouse testis. Endocrinology 141:3012-3019

Herbst KL, Anawalt BD, Amory JK, Bremner WJ 2002 Acyline: the first study in humans of a potent, new gonadotropin-releasing hormone antagonist. The Journal of Clinical Endocrinology and Metabolism 87:3215-3220

Herbst KL 2003 Gonadotropin-releasing hormone antagonists. Current Opinion in Pharmacology 3:660-666

Herbst KL, Coviello AD, Page S, Amory JK, Anawalt BD, Bremner WJ 2004 A single dose of the potent gonadotropin-releasing hormone antagonist acyline suppresses gonadotropins and testosterone for 2 weeks in healthy young men. The Journal of Clinical Endocrinology and Metabolism 89:5959-5965

Hikim AP, Swerdloff RS 1995 Temporal and stage-specific effects of recombinant human follicle-stimulating hormone on the maintenance of spermatogenesis in gonadotropin-releasing hormone antagonist-treated rat. Endocrinology 136:253-261

Hild SA, Attardi BJ, Reel JR 2004 The ability of a gonadotropin-releasing hormone antagonist, acyline, to prevent irreversible infertility induced by the indenopyridine, CDB-4022, in adult male rats: the role of testosterone. Biology of Reproduction 71:348-358

Hirase T, Staddon JM, Saitou M, Ando-Akatsuka Y, Itoh M, Furuse M, Fujimoto K, Tsukita S, Rubin LL 1997 Occludin as a possible determinant of tight junction permeability in endothelial cells. Journal of Cell Science 110 (Pt 14):1603-1613

Holdcraft RW, Braun RE 2004 Androgen receptor function is required in Sertoli cells for the terminal differentiation of haploid spermatids. Development (Cambridge, England) 131:459-467

Honda T, Shimizu K, Fukuhara A, Irie K, Takai Y 2003 Regulation by nectin of the velocity of the formation of adherens junctions and tight junctions. Biochemical and Biophysical Research Communications 306:104-109

Hopkins AM, Walsh SV, Verkade P, Boquet P, Nusrat A 2003 Constitutive activation of Rho proteins by CNF-1 influences tight junction structure and epithelial barrier function. Journal of Cell Science 116:725-742

Hotchkiss RD 1948 The mode of action of chemotherapeutic agents. Annual Review of Microbiology 2 (1 vol.):183-214

Hou J, Gomes AS, Paul DL, Goodenough DA 2006 Study of claudin function by RNA interference. Journal of Biological Chemistry 281:36117-36123

Huang HF, Marshall GR, Rosenberg R, Nieschlag E 1987 Restoration of spermatogenesis by high levels of testosterone in hypophysectomized rats after long-term regression. Acta Endocrinologica 116:433-444

Hussein MR, Abou-Deif ES, Bedaiwy MA, Said TM, Mustafa MG, Nada E, Ezat A, Agarwal A 2005 Phenotypic characterization of the immune and mast cell infiltrates in the human testis shows normal and abnormal spermatogenesis. Fertility and Sterility 83:1447-1453

Hutcheon AE, Sippel KC, Zieske JD 2007 Examination of the restoration of epithelial barrier function following superficial keratectomy. Experimental Eye Research 84:32-38

Hutchin ME, Pickles RJ, Yarbrough WG 2000 Efficiency of adenovirus-mediated gene transfer to oropharyngeal epithelial cells correlates with cellular differentiation and human coxsackie and adenovirus receptor expression. Human Gene Therapy 11:2365-2375

Hutvagner G, Zamore PD 2002 A microRNA in a multiple-turnover RNAi enzyme complex. Science (New York, NY 297:2056-2060

Hutvagner G, Zamore PD 2002 RNAi: nature abhors a double-strand. Current Opinion in Genetics and Development 12:225-232

Igdoura SA, Wiebe JP 1994 Suppression of spermatogenesis by low-level glycerol treatment. Journal of Andrology 15:234-243

Ikenouchi J, Furuse M, Furuse K, Sasaki H, Tsukita S, Tsukita S 2005 Tricellulin constitutes a novel barrier at tricellular contacts of epithelial cells. The Journal of Cell Biology 171:939-945

Ishizaki T, Chiba H, Kojima T, Fujibe M, Soma T, Miyajima H, Nagasawa K, Wada I, Sawada N 2003 Cyclic AMP induces phosphorylation of claudin-5 immunoprecipitates and expression of claudin-5 gene in blood-brain-barrier endothelial cells via protein kinase A-dependent and -independent pathways. Experimental Cell Research 290:275-288

Ito M, Kodama M, Masuko M, Yamaura M, Fuse K, Uesugi Y, Hirono S, Okura Y, Kato K, Hotta Y, Honda T, Kuwano R, Aizawa Y 2000 Expression of coxsackievirus and adenovirus receptor in hearts of rats with experimental autoimmune myocarditis. Circulation Research 86:275-280

Itoh M, Furuse M, Morita K, Kubota K, Saitou M, Tsukita S 1999 Direct binding of three tight junction-associated MAGUKs, ZO-1, ZO-2, and ZO-3, with the COOH termini of claudins. The Journal of Cell Biology 147:1351-1363

Itoh M, Sasaki H, Furuse M, Ozaki H, Kita T, Tsukita S 2001 Junctional adhesion molecule (JAM) binds to PAR-3: a possible mechanism for the recruitment of PAR-3 to tight junctions. The Journal of Cell Biology 154:491-497

Ivanov AI, Nusrat A, Parkos CA 2004 The epithelium in inflammatory bowel disease: potential role of endocytosis of junctional proteins in barrier disruption. Novartis Foundation Symposium 263:115-124; Discussion 124-132, 211-118

Janecki A, Jakubowiak A, Steinberger A 1991 Regulation of transepithelial electrical resistance in two-compartment Sertoli cell cultures: in vitro model of the blood-testis barrier. Endocrinology 129:1489-1496

Javed Q, Fleming TP, Hay M, Citi S 1993 Tight junction protein cingulin is expressed by maternal and embryonic genomes during early mouse development. Development (Cambridge, England) 117:1145-1151

Jiang G, Stalewski J, Galyean R, Dykert J, Schteingart C, Broqua P, Aebi A, Aubert ML, Semple G, Robson P, Akinsanya K, Haigh R, Riviere P, Trojnar J, Junien JL, Rivier JE 2001 GnRH antagonists: a new generation of long acting analogues incorporating p-ureido-phenylalanines at positions 5 and 6. Journal of Medicinal Chemistry 44:453-467

Jimenez M, Spaliviero JA, Grootenhuis AJ, Verhagen J, Allan CM, Handelsman DJ 2005 Validation of an ultrasensitive and specific immunofluorometric assay for mouse follicle-stimulating hormone. Biology of Reproduction 72:78-85

Johnson L 1995 Efficiency of spermatogenesis. Microscopy Research and Technique 32:385-422

Johnson PH, Quay SC 2005 Advances in nasal drug delivery through tight junction technology. Expert Opinion on Drug Delivery 2:281-298

Jutte NH, Jansen R, Grootegoed JA, Rommerts FF, van der Molen HJ 1983 FSH stimulation of the production of pyruvate and lactate by rat Sertoli cells may be involved in hormonal regulation of spermatogenesis. Journal of Reproduction and Fertility 68:219-226

Kaitu'u-Lino TJ, Sluka P, Foo CFH, Stanton PG 2007 Claudin-11 expression and localisation is regulated by androgens in rat Sertoli cells *in vitro*. Reproduction (Cambridge, England) 133:1169-1179

Kale G, Naren AP, Sheth P, Rao RK 2003 Tyrosine phosphorylation of occludin attenuates its interactions with ZO-1, ZO-2, and ZO-3. Biochemical and Biophysical Research Communications 302:324-329

Kangasniemi M, Wilson G, Parchuri N, Huhtaniemi I, Meistrich ML 1995 Rapid protection of rat spermatogenic stem cells against procarbazine by treatment with a gonadotropin-releasing hormone antagonist (Nal-Glu) and an antiandrogen (flutamide). Endocrinology 136:2881-2888

Kausalya PJ, Amasheh S, Gunzel D, Wurps H, Muller D, Fromm M, Hunziker W 2006 Disease-associated mutations affect intracellular traffic and paracellular Mg2+ transport function of Claudin-16. The Journal of Clinical Investigation 116:878-891

Kawasaki H, Suyama E, Iyo M, Taira K 2003 siRNAs generated by recombinant human Dicer induce specific and significant but target site-independent gene silencing in human cells. Nucleic Acids Research 31:981-987

Kawkitinarong K, Linz-McGillem L, Birukov KG, Garcia JG 2004 Differential regulation of human lung epithelial and endothelial barrier function by thrombin. American Journal of Respiratory Cell and Molecular Biology 31:517-527

Kondo T, Suda T, Fukuyama H, Adachi M, Nagata S 1997 Essential roles of the Fas ligand in the development of hepatitis. Nature Medicine 3:409-413

Kumar NM, Gilula NB 1996 The gap junction communication channel. Cell 84:381-388

Kumar TR, Wang Y, Lu N, Matzuk MM 1997 Follicle stimulating hormone is required for ovarian follicle maturation but not male fertility. Nature Genetics 15:201-204

Lapierre LA 2000 The molecular structure of the tight junction. Advanced Drug Delivery Reviews 41:255-264

Lawrence DW, Comerford KM, Colgan SP 2002 Role of VASP in reestablishment of epithelial tight junction assembly after Ca2+ switch. American Journal of Physiology 282:C1235-C1245

Leblond CP, Clermont Y 1952 Definition of the stages of the cycle of the seminiferous epithelium in the rat. Annals of the New York Academy of Sciences 55:548-573

Leblond CP, Clermont Y 1952 Spermiogenesis of rat, mouse, hamster and guinea pig as revealed by the periodic acid-fuchsin sulfurous acid technique. The American journal of anatomy 90:167-215

Lechner F, Sahrbacher U, Suter T, Frei K, Brockhaus M, Koedel U, Fontana A 2000 Antibodies to the junctional adhesion molecule cause disruption of endothelial cells and do not prevent leukocyte influx into the meninges after viral or bacterial infection. The Journal of Infectious Diseases 182:978-982

Lee JH, Gye MC, Choi KW, Hong JY, Lee YB, Park DW, Lee SJ, Min CK 2007 In vitro differentiation of germ cells from nonobstructive azoospermic patients using three-dimensional culture in a collagen gel matrix. Fertility and Sterility 87:824-833

Li JC, Mruk D, Cheng CY 2001 The inter-Sertoli tight junction permeability barrier is regulated by the interplay of protein phosphatases and kinases: an in vitro study. Journal of Andrology 22:847-856

Li MWM, Xia W, Mruk DD, Wong CQF, Yan HHN, Siu MKY, Lui W, Lee WM, Cheng CY 2006 Tumor necrosis factor α reversibly disrupts the blood-testis barrier and impairs Sertoli-germ cell adhesion in the seminiferous epithelium of adult rat testes. Journal of Endocrinology 190:313-329

Liew SH, Meachem SJ, Hedger MP 2007 A stereological analysis of the response of spermatogenesis to an acute inflammatory episode in adult rats. Journal of Andrology 28:176-185

Liu Y, Nusrat A, Schnell FJ, Reaves TA, Walsh S, Pochet M, Parkos CA 2000 Human junction adhesion molecule regulates tight junction resealing in epithelia. Journal of Cell Science 113 (Pt 13):2363-2374

Lok D, de Rooij DG 1983 Spermatogonial multiplication in the Chinese hamster. I. Cell cycle properties and synchronization of differentiating spermatogonia. Cell and Tissue Kinetics 16:7-18

Lu L, Reinach PS, Kao WW 2001 Corneal epithelial wound healing. Experimental Biology and Medicine (Maywood, NJ 226:653-664

Lucas KA, Pitari GM, Kazerounian S, Ruiz-Stewart I, Park J, Schulz S, Chepenik KP, Waldman SA 2000 Guanylyl cyclases and signaling by cyclic GMP. Pharmacological Reviews 52:375-414

Lui WY, Lee WM, Cheng CY 2001 Transforming growth factor-beta3 perturbs the inter-Sertoli tight junction permeability barrier in vitro possibly mediated via its effects on occludin, zonula occludens-1, and claudin-11. Endocrinology 142:1865-1877

Lui WY, Lee WM, Cheng CY 2003 Transforming growth factor beta3 regulates the dynamics of Sertoli cell tight junctions via the p38 mitogen-activated protein kinase pathway. Biology of Reproduction 68:1597-1612

Lui WY, Wong CH, Mruk DD, Cheng CY 2003 TGF-beta3 regulates the blood-testis barrier dynamics via the p38 mitogen activated protein (MAP) kinase pathway: an in vivo study. Endocrinology 144:1139-1142

Lui WY, Lee WM 2006 Regulation of junction dynamics in the testis--transcriptional and post-translational regulations of cell junction proteins. Molecular and Cellular Endocrinology 250:25-35

Lustig L, Denduchis B, Ponzio R, Lauzon M, Pelletier RM 2000 Passive immunization with anti-laminin immunoglobulin G modifies the integrity of the seminiferous epithelium and induces arrest of spermatogenesis in the guinea pig. Biology of Reproduction 62:1505-1514

Lynch RD, Tkachuk-Ross LJ, McCormack JM, McCarthy KM, Rogers RA, Schneeberger EE 1995 Basolateral but not apical application of protease results in a rapid rise of transepithelial electrical resistance and formation of aberrant tight junction strands in MDCK cells. European Journal of Cell Biology 66:257-267

Lyon MF, Glenister PH, Lamoreux ML 1975 Normal spermatozoa from androgen-resistant germ cells of chimaeric mice and the role of androgen in spermatogenesis. Nature 258:620-622

Madara JL, Stafford J 1989 Interferon-gamma directly affects barrier function of cultured intestinal epithelial monolayers. The Journal of Clinical Investigation 83:724-727

Mandell KJ, Babbin BA, Nusrat A, Parkos CA 2005 Junctional adhesion molecule 1 regulates epithelial cell morphology through effects on beta1 integrins and Rap1 activity. Journal of Biological Chemistry 280:11665-11674

Mann M, Friess AE., Stoffel MH 2003 Blood-Tissue Barriers in the Male Reproductive Tract of the Dog. Cells, Tissues, Organs 174:162-169

Marh J, Tres LL, Yamazaki Y, Yanagimachi R, Kierszenbaum AL 2003 Mouse round spermatids developed in vitro from preexisting spermatocytes can produce normal offspring by nuclear injection into in vivo-developed mature oocytes. Biology of Reproduction 69:169-176

Martinez-Estrada OM, Villa A, Breviario F, Orsenigo F, Dejana E, Bazzoni G 2001 Association of junctional adhesion molecule with calcium/calmodulin-dependent serine protein kinase (CASK/LIN-2) in human epithelial caco-2 cells. Journal of Biological Chemistry 276:9291-9296

Martin-Padura I, Lostaglio S, Schneemann M, Williams L, Romano M, Fruscella P, Panzeri C, Stoppacciaro A, Ruco L, Villa A, Simmons D, Dejana E 1998 Junctional adhesion molecule, a novel member of the immunoglobulin superfamily that distributes at intercellular junctions and modulates monocyte transmigration. The Journal of Cell Biology 142:117-127

Mason AJ, Hayflick JS, Zoeller RT, Young WS, 3rd, Phillips HS, Nikolics K, Seeburg PH 1986 A deletion truncating the gonadotropin-releasing hormone gene is responsible for hypogonadism in the hpg mouse. Science (New York, NY 234:1366-1371

Mason AJ, Pitts SL, Nikolics K, Szonyi E, Wilcox JN, Seeburg PH, Stewart TA 1986 The hypogonadal mouse: reproductive functions restored by gene therapy. Science (New York, NY 234:1372-1378

Matter K, Balda M 1998 Biogenesis of tight junctions: the C-terminal domain of occludin mediates basolateral targeting. Journal of Cell Science 111:511-519

Matter K, Balda MS 2003 Functional analysis of tight junctions. Methods (San Diego, Calif 30:228-234

Matter K, Balda MS 2003 Signalling to and from tight junctions. Nature Reviews 4:225-236

Matthiesson KL, Amory JK, Berger R, Ugoni A, McLachlan RI, Bremner WJ 2005 Novel male hormonal contraceptive combinations: the hormonal and spermatogenic effects of testosterone and levonorgestrel combined with a 5alpha-reductase inhibitor or gonadotropin-releasing hormone antagonist. The Journal of Clinical Endocrinology and Metabolism 90:91-97

Matthiesson KL, Stanton PG, O'Donnell L, Meachem SJ, Amory JK, Berger R, Bremner WJ, McLachlan RI 2005 Effects of testosterone and levonorgestrel combined with a 5alpha-reductase inhibitor or gonadotropin-releasing hormone antagonist on spermatogenesis and intratesticular steroid levels in normal men. The Journal of Clinical Endocrinology and Metabolism 90:5647-5655

Matthiesson KL, McLachlan RI, O'Donnell L, Frydenberg M, Robertson DM, Stanton PG, Meachem SJ 2006 The relative roles of follicle-stimulating hormone and luteinizing hormone in maintaining spermatogonial maturation and spermiation in normal men. The Journal of Clinical Endocrinology and Metabolism 91:3962-3969

McCabe MJ 2003 Contribution of occludin and claudin-11 to tight junctions in the testis. In: Applied Biology/Biotechnology. Melbourne, Australia: Royal Melbourne Institute of Technology, University; Honours thesis, *unpublished data*

McCarrey JR, O'Brien DA, Skinner MK 1999 Construction and preliminary characterization of a series of mouse and rat testis cDNA libraries. Journal of Andrology 20:635-639

McCarthy KM, Skare IB, Stankewich MC, Furuse M, Tsukita S, Rogers RA, Lynch RD, Schneeberger EE 1996 Occludin is a functional component of the tight junction. Journal of Cell Science 109 (Pt 9):2287-2298

McLachlan RI, Wreford NG, Meachem SJ, de Kretser DM, Robertson DM 1994 Effects of testosterone on spermatogenic cell populations in the adult rat. Biology of Reproduction 51:945-955

McLachlan RI, Wreford NG, Tsonis C, de Kretser DM, Robertson DM 1994 Testosterone effects on spermatogenesis in the gonadotropin-releasing hormone-immunized rat. Biology of Reproduction 50:271-280

McLachlan RI, Wreford NG, de Kretser DM, Robertson DM 1995 The effects of recombinant follicle-stimulating hormone on the restoration of spermatogenesis in the gonadotropin-releasing hormone-immunized adult rat. Endocrinology 136:4035-4043

McLachlan RI, O'Donnell L, Meachem SJ, Stanton PG, de Kretser DM, Pratis K, Robertson DM 2002 Hormonal regulation of spermatogenesis in primates and man: insights for development of the male hormonal contraceptive. Journal of Andrology 23:149-162

McLachlan RI, O'Donnell L, Meachem SJ, Stanton PG, de Kretser DM, Pratis K, Robertson DM 2002 Identification of specific sites of hormonal regulation in spermatogenesis in rats, monkeys, and man. Recent Progress in Hormone Research 57:149-179

McLachlan RI, O'Donnell L, Stanton PG, Balourdos G, Frydenberg M, de Kretser DM, Robertson DM 2002 Effects of testosterone plus medroxyprogesterone acetate on semen quality, reproductive hormones, and germ cell populations in normal young men. The Journal of Clinical Endocrinology and Metabolism 87:546-556

Meachem SJ, McLachlan RI, de Kretser DM, Robertson DM, Wreford NG 1996 Neonatal exposure of rats to recombinant follicle stimulating hormone increases adult Sertoli and spermatogenic cell numbers. Biology of Reproduction 54:36-44

Meachem SJ, Wreford NG, Stanton PG, Robertson DM, McLachlan RI 1998 Follicle-stimulating hormone is required for the initial phase of spermatogenic restoration in adult rats following gonadotropin suppression. Journal of Andrology 19:725-735

Meachem SJ, Nieschlag E, Simoni M 2001 Inhibin B in male reproduction: pathophysiology and clinical relevance. European Journal of Endocrinology / European Federation of Endocrine Societies 145:561-571

Medina R, Rahner C, Mitic LL, Anderson JM, Van Itallie CM 2000 Occludin localization at the tight junction requires the second extracellular loop. The Journal of Membrane Biology 178:235-247

Melaine N, Ruffault A, Dejucq-Rainsford N, Jegou B 2003 Experimental inoculation of the adult rat testis with Sendai virus: effect on testicular morphology and leukocyte population. Human Reproduction (Oxford, England) 18:1574-1579

Meng J, Holdcraft RW, Shima JE, Griswold MD, Braun RE 2005 Androgens regulate the permeability of the blood-testis barrier. Proceedings of the National Academy of Sciences of the United States of America 102:16696-16700

Michl P, Buchholz M, Rolke M, Kunsch S, Lohr M, McClane B, Tsukita S, Leder G, Adler G, Gress TM 2001 Claudin-4: a new target for pancreatic cancer treatment using Clostridium perfringens enterotoxin. Gastroenterology 121:678-684

Mirza M, Petersen C, Nordqvist K, Sollerbrant K 2007 Coxsackievirus and adenovirus receptor is up-regulated in migratory germ cells during passage of the blood-testis barrier. Endocrinology 148:5459-5469

Mitic LL, Anderson JM 1998 Molecular architecture of tight junctions. Annual Review of Physiology 60:121-142

Mitic LL, Schneeberger EE, Fanning AS, Anderson JM 1999 Connexin-occludin chimeras containing the ZO-binding domain of occludin localize at MDCK tight junctions and NRK cell contacts. The Journal of Cell Biology 146:683-693

Mitic LL, Van Itallie CM, Anderson JM 2000 Molecular physiology and pathophysiology of tight junctions I. Tight junction structure and function: lessons from mutant animals and proteins. American Journal of Physiology Gastrointestinal and Liver Physiology 279:G250-254

Moldvay J, Jackel M, Paska C, Soltesz I, Schaff Z, Kiss A 2007 Distinct claudin expression profile in histologic subtypes of lung cancer. Lung Cancer (Amsterdam, Netherlands) 57:159-167

Morimoto S, Nishimura N, Terai T, Manabe S, Yamamoto Y, Shinahara W, Miyake H, Tashiro S, Shimada M, Sasaki T 2005 Rab13 mediates the continuous endocytic recycling of occludin to the cell surface. Journal of Biological Chemistry 280:2220-2228

Morita K, Furuse M, Fujimoto K, Tsukita S 1999 Claudin multigene family encoding four-transmembrane domain protein components of tight junction strands. Proceedings of the National Academy of Sciences of the United States of America 96:511-516

Moroi S, Saitou M, Fujimoto K, Sakakibara A, Furuse M, Yoshida O, Tsukita S 1998 Occludin is concentrated at tight junctions of mouse/rat but not human/guinea pig Sertoli cells in testes. The American Journal of Physiology 274:C1708-1717

Morris AP, Tawil A, Berkova Z, Wible L, Smith CW, Cunningham SA 2006 Junctional Adhesion Molecules (JAMs) are differentially expressed in fibroblasts and co-localize with ZO-1 to adherens-like junctions. Cell Communication and Adhesion 13:233-247

Morse HC, Horike N, Rowley MJ, Heller CG 1973 Testosterone concentrations in testes of normal men: effects of testosterone propionate administration. The Journal of Clinical Endocrinology and Metabolism 37:882-886

Moss SB, Burnham BL, Bellve AR 1993 The differential expression of lamin epitopes during mouse spermatogenesis. Molecular Reproduction and Development 34:164-174

Mruk DD, Cheng CY 2004 Sertoli-Sertoli and Sertoli-germ cell interactions and their significance in germ cell movement in the seminiferous epithelium during spermatogenesis. Endocrine Reviews 25:747-806

Muffly KE, Nazian SJ, Cameron DF 1993 Junction-related Sertoli cell cytoskeleton in testosterone-treated hypophysectomized rats. Biology of Reproduction 49:1122-1132

Muffly KE, Nazian SJ, Cameron DF 1994 Effects of follicle-stimulating hormone on the junction-related Sertoli cell cytoskeleton and daily sperm production in testosterone-treated hypophysectomized rats. Biology of Reproduction 51:158-166

Mulholland DJ, Dedhar S, Vogl AW 2001 Rat seminiferous epithelium contains a unique junction (Ectoplasmic specialization) with signaling properties both of cell/cell and cell/matrix junctions. Biology of Reproduction 64:396-407

Muller D, Kausalya PJ, Bockenhauer D, Thumfart J, Meij IC, Dillon MJ, van't Hoff W, Hunziker W 2006 Unusual clinical presentation and possible rescue of a novel claudin-16 mutation. The Journal of Clinical Endocrinology and Metabolism 91:3076-3079

Myers M, Ebling FJ, Nwagwu M, Boulton R, Wadhwa K, Stewart J, Kerr JB 2005 Atypical development of Sertoli cells and impairment of spermatogenesis in the hypogonadal (hpg) mouse. Journal of Anatomy 207:797-811

Nalbantoglu J, Pari G, Karpati G, Holland PC 1999 Expression of the primary coxsackie and adenovirus receptor is downregulated during skeletal muscle maturation and limits the efficacy of adenovirus-mediated gene delivery to muscle cells. Human Gene Therapy 10:1009-1019

Nichols LS, Ashfaq R, Iacobuzio-Donahue CA 2004 Claudin 4 protein expression in primary and metastatic pancreatic cancer: support for use as a therapeutic target. American Journal of Clinical Pathology 121:226-230

Nigam SK, Denisenko N, Rodriguez-Boulan E, Citi S 1991 The role of phosphorylation in development of tight junctions in cultured renal epithelial (MDCK) cells. Biochemical and Biophysical Research Communications 181:548-553

Nilsson M, Husmark J, Bjorkman U, Ericson LE 1998 Cytokines and thyroid epithelial integrity: interleukin-1alpha induces dissociation of the junctional complex and paracellular leakage in filter-cultured human thyrocytes. The Journal of Clinical Endocrinology and Metabolism 83:945-952

Nitta T, Hata M, Gotoh S, Seo Y, Sasaki H, Hashimoto N, Furuse M, Tsukita S 2003 Size-selective loosening of the blood-brain barrier in claudin-5-deficient mice. The Journal of Cell Biology 161:653-660

Nunbhakdi-Craig V, Machleidt T, Ogris E, Bellotto D, White CL, 3rd, Sontag E 2002 Protein phosphatase 2A associates with and regulates atypical PKC and the epithelial tight junction complex. The Journal of Cell Biology 158:967-978

Nusrat A, Chen JA, Foley CS, Liang TW, Tom J, Cromwell M, Quan C, Mrsny RJ 2000 The coiled-coil domain of occludin can act to organize structural and functional elements of the epithelial tight junction. Journal of Biological Chemistry 275:29816-29822

O'Bryan MK, Gerdprasert O, Nikolic-Paterson DJ, Meinhardt A, Muir JA, Foulds LM, Phillips DJ, de Kretser DM, Hedger MP 2005 Cytokine profiles in the testes of rats treated with lipopolysaccharide reveal localized suppression of inflammatory responses. American Journal of Physiology 288:R1744-1755

O'Donnell L, Stanton PG, Wreford NG, Robertson DM, McLachlan RI 1996 Inhibition of 5 alpha-reductase activity impairs the testosterone-dependent restoration of spermiogenesis in adult rats. Endocrinology 137:2703-2710

O'Donnell L, McLachlan RI, Wreford NG, de Kretser DM, Robertson DM 1996 Testosterone withdrawal promotes stage-specific detachment of round spermatids from the rat seminiferous epithelium. Biology of Reproduction 55:895-901

O'Donnell L, McLachlan RI, Wreford NG, Robertson DM 1994 Testosterone promotes the conversion of round spermatids between stages VII and VIII of the rat spermatogenic cycle. Endocrinology 135:2608-2614

O'Donnell L, Pratis K, Stanton PG, Robertson DM, McLachlan RI 1999 Testosterone-dependent restoration of spermatogenesis in adult rats is impaired by a 5alpha-reductase inhibitor. Journal of Andrology 20:109-117

Ohtsuki S, Yamaguchi H, Katsukura Y, Asashima T, Terasaki T 2007 mRNA expression levels of tight junction protein genes in mouse brain capillary endothelial cells highly purified by magnetic cell sorting. Journal of Neurochemistry

Onoda M, Suarez-Quian CA, Djakiew D, Dym M 1990 Characterization of Sertoli cells cultured in the bicameral chamber system: relationship between formation of permeability barriers and polarized secretion of transferrin. Biology of Reproduction 43:672-683

Oroi L, Perrelet A 1975 In: Freeze-Etch Histology. Heidelberg, Germany: Springer-Verlag

Orth JM 1984 The role of follicle-stimulating hormone in controlling Sertoli cell proliferation in testes of fetal rats. Endocrinology 115:1248-1255

Orth JM, Gunsalus GL, Lamperti AA 1988 Evidence from Sertoli cell-depleted rats indicates that spermatid number in adults depends on numbers of Sertoli cells produced during perinatal development. Endocrinology 122:787-794

O'Shaughnessy PJ 1980 FSH receptor autoregulation and cyclic AMP production in the immature rat testis. Biology of Reproduction 23:810-814

Pareek TK, Joshi AR, Sanyal A, Dighe RR 2007 Insights into male germ cell apoptosis due to depletion of gonadotropins caused by GnRH antagonists. Apoptosis 12:1085-1100

Parvinen M 1993 Cyclic functions of Sertoli cells. In: The Sertoli cell. Clearwater, Florida, USA: Cache River Press

Pelletier RM 1986 Cyclic formation and decay of the blood-testis barrier in the mink (Mustela vison), a seasonal breeder. The American Journal of Anatomy 175:91-117

Pelletier RM 1988 Cyclic modulation of Sertoli cell junctional complexes in a seasonal breeder: the mink (Mustela vison). The American Journal of Anatomy 183:68-102

Pelletier RM 1990 A novel perspective: the occluding zonule encircles the apex of the Sertoli cell as observed in birds. The American Journal of Anatomy 188:87-108

Pelletier RM, Byers SW 1992 The blood-testis barrier and Sertoli cell junctions: structural considerations. Microscopy Research and Technique 20:3-33

Pelletier RM 1994 Blood barriers of the epididymis and vas deferens act asynchronously with the blood barrier of the testis in the mink (Mustela vison). Microscopy Research and Technique 27:333-349

Perryman KJ, Stanton PG, Loveland KL, McLachlan RI, Robertson DM 1996 Hormonal dependency of neural cadherin in the binding of round spermatids to Sertoli cells in vitro. Endocrinology 137:3877-3883

Phillips BE, Cancel L, Tarbell JM, Antonetti DA 2008 Occludin Independently Regulates Permeability under Hydrostatic Pressure and Cell Division in Retinal Pigment Epithelial Cells. Investigative Ophthalmology and Visual Science 49:2568-2576

Pileri SA, Roncador G, Ceccarelli C, Piccioli M, Briskomatis A, Sabattini E, Ascani S, Santini D, Piccaluga PP, Leone O, Damiani S, Ercolessi C, Sandri F, Pieri F, Leoncini L, Falini B 1997 Antigen retrieval techniques in immunohistochemistry: comparison of different methods. The Journal of Pathology 183:116-123

Pointis G, Fiorini C, Defamie N, Segretain D 2005 Gap junctional communication in the male reproductive system. Biochimica et Biophysica Acta 1719:102-116

Porter KL, Shetty G, Meistrich ML 2006 Testicular edema is associated with spermatogonial arrest in irradiated rats. Endocrinology 147:1297-1305

Potter LR, Abbey-Hosch S, Dickey DM 2006 Natriuretic peptides, their receptors, and cyclic guanosine monophosphate-dependent signaling functions. Endocrine Reviews 27:47-72

Pratis K, O'Donnell L, Ooi GT, Stanton PG, McLachlan RI, Robertson DM 2003 Differential regulation of rat testicular 5alpha-reductase type 1 and 2 isoforms by testosterone and FSH. The Journal of Endocrinology 176:393-403

Rangel LB, Agarwal R, D'Souza T, Pizer ES, Alo PL, Lancaster WD, Gregoire , Schwartz DR, Cho KR, Morin PJ 2003 Tight junction proteins claudin-3 and claudin-4 are frequently overexpressed in ovarian cancer but not in ovarian cystadenomas. Clinical Cancer Research 9:2567-2575

Rannikki AS, Zhang FP, Huhtaniemi IT 1995 Ontogeny of follicle-stimulating hormone receptor gene expression in the rat testis and ovary. Molecular and Cellular Endocrinology 107:199-208

Raschperger E, Thyberg J, Pettersson S, Philipson L, Fuxe J, Pettersson RF 2006 The coxsackie- and adenovirus receptor (CAR) is an in vivo marker for epithelial tight junctions, with a potential role in regulating permeability and tissue homeostasis. Experimental Cell Research 312:1566-1580

Rea MA, Weinbauer GF, Marshall GR, Nieschlag E 1986 Testosterone stimulates pituitary and serum FSH in GnRH antagonist-suppressed rats. Acta Endocrinologica 113:487-492

Rebel VI, Hartnett S, Denham J, Chan M, Finberg R, Sieff CA 2000 Maturation and lineage-specific expression of the coxsackie and adenovirus receptor in hematopoietic cells. Stem Cells 18:176-182

Riazuddin S, Ahmed ZM, Fanning AS, Lagziel A, Kitajiri S, Ramzan K, Khan SN, Chattaraj P, Friedman PL, Anderson JM, Belyantseva IA, Forge A, Riazuddin S, Friedman TB 2006 Tricellulin is a tight-junction protein necessary for hearing. American Journal of Human Genetics 79:1040-1051

Robertson DM, Pruysers E, Stephenson T, Pettersson K, Morton S, McLachlan RI 2001 Sensitive LH and FSH assays for monitoring low serum levels in men undergoing steroidal contraception. Clinical Endocrinology 55:331-339

Rodin DA, Lalloz MR, Clayton RN 1989 Gonadotropin-releasing hormone regulates follicle-stimulating hormone beta-subunit gene expression in the male rat. Endocrinology 125:1282-1289

Roosen-Runge EC 1952 Kinetics of spermatogenesis in mammals. Annals of the New York Academy of Sciences 55:574-584

Roosen-Runge EC, Barlow FD 1953 Quantitative studies on human spermatogenesis. I. Spermatogonia. The American Journal of Anatomy 93:143-169

Ross MH 1995 Histology: a text and atlas. In: Histology: a text and atlast(Eds, Ross MH, Romrell LJ, Kaye GI). Maryland, USA: Williams and Wilkins

Ruddy SB, Hadzija BW 1992 Iontophoretic permeability of polyethylene glycols through hairless rat skin: application of hydrodynamic theory for hindered transport through liquid-filled pores. Drug Design and Discovery 8:207-224

Russell L, Clermont Y 1976 Anchoring device between Sertoli cells and late spermatids in rat seminiferous tubules. The Anatomical Record 185:259-278

Russell L 1977 Movement of spermatocytes from the basal to the adluminal compartment of the rat testis. The American Journal of Anatomy 148:313-328

Russell LD, Peterson RN 1985 Sertoli cell junctions: morphological and functional correlates. International Review of Cytology 94:177-211

Russell LD, Saxena NK, Weber JE 1987 Intratesticular injection as a method to assess the potential toxicity of various agents and to study mechanisms of normal spermatogenesis. Gamete Research 17:43-56

Russell LD, Bartke A, Goh JC 1989 Postnatal development of the Sertoli cell barrier, tubular lumen, and cytoskeleton of Sertoli and myoid cells in the rat, and their relationship to tubular fluid secretion and flow. American Journal of Anatomy 184:179-189

Russell LD, Ettlin RA, Sinha Hikim AP, Clegg ED 1990 Histological and histopathological evaluation of the testis. Clearwater, Florida, USA: Cache River Press

Ruwanpura SM, McLachlan RI, Matthiesson KL, Meachem SJ 2008 Gonadotrophins regulate germ cell survival, not proliferation, in normal adult men. Human Reproduction (Oxford, England) 23:403-411

Saez JM 1994 Leydig cells: endocrine, paracrine, and autocrine regulation. Endocrine Reviews 15:574-626

Saitou M, Fujimoto K, Doi Y, Itoh M, Fujimoto T, Furuse M, Takano H, Noda T, Tsukita S 1998 Occludin-deficient embryonic stem cells can differentiate into polarized epithelial cells bearing tight junctions. The Journal of Cell Biology 141:397-408

Saitou M, Furuse M, Sasaki H, Schulzke JD, Fromm M, Takano H, Noda T, Tsukita S 2000 Complex phenotype of mice lacking occludin, a component of tight junction strands. Molecular Biology of the Cell 11:4131-4142

Sakakibara A, Furuse M, Saitou M, Ando-Akatsuka Y, Tsukita S 1997 Possible involvement of phosphorylation of occludin in tight junction formation. The Journal of Cell Biology 137:1393-1401

Sarkar O, Mathur PP, Cheng CY, Mruk DD 2008 Interleukin 1 alpha (IL1A) is a novel regulator of the blood-testis barrier in the rat. Biology of Reproduction 78:445-454

Sasagawa I, Tateno T, Adachi Y, Kubota Y, Nakada T 1998 Round spermatids from prepubertal mouse testis can develop into normal offspring. Journal of Andrology 19:196-200

Schulte J, Tepass U, Auld VJ 2003 Gliotactin, a novel marker of tricellular junctions, is necessary for septate junction development in Drosophila. The Journal of Cell Biology 161:991-1000

Schulze W 1982 Evidence of a wave of spermatogenesis in human testis. Andrologia 14:200-207

Setchell BP 1967 The blood-testicular fluid barrier in sheep. The Journal of Physiology 189:63P-65P

Setchell BP 1970 Testicular blood supply, lymphatic drainage and secretion of fluid. In: The Testis. (Eds) Johnson AD, Gomes WR and Van Denmark NL. New York: Academic Press

Setchell BP, Laurie MS, Jarvis LG 1981 The blood testis barrier at puberty. In: Development and Formation of Reproductive Organs. AG Byskov and H. Peters, eds. Excerpta Medica International Congress Series

Setchell BP, Zupp JL, Pollanen P 1988 Blood-testis barrier at puberty. In: Development and Formation of Reproductive Organs. AG Byskov and H Peters eds. Excerpta Medica International Congress Series

Setchell B 1993 The central role of Sertoli cells in spermatogenesis. In: The Sertoli cell. Clearwater, Florida, USA: Cache River Press

Setchell BP 2004 Hormones: what the testis really sees. Reproduction, Fertility, and Development 16:535-545

Setchell BP, Tao L, Zupp JL 1996 The penetration of chromium-EDTA from blood plasma into various compartments of rat testes as an indicator of function of the blood-testis barrier after exposure of the testes to heat. Journal of Reproduction and Fertility 106:125-133

Shah C, Modi D, Sachdeva G, Gadkar S, D'Souza S, Puri C 2005 N-terminal region of progesterone receptor B isoform in human spermatozoa. International Journal of Andrology 28:360-371

Shao M, Ghosh A, Cooke VG, Naik UP, Martin-DeLeon PA 2008 JAM-A is present in mammalian spermatozoa where it is essential for normal motility. Developmental Biology 313:246-255

Sharpe RM 1994 In: Knobil E, Neill JD (eds.), The Physiology of Reproduction. New York: Raven Press

Shaw CA, Larochelle N, Dudley RW, Lochmuller H, Danialou G, Petrof BJ, Karpati G, Holland PC, Nalbantoglu J 2006 Simultaneous dystrophin and dysferlin deficiencies associated with high-level expression of the coxsackie and adenovirus receptor in transgenic mice. The American Journal of Pathology 169:2148-2160

Sheth B, Fontaine JJ, Ponza E, McCallum A, Page A, Citi S, Louvard D, Zahraoui A, Fleming TP 2000 Differentiation of the epithelial apical junctional complex during mouse preimplantation development: a role for rab13 in the early maturation of the tight junction. Mechanisms of Development 97:93-104

Sheth B, Moran B, Anderson JM, Fleming TP 2000 Post-translational control of occludin membrane assembly in mouse trophectoderm: a mechanism to regulate timing of tight junction biogenesis and blastocyst formation. Development (Cambridge, England) 127:831-840

Shetty J, Marathe GK, Dighe RR 1996 Specific immunoneutralization of FSH leads to apoptotic cell death of the pachytene spermatocytes and spermatogonial cells in the rat. Endocrinology 137:2179-2182

Shetty G, Meistrich ML 2005 Hormonal approaches to preservation and restoration of male fertility after cancer treatment. Journal of the National Cancer Institute Monographs:36-39

Shi Y 2003 Mammalian RNAi for the masses. Trends in Genetics 19:9-12

Shoji M, Chuma S, Yoshida K, Morita T, Nakatsuji N 2005 RNA interference during spermatogenesis in mice. Developmental Biology 282:524-534

Sidhu SS, Bader GD, Boone C 2003 Functional genomics of intracellular peptide recognition domains with combinatorial biology methods. Current Opinion in Chemical Biology 7:97-102

Siegel RM, Fleisher TA 1999 The role of Fas and related death receptors in autoimmune and other disease states. The Journal of Allergy and Clinical Immunology 103:729-738

Sim AT, Scott JD 1999 Targeting of PKA, PKC and protein phosphatases to cellular microdomains. Cell Calcium 26:209-217

Simon DB, Lu Y, Choate KA, Velazquez H, Al-Sabban E, Praga M, Casari G, Bettinelli A, Colussi G, Rodriguez-Soriano J, McCredie D, Milford D, Sanjad S, Lifton RP 1999 Paracellin-1, a renal tight junction protein required for paracellular Mg2+ resorption. Science (New York, NY 285:103-106

Singh J, Handelsman DJ 1996 Neonatal administration of FSH increases Sertoli cell numbers and spermatogenesis in gonadotropin-deficient (hpg) mice. The Journal of Endocrinology 151:37-48

Singh J, O'Neill C, Handelsman DJ 1995 Induction of spermatogenesis by androgens in gonadotropin-deficient (hpg) mice. Endocrinology 136:5311-5321

Siu MK, Lee WM, Cheng CY 2003 The interplay of collagen IV, tumor necrosis factor-alpha, gelatinase B (matrix metalloprotease-9), and tissue inhibitor of metalloproteases-1 in the basal lamina regulates Sertoli cell-tight junction dynamics in the rat testis. Endocrinology 144:371-387

Siu MK, Cheng CY 2004 Dynamic cross-talk between cells and the extracellular matrix in the testis. Bioessays 26:978-992

Siu MK, Wong CH, Lee WM, Cheng CY 2005 Sertoli-germ cell anchoring junction dynamics in the testis are regulated by an interplay of lipid and protein kinases. Journal of Biological Chemistry 280:25029-25047

Sluka P, O'Donnell L, Stanton PG 2002 Stage-specific expression of genes associated with rat spermatogenesis: characterization by laser-capture microdissection and real-time polymerase chain reaction. Biology of Reproduction 67:820-828

Sluka P, O'Donnell L, Bartles JR, Stanton PG 2006 FSH regulates the formation of adherens junctions and ectoplasmic specialisations between rat Sertoli cells in vitro and in vivo. The Journal of Endocrinology 189:381-395

Sofikitis N, Giotitsas N, Tsounapi P, Baltogiannis D, Giannakis D, Pardalidis N 2008 Hormonal regulation of spermatogenesis and spermiogenesis. The Journal of Steroid Biochemistry and Molecular Biology 109:323-330

Song E, Lee SK, Wang J, Ince N, Ouyang N, Min J, Chen J, Shankar P, Lieberman J 2003 RNA interference targeting Fas protects mice from fulminant hepatitis. Nature Medicine 9:347-351

Sonoda N, Furuse M, Sasaki H, Yonemura S, Katahira J, Horiguchi Y, Tsukita S 1999 Clostridium perfringens enterotoxin fragment removes specific claudins from tight junction strands: Evidence for direct involvement of claudins in tight junction barrier. The Journal of Cell Biology 147:195-204

Sridharan S, Brehm R, Bergmann M, Cooke PS 2007 Role of connexin 43 in Sertoli cells of testis. Annals of the New York Academy of Sciences 1120:131-143

Sridharan S, Simon L, Meling DD, Cyr DG, Gutstein DE, Fishman GI, Guillou F, Cooke PS 2007 Proliferation of adult sertoli cells following conditional knockout of the Gap junctional protein GJA1 (connexin 43) in mice. Biology of Reproduction 76:804-812

Sridharan S, Brehm R, Bergmann M, Cooke PS 2008 Role of Connexin 43 in Sertoli Cells of Testis. Annals of the New York Academy of Sciences 1120:131-143

Stark GR, Kerr IM, Williams BR, Silverman RH, Schreiber RD 1998 How cells respond to interferons. Annual Review of Biochemistry 67:227-264

Steinberger E, Steinberger A 1975 Spermatogenic function of the testis. In: Greep RO, Aswood EB (eds) Handbook of physiology. Maryland, USA: Waverly Press Inc

Stevenson BR, Goodenough DA 1984 Zonulae occludentes in junctional complex-enriched fractions from mouse liver: preliminary morphological and biochemical characterization. The Journal of Cell Biology 98:1209-1221

Stevenson BR, Siliciano JD, Mooseker MS, Goodenough DA 1986 Identification of ZO-1: a high molecular weight polypeptide associated with the tight junction (zonula occludens) in a variety of epithelia. The Journal of Cell Biology 103:755-766

St-Pierre N, Dufresne J, Rooney AA, Cyr DG 2003 Neonatal hypothyroidism alters the localization of gap junctional protein connexin 43 in the testis and messenger RNA levels in the epididymis of the rat. Biology of Reproduction 68:1232-1240

Straight SW, Shin K, Fogg VC, Fan S, Liu CJ, Roh M, Margolis B 2004 Loss of PALS1 expression leads to tight junction and polarity defects. Molecular Biology of the Cell 15:1981-1990

Stuurman N, Heins S, Aebi U 1998 Nuclear lamins: their structure, assembly, and interactions. Journal of Structural Biology 122:42-66

Svoboda J, Hejnar J, Geryk J, Elleder D, Vernerova Z 2000 Retroviruses in foreign species and the problem of provirus silencing. Gene 261:181-188

Tachibana K, Nakanishi H, Mandai K, Ozaki K, Ikeda W, Yamamoto Y, Nagafuchi A, Tsukita S, Takai Y 2000 Two cell adhesion molecules, nectin and cadherin, interact through their cytoplasmic domain-associated proteins. The Journal of Cell Biology 150:1161-1176

Takai Y, Nakanishi H 2003 Nectin and afadin: novel organizers of intercellular junctions. Journal of Cell Science 116:17-27

Takase M, Tsutsui K, Kawashima S 1990 Effects of PRL and FSH on LH binding and number of Leydig cells in hypophysectomized mice. Endocrinologia Japonica 37:193-203

Takase M, Tsutsui K, Kawashima S 1990 Effects of prolactin and bromocryptine on the regulation of testicular luteinizing hormone receptors in mice. The Journal of Experimental Zoology 256:200-209

Takase M, Tsutsui K 1997 Inhibitory role of prolactin in the downregulation of testicular follicle-stimulating hormone receptors in mice. The Journal of Experimental Zoology 278:234-242

Tallone T, Malin S, Samuelsson A, Wilbertz J, Miyahara M, Okamoto K, Poellinger L, Philipson L, Pettersson S 2001 A mouse model for adenovirus gene delivery. Proceedings of the National Academy of Sciences of the United States of America 98:7910-7915

Tan KA, De Gendt K, Atanassova N, Walker M, Sharpe RM, Saunders PT, Denolet E,

Verhoeven G 2005 The role of androgens in sertoli cell proliferation and functional maturation: studies in mice with total or Sertoli cell-selective ablation of the androgen receptor. Endocrinology 146:2674-2683

Tanaka M, Kamata R, Sakai R 2005 EphA2 phosphorylates the cytoplasmic tail of Claudin-4 and mediates paracellular permeability. Journal of Biological Chemistry 280:42375-42382

Tao L, Zupp JL, Setchell BP 2000 Effect of efferent duct ligation on the function of the blood-testis barrier in rats. Journal of Reproduction and Fertility 120:13-18

Tapanainen JS, Aittomaki K, Huhtaniemi IT 1997 New insights into the role of follicle-stimulating hormone in reproduction. Annals of Medicine 29:265-266

Tarulli GA, Stanton PG, Lerchl A, Meachem SJ 2006 Adult sertoli cells are not terminally differentiated in the Djungarian hamster: effect of FSH on proliferation and junction protein organization. Biology of Reproduction 74:798-806

Tarulli GA, Meachem SJ, Schlatt S, Stanton PG 2008 Regulation of testicular tight junctions by gonadotrophins in the adult Djungarian hamster *in vivo*. Biology of Reproduction. Submitted

Thomas FC, Sheth B, Eckert JJ, Bazzoni G, Dejana E, Fleming TP 2004 Contribution of JAM-1 to epithelial differentiation and tight-junction biogenesis in the mouse preimplantation embryo. Journal of Cell Science 117:5599-5608

Tokes AM, Kulka J, Paku S, Szik A, Paska C, Novak PK, Szilak L, Kiss A, Bogi K, Schaff Z 2005 Claudin-1, -3 and -4 proteins and mRNA expression in benign and malignant breast lesions: a research study. Breast Cancer Research 7:R296-305

Toyama Y, Maekawa M, Yuasa S 2003 Ectoplasmic specializations in the Sertoli cell: new vistas based on genetic defects and testicular toxicology. Anatomical science international / Japanese Association of Anatomists 78:1-16

Tso JY, Sun XH, Kao TH, Reece KS, Wu R 1985 Isolation and characterization of rat and human glyceraldehyde-3-phosphate dehydrogenase cDNAs: genomic complexity and molecular evolution of the gene. Nucleic Acids Research 13:2485-2502

Tsukamoto T, Nigam SK 1999 Role of tyrosine phosphorylation in the reassembly of occludin and other tight junction proteins. The American Journal of Physiology 276:F737-750

Tsukita S, Furuse M 1999 Occludin and claudins in tight-junction strands: leading or supporting players? Trends in Cell Biology 9:268-273

Tsukita S, Furuse M, Itoh M 2001 Multifunctional strands in tight junctions. Nature Reviews 2:285-293

Ueda J, Semba S, Chiba H, Sawada N, Seo Y, Kasuga M, Yokozaki H 2007 Heterogeneous expression of claudin-4 in human colorectal cancer: decreased claudin-4 expression at the invasive front correlates cancer invasion and metastasis. Pathobiology 74:32-41

van Itallie CM, Anderson JM 1997 Occludin confers adhesiveness when expressed in fibroblasts. Journal of Cell Science 110:1113-1121

van Itallie C, Rahner C, Anderson JM 2001 Regulated expression of claudin-4 decreases paracellular conductance through a selective decrease in sodium permeability. The Journal of Clinical Investigation 107:1319-1327

Vedula SR, Lim TS, Kausalya PJ, Hunziker W, Rajagopal G, Lim CT 2005 Biophysical approaches for studying the integrity and function of tight junctions. Molecular and Cellular Biomechanics 2:105-123

Vera Y, Erkkila K, Wang C, Nunez C, Kyttanen S, Lue Y, Dunkel L, Swerdloff RS, Sinha Hikim AP 2006 Involvement of p38 mitogen-activated protein kinase and inducible nitric oxide synthase in apoptotic signaling of murine and human male germ cells after hormone deprivation. Molecular Endocrinology (Baltimore, Md) 20:1597-1609

Vester B, Smith A, Krohne G, Benavente R 1993 Presence of a nuclear lamina in pachytene spermatocytes of the rat. Journal of Cell Science 104 (Pt 2):557-563

Vincent T, Pettersson RF, Crystal RG, Leopold PL 2004 Cytokine-mediated downregulation of coxsackievirus-adenovirus receptor in endothelial cells. Journal of Virology 78:8047-8058

Vitale R, Fawcett DW, Dym M 1973 The normal development of the blood-testis barrier and the effects of clomiphene and estrogen treatment. The Anatomical Record 176:331-344

Vogl AW 1988 Changes in the distribution of microtubules in rat Sertoli cells during spermatogenesis. The Anatomical Record 222:34-41

Vogl AW, Pfeiffer DC, Mulholland D, Kimel G, Guttman J 2000 Unique and multifunctional adhesion junctions in the testis: ectoplasmic specializations. Archives of Histology and Cytology 63:1-15

Waites GMH, Setchell BP 1969 Some physiological aspects of the function of the testis. In: The Gonads. (Ed) McKerns KW. New York, USA: Appleton-Century-Crofts

Walker WH 2003 Molecular Mechanisms Controlling Sertoli Cell Proliferation and Differentiation. Endocrinology 144:3719-3721

Wang CQ, Mruk DD, Lee WM, Cheng CY 2007 Coxsackie and adenovirus receptor (CAR) is a product of Sertoli and germ cells in rat testes which is localized at the Sertoli-Sertoli and Sertoli-germ cell interface. Experimental Cell Research 313:1373-1392

Wang J, Barr MM 2005 RNA interference in Caenorhabditis elegans. Methods in Enzymology 392:36-55

Watson CJ, Rowland M, Warhurst G 2001 Functional modeling of tight junctions in intestinal cell monolayers using polyethylene glycol oligomers. American Journal of Physiology 281:C388-397

Weinbauer GF, Galhotra MM, Nieschlag E 1985 Focal testicular destruction following intratesticular injection of glycerol in rats. International Journal of Andrology 8:365-375

Weinbauer GF, Aslam H, Krishnamurthy H, Brinkworth MH, Einspanier A, Hodges JK 2001 Quantitative analysis of spermatogenesis and apoptosis in the common marmoset (Callithrix jacchus) reveals high rates of spermatogonial turnover and high spermatogenic efficiency. Biology of Reproduction 64:120-126

Whiteland JL, Shimeld C, Nicholls SM, Easty DL, Williams NA, Hill TJ 1997 Immunohistochemical detection of cytokines in paraffin-embedded mouse tissues. Journal of Immunological Methods 210:103-108

Wiebe JP, Barr KJ, Buckingham KD, Geddes PD, Kudo PA 1986 Prospects of a male contraceptive based on selective antispermatogenic action of 1,2,3-trihydroxypropane (THP, Glycerol). In: Male Contraception: Advances and Future Prospects. Philadelphia, USA: Harper and Row

Wiebe JP, Kowalik A, Gallardi RL, Egeler O, Clubb BH 2000 Glycerol disrupts tight junction-associated actin microfilaments, occludin, and microtubules in Sertoli cells. Journal of Andrology 21:625-635

Wistuba J, Schrod A, Greve B, Hodges JK, Aslam H, Weinbauer GF, Luetjens CM 2003 Organization of seminiferous epithelium in primates: relationship to spermatogenic efficiency, phylogeny, and mating system. Biology of Reproduction 69:582-591

Wong CH, Mruk DD, Lui WY, Cheng CY 2004 Regulation of blood-testis barrier dynamics: an in vivo study. Journal of Cell Science 117:783-798

Wong CH, Xia W, Lee NP, Mruk DD, Lee WM, Cheng CY 2005 Regulation of ectoplasmic specialization dynamics in the seminiferous epithelium by focal adhesion-associated proteins in testosterone-suppressed rat testes. Endocrinology 146:1192-1204

Wong V 1997 Phosphorylation of occludin correlates with occludin localization and function at the tight junction. The American Journal of Physiology 273:C1859-1867

Wong V, Gumbiner BM 1997 A synthetic peptide corresponding to the extracellular domain of occludin perturbs the tight junction permeability barrier. The Journal of Cell Biology 136:399-409

Wreford NG 1995 Theory and practice of stereological techniques applied to the estimation of cell number and nuclear volume in the testis. Microscopy Research and Technique 32:423-436

Wrobel KH, Mademann R, Sinowatz F 1979 The lamina propria of the bovine seminiferous tubule. Cell and Tissue Research 202:357-377

Wu JC, Gregory CW, De Philip RM 1993 Expression of E-cadherin in immature rat and mouse testis and in rat Sertoli cell cultures. Biology of Reproduction 49:1353-1361

Xia W, Cheng CY 2005 TGF-beta3 regulates anchoring junction dynamics in the seminiferous epithelium of the rat testis via the Ras/ERK signaling pathway: An in vivo study. Developmental Biology 280:321-343

Xia W, Mruk DD, Lee WM, Cheng CY 2005 Cytokines and junction restructuring during spermatogenesis--a lesson to learn from the testis. Cytokine and Growth Factor Reviews 16:469-493

Xia W, Mruk DD, Cheng CY 2007 C-type natriuretic peptide regulates blood-testis barrier dynamics in adult rat testes. Proceedings of the National Academy of Sciences of the United States of America 104:3841-3846

Xu C, Zhou ZY, Guo QS, Wang YF 2004 Expression of germ cell nuclear factor in mouse germ cells and sperm during postnatal period. Asian Journal of Andrology 6:217-222

Yan HH, Cheng CY 2005 Blood-testis barrier dynamics are regulated by an engagement/disengagement mechanism between tight and adherens junctions via peripheral adaptors. Proceedings of the National Academy of Sciences of the United States of America 102:11722-11727

Yan HH, Mruk DD, Lee WM, Cheng CY 2007 Ectoplasmic specialization: a friend or a foe of spermatogenesis? Bioessays 29:36-48

Yan HH, Mruk DD, Lee WM, Cheng CY 2008 Blood-testis barrier dynamics are regulated by testosterone and cytokines via their differential effects on the kinetics of protein endocytosis and recycling in Sertoli cells. The Faseb Journal 22:1945-1959

Yap AS, Stevenson BR, Cooper V, Manley SW 1997 Protein tyrosine phosphorylation influences adhesive junction assembly and follicular organization of cultured thyroid epithelial cells. Endocrinology 138:2315-2324

Youakim A, Ahdieh M 1999 Interferon-gamma decreases barrier function in T84 cells by reducing ZO-1 levels and disrupting apical actin. The American Journal of Physiology 276:G1279-1288

Yu AS, McCarthy KM, Francis SA, McCormack JM, Lai J, Rogers RA, Lynch RD, Schneeberger EE 2005 Knockdown of occludin expression leads to diverse phenotypic alterations in epithelial cells. American Journal of Physiology 288:C1231-1241

Zeng Y, Cullen BR 2002 RNA interference in human cells is restricted to the cytoplasm. RNA (New York, NY 8:855-860

Zhang FP, Pakarainen T, Poutanen M, Toppari J, Huhtaniemi I 2003 The low gonadotropin-independent constitutive production of testicular testosterone is sufficient to maintain spermatogenesis. Proceedings of the National Academy of Sciences of the United States of America 100:13692-13697

Zhang YH, Lin L, Liu ZW, Jiang XZ, Chen BH 2008 Disruption effects of monophthalate exposures on inter-Sertoli tight junction in a two-compartment culture model. Environmental Toxicology 23:302-308

Zhengwei Y, Wreford NG, Royce P, de Kretser DM, McLachlan RI 1998 Stereological evaluation of human spermatogenesis after suppression by testosterone treatment: heterogeneous pattern of spermatogenic impairment. The Journal of Clinical Endocrinology and Metabolism 83:1284-1291

Zhou Q, Nie R, Prins GS, Saunders PT, Katzenellenbogen BS, Hess RA 2002 Localization of androgen and estrogen receptors in adult male mouse reproductive tract. Journal of Andrology 23:870-881

Zhu LJ, Zong SD, Phillips DM, Moo-Young AJ, Bardin CW 1997 Changes in the distribution of intermediate filaments in rat Sertoli cells during the seminiferous epithelium cycle and postnatal development. The Anatomical Record 248:391-405

Zirkin BR, Awoniyi C, Griswold MD, Russell LD, Sharpe R 1994 Is FSH required for adult spermatogenesis? Journal of Andrology 15:273-276

Appendices

Appendices

Appendix 1.1: Immature Sertoli cell culture

IMMATURE SERTOLI CELL CULTURE

Method for a 12 rat culture

SOLUTIONS

1. *DMEM / F12 (2 litres)* ***Make the day before***
    - For DMEM/F12/ 1% bSA work out the amount required from the DMEM/F12 stock and only make amount required then
    - **NB.** FCS is only used for the plating step. Do not use for hypotonic shock treatments

Wash a 2L measuring cylinder with MilliQ. Using this cylinder (and a mixer/flea) put 1600ml MilliQ To the MilliQ add:

1 bottle of DMEM (stored at -80°C in freezer in centrifuge room)
1 bottle F12 powder(stored at -80°C in freezer in centrifuge room)
40ml pen strep (stored at -80°C in freezer in centrifuge room)
10ml glutamate (aliquots in freezer)
20ml non-essential amino acids (NEAA:aliquots in freezer)
32ml Sodium bicarbonate (in fridge)

Adjust this solution's pH to between 7.2 - 7.4 (use 7.3) then make up with to 2L with MilliQ and use flea to mix.
Filter into 2 × 1L sterile bottles and store in fridge (lasts ≈ 1 month)

NB Medium must be replaced every 2 days (48hours)

- If the medium is more than 2 days old, add 1ml of pen strep (left over is kept in freezer door) per 50ml medium

Also must add this every day using old medium: Prior to use DMEM/F12/ 1%bSA/1%ITS **OR** DMEM/F12/ 10%FCS/1%ITS must be made up adding

- either 1% bSA (w/v) or 10% FCS
- 1:100 HEPES
- 1:50 PenStrep
- 1:100 ITS

2. *Stock DNAse (10mg/ml)*

Add 300mg DNAse to 30ml PBS, filter (0.2µm), and then aliquot into sterile eppendorph tubes (3ml) Store frozen. Aliquots can be re-used if snap frozen each time

3. *PBS / Trypsin /DNAse*

- **The day before** measure out 0.19g of trypsin (stored at -80°C in freezer in centrifuge room) into a 25ml camalac and store in freezer
- **On the day** dissolve this in 75ml PBS
- Put in orbital shaker (37°C) until dissolved
- Filter the dissolved trypsin into a sterile camalac and add 400µl of DNAse stock (when step in protocol says so)

4. *(PBS / FCS / DNAse) ×2*
    - Measure out 40ml PBS, to this filter in 4ml foetal calf serum using 0.2µm filter.
    - To this add 40µl DNAse (when protocol says to)

5. *PBS / DNAse*
   - Measure out 120ml PBS
   - To this add 240µl DNAse (DNAse should be sterile)

6. *PBS / 1% bSA / DNAse*
   - **The day before** weigh out 0.4g bSA (white tub with red lid kept in cold room) in a 25ml camalac
   - **On the day** measure out 40ml PBS
   - Dissolve the bSA in 20ml and then filter into the remaining solution
   - To this add 40µl DNAse (when protocol says to)

7. *DMEM / F12 / 1%bSA / 1% HEPES (for 600µl pellet)*
   (Isolation - Day 0)
   - See table page 7

8. *10% DMEM / F12 (enough for 63 wells + some extra)* ***FOR HYPOTONIC SHOCK***
   (no. of wells x 0.5ml)
   - Combine:
     - 5ml DMEM / F12
     - 45ml sterile MilliQ

9. *DMEM / 1% bSA / 1% HEPES –* ***FOLLOWING HYPOTONIC SHOCK- day 4***
(enough for 130 wells + some extra (total 80ml)) (no. of wells x 1.5ml)
   - For washing use 60ml of medium alone made up as on page 8

PROTOCOL

Prior to day 1:
- Book fume hood
- Rats (12) 19 – 21 day old Sprague Dawley (out bred) rats
  NB. Place order down stairs well before
- CHECK
  - There is enough mesh, coverslips, homogeniser, razorblades and a sterile bottle of MQ and also PCF filters
  - **AUTOCLAVE** homogeniser, razors and mesh (80µm) if required.
  - Take out 1 aliquot of Matrigel from freezer, and place in fridge to thaw overnight

Day 1 - Sertoli cell isolation

Prior to culture (before killing the rats)

- **Matrigel**: aliquots of neat Matrigel are stored in the fridge.
  - Everything, including plates should be kept cool on ice

- Make a 1:8 dilution of Matrigel. (*must be done prior to warming medium bottle)*

  - Add 1ml DMEM/F12 to 239µL Matrigel and label bottle. (**NB. Matrigel can only be frozen/thawed twice)**

  - Label a 24 well plate with ISCC# , name, and plate number if more then one plate

- Place coverslips in wells to be used and add 20μL Matrigel (1:8) to each well using a pipette. Spread well using a sterile 1ml syringe plunger **(NB. If coating a bicameral chamber, wet membrane by adding 2-3 drops of medium into the well and then putting chamber in. Add 50μL Matrigel and ensure entire surface of membrane is covered, dab gently and then remove excess medium using pipette as above.)**
- By tilting plate slightly in ice box, use a pipette to remove excess Matrigel and transfer back into vial for reuse. **Don't** snap freeze, but place back into freezer.
- Place in 37°C incubator and allow at least 1 hour to set.

Testis removal, decapsulation and trypsin digestion

- Measure out trypsin (0.19g) and bSA (0.4g) into 25ml camalacs. **Can be weighed the day before (weigh on day if after weekend) and put in freezer/fridge. NB. They are not sterile.**
- Turn on the 37°C water bat and warm DMEM/F12, PBS, FCS and PenStrep.

1. Need three 50ml camalacs, and two 100ml camalacs. Label, and measure out required PBS (see solutions page)
   - Trypsin - 75ml PBS
   - FCS - 40ml PBS (X2)
   - DNAse (add just before use) - 120ml PBS
   - bSA - 40ml PBS -

2. For dry materials, approximately 20ml PBS can be added to camalacs to allow material to dissolve (37°C orbital shaker), and the rest of the required volume put in the sterile camalac. **(NB. This 20ml is not sterile and must be filtered into the remaining PBS. Trypsin should be added to entire 75ml to prevent clumping and then filtered later)** Remember to keep warm (air 37°C)

   Take DNAse from freezer and allow to thaw on bench

   In the laminar flow set up:
   - Petri dish (1 dish/12 animals and 1 waste dish)
   - Sterile blade
   - Milk dilution bottle and parafilm (1 bottle / 12 animals)

3. Take dissection tools, 70% ethanol and a 60ml camalac of warm DMEM/F12 to the animal house. Kill rats using CO_2 and collect testes (Squirt ethanol on groin area of rats and on tools. Lift penis and make an incision using scissors. Locate and gently remove each testis and place in camalac containing DMEM)

4. Place a small amount of warm DMEM/F12 into shallow half (lid) of waste petri dish and decapsulate testes using curved forceps and tweezers. Do so by holding testis with tweezers and gently piercing capsule with forceps. Proceed to push tubules from the tunica ensuring **all** tubules are removed. Place waste into other half of petri dish.

5. Using medium in the dish, was off any blood from the testis, and then remove any excess (medium).

6. Transfer testis to a clean petri dish and using a sterile razor blade held at 45° angle (90° will moosh them) chop longitudinally and then horizontally into 1mm blocks. DO NOT OVER CHOP!

7. **Add DNAse (400μl) to the trypsin**

8. Add 10ml of ***PBS / Trypsin / DNAse*** to the petri dish using the automated pipette and aspirate up and down until the solution is uniform (approximately 4 ×). *Try not to aspirate air or it will go clumpy. If there are large clumps mash with pipette until it can be sucked up.*

Place the tissue in a sterile round milk bottle and wash the remaining tissue from the petri dish with the rest of the ***PBS / Trypsin / DNAse.***

9. Place horizontally in the 37°C orbital shaker (round bottle @ 120rpm) and bath for 25 minutes. Hypochloride the waste testes tissue. **N.B The trypsin is used to strip all the peritubular cells off the interstitial tissue**

Tubule purification and preparation of single-cell suspension

10. **Add DNAse (40µl) to FCS (×1)**

11. Add 40ml ***PBS / FCS / DNAse*** to milk bottle. Mix up and down and allow to settle - collect waste bottle

12. Aspirate supernatant. Put in other 40ml ***PBS / FCS / DNAse*** (add DNAse)

13. Swirl bottle vigorously and allow to settle for 5 minutes

14. **Add DNAse (240µl) to PBS**

15. Remove most of the supernatant.

16. Replace removed supernatant with ≈ 40ml ***PBS / DNAse*** (roughly divide bottle into 40ml sections using pen). Swirl bottle vigorously and allow to settle (If tilting bottle, tape down and gently tap tubules down)

17. Repeat step 16

18. Repeat step 16

19. **Add DNAse (40µl) to bSA**

20. Remove the supernatant and add the ***PBS / 0.25% bSA / DNAse*** NOTE, If the solution is gluggy at this point add some more DNAse (1µl per ml of suspension)
21. Place some of the suspension into a sterile teflon/glass tissue homogeniser and **SLOWLY** depress pistle eight times. AVOID getting bubbles on the surface. Pour into sterile 50ml Falcon tubes (will need 2), and repeat with the rest of the suspension

22. Centrifuge at 1000rpm for 5 minutes
    Set up in the flow hood:
    - ISC mesh,
    - *PBS*
    - *DMEM / F12*
    - Haematocytometer and Trypan Blue

CELL WASHING

23. Remove supernatant and resuspend pellet by flicking the side of the tube. Resuspend in PBS (i.e. combine pellets and wash tubes to total around ≈ 10ml PBS) NOTE: If the cells don't spin down, i.e it is really gluggy, add some more DNAse and dilute out further with PBS. Usually will add ~60-100ul DNAse at this stage before filtering.

24. Filter the suspension through the sterile nylon mesh (80µm) into a 15ml centrifuge tube and centrifuge at 1000rpm for 5 minutes

PELLET VOLUME:

25. Wash the pellet twice (by removing the supernatant and filling the tube with PBS, then centrifuge as above) PELLET VOLUME:

26. After the spin take note of the volume of the pellet (≈800-1200) and make up enough plating medium, ***DMEM / F12 / 1%bSA / 1% ITS / 1% HEPES*** for the pellet - 20ml per 100µl of pellet

FINAL PELLET VOLUME

27. Sterilise area with ethanol

CELL COUNTS

28. Make the cell suspension up to 10ml with ***DMEM / F12 / 1% / 1% ITS / 1% HEPES***. Add 20µl of the suspension to 20µl of trypan blue (i.e 1:2 dilution)

29. Fill both sides of haematocytometer. Count stained (dead) and unstained (alive) cells in the 4 outer squares and middle square for both chambers, ignoring large cells, small cells, and clumps of cells. Count top and left line of each square. (expected cell no ≈ 50-70 million cells / 100µl pellet)

30. Calculate volume of cells to remove from the 10ml and amount of medium to add to dilute to total required volume

Haemocytometer

Count 5 squares in both chambers

Preparation of cells in medium for plating

1. Once cells have been counted, calculate the % viability, ie the total number of cells isolated, and the cell concentration (cells/ml)
2. Knowing the cell concentration and wanted concentration to be added to each well, calculate the required dilution
3. Prepare cell dilution and add cells to plates in a RANDOM ORDER but plate the last plate last.

    - For a 24 well plate, add 0.5ml of cells (2.5×10^6 cells/ml or 1.25×10^6 cells/cm^2)
    - Add 300µl for a 16 well chamberslide (0.75×10^6 cells/cm^2)
    - For 12mm bicameral chambers, add 600µl of cells (NB must also add 600µl medium w/o cells to outside of bicameral chamber)

NB. Keep the suspension uniform by aspiring the suspension with pipette for every 6 wells plated

4. Incubate cells at 37°C / 5%CO_2 in incubator for 2 days (until day 3)

Viable	Viable	Unviable	Unviable

CALCULATING % VIABILITY

% viability = Total # cells unstained
Total # cells

To CALCULATE THE No. OF CELLS IN 10ml:
No. of cells in 10ml (millions) = Average no. counted

Average # total cells × 50 000 × dilution × volume
Eg 308 × 50 000 × 2 × 10 = 308 million / 10ml

So if we want : 2.5 million /ml
And we have: 30.8 million /ml

We need to make a 1: 12.32 dilution
So that is 1ml of solution which has our 30.8 million cells + 12.32ml
Or 10ml + 123.2ml

Day 2/3

(Usually missed over the weekend)
If the colour of the medium changes then replace it with 500µl of fresh medium
NB Medium should be changed every 2 days

DAY 4 - Hypotonic shock

The use of a low salt medium to alter the osmolarity of the cells and attempt to kill off the germ cells. Used to obtain greater then 95% purity in SCC

ON ARRIVAL

- Warm DMEM / F12 in water bath
- Thaw PenStrep
- Prepare the following solutions-
  - 10% DMEM / F12 (total volume of wells / 2). 10% DMEM / F12 in sterile MQ water
  - DMEM / F12 + bSA + HEPES + PenStrep (total volume of wells × 1.5)

    Dissolve 1% bSA in about 50ml DMEM / F12 (sit on top)
    Filter dissolved bSA directly into remaining DMEM / F12
    To DMEM / F12 add
    - 1% bSA (pre dissolved)
    - 1:100 HEPES
    - 1:50 PenStrep

1. Add PenStrep to ***DMEM / F12 / 1% bSA / 1% HEPES / 1% ITS***
2. Add sterile water to ***DMEM / F12***
3. Check for contamination - cloudy medium or string fungus
4. Prepare suction apparatus (side tube-vacuum, top tube-pasteur pipette without cotton bud)
5. Put culture plate on foam-warmer than hood bench, with plate to tilt it
6. Set timer, remove medium from wells and replace it with 500µl ***10% DMEM / F12*** for 45sec (500µl for 24 well plate, 150µl for 16 well chamber slides)
7. Remove ***10% DMEM / F12*** in wells and replace with 500µl ***DMEM / F12 / 1% bSA / 1% ITS / 1% HEPES***
8. Remove ***DMEM / F12 / 1% bSA / 1% ITS / 1% HEPES*** in wells and replace it with 1ml ***DMEM / F12 / 1% bSA / 1% ITS / 1% HEPES*** (1ml for 24 well plate, 300µl for 16 well chamber slides)
9. Put back into incubator (37°C/ 5% CO_2)
10. 10. Rinse suction tube with EtOH and bottle with hypochloride

Appendix 1.2: siRNA protocol

siRNA preparation and calculations

STOCKS

SiRNA	Amount	Nmol	MW
Claudin-11-A	295.89µg	20	14794.54
Claudin-11-B	297.61µg	20	14880.26
Lamin A/C	74.40µg	5	14880.00

BUFFERS

Solution	Amount	Purpose
RNAiFect	1 x 1.0ml	Transfection of siRNA into cells
Suspension Buffer	1 x 0.5ml	Dissolve siRNA for first time use
Buffer ECR	2 x 15.0ml	To replace medium if transfection is poor

Aim: 1) To observe the ability of the Sertoli cells from ISCC#8 to take up siRNA (fluorescence)
2) To determine if the siRNA is toxic to the Sertoli cells (Lamin A/C)
3) To determine which of the claudin-11 siRNA fragments is most effective at silencing claudin-11
and at which optimal siRNA dilution/amount

Method

Upon receipt of siRNA strands

1) To Claudin-11-A and Claudin-11-B siRNA fragments, add 1ml of the sterile suspension buffer provided
(have 20nmol of both fragments)
2) To the Lamin A/C siRNA fragments, add 250µl of the same sterile buffer (have 5nmol of both fragments)
NB: This gives a final concentration of 20µM for each of the four siRNA fragments
3) Heat tubes for 1min at 90°C
4) Incubate tubes for 60mins at 37°C
5) Either begin experiment or freeze solutions
NB: Steps 1-5 only need to be conducted on the first occasion of using the siRNA. The solutions can be freezed and thawed repeatedly
ISCC#8 aims to determine the appropriate dilution of siRNA to use for future cultures. The following table has been constructed to show what siRNA to transfection reagent ratios will be used, when adding a final volume of 400µl to each well
NB: All weight measurements in the table below, refers to the siRNA

siRNA	1:3 (1.0µg)	1:6 (0.5µg)	1:6 (1.0µg)	1:6 (1.5µg)	1:9 (1.0µg)
Lamin A/C	-	-	+	-	-
Claudin-11-A	+	+	+	+	+
Claudin-11-B	+	+	+	+	+

However, TER wells receive a total of 1,200µl per well so the amount of siRNA is trebled, as is the amount of transfection reagent it is diluted in.

Lamin A/C

74.40µg has been dissolved in 250µl. Want 1µg of Lamin A/C siRNA, at a 1:6 ratio
250/74.4 = 3.36. This is for final volume of 400µl, but ISCC#8 has final volume of 1,200µl.
So, 3.36 x 3 = 10.08µl
This is enough for one well. Have triplicate wells, so in total, will take 30.24µl of the 250µl stock solution
For a final volume of 400µl, would make up the 3.36µl of siRNA to 100µl, so would add 96.64µl. However,
since the final volume is 1,200µl and this is in triplicate, we want 9(96.64)µl medium to dilute the siRNA
= 869.76µl of medium
To achieve the 1:6 ratio for a 400µl final volume, would add 6µl transfection reagent, but in this case would need to add 54µl for the reasons described above.

1) Remove 30.24µl of siRNA dissolved in suspension buffer, and add 869.76µl of prepared medium
2) Mix by vortexing. Add 54µl of transfection reagent to the solution and mix by pipetting up and down 5 times, or by vortexing for 10s
3) Incubate solution for 10-15mins at room temperature to allow transfection complexes to form
4) While this incubation is underway, remove all media from the wells, inside and out, and replace with 450µl of freshly prepared medium to the inside and outside of the well
5) Add the 150µl of transfection complexes dropwise to the inside and outside of each well.
6) Swirl plate to evenly distribute the transfection complexes
7) Incubate cells under normal growth conditions, taking TER analysis over 3 days before fixing cells

NB: If cytotoxicity is evident, change the medium 6-24 hours after transfection. Would change medium as per normal over days anyway

Claudin-11-A

295.89µg of siRNA has been dissolved in 1ml of suspension buffer. Want 1µg of siRNA is using a final
volume of 400µl, but we're using 1,200µl so we want 3µg
For 1µg: would need 3.38µl suspension. So for 3µg, would need 10.139µl of suspension. Since each well
is done in triplicate, need a final volume of 30.417µl from the 1ml stock.
This is to be diluted to 900µl final, by adding 869.583µl of freshly prepared medium
For the 1:3, 1:6 (1µg siRNA/400µl) and 1:9 ratios, add 27µl, 54µl and 81µl of the transfection reagents, to
the respective solution
Mix as normal, and follow protocol as per Lamin A/C, steps 3-7

<u>1:6 siRNA:Transfection reagent ratios, with 0.5µg/400µl and 1.5µg/400µl</u>

<u>0.5µg/400µl</u>
Need 30.417µl for 3µg/1.2ml across 3 wells. So for 1.5µg/1.2ml, would need 15.209µl of stock
Add this to 884.791µl of freshly prepared medium and to this solution, add 27µl transfection
reagent

<u>1.5µg/400µl</u>
Need 30.417µl for 3µg/1.2 and 15.209µl for 1.5µ/1.2. So for 4.5µg/1.2ml, need:
30.417µl + 15.209µl = 45.626µl of stock
Add this to 854.374µl of freshly prepared medium and to this solution, add 81µl of transfection
reagent

Mix solutions as per normal, and follow Lamin A/C protocol steps 3-7

Claudin-11-B (following same calculation rationale as those used for Claudin-11-A siRNA)

Have 297.61µl siRNA dissolved in 1ml of buffer.
For the 1:3, 1:6 (1µg/400µl), 1:9 ratios, add 30.241µl of stock, to 869.759µl of freshly prepared medium
For the respective ratios mentioned above, add 27µl, 54µl and 81µl

1:6 siRNA:Transfection reagent ratios, with 0.5µg/400µl and 1.5µg/400µl

0.5µg/400µl — Add 15.121µl of stock to 884.879µl of freshly prepared medium. To this add 27µl of transfection reagent and mix as per normal

1.5µg/400µl — Add 45.362µl of stock to 854.638µl of freshly prepared medium. To this add 81µl of transfection reagent and mix as per normal

Follow Lamin A/C protocol steps 3-7

Since the claudin-11-A and claudin-11-B siRNA will be added to cells which have been treated with ethanol
or testosterone, each in triplicate, the final volumes for each calculation in regards to claudin-11-A and
claudin-11-B need to be doubled. The following table presents the volume of each component of the experiment and how much will be used in total

Sample	**Amount susp. buff**	**Amount Available**	**Amount required**	**Amount remaining**	**Amount medium**	**Amount RNAiFect**	**Amount remaining**
Lamin A/C siRNA	250µl	250µl	30.24µl	219.76µl	869.76µl	54µl	1.446ml
Claudin-11-A siRNA	1ml	1ml	182.504µl	817.496µl	5,217.376µl	540µl	0.744ml
Claudin-11-B siRNA	1ml	1ml	181.448µl	818.552µl	5,218.552µl	540µl	0.204ml
Suspension Buffer	-	18ml	485µl	17.515ml	-	-	-
Transfection Reagent	-	1.5ml	1.296ml	204µl	-	-	-

Results

Conclusion

Appendix 1.3: Serum hormone assays

***Data also presented on CD inside back cover**

a. LH

Mark McCabe PhD Study - ep4-07

Treatment	Id	LH pg/100ul	rLH ng/ml	Treatment	id	LH pg/100ul	rLH ng/ml
Control	19 black	180.8	1.81	**Acyline +**	11 black	12	0.012*
	19 blue	179.2	1.79	**hCG**	*11 blue*	*73.2*	0.732
	19 none	na	Na		11 none	na	Na
	20 black	287.2	2.87		12 black	na	Na
	20 blue	528	5.28		12 blue	27.4	0.274
	20 none	106.8	1.07		12 none	na	Na
	21 black	151.2	1.51		13 black	na	Na
	21 blue	na	Na		13 blue	na	Na
	21 none	227.2	2.27		13 none	19.28	0.1928
	22 none	na	Na		18 black	21.8	0.218
Average		**237.2**	**2.37**	**Average**		**30.7**	**0.354**
St Dev		**140.3**	**1.40**	**St Dev**		**24.374**	**0.254**

Acyline	4 black	37.88	0.038	**Acyline +**	8 black	na	Na
	4 blue	12	0.012*	**hCG + FSH Ab**	8 blue	12	0.012*
	4 none	16.64	0.017		8 none	15.2	0.0152
	5 black	46	0.046		9 black	24.8	0.0248
	5 blue	36.72	0.037		9 blue	12	0.012*
	5 none	26	0.026		9 none	12	0.012*
	6 black	75.6	0.076		10 black	12	0.012*
	6 blue	na	Na		10 blue	na	Na
	6 none	53.6	0.054		10 none	na	Na
	7 none	na	Na		14 none	na	Na
Average		**38.1**	**0.381**	**Average**		**14.7**	**0.020**
St Dev		**20.7**	**0.207**	**St Dev**		**5.1**	**0.007**

Acyline +	1 black	na	Na	**Glycerol**	23	572	0.572

					black		
FSH Ab	1 blue	na	Na		23 blue	480	0.480
	1 none	na	Na		23 none	na	Na
	2 black	12	0.012*		24 black	318.4	0.318
	2 blue	12	0.012*		24 blue	532	0.532
	2 none	na	Na		24 none	na	Na
	3 black	12	0.012*		25 black	275.6	0.276
	3 blue	na	Na		25 blue	244.8	0.245
	3 none	12	0.012*		25 none	524	0.524
	7 black	14	0.140		26 none	239.6	0.240
Average		**12.4**	**0.124**	**Average**		**398.3**	**3.98**
St Dev		**0.9**	**0.009**	**St Dev**		**141.8**	**1.42**

Acyline +	15 black	40.4	0.404	**Glycerol**	27 none	186.8	0.1868
FSH	15 blue	20.4	0.204	**Control**	28 black	248.4	0.2484
	15 none	na	Na		28 blue	140.8	0.1408
	16 black	na	Na		28 none	222.4	0.2224
	16 blue	16.4	0.164		29 black	168.4	0.1684
	16 none	na	Na		29 blue	144.8	0.1448
	17 black	61.2	0.612		29 none	180.8	0.1808
	17 blue	na	Na		30 black	na	Na
	17 none	*42.8*	0.428		30 blue	110.4	0.1104
	18 none	12	0.012*		30none	381.2	0.3812
Average		**32.2**	**0.322**	**Average**		**198.2**	**1.982**
St Dev		**19.1**	**0.191**	**St Dev**		**80.4**	**0.804**

Rat LH IFMA QC data

Assay no	**rLH ng/ml**
ep4-07pl 1	2.256
ep4-07pl 1	2.0
ep4-07pl 2	1.752
ep4-07pl 2	1.8
Average	**1.976**
Stdev	**0.2**
CV	**11.3**

* assay sensitivity = 0.012ng/ml (ie below sensitivity)

b. Androgens

	Acyline + FSH Ab	Acyline	Acyline + hCG + FSH Ab	Acyline + hCG + C Ab	FSH	Control	Glycerol	Glycerol Control
	0.523	0.545		0.742	0.277	2.303	4.479	
	0.545	0.274	0.883	0.682	0.255	1.758	5.892	10.63
	0.281	0.227	0.247	0.85	0.323	1.12	3.505	7.34
	0.264	0.191	0.765	0.551	0.322	1.2	3.632	2.104
	0.2	0.368	0.66	0.93	0.277	1.677	2.253	7.605
	0.188	0.276	1.71	1.082		1.233	4.383	5.652
	0.272	0.265	0.74	0.795	0.271	2.194	5.345	6.307
	0.197	0.255	0.759	0.388	0.279	4.734	2.905	5.627
	0.566	0.223	0.526	0.31	0.29	4.064	7.953	3.795
	0.241	0.21	0.769	0.356	0.507	1.946	6.889	7.106
Avg	**0.328**	**0.283**	**0.784**	**0.669**	**0.311**	**2.223**	**4.724**	**6.241**
SD	**0.153**	**0.104**	**0.394**	**0.261**	**0.077**	**1.226**	**1.799**	**2.421**

c. FSH

Mark McCabe PhD Study - Rat FSH IFMA results ep2-07 and 3-07 Apr-07

Treatment	id	rFSH pg/100ul	rFSH ng/ml
Control	19 black	464	4.64
	19 blue	673	6.73
	19 none	na	na
	20 black	677	6.77
	20 blue	523	5.23
	20 none	413	4.13
	21 black	529	5.29
	21 blue	na	na
	21 none	604	6.04
	22 none	na	na
Average		**554.71**	**5.547**
St Dev		**101.12**	**1.011**
Acyline	4 black	67.1	0.671
	4 blue	40	0.4
	4 none	34	0.34
	5 black	55.3	0.553
	5 blue	86.9	0.869
	5 none	92.2	0.922
	6 black	86.6	0.866

Treatment	id	rFSH pg/100ul	rFSH ng/ml
Acyline + hCG	11 black	169	1.69
	11 blue	166	1.66
	11 none	Na	Na
	12 black	Na	Na
	12 blue	138	1.38
	12 none	Na	Na
	13 black	na	Na
	13 blue	105	1.05
	13 none	130	1.3
	18 black	109	1.09
Average		**136.2**	**1.362**
St Dev		**27.3**	**0.27**
Acyline + hCG + FSH Ab	8 black	na	Na
	8 blue	15	0.015 *
	8 none	15	0.015 *
	9 black	21.3	0.213
	9 blue	15	0.015 *
	9 none	15	0.015 *
	10 black	15	0.015 *

	6 blue	na	na
	6 none	80.2	0.802
	7 none	na	na
Average		**67.8**	**0.678**
St Dev		**22.5**	**0.225**

	10 blue	na	Na
	10 none	na	Na
	14 none	na	Na
Average		**16.1**	**0.161**
St Dev		**2.6**	**0.0**

Acyline +	1 black	15	0.015*
FSH Ab	1 blue	na	na
	1 none	na	na
	2 black	15	0.015*
	2 blue	15	0.015*
	2 none	na	na
	3 black	19.2	0.192
	3 blue	15	0.015*
	3 none	na	na
	7 black	452	4.52
Average		**88.5**	**0.890**
St Dev		**178.1**	**0.178**

Glycerol	23 black	1013	10.13
	23 blue	1176	11.76
	23 none	na	Na
	24 black	499	4.99
	24 blue	1232	12.32
	24 none	na	Na
	25 black	978	9.78
	25 blue	621	6.21
	25 none	764	7.64
	26 none	708	7.08
Average		**873.9**	**8.739**
St Dev		**265.6**	**2.656**

Acyline +	15 black	32.9	0.329
FSH	15 blue	37.3	0.373
	15 none	na	na
	16 black	na	na
	16 blue	68.5	0.685
	16 none	na	na
	17 black	23.2	0.232
	17 blue	na	na
	17 none	34.1	0.341
	18 none	45.4	0.454
Average		**40.2**	**0.402**
St Dev		**15.6**	**0.156**

Glycerol	27 none	675	6.75
Control	28 black	612	6.12
	28 blue	422	4.22
	28 none	545	5.45
	29 black	419	4.19
	29 blue	420	4.2
	29 none	395	3.95
	30 black	na	Na
	30 blue	380	3.8
	30none	916	9.16
Average		**531.6**	**5.316**
St Dev		**178.1**	**1.781**

QC data

Assay no	**QC**
Ep2-07	676
	574
	729
Ep3-07	632
	630
	634
Average	**646**
St Dev	**52.1**
CV	**8.07**

* assay sensitivity = 0.015ng/ml (ie below sensitivity)

Appendix 1.4: Data for the stereological assessment of germ cell types and numbers

* Data also presented on CD inside back cover

Mark McCabe. PhD Study 2. GnRH-antagonist treated rat study. Stereology germ cell counts (Georgia Balourdos and Sarah Meachem)

TW vol is testis weight converted into volume (µl) by multiplying by 10E12. Number of cells is the total number of cells of a specific type counted in each of the three sections from the same testis. Cells are counted in a volume of 10µm3 and number of fields reflects that as does the frame area. Nuclear volume is the number of nuclei (or cells) counted in the given section. This calculated by dividing the number of cells by the frame

Note: The testis weights refer to the left testis of the applicable animal (see number in tables) which was prepared for stereology

CONTROLS

Cell type	Type A+intermediate spermatogonia				
Group	Control	Control	Control	Control	Control
rat no.	20 None	21 Black	21 Blue	21 None	22 None
TW(vol)	1.86E+12	1.818E+12	1.678E+12	1.784E+12	1.666E+12
no.cells	122	101	116	130	108
no.fields	463	463	463	463	463
Frame um2	3228.9	3228.9	3228.9	3228.9	3228.9
Nv	8.16064E-06	6.75594E-06	7.75930E-06	8.69576E-06	7.22417E-06
Cells/TW	1.51788E+07	1.22823E+07	1.30201E+07	1.55132E+07	1.20355E+07

Cell type	Type B+preleptotene spermatocytes				
Group	Control	Control	Control	Control	Control
rat no.	20 None	21 Black	21 Blue	21 None	22 None
TW(vol)	1.86E+12	1.818E+12	1.678E+12	1.784E+12	1.666E+12
no.cells	78	70	90	90	69
no.fields	463	463	463	463	463
Frame um2	968.7	968.7	968.7	968.7	968.7
Nv	1.73910E-05	1.56073E-05	2.00665E-05	2.00665E-05	1.53843E-05
Cells/TW	3.23472E+07	2.83741E+07	3.36716E+07	3.57987E+07	2.56303E+07

Cell type	Leptotene/zygotene spermatocytes				
Group	Control	Control	Control	Control	Control
rat no.	20 None	21 Black	21 Blue	21 None	22 None
TW(vol)	1.86E+12	1.818E+12	1.678E+12	1.784E+12	1.666E+12
no.cells	112	97	103	100	96
no.fields	463	463	463	463	463
Frame um2	968.7	968.7	968.7	968.7	968.7
Nv	2.49717E-05	2.16273E-05	2.29650E-05	2.22961E-05	2.14043E-05
Cells/TW	4.64473E+07	3.93184E+07	3.85353E+07	3.97763E+07	3.56596E+07

Cell type	Sertoli cells				
Group	Control	Control	Control	Control	Control
rat no.	20 None	21 Black	21 Blue	21 None	22 None
TW(vol)	1.86E+12	1.818E+12	1.678E+12	1.784E+12	1.666E+12
no.cells	108	93	104	110	109

no.fields	463	463	463	463	463
Frame um2	968.7	968.7	968.7	968.7	968.7
Nv	2.40798E-05	2.07354E-05	2.31880E-05	2.45258E-05	2.43028E-05
Cells/TW	4.47885E+07	3.76970E+07	3.89094E+07	4.37539E+07	4.04885E+07

Cell type		**Round spermatids I - VIII**			
Group	Control	Control	Control	Control	Control
rat no.	20 None	21 Black	21 Blue	21 None	22 None
TW(vol)	1.86E+12	1.818E+12	1.678E+12	1.784E+12	1.666E+12
no.cells	109	133	124	234	134
no.fields	250	247	254	247	246
Frame um2	242.17	242.17	242.17	645.78	242.17
Nv	1.80039E-04	2.22349E-04	2.01589E-04	1.46701E-04	2.24931E-04
Cells/TW	3.34872E+08	4.04230E+08	3.38267E+08	2.61715E+08	3.74735E+08

Cell type		**Elongated spermatids I - VIII**			
Group	Control	Control	Control	Control	Control
rat no.	20 None	21 Black	21 Blue	21 None	22 None
TW(vol)	1.86E+12	1.818E+12	1.678E+12	1.784E+12	1.666E+12
no.cells	103	147	114	117	144
no.fields	250	247	254	249	246
Frame um2	242.17	242.17	242.17	242.17	242.17
Nv	1.70128E-04	2.45754E-04	1.85332E-04	1.94029E-04	2.41717E-04
Cells/TW	3.16439E+08	4.46780E+08	3.10987E+08	3.46147E+08	4.02700E+08

Cell type		**Elongating spermatids IX - XIV**			
Group	Control	Control	Control	Control	Control
rat no.	20 None	21 Black	21 Blue	21 None	22 None
TW(vol)	1.86E+12	1.818E+12	1.678E+12	1.784E+12	1.666E+12
no.cells	194	221	239	230	77
no.fields	250	247	254	249	241
Frame um2	1614.46	1614.46	1614.46	1614.46	645.78
Nv	4.80656E-05	5.54202E-05	5.82823E-05	5.72139E-05	4.94754E-05
Cells/TW	8.94020E+07	1.00754E+08	9.77977E+07	1.02070E+08	8.24260E+07

Cell type		**Pachytene spermatocytes I - VIII**			
Group	Control	Control	Control	Control	Control
rat no.	20 None	21 Black	21 Blue	21 None	22 None
TW(vol)	1.86E+12	1.818E+12	1.678E+12	1.784E+12	1.666E+12
no.cells	148	161	177	87	78
no.fields	250	247	254	247	241
Frame um2	1614.46	1614.46	1614.46	645.78	645.78
Nv	3.66686E-05	4.03740E-05	4.31631E-05	5.45428E-05	5.01179E-05
Cells/TW	6.82036E+07	7.33999E+07	7.24276E+07	9.73044E+07	8.34964E+07

Cell type		**Pachytene spermatocytes IX - XIV**			
Group	Control	Control	Control	Control	Control
rat no.	20 None	21 Black	21 Blue	21 None	22 None

TW(vol)	1.86E+12	1.818E+12	1.678E+12	1.784E+12	1.666E+12
no.cells	99	79	77	92	114
no.fields	250	247	254	249	246
frame					
um2	1614.46	1614.46	1614.46	1614.46	1614.46
Nv	2.45283E-05	1.98108E-05	1.87772E-05	2.28855E-05	2.87040E-05
Cells/TW	4.56227E+07	3.60161E+07	3.15081E+07	4.08278E+07	4.78209E+07

Acyline

Cell type		**Type A+intermediate spermatogonia**			
Group	Acyline	Acyline	Acyline	Acyline	Acyline
rat no.	5 None	6 Black	6 Blue	6 None	7 None
TW(vol)	2.96E+11	3.53E+11	2.81E+11	3.62E+11	2.5E+11
no.cells	67	42	81	54	44
no.fields	443	436	457	470	465
frame um2	430.52	430.52	430.52	430.52	430.52
Nv	3.51300E-05	2.23753E-05	4.11695E-05	2.66872E-05	2.19789E-05
Cells/TW	1.03985E+07	7.89849E+06	1.15686E+07	9.66076E+06	5.49473E+06

Cell type		**Type B+preleptotene spermatocytes**			
group	Acyline	Acyline	Acyline	Acyline	Acyline
rat no.	5 None	6 Black	6 Blue	6 None	7 None
TW(vol)	2.96E+11	3.53E+11	2.81E+11	3.62E+11	2.5E+11
no.cells	163	135	136	199	186
no.fields	443	436	450	470	465
frame um2	430.52	430.52	430.52	430.52	430.52
Nv	8.54654E-05	7.19207E-05	7.01993E-05	9.83472E-05	9.29109E-05
Cells/TW	2.52978E+07	2.53880E+07	1.97260E+07	3.56017E+07	2.32277E+07

Cell type		**Leptotene/zygotene spermatocytes**			
group	Acyline	Acyline	Acyline	Acyline	Acyline
rat no.	5 None	6 Black	6 Blue	6 None	7 None
TW(vol)	2.96E+11	3.53E+11	2.81E+11	3.62E+11	2.5E+11
no.cells	110	121	125	139	113
no.fields	450	460	450	450	400
frame um2	430.52	430.52	430.52	430.52	430.52
Nv	5.67789E-05	6.10990E-05	6.45215E-05	7.17479E-05	6.56183E-05
Cells/TW	1.68065E+07	2.15680E+07	1.81305E+07	2.59727E+07	1.64046E+07

Cell type			**Sertoli cells**		
group	Acyline	Acyline	Acyline	Acyline	Acyline
rat no.	5 None	6 Black	6 Blue	6 None	7 None
TW(vol)	2.96E+11	3.53E+11	2.81E+11	3.62E+11	2.5E+11
no.cells	173	84	169	94	167
no.fields	450	450	450	384	400
frame um2	215.26	215.26	215.26	215.26	215.26
Nv	1.78595E-04	8.67168E-05	1.74466E-04	1.13719E-04	1.93952E-04
Cells/TW	5.28642E+07	3.06110E+07	4.90250E+07	4.11663E+07	4.84879E+07

Cell type			**Round spermatids I - VIII**		
group	Acyline	Acyline	Acyline	Acyline	Acyline
rat no.	5 None	6 Black	6 Blue	6 None	7 None
TW(vol)	2.96E+11	3.53E+11	2.81E+11	3.62E+11	2.5E+11
no.cells	68	31	56	53	12
no.fields	256	255	246	253	247
frame um2	3444.19	3444.19	3444.19	3444.19	3444.19

Nv	7.71226E-06	3.52967E-06	6.60946E-06	6.08231E-06	1.41058E-06
Cells/TW	2.28283E+06	1.24597E+06	1.85726E+06	2.20179E+06	3.52645E+05

Cell type	**Elongated spermatids I - VIII**				
group	Acyline	Acyline	Acyline	Acyline	Acyline
rat no.	5 None	6 Black	6 Blue	6 None	7 None
TW(vol)	2.96E+11	3.53E+11	2.81E+11	3.62E+11	2.5E+11
no.cells	0	0	0	0	0
no.fields	2456	255	246	253	247
frame um2	3444.19	3444.19	3444.19	3444.19	3444.19
Nv	0.00000E+00	0.00000E+00	0.00000E+00	0.00000E+00	0.00000E+00
Cells/TW	0.00000E+00	0.00000E+00	0.00000E+00	0.00000E+00	0.00000E+00

Cell type	**Elongated spermatids IX - XIV**				
group	Acyline	Acyline	Acyline	Acyline	Acyline
rat no.	5 None	6 Black	6 Blue	6 None	7 None
TW(vol)	2.96E+11	3.53E+11	2.81E+11	3.62E+11	2.5E+11
no.cells	0	2	14	4	0
no.fields	256	255	246	253	247
frame um2	3444.19	3444.19	3444.19	3444.19	3444.19
Nv	0.00000E+00	2.27721E-07	1.65236E-06	4.59042E-07	0.00000E+00
Cells/TW	0.00000E+00	8.03854E+04	4.64314E+05	1.66173E+05	0.00000E+00

Cell type	**Pachytene spermatocytes I - VIII**				
group	Acyline	Acyline	Acyline	Acyline	Acyline
rat no.	5 None	6 Black	6 Blue	6 None	7 None
TW(vol)	2.96E+11	3.53E+11	2.81E+11	3.62E+11	2.5E+11
no.cells	101	94	103	130	76
no.fields	256	255	246	253	247
frame um2	1033.26	1033.26	1033.26	1033.26	1033.26
Nv	3.81832E-05	3.56762E-05	4.05222E-05	4.97294E-05	2.97788E-05
Cells/TW	1.13022E+07	1.25937E+07	1.13867E+07	1.80020E+07	7.44470E+06

Cell type	**Pachytene spermatocytes IX - XIV**				
group	Acyline	Acyline	Acyline	Acyline	Acyline
rat no.	5 None	6 Black	6 Blue	6 None	7 None
TW(vol)	2.96E+11	3.53E+11	2.81E+11	3.62E+11	2.5E+11
no.cells	45	28	40	37	36
no.fields	256	255	246	253	247
frame um2	3444.19	3444.19	3444.19	3444.19	3444.19
Nv	5.10370E-06	3.18809E-06	4.72104E-06	4.24614E-06	4.23173E-06
Cells/TW	1.51070E+06	1.12540E+06	1.32661E+06	1.53710E+06	1.05793E+06

<u>Acyline + FSH Ab</u>

Cell type	**Type A+intermediate spermatogonia**				
group	A + FSH Ab	A + FSH Ab	A + FSH Ab	A + FSH Ab	A + FSH Ab
rat no.	2 None	3 Black	3 Blue	3 None	7 Black
TW(vol)	2.22E+11	2.73E+11	2.76E+11	3.66E+11	3.77E+11
no.cells	33	53	21	34	49
no.fields	454	453	322	437	466
frame um2	430.52	430.52	430.52	430.52	430.52
Nv	1.68836E-05	2.71759E-05	1.51485E-05	1.80719E-05	2.44240E-05
Cells/TW	3.74816E+06	7.41903E+06	4.18099E+06	6.61432E+06	9.20785E+06

Cell type	Type B+preleptotene spermatocytes				
group	A + FSH Ab	A + FSH Ab	A + FSH Ab	A + FSH Ab	A + FSH Ab
rat no.	2 None	3 Black	3 Blue	3 None	7 Black
TW(vol)	2.22E+11	2.73E+11	2.76E+11	3.66E+11	3.77E+11
no.cells	100	94	99	128	171
no.fields	454	453	322	437	466
frame um2	430.52	430.52	430.52	430.52	430.52
Nv	5.11624E-05	4.81988E-05	7.14144E-05	6.80354E-05	8.52348E-05
Cells/TW	1.13581E+07	1.31583E+07	1.97104E+07	2.49010E+07	3.21335E+07

Cell type	Leptotene/zygotene spermatocytes				
group	A + FSH Ab	A + FSH Ab	A + FSH Ab	A + FSH Ab	A + FSH Ab
rat no.	2 None	3 Black	3 Blue	3 None	7 Black
TW(vol)	2.22E+11	2.73E+11	2.76E+11	3.66E+11	3.77E+11
no.cells	129	72	95	60	81
no.fields	454	453	450	450	400
frame um2	430.52	430.52	430.52	430.52	430.52
Nv	6.59995E-05	3.69182E-05	4.90363E-05	3.09703E-05	4.70361E-05
Cells/TW	1.46519E+07	1.00787E+07	1.35340E+07	1.13351E+07	1.77326E+07

Cell type	Sertoli cells				
group	A + FSH Ab	A + FSH Ab	A + FSH Ab	A + FSH Ab	A + FSH Ab
rat no.	2 None	3 Black	3 Blue	3 None	7 Black
TW(vol)	2.22E+11	2.73E+11	2.76E+11	3.66E+11	3.77E+11
no.cells	209	118	116	139	158
no.fields	450	453	450	450	400
frame um2	215.26	215.26	215.26	215.26	215.26
Nv	2.15760E-04	1.21010E-04	1.19752E-04	1.43496E-04	1.83499E-04
Cells/TW	4.78987E+07	3.30357E+07	3.30515E+07	5.25194E+07	6.91791E+07

Cell type	Round spermatids I - VIII				
group	A + FSH Ab	A + FSH Ab	A + FSH Ab	A + FSH Ab	A + FSH Ab
rat no.	2 None	3 Black	3 Blue	3 None	7 Black
TW(vol)	2.22E+11	2.73E+11	2.76E+11	3.66E+11	3.77E+11
no.cells	55	33	27	53	71
no.fields	252	170	211	251	253
frame um2	3444.19	3444.19	3444.19	3444.19	3444.19
Nv	6.33687E-06	5.63609E-06	3.71530E-06	6.13077E-06	8.14799E-06
Cells/TW	1.40679E+06	1.53865E+06	1.02542E+06	2.24386E+06	3.07179E+06

Cell type	Elongated spermatids I - VIII				
group	A + FSH Ab	A + FSH Ab	A + FSH Ab	A + FSH Ab	A + FSH Ab
rat no.	2 None	3 Black	3 Blue	3 None	7 Black
TW(vol)	2.22E+11	2.73E+11	2.76E+11	3.66E+11	3.77E+11
no.cells	0	0	0	0	0
no.fields	252	170	211	251	253
frame um2	3444.19	3444.19	3444.19	3444.19	3444.19
Nv	0.00000E+00	0.00000E+00	0.00000E+00	0.00000E+00	0.00000E+00
Cells/TW	0.00000E+00	0.00000E+00	0.00000E+00	0.00000E+00	0.00000E+00

Cell type	Elongated spermatids IX - XIV				
group	A + FSH Ab	A + FSH Ab	A + FSH Ab	A + FSH Ab	A + FSH Ab
rat no.	2 None	3 Black	3 Blue	3 None	7 Black
TW(vol)	2.22E+11	2.73E+11	2.76E+11	3.66E+11	3.77E+11

no.cells	3	0	0	1	0
no.fields	252	170	211	251	253
frame um2	3444.19	3444.19	3444.19	3444.19	3444.19
Nv	3.45648E-07	0.00000E+00	0.00000E+00	1.15675E-07	0.00000E+00
Cells/TW	7.67338E+04	0.00000E+00	0.00000E+00	4.23370E+04	0.00000E+00

Cell type	**Pachytene spermatocytes I - VIII**				
group	A + FSH Ab	A + FSH Ab	A + FSH Ab	A + FSH Ab	A + FSH Ab
rat no.	2 None	3 Black	3 Blue	3 None	7 Black
TW(vol)	2.22E+11	2.73E+11	2.76E+11	3.66E+11	3.77E+11
no.cells	58	46	105	165	180
no.fields	252	170	211	251	253
frame um2	1033.26	1033.26	3444.19	3444.19	3444.19
Nv	2.22750E-05	2.61878E-05	1.44484E-05	1.90864E-05	2.06569E-05
Cells/TW	4.94505E+06	7.14927E+06	3.98776E+06	6.98561E+06	7.78765E+06

Cell type	**Pachytene spermatocytes IX – XIV**				
group	A + FSH Ab	A + FSH Ab	A + FSH Ab	A + FSH Ab	A + FSH Ab
rat no.	2 None	3 Black	3 Blue	3 None	7 Black
TW(vol)	2.22E+11	2.73E+11	2.76E+11	3.66E+11	3.77E+11
no.cells	26	7	23	23	19
no.fields	252	170	211	251	253
frame um2	3444.19	3444.19	3444.19	3444.19	3444.19
Nv	2.99561E-06	1.19553E-06	3.16489E-06	2.66052E-06	2.18045E-06
Cells/TW	6.65026E+05	3.26381E+05	8.73509E+05	9.73751E+05	8.22029E+05

			Acyline + FSH		
Cell type	**Type A+intermediate spermatogonia**				
group	A + FSH	A + FSH	A + FSH	A + FSH	A + FSH
rat no.	16 None	17 Black	17 Blue	17 None	18 None
TW(vol)	4.92E+11	4.02E+11	4.43E+11	4.02E+11	4.82E+11
no.cells	25	31	21	28	25
no.fields	439	458	423	457	456
frame um2	430.52	430.52	430.52	430.52	430.52
Nv	1.32276E-05	1.57218E-05	1.15315E-05	1.42314E-05	1.27345E-05
Cells/TW	6.50800E+06	6.32017E+06	5.10845E+06	5.72103E+06	6.13803E+06

Cell type	**Type B+preleptotene spermatocytes**				
group	A + FSH	A + FSH	A + FSH	A + FSH	A + FSH
rat no.	16 None	17 Black	17 Blue	17 None	18 None
TW(vol)	4.92E+11	4.02E+11	4.43E+11	4.02E+11	4.82E+11
no.cells	133	185	134	178	166
no.fields	439	458	423	457	456
frame um2	430.52	430.52	430.52	430.52	430.52
Nv	7.03710E-05	9.38238E-05	7.35819E-05	9.04712E-05	8.45571E-05
Cells/TW	3.46225E+07	3.77172E+07	3.25968E+07	3.63694E+07	4.07565E+07

Cell type	**Leptotene/zygotene spermatocytes**				
group	A + FSH	A + FSH	A + FSH	A + FSH	A + FSH
rat no.	16 None	17 Black	17 Blue	17 None	18 None
TW(vol)	4.92E+11	4.02E+11	4.43E+11	4.02E+11	4.82E+11
no.cells	93	106	108	109	97
no.fields	450	373	450	450	457

frame um2	430.52	430.52	430.52	430.52	430.52
Nv	4.80040E-05	6.60091E-05	5.57465E-05	5.62627E-05	4.93017E-05
Cells/TW	2.36180E+07	2.65357E+07	2.46957E+07	2.26176E+07	2.37634E+07

Cell type	**Sertoli cells**				
group	A + FSH	A + FSH	A + FSH	A + FSH	A + FSH
rat no.	16 None	17 Black	17 Blue	17 None	18 None
TW(vol)	4.92E+11	4.02E+11	4.43E+11	4.02E+11	4.82E+11
no.cells	70	136	112	116	136
no.fields	450	450	450	450	450
frame um2	215.26	215.26	215.26	215.26	215.26
Nv	7.22640E-05	1.40399E-04	1.15622E-04	1.19752E-04	1.40399E-04
Cells/TW	3.55539E+07	5.64403E+07	5.12207E+07	4.81402E+07	6.76722E+07

Cell type	**Round spermatids I - VIII**				
group	A + FSH	A + FSH	A + FSH	A + FSH	A + FSH
rat no.	16 None	17 Black	17 Blue	17 None	18 None
TW(vol)	4.92E+11	4.02E+11	4.43E+11	4.02E+11	4.82E+11
no.cells	155	86	115	139	143
no.fields	245	220	249	250	256
frame um2	1033.26	1033.26	1033.26	1033.26	1033.26
Nv	6.12288E-05	3.78326E-05	4.46981E-05	5.38103E-05	5.40613E-05
Cells/TW	3.01246E+07	1.52087E+07	1.98012E+07	2.16317E+07	2.60575E+07

Cell type	**Elongated spermatids I - VIII**				
group	A + FSH	A + FSH	A + FSH	A + FSH	A + FSH
rat no.	16 None	17 Black	17 Blue	17 None	18 None
TW(vol)	4.92E+11	4.02E+11	4.43E+11	4.02E+11	4.82E+11
no.cells	0	0	0	0	0
no.fields	245	220	249	250	256
frame um2	3444.19	3444.19	3444.19	3444.19	3444.19
Nv	0.00000E+00	0.00000E+00	0.00000E+00	0.00000E+00	0.00000E+00
Cells/TW	0.00000E+00	0.00000E+00	0.00000E+00	0.00000E+00	0.00000E+00

Cell type	**Elongated spermatids IX - XIV**				
group	A + FSH	A + FSH	A + FSH	A + FSH	A + FSH
rat no.	16 None	17 Black	17 Blue	17 None	18 None
TW(vol)	4.92E+11	4.02E+11	4.43E+11	4.02E+11	4.82E+11
no.cells	4	0	20	10	2
no.fields	245	220	249	250	256
frame um2	3444.19	3444.19	3444.19	3444.19	3444.19
Nv	4.74031E-07	0.00000E+00	2.33208E-06	1.16138E-06	2.26831E-07
Cells/TW	2.33223E+05	0.00000E+00	1.03311E+06	4.66873E+05	1.09333E+05

Cell type	**Pachytene spermatocytes I - VIII**				
group	A + FSH	A + FSH	A + FSH	A + FSH	A + FSH
rat no.	16 None	17 Black	17 Blue	17 None	18 None
TW(vol)	4.92E+11	4.02E+11	4.43E+11	4.02E+11	4.82E+11
no.cells	289	289	266	303	290
no.fields	245	220	249	250	256
frame um2	1033.26	1033.26	1033.26	1033.26	1033.26
Nv	1.14162E-04	1.27135E-04	1.03389E-04	1.17299E-04	1.09635E-04
Cells/TW	5.61678E+07	5.11083E+07	4.58012E+07	4.71541E+07	5.28440E+07

Cell type	**Pachytene spermatocytes**

		IX - XIV			
group	A + FSH	A + FSH	A + FSH	A + FSH	A + FSH
rat no.	16 None	17 Black	17 Blue	17 None	18 None
TW(vol)	4.92E+11	4.02E+11	4.43E+11	4.02E+11	4.82E+11
no.cells	174	99	135	145	133
no.fields	245	220	249	250	256
frame um2	3444.19	3444.19	3444.19	3444.19	3444.19
Nv	2.06204E-05	1.30655E-05	1.57415E-05	1.68400E-05	1.50843E-05
Cells/TW	1.01452E+07	5.25232E+06	6.97350E+06	6.76966E+06	7.27062E+06

			Acyline + hCG + FSH Ab		
Cell type		**Type A+intermediate spermatogonia**			
group	A + hCG + F Ab	A + hCG + F Ab	A + hCG + F Ab	A + hCG + F Ab	A + hCG + F Ab
rat no.	9 None	10 Black	10 Blue	10 None	14 None
TW(vol)	4.6E+11	3.6E+11	5.13E+11	3.7E+11	3.72E+11
no.cells	22	32	26	28	24
no.fields	443	462	454	458	369
frame um2	430.52	430.52	430.52	430.52	430.52
Nv	1.15352E-05	1.60885E-05	1.33022E-05	1.42004E-05	1.51075E-05
Cells/TW	5.30620E+06	5.79185E+06	6.82404E+06	5.25413E+06	5.61998E+06

Cell type		**Type B+preleptotene spermatocytes**			
group	A + hCG + F Ab	A + hCG + F Ab	A + hCG + F Ab	A + hCG + F Ab	A + hCG + F Ab
rat no.	9 None	10 Black	10 Blue	10 None	14 None
TW(vol)	4.6E+11	3.6E+11	5.13E+11	3.7E+11	3.72E+11
no.cells	92	101	88	118	108
no.fields	443	464	454	458	369
frame um2	430.52	430.52	430.52	430.52	430.52
Nv	4.82382E-05	5.05603E-05	4.50229E-05	5.98444E-05	6.79836E-05
Cells/TW	2.21896E+07	1.82017E+07	2.30967E+07	2.21424E+07	2.52899E+07

Cell type		**Leptotene/zygotene spermatocytes**			
group	A + hCG + F Ab	A + hCG + F Ab	A + hCG + F Ab	A + hCG + F Ab	A + hCG + F Ab
rat no.	9 None	10 Black	10 Blue	10 None	14 None
TW(vol)	4.6E+11	3.6E+11	5.13E+11	3.7E+11	3.72E+11
no.cells	87	116	62	89	99
no.fields	400	450	450	450	369
frame um2	430.52	430.52	430.52	430.52	430.52
Nv	5.05203E-05	5.98759E-05	3.20026E-05	4.59393E-05	6.23183E-05
Cells/TW	2.32393E+07	2.15553E+07	1.64174E+07	1.69975E+07	2.31824E+07

Cell type			**Sertoli cells**		
group	A + hCG + F Ab	A + hCG + F Ab	A + hCG + F Ab	A + hCG + F Ab	A + hCG + F Ab
rat no.	9 None	10 Black	10 Blue	10 None	14 None
TW(vol)	4.6E+11	3.6E+11	5.13E+11	3.7E+11	3.72E+11
no.cells	116	141	58	198	120
no.fields	400	450	450	450	369
frame um2	215.26	215.26	215.26	215.26	215.26
Nv	1.34721E-04	1.45560E-04	5.98759E-05	2.04404E-04	1.51075E-04
Cells/TW	6.19716E+07	5.24017E+07	3.07163E+07	7.56295E+07	5.61998E+07

Cell type	Round spermatids I - VIII				
group	A + hCG + F Ab	A + hCG + F Ab	A + hCG + F Ab	A + hCG + F Ab	A + hCG + F Ab
rat no.	9 None	10 Black	10 Blue	10 None	14 None
TW(vol)	4.6E+11	3.6E+11	5.13E+11	3.7E+11	3.72E+11
no.cells	27	102	120	51	197
no.fields	219	242	258	194	242
frame um2	3444.19	3444.19	3444.19	3444.19	3444.19
Nv	3.57958E-06	1.22376E-05	1.35044E-05	7.63276E-06	2.36354E-05
Cells/TW	1.64661E+06	4.40555E+06	6.92774E+06	2.82412E+06	8.79239E+06

Cell type	Elongated spermatids I - VIII				
group	A + hCG + F Ab	A + hCG + F Ab	A + hCG + F Ab	A + hCG + F Ab	A + hCG + F Ab
rat no.	9 None	10 Black	10 Blue	10 None	14 None
TW(vol)	4.6E+11	3.6E+11	5.13E+11	3.7E+11	3.72E+11
no.cells	0	0	0	0	0
no.fields	219	242	258	194	242
frame um2	3444.19	3444.19	3444.19	3444.19	3444.19
Nv	0.00000E+00	0.00000E+00	0.00000E+00	0.00000E+00	0.00000E+00
Cells/TW	0.00000E+00	0.00000E+00	0.00000E+00	0.00000E+00	0.00000E+00

Cell type	Elongated spermatids IX - XIV				
group	A + hCG + F Ab	A + hCG + F Ab	A + hCG + F Ab	A + hCG + F Ab	A + hCG + F Ab
rat no.	9 None	10 Black	10 Blue	10 None	14 None
TW(vol)	4.6E+11	3.6E+11	5.13E+11	3.7E+11	3.72E+11
no.cells	0	0	1	10	0
no.fields	219	242	258	194	242
frame um2	3444.19	3444.19	3444.19	3444.19	3444.19
Nv	0.00000E+00	0.00000E+00	1.12536E-07	1.49662E-06	0.00000E+00
Cells/TW	0.00000E+00	0.00000E+00	5.77312E+04	5.53749E+05	0.00000E+00

Cell type	Pachytene spermatocytes I - VIII				
group	A + hCG + F Ab	A + hCG + F Ab	A + hCG + F Ab	A + hCG + F Ab	A + hCG + F Ab
rat no.	9 None	10 Black	10 Blue	10 None	14 None
TW(vol)	4.6E+11	3.6E+11	5.13E+11	3.7E+11	3.72E+11
no.cells	125	187	129	84	155
no.fields	219	242	258	194	242
frame um2	1033.26	1033.26	1033.26	1033.26	1033.26
Nv	5.52403E-05	7.47854E-05	4.83905E-05	4.19052E-05	6.19879E-05
Cells/TW	2.54106E+07	2.69227E+07	2.48243E+07	1.55049E+07	2.30595E+07

Cell type	Pachytene spermatocytes IX - XIV				
group	A + hCG + F Ab	A + hCG + F Ab	A + hCG + F Ab	A + hCG + F Ab	A + hCG + F Ab
rat no.	9 None	10 Black	10 Blue	10 None	14 None
TW(vol)	4.6E+11	3.6E+11	5.13E+11	3.7E+11	3.72E+11
no.cells	53	90	90	56	51
no.fields	219	242	258	194	242
frame um2	3444.19	3444.19	3444.19	3444.19	3444.19
Nv	7.02659E-06	1.07979E-05	1.01283E-05	8.38106E-06	6.11882E-06
Cells/TW	3.23223E+06	3.88725E+06	5.19581E+06	3.10099E+06	2.27620E+06
	Acyline +				

	hCG				
Cell type	**Type A+intermediate spermatogonia**				
group	A + hCG	A + hCG	A + hCG	A + hCG	A + hCG
rat no.	12 None	13 Black	13 Blue	13 None	18 Black
TW(vol)	5.05E+11	5.71E+11	3.75E+11	3.61E+11	5.76E+11
no.cells	17	19	37	35	28
no.fields	455	428	447	363	454
frame um2	430.52	430.52	430.52	430.52	430.52
Nv	8.67849E-06	1.03114E-05	1.92265E-05	2.23959E-05	1.43255E-05
Cells/TW	4.38264E+06	5.88779E+06	7.20995E+06	8.08491E+06	8.25147E+06
Cell type	**Type B+preleptotene spermatocytes**				
group	A + hCG	A + hCG	A + hCG	A + hCG	A + hCG
rat no.	12 None	13 Black	13 Blue	13 None	18 Black
TW(vol)	5.05E+11	5.71E+11	3.75E+11	3.61E+11	5.76E+11
no.cells	116	83	124	120	113
no.fields	455	428	447	363	454
frame um2	430.52	430.52	430.52	430.52	430.52
Nv	5.92179E-05	4.50444E-05	6.44349E-05	7.67859E-05	5.78135E-05
Cells/TW	2.99051E+07	2.57204E+07	2.41631E+07	2.77197E+07	3.33006E+07
Cell type	**Leptotene/zygotene spermatocytes**				
group	A + hCG	A + hCG	A + hCG	A + hCG	A + hCG
rat no.	12 None	13 Black	13 Blue	13 None	18 Black
TW(vol)	5.05E+11	5.71E+11	3.75E+11	3.61E+11	5.76E+11
no.cells	92	68	129	95	103
no.fields	450	450	450	400	446
frame um2	430.52	430.52	430.52	430.52	430.52
Nv	4.74878E-05	3.50997E-05	6.65861E-05	5.51658E-05	5.36425E-05
Cells/TW	2.39813E+07	2.00419E+07	2.49698E+07	1.99149E+07	3.08981E+07
Cell type	**Sertoli cells**				
group	A + hCG	A + hCG	A + hCG	A + hCG	A + hCG
rat no.	12 None	13 Black	13 Blue	13 None	18 Black
TW(vol)	5.05E+11	5.71E+11	3.75E+11	3.61E+11	5.76E+11
no.cells	109	107	117	83	98
no.fields	450	450	450	400	446
frame um2	215.26	215.26	215.26	215.26	215.26
Nv	1.12525E-04	1.10461E-04	1.20784E-04	9.63951E-05	1.02077E-04
Cells/TW	5.68253E+07	6.30731E+07	4.52941E+07	3.47986E+07	5.87963E+07
Cell type	**Round spermatids I - VIII**				
group	A + hCG	A + hCG	A + hCG	A + hCG	A + hCG
rat no.	12 None	13 Black	13 Blue	13 None	18 Black
TW(vol)	5.05E+11	5.71E+11	3.75E+11	3.61E+11	5.76E+11
no.cells	191	176	98	83	83
no.fields	252	248	304	219	252
frame um2	3444.19	3444.56	1033.26	1033.26	3444.19
Nv	2.20062E-05	2.06028E-05	3.11992E-05	3.66796E-05	9.56292E-06
Cells/TW	1.11131E+07	1.17642E+07	1.16997E+07	1.32413E+07	5.50824E+06
Cell type	**Elongated spermatids I - VIII**				
group	A + hCG	A + hCG	A + hCG	A + hCG	A + hCG
rat no.	12 None	13 Black	13 Blue	13 None	18 Black

TW(vol)	5.05E+11	5.71E+11	3.75E+11	3.61E+11	5.76E+11
no.cells	0	0	0	0	0
no.fields	252	248	304	219	252
frame um2	3444.19	3444.56	3444.19	3444.19	3444.19
Nv	0.00000E+00	0.00000E+00	0.00000E+00	0.00000E+00	0.00000E+00
Cells/TW	0.00000E+00	0.00000E+00	0.00000E+00	0.00000E+00	0.00000E+00

Cell type	**Elongated spermatids IX - XIV**				
group	A + hCG	A + hCG	A + hCG	A + hCG	A + hCG
rat no.	12 None	13 Black	13 Blue	13 None	18 Black
TW(vol)	5.05E+11	5.71E+11	3.75E+11	3.61E+11	5.76E+11
no.cells	17	5	0	7	0
no.fields	252	248	304	219	252
frame um2	3444.19	3444.56	3444.19	3444.19	3444.19
Nv	1.95867E-06	5.85308E-07	0.00000E+00	9.28040E-07	0.00000E+00
Cells/TW	9.89128E+05	3.34211E+05	0.00000E+00	3.35023E+05	0.00000E+00

Cell type	**Pachytene spermatocytes I - VIII**				
group	A + hCG	A + hCG	A + hCG	A + hCG	A + hCG
rat no.	12 None	13 Black	13 Blue	13 None	18 Black
TW(vol)	5.05E+11	5.71E+11	3.75E+11	3.61E+11	5.76E+11
no.cells	179	182	297	260	214
no.fields	252	248	304	219	252
frame um2	1033.26	1033.26	1033.26	1033.26	1033.26
Nv	6.87453E-05	7.10248E-05	9.45526E-05	1.14900E-04	8.21871E-05
Cells/TW	3.47164E+07	4.05552E+07	3.54572E+07	4.14789E+07	4.73398E+07

Cell type	**Pachytene spermatocytes IX - XIV**				
group	A + hCG	A + hCG	A + hCG	A + hCG	A + hCG
rat no.	12 None	13 Black	13 Blue	13 None	18 Black
TW(vol)	5.05E+11	5.71E+11	3.75E+11	3.61E+11	5.76E+11
no.cells	61	68	122	71	86
no.fields	252	248	304	219	252
frame um2	3444.19	3444.56	3444.19	3444.19	3444.19
Nv	7.02817E-06	7.96019E-06	1.16520E-05	9.41298E-06	9.90857E-06
Cells/TW	3.54923E+06	4.54527E+06	4.36949E+06	3.39809E+06	5.70733E+06

Appendix 1.5: Individual human immunos.

***Full size pictures presented on CD inside back cover**